

NOTE TO USERS

This reproduction is the best copy available

UMI

**THE ROLE OF GROUNDWATER FLOW IN STREAMFLOW GENERATION
WITHIN TWO SMALL FORESTED WATERSHEDS
OF THE CANADIAN SHIELD**

by

Marc Joseph Hinton

A thesis
presented to the University of Waterloo
in fulfillment of the
thesis requirement for the degree of
Doctor of Philosophy
in
Earth Sciences

Waterloo, Ontario, Canada, 1998

© Marc Joseph Hinton 1998



**National Library
of Canada**

**Acquisitions and
Bibliographic Services**

395 Wellington Street
Ottawa ON K1A 0N4
Canada

**Bibliothèque nationale
du Canada**

**Acquisitions et
services bibliographiques**

395, rue Wellington
Ottawa ON K1A 0N4
Canada

Your file Votre référence

Our file Notre référence

The author has granted a non-exclusive licence allowing the National Library of Canada to reproduce, loan, distribute or sell copies of this thesis in microform, paper or electronic formats.

The author retains ownership of the copyright in this thesis. Neither the thesis nor substantial extracts from it may be printed or otherwise reproduced without the author's permission.

L'auteur a accordé une licence non exclusive permettant à la Bibliothèque nationale du Canada de reproduire, prêter, distribuer ou vendre des copies de cette thèse sous la forme de microfiche/film, de reproduction sur papier ou sur format électronique.

L'auteur conserve la propriété du droit d'auteur qui protège cette thèse. Ni la thèse ni des extraits substantiels de celle-ci ne doivent être imprimés ou autrement reproduits sans son autorisation.

0-612-38244-3

Canada

The University of Waterloo requires the signatures of all persons using or photocopying this thesis. Please sign below, and give address and date.

ABSTRACT

The role of subsurface flow in streamflow generation during storms was investigated in two forested watersheds of the Canadian Shield in south-central Ontario. Storms were intensively monitored in the Harp 4-21 catchment (3.7 ha), where coarse-textured glacial till is up to 15 m thick, and in Harp 3A (21.7 ha), where the till is less than 0.5 m thick. Measured data included stream discharge in up to five subcatchments per watershed, soil moisture content by time domain reflectometry, groundwater levels, and groundwater and stream chemistry.

Subsurface flow is the dominant component of storm runoff. More than 75% of stream discharge in Harp 4-21 and 85% in Harp 3A was pre-event water (soil and till water). Three-component hydrograph separations based on two tracers (^{18}O and dissolved silica) in Harp 4-21 show that groundwater flow through glacial till contributed 29 and 62% of total runoff for two storms. Vertical hydraulic gradients show that increased flow from the tills to the soils cannot account for the large and rapid increase of the till water component in the stream. Pre-event till water that has been discharged to the soils prior to storm onset is probably flushed from the soils into the stream during storm events.

Increased subsurface flow is caused by increased water content and hydraulic conductivity, rather than by increased hydraulic gradient. Since increases in hydraulic gradient were small (<0.04), groundwater ridging was insufficient to produce the observed increases in subsurface flow. Instead, the rising water table saturated permeable soil horizons, thereby increasing hydraulic conductivities and downslope subsurface flow. Flow within the transiently saturated horizons can account for observed subsurface stormflow if hydraulic conductivities are high. In Harp 4-21 and Harp 3A, sufficiently high saturated hydraulic conductivities of approximately 10^{-3} m/s were estimated from soil water balances and

infiltration experiments. However, macropores must be present to account for the high measured hydraulic conductivities of these soils.

Most of the subsurface storm runoff in the two catchments was generated within the soils because soil structure and macropores led to higher hydraulic conductivities in the soil than in the underlying glacial till or bedrock. Furthermore, subsurface flow and the efficiency of runoff production from a hillslope were greatest when groundwater levels rose into shallow soil horizons. Results were most consistent with the transmissivity feedback model with dual porosity flow in which the large increase in subsurface flow is attributed to saturation of macropores in shallow soil horizons by a rising water table. This conceptual model also provides an explanation for the displacement of pre-event water through macropores to the stream.

The thickness of glacial till influences the area from which runoff is generated and, consequently, the magnitude of storm runoff. In Harp 4-21, where till is thick, upslope areas store infiltrating precipitation and generate little runoff. Groundwater flow through the till maintains high groundwater levels and water contents in soils adjacent to the stream throughout the year. Wet areas near the Harp 4-21 stream respond rapidly to storms and contribute consistently to storm runoff along shallow flowpaths even after dry weather conditions. In Harp 3A, where till is thin, upslope areas cannot sustain groundwater flow during dry periods, areas adjacent to the stream dry out, and summer storms produce minimal runoff. However, when antecedent conditions in Harp 3A are wet, the water table develops in middle and upper hillslope soils and subsurface runoff is generated rapidly. As a result, storm runoff is more variable (effective runoff ratios of 0.0-0.67) in Harp 3A than in Harp 4-21 (0.07-0.38).

Dissolved organic carbon (DOC) concentrations and budgets demonstrate the importance of storms to the DOC export from catchments. DOC concentrations in the stream increase during storms by as much as 100 and 410% in Harp 3A and Harp 4-21 respectively. Storms were responsible for the export of between 57 to 68% of the total DOC in autumn and between 29 to 40% in spring. Riparian groundwater levels and flowpaths influence DOC concentrations and sources to the stream during storms. In Harp 4-21, riparian areas contributed between 73 and 84% of the stream DOC export during an autumn storm because groundwater flowed through shallow organic horizons as demonstrated by near-stream piezometers. In Harp 3A, riparian areas of hillslopes contributed less than 50% of the stream DOC because riparian flowpaths were predominantly through the lower B horizon.

This thesis contributes to the methodology, data collection, interpretation, and conceptual understanding of subsurface flow in streamflow generation studies. General equations for three-component hydrograph separations were developed and applied to this study. The magnitude and timing of runoff production from hillslope sites were quantified by a soil water balance method. This method relates runoff generation to changes in water storage instead of water fluxes. The concept of a variable contributing area, which defines the area that contributes to surface and subsurface runoff generation, was introduced. Existing conceptual models of streamflow generation were re-interpreted and classified according to the mechanism (increase in hydraulic conductivity, increase in hydraulic gradient), the spatial extent and the zone in which increased subsurface flow occurs (saturated, transiently-saturated or unsaturated).

The results of this research have several implications for the study of subsurface flow during storms. This study has demonstrated the importance of relating physical and hydraulic properties such as slope, sediment texture, till thickness, hydraulic conductivity and characteristic curves to subsurface flow generation. Since increases in water content and

hydraulic conductivity are more important than increases in hydraulic gradient for producing subsurface flow on the catchment scale, a greater focus on measurements of the unsaturated properties of undisturbed sediments in future studies is warranted. Many gaps in our understanding of subsurface flow generation during storms have been identified, and several opportunities for additional research suggested.

ACKNOWLEDGEMENTS

Graduate studies at the University of Waterloo have been a good experience for me. During the course of my studies, I have had the pleasure to befriend, work with, learn from, and share ideas with some very good people. Most notable among these people are my supervisors, Drs. Sherry Schiff and Mike English. I am very grateful for the guidance, encouragement, trust, patience and opportunities they have given me. I have learned much more from them than I could have expected from any graduate program.

I would like to thank my thesis committee members, the late Dr. Bob Farvolden, Dr. Bob Gillham, Dr. Dave Rudolph, for constructive comments on my thesis, and the external members of my thesis defense committee, Dr. Mike Stone and Dr. Jeff McDonnell, for enthusiastically agreeing to review this research.

Several people contributed to this thesis in small or large ways. Alex MacLean's hard work, endurance and good humor in difficult field conditions are testimony to his good nature and dedication. Richard Elgood's patience, willing cooperation, and ability to find solutions for problems encountered in the lab and the field was most helpful and appreciated. Mike Stone's interest and generosity with his time to help students was also appreciated. Lem Scott was very helpful in providing advice on instrumentation and hydrological conditions in the field. Ramon Aravena and I shared very interesting discussions on DOC and on scientific research. George Schneider conducted the geophysical survey in Harp 4-21 and explained its results with great enthusiasm. Dave Redmond shared his expertise in time domain reflectometry (TDR) and allowed me to use the WATTDR program for the analysis of TDR traces. I also wish to thank Jennifer Ailles, Sam Alpay, Cam Chadwick, Connie Constantinidis, Steve Dankevy, Mike English, Randy Fagan, Lee Ann Fishback, Bob Ingleton, Paul Johnson, Alex MacLean, Jane MacLean, Anne Meyer, Paul Overduin, Jodi Patterson,

Larry Pezutto, Michael Schultz, Mark van Bakel and Jamie Wills for assistance in the field and in Waterloo.

I would like to thank Pat and Glenn Kyryluk who graciously agreed to let me conduct research on their property and Mr. and Mrs. Droppo who rented out their cottage in convenient proximity to the Harp 3A watershed.

Dr. Peter Dillon, Dr. Bruce LaZerte and Lem Scott of the Ontario Ministry of the Environment at Dorset provided precipitation, streamflow and water chemistry data and much appreciated logistical support including chemical analyses, access to MOE instrumentation and facilities, a workspace, and field equipment. Field equipment was also borrowed from the Geography Department at Wilfrid Laurier University and the Department of Earth Sciences at the University of Waterloo.

Funding for field work was provided by the Ontario Ministry of the Environment and the Natural Science and Engineering Research Council of Canada (to S. Schiff). The University of Waterloo Science and Graduate Studies Offices and the Waterloo Centre for Groundwater Research supported travel to scientific conferences. I am also very grateful for personal financial support from the Natural Science and Engineering Research Council of Canada, Eco-Research (Tri-Council Secretariat) and Geological Society of America scholarships.

Several people helped make my experience in Waterloo most enjoyable including Brewster Conant, Jalal Biglou, Willem Sluis, the rest of the Huether Hoods, Laura Smith, and fellow students, colleagues and staff. The spirit of cooperation that I experienced at the University of Waterloo, Wilfrid Laurier University and the Ministry of the Environment at Dorset was remarkable.

I wish to thank Connie Constantinidis for her encouragement and friendship, and for always believing that I could do this work.

I am very grateful to Denyse, Paul, Sonia, Jean-Pierre and Michelle for their encouragement, support and understanding throughout many years of study, and to Sarah and Laura whose smiles and laughter make my day even brighter.

Most of all, I wish to thank Sam for sharing this wonderful experience with me.

To
Denyse
and
Norman

TABLE OF CONTENTS

ABSTRACT	iv
ACKNOWLEDGEMENTS	viii
LIST OF TABLES	xviii
LIST OF ILLUSTRATIONS	xx
COPYRIGHTS	xxvi
Chapter 1: Introduction	1
Research context: Challenges and opportunities	2
Paradigm shifts in conceptual models and methods in streamflow generation studies	2
Hydrology on the Canadian Shield	7
Research objectives	11
Study area	11
Organization of thesis	13
Chapter 2: Subsurface flow in conceptual models of streamflow generation	15
Introduction	15
Terminology	16
Mechanisms for increased subsurface flow to streams during storms	17
Increase in hydraulic conductivity	18
Increase in hydraulic gradients	18
Zones of increased subsurface flow	20
Conceptual models of subsurface flow generation and their development	22
1) Unsaturated flow	23
2) Groundwater ridging model	26
3) Transmissivity feedback model	28
4) Perched water table model	31
5) Old water macropore flow model	33
Comparison of the conceptual models of subsurface stormflow generation	34
Physical and hydrological properties conducive to subsurface stormflow generation	37
Groundwater ridging	39
Models with increasing saturation	40
Transmissivity feedback with matrix flow	42
Transmissivity feedback with dual porosity flow	42
Old water macropore flow	44
Perched water table	45

Unsaturated flow	45
Conclusions	46
Chapter 3: Physical properties governing groundwater flow in Harp 4-21	48
Introduction	48
Study Site	50
Methods	53
Results and Discussion	56
Hydraulic conductivity of the sediments	56
Surface topography	57
Sediment thickness	62
Spatial and temporal pattern of stream discharge	67
Conclusions	72
Chapter 4: Examining the contributions of glacial till water to storm runoff using two- and three-component hydrograph separations	77
Introduction	77
Study Site	79
Methods	81
Hydrograph Separation	83
Results and Discussion	85
Two-Component Hydrograph Separations Based on ^{18}O	85
Three-Component Hydrograph Separations based on ^{18}O and SiO_2	90
Uncertainties in the Till Water Component	100
Two-Component Hydrograph Separations Based on SiO_2	103
Groundwater Flow from the Till to the Soil	105
Summary and Conclusions	109
Chapter 5: Role of glacial till on groundwater levels and stream runoff: A comparison of Harp 4-21 and Harp 3A.	111
Introduction	111
Study site	112
Methods	115
Instrumentation	115
Monitoring periods	117
Effective runoff ratios	117
Results	119
Precipitation	119
Stream discharge	119
Hydrograph separations	130
Groundwater levels	132
1) Depth to the water table	132
2) Groundwater flow from upslope during dry weather	132
3) The area (or spatial extent) where the water table is located within the soil horizons	134
4) The timing of water table fluctuations	137

Discussion	139
Effect of glacial till on groundwater flow and stream discharge	139
Effect of soils on storm runoff	142
Conclusions	142
 Chapter 6: Subsurface flow production in Harp 4-21 and Harp 3A	 144
Introduction	144
Study site	146
Methods	146
Instrumentation	146
Monitoring	147
Characteristic curves	149
Water storage calculations	151
Water balance	154
Subsurface runoff ratio	157
Results	157
Water content and soil characteristic curves	157
Cumulative water balances	159
1) November 2 and 4, 1992 event in Harp 4-21	159
2) November 2 and 4, 1992 event in Harp 3A	166
3) November 10 and 12, 1992 event in Harp 3A	169
4) Water redistribution during dry periods	173
5) Spring storm events	177
Individual water balances	177
1) Changes in net subsurface runoff and groundwater levels	177
2) Total hillslope runoff	179
3) Calculation of hydraulic conductivity	179
Discussion	185
Magnitude and area of subsurface runoff production	185
Timing of runoff production	186
Hydraulic conductivity profile of the soil	188
Conclusions and implications	189
 Chapter 7: Streamflow generation in Harp 4-21 and Harp 3A	 193
Introduction	193
Approach: Evaluation of the dominant subsurface flow processes	193
1. The role of subsurface flow in storm runoff	194
2. Areas that contribute to storm runoff	195
3. Spatial extent of water table fluctuations during storm events	195
4. Timing of groundwater fluctuations during storms	196
5. Capillary fringe effect	196
6. Changes in hydraulic gradients	197
7. Flow through transiently saturated sediments	197
8. Matrix versus dual porosity flow	199
Study site and methods	200

Results	203
1. The role of subsurface flow in storm runoff.....	203
2. Areas that contribute to storm runoff	205
3. Spatial extent of water table fluctuations during storms	210
4. Timing of groundwater fluctuations during storms	216
5. Capillary fringe effect	219
6. Changes in hydraulic gradients	222
7. Flow through transiently saturated sediments	227
8. Matrix versus dual porosity flow.....	234
Discussion	236
Conceptual models of subsurface stormflow in Harp 4-21 and Harp 3A	236
Groundwater ridging model	236
Transmissivity feedback, perched water table and old water macropore flow models	237
Unsaturated flow model	238
Role of macropores	238
Effect of hydraulic conductivity	238
Interaction between the matrix and macropores: pre-event flow in macropores	241
Spatial extent of runoff production	242
Variable contributing areas	242
Localized flow systems	244
Subsurface flow mechanisms in Canadian Shield catchments	245
Conclusions	247
 Chapter 8: The significance of storms for the concentration and export of dissolved organic carbon from Harp 4-21 and Harp 3A	251
Introduction	251
Site description	253
Methods	256
Sampling methods	256
DOC analysis	257
Methods of calculating DOC export	257
Results and discussion	261
DOC concentrations as a function of stream discharge	261
Uncertainty in estimating DOC export	269
DOC export during runoff events	271
Assessing the potential effects of climate change on DOC concentration and DOC export.....	275
Conclusions	276
 Chapter 9: Sources and flowpaths of dissolved organic carbon during storms in Harp 4-21 and Harp 3A	279
Introduction	279
Site description	280
Methods	282

Results	285
Hydrological flowpaths	285
DOC concentrations	288
DOC contributions along flowpaths	293
Riparian and wetland vs. hillslope sources of DOC	295
Wetlands and in-stream sources of DOC	297
Discussion	302
Riparian areas	302
Riparian vs. hillslope areas	304
Hillslope vs. wetland areas	305
Wetland vs. riparian areas	306
Conclusions and implications	307
 Chapter 10: Conclusions	 309
Contributions of this thesis	309
The role of glacial till	310
The role of soils	311
Timing and spatial extent of subsurface stormflow generation	312
Role of physical and hydrological conditions on the Canadian Shield	312
Conceptual models of subsurface stormflow generation	313
The role of storms on DOC	316
Implications of this study	317
Hydrological implications	317
Hydrochemical implications	319
Modelling implications	320
Ecological implications	324
Research opportunities	325
Additional testing of hydrological processes	325
Field studies	326
Numerical models	327
Processes that affect DOC during storms	328
Summary	329
 References	 330
 Appendix 1: Piezometer data	 348
 Appendix 2: Rating curves	 355
 Appendix 3: TDR waveguide depths	 361
 Appendix 4: Water storage calculations	 364
Method	364
Errors in water storage calculations	372

Appendix 5: Water content data	377
Appendix 6: Water storage data	393
Appendix 7: Isotope data	408
Appendix 8: Dissolved silica data, 1989-1990	413
Appendix 9: DOC analyses	425
Comparison of dissolved organic carbon analyses	425
Cellulose nitrate filters	427
Appendix 10: DOC data, 1992-1993	431

LIST OF TABLES

Table 2.1	Capillary rise within different porous media (Bear, 1972).	29
Table 2.2	Comparison of subsurface stormflow models for the increase in subsurface flow with respect to dominant hydraulic mechanisms and subsurface zones.	35
Table 2.3	Comparison of subsurface stormflow models with respect to the maximum spatial extent of subsurface flow generation.	36
Table 2.4	Physical properties and environments most suitable for different subsurface stormflow models.	38
Table 3.1	Areas contributing directly to each subcatchment as determined from surface topography (A) and groundwater equipotentials (B).	61
Table 3.2.	Seasonal change in the spatial pattern of stream discharge.	70
Table 4.1	Data used to calculate three-component hydrograph separations.	92
Table 4.2	Summary of results of three-component hydrograph separations calculated using Equations 4.4 to 4.6 and values in Table 4.1.	95
Table 4.3	Minimum till water contributions at S1 during runoff events.	104
Table 5.1.	Characteristics of the Harp 4-21 and Harp 3A catchments.	113
Table 5.2.	Seasonal distribution of precipitation and stream runoff, 1988-89, expressed as a) a depth, and b) a fraction of annual totals.	120
Table 5.3.	Effective runoff ratios.	126
Table 5.4.	Isotopic hydrograph separations near peak discharge for 1992 and 1993 events.	131
Table 6.1.	Cumulative subsurface runoff ($\Sigma\Delta SSR$) during storms in Harp 4-21.	167
Table 6.2.	Cumulative subsurface runoff ($\Sigma\Delta SSR$) during storms in Harp 3A.	171
Table 6.3.	Change in soil water storage during the summer.	176
Table 6.4.	Hydraulic conductivity profiles calculated from soil water balances (Figure 6.17) and bail tests in piezometers adjacent to TDR sites.	183
Table 6.5.	Physical properties of (Orthic Humo-Ferric) Podzolic soils in Harp 4 (Lozano et al., 1987).	184

Table 7.1	Minimum contributing areas and hillslope lengths of storms in catchments W1, W5, and S1.	206
Table 7.2	Actual contributing areas and hillslope lengths during the November 2 and 4, 1992 storm event in catchments W1, W5, and S1.	209
Table 7.3.	Change in pre-event discharge and downslope hydraulic gradients in Harp 3A during selected storms.	229
Table 7.4.	Change in pre-event discharge and downslope hydraulic gradients in Harp 4-21 during selected storms.	230
Table 7.5	Maximum subsurface flow in transiently saturated horizons in Harp 3A.	232
Table 7.6	Maximum subsurface flow in transiently saturated horizons in Harp 4-21.	235
Table 8.1	Regressions between DOC concentrations and stream discharge during the autumn and spring sampling seasons.	265
Table 8.2	Comparison of autumn DOC export at W1 and S1 calculated using period-weighted and seasonal regression methods from all measured data and weekly interval data.	270
Table 8.3	Summary of DOC export from W1 and S1 during a) autumn 1992 and b) spring 1993.	272
Table 8.4	Average DOC concentrations for periods of stormflow, baseflow and total flow during the autumn and spring sampling periods.	274
Table 9.1	Flow-averaged DOC concentrations for periods of stormflow, baseflow and total flow during the autumn and spring sampling periods.	291
Table 9.2	Average DOC concentrations of groundwaters and ponded water in Harp 4-21 and Harp 3A.	292
Table 9.3	Hillslope and stream export of DOC between November 2 and 9, 1992.	296
Table 9.4	DOC and water yields within each subcatchment of Harp 3A in the autumn and spring sampling seasons.	298
Table 10.1	Hydrological response in hillslopes of different sediment thickness on the Canadian Shield.	314

LIST OF ILLUSTRATIONS

Figure 1.1.	Environmental factors that influence streamflow generation processes (adapted from Dunne, 1978).	5
Figure 1.2.	Till provinces of Canada (Scott, 1976).	9
Figure 1.3.	Hydrogeological regions of Canada (Brown, 1976).	10
Figure 1.4.	Harp Lake watershed study area.	12
Figure 2.1	Unsaturated hydraulic conductivity of a sand (adapted from Rawls et al., 1993).	19
Figure 2.2	Zones of increased subsurface flow during storms.	21
Figure 2.3	Conceptual models of subsurface stormflow.	25
Figure 2.4	Hydraulic properties of a dual porosity medium.	43
Figure 3.1	Location and instrumentation of the Harp 4-21 catchment.	51
Figure 3.2	Sediment thickness in Harp 4-21 as determined from seismic survey.	54
Figure 3.3	Groundwater equipotentials in Harp 4-21 following spring melt on May 1, 1989.	58
Figure 3.4	Approximate subcatchment boundaries determined from (A) surface topography (Figure 3.1) and (B) groundwater equipotentials on May 1, 1989.	60
Figure 3.5	Cross sections indicating the change in saturated areas resulting from groundwater level fluctuations.	63
Figure 3.6	Approximate maximum and minimum extent of surface saturation in Harp 4-21 in 1989.	64
Figure 3.7	Seasonal groundwater level fluctuations in three slope positions.	66
Figure 3.8	Stream discharge at S1 as a function of piezometric levels adjacent to the lower portion of the stream.	68
Figure 3.9	The proportion of stream discharge at S4 relative to S1 as a function of piezometric levels in P05 near the upper portion of the stream.	71
Figure 3.10	Changes in stream discharge (A), the proportion of stream discharge at S4 relative to S1 (B) and piezometric levels along the lower (C) and upper (D-E) portions of the stream during the rainstorm on October 20, 1989.	73

Figure 4.1	Location map and instrumentation of the Harp 4-21 catchment.	80
Figure 4.2	Seasonal variations in water levels in piezometer P61.	86
Figure 4.3	Three-component hydrograph separations for the June 22, 1989 event.	87
Figure 4.4	Three-component hydrograph separations for the October 31, 1989 event.	88
Figure 4.5	Graphical presentation of the three-component hydrograph separations for the June 22, 1989 event.	93
Figure 4.6	a) The relative proportions of soil and till water during the June 22 event assuming constant soil and till water SiO ₂ concentrations. b) The change in soil water SiO ₂ concentrations required to maintain constant relative proportions of soil and till water. c) Coincident changes in water levels in piezometer P61.	97
Figure 4.7	The correlation between SiO ₂ and the sum of major cations (Ca ²⁺ , Mg ²⁺ , Na ⁺ , K ⁺) at S1 for the June 22 event.	99
Figure 4.8	Temporal variations in SiO ₂ concentrations in till water (P20-05), soil water (ZT8BC) and in a zone of soil and till water mixing (P11).	102
Figure 4.9	Influence of water levels in piezometer P58 on the minimum proportion of till water near peak discharge calculated using two-component hydrograph separations with SiO ₂ as a tracer.	106
Figure 4.10	Water level changes during three June 1989 events in vertical piezometer nests (a) P45 and (b) P50 screened both in the soils and in the tills. c) Changes in vertical gradients in P50 during the same events.	108
Figure 5.1	Instrumentation of the Harp 4-21 and Harp 3A catchments.	114
Figure 5.2	Definition of event runoff (Re) and baseflow runoff (Rb) in the calculation of the effective runoff ratio.	118
Figure 5.3	Precipitation and normalized daily stream discharge at sites S1 (Harp 4-21) and W1 (Harp 3A), 1988-89.	121
Figure 5.4	Precipitation and stream discharge at sites W1-W5 (Harp 3A), S1 and S4 (Harp 4-21), autumn 1992.	124
Figure 5.5	Precipitation and normalized stream discharge at S1 (Harp 4-21) and W5 (Harp 3A) for November 2 and 4 events.	125
Figure 5.6	Precipitation and stream discharge at sites W1, W3-W5 (Harp 3A) and S1 (Harp 4-21), spring 1993.	127

Figure 5.7	Precipitation and normalized stream discharge at S1 (Harp 4-21) and W5 (Harp 3A) for May 24, 28 and 31 events.	128
Figure 5.8	Effect of antecedent soil water storage on effective runoff ratios a) in Harp 3A and b) in Harp 4-21.	129
Figure 5.9	Precipitation and groundwater fluctuations for November 2 and 4 events in a) Harp 4-21 and b) Harp 3A.	133
Figure 5.10	Precipitation and groundwater fluctuations in Harp 3A, autumn 1992.	135
Figure 5.11	Precipitation and groundwater fluctuations in Harp 3A, spring 1993.	136
Figure 5.12	Timing of groundwater (P88-01) and stream (W5) response to November 1992 storms in Harp 3A.	138
Figure 5.13	Stream discharge at W5 as a function of groundwater levels in midslope piezometer P88-01.	140
Figure 6.1	The relative contributions to storm runoff from different hillslope positions according to Hewlett and Hibbert (1967) (adapted from Chorley, 1978).	145
Figure 6.2	Instrumentation of the Harp 4-21 and Harp 3A catchments.	147
Figure 6.3	Three examples of soil characteristic curves calculated from water content and water level data. a) TD87-02, b) TD86-03 and c) TD81-04.	150
Figure 6.4	Water content profile for water storage calculations.	152
Figure 6.5	Water content profiles and water table fluctuations at TD86 during the November 2 and 4 event.	158
Figure 6.6	Water storage during the autumn monitoring period in a) Harp 4-21 and b) Harp 3A.	160
Figure 6.7	Water storage during the spring monitoring period in a) Harp 4-21 and b) Harp 3A.	161
Figure 6.8	Cumulative a) water storage ($\Sigma\Delta S$) and b) net subsurface runoff ($\Sigma\Delta SSR$) in Harp 4-21 during the November 2 and 4, 1992 event.	162
Figure 6.9	Available water storage in different TDR profiles in Harp 4-21 during the November 2 and 4, 1992 event.	164
Figure 6.10	Cumulative water storage ($\Sigma\Delta S$) within the TD4 profile during the November 2 and 4, 1992 event.	165

Figure 6.11	Cumulative a) water storage ($\Sigma\Delta S$) and b) cumulative net subsurface runoff ($\Sigma\Delta SSR$) in Harp 3A during the November 2 and 4, 1992 event.	168
Figure 6.12	Cumulative water storage ($\Sigma\Delta S$) within the TD86 profile during the November 2 and 4, 1992 event.	170
Figure 6.13	Cumulative a) water storage ($\Sigma\Delta S$) and b) cumulative net subsurface runoff ($\Sigma\Delta SSR$) in Harp 3A during the November 10 and 12, 1992 event (dashed lines).	172
Figure 6.14	Cumulative net subsurface runoff ($\Sigma\Delta SSR$) in a) Harp 3A and b) Harp 4-21 during the dry period in early May, 1993.	174
Figure 6.15	Net subsurface flow ($\Delta SSR/\text{time}$) and water table fluctuations at a) TD88 and b) TD86 during November, 1992 events.	178
Figure 6.16	Total subsurface runoff (SSR) from TDR hillslope (TD86-TD87-TD88) and stream runoff for Harp 3A (W1) during November, 1992 events.	180
Figure 6.17	Total subsurface runoff (SSR) vs. maximum groundwater levels at a) TD88, b) TD87 and c) TD86.	182
Figure 7.1	Comparison of hydraulic (c-d) and topographic (a-b) gradients at the hinge point.	198
Figure 7.2	Instrumentation of the Harp 4-21 and Harp 3A catchments.	201
Figure 7.3	Minimum contributing areas (A_c) and hillslope lengths L_c at a) W1, b) W5 and c) S1 during the November 2 and 4 storm events.	208
Figure 7.4	Maximum observed increase in groundwater levels in Harp 4-21 during the June 22, 1989 storm event.	211
Figure 7.5	Maximum observed increase in groundwater levels in Harp 4-21 during the October 31, 1989 storm event.	213
Figure 7.6	Water table profiles along transect A in Harp 3A during the a) November 2, 1992 and b) May 24, 1993 storm events.	214
Figure 7.7	Water table profiles along transect B in Harp 3A during the a) November 2, 1992 and b) May 24, 1993 storm events.	215
Figure 7.8	Timing of water table fluctuations in Harp 3A during the November 2 and 4, 1992 storm event.	217
Figure 7.9	Timing of water table fluctuations in Harp 4-21 during the June 22, 1989 storm event.	218

Figure 7.10	Water table levels at P86-03 and water contents at TD86-03 during November 1992 storm events.	220
Figure 7.11	Water table levels at P06 and water contents at TD4-02 and TD4-03 during autumn 1992 storm events.	221
Figure 7.12	Groundwater levels and downslope hydraulic gradients along transect A in Harp 3A, autumn 1992.	223
Figure 7.13	Groundwater levels and downslope hydraulic gradients in Harp 4-21, autumn 1992.	224
Figure 7.14	Water table profiles along transect C in Harp 4-21 during the June 22, 1989 storm event.	225
Figure 7.15	Water table profiles along transect D in Harp 4-21 during the June 22, 1989 storm event.	226
Figure 7.16.	Water table profiles along transect D in Harp 4-21 during the October 31, 1989 storm event.	228
Figure 7.17	Transiently saturated soil horizons at sites P86, P87 and P88 in Harp 3A.	233
Figure 7.18	Schematic representation of the conductivity calibration problem for bimodal (dual porosity) pore size distributions (adapted from Durner, 1994).	240
Figure 8.1	Location and instrumentation of the a) Harp 4-21 and b) Harp 3A catchments.	254
Figure 8.2	Schematic example of the sample-interpolation method of calculating DOC concentrations.	259
Figure 8.3	Criteria for graphical hydrograph separation to define periods of stormflow and baseflow.	262
Figure 8.4	Stream discharge and DOC concentrations during the a) autumn and b) spring sampling seasons at W1 and S1.	263
Figure 8.5	Regressions between DOC concentration and stream discharge for individual autumn storm events at W1.	266
Figure 8.6	Cumulative percentage of DOC export as a function of cumulative percentage of flow duration at W1 during the autumn sampling period.	273
Figure 9.1	Location and instrumentation of the Harp 4-21 and Harp 3A catchments.	281

Figure 9.2	Depth to water table during baseflow and stormflow conditions in Harp 4-21 and Harp 3A.	286
Figure 9.3	DOC concentrations of waters in Harp 4-21 and Harp 3A (1989-1993).	289
Figure 9.4	Stream DOC concentrations at S1, W5 and W3 during the a) autumn and b) spring sampling periods.	290
Figure 9.5	DOC concentrations versus stream discharge during autumn 1992 storms at a) W3 and b) W4.	299
Figure 9.6	DOC concentrations and water levels in Wetland 2 during a) autumn, and b) spring.	300
Figure 10.1	Hydrological reservoir model (Seip et al., 1985).	322

COPYRIGHTS

Previously published papers from this dissertation have been reproduced with the kind permission of Elsevier Science Publishers B.V., the American Geophysical Union, and Kluwer Academic Publishers.

Chapter 3

Hinton, M. J., Schiff, S. L. and English, M. C., 1993. Physical properties governing groundwater flow in a glacial till catchment. *J. Hydrol.*, 142, 229-249.

Copyright by Elsevier Science Publishers B.V.

Chapter 4

Hinton, M. J., Schiff, S. L. and English, M. C., 1994. Examining the contributions of glacial till water to storm runoff using two- and three-component hydrograph separations. *Water Resour. Res.*, 30 (4), 983-993.

Copyright by the American Geophysical Union.

Chapter 8

Hinton, M. J., Schiff, S. L. and English, M. C., 1997. The significance of storms for the concentration and export of dissolved organic carbon from two Precambrian Shield catchments. *Biogeochem.*, 36, 67-88.

Copyright by Kluwer Academic Publishers.

Chapter 9

Hinton, M. J., Schiff, S. L. and English, M. C., 1998. Sources and flowpaths of dissolved organic carbon during storms in two forested watersheds of the Precambrian Shield. *Biogeochem.*, 41, 175-197.

Copyright by Kluwer Academic Publishers.

Chapter 1

Introduction

The distribution of water in our environment is one of the most important natural factors that influences human activities. Water vapour from the atmosphere is spread across the earth's surface as precipitation. Water that reaches the ground surface can follow many different pathways. It can evaporate or be transpired back to the atmosphere, flow across the land surface to streams, or infiltrate the ground surface and flow to streams, rivers, lakes or oceans. Collectively, these and other related processes are important because they shape the landscape, modify stream water quality, influence land use, and affect the life that surface water (and land) can support.

Streamflow generation is the transmission of precipitation into a stream. It is influenced by several different hydrological processes that affect the amount, timing and flowpaths of water transport to streams during and after storms. For example, when the rainfall rate exceeds the rate of infiltration, the excess rainfall flows across the ground surface and reaches streams as (Horton) overland flow (Horton, 1933). Alternatively, precipitation can infiltrate the ground, flow beneath the surface, emerge as groundwater discharge and flow overland to streams (return flow) (e.g. Dunne and Black, 1970a). The study of streamflow generation consists of examining the various hydrological processes that deliver precipitation to streams.

Subsurface flow and streamflow generation are important to the hydrological cycle on the Canadian Shield at several scales. On a continental scale, streamflow from the Canadian Shield is the main source of water from North America to the Arctic Ocean, the Great Lakes and the St. Lawrence River. It is also responsible for much of the hydroelectric generating

capacity in Canada. On a regional scale, streamflow provides water supply for many communities on the Canadian Shield. Subsurface flow is an important component of stream runoff and can maintain stream baseflow and provide nutrients essential for aquatic habitats. On a local scale, subsurface flow transports nutrients and contaminants from point (e.g. septic systems, landfills) and non-point sources (e.g. agriculture) to surface water bodies.

To better understand and describe how different hydrological processes interact to generate streamflow, conceptual or perceptual models of streamflow generation are developed. A conceptual model is a simplified representation of how systems work and processes interact. Conceptual models of streamflow generation are useful as teaching tools, as aids in the development of mathematical models of stream response to storms, and most importantly, as a framework that ultimately influences land use management.

Streamflow generation on the Canadian Shield is examined in this thesis by field studies of two small watersheds. The results are used to improve the understanding of hydrological processes and to refine conceptual models of streamflow generation.

Research context: Challenges and opportunities

Paradigm shifts in conceptual models and methods in streamflow generation studies

Several conceptual models of streamflow generation have been developed to represent the dominant hydrological processes that cause storm runoff (see Freeze, 1974; Chorley, 1978; Ward, 1984). Prior to the 1960s, the prevailing paradigm supported the concept that surface infiltration and Horton overland flow were the dominant controls on streamflow generation. This paradigm began to change in the 1960s and 1970s when more data became available from increasingly comprehensive hydrometric field studies (e.g. Dunne and Black, 1970a, 1970b). These studies suggested that saturation overland flow (overland flow that results from

precipitation directly onto saturated areas plus return flow) was the dominant hydrological process. In comparison, Horton overland flow was insignificant. Therefore, groundwater contributions, although not considered dominant, were greater than previously perceived.

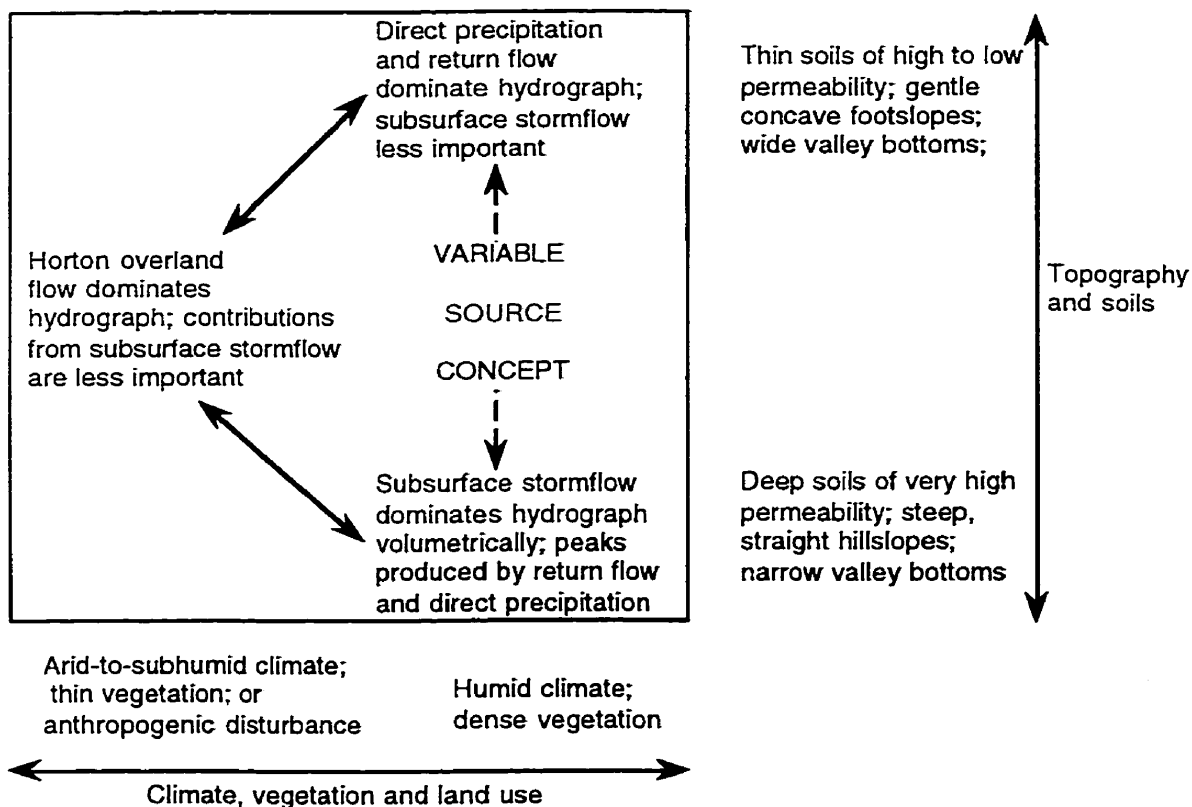
The use of chemical and isotopic tracers (Pinder and Jones, 1969; Dincer et al., 1970) represented a significant development in the study of streamflow generation. There was a further shift in the emerging paradigm when results demonstrated that storm runoff included a large component of groundwater and soil water. As isotopic tracing techniques developed, many streamflow generation studies of the 1970s and early 1980s focused almost exclusively on isotopes and stream chemistry with minimal hydrometric data from wells or hillslope trenches (e.g. Sklash and Farvolden, 1979; Hooper and Shoemaker, 1986).

During the same period, there was a growing awareness of the effects of toxic substances in our environment (e.g. Carson, 1962) that shifted the focus of many scientific disciplines towards the study of contaminant transport and fate. With increased interest in water flowpaths and stream chemistry, more studies in the 1980s and 1990s integrated hydrometric and water chemistry data. An example of the progression of conceptual models and methods was demonstrated in the Maimai catchments of New Zealand (McDonnell, 1990). Successive studies, in which different techniques were used, provided conflicting interpretations of the dominant streamflow generation processes (Mosley, 1979, 1982; Pearce et al., 1986; Sklash et al., 1986). Combined use of tracer and hydrometric data (McDonnell, 1990; McDonnell et al., 1991a, 1991b) resolved this conflict by proposing an alternate conceptual model in which soil water was displaced towards the stream through large soil pores (macropores). This example shows that conclusions were dependent on methodology and existing conceptual models, multiple techniques were needed to resolve the problem, and an alternate conceptual model had to be developed because existing models were inadequate.

Although many studies have clearly demonstrated that subsurface flow is the dominant component of storm runoff, the specific hydrological processes are still not fully understood. Few conceptual models have been suggested to explain how subsurface flow contributes most to storm runoff, and those that have been proposed have not yet been widely tested under natural conditions. For example, Sklash and Farvolden (1979) proposed the groundwater ridging model in which hydraulic gradients increase as the capillary fringe is rapidly converted to the water table (Chapter 2). Although groundwater ridging has been demonstrated to occur in a laboratory model (Abdul and Gillham, 1984), in a plot-size field experiment (Abdul and Gillham, 1989), and in mine tailings (Blowes and Gillham, 1988), it is unclear whether it is effective in producing the observed runoff at the catchment scale under natural field conditions (e.g. Buttle and Sami, 1992).

The development of conceptual models of streamflow generation has resulted from investigations of many catchments with different physical and hydrological properties. Although it is generally recognized that the dominant hydrological processes vary according to environmental factors such as climate, vegetation, land use, geology, soil properties and topography (Figure 1.1, Dunne, 1978), there has been relatively little attempt to relate streamflow generation processes and conceptual models to the physical and hydrological properties of catchments. This problem arises, in part, because identifying streamflow generation processes is difficult. Firstly, there is large spatial and temporal variability in streamflow generation. As a result, adjacent catchments in similar climatic and geological environments can have greatly different responses to precipitation. Similarly, the area contributing to storm runoff can vary between or even within storms in a single catchment. Secondly, streamflow generation often results from several interacting processes which make it difficult to identify those that are dominant. Thirdly, streamflow generation processes often involve subsurface water that is more difficult to observe and measure given the spatial

Figure 1.1. Environmental factors that influence streamflow generation processes (adapted from Dunne, 1978). Horton overland flow is the excess rainfall that flows across the ground surface when the rainfall rate exceeds the rate of infiltration. Return flow is groundwater that discharges to the ground surface and flows overland to the stream. The variable source area concept describes the relative importance of saturated overland flow (direct precipitation onto saturated areas and return flow) and subsurface stormflow to storm runoff in response to variations in saturated areas near the stream.



variability in the factors that control its storage and movement. Therefore, the application of conceptual models can be improved by identifying the physical and hydrological properties of catchments and their influence on streamflow generation. If streamflow generation processes are related to specific physical or hydrological conditions, investigations of individual subcatchments or catchments may be more widely applicable even beyond the climatic or geological regions in which they were conducted.

The shift in paradigms within streamflow generation research may not yet be complete as there are still important unanswered questions such as "What hydrological processes lead to the large component of subsurface flow in storm runoff?" Consequently, there are several challenges and opportunities for streamflow generation research. Firstly, hydrogeological principles should be applied to assess the subsurface flow processes within current conceptual models of streamflow generation. These models have hydrogeological implications that have not yet been fully considered. A second challenge is to collect new field data to identify subsurface flow processes in catchments where isotopic data indicate that a large proportion of storm runoff is produced by subsurface flow. These data must emphasize monitoring of the groundwater response to storms and integrate hydrograph separations with detailed hydrometric monitoring. Another challenge within these new field studies is to evaluate whether or not existing conceptual models can explain the rapid production of subsurface water. If not, new conceptual models will be required. Finally, new studies should attempt to relate physical and hydrological properties to streamflow generation. Spatial and temporal variability in runoff production that is caused by hydrological conditions or physiographic and geological settings can then be identified and taken into consideration.

Hydrology on the Canadian Shield

Isotopic hydrograph separations have shown that groundwater flow is an important component of stream runoff on the Canadian Shield (Fritz et al., 1976; Bottomley et al., 1984, 1986; Moore, 1989). However, there has generally been little emphasis on groundwater studies on the Canadian Shield because most flow systems are local and shallow, surface water is more abundant as a water supply, and water demand is lower than in other regions of the country where urban, industrial and agricultural demands are greater.

The most extensive groundwater studies on the Canadian Shield have been conducted as part of the Canadian Nuclear Waste Management Program (summarized briefly by Farvolden et al., 1988) or the International Hydrologic Decade project, 1965-1974 (Barry, 1975). Within these studies, there has been little emphasis on flow within glacial till. For example, the purpose of the studies at the Underground Research Laboratory (Manitoba) and at Atikokan (Ontario) was to examine the possibility of using bedrock as a nuclear fuel waste repository. Therefore, the emphasis was on flow in fractured rock (Farvolden et al., 1988). At Chalk River (Ontario), the local geological setting includes aeolian, lacustrine, and deltaic sands with inherently higher hydraulic conductivities so that there was little motivation to examine the hydrogeology of glacial till (Cherry et al., 1975).

Comprehensive streamflow generation studies on the Canadian Shield have provided little insight into the role of groundwater flow through till during runoff events. Studies either have been conducted in catchments or hillslopes where glacial till is very thin (e.g. Peters et al., 1995) or absent (e.g. Allan and Roulet, 1994), or have not specifically examined streamflow generation processes within the till (e.g. Bottomley et al., 1986).

Since nearly all of Canada was glaciated during the Pleistocene, glacial till is found across most of the country (Figure 1.2, Scott, 1976). Although the Canadian Shield is one of the main hydrogeological regions of Canada (Figure 1.3, Brown, 1976; Heath, 1988) and is within the largest till province (Figure 1.2), groundwater research in glacial tills in North America has focused mostly on other till provinces where glacial sediments are thicker, and reliance on groundwater for water supply is higher (e.g. Keller et al., 1988; Gerber and Howard, 1996). This distinction is important because tills in areas away from the Canadian Shield have different textures. They often incorporate glaciolacustrine deposits or carbonates that have been ground by glaciers to produce finer textured tills (Figure 1.2). These finer tills are aquitards in comparison to the coarser outwash or glaciofluvial units with which they are often interbedded. However, tills that are derived solely from the Canadian Shield are coarser grained (clay content usually < 20%) and may transmit appreciable volumes of water.

Because little is known about the hydrogeology of glacial tills on the Canadian Shield, there are many research opportunities and challenges. One of the most important challenges is to relate groundwater flow and discharge with surface water hydrology, and water flowpaths with stream water chemistry. Since wetlands are widespread on the Canadian Shield and influence surface water fluxes and chemistry (Devito et al., 1989, 1996; Devito and Dillon, 1993), the effect of groundwater flow on water levels and redox conditions in wetlands should be further studied. Soils that are derived from glacial till may also have an important hydrological role to consider since sediments on the Canadian Shield are often thin (<10 m), and water tables shallow.

Figure 1.2. Till provinces of Canada (Scott, 1976).

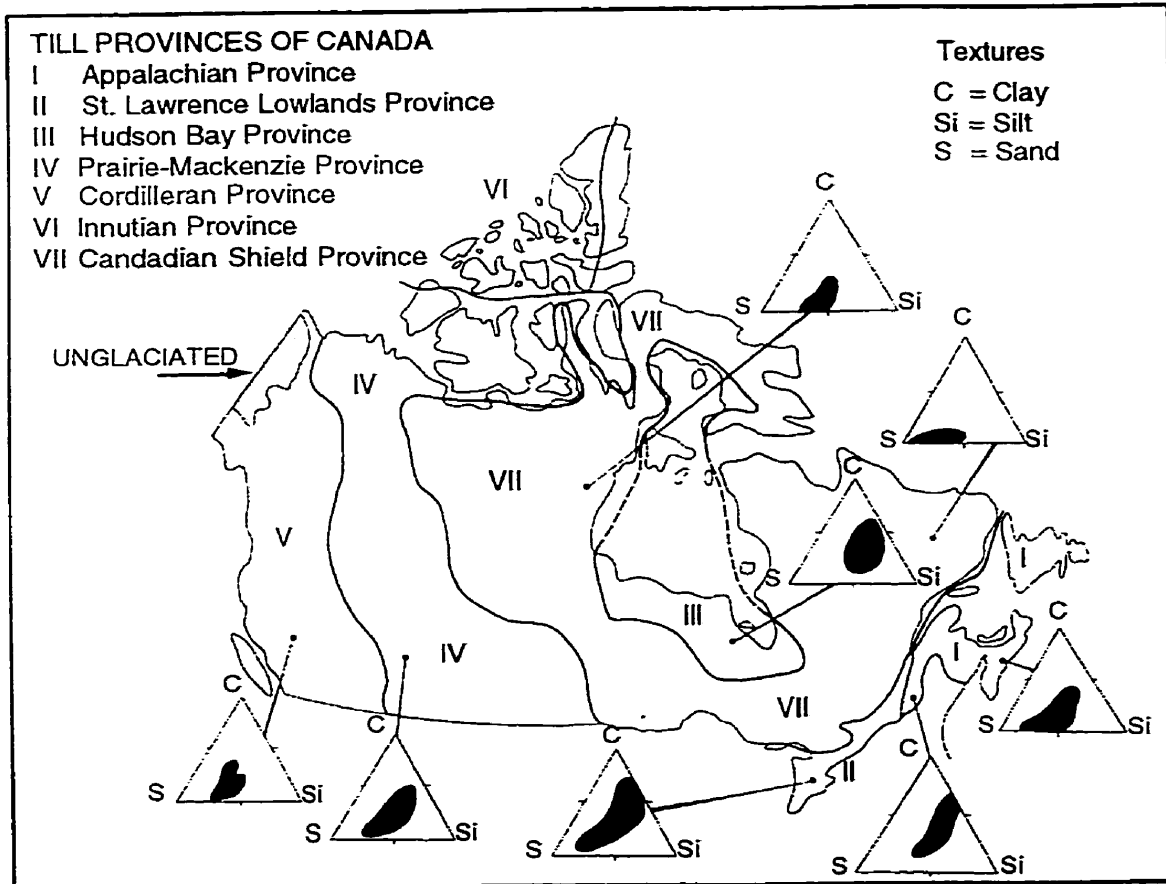
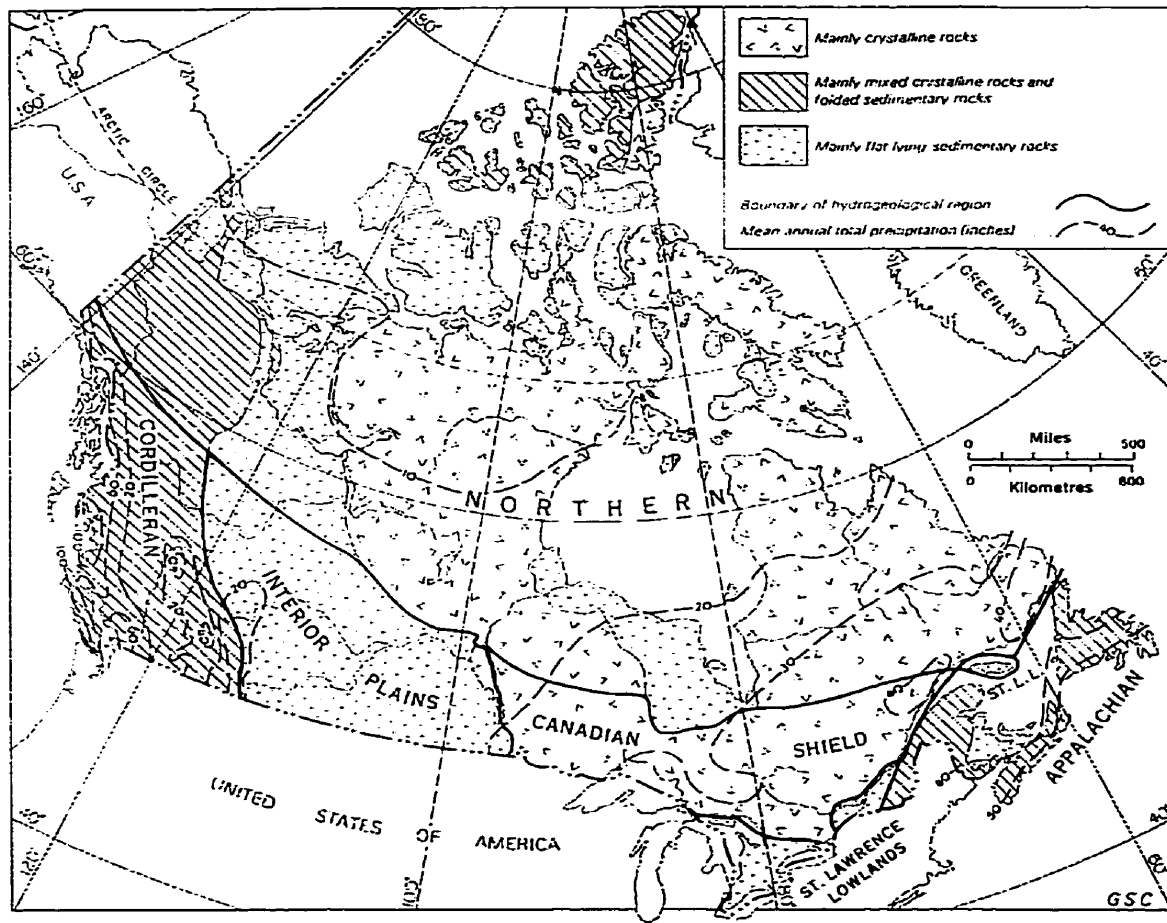


Figure 1.3. Hydrogeological regions of Canada (Brown, 1976).



Research objectives

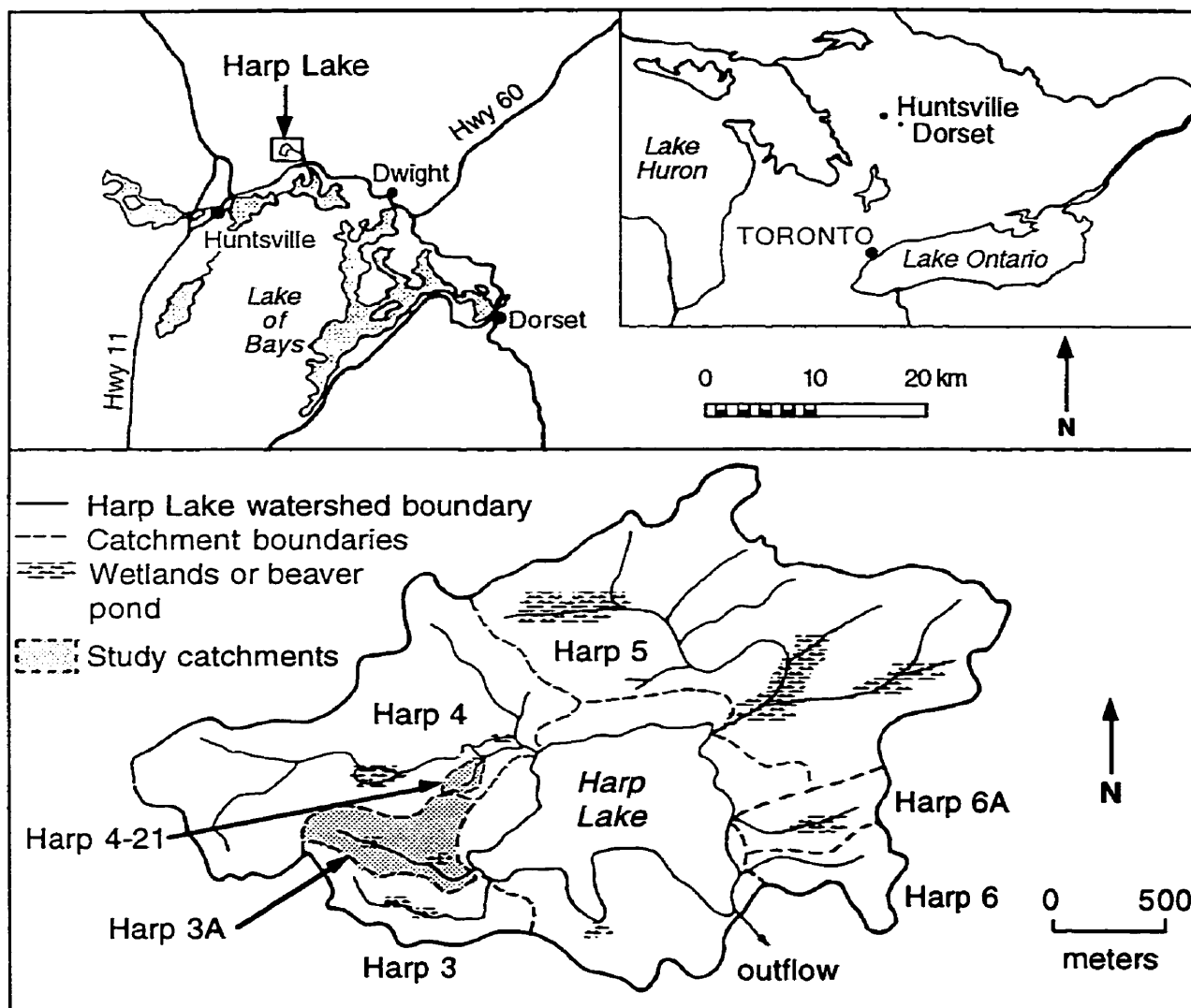
The overall objective of this study is to improve the understanding of the role of subsurface flow in streamflow generation. The specific objectives of this thesis that will contribute towards this overall objective are:

- 1) to review and assess the present understanding of subsurface flow processes within conceptual models of streamflow generation,
- 2) to advance the understanding of subsurface flow processes through new field investigations that emphasize subsurface flow and integrate hydrometric, hydrochemical and isotopic data,
- 3) to assess the applicability of the conceptual models to field sites on the basis of measured physical and hydraulic data
- 4) to relate measurable physical or hydrological variables to conceptual streamflow generation models so that measurements of these variables in other catchments can be used to identify streamflow generating mechanisms,
- 5) to examine the hydrological role of glacial tills in streamflow generation on the Canadian Shield, and
- 6) to explain changes in dissolved organic carbon (DOC) concentrations and fluxes in the stream during storms.

Study area

This study was conducted on the Canadian Shield of central Ontario within the Harp Lake watershed (45°23'N, 79°8'W, Figure 1.4), one of several watersheds in which the hydrology, hydrochemistry and biology have been monitored by the Ontario Ministry of the

Figure 1.4. Harp Lake watershed study area.



Environment (MOE) since 1976. Two small catchments, Harp 4-21 and Harp 3A (3.7 and 21.7 ha respectively, Figure 1.4), are characterized by different glacial till thicknesses (0-15 m) that provide the opportunity for a paired watershed comparison. Harp 4-21 was partially instrumented by the MOE to examine soil and stream water chemistry (1984-1991) (LaZerte and Scott, 1996). Stream discharge and chemistry have been monitored by the MOE at the Harp 3A outlet since 1976. Dankevych (1989) provided a preliminary investigation of groundwater flow and chemistry in Harp 4-21.

The size of these catchments is well suited to study streamflow generation processes for their particular geographical settings. However, these catchments are not representative of the average hydrological response of the entire region. In effect, they are smaller than a "representative elementary area" (REA) (Wood et al., 1988, 1990) in which catchments are sufficiently large to incorporate the range of physical and hydraulic conditions so that average hydrological responses are observed and spatial patterns are not considered explicitly. Given the wide range of sediment thickness, slope, topography and the presence of surface water bodies on the Canadian Shield, the variability in runoff response may be sufficiently large that catchments suitable to study streamflow generation processes are smaller than the REA. Consequently, the results of this study cannot be scaled up directly to indicate the regional hydrological response. However, they may provide insight into the physical or hydrological criteria that should be considered at the regional scale.

Organization of thesis

The role of subsurface flow processes within conceptual models of streamflow generation is presented and assessed in Chapter 2. In this chapter, the physical settings conducive to subsurface flow generation are examined.

Field investigations included two phases of research. The first phase focused exclusively on the Harp 4-21 catchment and is presented in Chapters 3 and 4. In Chapter 3, the groundwater and stream dynamics are examined and some of the physical and hydrological factors that control groundwater flow and discharge in Harp 4-21 are discussed. These basic data are required to understand subsurface flow processes in this catchment. In Chapter 4, the use of chemical and isotopic hydrograph separations is combined with hydrometric data to quantify and explain the stormflow contribution of groundwater flow through the soil and till. This phase of research was followed by field studies of MacLean (1992) in which the role of the vadose zone in runoff generation in Harp 4-21 was examined.

The second phase of research expanded upon initial work by instrumenting a second catchment, Harp 3A, and simultaneously monitoring groundwater levels, stream discharge, soil moisture, and DOC concentrations in both catchments. Chapter 5 is a comparison of the effect of different till thickness on storm runoff response and groundwater dynamics in the two catchments. The spatial and temporal patterns of soil moisture storage during storms that affect subsurface runoff production are discussed in Chapter 6. In Chapter 7, the hydrological results from both phases of this research are integrated by assessing the mechanisms of subsurface stormflow generation in Harp 4-21 and Harp 3A. The relative importance of storm and baseflow periods for the concentration and export of dissolved organic carbon (DOC) are compared in Chapter 8. In Chapter 9, a practical application of the conceptual models is demonstrated by relating hydrological flowpaths with DOC concentrations and export during storms. In Chapter 10, the main contributions of this thesis are summarized, its implications are discussed and opportunities for future research are proposed.

Chapters 3, 4, 8 and 9 were previously published as peer-reviewed journal articles (Hinton et al., 1993, 1994, 1997, 1998 respectively). Within this thesis, references to these articles have been replaced by the appropriate chapter numbers.

Chapter 2

Subsurface flow in conceptual models of streamflow generation

Introduction

Chemical and isotopic hydrograph separations have indicated that pre-event water (groundwater and vadose water) is frequently dominant in storm runoff for many low-order catchments in humid climates over a wide range of geological environments (Hooper and Shoemaker, 1986; Rodhe, 1987). These results have led to conceptual models of streamflow generation that emphasize soil water or groundwater flow to the stream by different hydrological processes (Sklash and Farvolden, 1979; Lundin, 1982; McDonnell, 1990). Differences in hydrological processes among watersheds may be caused by differences in physical and hydrological properties. Evaluation of physical and hydrological properties of watersheds can indicate the dominant processes of subsurface flow and the appropriate conceptual or mathematical models.

Although there have been several reviews of conceptual models of streamflow generation (Freeze, 1974; Ward, 1984; Rodhe, 1987; Bonnell, 1993, 1998), there has been very little detailed examination of the processes that can lead to large proportions of subsurface flow in storm runoff (Buttle, 1994). A more complete evaluation of the physical or hydrological properties that control subsurface flow production, the geographical setting most appropriate for each model, and the hydrogeological implications of the various models is warranted.

The general purpose of this chapter is to describe and refine the present understanding of subsurface stormflow generation. A complete literature review and evaluation of the subject is not attempted. Rather, the relevant literature is reconsidered with four specific goals. The

first is to describe the mechanisms for increased subsurface flow to streams during storms. The second goal is to describe subsurface stormflow models and identify their key implications. Thirdly, the models are compared and contrasted with respect to the dominant mechanisms and hydrological processes that cause increased subsurface flow during storms. Fourthly, the physical and hydrological properties conducive to increases in subsurface flow are identified within each conceptual model.

Terminology

Within the literature of streamflow generation, descriptions of the physical processes that control subsurface flow are frequently imprecise. Many different terms have been used to define similar concepts, or similar terms, different concepts. Some commonly used hydrological terms, such as "throughflow" and "interflow", refer to a combination of processes but do not specify them. For example, the term interflow is used for "subsurface flow which returns to form surface runoff without reaching the water table before arriving at the watershed outlet" (Amerman, 1965, cited in Kirkby, 1978). Consequently, such terminology should be avoided and replaced by more precise terms that identify individual processes, such as infiltration, unsaturated flow (in the matrix or in macropores) and groundwater discharge.

Hydrogeological terminology for subsurface stormflow has also been misused. For example, Whipkey and Kirkby (1978) have distinguished between groundwater flow and saturated flow within the soil. Rodhe (1987) considered that shallow, transient perched water tables did not represent groundwater. For the purpose of this discussion, strict definitions of hydrogeological terms are used (Freeze and Cherry, 1979). Groundwater flow refers to flow under positive pressure heads ($\Psi > 0$), regardless of location with respect to soil horizons. Water table development above the unsaturated zone is considered a perched water table with little regard to its duration, spatial extent, or depth within the soil.

Before proceeding to a detailed description and comparison of the models, it is first necessary to consider the mechanisms for increased subsurface flow to streams during storms since these form one basis of comparison.

Mechanisms for increased subsurface flow to streams during storms

One of the most compelling results of hydrograph separations that requires further explanation is the large increase in pre-event water flow to many streams during storms. From a macroscopic perspective, subsurface flow can be examined with an unsaturated form of Darcy's law:

$$Q = K(\theta) i A \quad (2.1)$$

where Q is downslope discharge, K is the hydraulic conductivity which is a function of water content, θ , i is the hydraulic gradient (along the hillslope), and A is the cross-sectional area. Although Darcy's law may not be strictly applicable in all microenvironments, such as in macropores, it provides a useful conceptual framework to examine the reasons for increased subsurface flow to streams during storms.

According to Darcy's law, the change in subsurface flow is directly proportional to changes in hydraulic gradient and hydraulic conductivity. Since the cross-sectional area through a vertical profile perpendicular to the hillslope is constant, there are two possible reasons for an increase in downslope subsurface flow: 1) an increase in the magnitude of the hydraulic gradient, and 2) an increase in the hydraulic conductivity of the unsaturated sediments that is caused by an increase in water content.

Groundwater that discharges and becomes overland flow prior to reaching the stream is not explicitly considered by this equation. However, if the vertical profile is chosen at the

upslope edge of the discharge area, then the increase in subsurface flow represents that from the entire hillslope.

Increase in hydraulic conductivity

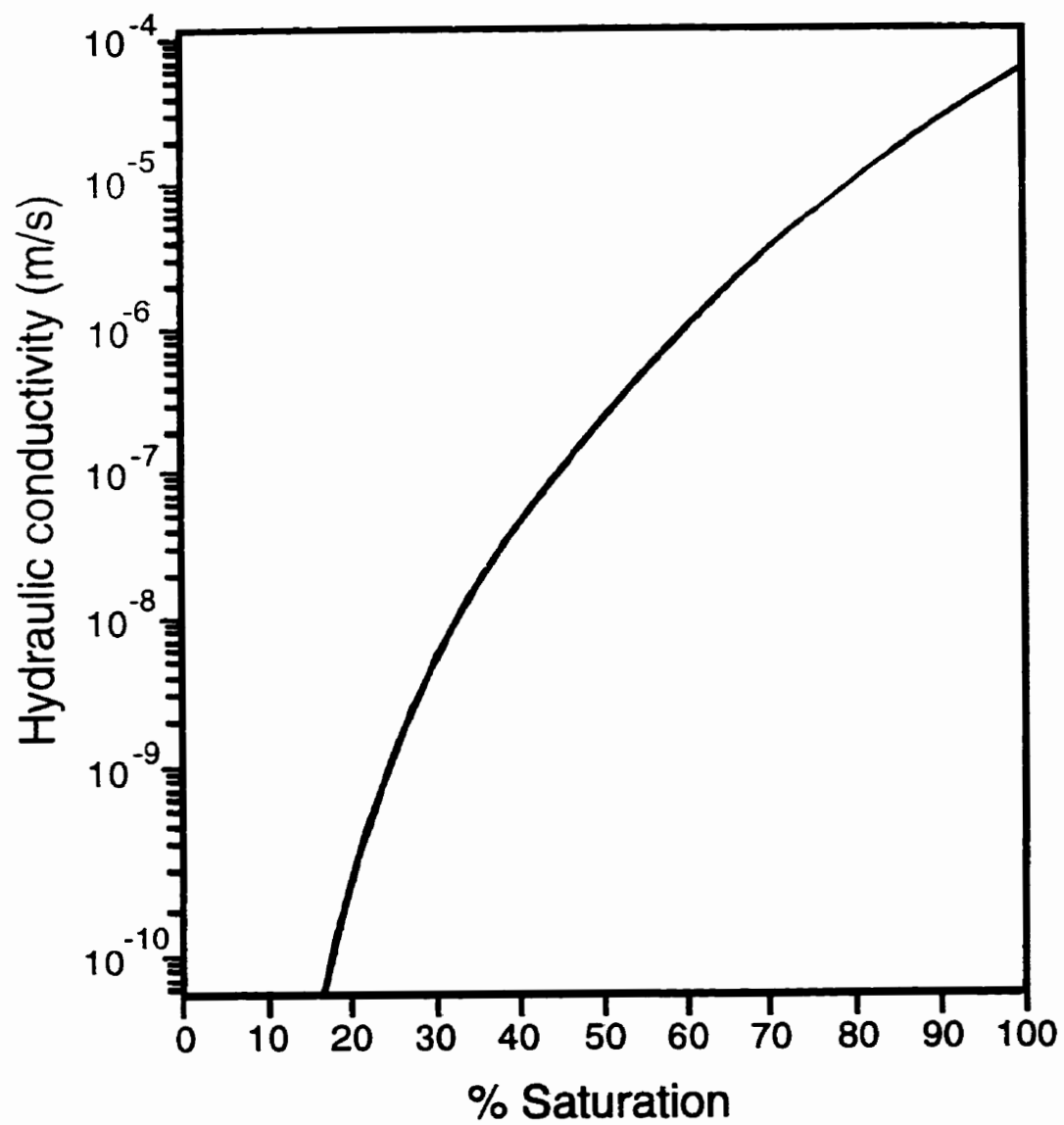
Richards' (1931) theoretical and experimental results can be used to demonstrate that unsaturated flow within a given horizon is generally much smaller than saturated flow. Since the hydraulic conductivity, and hence, the flow through a given sediment, can vary by several orders of magnitude depending on water content (Figure 2.1), a rising water table is extremely important because it can increase the flow through previously unsaturated sediments by increasing hydraulic conductivity.

The increase in groundwater flow that results from an increase in hydraulic conductivity can be independent of changes in hydraulic gradients. If the water table rises equally along the length of a hillslope, the downslope hydraulic gradient remains constant, yet groundwater flow may increase substantially through soil horizons that become saturated.

Increase in hydraulic gradients

Changes in hydraulic gradient are sometimes interpreted as the main reason for the increase in subsurface flow to the stream (Sklash and Farvolden, 1979; Abdul and Gillham, 1989). Since flow in unsaturated sediments is generally less than in saturated sediments, this chapter will focus primarily on changes in hydraulic gradients in the saturated zone. Changes in downslope hydraulic gradients in the saturated zone are caused by changes in the slope of the water table and, therefore, are easily measured and are more commonly reported than are measurements of soil water tension.

Figure 2.1 Unsaturated hydraulic conductivity of a sand (adapted from Rawls et al., 1993).



The slope of the water table can only change when water table fluctuations are not spatially uniform. Several factors that can lead to unequal water table fluctuations include the depth to the water table, the available storage in the unsaturated zone, and subsurface flow from upslope. Depending on the cause, the change in the slope of the water table may be spatially restricted within the catchment.

Changes in hydraulic gradient are not usually independent of changes in hydraulic conductivity because changes in water content usually accompany water table fluctuations. Only when the capillary fringe is converted to a water table can hydraulic gradients change without a change in water content.

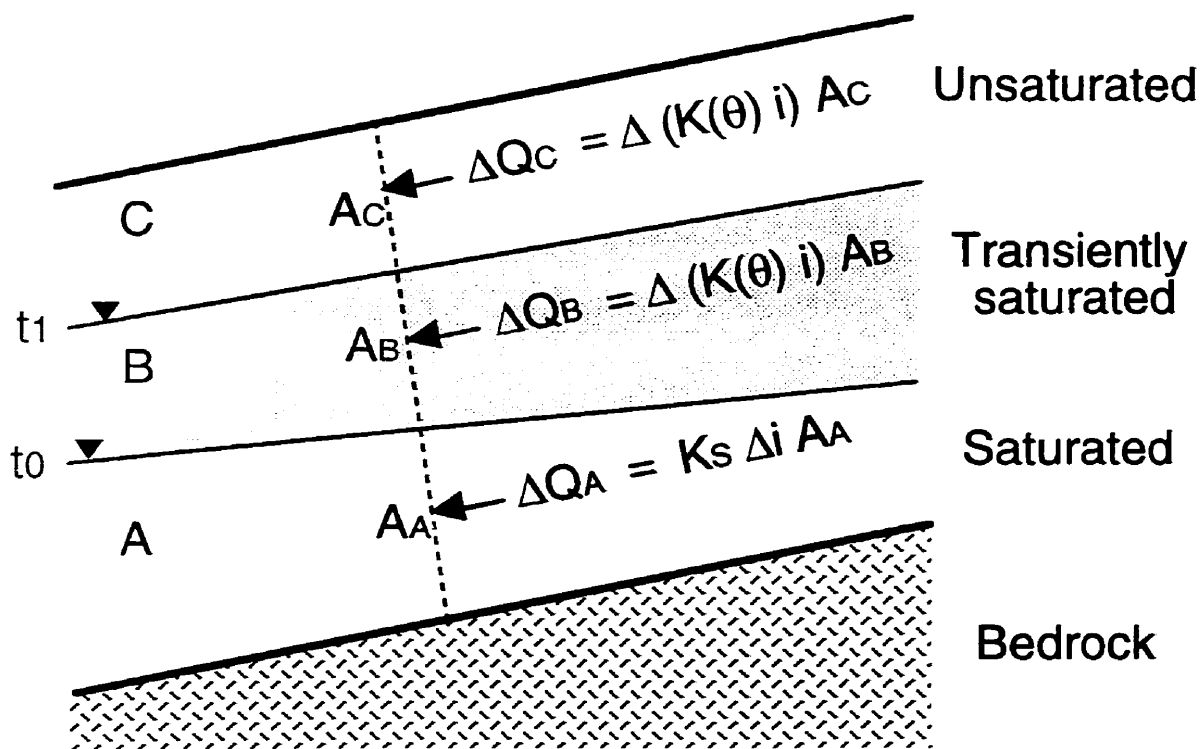
Zones of increased subsurface flow

To compare different conceptual models of subsurface flow, it is useful to consider where the increase in lateral subsurface flow occurs. In response to infiltration events, lateral flow can increase in three zones (Figure 2.2): 1) the existing zone of saturation (A), 2) the zone which becomes saturated during the event (B) and 3) the zone which remains unsaturated for the duration of the event (C). The initial capillary fringe is included in zone A.

According to Darcy's Law, the increase in lateral groundwater flow through the existing saturated sediments during a storm (ΔQ_A) is directly proportional to the increase in the hydraulic gradient. Since the sediments are already saturated, their hydraulic conductivity remains constant such that the increase in flow is solely caused by the change in hydraulic gradient.

Since the water table fluctuates during a storm event, the boundary between the transiently saturated zone (B) and the unsaturated zone (C), and their respective thicknesses

Figure 2.2 Zones of increased subsurface flow during storms: A) zone that remains saturated, B) transiently saturated zone, and C) zone that remains unsaturated. Minimum water table position prior to storm (t_0) and maximum water table position during storm (t_1) are shown. Hydraulic conductivity (K) is a function of water content (θ). i = downslope hydraulic gradient, A = Cross-sectional area perpendicular to hillslope. As a simplification, the boundary between zones B and C is fixed at the highest elevation of saturation during a storm.



fluctuate. To simplify this discussion, the boundary between these two zones is assumed to be fixed at the highest elevation where saturation occurs during a storm. Therefore, changes in flow in each zone are caused by changes in gradient or hydraulic conductivity rather than by changes in thickness.

In contrast to zone A, the increases in flow contribution from zones B and C are primarily related to greater hydraulic conductivity that arises from increasing water content. In general, the relative change in hydraulic conductivity can be several orders of magnitude (Figure 2.1), whereas the change in hydraulic gradient rarely exceeds several percent, except under ideal conditions. However, since zones B and C can be much thinner than the existing saturated zone (A), the relative changes in flow in the three zones depends on their physical and hydrological characteristics, such as thickness and hydraulic conductivity.

Conceptual models of subsurface flow generation and their development

Several current models of streamflow generation include subsurface components of flow (see Freeze, 1974; Ward, 1984). Within these models, there are five possible explanations for the large increase in subsurface flow of pre-event water to the stream during storms: 1) unsaturated flow, 2) groundwater ridging, 3) transmissivity feedback, 4) perched water tables, and 5) old water macropore flow. Many of the processes that have been included in current conceptual models of subsurface flow had been recognized prior to the widespread use of hydrograph separations (see review by Hursh, 1944). However, their significance and interrelationships were not fully considered because of limited field data. The key elements of each model and of their development are examined in the sections that follow.

1) Unsaturated flow

A significant improvement in our understanding of subsurface stormflow was made by Hewlett and Hibbert (1967) who considered the implications of column experiments by Horton and Hawkins (1964). The former recognized that infiltrating rainfall did not necessarily have to reach the stream to produce the large increase in stream discharge. Rather, they argued that infiltrating rainwater could rapidly displace soil water and groundwater into the stream. In effect, they had implicitly recognized that an increase in upslope hydraulic pressure can be transmitted rapidly downslope and increase subsurface flow and streamflow. Although this concept applies both to saturated and unsaturated flow, they attributed much of the increase in subsurface flow to unsaturated flow. Their descriptions form the basis of the unsaturated flow model.

Increased unsaturated flow during storms is caused by "thickening of the water films surrounding soil particles" (Hewlett and Hibbert, 1967, p 279), and therefore, by an increase in water content and hydraulic conductivity. The increase in pre-event subsurface flow to the stream occurs by displacement of subsurface water by infiltrating storm precipitation (also referred to as translatory or piston flow) and expansion of groundwater discharge areas adjacent to the stream (Hewlett and Hibbert, 1967).

In this model, most of the increase in flow occurs in the unsaturated zone (ΔQ_C , Figure 2.2). However, since water must be under positive pressure head to be discharged from the soil (Richards, 1950), water must recharge the groundwater table before discharging to the stream. Therefore, some of the increase in flow must also occur below the water table (ΔQ_A or ΔQ_B). Hewlett and Hibbert (1967) did not discuss the processes responsible for the expansion of discharge areas near the stream, the rise in groundwater levels, and the increase in

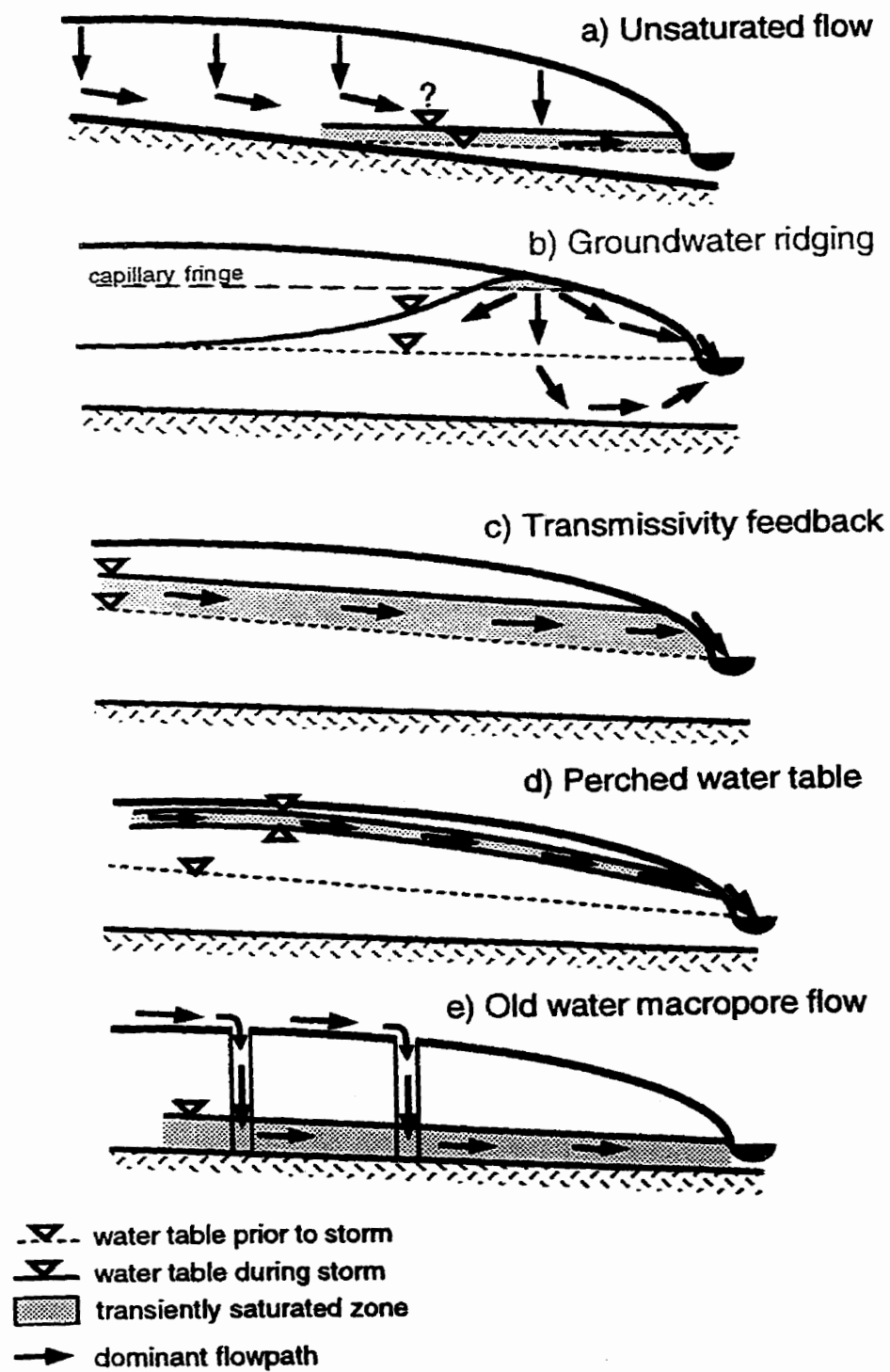
groundwater discharge that causes expansion of stream channels (Figure 2.3A, question mark).

One implication of the unsaturated flow model is that the proportion of precipitation that generates storm runoff as unsaturated flow is likely small. Some of the infiltrated water does not contribute to subsurface stormflow directly but, instead, contributes to increasing soil water content which is necessary to increase the unsaturated hydraulic conductivity. This water storage decreases subsurface stormflow and causes delays between infiltration and groundwater discharge.

Unsaturated hydraulic conductivity is probably the dominant factor that determines whether or not unsaturated flow can contribute to stormflow. Freeze's (1972b) numerical simulations demonstrated that unsaturated flow through the matrix contributed to storm runoff when saturated (i.e. maximum) hydraulic conductivity was 4.4×10^{-3} m/s, but was insignificant for saturated hydraulic conductivity below 4.4×10^{-5} m/s. Unsaturated flow was significant only from steep and convex hillslopes with saturated hydraulic conductivity of 4.4×10^{-4} m/s. Freeze (1972b) thought that his assumed maximum saturated hydraulic conductivity of 4.4×10^{-3} m/s was unrealistic. However, Harr (1978, p. 40) measured saturated hydraulic conductivity as high as 1.1×10^{-3} m/s in soils where the "structural characteristics affect hydrological properties more than do textural characteristics." Freeze's results demonstrate the magnitude of hydraulic conductivity required, whereas Harr's results suggest the importance of soil structure and macropores for unsaturated flow.

There has been considerable interest in the hydrological processes of water flow in unsaturated macropores and in the influence of soil structure and texture on unsaturated flow. For example, Phillips et al. (1989) demonstrated that water under negative pressure head could enter into simulated macropores once a continuous water film was established along the

Figure 2.3 Conceptual models of subsurface stormflow.



macropore wall. Kung (1990a, 1990b) demonstrated that infiltrating water in the unsaturated zone can be funneled along preferential flowpaths that are controlled by textural and structural changes in a sloping soil profile. Field tracer experiments by Tsuboyama et al. (1994) showed that even though unsaturated flow occurred predominantly in the matrix, preferential flow significantly contributed to subsurface flow and transport. A model for the transfer of water between matrix and macropores in variably saturated media was proposed and evaluated by Gerke and van Genuchten (1993a, 1993b). Although a complete review of this literature is beyond the scope of this thesis, it is apparent from these examples that unsaturated preferential flow could significantly influence subsurface stormflow generation.

2) Groundwater ridging model

Rapid development of a groundwater ridge adjacent to the stream was first described in 1941 as a possible explanation for subsurface stormflow generation (Hursh and Brater, 1941; Wenzel, 1941, cited in Hursh 1944). The role of the capillary fringe in producing this ridge was only suggested much later as part of the groundwater ridging model proposed by Sklash and Farvolden (1979).

The effect of the capillary fringe is central to the groundwater ridging model. The capillary fringe is a zone of tension-saturation immediately above the water table that results from the capillary forces (surface or interfacial tension) that retain water in sediments under negative pore pressures (Bear, 1972). The thickness of the capillary fringe depends on the air-entry pressure (Ψ_a , the negative pressure head at which air first enters a saturated media) and, consequently, on pore size. The capillary fringe effect is the very rapid rise of a water table in response to the infiltration of a small amount of water that changes the tension-saturated capillary fringe into a phreatic ($\Psi > 0$) surface. The significance of this effect is well described and demonstrated by Gillham (1984) in a field experiment; its occurrence has been observed

in several field studies and experiments (Blowes and Gillham, 1988; Novakowski and Gillham, 1988; Abdul and Gillham, 1984, 1989).

The groundwater ridging model suggests that, in response to infiltration, the water table rises rapidly adjacent to the stream where the capillary fringe extends to the ground surface. However, the water table does not rise farther upslope where infiltration is stored in the unsaturated zone above the capillary fringe (Figure 2.3b). This pattern of water table response causes the formation of a groundwater mound or ridge adjacent to the stream channel. The increase in subsurface flow in the groundwater ridging model occurs within the saturated zone (ΔQ_A , Figure 2.2) and is attributed to the increase in horizontal and vertical hydraulic gradients towards the stream. As a result, discharge areas expand to accommodate the increase in subsurface flow.

The development of a groundwater ridge changes the pattern of groundwater flow through the entire depth of the aquifer near the stream. Vertical gradients are changed such that downward flow is induced beneath the crest of the ridge and vertical convergence of flow lines is increased beneath the stream (Figure 2.3b). As such, the increase in groundwater flow is distributed throughout the thickness of the aquifer and throughout the expanded discharge area.

This model relies on the unequal response of the groundwater table adjacent to a stream to produce a groundwater ridge and a change in hydraulic gradient. If the water table were to rise equally with distance from the stream, then the downslope hydraulic gradient would remain unchanged and the change in subsurface flow could not be caused by groundwater ridging. An unequal water table response can result from the variable thickness of the capillary fringe and by the increasing thickness of the unsaturated zone with increasing distance from the stream. Near the stream, the capillary fringe thickness can vary where it is

limited by a sloping ground surface. Farther from the stream, the water table does not rise rapidly because flow to the top of the capillary fringe is delayed through thicker unsaturated zones (Figure 2.3b).

Groundwater ridges can only effectively increase subsurface flow if they are located within approximately 20 m or less of discharge zones. At greater distances, groundwater ridges can only produce marginal increases in hydraulic gradients. For example, if the water table extends to the ground surface at the stream edge and the capillary fringe is 0.5 m thick (for fine sand, Table 2.1), 20 m upslope, the change in hydraulic gradient would be 0.025 and would not likely cause large increases in subsurface flow. In field and laboratory studies where groundwater ridges have been observed, the distance from the ridge to the centre of the stream ranges between 1 and 4.5 m (Abdul and Gillham, 1984, 1989; Blowes and Gillham, 1988; Novakowski and Gillham, 1988). The groundwater ridge cannot explain increases in subsurface runoff that are generated in midslope and upslope portions of the catchment. Stream response by groundwater ridging is, therefore, restricted to a small proportion of precipitation (Sklash et al., 1986).

3) Transmissivity feedback model

Hursh and Brater (1941, Hursh, 1944) discussed possible subsurface stormflow contributions by saturated flow through shallow permeable soil horizons. This idea later developed into the transmissivity feedback model in Sweden, where groundwater ridges were not observed during storms (Lundin, 1982; Rodhe, 1987; Bishop, 1991).

In the transmissivity feedback model, the increase in subsurface flow is caused by an increase in transmissivity as the water table rises and saturates more permeable soil horizons in the unconfined aquifer (Figure 2.3c). The positive feedback in this model occurs between infiltration and downslope subsurface flow. Infiltration causes the water table to rise and

Table 2.1 Capillary rise within different porous media (Bear, 1972).

Material	Capillary rise (cm)
Coarse sand	2-5
Sand	12-35
Fine sand	35-70
Silt	70-150
Clay	>200-400

shallow soil horizons to become saturated. Since the hydraulic conductivity of the shallow soils becomes higher with saturation, the transmissivity and subsurface flow towards the stream increase. Therefore, as infiltration increases, so does the capacity of the hillslope to transmit subsurface flow downslope. Where saturated hydraulic conductivity decreases with depth, this feedback mechanism is non-linear such that small increases in infiltration and water table elevation can greatly increase transmissivity.

The water table rise associated with the capillary fringe effect does not increase the transmissivity of previously saturated sediments. Presumably, the transmissivity should only increase during the storm event if the water table or the capillary fringe rises above the capillary fringe position prior to the storm. Hysteresis generally causes the thickness of the capillary fringe to be smaller upon wetting than upon drying such that its rise would be less than that of the water table. In contrast, where the capillary fringe intersects the ground surface, there can be no effective increase in subsurface transmissivity.

The transmissivity feedback model is enhanced by 1) a large increase in the hydraulic conductivity from unsaturated to saturated conditions, and 2) an increase in the saturated hydraulic conductivity towards the ground surface. These factors are often necessary to transmit infiltrating precipitation as subsurface flow within relatively thin transiently saturated horizons (ΔQ_B , Figure 2.2). An increase in hydraulic conductivity towards the surface in soils is not a limitation to the model. In fact, this pattern is consistent with soil formation and development, is widely observed in most well developed soils (particularly in forested areas), and is commonly caused by soil structure, root holes or other types of macropores.

The transmissivity feedback model can be applied separately to matrix flow (single porosity) and dual porosity flow. In the transmissivity feedback model with single porosity, the increase in subsurface flow occurs within the matrix (e.g. Bishop, 1991); in the proposed

transmissivity feedback model with dual porosity, it occurs both within the matrix and the macropores. Although this distinction has not been made previously, it emphasizes the importance of differences between the hydraulic characteristics of single and dual porosity media for streamflow generation.

In the transmissivity feedback model with dual porosity, transient saturation of macropores is responsible for the large increase in bulk hydraulic conductivity from slightly negative to positive pore pressures. Since the macropores are the largest pores, they are drained under very small negative pressure heads and contribute little to lateral subsurface flow. When saturated, the macropore contributes significantly to the bulk hydraulic conductivity of the soil horizon. The role of the matrix is twofold. Firstly, it provides storage of pre-event water, and secondly, it is sufficiently permeable that it can transmit flow between disconnected macropores when they are saturated. Pre-event water can enter macropores by two mechanisms. Firstly, when infiltration reaches the top of a tension-saturated or nearly saturated zone in the matrix, the water pressure in the pores of the soil matrix becomes positive and pre-event water will flow from the soil matrix to saturate the macropores. Secondly, after the water table has risen, saturated flow through the matrix between disconnected macropores can displace pre-event water into macropores. Therefore, even if bypass flow (preferential flow through large pores in an unsaturated matrix) of event water fills the macropore first, it is still possible to displace pre-event water into macropores.

4) Perched water table model

In the perched water table model, subsurface stormflow is produced when the infiltration rate into a soil horizon exceeds the capacity of the underlying horizon to transmit the water vertically. Although Hursh (1944) identified the essence of the perched water table model, Weyman (1970) recognized that discharge from a perched water table was

predominantly displaced groundwater rather than infiltrating event water, and that the magnitude of discharge was related to the upslope areal extent of the perched water table.

When a perched water table develops above a layer of low hydraulic conductivity, saturation of the overlying, more permeable layer increases its hydraulic conductivity. Thereby, downslope flow within the transiently saturated zone increases (ΔQ_B , Figure 2.2), provided the perched water table slopes downward towards the stream (Figure 2.3d).

This conceptual model requires four elements. Firstly, for a perched water table to develop, a continuous layer of low hydraulic conductivity is necessary. Its spatial extent will determine the volume of subsurface storm runoff that can be produced. Secondly, rainfall intensities must be sufficient to produce subsurface ponding above the layer of low hydraulic conductivity. The perched water table will not develop if rainfall intensities are less than the hydraulic conductivity of the low permeability unit. Thirdly, the low permeability layer should also have a sloping surface to assist downslope flow within the perched layer. Lastly, the overlying layer must have a sufficiently high saturated hydraulic conductivity to transmit subsurface flow downslope to the stream.

There are important differences between the responses of perched and free water tables. In particular, a free water table can have a capillary fringe that responds to infiltration very rapidly, whereas a soil horizon underlain by a low permeability layer may not be saturated initially and will store infiltrating water before a perched water table develops. Furthermore, a perched water table repeatedly develops within the same horizon, whereas the initial position of a free water table can be variable.

Perched water tables are not uncommon. Saturated hydraulic conductivity less than 10^{-7} m/s (≈ 0.4 mm/hr, equivalent to a low rainfall rate) may occur in silt, clay, till, and unfractured bedrock (Freeze and Cherry, 1979). Although perched water tables may occur

within soils, they develop most frequently at the base of the soil profile where the hydraulic conductivity of the underlying unit is often much lower (e.g. Dunne and Black, 1970a; McDonnell, 1990; Buttle and Sami, 1992).

5) Old water macropore flow model

The significance of macropores for the rapid movement of water through the subsurface has long been recognized (Hursh, 1944, see Beven and Germann, 1982) with particular emphasis on the importance of macropores for infiltration of event water (e.g. Mosley, 1979, 1982; Wilson et al., 1990). The role of macropores for the generation of pre-event (old) water runoff has received less attention. Based on his study of the Maimai M8 catchment in New Zealand, McDonnell (1990) developed the old water macropore model in which the increase in pre-event water in stream discharge is caused by flow through macropores.

When rainfall intensities exceed the infiltration capacity of the soil matrix at the surface, water ponds, flows downslope into vertical cracks and bypasses most of the soil matrix which remains unsaturated (Figure 2.3e). This infiltrating event water creates a perched water table at the bedrock surface where a small volume of infiltrating event water mixes with a larger volume of pre-event water. The horizontal macropores near the bedrock surface saturate with and drain predominantly pre-event water from the hillslope. The large increase in subsurface flow is mostly attributed to an increase in hydraulic conductivity that results from saturation of macropores in the transiently saturated zone (ΔQ_B , Figure 2.2).

McDonnell's (1990) model requires vertical bypassing of water from the surface to depth within the soil profile. At the Maimai catchment, vertical bypassing of event water was enhanced by Horton (1933) overland flow which produced surface ponding above the matrix and lateral flow into the vertical cracks (McDonnell, 1990). The model requires that the

hydraulic conductivity of surface soil horizons be lower than rainfall intensities and that most of the flow in the vertical cracks bypasses the soil matrix with little diffusion into it.

These conceptual models are not mutually exclusive such that a combination of processes are possible within a soil profile or that several processes can occur along a hillslope. For example, both the development of a perched water table and the existence of pre-event macropore flow contributed to streamflow generation in McDonnell's (1990) study.

Comparison of the conceptual models of subsurface stormflow generation

The dominant mechanisms, zones and spatial extent for the increase in subsurface flow in the different conceptual models are summarized and compared in Tables 2.2 and 2.3. Although different models include many of the same hydrological processes, they may not occur within the same zones (Table 2.2) or over the same spatial extent (Table 2.3).

The unsaturated flow model is the only one to emphasize the dominant role of downslope flow within the unsaturated zone (ΔQ_C , Figure 2.2, Table 2.2). However, infiltration and vertical unsaturated flow also occur within other models implicitly.

The groundwater ridging model is fundamentally different because the dominant mechanism for the increase in subsurface flow is the increase in hydraulic gradient which occurs within the existing zone of saturation (ΔQ_A , Figure 2.2, Table 2.2). Furthermore, this model is the only one in which subsurface stormflow generation is restricted to a small proportion of the catchment area (Table 2.3). These differences are very important because the dominant flowpaths for the increase in subsurface flow, the spatial extent of subsurface flow generation, and the physical and hydrological properties required are also different.

The dominant mechanism and flowpaths for the increase in downslope subsurface flow are similar for the transmissivity feedback, perched water table and old water macropore flow

Table 2.2 Comparison of subsurface stormflow models for the increase in subsurface flow with respect to dominant hydraulic mechanisms and subsurface zones.

Subsurface stormflow model	Dominant mechanism		Dominant zone		
	Change in hydraulic gradient	Change in hydraulic conductivity	Unsaturated	Transiently saturated	Previously saturated ¹
Unsaturated flow		√	√		
Groundwater ridging	√				√
Transmissivity feedback		√		√	
Perched water table		√		√	
Old water macropore flow		√		√	

¹ including capillary fringe

Table 2.3 Comparison of subsurface stormflow models with respect to the maximum spatial extent of subsurface flow generation.

Subsurface stormflow model	Maximum spatial extent		Control on spatial extent
	Near-stream and lower hillslope	Entire catchment	
Unsaturated flow		√	unsaturated bulk K, spatial extent of interconnected macropores
Groundwater ridging	√		depth to capillary fringe, Δ in hydraulic gradient
Transmissivity feedback		√	spatial extent of water table response
Perched water table		√	spatial extent of low K layer
Old water macropore flow		√	spatial extent of macropores and water table response

K = hydraulic conductivity

models (Table 2.2). In effect, both the perched water table model and the old water macropore flow model could be considered special cases of the transmissivity feedback model because they require transient saturation to increase subsurface flow. Similarly, the different processes within these models may occur simultaneously or in combination. For example, vertical cracks or macropores could enhance unsaturated flow to the water table in the transmissivity feedback model. Although subsurface flow can be generated from the entire watershed in each model, the controls on the spatial extent of flow generation are slightly different (Table 2.3).

Although differences between these three models are minor, they can be important with respect to water flowpaths and, therefore, water chemistry. Increased downslope subsurface flow always occurs through the same horizon in the perched water table model, whereas it may occur within different soil horizons in the transmissivity feedback model. In the old water macropore flow model, vertical flow bypasses shallow soil horizons and limits interaction with them.

Physical and hydrological properties conducive to subsurface stormflow generation

Results of stormflow generation studies are most useful when it is known under what circumstances they apply to other watersheds. Therefore, it is essential to understand how the dominant hydrological processes are related to the physical and hydrological properties of watersheds. This relationship is important for both identifying the measurements that are most useful and predicting which hydrological processes are likely to dominate in a given watershed.

Subsurface stormflow models rely on different processes that are influenced by different physical and hydrological characteristics (Table 2.4). Important physical characteristics to consider are those that influence the hydraulic gradient or the hydraulic conductivity. These

Table 2.4 Physical properties and environments most suitable for different subsurface stormflow models.

Subsurface stormflow model	Topography and water table	Hydraulic conductivity	Air entry pressure and retention curve	Sediment texture, pore size or structure
Unsaturated flow	moderate to steep hillslopes	high bulk K_u^* , large change in K_u with Ψ^*	small change in θ with Ψ	well structured or macroporous
Groundwater ridging	variable thickness or depth of capillary fringe*, nearly flat water table prior to the storm	high K_S near the stream*	large Ψ_a^*	fine to medium sands, no large pores
Transmissivity feedback -matrix flow	moderate to steep hillslopes and water table	large change in K_u at small Ψ^* , high K_S increasing towards the surface	small Ψ_a , small change in θ with Ψ	coarse sands, broad pore size distribution
Transmissivity feedback -dual porosity	moderate to steep hillslopes and water table	High K_S due mostly to macropores*, moderate K_S in matrix, large change in K_u at small Ψ for bulk soil*	large Ψ_a for matrix, small Ψ_a for macropores, small change in θ with Ψ for bulk soil	fine to medium sand matrix, well structured or many macropores*
Perched water table	moderate to steep hillslopes (sloping horizon of low K_S)*	High K_S , overlying low K_S^* , large change in K_u at small Ψ for bulk soil*	small Ψ_a in perched zone, small change in θ with Ψ	coarse sands overlying fine silts and clays
Old water macropore flow	moderate to steep hillslopes	High K_S due to macropores*, matrix $K_S < \text{rainfall intensity}^*$, large change in K_u at small Ψ for bulk soil*	large Ψ_a for matrix, small Ψ_a for macropores, small change in θ with Ψ	silty to fine sand matrix at surface, interconnected macropores or coarse matrix at depth*

K_S = Saturated hydraulic conductivity, K_u = Unsaturated hydraulic conductivity, Ψ = Pressure head, Ψ_a = Air-entry pressure, θ = water content. Essential criteria are indicated with an asterisk.

This table identifies optimal physical and hydrological properties, it does not suggest the entire range of properties suitable for each model. For example, although subsurface flow is enhanced by steeper slopes in all models, with the exception of groundwater ridging, the models are also applicable in catchments with more gentle slopes. Another limitation is that optimal criteria are considered individually which may lead to unlikely combinations in hydraulic properties such as a large change in K_u with Ψ and a small change in θ with Ψ for the unsaturated flow model.

include topography, sediment thickness and texture, and pore size distribution. Relevant hydrological characteristics include the saturated hydraulic conductivity, the relative (unsaturated hydraulic) conductivity function, soil water characteristic (or retention) curve, air entry (or bubbling) pressure, water table configuration, and soil water content. Therefore, a given model may be more appropriate for specific geographical or geological settings.

Groundwater ridging

Groundwater ridging requires a large change in hydraulic gradient at the stream edge. Consequently, a water table that is nearly flat adjacent to the stream prior to the storm would have a larger relative increase in hydraulic gradient than would a sloping water table. In fact, groundwater ridging has been documented mostly in intermittent streams in which, prior to the storm, the water table was nearly horizontal and was positioned below the stream bed (Blowes and Gillham, 1988; Abdul and Gillham, 1989).

Groundwater ridging also requires sediments with a large capillary fringe and, consequently, a large air-entry pressure (Table 2.4). Since the air-entry pressure is a function of the large-sized pores, the thickness of the capillary fringe is decreased by the development of secondary porosity, such as that caused by soil structure and aggregation. In the absence of secondary porosity, the thickness of the capillary fringe is influenced by soil texture. The unsaturated hydraulic conductivity of sediments and the shape of the retention curve below the air-entry pressure are relatively unimportant in the groundwater ridging model since the increase in subsurface flow is attributed mostly to saturated flow.

The groundwater ridging model is most applicable to soils without any substantial structure, aggregation or macropores, and with textures similar to, or finer than, medium or fine sand. Where soils have large pores that drain under small negative pressures, saturation of

these pores will increase the hydraulic conductivity. Therefore, the increase in subsurface flow in this example would be attributed to increased hydraulic conductivity and not to increased hydraulic gradient. The approximate height of the capillary fringe for different textures is presented in Table 2.1. Coarse sands have a capillary fringe on the order of 2–5 cm (Bear, 1972) and would not produce substantial changes in water table elevations. Although silts and clayey sediments may have a large capillary fringe, their low hydraulic conductivity preclude large groundwater fluxes (Zaltsberg, 1986; McDonnell and Buttle, 1998). This problem illustrates the paradox of the groundwater ridging model in which the coarsest sediments with the largest hydraulic conductivity are likely to have the smallest capillary fringe and the finest sediments with the largest capillary fringe, the lowest hydraulic conductivity.

Models with increasing saturation

The other models attribute the increase in subsurface flow mostly to increasing saturation and increasing hydraulic conductivity (Table 2.2). Although steeper hydraulic gradients enhance these processes, both the saturated and unsaturated hydraulic properties of the sediments become much more important for increasing subsurface flow in the transiently saturated zone (ΔQ_B). Four hydraulic properties enhance this type of flow: 1) a large saturated hydraulic conductivity ($K_s \approx 10^{-4}$ m/s), 2) a small air-entry pressure ($|\Psi_a| \approx 0.05$ m), 3) a sharp decrease in hydraulic conductivity at very small negative pressure heads ($0 > \Psi > -0.05$ m), and 4) a gentle slope in the retention curve for small negative pressure heads ($0 > \Psi > \approx -1$ m).

Large saturated hydraulic conductivity is needed to transmit large increases in subsurface flow during storms. The approximate magnitude of the necessary saturated hydraulic conductivity can be estimated from the rise and slope of the water table, the upslope contributing area, and the precipitation intensity. Given typical values of these variables on the

Canadian Shield, soils with $K_s > \approx 10^{-4}$ m/s should be capable of transmitting most storm precipitation as subsurface flow.

Small air-entry pressures ($|\Psi_a| < \approx 0.05$ m) allow air to enter and water to drain from the largest pores. Since these large pores are the dominant conduits for flow, the hydraulic conductivity can decrease sharply a few centimeters above the water table. Small air entry pressures are typical for uniform coarse sand and gravel or structured sediments.

To accommodate large increases in subsurface flow, the increase in hydraulic conductivity from negative to positive pressure heads must be large because the rise in water table elevation is frequently small. When the water table drops after a storm, a decrease in hydraulic conductivity at small negative pressure heads minimizes subsurface flow and reduces drainage of soil moisture from the transiently saturated zone. Large changes in hydraulic conductivity at small negative pore pressures have been reported and modelled for coarse and macroporous soils (e.g. Richards, 1931; Germann and Beven, 1981; Wilson and Luxmoore, 1988; Durner, 1994).

A gentle slope in the retention curve from saturation to pressure heads of approximately -1 m maintains high water contents, minimizes the specific yield above the water table, and consequently maximizes the rise in the water table during subsequent infiltration. More water is retained in sediments with a broad range of pore sizes than in sediments with uniform large pores. A coarse sediment with a uniform pore size distribution and a steep retention curve at small negative pressure heads effectively produces a sharp decrease in hydraulic conductivity from saturated to unsaturated conditions. However, substantial drainage increases the specific yield, reduces the subsequent rise in the water table and results in a thinner transiently saturated zone (ΔQ_B). Although fine sediments have more gentle retention curves with smaller specific yields, their hydraulic conductivity is smaller and

air entry pressure larger. Sediments with a wide range of pore sizes retain water more effectively than uniform sediments at smaller pressure heads once the large pores have drained. In general, broad retention curves and pore size distributions are indicative of poorly sorted or well aggregated sediments (Wu et al., 1990).

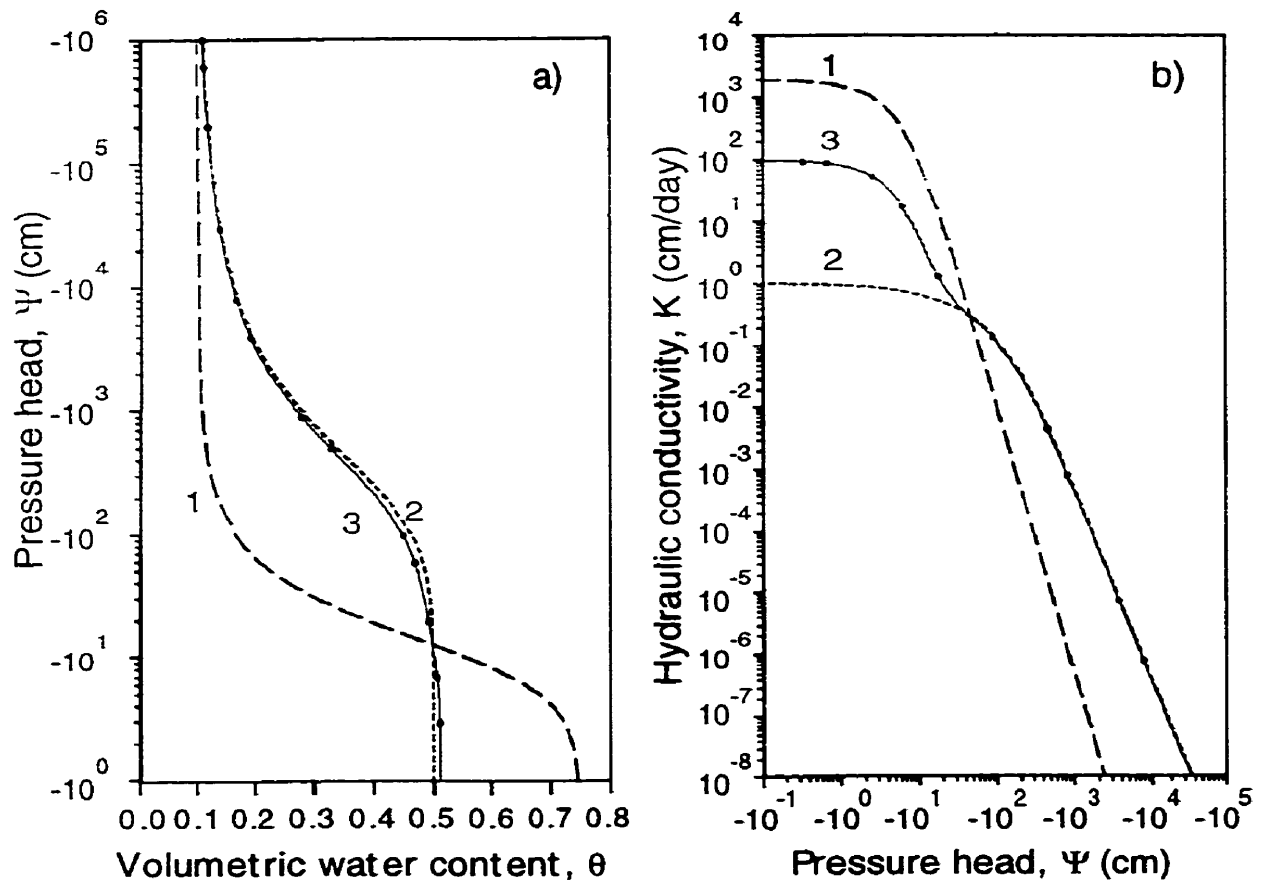
Transmissivity feedback with matrix flow

The transmissivity feedback model with matrix flow is most applicable in watersheds with coarse and highly permeable sediments (Table 2.4). Coarse sand satisfies the hydraulic requirements of the model since it generally has a small air-entry pressure and a high saturated hydraulic conductivity that decreases rapidly at small negative pressure heads. However, coarse sand has a large specific yield ($\approx 27\%$, Domenico and Schwartz, 1990) that stores infiltration. Small proportions of silt or clay may increase water retention without substantially decreasing hydraulic conductivity.

Transmissivity feedback with dual porosity flow

The transmissivity feedback model with dual porosity flow relies on the different hydraulic properties of the matrix and macropores to produce the necessary bulk hydraulic properties. The retention and unsaturated hydraulic conductivity curves for the macropores (lines 1), matrix (lines 2) and the bulk soil (lines 3) are shown schematically in Figure 2.4. The matrix can be characterized by a large air entry pressure, moderate saturated hydraulic conductivity, and a gentle retention curve. The macropores are characterized by a small air entry pressure ($< 0.01\text{m}$), a large saturated hydraulic conductivity that decreases rapidly at small negative pressure heads, and a steep retention curve. Since the macropores comprise a small proportion of the total pore space, the retention curve of the bulk soil is similar to that of the matrix (Figure 2.4a). However, since most of the flow under saturated conditions occurs through the macropores, the saturated hydraulic conductivity of the bulk soil is increased

Figure 2.4 Hydraulic properties of a dual porosity medium: a) retention and b) hydraulic conductivity functions of 1) fracture or macropore, 2) matrix pore systems, and 3) of the total porous medium (adapted from Gerke and van Genuchten, 1993a).



significantly by their presence (Figure 2.4b). Under moderate negative pressure heads, the macropores drain and, therefore, the unsaturated hydraulic conductivity of the bulk soil decreases to that of the matrix.

The transmissivity feedback model with dual porosity flow is best suited to watersheds with macroporous sediments of fine to medium sand (Table 2.4). Since the decrease in hydraulic conductivity of the bulk soil is primarily caused by the drainage of macropores, fine and medium sands with wide pore size distributions and large air entry pressures retain water in the matrix under negative pressure heads. Consequently, only a small amount of infiltration is required to saturate the matrix and macropores. Pre-event flow that originates in the matrix must be transmitted through it before entering a macropore. Therefore, the matrix cannot be so fine-grained to reduce its saturated hydraulic conductivity. Since the hydraulic conductivity of the saturated bulk soil is greatly influenced by the size, density and interconnectivity of the macropores, this model applies to watersheds where conditions enhance the formation and preservation of soil structure and macropores. An advantage of this model over the transmissivity feedback model with matrix flow is that it can also apply to finer textured sediments.

Old water macropore flow

The geographical setting that is most suitable for the old water macropore flow model is similar to that for the transmissivity feedback model with dual porosity with three notable exceptions (Table 2.4). Firstly, the matrix must be finer grained at the surface to produce Horton overland flow that enhances vertical bypass flow. Secondly, vertical macropores or fractures are necessary so that infiltration can bypass soil horizons rather than displace water through the matrix. Thirdly, macropores must be interconnected or a coarse textured matrix is required at depth to transmit flow effectively between disconnected macropores.

Perched water table

To produce a perched water table, a low permeability layer of silty or finer textured sediment or unfractured rock is required. In addition, hydrological and physical properties for the overlying layer that are similar to those required for the transmissivity feedback model will enhance lateral flow within the permeable sediments above the low permeability layer (Table 2.4).

Unsaturated flow

The important bulk hydraulic properties for the unsaturated flow model are a high unsaturated hydraulic conductivity that can transmit sufficient subsurface flow towards the stream and a steep relative conductivity function. Given the magnitude of unsaturated hydraulic conductivity of most sediments, it is unlikely that unsaturated flow is the dominant contributor to storm runoff in most soils without the presence of mesopores or macropores (e.g. Freeze, 1972b). It is beyond the scope of this discussion to consider more specifically what unsaturated flow processes and what combinations of matrix and macropore characteristics may lead to the bulk hydraulic properties specified in Table 2.4.

Because the hydraulic conductivity of a sediment often decreases by more than one order of magnitude when unsaturated, it is easy to suggest that unsaturated flow is insignificant compared to saturated flow. However, measurements of hydraulic conductivity in undisturbed soils, soil water tensions, and areas that contribute to stream discharge provided convincing evidence that unsaturated flow can be significant (Harr, 1978). It is also important to recognize that the saturated hydraulic conductivity within a soil profile may also vary by more than one order of magnitude such that the unsaturated hydraulic conductivity in the upper soil may be similar to the saturated hydraulic conductivity in the lower soil profile (e.g.

Harr, 1978). Therefore, unsaturated flow should not be rejected as a potentially important flowpath.

Conclusions

Conceptual models of subsurface stormflow should identify and explain mechanisms for increased flow, individual flow processes (e.g. saturated macropore flow), interactions between individual flow processes (e.g. flow between matrix and macropores), and spatial distributions of these processes during storms. Previous descriptions of conceptual models did not discuss all these elements. This summary has considered many new implications of these models. Firstly, it has shown that these models are not appropriate in all geographical settings. For example, the requirements of the groundwater ridging model make it applicable to a small range of sediment textures and topographic slopes. Secondly, several elements within these models remain poorly described, in particular, the interactions between individual flow processes. Thirdly, it suggests that an examination of the hydrological and physical properties within a watershed may provide insight into the streamflow generation processes that may (or may not) be operative.

This summary has considered the mechanisms of increased subsurface flow. Although several models implicitly described whether increased subsurface flow results from increased hydraulic gradients or from increased hydraulic conductivity, it is useful to make this distinction explicitly because it reveals a fundamental difference in the groundwater ridging model. This model relies on an increase in hydraulic gradient rather than an increase in saturation to increase subsurface flow. This distinction has further implications on the flowpaths for increased subsurface flow (in the previously saturated zone) and the spatial extent of subsurface runoff production. Consequently, it is very easy to distinguish groundwater ridging from other models using simple field measurements. Transects of

groundwater level measurements adjacent to the stream can be used to detect groundwater ridge development and to quantify the magnitude of the change in hydraulic gradient. Stream runoff during storms can be easily measured and compared to precipitation volume in order to evaluate the minimum spatial extent of runoff generation.

In contrast, it appears that the transmissivity feedback model may apply to watersheds with a broader range of physical and hydrological properties. The transmissivity feedback model with dual porosity was proposed to account for the large increase in subsurface flow in finer textured soils in which fluctuations of the water table are small. It also explains how pre-event water can be displaced through macropores. Although the old water macropore model also explains this displacement, it is restricted to a smaller range of catchment settings.

Unsaturated flow may be important in the upslope portions of forested catchments with structured or macroporous soils even though other hydrological processes and models may dominate in midslope or lower slope positions. The relative importance of unsaturated and saturated flow for streamflow generation should be assessed. Although unsaturated flow may not dominate storm runoff generation, it may be an important secondary process that influences the redistribution of soil moisture.

Classification of subsurface stormflow generation mechanisms and spatial extents is a useful approach to evaluate streamflow generation models in individual study sites such as Harp 4-21 and Harp 3A (Chapter 7). Furthermore, results should be related to physical or hydrological properties so that these relationships can be extrapolated to other watersheds.

Chapter 3

Physical properties governing groundwater flow in Harp 4-21

Introduction

Stream chemistry and the neutralization of acidic deposition is greatly influenced by the geologic, hydrologic and biological factors that control the movement of water through catchments. Groundwater discharge to streams and lakes is particularly important in acid sensitive areas such as the Canadian Shield where the alkalinity of groundwater is the main buffer of acidic deposition (Bottomley et al., 1984, 1986). Groundwater flow and discharge are also significant components of nutrient cycling in catchments (Likens et al., 1977).

From isotopic hydrograph separations, groundwater ("old" water) is found to be a significant component of streamflow in many glacial till catchments underlain by crystalline bedrock (Fritz et al., 1976; Sklash and Farvolden, 1979; Rodhe, 1981, 1984, 1987; Hooper and Shoemaker, 1986; Moore, 1989). Flowpaths to the stream can be inferred from hydrograph separations using "in-stream" parameters such as isotopic ratios or chemical concentrations (e.g. Maulé and Stein, 1990; Wels et al., 1991a, 1991b). However, these reconstructed flowpaths provide little information on the physical properties that govern hydrologic processes and therefore hydrograph separations alone have little predictive power. To study and predict the interactions between groundwater and surface water, it is necessary to shift our investigations beyond the boundaries of the stream and also examine how the physical properties of a catchment influence the dominant hydrological processes in a catchment.

A considerable amount of research has focused on the physical properties that influence the location and size of surface saturated areas since these areas can generate much of the streamflow in humid regions by saturation overland flow. Following the definitions of

Dunne et al. (1975), saturation overland flow includes both return flow which is groundwater that has discharged to the ground surface and direct precipitation onto saturated areas. In a theoretical study, Kirkby and Chorley (1967) suggest that surface saturation is most probable in locations of 1) slope convergence in plan view, 2) slope concavities in section and 3) thinning sediments. Extensive field studies by Dunne et al. (1975), Anderson and Burt (1978a, b) and Beven (1978) demonstrate that areas of topographic convergence (in plan) are preferential locations of surface saturation, are areas of convergent groundwater flow, and are areas that generally produce greater stream discharge per unit catchment area than divergent or straight hillslopes. Dunne et al. (1975) show that the extent of surface saturated areas varies both seasonally and during storms with the largest changes occurring along gentle topographic slopes adjacent to discharge areas. They also attempt to relate the extent of surface saturation to soil properties, vegetation and hydrologic parameters. Ward (1984) remarks that there is a lack of field evidence demonstrating that the thinning of sediments results in saturated overland flow. In a recent review of catchment hydrology, Goodrich and Woolhiser (1991) conclude that there is a need to improve the surface water-groundwater linkages in watershed models. To improve such models it is first necessary to understand the properties and processes that govern surface water-groundwater interactions.

The purpose of this chapter is twofold. First, field data from a glacial till catchment are examined to determine the influence of hydraulic conductivity, surface topography and sediment thickness on groundwater flow and groundwater discharge. The second goal is to explain the observed spatial and temporal pattern of stream discharge based on our knowledge of the physical properties of the catchment.

Other physical properties of the catchment can also influence groundwater flowpaths and groundwater discharge, in particular macroporosity (Beven and Germann, 1982), vegetation and the unsaturated characteristics of the sediments. These additional properties are

not specifically addressed in this chapter. The influence of the unsaturated zone on streamflow generation was studied in Harp 4-21 by MacLean (1992).

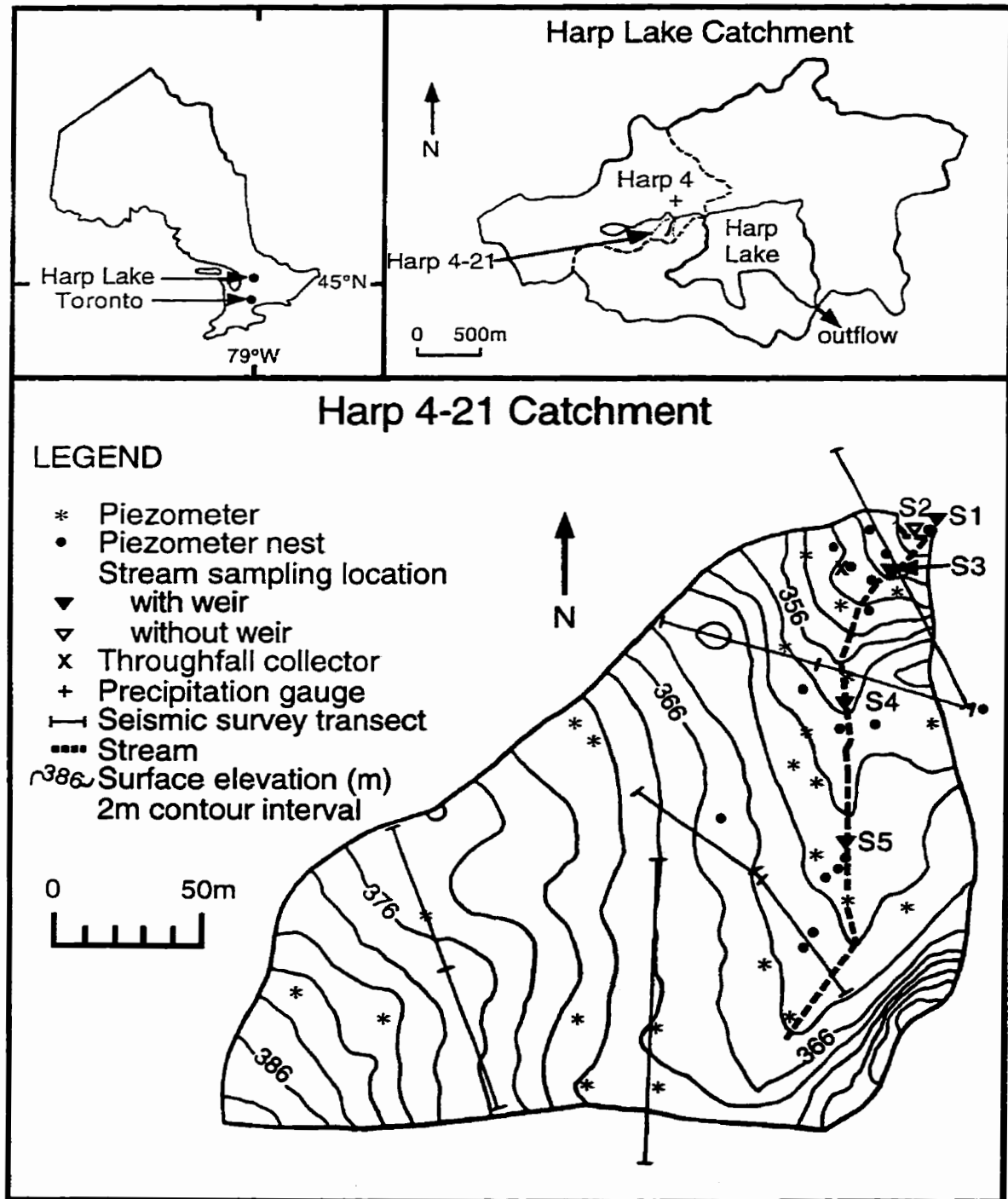
Study site

The study site is Harp 4-21, a small 3.7 ha headwater catchment located within the Harp Lake catchment in the Muskoka-Haliburton region of Ontario near the southern margin of the Canadian Shield (Figure 3.1). The site is monitored by the Ontario Ministry of the Environment (MOE) as part of the Acid Precipitation In Ontario Study (APIOS) to determine the effects of acidic deposition on several lakes and streams in the region. Results of hydrological and hydrogeochemical studies of the Harp 4 and Harp 5 catchments are reported by LaZerte and Dillon (1984), Bottomley et al. (1984), Seip et al. (1985), Rustad et al. (1986), Sklash (1986), Devito et al. (1990), Schiff et al. (1990) and Wels et al. (1990, 1991a).

The mean annual precipitation for the region is 1033 mm (1976-89) (MOE, unpublished data) of which approximately 26 percent falls as snow (Shibatanni, 1988). Stream discharge from Harp 4-21 is perennial and accounts for approximately 48% of the incoming precipitation (1989-90). Approximately two-thirds of the annual streamflow occurs between March 1st and June 30th when groundwater levels are highest due to spring melt and rainstorms (1989-90). Although the precipitation for the region has an average pH of 4.3 (1982-86) (Dillon et al., 1988), the mean pH and alkalinity of the Harp 4-21 stream are 6.8 and 184 $\mu\text{eq/l}$ respectively (B. LaZerte, unpublished data, 1984-90) indicating that this catchment effectively neutralizes the incoming acidic deposition despite the lack of carbonate minerals in the sediments and bedrock of the catchment (Aravena et al., 1992).

The catchment is underlain by metamorphic Canadian Shield bedrock composed predominantly of amphibolite and schist (Jeffries and Snyder, 1983). Groundwater from a bedrock well has tritium (^3H) levels above cosmogenic background values indicating that the

Figure 3.1 Location and instrumentation of the Harp 4-21 catchment.



fractured bedrock surface does not form an impermeable boundary. However, low yields from nearby domestic wells drilled through up to 150 m of bedrock suggests that the permeability of the bedrock is low and the majority of groundwater flow occurs within the overburden (Wills, 1992).

The overburden in Harp 4-21 forms an unconfined aquifer consisting of glacial tills overlain by soils. The tills range in texture from loamy sands to sandy clay loams with less than 25 percent clay-sized particles (Dankevy, 1989). Coarser sediments from pebbles to boulders are frequently observed during drilling and excavating and are visible at the ground surface. A horizontally discontinuous layer of compact till (densipan) approximately 0.2 to 0.5 m thick is often observed at the base of the soil profile at depths ranging from 0.5 to 1.2 m. This layer is most prominent in the upper half of the catchment. Densipan layers are common in many other catchments such as Hubbard Brook (Likens et al., 1977) and Sleepers River (Dunne and Black, 1970a, 1970b). Compact tills are also found at greater depths (> 2.5 m) in portions of the upper catchment but there are insufficient data to determine the spatial extent and thickness of these layers. Water levels in piezometers screened above and below compacted layers do not indicate the presence of perched water tables so that the aquifer is assumed to be unconfined throughout the catchment. Therefore, in this chapter groundwater flow specifically relates to saturated subsurface flow in the unconfined aquifer including both the tills and the soils.

Soils in Harp 4-21 belong to the Podzolic order (Agriculture Canada Expert Committee on Soil Survey, 1987); the physical and chemical characteristics of soils in the Harp 4 catchment are summarized by Lozano et al. (1987). The soils are generally characterized by surface organic horizons (L, F and H), a dark-coloured humic-rich mineral horizon with many roots (Ah), a dark brownish and reddish iron-rich mineral horizon with many roots (Bhf or Bf) and occasionally a light grey mineral horizon with few roots (BC)

above the parent material (C). Soils near the stream are frequently saturated and have thicker organic horizons and humic-rich A horizons.

Harp 4-21 is covered by a mixed hardwood forest dominated by *Acer saccharum* (sugar maple), *Betula alleghaniensis* (yellow birch), *populus spp.* (poplar species), *Abies balsamea* (balsam fir) and *Tsuga canadensis* (hemlock).

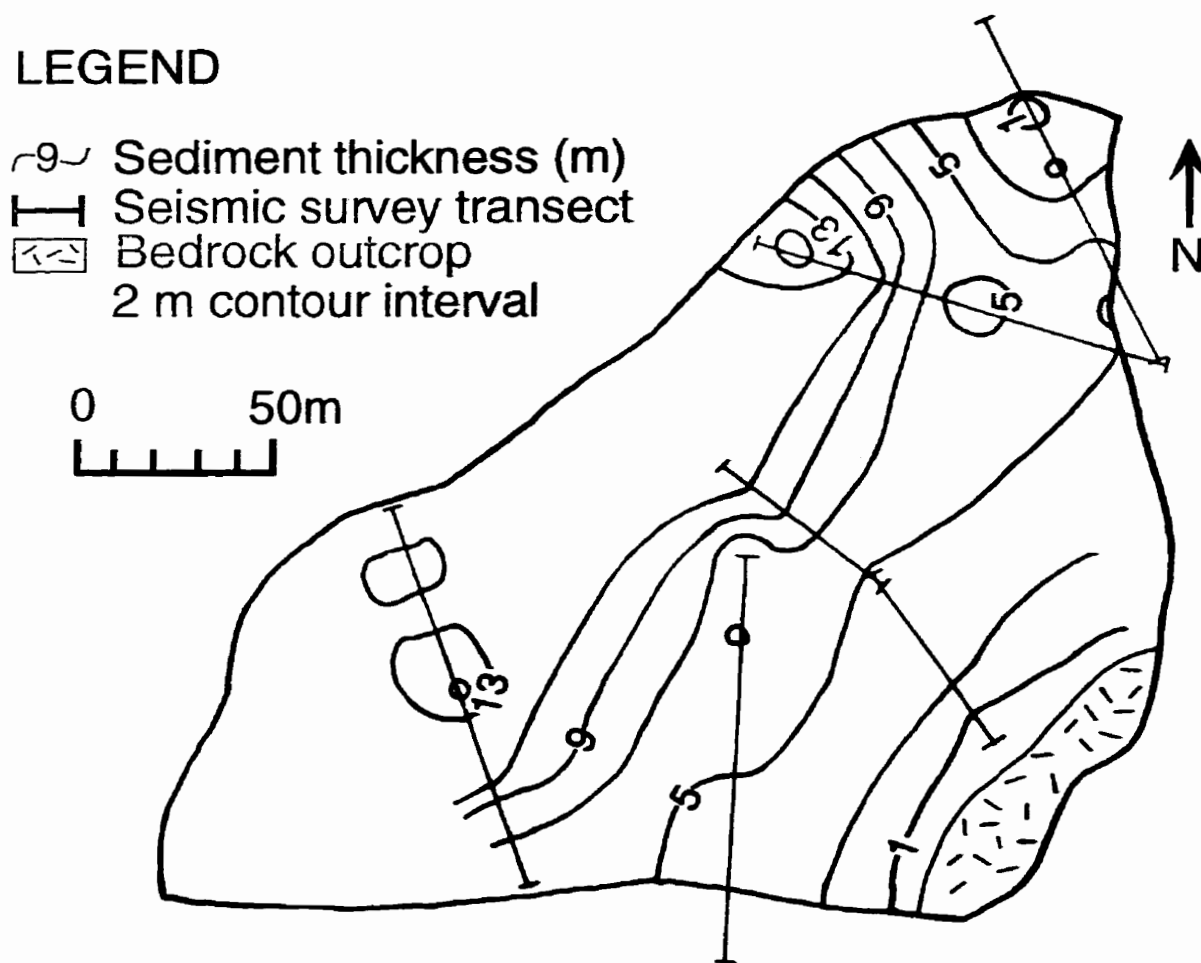
Methods

A comprehensive topographic survey of the Harp 4-21 catchment was conducted using a Wild Leitz total station (Figure 3.1). Slopes along the upper half of the stream are slightly concave, decreasing from as much as 17 percent in the uppermost catchment to 8 percent adjacent to the stream. Slopes draining to the lower half of the stream are slightly convex and steepen to as much as 30 percent. However, the base of these slopes are concave in the lowermost portion of the catchment where hillslope gradients decrease to approximately 15 percent.

The depth of sediments to bedrock was measured by seismic refraction along five 110 m transects using a OYO McSEIS 1500 Digital Seismograph and a geophone spacing of 5 m (Figure 3.2) (Redpath, 1973). The sediments are thickest along the northwestern margin of the catchment where overburden thickness ranges from 11 m to 15 m. The overburden gradually thins to less than 3 m in the northeastern portion of the catchment and to a bedrock outcrop in the southeastern portion of the catchment (Figure 3.2).

A network of 47 stainless steel drive-point, 35 PVC and 7 ABS piezometers was established to measure hydraulic conductivities, horizontal and vertical gradients and to collect groundwater samples (Figure 3.1). Piezometers were installed both in the soils and the tills and were screened over intervals ranging from 0.15 m to 0.6 m. Some of the deeper 3.8

Figure 3.2 Sediment thickness in Harp 4-21 as determined from seismic survey. Contours between geophysical transects are approximate.



cm (1.5") to 6.4 cm (2.5") diameter PVC and ABS piezometers were installed using augering drill rigs. The 1.3 cm (0.5") diameter drive-point piezometers were installed in vertical nests of two to eight piezometers using a Cobra portable vibrating rock drill. This installation method was the most effective at penetrating compacted tills although it did not allow for the collection of sediment samples. The hydraulic conductivity of the sediments was determined by slug and/or bail testing of the piezometers (Hvorslev, 1951). These results compare reasonably well (generally within one order of magnitude) to the hydraulic conductivities obtained using permeameter tests and grain size analyses (Dankevy, 1989).

Piezometric levels and stream discharge were monitored during fifteen runoff events between March, 1989 and May, 1990. Baseflow conditions between storms were monitored regularly. Stream discharge was gauged at S1 using a 90° V-notch weir enclosed in a heated structure to maintain ice-free conditions (Figure 3.1). A continuous record of stream discharge was obtained using a Leopold and Stevens (model A71) float-operated water level recorder and a stage-discharge relationship established from manual discharge measurements. Beginning in October 1989 stream discharge was measured manually from V-notch weirs installed at S3, S4 and S5 (Figure 3.1). Discharge at S2 is assumed to equal the difference between discharge at S1 and S3 since the area contributing directly to S1 is small and little discharge from this area was observed. Piezometric levels were recorded manually using either an electronic water level tape or Ping-Pong ball floats in selected PVC piezometers (Gillham, 1984).

Results and discussion

Hydraulic conductivity of the sediments

The glacial tills in Harp 4-21 have a large range of horizontal hydraulic conductivities from 2.6×10^{-5} m/s to 1.8×10^{-9} m/s ($n=56$) with a geometric mean of 2.3×10^{-7} m/s. Four drive point piezometers have conductivities of less than 1×10^{-9} m/s. This range is typical for glacial tills and silty sands (Freeze and Cherry, 1979) and emphasizes the heterogeneous nature of the Harp 4-21 tills.

Thin layers of significantly different permeability are evident within the tills of Harp 4-21. For example, hydraulic conductivities in one piezometer nest vary by four orders of magnitude over a 0.3 m depth. The influence of layering on groundwater flow is dictated by the spatial extent of these layers. No distinct pattern of large-scale layering emerges from the slug and bail test results of the tills. Regressions between log-hydraulic conductivity and both piezometer screen elevation and screen depth below ground surface indicate that there are no catchment scale patterns in hydraulic conductivity either horizontally or parallel to the ground surface ($r^2 = 0.06$ and 0.03 respectively). If there is any continuous layering, it is either at a scale smaller than the distance between piezometers or it is neither horizontal nor parallel to the ground surface. Variable stratigraphy between nearby excavations and boreholes suggests that layering is only continuous over distances on the order of five meters. The resulting groundwater flowpaths in the till are likely tortuous and difficult to define precisely. Due to the numerous heterogeneities and the difficulty of drilling into the tills, the measurement of hydraulic conductivity is not a practical way of obtaining detailed information concerning the continuity of layering within the tills.

The hydraulic conductivities of the soils vary over a much smaller range from 3.0×10^{-5} m/s to 3.7×10^{-7} m/s ($n=13$) with a geometric mean of 2.7×10^{-6} m/s. The absence of horizons of low hydraulic conductivity should result in higher effective hydraulic conductivities in the soils. Therefore, the flux of groundwater discharge from the catchment should increase substantially as groundwater levels rise within the soil. Furthermore, the groundwater levels within the soils should determine the relative importance of groundwater flow from the soils and the tills. There are insufficient data in Harp 4-21 to examine the differences in hydraulic conductivities between the soil horizons. However, increases in bulk density and decreases in root density with depth (Lozano et al., 1987) suggest that hydraulic conductivities decrease with depth within the soil profile.

Surface topography

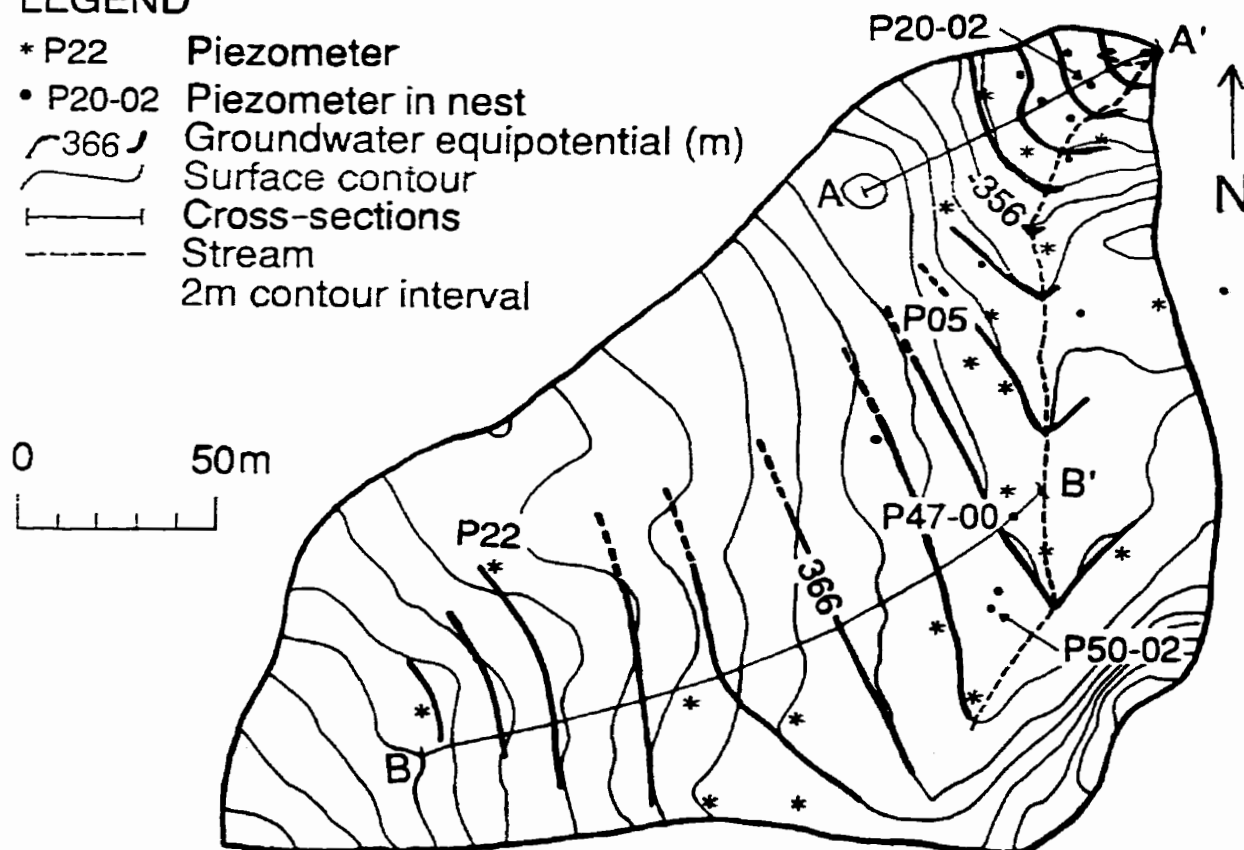
Surface topography is generally assumed to indicate the horizontal direction of groundwater flow in local groundwater flow systems. Where groundwater levels are very near or at the ground surface, the maximum horizontal hydraulic gradient is directed parallel to the maximum surface slope. Assuming horizontally homogeneous and isotropic hydraulic conductivities, groundwater flow is perpendicular to topographic contours. In Harp 4-21, topography indicates the direction of groundwater flow adjacent to the stream and in the lowermost portion of the catchment where the water table is at the ground surface and the equipotentials are parallel to the topographic contours (Figure 3.3). Topographic convergence in the lowermost portion of the catchment results in horizontal convergence of groundwater flow and discharge to the ground surface such that surface flow is maintained at S2 throughout the year.

In the middle and upper portions of the Harp 4-21 catchment, groundwater equipotentials are not parallel to topographic contours indicating that groundwater flow is not

Figure 3.3 Groundwater equipotentials in Harp 4-21 following spring melt on May 1, 1989. Dashed lines indicate approximate locations of equipotentials where the piezometer network is sparse. Surface elevations are also shown. Cross-sections A-A' and B-B' are shown in Figure 3.5.

LEGEND

- * P22 Piezometer
- P20-02 Piezometer in nest
- 366 Groundwater equipotential (m)
- Surface contour
- Cross-sections
- Stream
- 2m contour interval



parallel to the steepest topographic slope (Figure 3.3). For groundwater levels to fluctuate without changing the direction of flow, groundwater levels for all locations at a given elevation must fluctuate simultaneously and by the same amount. Many factors influence the spatial pattern of groundwater recharge and discharge such that groundwater levels at a given elevation in Harp 4-21 fluctuate neither simultaneously nor equally. Therefore, the direction of groundwater flow varies with groundwater level fluctuations. In general, the direction of groundwater flow is not perpendicular to surface topography wherever the depth to the groundwater table changes along any given topographic contour. This phenomenon is not unique to Harp 4-21. It can be shown from patterns of surface saturation (e.g. Dunne et al., 1975) that in portions of many other catchments, the direction of groundwater flow differs from the steepest topographic slope.

The discrepancy between the directions of groundwater flow and steepest topographic slope has significant implications for interpreting hydrological data from catchments and for modelling catchment hydrology. Catchment boundaries are generally defined using surface topography based on the assumption that groundwater flow is perpendicular to the topographic contours. However, to correctly identify the contributing area of a catchment, it is necessary to determine catchment boundaries from a map of groundwater equipotentials (Figure 3.3). Slight deviations in the direction of groundwater flow from the direction of steepest slope can result in substantial errors when determining the contributing area of a catchment (Figure 3.4, Table 3.1). Based on topographic divides, the S2 and S3 subcatchment areas are underestimated by 57% and 13% respectively whereas subcatchments areas for S4 and S5 are overestimated by 41% and 23% respectively. These results emphasize the need to identify locations where groundwater flow does not conform to topographic contours. Furthermore, if the direction of groundwater flow changes with fluctuating groundwater levels, then the

Figure 3.4 Approximate subcatchment boundaries determined from (A) surface topography (Figure 3.1) and (B) groundwater equipotentials on May 1, 1989 (Figure 3.3). Subcatchment areas are shown in Table 3.1.

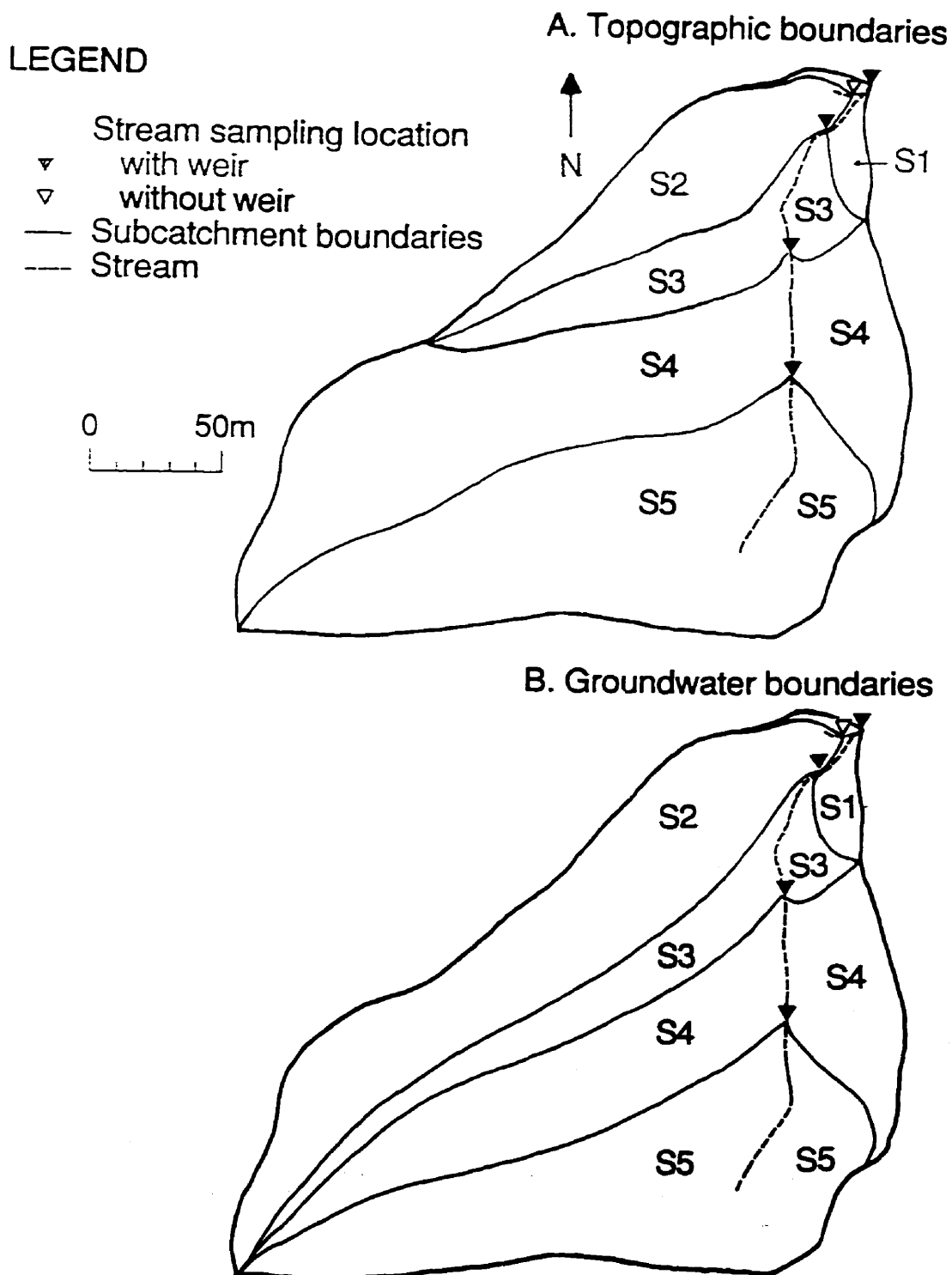


Table 3.1 Areas contributing directly to each subcatchment as determined from surface topography (A) and groundwater equipotentials (B) shown in Figure 3.4.

Subcatchment	A Topographic Area (m ²)	B Groundwater Area (m ²)	Error (A-B)/B (%)
S1	790	860	-8
S2	4570	10720	-57
S3	3860	4420	-13
S4	14170	10050	41
S5	14090	11430	23

locations of catchment boundaries will vary such that the contributing area of a catchment may also change with groundwater level fluctuations. Digital Elevation Models (DEM) are being used to automate the subdivision of catchments to provide spatially distributed hydrologic models (Moore and Grayson, 1991). In catchments where subsurface flow is significant, incorrect subcatchment areas and groundwater flow directions may result in errors in the predicted spatial distribution of stream discharge.

The magnitude of the topographic slope influences the extent of surface saturated areas and their expansion and contraction with fluctuating groundwater levels. As groundwater levels increase, a much larger area saturates to the surface along gentle slopes (Figure 3.5b) than along steeper slopes (Figure 3.5a). Since hillslopes are more gentle adjacent to the upper portion of the Harp 4-21 stream than in the steeper lower catchment, surface saturated areas expand much more adjacent to the upper stream than in the lower catchment (Figures 3.5 and 3.6). Similarly, groundwater levels rising from the tills into the more permeable soils result in a greater spatial extent of saturation within the soils along the gentle hillslopes adjacent to the upper stream than along the steeper slopes in the lower catchment. As a result of these spatial changes in surface and soil saturation, the spatial pattern of stream discharge and water flowpaths is expected to change significantly with fluctuating groundwater levels.

Sediment thickness

Assuming there is no horizontal convergence or divergence of groundwater flow, decreasing sediment thickness along a flowpath requires a proportional increase in the horizontal hydraulic gradient or conductivity at the point of thinning to transmit the flux of groundwater from upslope. Where groundwater levels are at the surface, thinning sediments can result in groundwater discharge since the horizontal hydraulic gradients are limited by the ground surface and cannot increase to transmit the flux of groundwater from upslope.

Figure 3.5 Cross-sections indicating the change in saturated areas resulting from groundwater level fluctuations. More gentle topographic slopes adjacent to the stream in the upper catchment (B) result in larger seasonal changes in the area of surface saturation than in the lower catchment (A). Cross-section locations are shown in Figure 3.3.

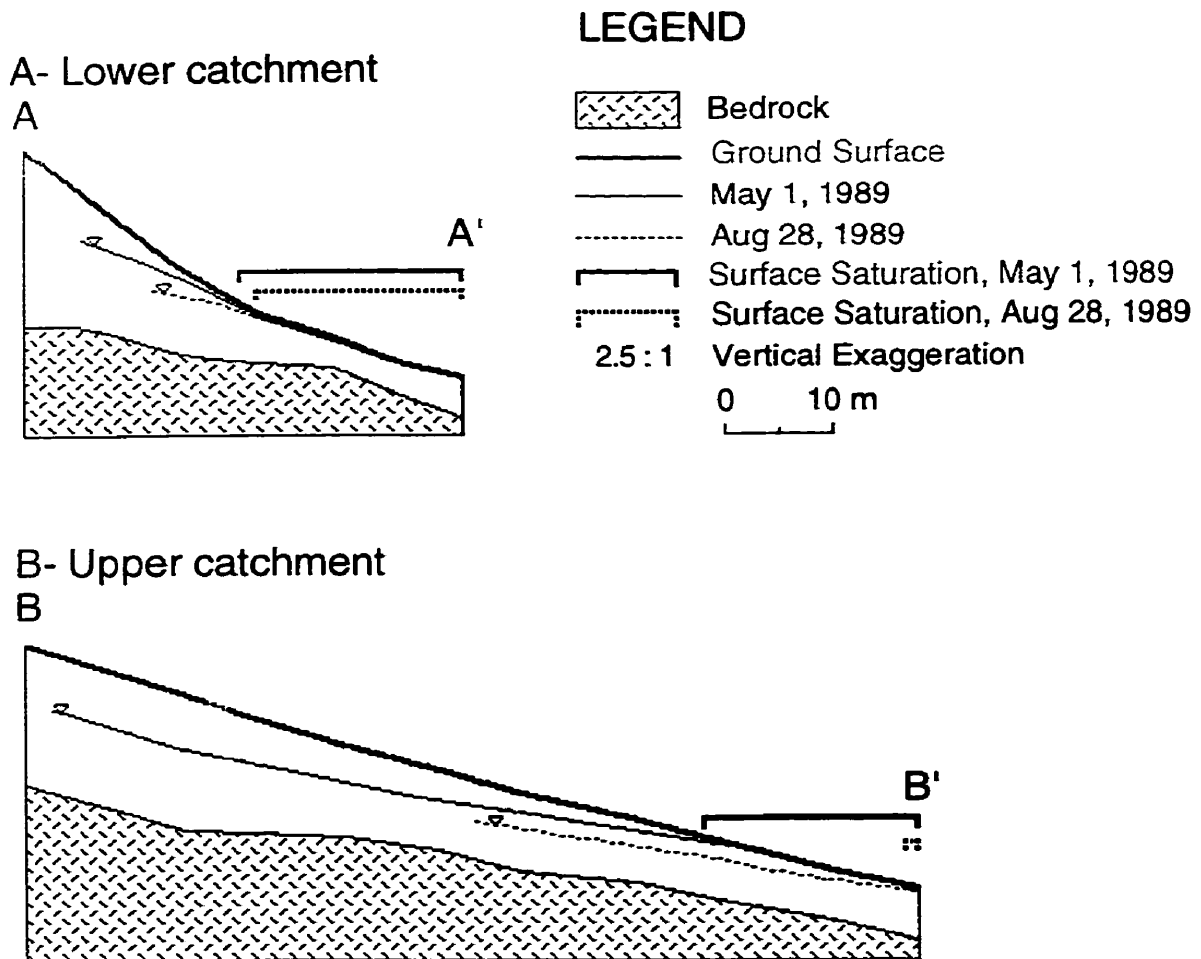
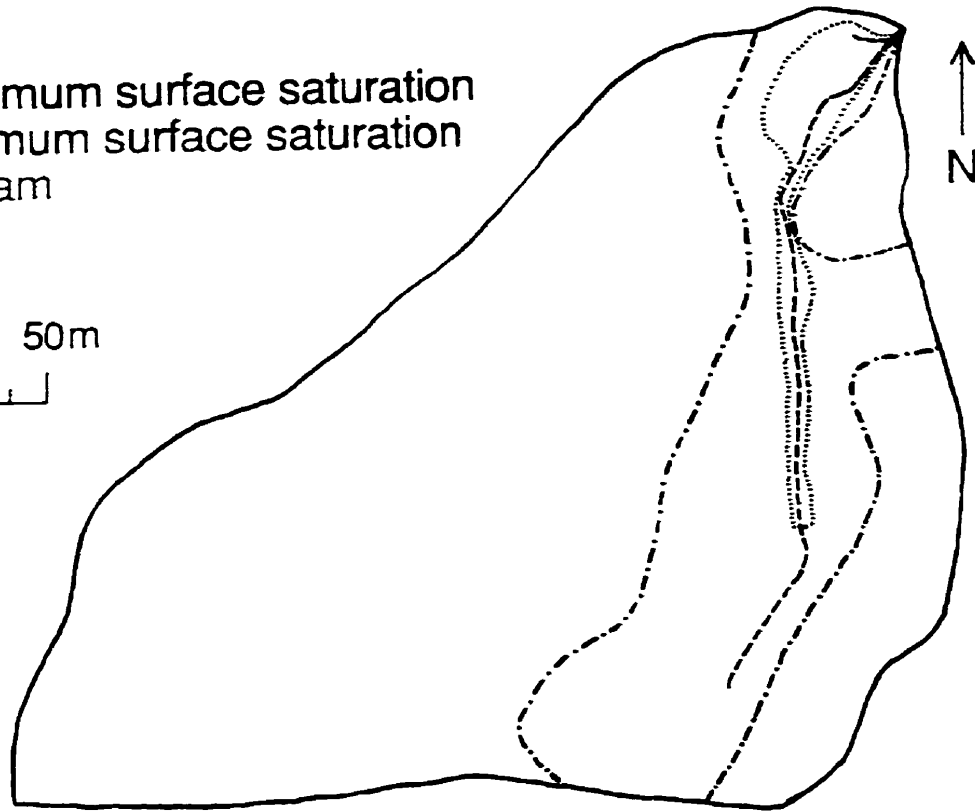
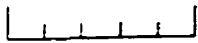


Figure 3.6 Approximate maximum and minimum extent of surface saturation in Harp 4-21 in 1989. Surface saturation was determined from visual observations and groundwater level measurements. Small unsaturated hummocks within the areas are ignored.

LEGEND

- Maximum surface saturation
- Minimum surface saturation
- Stream

0 50m

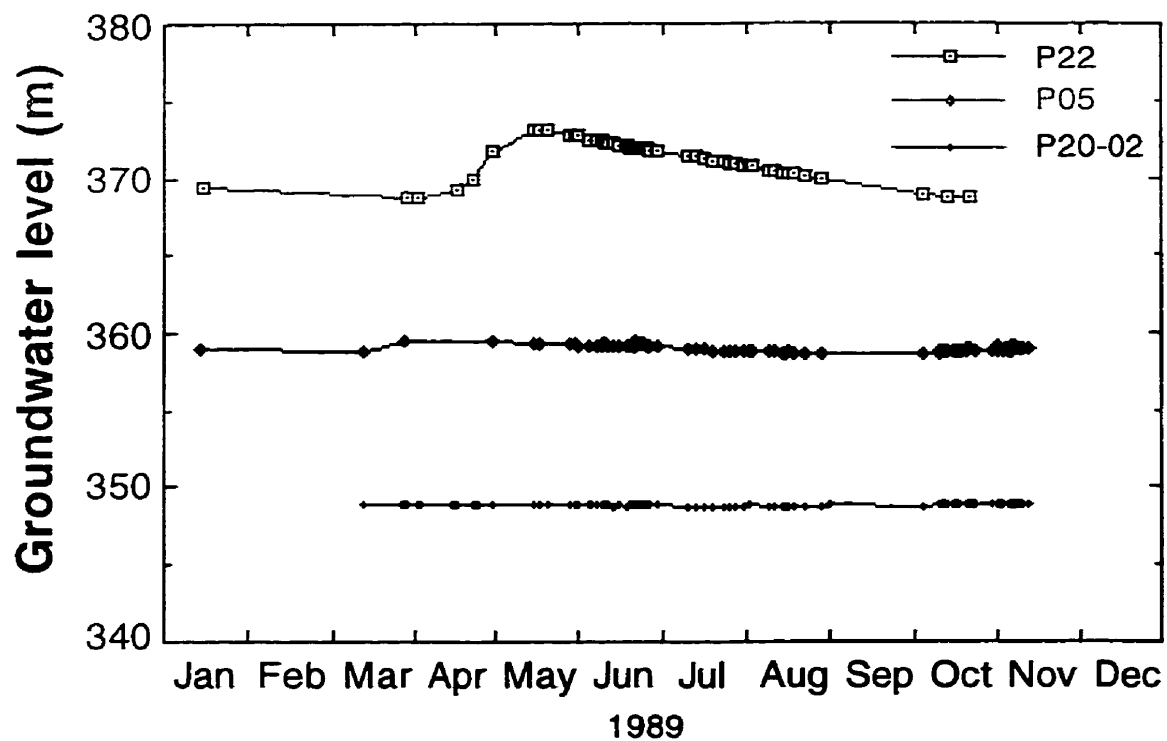


Decreasing sediment thickness along flowpaths (Figure 3.5) can therefore influence the locations and extent of groundwater discharge to the surface. In the lowermost portion of the catchment, decreasing sediment thickness and horizontal convergence of groundwater both contribute to groundwater discharge. Between elevations 356 m and 348 m in the S2 subcatchment (Figure 3.3), the dimensions of the saturated zone perpendicular to the horizontal direction of flow decrease from 42 m wide and 6.2 m deep to 14 m wide and 2.3 m deep indicating that the relative importance of decreasing sediment thickness and horizontal convergence is approximately equal.

Along the upper portion of the stream where horizontal groundwater convergence is minimal, locations of decreasing sediment thickness (Figure 3.2) correspond with the locations of surface saturation (Figure 3.6) suggesting that changes in sediment thickness are responsible for groundwater discharge. However, it is incorrect to attribute all groundwater discharge to decreasing sediment thickness along a flowpath since other factors can contribute to groundwater discharge. For example, a symmetrical flow boundary at the base of a hillslope can result in groundwater discharge regardless of changes in sediment thickness.

The presence of thick unsaturated sediments in the upslope portions of Harp 4-21 significantly influences the catchment's hydrological regime. Individual storms have little influence on groundwater levels in these areas since there is generally considerable storage available within the unsaturated zone. However, during spring melt there is sufficient infiltration to replenish much of this storage and cause a large increase in groundwater levels (Figure 3.7). Since groundwater levels decline slowly, most of the infiltration into these thick unsaturated tills has little direct influence on stormflow but has a significant effect on baseflow. Therefore, the thick unsaturated sediments have the effect of reducing the effective runoff (the proportion of runoff to precipitation) from storms and increasing the quantity of

Figure 3.7 Seasonal groundwater level fluctuations in three slope positions. The magnitude of groundwater level fluctuations is greatest in the upper catchment (P22) where the thickness of unsaturated sediments is greatest and decreases towards the stream (P05 and P20-02). Piezometer locations are shown in Figure 3.3.



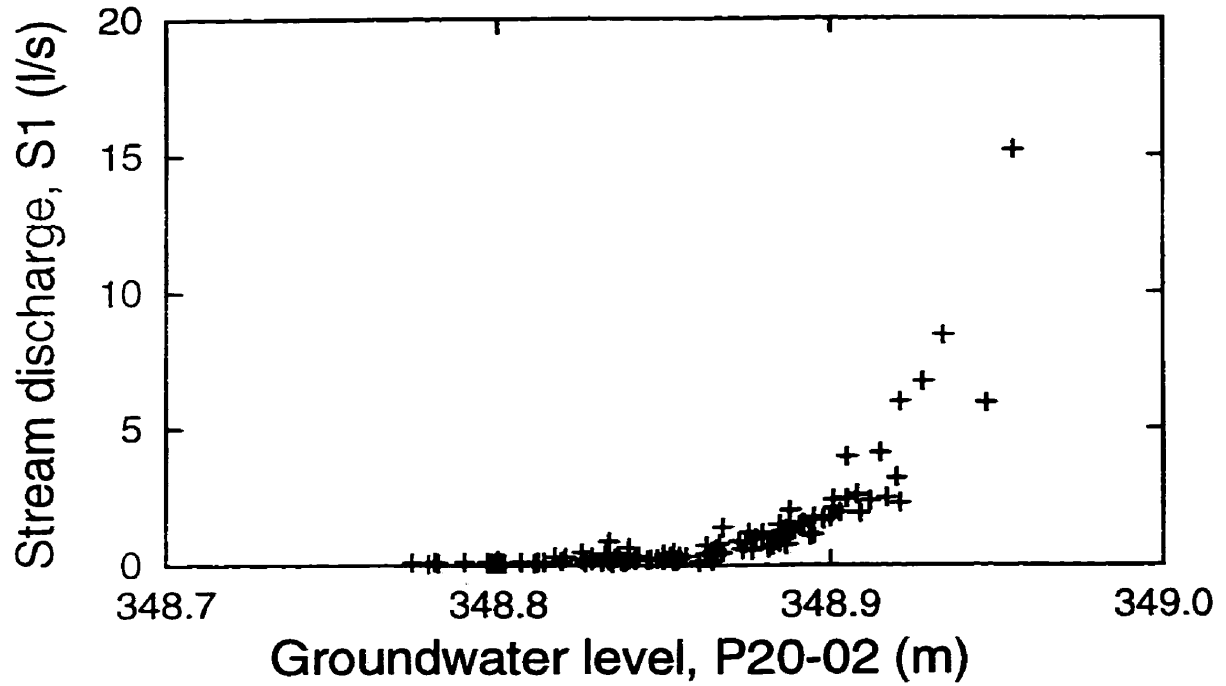
baseflow during the remainder of the year. Groundwater recharging these upslope sediments gradually flows downgradient such that the range of seasonal groundwater level fluctuations decreases towards the stream (Figure 3.7). Consequently, soils adjacent to the stream remain nearly saturated most of the year and baseflow is sustained during dry periods. The amount of available storage in the unsaturated sediments is not strictly dependent on sediment thickness but is also determined by the porosity and the moisture content of the sediments. The moisture content and the thickness of unsaturated sediments are, in turn, influenced by many other factors such as surface topography, the hydraulic properties of the unsaturated sediments, evapotranspiration and the configuration of the groundwater table.

Although hydraulic conductivity, surface topography and sediment thickness are discussed separately, the fluxes, flowpaths and discharge areas of groundwater flow are determined by the interactions among various physical properties. Even within a catchment as small as Harp 4-21, knowledge of only the physical properties is insufficient to predict their effect on stream discharge since the relative importance of these properties varies both spatially and temporally with fluctuating groundwater levels. Therefore, it is necessary to specify the range of hydrologic conditions for which the possible effects of given physical properties influence stream discharge.

Spatial and temporal pattern of stream discharge

Fluctuations in groundwater levels significantly influence stream discharge in Harp 4-21. Stream discharge remains low over a large range of groundwater levels and then increases significantly for small increases in groundwater levels (Figure 3.8). These large changes in stream discharge suggest that the relative importance of different physical properties, hydrological processes and pathways change as groundwater levels fluctuate. The rapid increase in stream discharge for high groundwater levels can be attributed to the higher

Figure 3.8 Stream discharge at S1 as a function of piezometric levels adjacent to the lower portion of the stream (P20-02, 0.69m depth). Similar results are found for other piezometers in proximity of the stream (for example P05). Piezometer locations are shown in Figure 3.3.



effective hydraulic conductivities of the soils relative to the underlying tills and to the gentle topographic slopes adjacent to discharge areas. As groundwater levels increase, there is an increase in the saturated thickness within the soils and a consequent increase in flow within the soils. Furthermore, preferential pathways such as macropores in the upper soil horizons may only become significant flowpaths when these horizons become saturated by high groundwater levels. As previously discussed, increasing groundwater levels also results in a large expansion of discharge areas along gentle slopes and an increase in saturated overland flow.

Fluctuations in groundwater levels also significantly influence the spatial distribution of stream discharge. The average proportion of discharge originating upstream of S4 increases from 43 percent when groundwater levels are low to moderate in the autumn to 69 percent when groundwater levels are highest in the spring (Table 3.2). These changes are related to the differences in topographic slope adjacent to the upper and lower portions of the stream. As groundwater levels rise, upstream areas of soil and surface saturation expand substantially owing to the gentle topographic slope (Figures 3.5b and 3.6) and the relative importance of upstream sources of stream discharge increases as a result of increasing groundwater discharge and saturation overland flow (Figure 3.9). Since the expansion of saturated areas in the lower catchment is limited by steeper slopes (Figure 3.5a), the resulting increase in discharge is smaller so that the relative proportion of discharge from the lower catchment decreases as groundwater levels increase.

Changes in the spatial distribution of stream discharge during storms are similar to the seasonal changes since increasing groundwater levels adjacent to the upper stream result in a relative increase in upstream discharge during storms. Although there are differences in the

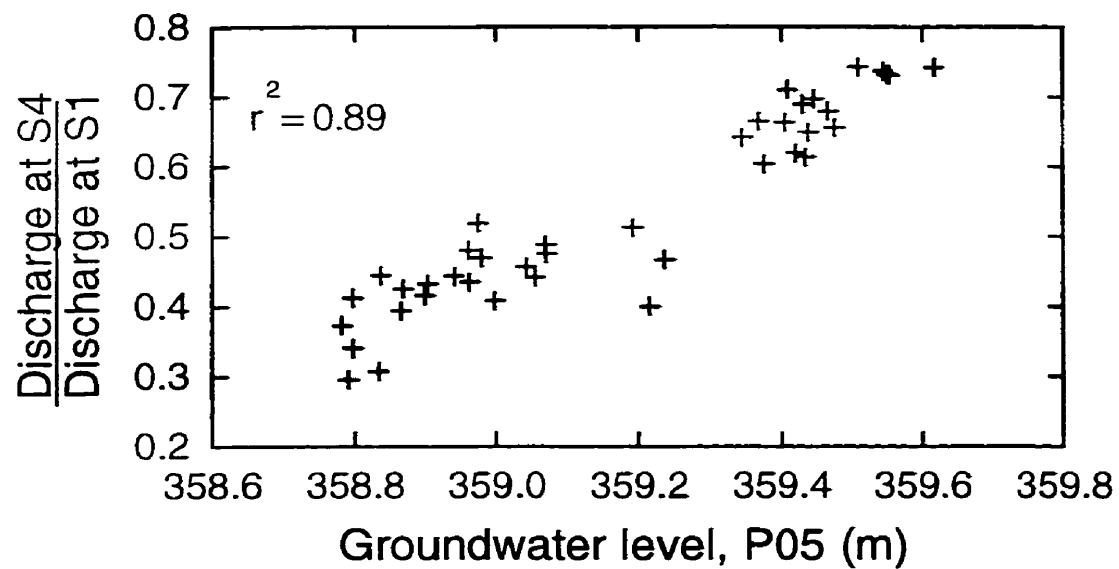
Table 3.2. Seasonal change in the spatial pattern of stream discharge.

Location	Percentage of the stream discharge at S1	
	October-November 1989	April 1990
S5	7 ± 2 ^a	22 ± 2 ^a
S4	43 ± 7	69 ± 5
S3	61 ± 6	77 ± 3
S2	39 ± 6	23 ± 3
S1	100	100

Groundwater levels were low to moderate in October and November 1989 and high in April 1990. Stream discharge at S2 is determined as the difference between discharge at S1 and S3. Stream gauging locations are shown in Figure 3.1.

- ^a The proportion of discharge at S5 is underestimated since some stream discharge flows along the surface around the S5 weir.

Figure 3.9 The proportion of stream discharge at S4 relative to S1 as a function of piezometric levels in P05 near the upper portion of the stream. Includes data collected during storms and at baseflow. The locations of stream gauging site S4 and piezometer P05 are shown in Figures 3.1 and 3.3 respectively.



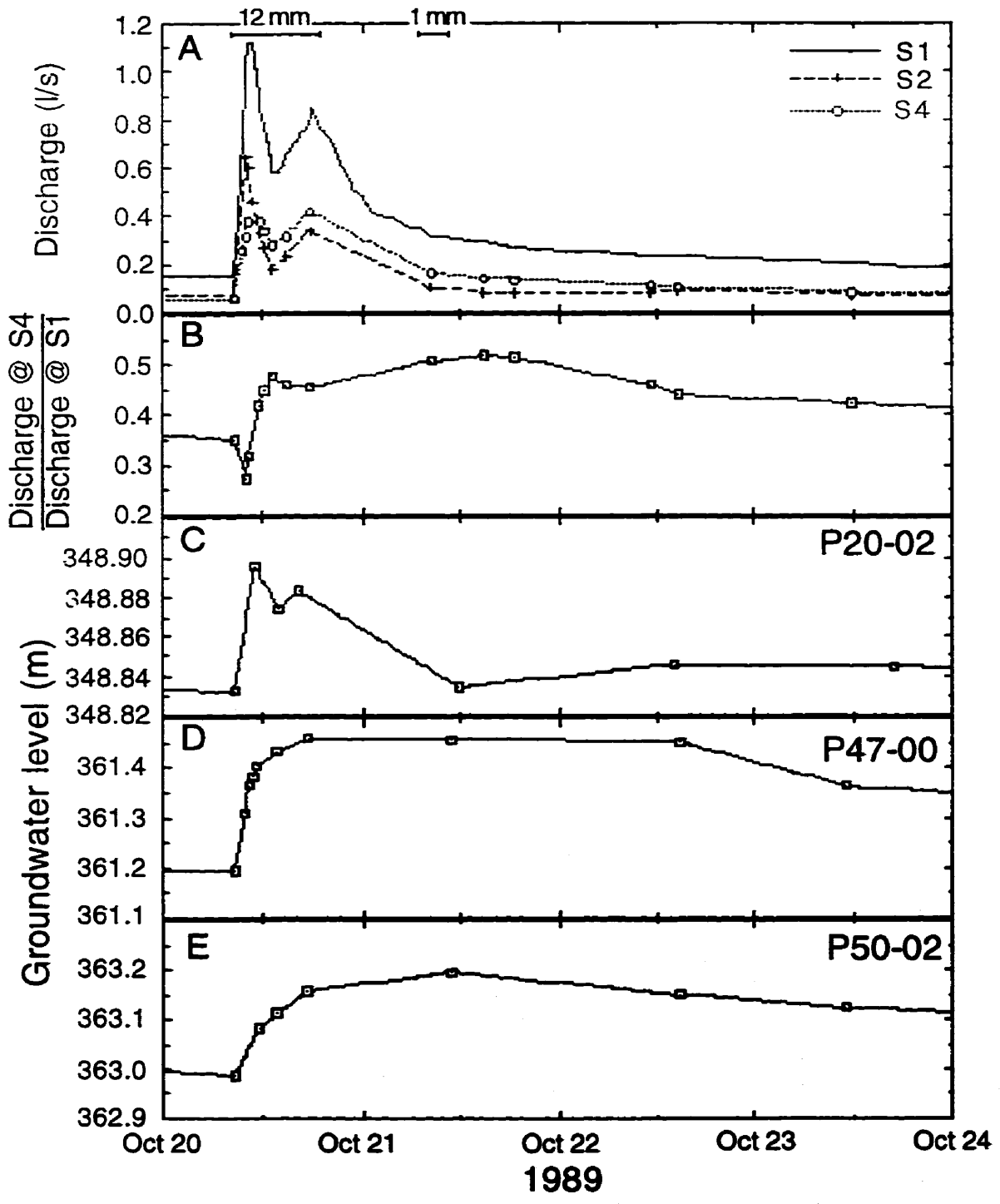
stream response between storms, there is a basic pattern common to several storms. During the initial portion of the storm, a greater proportion of stream discharge originates in the lowermost portion of the catchment where groundwater levels are close to or at the ground surface and saturation overland flow occurs readily (Figure 3.10). Along the upper portion of the stream, groundwater levels respond more slowly with increasing distance from the stream resulting in a more gradual increase and a later peak in stream discharge at S4. Consequently, the proportion of discharge at S4 increases throughout the remainder of the storm and peaks following the storm when groundwater levels in the upper catchment are peaking and groundwater levels in the lowermost catchment have declined. The proportion of discharge at S4 then gradually decreases as water levels along the upper portion of the stream decrease. Similar spatial changes in the proportions of stream discharge are observed during spring melt episodes. However, the magnitude of these changes are much smaller than in the autumn since the relative increase in discharge from baseflow to peak flow is smaller and since further expansion of discharge areas adjacent to the upper portion of the stream produces a smaller relative increase in the upstream discharge area.

The similarities between the seasonal and storm patterns of stream discharge suggest that examination of the seasonal changes in hydrologic pathways could be helpful for understanding some of the changes in flow pathways that occur as a result of groundwater level fluctuations during storms. However, caution must be used when making such comparisons since the pattern and degree of saturation in the catchment change prior to each storm and may significantly influence the flow pathways and stream response for each storm.

Conclusions

Groundwater flow plays a significant role in controlling streamflow in Harp 4-21. Groundwater flow contributes directly to stream discharge and governs the formation of

Figure 3.10 Changes in stream discharge (A), the proportion of stream discharge at S4 relative to S1 (B) and piezometric levels along the lower (C) and upper (D-E) portions of the stream during the rainstorm on October 20, 1989. Piezometer and stream gauging locations are shown in Figures 3.1 and 3.3.



discharge areas that influence both groundwater and event water contributions by saturation overland flow. To understand how groundwater flow influences streamflow generation and water flowpaths in glacial till catchments it is useful to study the physical properties that control groundwater flow.

The combined effects of surface topography, sediment thickness and hydraulic conductivity within the catchment largely control the direction of groundwater flow and the locations and extent of groundwater discharge areas in Harp 4-21. No single physical property of the catchment is sufficient to fully explain the pattern of groundwater flow and flow pathways completely. It is also important to recognize that the relative importance of these physical properties changes both spatially and temporally as a result of fluctuating groundwater levels.

Although the role of sediment thickness on streamflow generation is frequently ignored, results from Harp 4-21 show that decreasing sediment thickness may be as important as convergent topography in producing surface saturation and groundwater discharge. Furthermore, the pattern of sediment thickness within the catchment also influences its hydrological regime. Much of the infiltration during wet periods is stored within the thick unsaturated sediments in the upslope portions of Harp 4-21. Infiltration during spring melt causes large increases in groundwater levels which sustains baseflow during dry periods. Much different hydrological regimes are found in nearby catchments where the streams are ephemeral and the lack of available storage in the thin sediments results in higher effective runoff during spring melt (e.g. Wels et al., 1991b). The influence of sediment thickness on groundwater flow and stream discharge also depends on other factors such as the hydraulic conductivity, surface topography and the configuration of the water table. Consequently, it is useful to consider the importance of these factors to predict how sediment thickness will affect

groundwater flow and streamflow in a particular catchment. If the role of sediment thickness is to be examined in larger catchments, then there is a need to develop more practical geophysical methods that can be used to determine sediment thickness at many locations over larger areas.

The hydraulic conductivities of the tills do not show any large scale pattern of layering despite the presence of compact layers in boreholes and excavations. The lack of low hydraulic conductivities within the soil suggests that the effective permeability of the soils is greater than that of the tills so that groundwater flow from the catchment is greatly dependent on water levels in the soils. The extremely heterogeneous nature of the tills and the difficulties of instrumenting the tills do not allow for a detailed description of their hydraulic properties from piezometer tests. For applications in which detailed knowledge of the hydraulic properties is not required, instrumentation and methods that provide larger scale measurements of the effective hydraulic properties of the tills may be preferable.

Surface topography indicates the direction of groundwater flow where groundwater levels are very close to the ground surface. However, it is incorrect to assume *a priori* that the direction of groundwater flow is perpendicular to surface contours everywhere in a catchment. In Harp 4-21, subcatchment divides based on topographic contours and groundwater equipotentials are substantially different. Furthermore, spatial differences in groundwater level fluctuations indicate that the locations of subcatchment boundaries change with fluctuating groundwater levels. Hydrological models based on DEMs would be best applied if the DEM was based on groundwater equipotentials rather than surface topography. However, data for groundwater equipotentials are rarely available in most catchments such that it is necessary to use surface topography to select catchment boundaries even though it can result in significant errors in the predicted spatial pattern of stream discharge.

Groundwater levels significantly influence the spatial pattern of stream discharge and the relative importance of different flowpaths in Harp 4-21. Consequently, fluctuating groundwater levels may have a significant impact on stream chemistry. Knowledge of the groundwater levels in a catchment prior to a storm may be useful for determining the stream response to a storm and for identifying differences in the dominant flowpaths during storms. To model the effect of such spatial differences in hydrologic processes using hydrologic and hydrochemical models would require distributed models such as TOPMODEL (Beven and Kirkby, 1979) and DEM based models (Moore and Grayson, 1991) since lumped models such as Birkenes (Christophersen and Wright, 1982) do not account for spatial differences in flow processes.

The heterogeneous tills, variable sediment thickness and variable hillslope gradients found in Harp 4-21 are typical of many glacial till catchments in the Canadian Shield. Despite similarities between many of these catchments, their hydrological responses often differ. From a simplistic understanding of hydraulic conductivity, surface topography and depth of sediments in Harp 4-21, it has been possible to explain some of the observed patterns of groundwater flow and stream discharge in a complex groundwater flow system. Therefore, these properties may also be useful for predicting the differences in hydrological processes between catchments.

Chapter 4

Examining the contributions of glacial till water to storm runoff using two- and three-component hydrograph separations

Introduction

Hydrograph separations based on chemical or isotopic mass balances of stream discharge are commonly used to determine the relative contributions of event (new) water and pre-event (old) water as sources of streamflow during runoff events (Bottomley et al., 1984, 1986; Hooper and Shoemaker, 1986; Moore, 1989; Wels et al., 1991a). Changes in the relative contributions of these waters are then used to infer changes in hydrological processes and flowpaths during runoff generation (Sklash and Farvolden, 1979; Sklash et al. 1986; McDonnell et al., 1991; Wels et al., 1991b). Hydrograph separations have been a common tool in studies of the hydrochemistry of forested catchments because knowledge of the sources and flowpaths of water during runoff events aid in the development of conceptual and mathematical models of stream discharge and stream water chemistry (Christophersen et al., 1982; Gherini et al., 1985).

The results of hydrograph separations in humid forested catchments underlain by crystalline bedrock generally indicate that old water (commonly assumed to be groundwater or a mixture of groundwater and soil water) comprises approximately 30 to nearly 100 percent of stream discharge during storms in low order catchments (Fritz et al., 1976; Sklash, 1985; Maulé and Stein, 1990; Rodhe, 1981, 1984, 1987; Bishop, 1991). Despite the numerous similarities in the physical characteristics among many of these catchments, there appears to have been little attempt to relate hydrograph separation results to physical and hydrological factors. Large variations in the hydrograph separation results between several events within a

single catchment suggest that the wide range of hydrological conditions present in the catchments during these runoff events may be responsible for much of these variations. Since hydrograph separations measure the relative fluxes of new and old water to the stream, the results should be influenced by both precipitation intensity and groundwater flux to the stream. Summarizing the results of 37 runoff events in 10 catchments, Rodhe (1987) showed that the average proportion of groundwater discharged during the events was negatively correlated to both the rate of water input to the catchments and to the maximum specific discharge of the streams. Few studies have used the results of hydrograph separations to investigate the physical and hydrological factors that result in rapid old water flow to the stream during runoff events.

Several investigators have demonstrated the importance that groundwater levels have on runoff generation. Groundwater levels influence the discharge of both the new and old water components of storm runoff. Rising groundwater levels result in the expansion of groundwater discharge areas that are impermeable to incident precipitation and cause both overland flow and return flow to the stream (Dunne et al., 1975). Furthermore, numerical modeling by Sklash and Farvolden (1979), and laboratory and field experiments by Abdul and Gillham (1984, 1990), and Blowes and Gillham (1988) have shown that rising groundwater levels adjacent to the stream can also result in increased hydraulic gradients and groundwater discharge into the stream bed.

Much of the Northern hemisphere is covered by glacial till deposits. The presence of compacted layers and clay-sized particles can significantly reduce the hydraulic conductivities of these tills. In shallow flow systems where tills are underlain by low permeability bedrock, groundwater flow through these tills is frequently assumed to be negligible relative to flow through the overlying soils (Espeby, 1989; Likens et al., 1979). However, the texture, mineralogy and petrology of glacial tills are very variable both regionally and stratigraphically

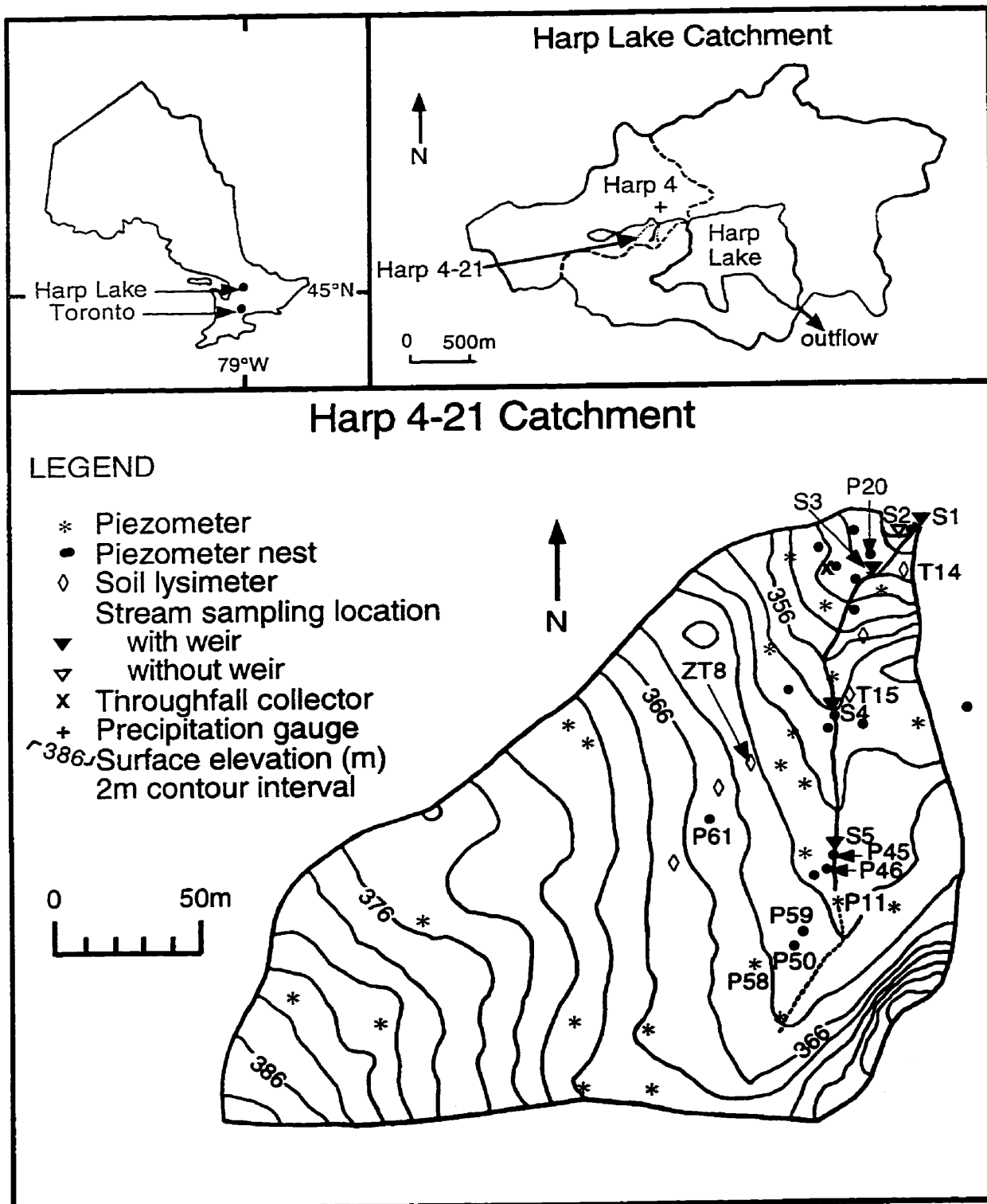
and frequently are related to the bedrock geology of the source rock (Karrow, 1979). On the Canadian Shield, the texture of glacial tills generally has a small proportion of clay-sized sediment (Scott, 1979) and may consequently have hydraulic conductivities that are sufficiently large to transmit a significant proportion of the groundwater flow through these catchments. Such flow may also significantly influence stream chemistry since the residence times of groundwater are likely to be greater in the tills than in the soils resulting in higher chemical concentrations in discharging till waters. The extreme spatial variability of the hydraulic properties of the tills greatly complicates the hydrometric monitoring of flow through these sediments and the interpretation of these results so that hydrograph separations are a useful tool in examining the overall significance of groundwater flow through the tills.

Hydrograph separations based on chemical and isotopic data are used in this chapter with the purpose of examining the relative importance of groundwater discharge through soils and tills to a Canadian Shield stream during stormflow conditions. Three specific hypotheses are addressed. Firstly, groundwater that has flowed through glacial till (till water) is an important component of stream discharge during runoff events. Secondly, the proportion of till water discharging to the stream varies both seasonally and during storm events and is related to groundwater levels. Lastly, the use of hydrometric data can improve our interpretations of flowpaths inferred from hydrograph separations.

Study site

The study site is Harp 4-21, a small 3.7 ha headwater catchment located within the Harp Lake catchment in the Muskoka-Haliburton region of central Ontario (Figure 4.1). Stream discharge from Harp 4-21 is perennial and accounts for approximately 35% (1988-90) of the mean annual precipitation of 1033 mm (1976-89) (Ontario Ministry of the Environment (MOE), unpublished data). Approximately two-thirds of the annual streamflow occurs

Figure 4.1 Location map and instrumentation of the Harp 4-21 catchment.



between March 1st and June 30th when groundwater levels are highest due to spring melt and rainstorms. A general description of the hydrogeology of the catchment is provided in Chapter 3.

The catchment is underlain by metamorphic Canadian Shield bedrock composed predominantly of amphibolite and schist (Jeffries and Snyder, 1983). The overburden in Harp 4-21 forms an unconfined aquifer consisting of glacial tills overlain by Podzolic soils. The tills are relatively coarse consisting predominantly of sandy loams with 0-24% clay-sized particles and substantial quantities of pebble to boulder size material (Dankevych, 1989). The overburden is up to 15 m thick in the northwestern upslope portion of the catchment and gradually thins to between 2 and 6 m beneath the stream (Chapter 3). A horizontally discontinuous layer of compact till (densipan) is often observed within or at the base of the soil profile at depths ranging up to 1.2 m. This layer is most prominent in the upper half of the catchment. Compact tills are also found at greater depths (> 2.5 m) in the upper catchment but there are insufficient data to determine the horizontal extent of these layers. The physical and chemical characteristics of the soils in the Harp 4 catchment are summarized by Lozano et al. (1987).

Methods

The monitoring network consists of 89 piezometers and 5 stream sampling locations (Figure 4.1). A more detailed description of instruments and sampling procedures is provided in Chapter 3. The glacial tills in Harp 4-21 have a large range of horizontal hydraulic conductivities from 2.6×10^{-5} m/s to 1.8×10^{-9} m/s ($n=56$) with a geometric mean of 2.3×10^{-7} m/s (95% confidence interval of the mean from 1.0×10^{-7} to 5.1×10^{-7} m/s). Four drive point piezometers have conductivities of less than 1×10^{-9} m/s. This range is typical for glacial tills and silty sands (Freeze and Cherry, 1979) and emphasizes the heterogeneous nature of the Harp 4-21 tills. The horizontal hydraulic conductivities of the soils vary over a much smaller

range from 3.0×10^{-5} to 3.7×10^{-7} m/s ($n=13$) with a geometric mean of 2.7×10^{-6} (95% confidence interval of the mean from 1.4×10^{-6} to 5.2×10^{-6} m/s). The absence of horizons of low hydraulic conductivity results in higher effective hydraulic conductivities in the soils (Chapter 3).

Fifteen runoff events were monitored between March, 1989 and May, 1990. Stream discharge was recorded continuously at S1 using a float-operated water level recorder and manually at S3, S4 and S5 (Figure 4.1). Discharge at S2 is assumed to equal the difference between discharge at S1 and S3 since the surface area contributing directly to S1 is small. Surface saturated area was estimated using piezometric data and visual observations of surface ponding. This method probably overestimates surface saturated areas since it also includes unsaturated hummocks between surface saturated hollows. Stream water samples were collected at all five stream sites (S1 to S5) during both baseflow and stormflow conditions with the exception of the June 22, 1989 storm which was sampled only at S1. Groundwater samples were collected from piezometers screened from 0.15 to 6.7 m depth in the soils and in the tills and soil water samples were collected using tension and zero-tension lysimeters (Figure 4.1). Throughfall samples were collected in 20 L pails lined with plastic sample collection bags. Molybdate reactive dissolved silica (SiO_2 , expressed in mg Si/l) was analysed by colourimetry (MOE, 1986a) and major cations (Ca^{2+} , Mg^{2+} , Na^+ , K^+) were analysed by atomic absorption spectroscopy (MOE, 1986b) by the MOE. Rain and snow chemistry samples are collected weekly by the MOE at the precipitation site (Figure 4.1). Selected samples were also analysed for $^{18}\text{O}/^{16}\text{O}$ ratios (reported as ‰ difference relative to SMOW with a precision of $\pm 0.2\text{‰}$ (1σ)) at the University of Waterloo for isotopic hydrograph separations.

Hydrograph separation

Hydrograph separation consists of quantifying the various sources contributing to stream discharge. For two sources contributing to streamflow, the proportions of old and new water discharge in the stream water are determined from the equations:

$$\frac{Q_o}{Q_s} = \frac{(C_s - C_n)}{(C_o - C_n)} \quad (4.1)$$

$$\frac{Q_n}{Q_s} = \frac{(C_s - C_o)}{(C_n - C_o)} \quad (4.2)$$

where C is the concentration of the chemical species and the subscripts o, n, and s refer to old, new and stream water, respectively.

A chemical mass balance equation can be formulated for a three-component system:

$$C_{ot}Q_{ot} + C_{os}Q_{os} + C_nQ_n = C_sQ_s \quad (4.3)$$

where the subscripts ot and os refer to old till water and old soil water, respectively. This equation can be solved if either 1) the discharge of one of the components is known (DeWalle et al., 1989) or 2) two tracers are used simultaneously. Where two tracers such as isotopes (i) and dissolved silica (Si) are used, a set of linear equations can be solved for Q_n/Q_s , Q_{os}/Q_s and Q_{ot}/Q_t :

$$\frac{Q_n}{Q_s} = X_n = \frac{(C_s^{Si} - C_{os}^{Si})(C_{ot}^i - C_{os}^i) - (C_s^i - C_{os}^i)(C_{ot}^{Si} - C_{os}^{Si})}{(C_n^{Si} - C_{os}^{Si})(C_{ot}^i - C_{os}^i) - (C_n^i - C_{os}^i)(C_{ot}^{Si} - C_{os}^{Si})} \quad (4.4)$$

$$\frac{Q_{os}}{Q_s} = X_{os} = \left(\frac{C_s^t - C_{ot}^t}{C_{os}^t - C_{ot}^t} \right) - X_n \left(\frac{C_n^t - C_{ot}^t}{C_{os}^t - C_{ot}^t} \right) \quad (4.5)$$

$$\frac{Q_{ot}}{Q_s} = X_{ot} = \left(\frac{C_s^t - C_{os}^t}{C_{ot}^t - C_{os}^t} \right) - X_n \left(\frac{C_n^t - C_{os}^t}{C_{ot}^t - C_{os}^t} \right) \quad (4.6)$$

Equations 4.5 and 4.6 can be applied using either of the tracers ($t = i$ or Si) provided that $C_{ot}^t \neq C_{os}^t$ for the tracer used. Five assumptions are necessary to apply the three-component hydrograph separation: 1) the concentrations of each component must be distinct from the other two components for one or both of the tracers, 2) the concentrations of the three components cannot be collinear for the two tracers, 3) the average concentration of each component must remain constant for the duration of the event, 4) there are only three components (based on the concentrations of the two tracers) contributing to stream discharge, and 5) the tracers must mix conservatively. The interpretation of the three-components in Equations 4.3 to 4.6 obviously depends on the tracers used and the spatial and temporal patterns of their concentrations in the catchment under investigation. Wels et al. (1991a) used a three-component hydrograph separation (new overland flow, new subsurface flow and old subsurface flow) for the special case where $C_{new\ OF}^i = C_{new\ SSF}^i$ and $C_{new\ SSF}^{Si} = C_{old\ SSF}^{Si}$ (OF = overland flow, SSF = subsurface flow) which simplifies Equations 4.4 and 4.6 to Equations 4.2 (using SiO_2) and 4.1 (using deuterium), respectively.

Results and discussion

Two-component hydrograph separations based on ^{18}O

Two-component hydrograph separations using ^{18}O (Equations 4.1 and 4.2) were used to determine the relative fluxes of new and old water for two storms with contrasting antecedent moisture conditions within the catchment. Groundwater levels prior to the June 22, 1989 rainstorm remained near their seasonal maximum in most of the catchment following spring melt and an 11 mm storm on June 20 (Figure 4.2). Four bursts of rainfall produced 36 mm of rain on June 22 resulting in four distinct peaks in stream discharge (Figure 4.3). The isotopic ratios of bulk throughfall samples from the first burst of rainfall (-5.80‰) and from the three remaining bursts of rainfall (-5.75‰) are significantly different from the isotopic ratios of baseflow following the storm (-12.27‰) and the average isotopic ratio of groundwater from four piezometers ($-12.32\pm 0.12\text{‰}$) so that the uncertainty in the resulting hydrograph separations is less than 4% of the total flow. Despite high initial surface saturation ($\approx 8\%$) and rainfall intensities up to 12 mm/hr, the old water component is always the dominant portion of stream discharge decreasing to a minimum of 56% near peak discharge and comprising 83% of the total stream discharge.

In the fall of 1989, groundwater levels were relatively low following a dry summer. Prior to the October 31, 1989 rainstorm, groundwater levels remained low following 11 days of dry, warm weather (Figure 4.2) and $\approx 3\%$ of the catchment area remained saturated to the surface. The total rainfall for the storm was 19 mm with a maximum hourly intensity of 5.5 mm/hr (Figure 4.4). The isotopic ratio of stream baseflow (-11.83‰) prior to the storm is similar to the mean groundwater isotopic ratios from six piezometers ($-11.71\pm 0.53\text{‰}$) and is significantly different from the bulk throughfall (-6.43‰). The variation in old water isotopic ratios is considerably smaller than the difference between the new and old water

Figure 4.2 Seasonal variations in water levels in piezometer P61. The arrows indicate the June 22 and October 31 events.

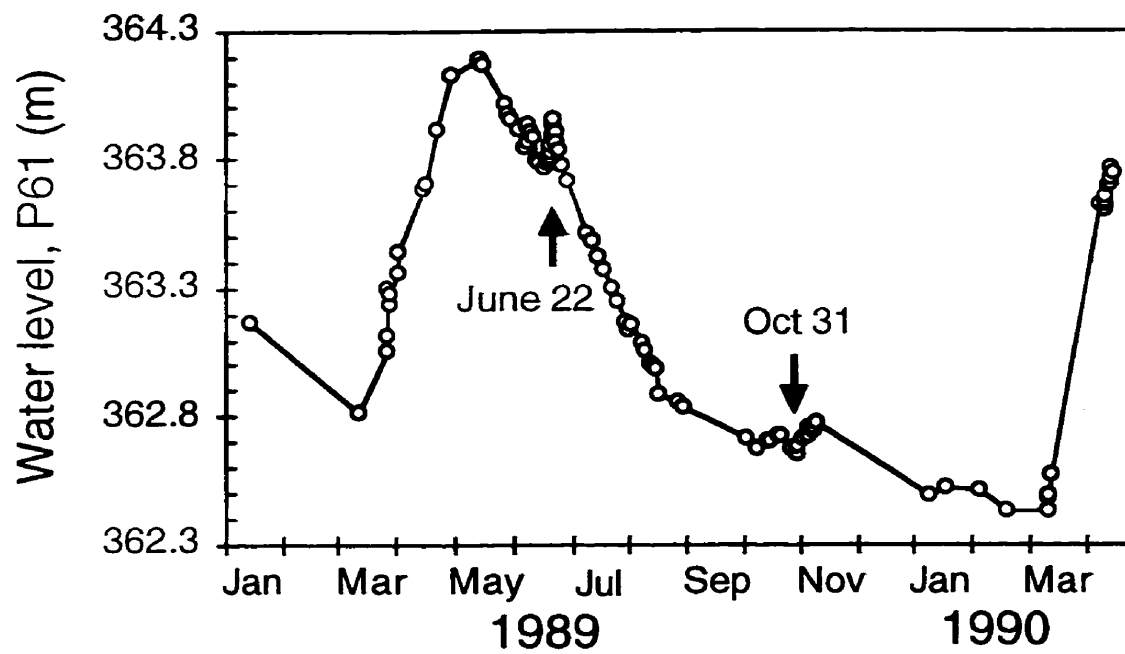


Figure 4.3 Three-component hydrograph separations for the June 22, 1989 event. Data and results are presented in Tables 4.1 and 4.2 respectively. Dissolved silica and $\delta^{18}\text{O}$ scales are selected so that new water and baseflow water concentrations coincide. Arrows indicate samples collected prior to or following the displayed time period.

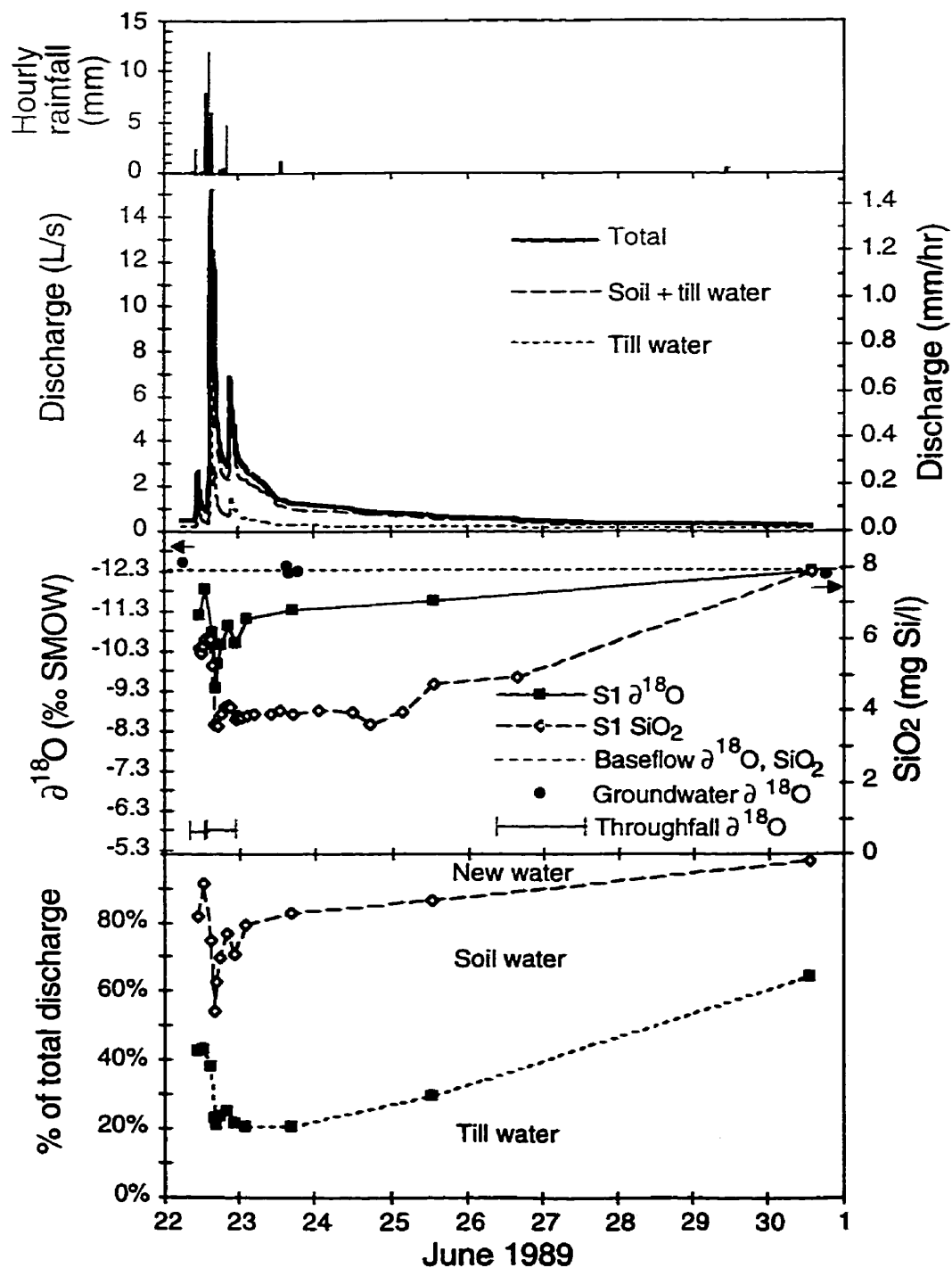
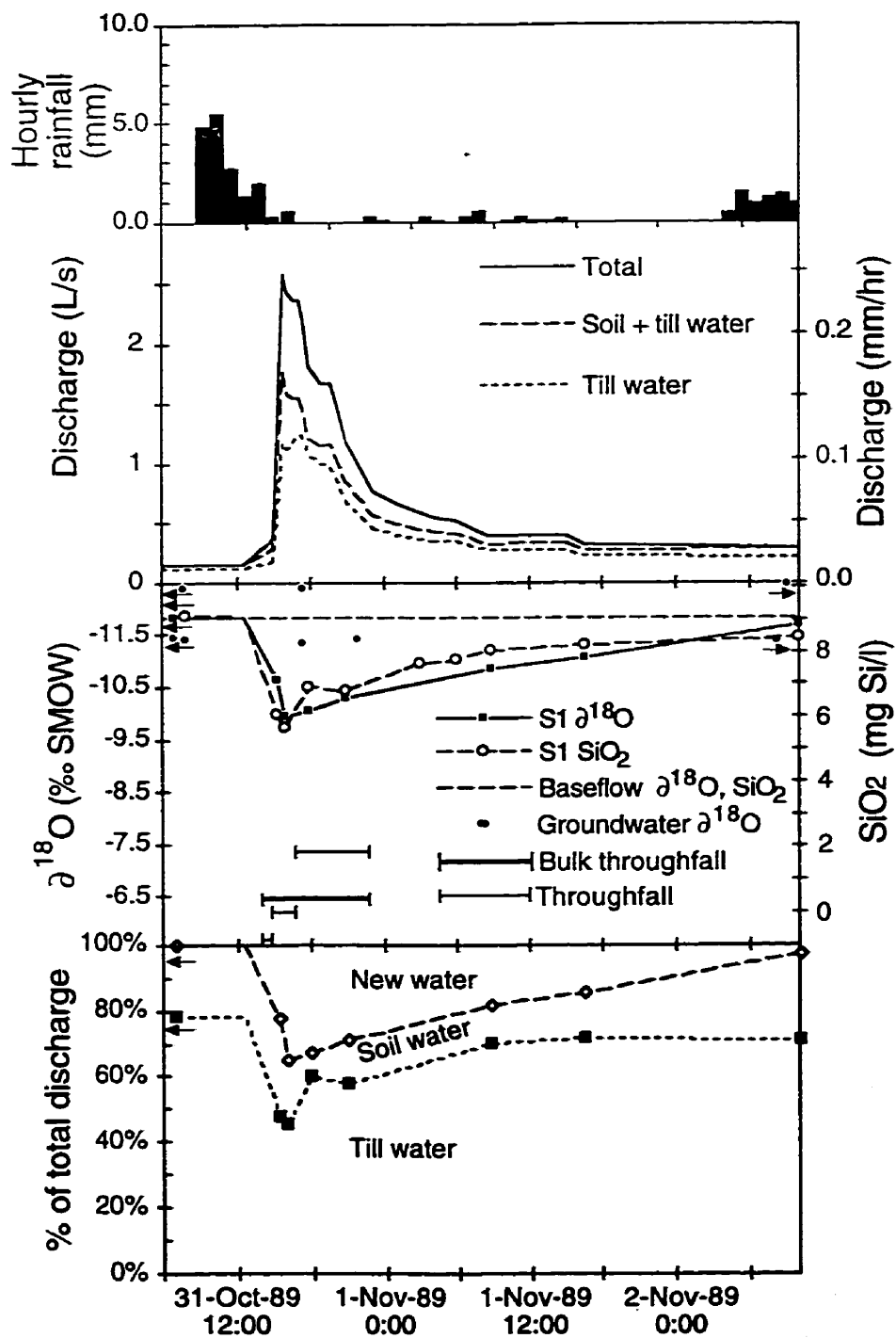


Figure 4.4 Three-component hydrograph separations for the October 31, 1989 event. Data and results are presented in Tables 4.1 and 4.2 respectively. Dissolved silica and $\delta^{18}\text{O}$ scales are selected so that new and old water concentrations coincide. Arrows indicate samples collected prior to or following the displayed time period.



concentrations such that the range in groundwater $\delta^{18}\text{O}$ (-11.34‰ to -12.37‰) corresponds to only a 7% error in the proportion of the total old water discharge. Even though the isotopic ratio of throughfall became more depleted as the storm progressed (-5.66‰, -6.18‰ and -7.34‰; the isotopic ratio for the third portion of the storm was calculated to be -7.34‰ by volume weighted difference from the bulk sample), this depletion results in less than a 3% error in the hydrograph separation if a cumulative mean of the new water is used as suggested by McDonnell et al. (1990). The resulting two-component isotopic hydrograph separation for the October 31 storm shows that old water dominates the storm hydrograph at S1 contributing 65% of peak discharge and 77% of the total hydrograph.

The flowpaths of new water to the stream during these two events may be inferred from the total volumes of rainfall and new water runoff. Since the effective runoff (ratio of runoff/rainfall) for the June 22 storm is 47% and the ratio of new water to total runoff is 17%, the area of saturated overland flow required to contribute new water directly to the stream is only 8% of the total basin area. Considering that the proportion of saturated area within the catchment varied between approximately 8-20% during the event, direct precipitation onto saturated areas is a plausible flowpath for most of the new water entering the stream. Similarly, the intensities of rainfall and new water runoff can be compared. The peak intensity of new water stream discharge during this storm was 0.46 mm/hr. If this value is compared with the maximum hourly rainfall intensity of 12 mm/hr then only 4% of the total catchment area is required to contribute the flux of new water at peak stream discharge.

The effective runoff and the proportion of new water discharge for the October 31 storm are 16% and 24%, respectively, and direct precipitation contributed from only 4% of the catchment area is required to account for the total volume of new water. Considering that the peak intensity of new water stream discharge is only 0.08 mm/hr compared to the maximum

rainfall intensity of 5.5 mm/hr, then direct precipitation onto less than 2% of the catchment area is required to produce the flux of new water to the stream at peak discharge. From groundwater level measurements, the extent of surface saturation on October 31 is estimated to vary between approximately 3-7% during the event. Although these results suggest that direct precipitation onto saturated areas could be the major flowpath of event water to the stream, the timing of the new water flow indicates that a small fraction of the new water is reaching the stream more slowly and is probably infiltrating the mineral soil. Visual observations indicate that saturation overland flow usually occurs beneath the litter within the surface organic horizons.

Three-component hydrograph separations based on ^{18}O and SiO_2

Dissolved silica can be a useful tracer in many catchments since only trace amounts are usually found in precipitation (Likens et al., 1979; Wels et al., 1991a) whereas water that has sufficient contact time with the overburden frequently has dissolved enough SiO_2 to be chemically distinct compared to precipitation. Making the assumption that new water does not dissolve any SiO_2 , Hooper and Shoemaker (1986) found that SiO_2 was a suitable tracer to separate hydrographs into new and old components. In many catchments, infiltrating new water can dissolve SiO_2 rapidly enough to make it indistinguishable from old water (McKeague and Cline, 1963; Kennedy, 1971) so that isotopic and SiO_2 data can be combined to distinguish between new and old water flowing through the subsurface (Wels et al., 1991a; Maulé and Stein, 1990). In catchments where till water has much higher SiO_2 concentrations than either soil water or infiltrating event water, SiO_2 can be used to distinguish between water flowing in the soil and water flow through the underlying tills (Hendershot et al., 1992).

The spatial pattern of SiO_2 concentrations in Harp 4-21 reflects groundwater flowpaths. Throughfall samples have trace amounts of SiO_2 . The average SiO_2 concentration

of 296 soil water samples collected by the MOE from lysimeters within Harp 4-21 during the study period is 2.54 ± 1.53 mg Si/l (B. LaZerte, unpublished data). However, groundwater SiO_2 concentrations in the tills are significantly higher ($p < 0.01$) with a mean of 9.33 ± 2.57 mg Si/l ($n=137$). Therefore, SiO_2 concentrations in the stream will vary according to the relative contributions of three water types: 1) new water that discharges to the stream during the event, 2) old soil water that has had little or no contact with the tills (soil water), and 3) longer residence time old water that has been in contact with the tills (till water). Note that this classification does not distinguish between vadose and phreatic water in the soils.

Hydrographs for the June 22 and October 31 events were separated into three components using ^{18}O as a tracer in Equation 4.4 and SiO_2 as a tracer in Equations 4.5 and 4.6. The input data are presented in Table 4.1 and the hydrograph separations for June 22 event are shown graphically in Figure 4.5. Although soil water samples were not available for the storm events, soil water sampled for ^{18}O immediately before and after spring melt were not substantially different from groundwater ^{18}O in the tills. The soil water $\delta^{18}\text{O}$ for the June 22 event was estimated to be -12.54‰ using the post-melt samples and the anticipated enrichment by the rainfall prior to the event. Furthermore, samples collected from piezometers screened within the soils that only became saturated during the October 31 event were also similar to groundwater ^{18}O in the tills so that the baseflow ^{18}O is assumed for both soil and till water for this event. Therefore, the proportions of new and old water for the October 31 event are identical to the two-component model. Small differences between soil and till water ^{18}O have little effect on the proportion of till water for either event since it is more greatly influenced by their SiO_2 concentrations (discussed below).

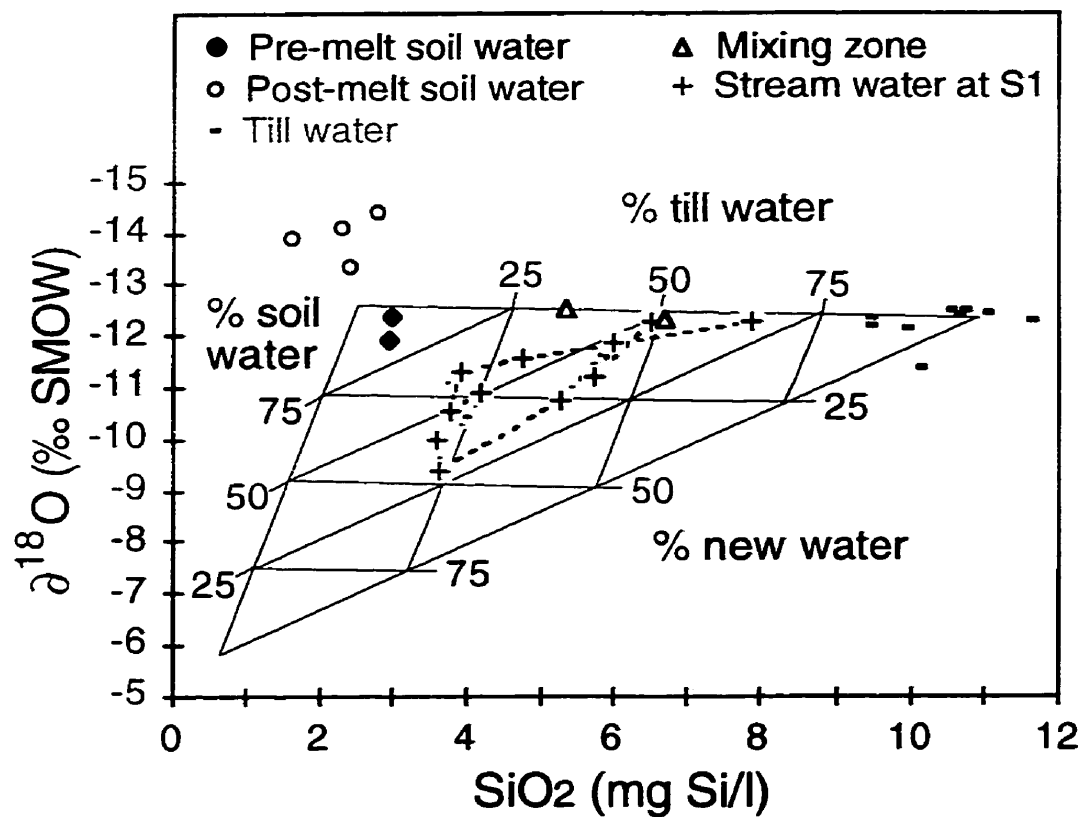
The till water SiO_2 concentration is assumed to equal the highest stream SiO_2 concentration that occurred during low baseflow conditions (10.9 mg/l at S1) when inputs of soil water and new water are assumed to be negligible. Baseflow is assumed to provide the

Table 4.1 Data used to calculate three-component hydrograph separations.

Component	June 22, 1989			October 31, 1989		
	Best estimate	Lowest	Highest	Best estimate	Lowest	Highest
C_n^{Si}	0.66	0.00	1.97	0.66	0.00	1.97
C_{os}^{Si}	2.54	1.97	3.06	2.54	1.97	3.06
C_{ot}^{Si}	10.9	9.33	12.6	10.9	9.33	12.6
C_n^i	-5.78	-6.18	-5.38	-6.43	-6.83	-6.03
C_{os}^i	-12.54	-13.91	-11.90	-11.83	-12.37	-11.34
C_{ot}^i	-12.32	-12.51	-12.18	-11.83	-12.37	-11.34
C_s^{Si}	varies, shown in Figure 4.3			varies, shown in Figure 4.4		
C_s^i	varies, shown in Figure 4.3			varies, shown in Figure 4.4		

Results are presented in Table 4.2. Lowest and highest values are discussed in the text and are used to calculate the maximum range of till water in Table 4.2. The notation used for the various components are described in Equations (4.3) to (4.6). SiO_2 concentrations are expressed in milligrams Si per litre and ^{18}O values in per mil.

Figure 4.5 Graphical presentation of the three-component hydrograph separations for the June 22, 1989 event. Till water samples from the entire study period are shown. Mixing zone samples were collected from piezometer P11 before and following the event.



best estimate of average till water SiO_2 concentrations since the till water SiO_2 concentrations vary spatially and the average SiO_2 concentration obtained from piezometers is biased by piezometers that are located upgradient from discharge areas or are screened at shallow depths. The average SiO_2 concentration of 2.54 mg/l from soil lysimeters at all depths is used as the soil water concentration. Although precipitation in contact with the mineral soil may dissolve silica rapidly, the two-component isotopic hydrograph separation indicated that much of the new water component could reach the stream by saturation overland flow and therefore may have limited contact with the mineral soil. Laboratory leaching studies of similar podzolic soils suggest that infiltrating new water would not exceed a SiO_2 concentration of ≈ 2.1 mg/l even after 7 days of contact with the soils (Wels, 1989). There are few data for the new water Si concentration since most overland flow samples are a mixture of new water and discharging old water. One sample, water discharging from the mineral soil nearly 24 hours following the last peak in streamflow during the June 22 event, had a SiO_2 concentration of 0.66 mg/l. This sample is a mixture of both new water and soil water but is used for both storms as a reasonable estimate of new water SiO_2 . Since the proportion of new water is relatively small, the results of the three-component hydrograph separations are relatively insensitive to the SiO_2 value of the new water component in the range of 0 to 2 mg/l.

Stream SiO_2 concentrations, isotope ratios and the resulting three-component hydrograph separations for the June 22 and the October 31 events are shown in Figures 4.3 and 4.4 respectively and are summarized in Table 4.2. In the June 22 event, till water contributes 29% of the total stream discharge and exceeds 20% of discharge throughout the event. In the October 31 event till water is the dominant component of storm runoff contributing 62% of total stream discharge at S1. Although the data are not presented here, the results also show that till water is the dominant component of flow at all stream sites during the October 31 event (Table 4.2). These results support the first hypothesis that groundwater

Table 4.2 Summary of results of three-component hydrograph separations calculated using Equations 4.4 to 4.6 and values in Table 4.1.

	Total Event % of total runoff			Maximum range of till water
	New water	Soil water	Till water	
June 22, 1989				
S1	20	51	29	17-43
Oct. 31, 1989				
S1	23	15	62	46-72
S2	22	12	66	
S3	25	9	66	
S4	23	10	67	
S5	29	4	67	

flow through glacial tills can indeed contribute significantly to stream discharge during storms.

During the June 22 event, stream SiO_2 concentrations decrease at peak discharge but do not return to baseflow concentrations as rapidly as $\delta^{18}\text{O}$ values (Figure 4.3). Three possible explanations for this difference between SiO_2 and ^{18}O are 1) that the soil water contribution increases relative to that of till water, 2) that the relative proportions of soil and till water remain constant but the average SiO_2 concentration of old soil water decreases during the event, and 3) that the average SiO_2 concentration of till water decreases during the event as a result of precipitation of silicates or adsorption of SiO_2 . Figure 4.6a shows the relative proportions of soil and till water in the old water component calculated from the three-component model assuming constant soil and till water SiO_2 concentrations. Prior to the storm, till water makes up 50% of the old water discharge. This proportion decreases to 43% at peak discharge, reaches a minimum of 25% approximately 24 hours following the last peak and increases to 65% of old water discharge at baseflow following the storm (Figure 4.6a). Such changes in the relative contribution of soil water and till water demonstrate a possible error that could arise in two-component hydrograph separations using SiO_2 as a tracer. SiO_2 traces the flowpaths rather than the age of the water. If SiO_2 were used to separate new and old water using baseflow SiO_2 as the average old water concentrations (Equations 4.1 and 4.2), then the hydrograph separations would progressively underestimate the proportion of old water since the average old water SiO_2 concentration decreases during the storm as the proportion of soil water increases relative to that of till water. Conversely, if new water dissolves SiO_2 then old water may be overestimated so that these errors may cancel one another.

Figure 4.6 a) The relative proportions of soil and till water during the June 22 event assuming constant soil and till water SiO_2 concentrations. b) The change in soil water SiO_2 concentrations required to maintain constant relative proportions of soil and till water. c) Coincident changes in water levels in piezometer P61.

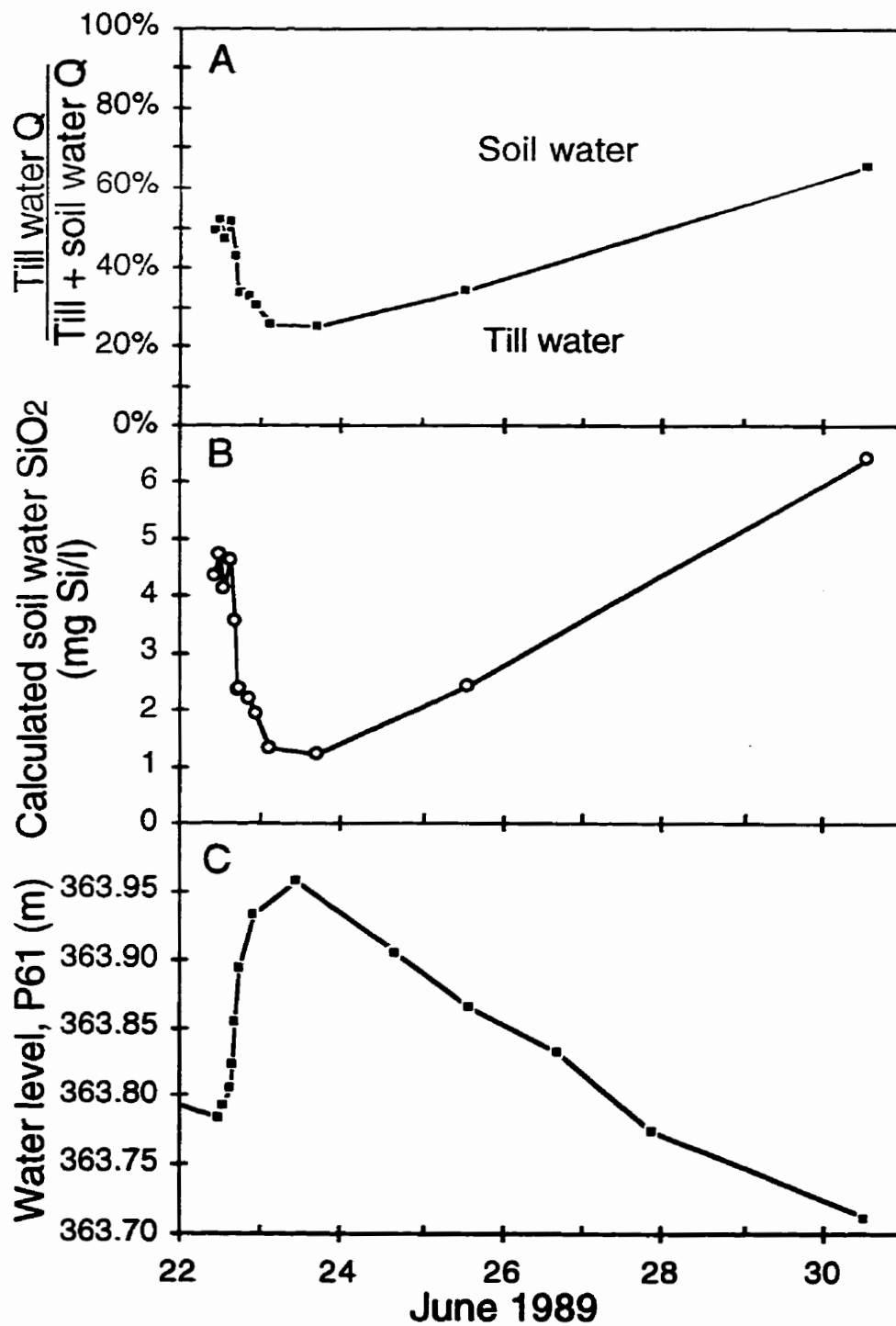
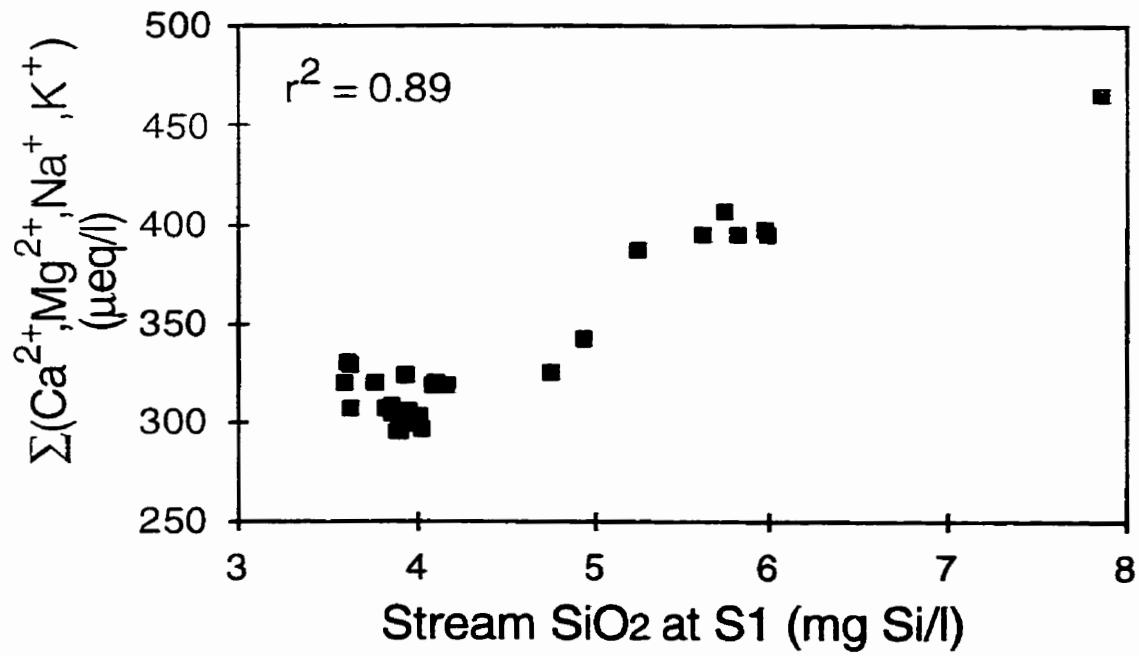


Figure 4.6b demonstrates the change in the average SiO_2 concentration of old soil water that would be required if the relative contributions of soil water and till water were to remain constant. This change is unrealistic since it would require average old soil water SiO_2 concentrations of 6.4 mg/l at baseflow and 1.2 mg/l during the event. Using more realistic estimates of the possible changes in soil water SiO_2 during an event shows that the relative change in soil and till water contributions is the dominant cause for the differences between the SiO_2 and ^{18}O data.

Precipitation of silicates is not likely since water from piezometers near the base of the till are still close to saturation with respect to clay minerals most likely to precipitate (Dankevy, 1989). Furthermore, precipitation or adsorption would likely result in variations in the ratio of SiO_2 to major cations. Figure 4.7 shows that SiO_2 and the sum of major cations are highly correlated ($r^2 = 0.89$) during the June 22 event suggesting that precipitation of silicates is minimal. If precipitation or adsorption was occurring then the till water component would be substantially higher than estimated by the three-component model.

Two processes may be responsible for the changes in the relative proportions of soil and till water. These changes correspond approximately to changes in piezometric heads during the event (Figure 4.6c). It is possible that the rising water table within the soils is progressively saturating shallower, more conductive soil horizons and 'releasing' vadose water from these horizons. This piezometer (P61) is located in a midslope area where tension saturation does not extend to the ground surface. Water levels in piezometers closer to the stream peak earlier but show the same gradual decline in water levels following the storm. Therefore, the increase in the soil water component could also be attributed to a progressive spatial expansion of phreatic conditions within the soils. These explanations support the

Figure 4.7 The correlation between SiO_2 and the sum of major cations (Ca^{2+} , Mg^{2+} , Na^+ , K^+) at S1 for the June 22 event.



second hypothesis that attributes the change in the relative proportions of soil and till water to fluctuating water levels.

The changes in the stream SiO_2 concentrations during the October 31 event follow the changes in $\delta^{18}\text{O}$ values closely (Figure 4.4) suggesting that the relative proportions of soil water and till water do not vary as much as in the June 22 event. The proportion of old water that originates as till water decreases from 78% at baseflow to 61% at peak discharge. Considerably lower groundwater levels would provide fewer opportunities to release vadose water from shallow soil horizons and the absence of phreatic conditions within the soil at P61 indicates that limited lateral expansion of phreatic conditions in the soil would provide much less soil water from midslope soils.

Uncertainties in the till water component

In Harp 4-21 all the assumptions of the three-component model are not fulfilled. Consequently, the validity of the model is a function of the degree to which the assumptions are met and the results must be interpreted with consideration of these uncertainties. Figure 4.5 demonstrates that assumptions 1, 2 and 4 are reasonable. There is no apparent reason suggesting assumption 5 could be violated. The largest uncertainties in the three-component hydrograph separations in this study are likely to result from the assumption of constant SiO_2 concentration for each of the three components. In fact, it is the spatially variable nature of SiO_2 that allows hydrographs to be separated using SiO_2 . Not only are there uncertainties in determining a spatially averaged SiO_2 concentration of each component, but the concentrations of each component could also change during the event as a result of changing flowpaths or changes in the spatial distribution of discharge throughout the catchment. As will be demonstrated below and in the subsequent section, these uncertainties have a minor

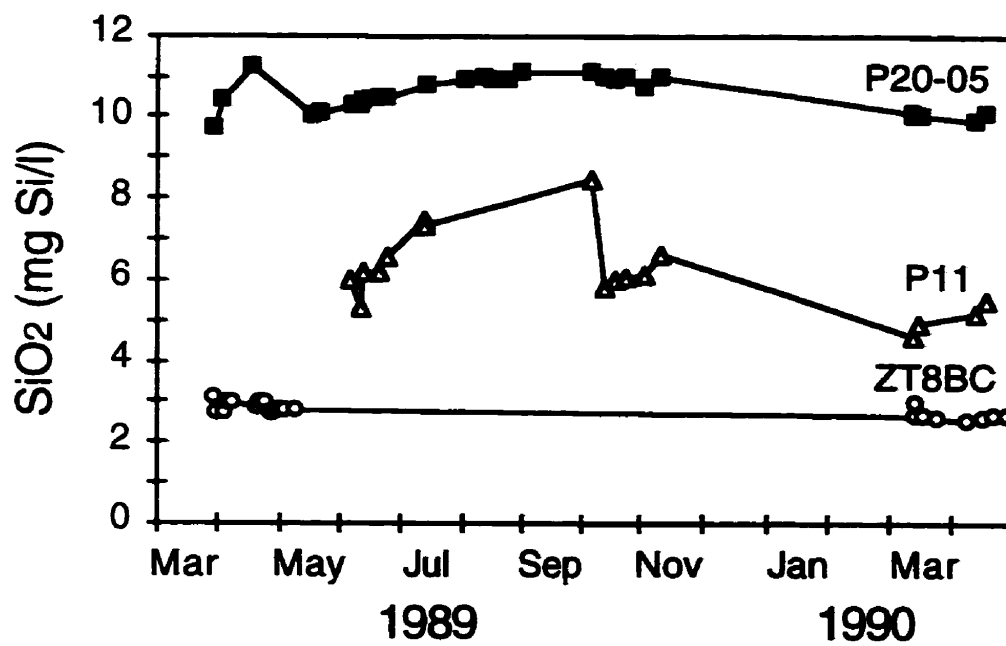
influence on the relative proportions of the three components and they do not change the conclusion that the till water makes a significant contribution to stream discharge.

The SiO_2 concentrations measured in till water shows only a slight seasonal fluctuation for any given piezometer (Figure 4.8). Although there are generally few data during dry conditions, soil lysimeters generally show relatively constant SiO_2 concentrations and do not show large sudden changes (Figure 4.8). Changes in the average SiO_2 concentrations for soil and till water components are more likely to result from changes in the spatial pattern of flow than from changes in the concentrations at any given location.

The sensitivity of the till water results are examined using the maximum expected range for the average SiO_2 concentrations and $\delta^{18}\text{O}$ values for each component (Table 4.2). The new water SiO_2 concentration varies from 0 mg/l assuming no SiO_2 dissolution to a maximum of 1.97 mg/l which is the average soil water SiO_2 in all soil water samples collected from the A horizon. The maximum range for the average soil water Si concentration varies from 1.97 to 3.06 mg/l, the average soil water concentrations of the A and lowermost B horizons, respectively. The maximum range of till water SiO_2 concentrations varies from 9.33 mg/l, the average of all piezometers screened in the tills, to 12.6 mg/l, the largest SiO_2 concentration measured from any piezometer. Note that this range is much larger than the calculated maximum range of 9.7 to 11.1 mg/l based on changes in the spatial pattern of stream discharge. Pre-melt and post-melt samples define the range for soil water $\delta^{18}\text{O}$ for the June 22 event whereas the maximum measured ranges for groundwater $\delta^{18}\text{O}$ are used for soil and till water for the October 31 event. The analytical precision of $\pm 0.4\text{‰}$ (2σ) is used to define the range for new water $\delta^{18}\text{O}$ since the uncertainty in the average value is not known.

Despite the uncertainty in the SiO_2 concentrations, the till water component is relatively insensitive to the range of concentrations possible within Harp 4-21 (Table 4.2). Till

Figure 4.8 Temporal variations in SiO_2 concentrations in till water (P20-05), soil water (ZT8BC) and in a zone of soil and till water mixing (P11).



water is a substantial proportion of total runoff in both events, 17-43% on June 22 and 46-72% on October 31. These ranges are artificially large since the values in Table 4.1 can result in unrealistic negative values of new water or soil water. Because stream SiO_2 concentrations were closest to those of till water, the results of the hydrograph separations are most sensitive to the till water SiO_2 concentration. The average difference in the proportions of till water calculated using the highest and lowest till water SiO_2 concentrations was 11%. The results were less sensitive to the range of soil water (6%) and new water (5%) SiO_2 concentrations. The proportion of till water was relatively insensitive to the ranges of ^{18}O values of either new water (<1%), soil water (3%) or till water (<1%).

Two-component hydrograph separations based on SiO_2

Two-component hydrograph separations based on SiO_2 concentrations are used to estimate the minimum proportion of till water during events for which isotopic data is either unavailable or unsuitable. By assuming that the average SiO_2 concentration of all new water and soil water does not exceed the average soil lysimeter concentration near the base of the B horizon in Harp 4-21 (3.06 mg/l, n=52) and that the till water component has an average concentration equal to the maximum SiO_2 of any piezometer (12.6 mg/l), then a two-component hydrograph separation (Equation 4.1) using these extreme values of SiO_2 will indicate the minimum proportion of till water that could be discharged to the stream. This procedure is analogous to using a three-component model with $C_n^{\text{Si}} = C_{\text{os}}^{\text{Si}}$ so that the second term of Equation 4.6 equals zero.

The minimum till water contributions at baseflow and near peak flow for 15 runoff events are listed in Table 4.3. Till water contributes a significant proportion of discharge during several storms. Note that the values for the June 22 and October 31 events in Table 4.3 are extremely conservative relative to the three-component hydrograph separations in

Table 4.3 Minimum till water contributions at S1 during runoff events.

Date of event	Peak discharge (l/s)	Baseflow SiO ₂ (mg Si/l)	SiO ₂ at peak discharge (mg Si/l)	Baseflow (%)	Peak (%)
28-Mar-89	11.82	8.46	2.80	57	-3 ^a
4-Apr-89	2.04	6.22	4.54	33	16
16-Apr-89	2.54	5.86	4.32	29	13
25-Apr-89	4.77	3.98	2.96	10	-1 ¹
10-Jun-89	3.32	6.46	4.74	36	18
20-Jun-89	1.19	7.54	6.14	47	32
22-Jun-89	15.20	7.86	3.60	50	6
10-Oct-89	1.06	9.60	8.00	69	52
12-Oct-89	0.68	8.98	8.10	62	53
20-Oct-89	1.20	9.04	7.34	63	45
31-Oct-89	2.64	9.08	5.68	63	27
2-Nov-89	0.66	8.42	7.80	56	50
6-Nov-89	1.65	8.46	6.46	57	36
15-Mar-90	5.18	8.04	3.64	52	6
16-Apr-90	4.10	4.70	3.32	17	3

Proportions calculated from Si data using two-component hydrograph separations (Equation 4.1 with $C_n = 3.06$ mg/l and $C_o = 12.6$ mg/l).

^a Peak discharge SiO₂ less than maximum soil and new water SiO₂.

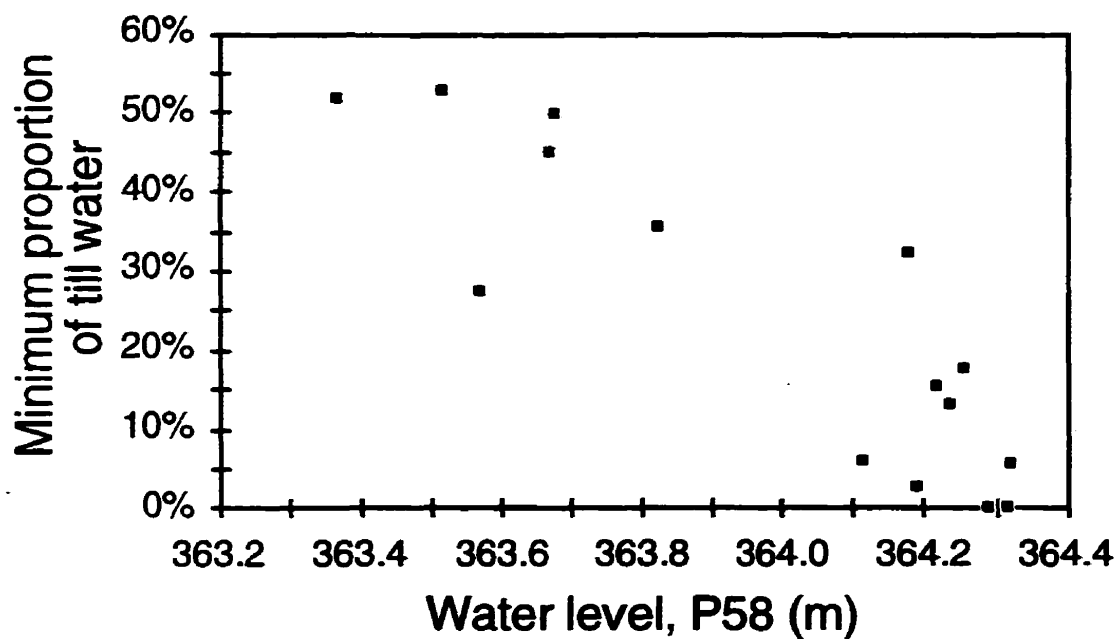
Table 4.2. The relative importance of till water to stream discharge fluctuates according to groundwater levels (Figure 4.9). When groundwater levels are high during and following spring melt (Figure 4.2), the stream water SiO_2 concentrations approach that of soil water indicating that the relative importance of till water is greatly reduced in comparison to the large fluxes of soil water. When groundwater levels are low in the autumn (Figure 4.2), even the minimum estimates of till water for different events remain in excess of 27% to 53% of peak stream discharge. Since groundwater levels are correlated between several piezometers, similar patterns are also observed in other piezometers close to the stream. This relation supports the second hypothesis that the seasonal changes in the till water component are related to water levels.

Groundwater flow from the till to the soil

Since the glacial till sediments are not in direct contact with the stream, till water must flow through the soils prior to reaching the stream. Consequently, till water flow through the soil near the stream and mixes with soil water. The average SiO_2 concentration of piezometers in this mixing zone is 6.73 ± 2.16 mg/l, intermediate between soil and till waters. Figure 4.8 shows the seasonal change in SiO_2 concentration of a piezometer screened in the stream bed. These variations probably result from a change in the relative proportions of soil and till water in this mixing zone. These changes correspond approximately to seasonal changes in water levels; more till water when water levels are lowest and more soil water when water levels are highest.

It is important to determine whether the till water flow during events (Figures 4.3 and 4.4) increases as a result of 1) an increase in groundwater flow from the tills to the soils and then to the stream or 2) from the flushing of till water that has already discharged to the soils prior to the event. In the first case, the till water flow depends on the hydraulic response in the

Figure 4.9 Influence of water levels in piezometer P58 on the minimum proportion of till water near peak discharge calculated using two-component hydrograph separations with SiO_2 as a tracer. Hydrograph separation data are presented in Table 4.3. Negative values are plotted as 0% till water.

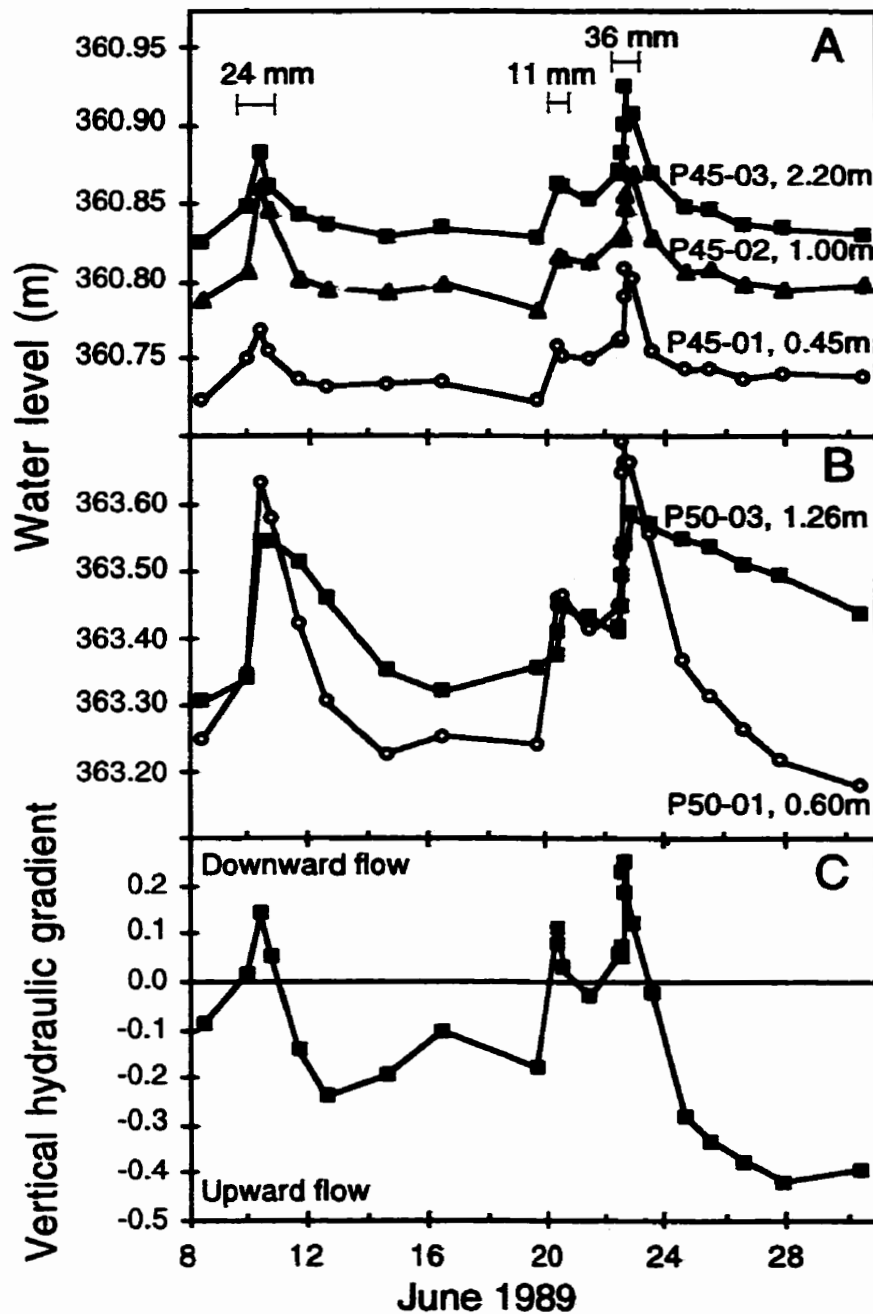


tills. In the second case, the till water flow depends on the hydraulic response in the soils, the previous flow conditions in the soils and the ability of the tills to recharge the soils.

Figure 4.10a shows the piezometric response at three depths beneath the stream bed for three events in June 1989. The two deepest piezometers are screened in the till. The vertical gradient is upward indicating till water discharge towards the stream. The water levels fluctuate equally in all three piezometers showing that the vertical gradients between the till and the stream bed remain nearly constant during the three events. Therefore, there is no increase in till water flow into the stream bed during the events.

Figures 4.10b and 4.10c show the piezometric response and the vertical hydraulic gradient between the till and the soil 25 m upslope from the stream for the same three events. The piezometric head in the soil increases rapidly but declines steadily following the peak. The piezometric head in the till increases less than in the soil but declines much more gradually following the peak. Consequently, there is a change in the direction of flow between the till and soil. At baseflow, there is upward flow from the tills to the soils. On the rising limb and at peak there is downward flow from the soil to the till. Shortly after the peak, the upward flow resumes and even increases gradually following the June 22 event. The change to downward flow is coincident with the peak in till water discharge in the stream so that increased flow from the tills to the soils cannot explain the increase in till water flow to the stream. However, the change to upward flow between events suggests a process where till water can discharge to the soils and replace till water that was flushed out during the event. This flushing and gradual replenishment of till water in the soils is consistent with the rapid change and subsequent gradual recovery in the relative proportions of till and soil water shown in Figure 4.6.

Figure 4.10 Water level changes during three June 1989 events in vertical piezometer nests (a) P45 and (b) P50 screened both in the soils (open symbols) and in the tills (solid symbols). c) Changes in vertical gradients in P50 during the same events (positive upwards). The depths of rainfall are indicated in (a)



Summary and conclusions

Three-component hydrograph separations have provided insight into runoff generation. Although all the assumptions were not perfectly satisfied, the hydrograph separations were sufficiently accurate to address the goals of this chapter. A two-component model based on ^{18}O would not have provided such insight. The additional information provided by the hydrometric data demonstrates the necessity of widening the scope of data collection beyond that of only stream water samples.

Whereas it would be extremely difficult to accurately quantify the flow of groundwater through these tills using hydrometric measurements, the use of three-component hydrograph separations with two tracers has shown that despite the presence of compacted layers and relatively low hydraulic conductivity sediments within the tills (10^{-5} to $<10^{-9}$ m/s), till water is an important component of stream discharge. Therefore, groundwater flow through glacial tills may have a significant influence on stream hydrology and chemistry in catchments with coarse-grained tills. Similar catchments may be numerous in regions where glacial tills are derived from granitic bedrock. Two-component hydrograph separations using SiO_2 indicate the till water component varies seasonally and is related to water levels. The variation between the soil and till water components may be related both to the soil horizon in which water flows and to the spatial extent of phreatic conditions in the soils. Variations in the relative proportions of soil and till water during the June 22 event suggest a conceptual model where till water discharges to the soils near the stream between events and the soil and till water mixture is rapidly flushed from the soils to the stream during events. Measurements of vertical gradients between the soils and the tills in two locations support this conceptual model.

Many existing models of water flow or water chemistry for forested catchments rely on a conceptual model where flow is either lateral within a soil horizon or downward from the

surface to the A, B or C horizons. These models generally do not allow for deeper groundwater to flow to the stream through shallower soil horizons. The results of this chapter suggest that such a model may not apply in Harp 4-21 since a substantial proportion of water discharges from the deeper tills into the shallow soil horizons and mixes with soil water prior to discharging to the stream. Further work in other catchments is needed to characterize the physical and hydraulic properties necessary to result in substantial groundwater flow into soils from the underlying bedrock or till.

Chapter 5

Role of glacial till on groundwater levels and stream runoff:

A comparison of Harp 4-21 and Harp 3A.

Introduction

Monitoring of the hydrological and geochemical budgets of several catchments on the Canadian Shield of central Ontario (e.g. Dillon et al., 1987) showed that sensitivity to acidification was variable among lakes despite the lack of carbonates. Although during the early 1980s there were significant decreases in both pH and alkalinity in Plastic Lake, where the soils and till are less than 1 m thick, there were no such changes in nearby Harp Lake, where approximately one half of the catchment soils and tills are greater than 1 m in thickness (Dillon et al., 1987). Despite the apparent hydrochemical significance of glacial till on the Canadian Shield, there has been very little study of its hydrological role.

One approach to address the hydrological significance of till is a paired or multiple watershed study. This approach is commonly used to examine the effect of disturbance or treatment on a natural system. For example, such experiments have been designed to examine the impact of various forestry practices on catchment hydrology (e.g. Bosch and Hewlett, 1982; Sahin and Hall, 1996), and of acid deposition on stream hydrochemistry (Likens et al., 1977; Dillon et al., 1982). Similar approaches have been used to explain natural differences in nutrient budgets of watersheds and lakes (Dillon et al., 1991; Schindler et al., 1992; Dillon and Molot, 1997). These studies sometimes reveal that differences in geology or other physical properties can produce different hydrological or hydrochemical responses in similar climatic regions (Scheider et al., 1983; Nelson et al., 1993).

The objective of this chapter is to identify the effects of glacial till thickness on groundwater flow and stream discharge in catchments on the Canadian Shield. A paired watershed study is used to compare groundwater dynamics and stream discharge in Harp 4-21, where till is thick, and in Harp 3A, where till is thin or absent. Although the hydraulic conductivity of the till is lower than that of the soils (Chapter 3), it is hypothesized that groundwater flow through the till results in significantly different groundwater dynamics and stream responses both seasonally and during storms in the two catchments.

Study site

The general characteristics of the Harp 4-21 and Harp 3A catchments are compared in Table 5.1. The main characteristic that distinguishes Harp 4-21 from Harp 3A is the thickness of till. Combined soil and till thicknesses vary between 0 and 15 m in Harp 4-21 (Chapter 3), whereas soil is less than 1.0 m thick and glacial till less than 0.5 m thick in Harp 3A. Soil and till are very thin or absent along the eastern and southern boundaries of Harp 3A where bedrock is exposed (Figure 5.1). Podzolic hillslope soils of Harp 3A are very similar to those in Harp 4-21 as described by Lozano et al. (1987) and in Chapter 3.

More than 4 m of silty and clayey sediments below the 336 m contour of Harp 3A (Figure 5.1) may have been deposited when portions of the Harp Lake watershed were submerged by glacial Lake Algonquin (Jeffries and Snyder, 1983). The elevation of these sediments corresponds closely to the upper limit of submergence (340 m) reported at Dorset (Figure 1.4) (Chapman, 1975). Because hydraulic conductivities are low, 5.6×10^{-7} to 4.5×10^{-9} m/s, flow through these glaciolacustrine sediments is negligible (≈ 0.1 l/s).

Topography also differs somewhat between the catchments (Table 5.1). The hillslope profiles in Harp 3A are generally straight with convex hilltops. Slopes are steeper in Harp 3A than in Harp 4-21 and most range from 25-35% with some slopes as steep as 50%. At the base

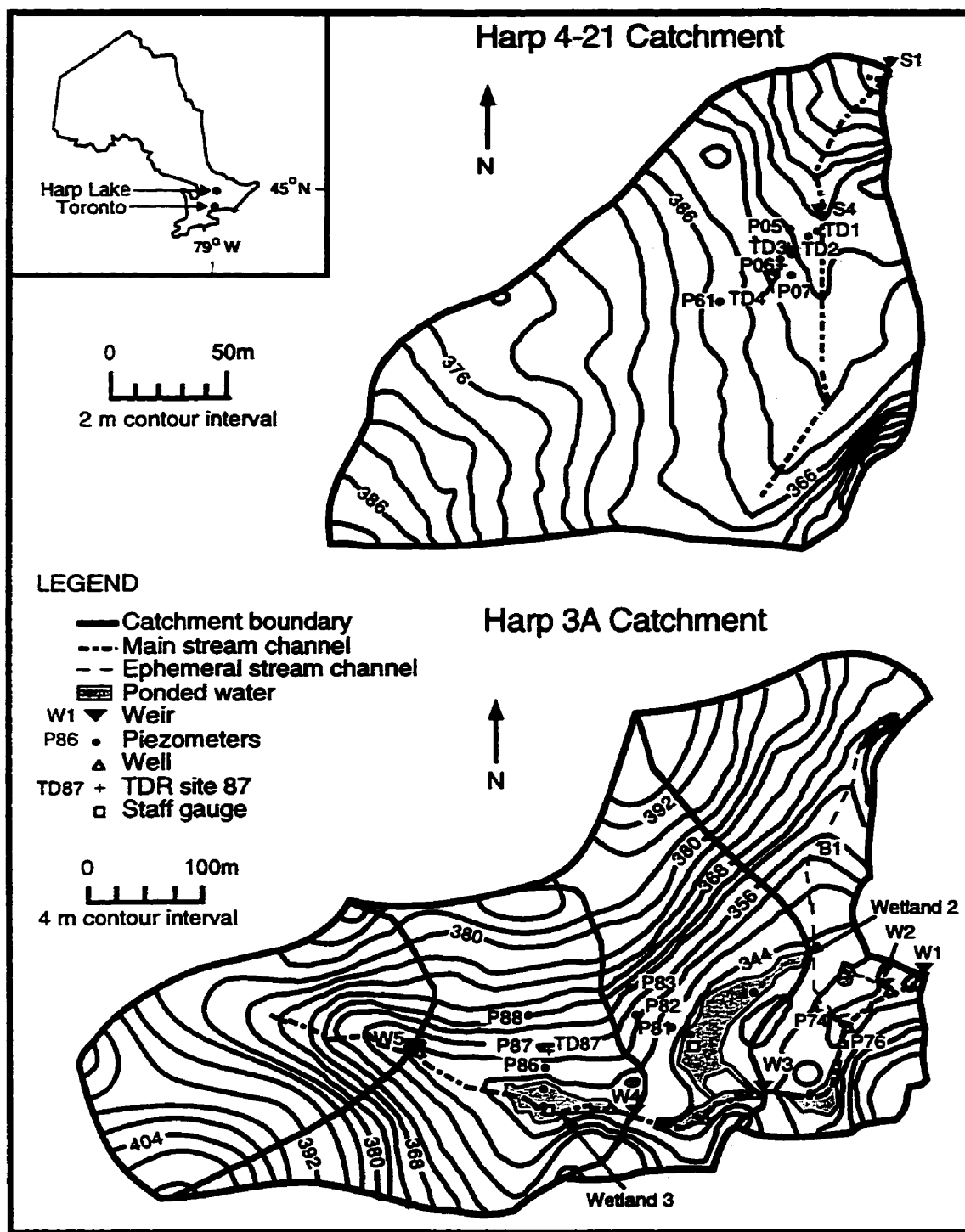
Table 5.1. Characteristics of the Harp 4-21 and Harp 3A catchments.

	Harp 4-21 ^a	Harp 3A
Area	3.7 ha	21.7 ha
Total relief	43 m	82 m
Slope	8-30%	20-50%
Dominant vegetation	maple, birch	maple, birch cedar and spruce in Wetland 2
Sediment thickness	0-15 m	0-1.5, >4 m in the lowermost area
Bedrock	amphibolite and schist	amphibolite, schist, granitized biotite and hornblende gneiss
% area covered by wetlands	3%	<0.3%
Average ^b pH (1987-89)	6.8	6.0
Average ^b alkalinity (1987-89)	188 µeq/l	86 µeq/l

^a See Chapter 3 for a full description of Harp 4-21 characteristics.

^b Average of individual measurements (1 sample per ≈ 2.5 days), not flow weighted (MOE, unpublished data).

Figure 5.1 Instrumentation of the Harp 4-21 and Harp 3A catchments.



of many hillslopes, there is an abrupt decrease in slope to less than 5% in the valley bottom. Shallow ephemeral wetlands have formed where the valley bottom is flat and more than 15 m wide. There are two small wetlands (0.4 ha and 0.2 ha) and several other small areas (<0.1 ha) in Harp 3A where ponding occurs (Figure 5.1). Organic sediments up to 1.7 m and 2.3 m thick are found in Wetlands 2 and 3 respectively. Surface water depths within Wetland 2 ranged from 0 cm in the summer to 25 cm in the autumn.

Forests in the two catchments are similar (Table 5.1). Harp 3A hillslopes are covered by a hardwood forest dominated by sugar maple (*Acer saccharum*) with some yellow and white birch (*Betula alleghaniensis* and *Betula papyrifera*) and poplar species (*populus* spp.). Wetland 2 is characterized by hummock-hollow topography with a *Sphagnum* ground layer and both cedar (*Thuja occidentalis*) and black spruce (*Picea mariana*) are present. Wetland 3 has a partial canopy of yellow birch and black spruce.

Harp 3A is subdivided into four subcatchments (W1, W3, W4, W5) according to topographic boundaries (Figure 5.1). In this chapter, stream runoff responses at W5 in Harp 3A (4.9 ha) and S1 in Harp 4-21 (3.7 ha) are compared to demonstrate the effect of different sediment thickness and slopes because W5 is not influenced by wetlands and has similar area, soils and vegetation as Harp 4-21 (S1).

Methods

Instrumentation

Stream discharge at S1, S4 (Harp 4-21) and W1 to W5 (Harp 3A) was calculated from continuous measurements of stage and stage-discharge rating curves (Appendix 2). Stage was measured by Leopold and Stevens type A71 and F recorders or electronic potentiometers recording to Campbell Scientific data loggers (Figure 5.1). The weir at W1 was a combination

V-notch and rectangular weir built of steel and set in concrete. The four other V-notch weirs in Harp 3A were built of wood and lined with plastic sheeting to prevent leakage.

A total of 48 piezometers and wells were installed in Harp 3A. Most were constructed of 3.8 cm (1.5") diameter PVC, screened with nylon mesh (screen lengths of 0.20 m for piezometers and fully-screened for wells), and installed by digging soil pits or with gas-powered augers. Thirteen shallow piezometers with storage beneath the screened area were designed to verify saturation within the upper 0.05 to 0.15 m of soil and to collect shallow groundwater. These piezometers were made of 3.8 cm (1.5") diameter plastic and were screened over only 0.05 m. Nests of piezometers were located in transects perpendicular to the stream and wetlands (Figure 5.1). Water levels were recorded manually with an electronic water level device or Ping-Pong ball floats (Gillham, 1984). Bail tests were performed on most piezometers, except those that were dry during testing in the spring (Appendix 1). Water levels in Wetlands 2 and 3 were measured manually on staff gauges (Figure 5.1). During the spring season, water levels in Wetland 2 were also monitored continuously with a 15 cm float connected to an electronic potentiometer. Piezometer installations in Harp 4-21 are described in Chapter 3 and by MacLean (1992). During storms, groundwater levels in Harp 4-21 were measured in piezometers along MacLean's (1992) time domain reflectometry (TDR) transect (TD1, TD2, TD3, P06, and P61) and in piezometers P05 and P07 (Figure 5.1). Hourly precipitation was measured by the MOE at a site 500 m north of Harp 4-21.

Detailed topographic surveys of Harp 3A and Harp 4-21 were conducted with a Wild Leitz total station. Depth to bedrock was determined by digging and augering in Harp 3A, and by a seismic refraction survey in Harp 4-21 (Chapter 3). Although augering and digging may underestimate the depth to bedrock when cobbles or boulders are encountered, the occurrence of bedrock outcrops in several areas of Harp 3A suggests that the till is thin in most of the catchment.

Throughfall and stream water samples were collected during storms for isotopic hydrograph separations. Only baseflow and peak flow samples from W1, W5 and S1 and bulk throughfall samples were analysed for ^{18}O . Two-component hydrograph separations (Equation 4.1) were conducted to provide estimates of the proportion of pre-event water at peak discharge. To calculate the hydrograph separations, throughfall samples were used as event water and stream baseflow samples as pre-event water.

Monitoring periods

Precipitation and stream discharge from Harp 4-21 (S1) and Harp 3A (W1) were monitored continuously by the MOE. The remaining weirs were operated only during the monitoring periods. The seasonal patterns of stream runoff are compared for the 1988-89 water year (June 1 to May 31). Stream discharge and groundwater levels at all sites in Harp 3A were monitored from September 27 to November 20, 1992 (autumn season) and from May 2 to June 4, 1993 (spring season). Monitoring in Harp 4-21 was from September 27 to November 10, 1992 and from May 2 to May 30, 1993. Flow at weirs W2 and S4 were not continuously monitored during the spring season.

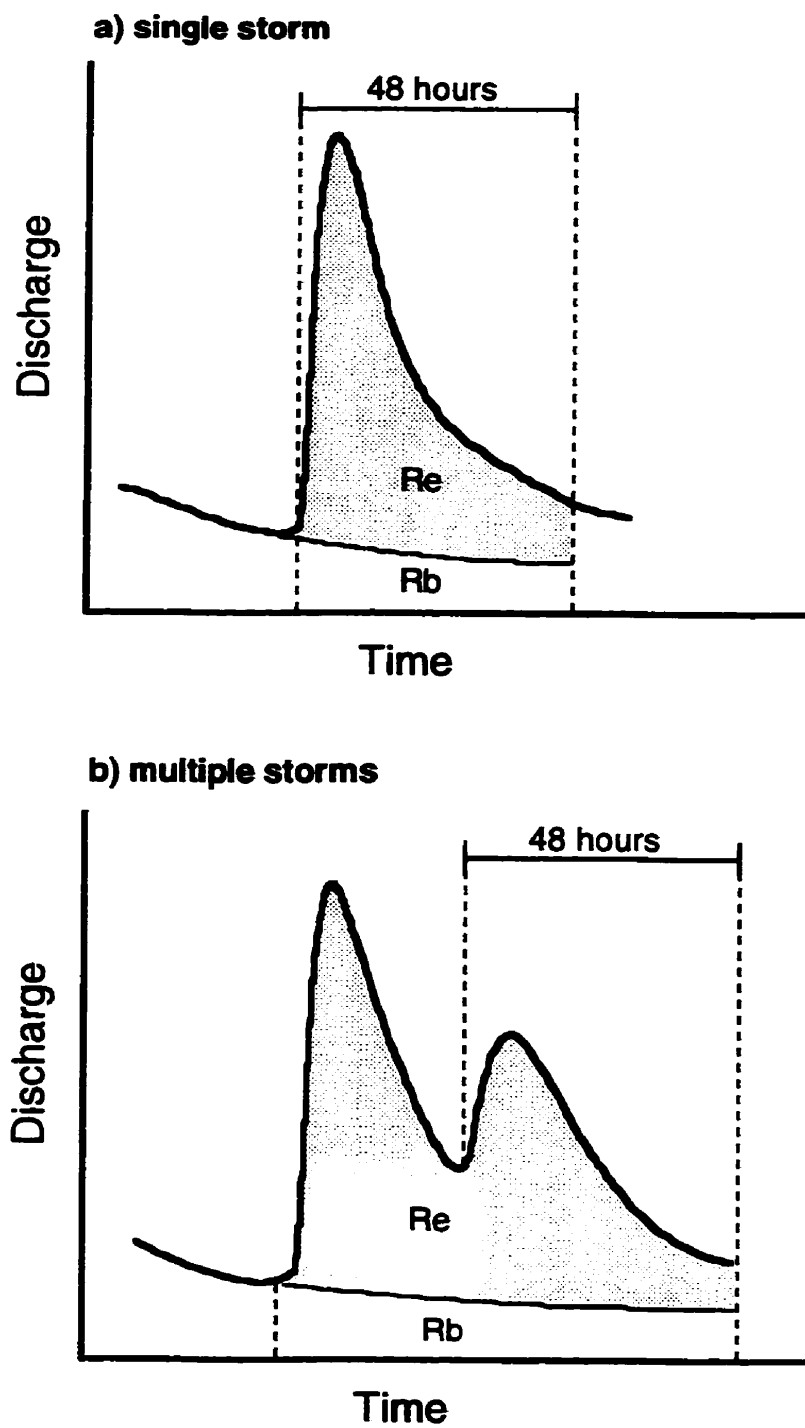
Effective runoff ratios

Effective runoff ratios are an approximate measure of the efficiency of runoff production in a watershed. They also provide a minimum estimate of the proportion of a catchment area that rapidly produces storm runoff. Effective runoff ratios are calculated as:

$$\text{effective runoff ratio} = \frac{R_e}{P} \quad (5.1)$$

where R_e is the runoff caused by the event, and $R_e = R - R_b$ where R is the total runoff and R_b is the baseflow runoff that would have occurred in the absence of precipitation (Figure 5.2a). The definitions of R_e and R_b are arbitrary because the duration of an event is poorly

Figure 5.2 Definition of event runoff (R_e) and baseflow runoff (R_b) in the calculation of the effective runoff ratio.



defined. For these calculations, a fixed event duration of 48 hours was chosen to avoid biases in runoff volumes caused by event duration. During this period, most of the runoff was generated and stream discharge had almost returned to pre-event baseflow. The value of R_b was estimated by the exponential decay of the stream discharge prior to the event (Bruce and Clark, 1966). If a second storm occurred within the 48 hour period, the storm duration was extended 48 hours after the start of the second storm (Figure 5.2b).

Results

Precipitation

Autumn 1992 was very wet with 425 mm of precipitation between August 28 and November 20. This total includes two large storms on September 18 (39 mm) and September 22 (82 mm) that replenished much of the summer soil water deficit. Very wet soil moisture conditions prior to the large storm on November 12 (62 mm) were caused by storms on November 2 (34 mm), 4 (12 mm) and 10 (16 mm).

Spring 1993 weather conditions were dry. Snowmelt was complete and the forest canopy was well developed by May 2. Two weeks of warm and dry weather in early May (3 mm precipitation; 8 days with maximum temperatures above 20°C, 1 day above 30°C) resulted in drier soil moisture conditions during spring than in autumn in Harp 3A. In Harp 4-21, soil moisture conditions in middle and lower slopes were higher in spring than in autumn because groundwater levels had risen as a result of spring melt.

Stream discharge

Total annual runoff was much higher in Harp 3A than in Harp 4-21 (Table 5.2a). Stream discharge in Harp 3A was higher throughout autumn, winter and spring (Figure 5.3).

Table 5.2. Seasonal distribution of precipitation and stream runoff, 1988-89, expressed as a) a depth, and b) a fraction of annual totals.

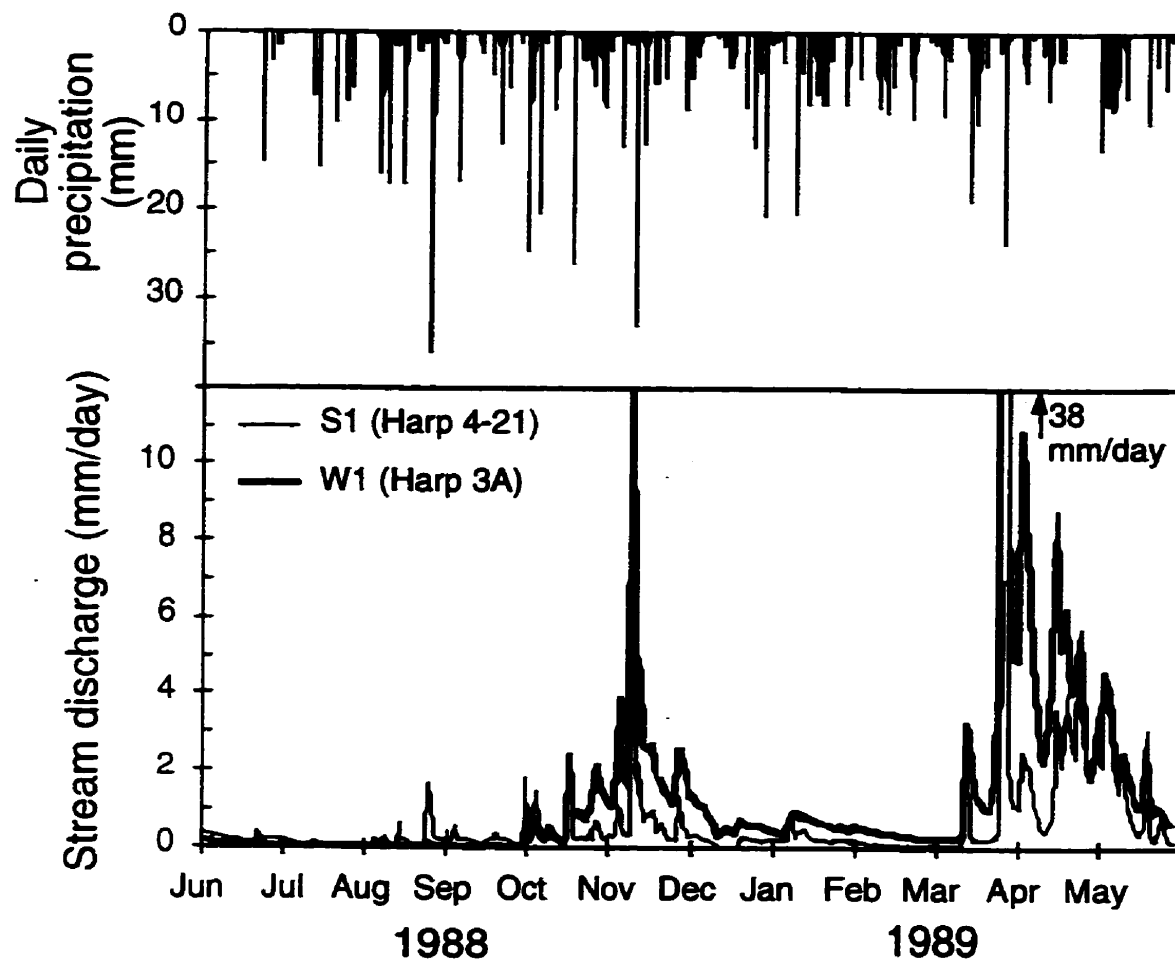
a)

	Jun, Jul, Aug	Sep, Oct, Nov	Dec, Jan, Feb	Mar, Apr, May	Total
	(mm)				
Precipitation	210	315	233	228	986
S1 (Harp 4-21)	15	43	13	136	208
W1 (Harp 3A)	2	100	48	326	476

b)

	Jun, Jul, Aug	Sep, Oct, Nov	Dec, Jan, Feb	Mar, Apr, May	
	(fraction of annual total)				
Precipitation	0.21	0.32	0.24	0.23	
S1 (Harp 4-21)	0.07	0.21	0.06	0.66	
W1 (Harp 3A)	0.005	0.21	0.10	0.68	

Figure 5.3 Precipitation and normalized daily stream discharge at sites S1 (Harp 4-21) and W1 (Harp 3A), 1988-89 (MOE unpublished data).



Since precipitation inputs must be very similar in these small adjacent catchments, differences in annual runoff must be caused either by differences in evapotranspiration or by groundwater flow across catchment boundaries. Groundwater flow into Harp 3A from adjacent catchments is very unlikely because of the very thin sediments and the narrow ridges that form the catchment divide. Groundwater flow out of Harp 4-21 (Dankevy, 1989) can only account for a small depth of water (≈ 50 mm). As a result, greater evapotranspiration in Harp 4-21 is the probable cause for its lower annual runoff.

Harp 4-21 and Harp 3A showed substantially different baseflow discharge and runoff responses to storms and snowmelt. The seasonality of stream discharge, lowest flow during summer, increased flow during autumn, decreased flow during winter and greatest flow during spring (Figure 5.3, Table 5.2b), is similar for both catchments. This pattern reflects seasonal changes in evapotranspiration, rainfall, snow accumulation, and snowmelt, which are not catchment specific. In Harp 3A, storm response to spring and autumn events was larger than in Harp 4-21 but was very small to nil during summer storms (Figure 5.3). Perennial baseflow and summer storm runoff accounted for a small but notable proportion of the annual runoff in Harp 4-21 (7%). In Harp 3A, most of the stream and the wetland areas dry out during the summer so that only a negligible proportion of runoff occurred in summer (0.5%, Table 5.2). Small summer storm response in Harp 3A was likely caused by dry summer soil conditions. Despite similar or smaller precipitation inputs (because water is stored as snow), winter baseflow in Harp 3A was higher and more sustained than summer baseflow (Figure 5.3, Table 5.2). Therefore, dry summer soil conditions in Harp 3A were caused by evapotranspiration rather than by rapid soil water drainage. Since runoff events contribute a significant proportion of the hydrological and geochemical mass balances of both watersheds (Chapter 8), it is important to examine how storm runoff response varies with antecedent weather and soil moisture conditions.

Storm runoff in Harp 3A was more variable and responsive to antecedent moisture conditions than in Harp 4-21. After the September 1992 storms (189 mm) had replenished soil moisture, the timing and magnitude of stream responses to October storms were similar in the two catchments (Figures 5.4 and 5.5, Table 5.3). Wet conditions prior to November storms led to larger stream discharge and effective runoff ratios in Harp 3A (Table 5.3). In contrast, dry weather in early May and August 1993 (19 mm precipitation in the four weeks prior to the storm) caused much smaller stream response in Harp 3A (Figures 5.6 and 5.7, Table 5.3). Smaller effective runoff ratios in Harp 3A than in Harp 4-21 for the May 14 and 24 storms suggest that evapotranspiration influenced antecedent moisture conditions and storm runoff response differently in the two catchments (Table 5.3). The influence of antecedent weather conditions in Harp 3A is further demonstrated during storms on May 24, 28 and 31 when stream discharge (Figures 5.6 and 5.7) and effective runoff ratios (Table 5.3) were larger in the later two storms despite a larger precipitation input during the first storm.

Effective runoff ratios in Harp 3A increased with increasing soil water storage at TD87 (Figure 5.8a). However, the correlation ($r^2 = 0.84$ for W1 and 0.94 for W5; August 27 outlier excluded) is also partially attributed to the amount of precipitation since the two largest storms also occurred when antecedent water storage was highest. Figure 5.8a suggests that when soil moisture conditions are high, the efficiency of runoff production changes rapidly with small (< 25 mm) changes in soil water storage. This effect is highlighted by a doubling in effective runoff ratios between storms on May 14 and 24 and storms on May 28 and 31 even though soil water storage increased by less than 15 mm (Figure 5.8a and Table 5.3).

Effective runoff ratios in Harp 4-21 were not clearly related to soil water storage (Figure 5.8b). Although the effective runoff ratio was lowest during dry summer conditions (August 27) and higher during wetter autumn conditions (Table 5.3), consistent with the results of MacLean (1992), there is no clear relationship during wet conditions (Figure 5.8b).

Figure 5.4 Precipitation and stream discharge at sites W1-W5 (Harp 3A), S1 and S4 (Harp 4-21), autumn 1992. Weir locations are shown in Figure 5.1.

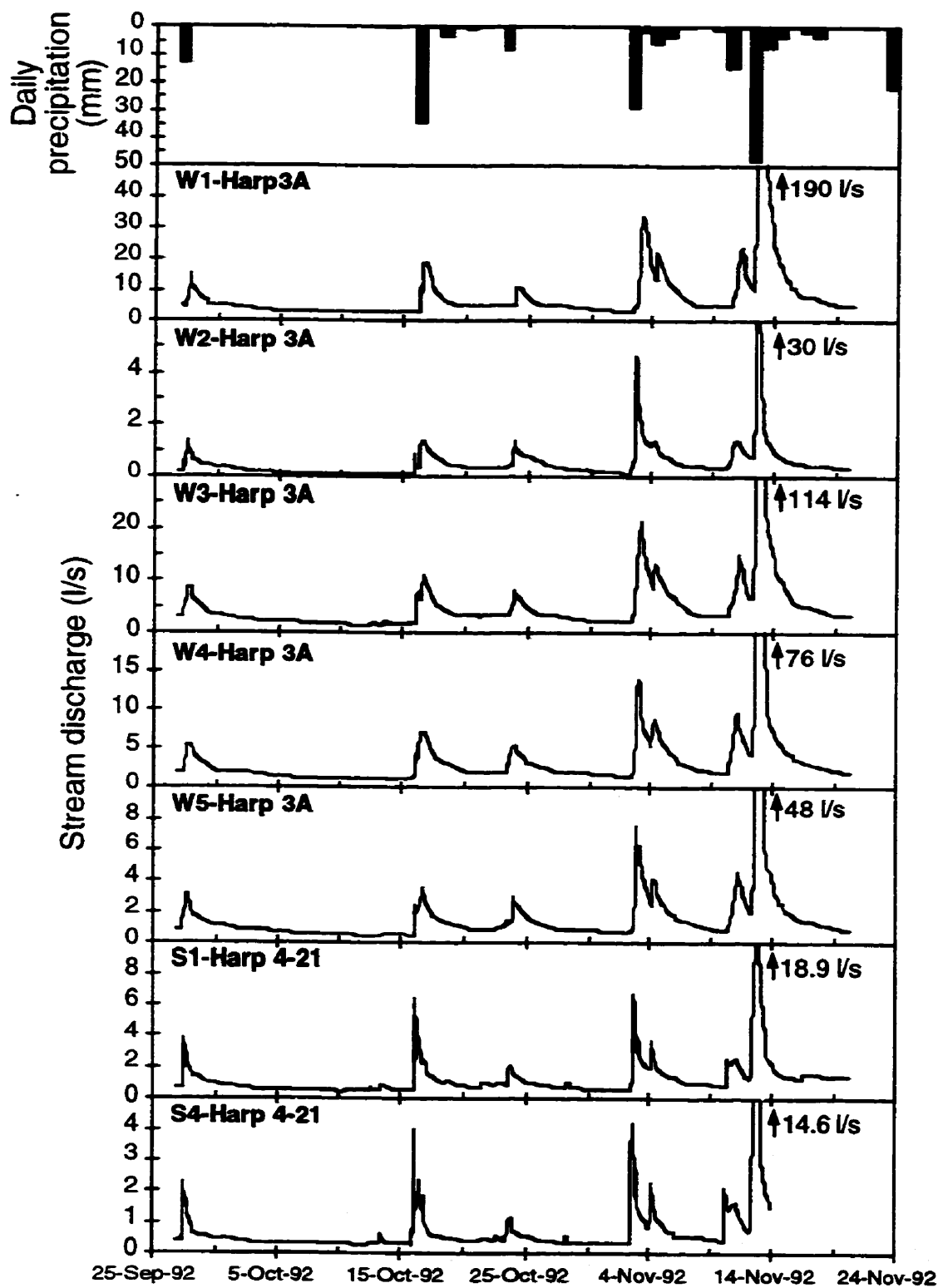


Figure 5.5 Precipitation and normalized stream discharge at S1 (Harp 4-21) and W5 (Harp 3A) for November 2 and 4 events.

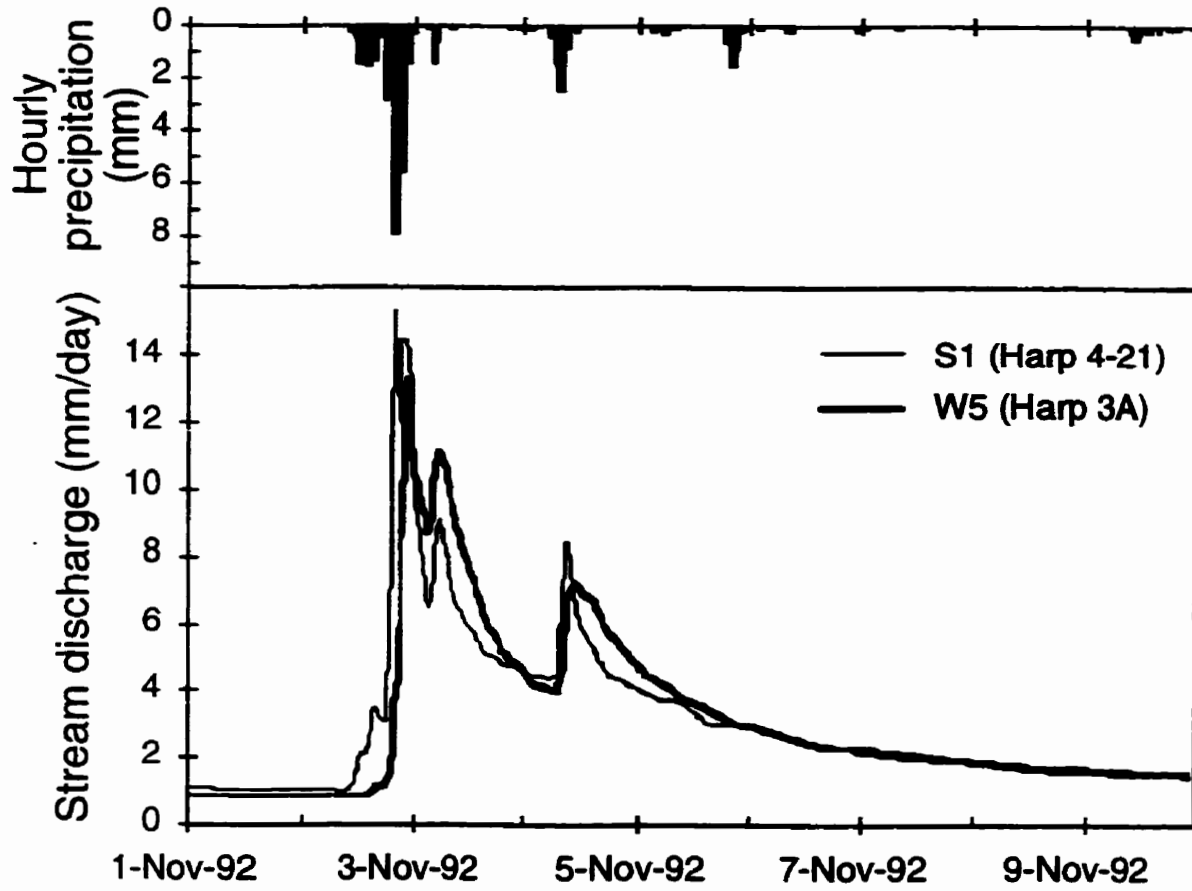


Table 5.3. Effective runoff ratios.

Storm date	Precipitation (mm)	Effective runoff ^a		
		W1	W5	S1
27-Sep-92	14.6	0.27	0.24	0.33
16-Oct-92	40.6	0.17	0.18	0.18
23-Oct-92	9.7	0.32	0.33	0.33
2-Nov-92 ^b	45.5	0.48	0.40	0.35
10-Nov-92 ^c	78.5	0.63	0.57	0.38
14-May-93	10.1	0.09	0.06	0.20
24-May-93	34.6	0.10	0.08	0.20
28-May-93	18.0	0.20	0.21	0.26
31-May-93	21.0	0.19	0.23	0.28
27-Aug-93	9.8	0.00	-	0.07

^a Effective runoff ratio = $\frac{Re}{P}$ where Re is the event runoff, and $Re = R - Rb$ where R is the total runoff and Rb is the baseflow runoff.

^b Includes November 4 storm.

^c Includes November 12 storm.

Figure 5.6 Precipitation and stream discharge at sites W1, W3-W5 (Harp 3A) and S1 (Harp 4-21), spring 1993. Weir locations are shown in Figure 5.1.

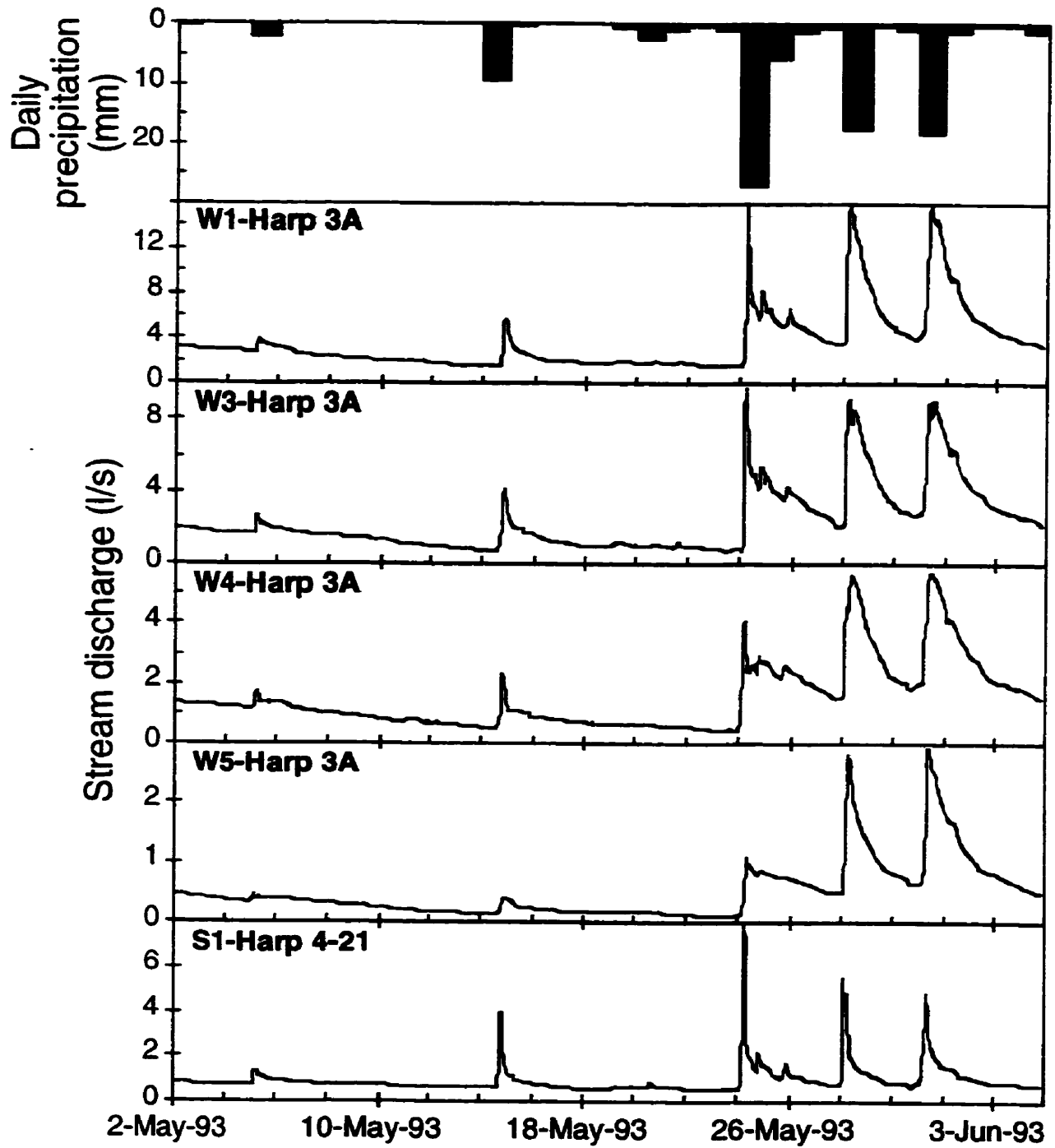


Figure 5.7 Precipitation and normalized stream discharge at S1 (Harp 4-21) and W5 (Harp 3A) for May 24, 28 and 31 events.

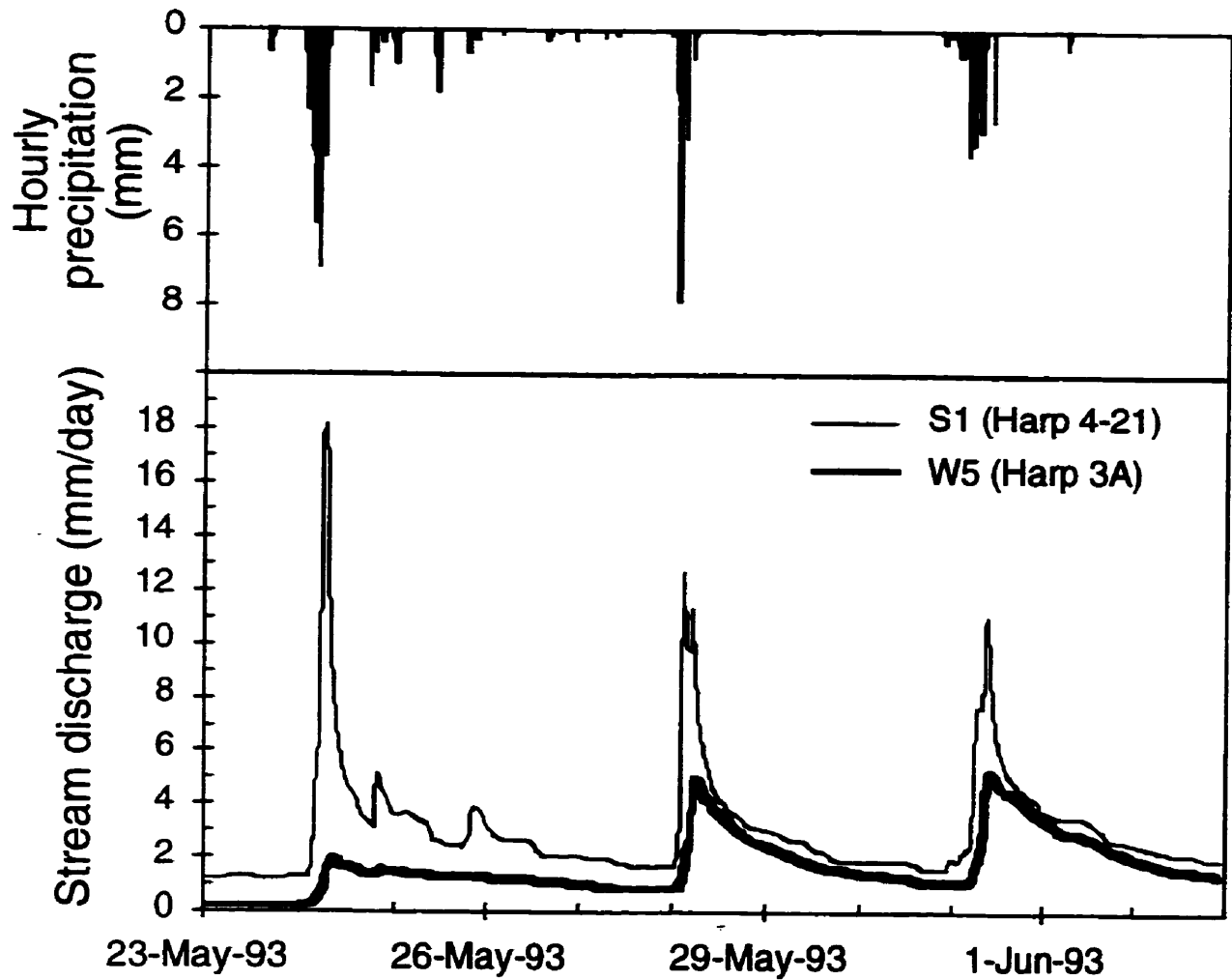
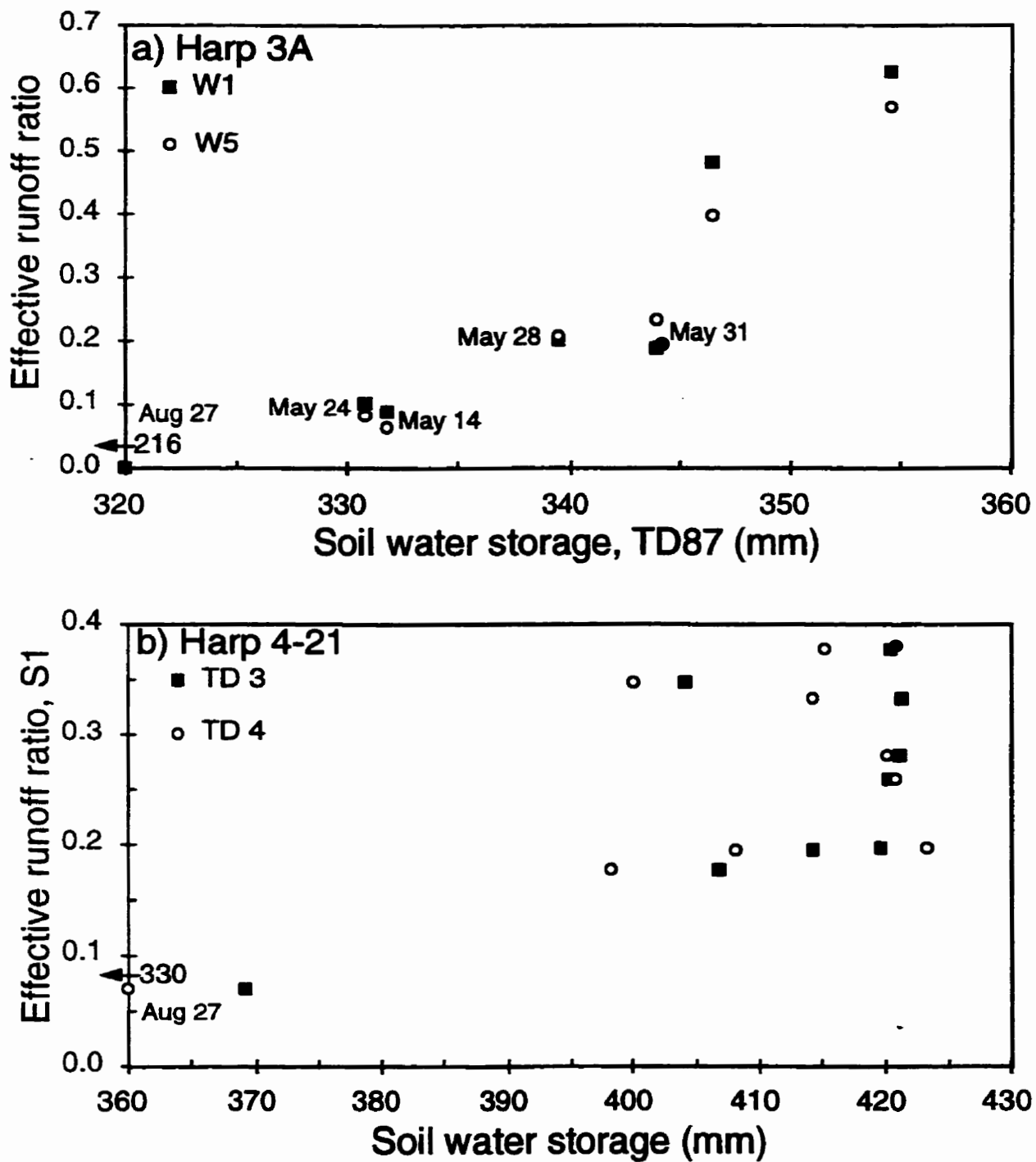


Figure 5.8 Effect of antecedent soil water storage on effective runoff ratios a) in Harp 3A and b) in Harp 4-21. Locations of TD87, TD3 and TD4 are shown in Figure 5.1.



The lack of correlation between antecedent moisture conditions and runoff response when soil moisture conditions are high ($r^2 = 0.003$ for TD4 to 0.03 for TD3; August 27 outlier excluded) is most likely caused by spatial variability in soil water storage and runoff production.

Near-stream areas contributed more rapidly to storm runoff in Harp 4-21 than in Harp 3A. During the initial portion of the November 2 storm event, Harp 4-21 responded to the small inputs of precipitation that did not increase flow at W5 (Harp 3A) (Figure 5.5). Furthermore, the rising limb of hydrographs are steeper in Harp 4-21 and peak earlier. These results suggest that less precipitation was stored in near-stream areas of Harp 4-21 and that precipitation onto these areas was transmitted more rapidly to the stream.

Except during dry summer conditions, Harp 3A hillslopes contributed more to stream runoff than did the wetlands. The large effective runoff ratios indicate that a high proportion of the watershed must have contributed to storm runoff (Table 5.3). Even if Wetlands 2 and 3 contributed 100 percent of precipitation to runoff, this volume of water would represent less than 4 percent of the total runoff in the autumn and less than 6 percent in the spring because they occupy only 3% of the total catchment area.

Hydrograph separations

Pre-event water was the main component of storm runoff in both catchments, providing more than 85% of peak discharge in Harp 3A during both autumn and spring storms and 75% or more of peak stream discharge during spring storms in Harp 4-21 (Table 5.4). Since the highest proportion of event water usually occurs at or near peak discharge (Chapter 4), the event water component at other times during the storm are less than at peak discharge. Consequently, pre-event water likely dominates (>75-85%) the total volume of discharge.

Table 5.4. Isotopic hydrograph separations near peak discharge for 1992 and 1993 events.
 $\delta^{18}\text{O}$ values expressed relative to SMOW.

Storm event	Throughfall	Baseflow		Near peak flow		Pre-event component		
	$\delta^{18}\text{O}$ ‰	$\delta^{18}\text{O}$ ‰	Q (l/s)	$\delta^{18}\text{O}$ ‰	Q (l/s)	Q (l/s)	%	% increase
a) W1								
10-Nov-92	-14.00	-10.11	4.0	-10.07	22.5	22.5	101	460
12-Nov-92	-13.15	-	9.4	-10.50	172	150	87 ^a	1500
24-May-93	-6.18	-13.06	1.4	-12.19	15.3	13.3	87	840
28-May-93	-8.82	-	3.3	-12.49	15.6	13.6	87 ^b	310
b) W5								
24-May-93	-6.18	-14.19	0.06	-14.07	1.0	1.0	99	1500
28-May-93	-8.82	-	0.47	-13.58	2.4	2.1	89 ^b	350
c) S1								
24-May-93	-6.18	-12.47	0.53	-10.89	7.7	5.6	75	960
28-May-93	-8.82	-	0.72	-11.75	3.4	2.7	80 ^b	280

^a Using baseflow $\delta^{18}\text{O}$ value prior to 10-Nov-92 event.

^b Using baseflow $\delta^{18}\text{O}$ value prior to 24-May-93 event.

Consequently, pre-event water likely dominates (>75-85%) the total volume of storm runoff in the two catchments.

The hydrograph separations in Table 5.4 should provide a reasonable estimate of the relative magnitude of the pre-event component of storm runoff because the isotopic separation between the components is substantial (3.0 to 8.0‰). However, isotopic separation between throughfall and baseflow samples were too small to calculate hydrograph separations for the storms on November 2 and 4, 1992.

Groundwater levels

The presence of thicker glacial till in Harp 4-21 resulted in four differences between the groundwater flow systems of the two catchments: 1) the depth to the water table, 2) groundwater flow from upslope during dry weather, 3) the area (or spatial extent) where the water table is located within the soil horizons, and 4) the timing of water table fluctuations.

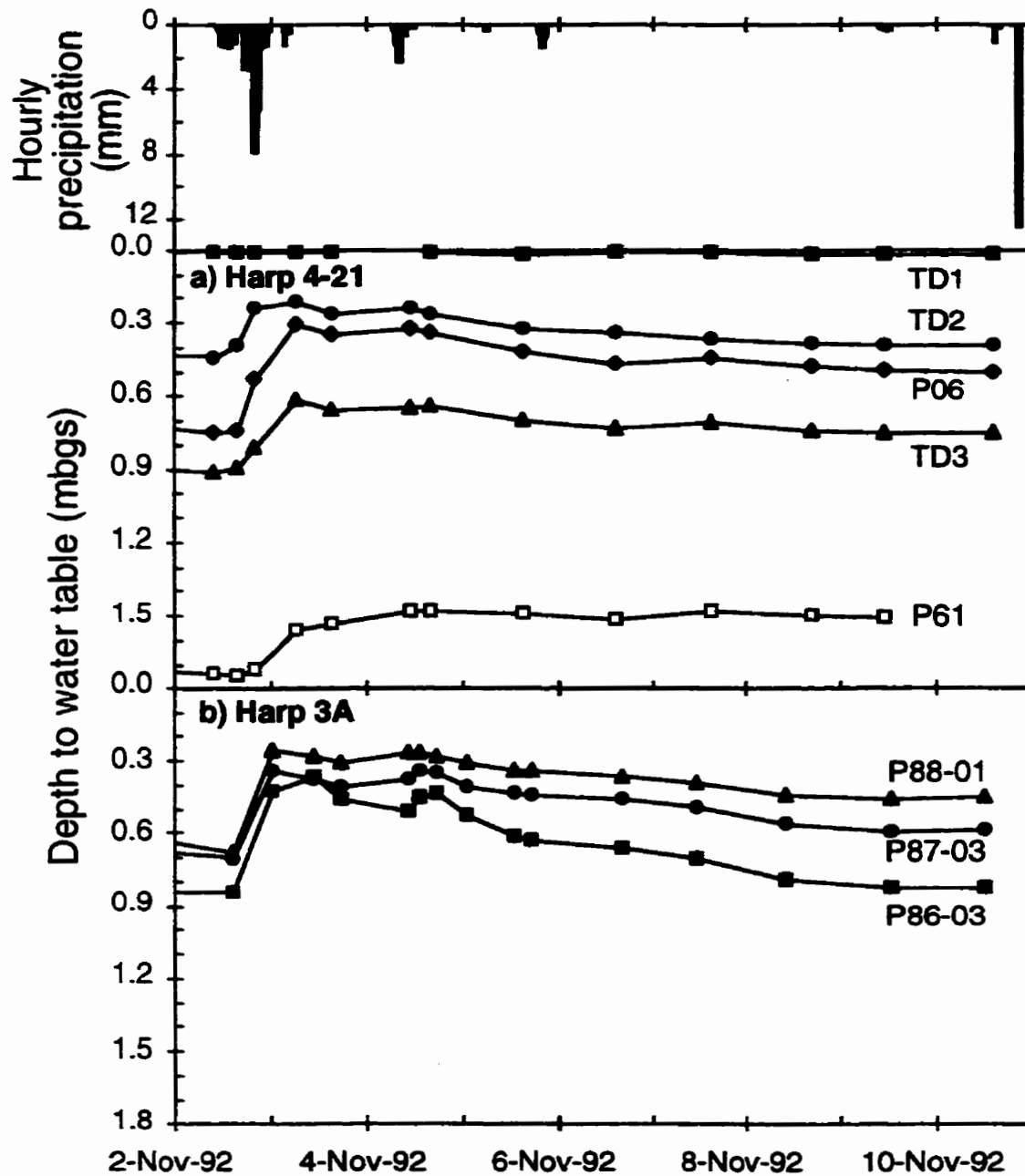
1) Depth to the water table

The depth to the water table in Harp 4-21 generally increases with increasing distance from the stream (Figure 5.9a), varying from less than 0.05 m at the stream edge (TD1), to 0.9-2.6 m at midslope piezometer P61, to 2.4-6.8 m in upslope piezometer P22, 150 m from the stream (Figure 3.3). When the water table was present within Harp 3A hillslopes, its depth was relatively uniform regardless of position along the hillslope (Figure 5.9b).

2) Groundwater flow from upslope during dry weather

Groundwater flow from upslope tills sustains stream baseflow in Harp 4-21 during dry periods. Seasonal groundwater level fluctuations in upslope piezometers (Figure 3.7) show that groundwater levels rose in April and May and declined slowly for the rest of the year. If a

Figure 5.9 Precipitation and groundwater fluctuations for November 2 and 4 events in a) Harp 4-21 and b) Harp 3A (mbgs = meters below ground surface). Piezometer locations are shown in Figure 5.1.



specific yield of approximately 0.16 is assumed for the till (Domenico and Schwartz, 1990), the total volume of water released from upslope tills would correspond to an average baseflow of approximately 0.2 l/s (0.5 mm/d), comparable to late autumn stream baseflow when evapotranspiration rates are low. In contrast, there was no sustained baseflow from Harp 3A hillslopes during dry weather. The water table was only present in upslope piezometer P83-02 during storms (Figures 5.10 and 5.11). All hillslope piezometers were dry in August 1993. Since none of the piezometers in Harp 3A penetrated bedrock, it is not known if the water table was present within it. However, groundwater flow in the bedrock was insufficient to sustain downslope groundwater levels or significant stream baseflow.

3) The area (or spatial extent) where the water table is located within the soil horizons

The spatial extent of the water table within the soil horizons varied greatly in Harp 3A both seasonally and during storms. During summer, the water table in Harp 3A was only observed in wetlands, below the stream and in valley bottoms; hillslope soils were unsaturated. During autumn baseflow conditions, the water table was present within soil horizons from the base of the hillslope to at least midslope positions P88 and P82 (Figure 5.10). During autumn storms, the water table rose rapidly into upslope soils (e.g. piezometer P83-02, Figure 5.10). Observations of surface saturation in depressions along the northwestern watershed divide of Harp 3A suggest that the water table may have been present within the soils up to the catchment divide during runoff events in the autumn. During spring storms with drier antecedent conditions, the water table rose from lower to midslope soils (Figure 5.11). The disappearance of the water table in the overburden at piezometer nest P86 and not at P87 suggests that the spatial distribution of the water table may have become heterogeneous as the hillslopes began to dry out in early spring (Figure 5.11).

Figure 5.10 Precipitation and groundwater fluctuations in Harp 3A, autumn 1992. Dashed line indicates the period when a piezometer was dry. Piezometer locations are shown in Figure 5.1.

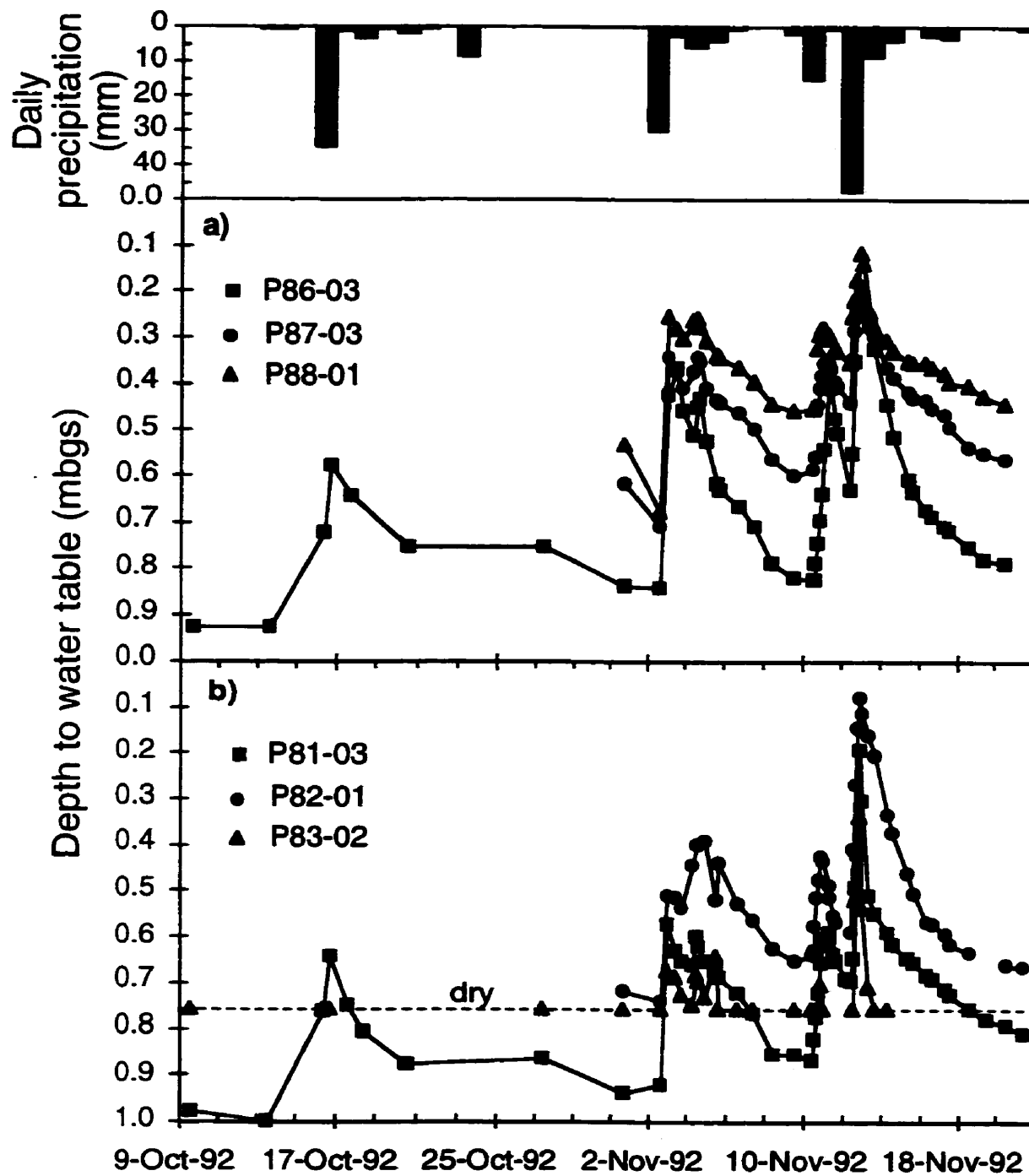
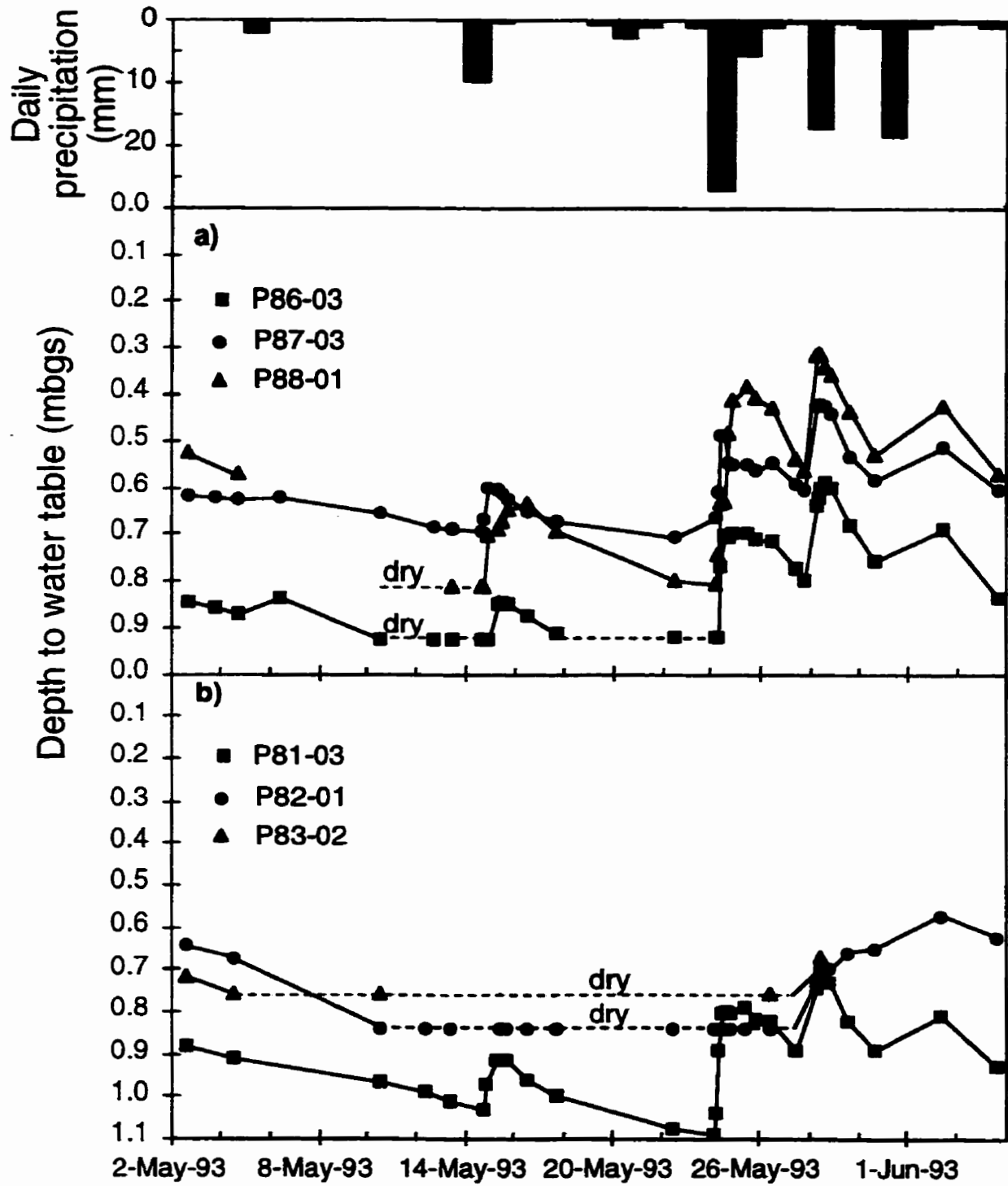


Figure 5.11 Precipitation and groundwater fluctuations in Harp 3A, spring 1993. Dashed line indicates the period when a piezometer was dry. Piezometer locations are shown in Figure 5.1.



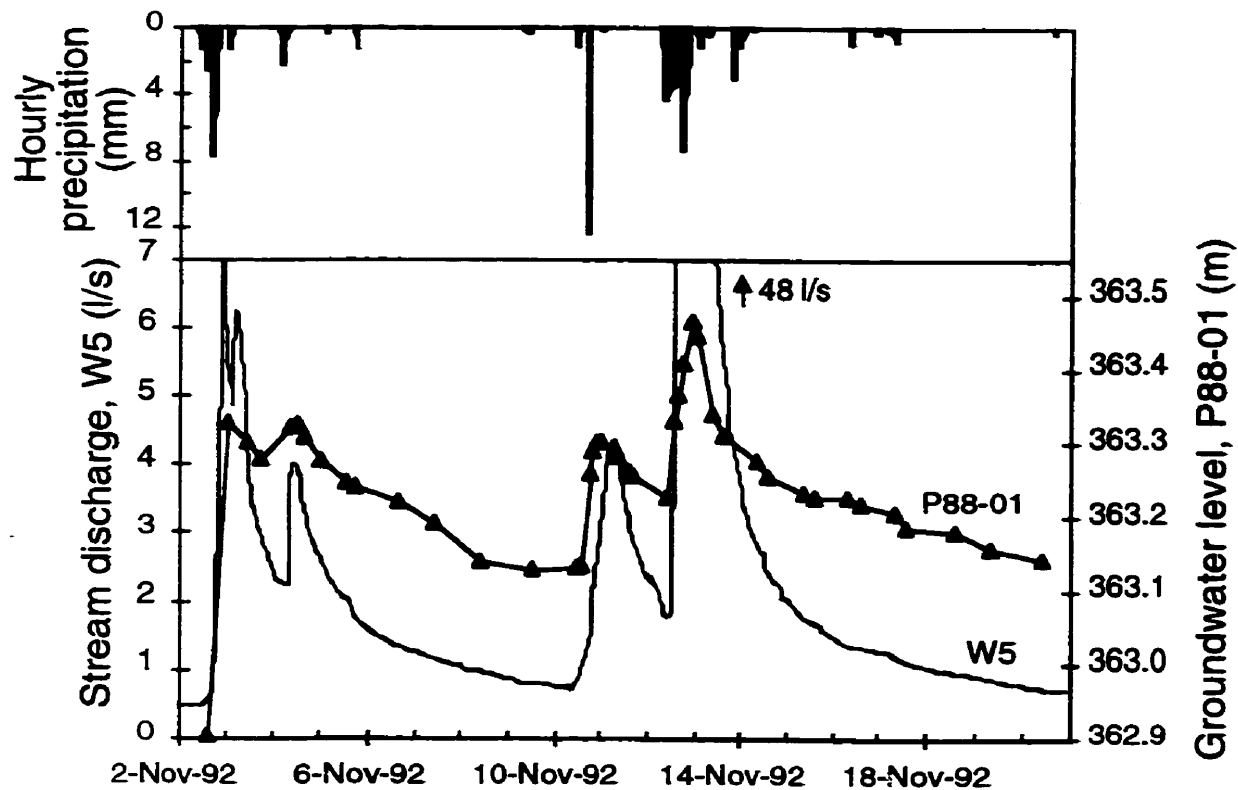
The variations in the spatial extent of the water table within soil horizons were much smaller in Harp 4-21 than in Harp 3A. Along the TDR transect in Harp 4-21, the spatial extent of the water table within soils varied between 13 and 52 m from the stream because the water table never rose into the soil at midslope site P61, and never dropped below soil horizons at TD2 (Figure 5.9). However, the extent of the water table in soil horizons was not uniform in Harp 4-21 hillslopes. Farther upstream, variations were larger; the water table within the soils extended more than 90 m from the stream during wet conditions and less than 15 m during dry conditions. This result may help explain the seasonal changes in the proportion of discharge from the S4 and S5 subcatchments (i.e. greater during wet periods and smaller during dry periods, Chapter 3).

4) The timing of water table fluctuations

The timing of groundwater level fluctuations also differed between the catchments, varying with the depth to the water table. In upslope areas of Harp 4-21, groundwater levels were deepest, fluctuated seasonally, and showed no response to individual storms (Figure 3.7). In midslope areas of Harp 4-21, groundwater levels were in the till just below the soil and responded to individual storms. However, that response could be delayed one or more days (P61, Figure 5.9). In all areas of both catchments where the water table was within soil horizons, groundwater levels responded very rapidly to storms (Figure 5.9).

The timing of groundwater level fluctuations within the soils was closely related to the timing of changes in stream discharge. For example, the hydrographs of water levels at P88-01 and stream discharge at W5 show that the groundwater levels rose simultaneously with stream discharge during the November 2, 4 and 12 storms and prior to stream discharge during the brief high-intensity storm on November 10 (Figure 5.12). As shown in

Figure 5.12 Timing of groundwater (P88-01) and stream (W5) response to November 1992 storms in Harp 3A (masl = meters above sea level). Piezometer and weir locations are shown in Figure 5.1.



Figures 5.10 and 5.11, the groundwater levels at other hillslope sites in Harp 3A increased simultaneously with water levels in P88-01.

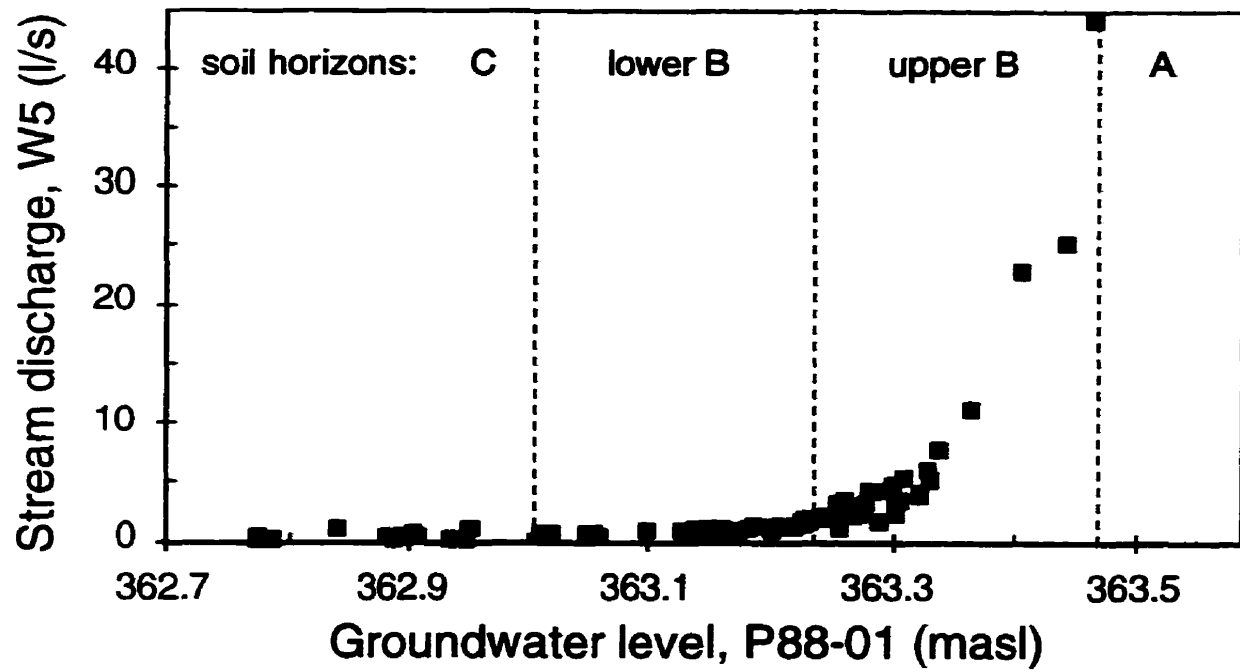
Stream discharge was related to the groundwater elevation within the soils. Only when the water table rose into the upper B horizon was there a large increase in stream discharge (Figure 5.13). The increase in flow may be attributed to higher hydraulic conductivity in the upper B horizon (Chapter 6). A similar relationship between stream discharge and groundwater levels was also observed in Harp 4-21 (Chapter 3) and for other piezometers in Harp 3A.

Discussion

Effect of glacial till on groundwater flow and stream discharge

The primary hydrogeological role of thicker glacial till in Harp 4-21 is not in the transmission of subsurface flow during storms, but in the storage of water during storms and its redistribution between them. In providing storage, it is not strictly the thickness of the till that is important; it is also the location of water storage with respect to hillslope position (i.e. its hydraulic head), availability for evapotranspiration, and the hydraulic conductivity of the till. Thicker till in upslope areas of Harp 4-21 stores water in upper hillslopes which gradually flows to lower hillslopes and the stream throughout the year. In contrast, thick sediment within the stream valley would provide little effective water storage because stored water cannot drain to the stream. A sufficient volume of groundwater must be stored in upslope till to maintain near-stream groundwater levels and stream baseflow throughout the summer. The necessary volume of stored water is equal to the volume of approximately six months of baseflow in addition to summer evapotranspiration from near-stream areas. Therefore, the till must be thick enough to store most of spring recharge below the root zone where it is not

Figure 5.13 Stream discharge at W5 as a function of groundwater levels in midslope piezometer P88-01. Piezometer location is shown in Figure 5.1.



available for evapotranspiration. Such groundwater storage is available in Harp 4-21 but not in Harp 3A where till water is lost to evapotranspiration. It is difficult to estimate the minimum thickness of glacial till necessary to sustain summer baseflow because several factors such as evapotranspiration in areas near the stream, depth of rooting zone, and catchment dimensions must be considered. However, based on the characteristics of Harp 4-21, it is likely that a minimum till thickness of approximately 5 m (7000 m^3 estimated volume to sustain summer baseflow and evapotranspiration/ $(10000 \text{ m}^2$ upslope area \times 0.16 specific yield) + 1 m estimated rooting zone in till) would be required in upslope areas.

The role of till in sustaining near-stream groundwater levels and stream baseflow also depends on its hydraulic conductivity. If the till were more permeable (e.g. $>10^{-5}$ m/s), the water table would drop more rapidly following spring melt and may not contribute much to summer baseflow. In contrast, groundwater flow through less permeable till (e.g. $<10^{-8}$ m/s) would be too small to have an appreciable influence on stream baseflow. For a till thickness of approximately 5 m and a hydraulic gradient of 0.1, the minimum hydraulic conductivity required to transmit sufficient water to sustain baseflow would be approximately 4×10^{-6} m/s.

Thick glacial till effectively moderated seasonal variations in storm runoff response by its influence on groundwater levels in near-stream soils and on depth to water table in upslope areas. During dry weather, groundwater flow through glacial till maintains a shallow water table in lower hillslope soils. Since less precipitation can be stored, greater storm runoff is produced. This effect was observed in Harp 4-21, where till is thicker. In Harp 3A, where till is thinner, the lack of sustained groundwater flow causes near-stream soils to dry out and storm response to decrease to zero during dry conditions (Table 5.3). During wet conditions, precipitation onto upper hillslopes of Harp 3A contributed to storm runoff when the water table developed within the soils. When the water table is deeper than approximately 2-3 m in

Harp 4-21 hillslopes, it does not respond rapidly to infiltration during storms even during wet conditions. As a result, upper hillslopes of Harp 4-21 do not contribute to storm runoff but, instead, to stream baseflow. Therefore, the effect of greater till thickness in Harp 4-21 is to limit the area of hillslope response and the magnitude of storm runoff during wet conditions.

Effect of soils on storm runoff

The primary reason for the differences in runoff response between Harp 4-21 and Harp 3A is the spatial extent of the water table within soil horizons. Several results suggest that stream runoff response to storms is determined primarily by groundwater flow within the soils. Firstly, pre-event water is the dominant component of storm flow in both catchments (Table 5.4, Chapter 4). Secondly, groundwater level response to storms occurs prior to or synchronously with stream discharge where groundwater levels are within soil horizons; the response is significantly delayed where the water table is below soil horizons (Figures 5.9 and 5.12). Thirdly, stream discharge varies directly with groundwater levels within the soils (Figures 3.8 and 5.13). Finally, effective runoff ratios vary with the extent of the water table within soil horizons; ratios are lowest when the extent of saturated conditions in the soil is small to nil, and largest when the water table extends into midslope or upslope soils (Table 5.3).

Conclusions

The presence and thickness of glacial till has a significant influence on groundwater flow in two catchments of the Canadian Shield. Thicker glacial till causes 1) greater depths to the water table in upslope areas, 2) storage of infiltrating precipitation in these areas, 3) groundwater flow from these areas to sustain summer baseflow, 4) smaller variability in the spatial extent of the water table in soil horizons.

Groundwater flow through thick till also influences the magnitude of both seasonal and individual storm runoff. During dry weather, shallow water tables adjacent to the stream maintain stream baseflow and cause larger runoff responses to summer storms. During wet soil water conditions, water storage within thicker till in upslope areas of Harp 4-21 results in smaller storm runoff responses than in Harp 3A. Upslope areas of Harp 3A contribute to storm runoff when the water table develops within soil horizons.

Groundwater flow through till has hydrological, ecological and chemical implications. Firstly, the hydrological budgets for catchments with thin and thick till can be very different. Long-term annual runoff is lower where till is thick because water stored in the till is available for evapotranspiration during the summer. Regional differences in till thickness on the Canadian Shield could result in greater annual runoff and susceptibility to flooding in regions with thin till. Secondly, thick tills maintain stream baseflow over extended periods of drought. Summer baseflow is important for the dilution of effluent in streams, the maintenance of stream habitat for aquatic communities, and for sustaining water levels and reducing conditions in wetlands (Devito and Dillon, 1993; Devito et al., 1996).

Chapter 6

Subsurface flow production in Harp 4-21 and Harp 3A

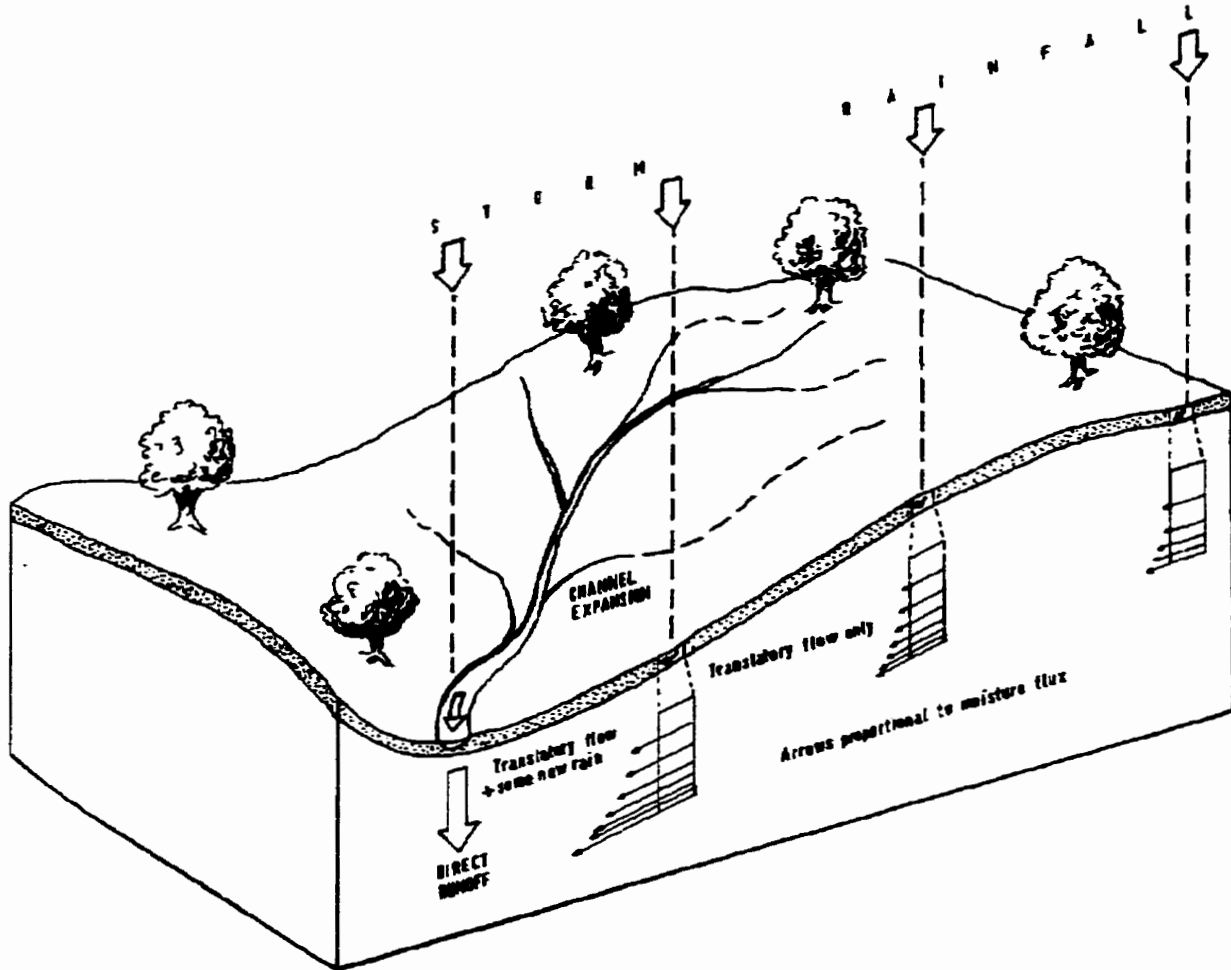
Introduction

Conceptual models of streamflow generation frequently emphasize hydrological processes near streams (Chapter 2). Models that accommodate processes such as saturation overland flow and groundwater ridging consider that most storm runoff is generated in the riparian zone and little is generated by precipitation onto the middle and upper hillslopes. However, as Hewlett and Hibbert (1967) recognized, precipitation onto middle and upper hillslopes can also generate storm runoff by subsequent displacement of water towards the stream (Figure 6.1). Precipitation onto saturated areas near the stream is known to produce a nearly equivalent depth of stream runoff (e.g. Dunne and Black, 1970b), whereas the efficiency of runoff production along the remainder of the hillslope is rarely documented. Quantifying the magnitude and timing of subsurface flow production from different hillslope positions will help determine the role of subsurface flow upslope of near-stream areas and identify the dominant streamflow generation processes.

Subsurface flow contributions to storm runoff are most often interpreted and reported in terms of fluxes (e.g. trough measurements or Darcy's law calculations) or as percentages of total runoff or discharge rates (e.g. hydrograph separations). Alternatively, subsurface flow generation can also be considered in the context of a water balance. Precipitation that infiltrates the ground surface can either increase soil moisture, be removed from the ground (e.g. by evapotranspiration) or displace other subsurface water to the surface.

The purpose of this chapter is to determine the spatial and temporal patterns of subsurface flow production along hillslopes in Harp 4-21 and Harp 3A. These results are used

Figure 6.1 The relative contributions to storm runoff from different hillslope positions according to Hewlett and Hibbert (1967, adapted from Chorley (1978)). The length of arrows are proportional to moisture flux.



to identify some of the factors that influence the magnitude and timing of subsurface flow production. More generally, this chapter also provides a new approach to the study and interpretation of subsurface flow production by quantifying spatial and temporal changes in soil water balances.

Study site

The physical characteristics of the Harp 4-21 and Harp 3A watersheds are discussed in Chapters 3 and 5 and are summarized in Table 5.1. Harp 4-21 is characterized by a greater sediment thickness, whereas Harp 3A has steeper slopes.

Methods

Instrumentation

The monitoring of stream discharge and groundwater levels for this study was described in Chapter 5. Volumetric soil water content was measured using time domain reflectometry (TDR) as described by MacLean (1992). TDR consists of measuring the propagation time of an electromagnetic wave through the soil to determine its dielectric constant. As air and water have different dielectric constants (1 and 81.5 respectively), its measurement can be related to soil water content by the empirical equation of Topp et al. (1980).

TDR water content measurements were made between waveguide pairs inserted horizontally into the major soil horizons in the upslope face of each soil pit (MacLean, 1992). Waveguides were made with 30 cm (28 cm exposed) uncoated steel welding rods (3 mm diameter). Guides were used during installation to ensure that the rods were uniformly spaced 5 cm apart. The soil pits were carefully backfilled to maintain soil horizons. Wave forms were

collected manually using a Tektronics model 1502B cable tester and downloaded in the field. Wave forms were later analysed with a computer program (WATTDR, v. 3.00) that facilitates the identification of the start and end times of the TDR trace and makes use of the Topp et al. (1980) equation (D. Redman, personal communication). Some wave forms, mostly during the spring sampling season, were incorrectly downloaded and, therefore, the water contents could not be determined. For each profile of water content measurements, the groundwater level was measured simultaneously in a piezometer installed at each TDR site.

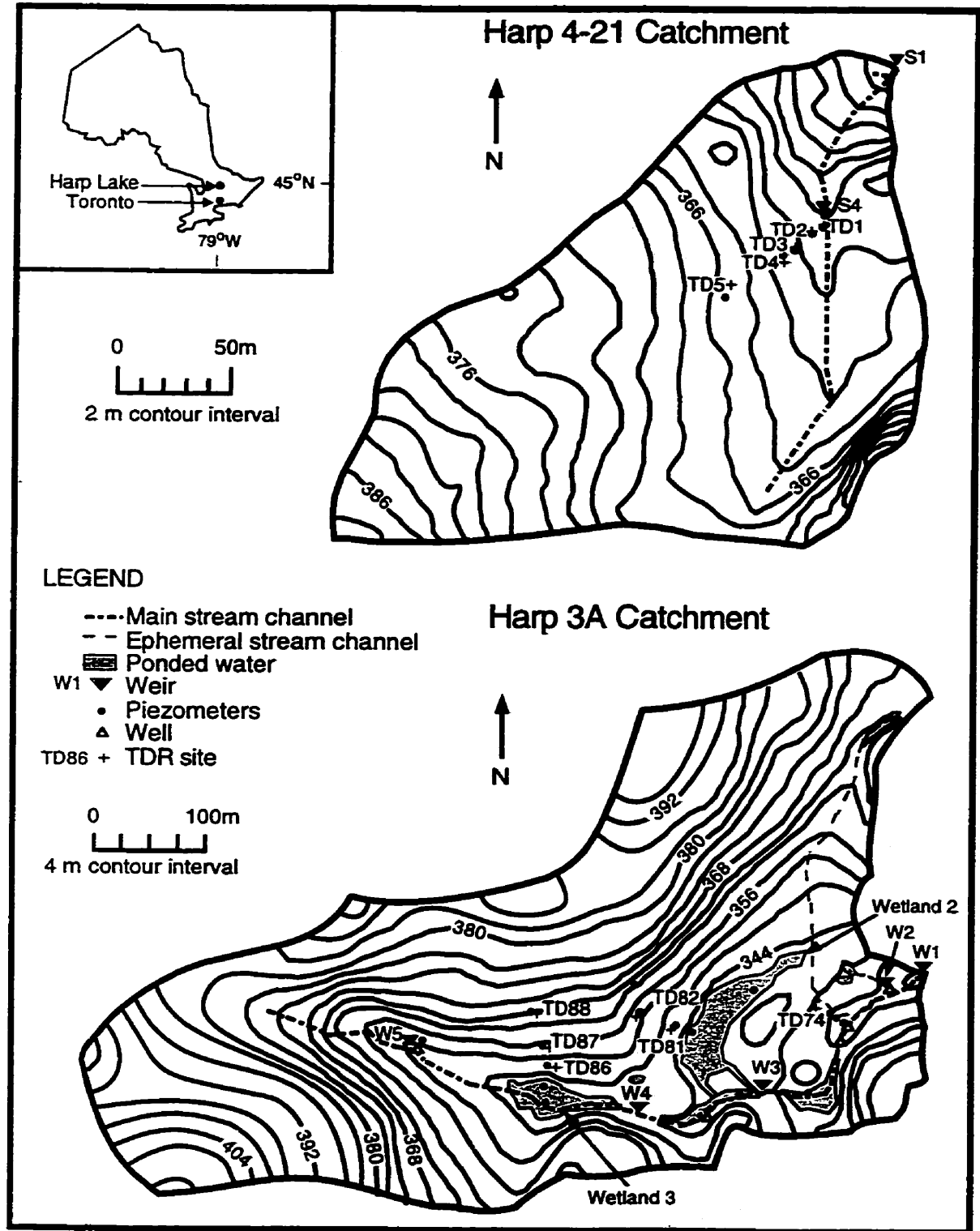
MacLean's (1992) transect of TDR sites in Harp 4-21 was reused in this study (Figure 6.2). Soil water content was measured at 3 depths in each of five TDR sites (TD1 to TD5, Appendix 3). In Harp 3A, six additional TDR sites were installed in October 1992 (TD74, TD81, TD82, TD86, TD87, and TD88) (Figure 6.2). Sites were located along piezometer transects and positioned immediately adjacent to piezometers (with corresponding numbers P74, P81, P82, P86, P87, and P88). Instrumentation of sites in Harp 3A provided measurements of soil water content at 4 depths that corresponded roughly to the A, upper B, middle to lower B and BC or C horizons (Appendix 3).

Monitoring

Storms were monitored during two seasons: autumn from September 27 to November 20, 1992, and spring from May 2 to June 5, 1993. The autumn was unusually wet with 425 mm of precipitation from August 28 to November 20 and included two large storms on September 18 (39 mm) and September 22 (82 mm).

Volumetric soil water content measurements by TDR were collected prior to storms and several times during the receding limb of runoff events. Water contents were measured in Harp 4-21 from October 10 to November 9, 1992 and from May 2 to May 30, 1993. In

Figure 6.2 Instrumentation of the Harp 4-21 and Harp 3A catchments.

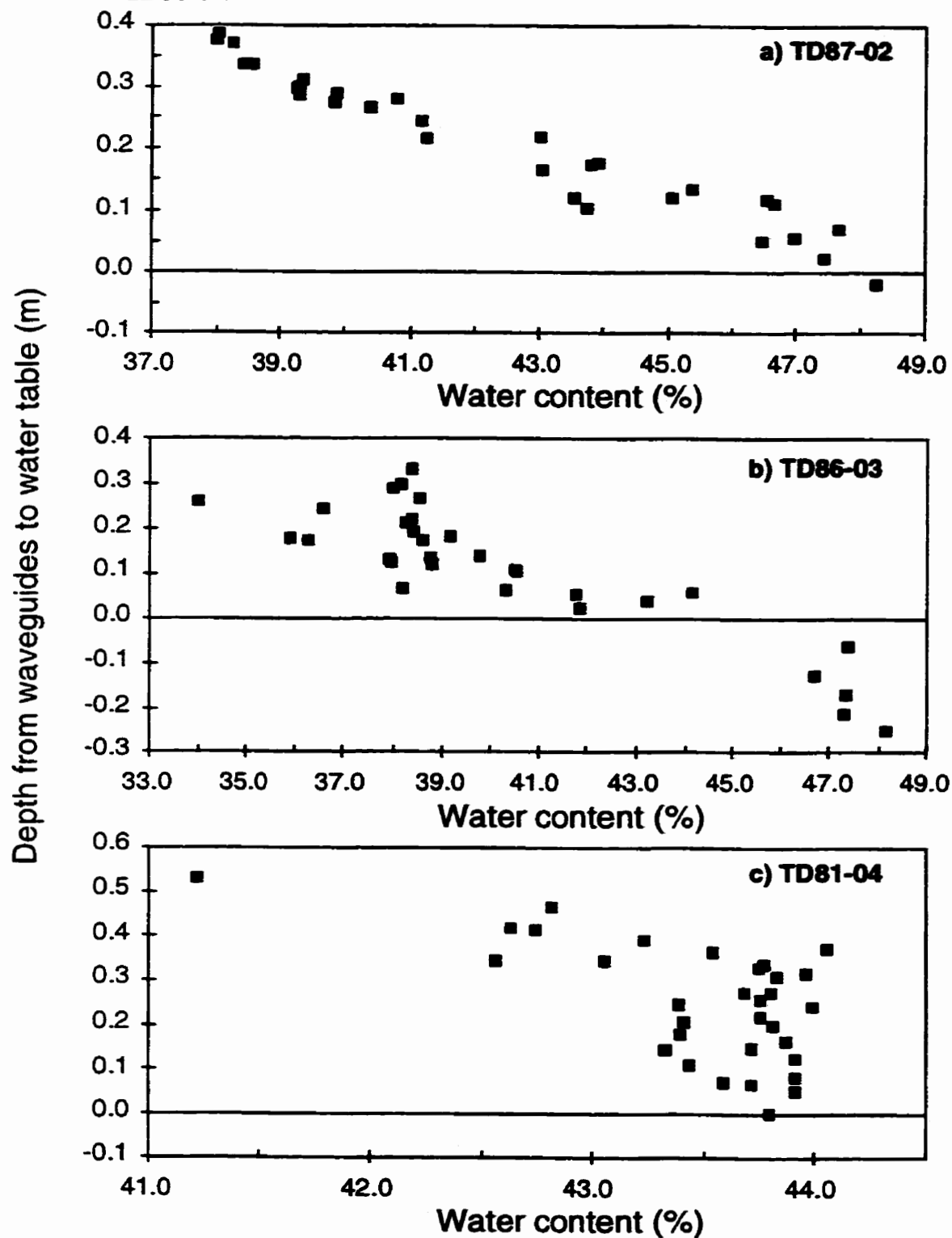


Harp 3A, monitoring began at TD86 on October 9, 1992, and included other sites as instrumentation became operational (up until October 31). TDR sites were monitored until November 20, 1992 and then from May 2 to May 30, 1993. Results of TDR measurements at TD1 and TD74 are not discussed because TD1 remained saturated throughout the study and changes in soil water content at TD74 were influenced by the ephemeral stream flowing past it.

Characteristic curves

In situ characteristic soil moisture curves were estimated from simultaneous measurements of water content and the depth to the water table below the TDR waveguides (MacLean, 1992). Each set of measurements provides one point on the characteristic curve such that several sets of measurements during different soil moisture conditions defines the characteristic curve. Since tensiometers or pressure sensors were not available, direct measurement of pressure head was not possible. Therefore, static conditions were assumed so that the negative pressure head at the waveguides equals the depth of the water table below the waveguides. Potential errors that result from this assumption are considered in Appendix 4. These characteristic curve data usually fit a linear equation since the range of pressure head was generally small (< 0.7 m) (Figure 6.3). There was little decrease in residual error with a polynomial (MacLean, 1992) or the Gardner et al. equation (1970, cited in Hillel, 1971) fit to the data. In some soil horizons, different characteristic curves were obtained for different storms since the water contents represented different drying, wetting or scanning curves. Although these curves do not have the accuracy of laboratory measurements, they do have the distinct advantage of providing field measurements that potentially include the effects of macroporosity.

Figure 6.3 Three examples of soil characteristic curves calculated from water content and water level data (see text for description). a) TD87-02, b) TD86-03 and c) TD81-04.



Saturated water content (or porosity) was taken as the average of the water content measurements when the water table was above the waveguides. Matrix-saturated water content was estimated as the intercept of the (linear) characteristic curve with the water content axis.

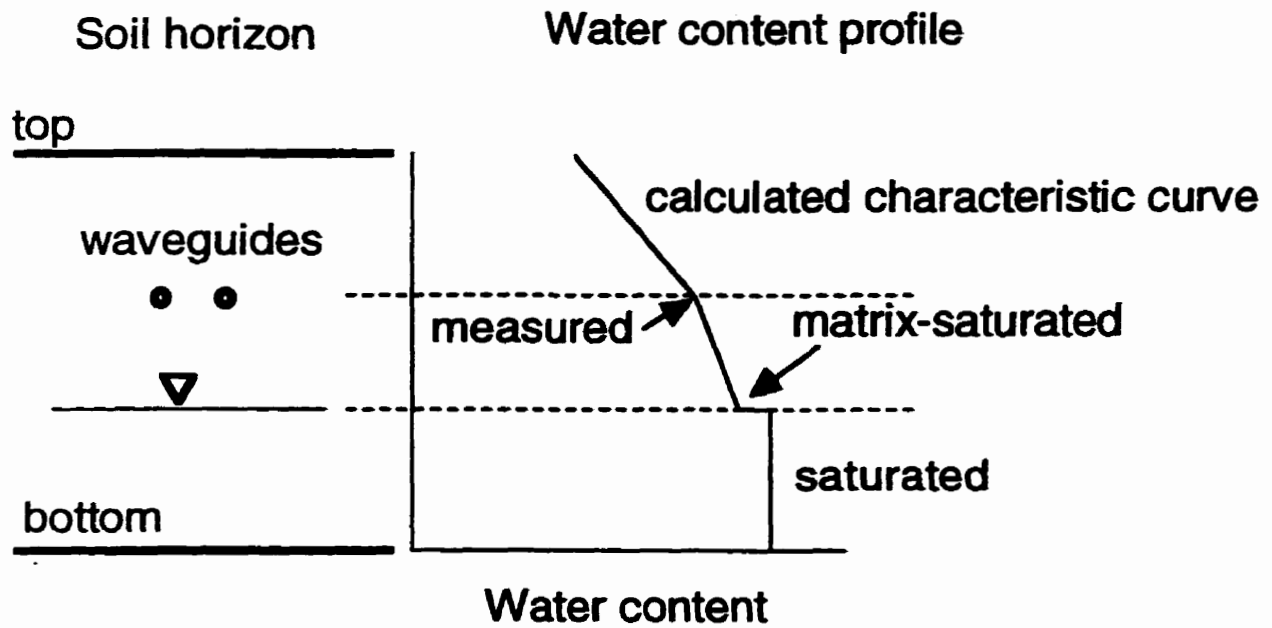
Water storage calculations

To calculate water balances for each site, the total amount of water stored within a soil profile had to be estimated from water content measurements taken at discrete depths. Rather than assuming soil moisture was constant within each soil layer, a moisture profile was estimated for each soil horizon from its water content and the water table depth. In Harp 3A, water storage above bedrock was calculated at each site. In Harp 4-21, water storage was calculated to an arbitrary depth of 1 m below which the water table never dropped, except at TD5 where a depth of 2 m was used.

The water content profile was calculated according to the position of the water table relative to TDR waveguides (Figure 6.4). A saturated water content was always assumed below the water table, a matrix-saturated (i.e. macropores drained) water content immediately above the water table surface. The measured water content at the waveguides was used when the waveguides were above the water table. Above the waveguides, the water content profile was calculated from the characteristic curve of each horizon. A detailed description of the water storage calculation method is presented in Appendix 4.

Possible sources of error in the calculation of water storage for individual soil profiles include errors in water content determination at individual sampling points and errors in water content profiles within a soil. Although no attempt was made to quantify these errors through field sampling of water contents, their relative significance is briefly discussed. The results

Figure 6.4 Water content profile for water storage calculations (see text for description).



presented in this chapter compare changes in water storage over time rather than absolute depths of water stored. Consequently, systematic errors in water storage at a sampling point or within a profile will not influence the interpretations of the changes in water storage.

Errors in volumetric water content determination at individual sampling points using TDR are small. The calibration equations developed by Topp et al. (1980) for four mineral soils of different texture had a water content error estimate of 0.013 (m^3/m^3). Subsequent column and field experiments have shown this method to be accurate to better than 0.03 (Topp et al., 1982a, 1982b; Topp and Davis, 1985). Reproducibility of TDR water content measurements are very small (Baker and Almaras, 1990). For example, the standard deviation of repeated measurement of saturated water content at TD87-04, which remained below the water table for most of the study, was only 0.003.

Errors in water content profiles within a soil can result from an insufficient number of measurement depths. TDR measures water content within a distance of approximately 30 mm transverse to the plane of the waveguides (Baker and Lascano, 1989; for a similar waveguide configuration to that used in this study). Consequently, the entire soil thickness was not sampled and water storage errors could arise particularly where there are contrasting soil horizons that may produce sudden changes in water content. For this reason, TDR waveguides were installed in separate soil horizons and water storage was calculated independently for each horizon. The number of measurement depths were probably adequate to determine water storage within soil profiles except at sites TD4 and TD5 in Harp 4-21 where the shallowest waveguides were 0.28 and 0.29 m below ground surface respectively. The increase in soil moisture in the uppermost horizons at these sites may not have been measured early in the storm and may have produced inaccurate water balances, particularly for measurements immediately after rainfall. Similarly, the water table at TD5 was as much as 1.1 m below the

bottom of the lowest waveguides and, therefore, water content changes in the till could not fully be taken into account. This type of error is thought to be the most significant in this study. However, without detailed soil moisture profiles, it is not possible to quantify the error in water storage within a profile.

Errors in water storage can also result from incorrectly estimated water content profiles within a horizon because characteristic curves are in error or static conditions do not apply. However, these errors should not have had a large influence ($\approx <3$ mm in a horizon) on water storage calculations because the range of pressure heads was small and because the characteristic curve was only used to determine the distribution of water content from a measured data point at the waveguides (Appendix 4). Although the water content profile is an approximation, it makes the best use of the available data and is a better representation than a constant water content profile.

Although it was not possible to quantify the errors in soil water storage within this study, the results show consistent patterns from storm to storm or between sites. Random errors of 5 percent in water content (2 percent absolute water content) over a 0.25 m horizon would have resulted in a 5 mm error in water storage for that horizon. Such an error would not have influenced the conclusions drawn from these results.

Water balance

Water balances of storms were calculated for both the watershed and the individual sites. The water balance for the watershed is:

$$\text{input} - \text{output} = \Delta\text{storage}$$

$$P - (R + ET) = \Delta S \tag{6.1}$$

where P, R, and ET are the depths (volume per unit area) of precipitation, stream runoff, and evapotranspiration respectively, and ΔS is the average net change in storage across the entire watershed expressed as an equivalent depth. During autumn storm events after leaf fall, we can assume that $ET \approx 0$ so that the water balance simplifies to:

$$P - R = \Delta S \quad (6.2)$$

The net change in storage for a watershed was calculated from measurements of P and R. Cumulative summation of P and R measurements since storm onset provided the means to calculate ΔS since the start of an event.

The water balance for each TDR site is:

input - output = Δ storage

$$(P + SSR_i + SR_i) - (SSR_o + SR_o + ET) = \Delta S$$

or

$$P - (\Delta SSR + \Delta SR + ET) = \Delta S \quad (6.3)$$

where SSR is subsurface runoff, SR is surface runoff, the subscripts i and o represent inflow and outflow to the site, $\Delta SSR = SSR_o - SSR_i$, and $\Delta SR = SR_o - SR_i$. Since there was no surface flow at the sites, except at TD1 and TD74 (which are not discussed), the ΔSR term can be dropped. Rearranging terms to put output on the right, yields:

$$P - \Delta S = (\Delta SSR + ET) \quad (6.4)$$

Assuming that evapotranspiration was negligible in the autumn after leaf fall:

$$P - \Delta S = \Delta SSR \quad (6.5)$$

Net subsurface runoff as defined here (ΔSSR) refers to the net depth of subsurface runoff that is generated from a soil profile at an individual site. If the volumes of net subsurface runoff are added from the hilltop to any point n on the hillslope, the sum is equal to the total subsurface runoff (SSR_n) to that point:

$$SSR_n = \Delta SSR_1 * A_1 + \Delta SSR_2 * A_2 + \dots + \Delta SSR_n * A_n \quad (6.6)$$

where A is the hillslope area that generates a depth of net subsurface runoff ΔSSR , and subscripts 1 through n refer to successive portions of the hillslope beginning from the top ($n = 1$). Therefore, if n is located at the base of a hillslope, SSR_n is the subsurface runoff from the entire hillslope. Subsurface runoff generated in upslope soils ($SSR_x > 0$) can either be stored in downslope soils ($\Delta SSR_{x+1} < 0$) or can be transmitted farther downslope and can rapidly produce subsurface flow to the stream. Since SSR_n is defined for the time interval specified by ΔSSR values, SSR_n/time equals the average subsurface flow over this time interval.

These equations can be used to calculate either cumulative water balances from the start of a runoff event or water balances between individual measurements of water storage. To distinguish between the two, cumulative values for a storm will use the prefix " Σ " (as in ΣP , ΣR , $\Sigma \Delta S$, $\Sigma \Delta SSR$), while individual water balances will retain the notation in the equations above. Individual water balances are used to construct hydrographs of subsurface runoff production for individual sites and hillslopes.

Cumulative results can be compared with respect to storage and runoff production. Because $\Sigma \Delta S$ is measured directly for each soil profile, it is possible to compare it to the $\Sigma \Delta S$ for the watershed which is calculated from measurements of $\Sigma P - \Sigma R$ (Equation 6.2). Alternatively, $\Sigma \Delta SSR$ which is calculated from Equation 6.5 can be compared to the measured cumulative stream runoff, ΣR .

The value of calculating water balances for small areas is threefold. Firstly, results can be compared among individual sites to expose the spatial and temporal differences in storage and runoff production. Secondly, water balances from individual sites (Equation 6.5) can be compared to water balances for the entire catchment (Equation 6.2) to determine how individual sites contribute to the stream hydrograph. Thirdly, storage and subsurface runoff from an individual site can be related to its hydraulic properties and reveal some of the factors that affect subsurface runoff response.

Subsurface runoff ratio

To measure the efficiency of subsurface runoff production at a site in response to a storm event, the subsurface runoff ratio is defined as:

$$\text{subsurface runoff ratio} = \text{SSRR} = \frac{\sum \Delta \text{SSR}}{\sum P} \quad (6.7)$$

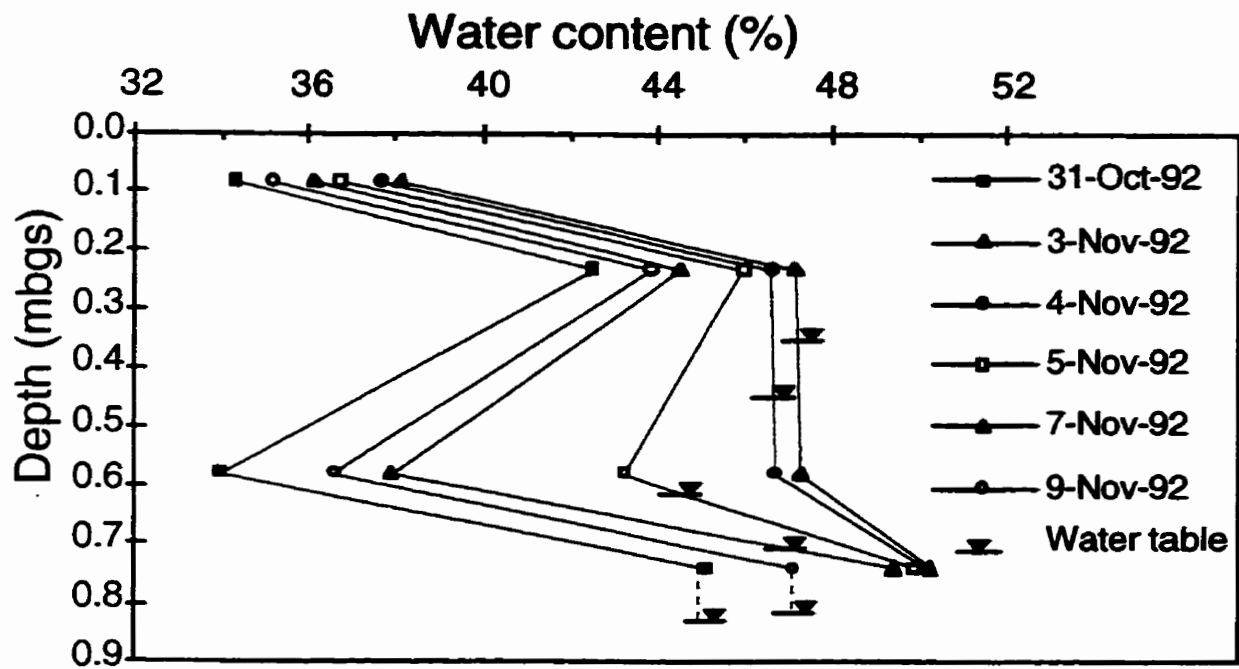
where $\sum \Delta \text{SSR}$ is the cumulative net subsurface runoff (Equation 6.5) and $\sum P$ is cumulative depth of precipitation for the storm event. It is analogous to the effective runoff ratio (Chapter 5) but does not take into account natural drainage of the soil in the absence of precipitation.

Results

Water content and soil characteristic curves

Although MacLean (1992) reported the presence of a 0.7 m capillary fringe based on similarly obtained characteristic curves, data from several sites suggest that a capillary fringe is absent in most soils within the two catchments. Most soils horizons showed a decrease in water content when the water table dropped below the TDR waveguides (Figure 6.5). Consequently, characteristic curves showed a decrease in water content at small negative pressure heads (e.g. Figure 6.3a and b). Only three characteristic curves suggested the

Figure 6.5 Water content profiles and water table fluctuations at TD86 during the November 2 and 4 event (46 mm precipitation).



presence of a significant capillary fringe (TD5-02, TD5-03, and TD81-04; Figure 6.3c) varying in thickness from 0.4 to 0.8 m. Although most sites did not have a capillary fringe, characteristic curves of some sites were gently sloping, which suggests that a small input of infiltrating water could produce a substantial rise in the water table.

An interesting result for several characteristic curves was the large change in water content (up to 5 percent) between measurements taken during saturated conditions and under slightly negative pressure heads (when the water table was just below the waveguides) (Figure 6.3b). This difference suggests that a portion of the total porosity, which likely corresponds to the larger pores (>1.5 mm), drained under very small tensions (<0.01 m) as was discussed in Chapter 2. Such large changes in water content near the water table demonstrate the importance of accounting for water table position and water content profiles in water storage calculations.

Cumulative water balances

The magnitude of changes in depth of water stored at each TDR site during autumn and spring increased with increasing distance from the Harp 4-21 stream (TD2 < TD3 ≈ TD4 < TD5) (Figures 6.6 and 6.7 respectively). In Harp 3A, no distinct spatial pattern emerged along the transects although TD86 consistently showed the largest fluctuations in soil water storage. The changes in water storage were similar at sites TD3, TD4, TD81, TD87 and TD88.

1) November 2 and 4, 1992 event in Harp 4-21

Changes in cumulative water storage ($\sum\Delta S$) measured by TDR during the November 2 and 4 event were much smaller at TD2 than the average cumulative change in water storage over the entire Harp 4-21 watershed ($\sum P - \sum R$) (Equation 6.2, Figure 6.8a). In contrast, changes in storage at TD3 were similar to the average watershed response. Cumulative water

Figure 6.6 Water storage during the autumn monitoring period in a) Harp 4-21 and b) Harp 3A. Monitoring site locations are shown in Figure 6.2.

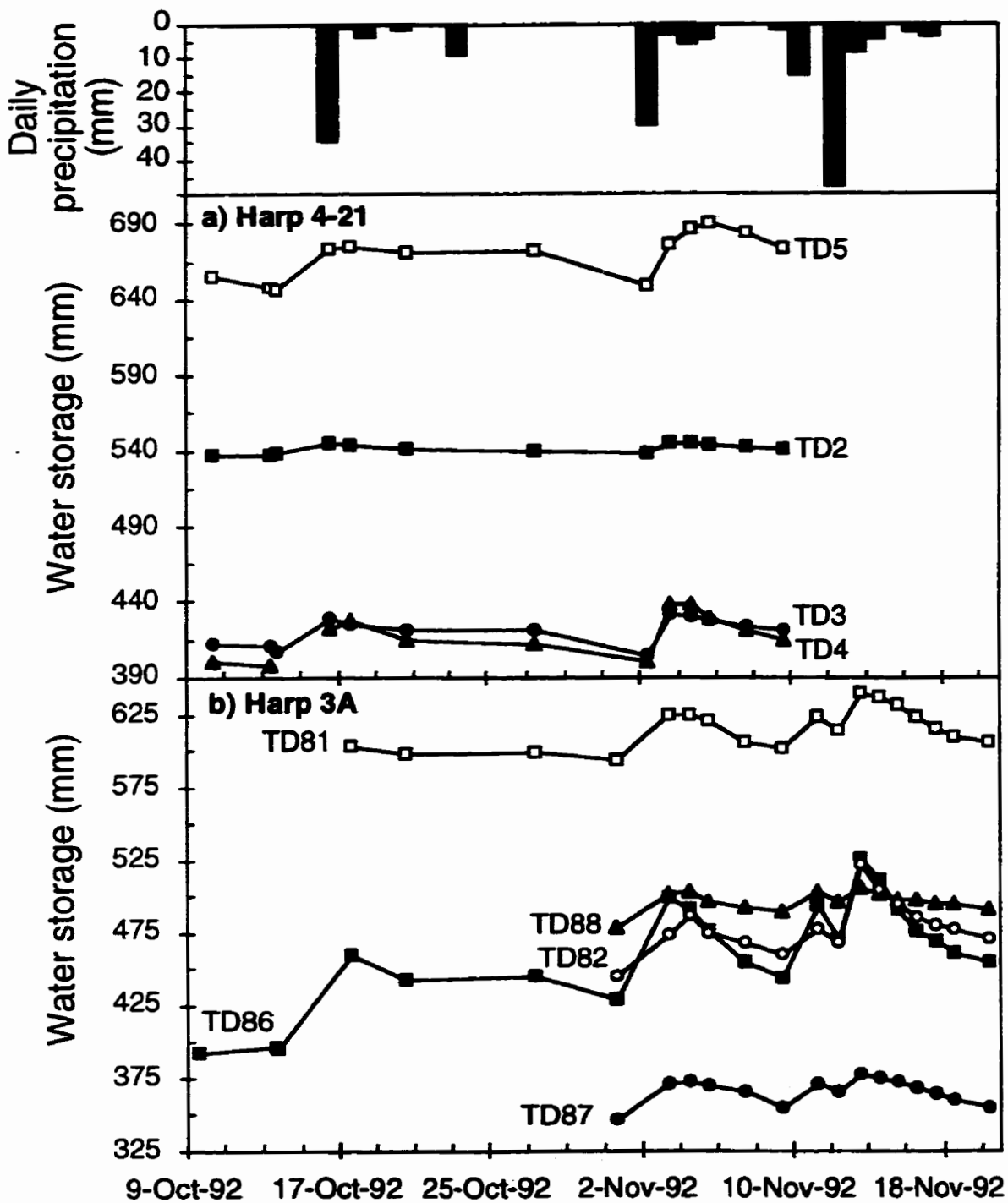


Figure 6.7 Water storage during the spring monitoring period in a) Harp 4-21 and b) Harp 3A. Monitoring site locations are shown in Figure 6.2.

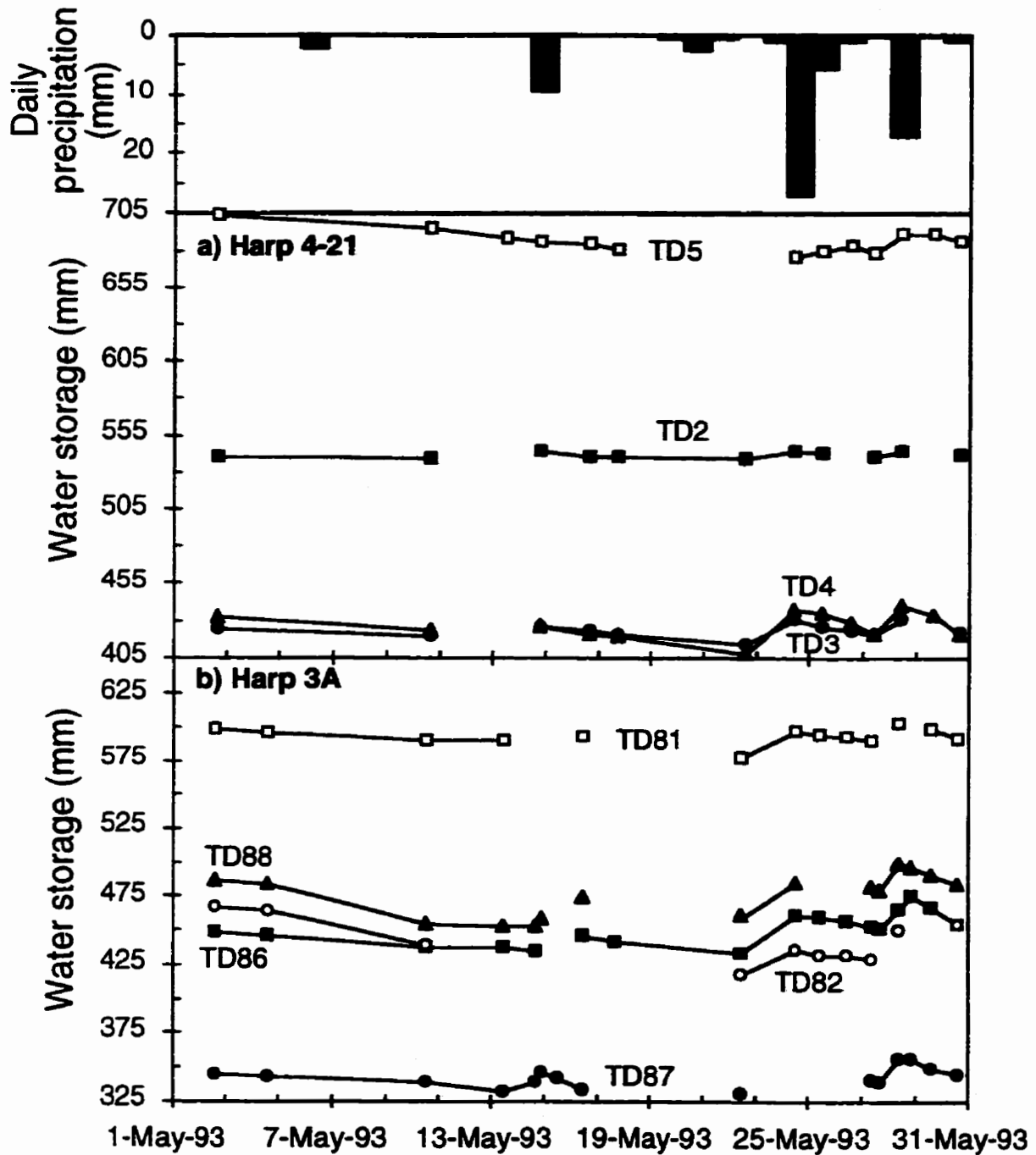
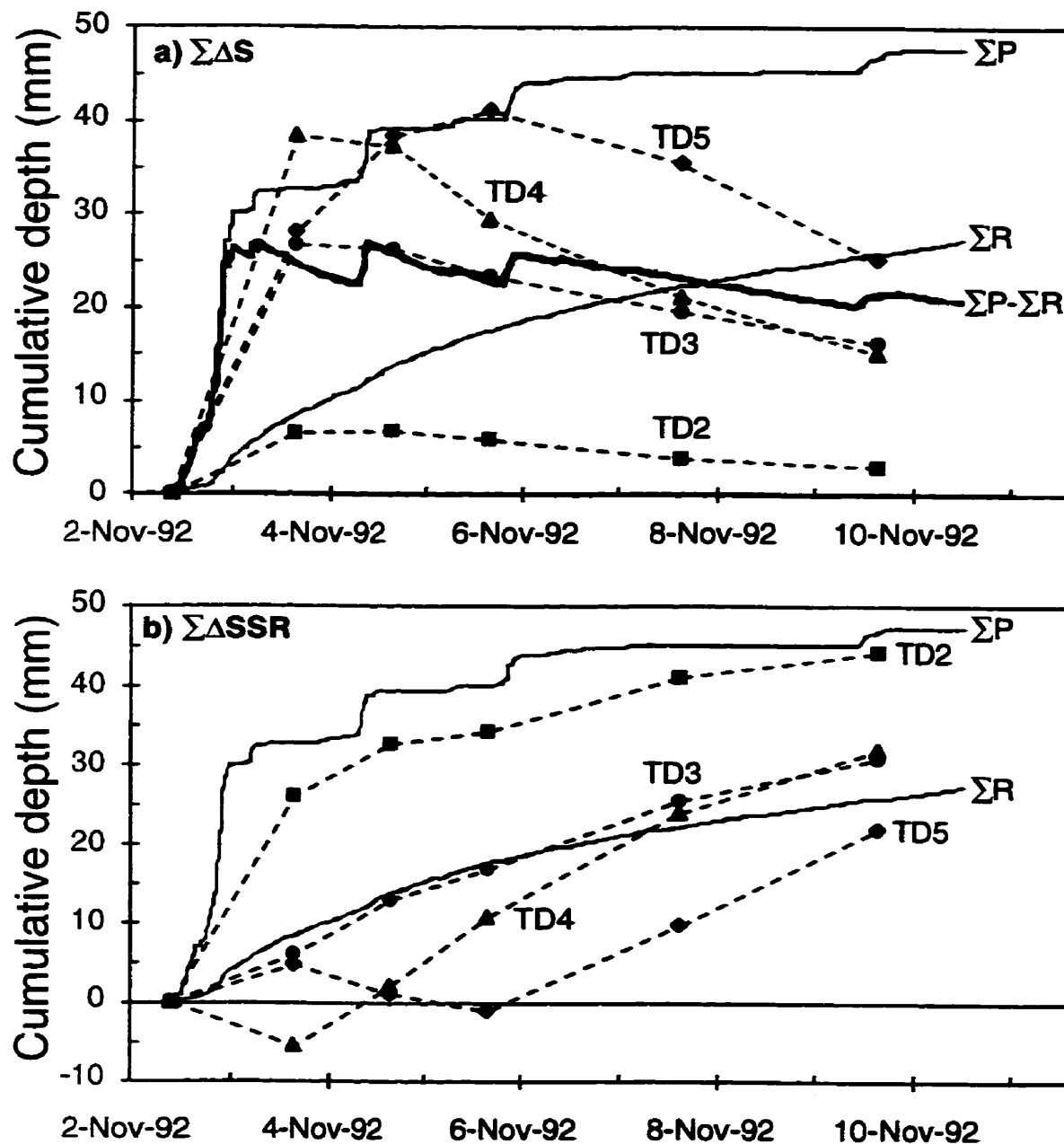


Figure 6.8 Cumulative a) water storage ($\Sigma\Delta S$) and b) net subsurface runoff ($\Sigma\Delta SSR$) in Harp 4-21 during the November 2 and 4, 1992 event (dashed lines). Cumulative precipitation (ΣP), depth of stream runoff (ΣR) and change in storage over the entire catchment ($\Sigma P - \Sigma R$) are shown for comparison (solid lines).



storage was greater at TD4 than for the entire Harp 4-21 watershed until November 6 and was greater at TD5 for the duration of the storm.

At TD2, very little of the storm precipitation contributed to increasing water storage (Figure 6.8a). Prior to these storms, the soil near the stream at TD2 was close to saturation with an available water storage depth of only 12 mm. Consequently, all the excess precipitation must have produced runoff. Despite the small available water storage, the water table did not rise to the ground surface and the soil profile never became fully saturated at TD2 because of its location within a small hummock (Figure 6.9). The absence of any ponding at the surface indicated that the shallow soils were sufficiently permeable to transmit all the infiltration and subsurface flow from upslope.

Most of the storm precipitation at TD3 and all at TD4 and TD5 initially contributed to increasing soil water storage (Figure 6.8a). The initial water table positions were deeper at TD3 and TD4 than at TD2 (Figure 5.9) with correspondingly higher available storages of 48 and 50 mm respectively (Figure 6.9). Most of the increase in water storage (>70%) actually occurred in the upper soil horizons above the rising water table (Figure 6.10). At TD5, the water table was deeper (1.7 m) and the available water storage larger (117 mm) to allow storage of all the infiltrating rain water in the soil profile for more than a day after the storm (Figure 6.8a).

Subsurface runoff production in Harp 4-21 occurred most rapidly near the stream and was delayed farther upslope. Figure 6.8b clearly demonstrates the difference in the timing of subsurface runoff generation between the sites. Near the stream at TD2, nearly all the precipitation generated subsurface runoff with little or no delay. Farther from the stream at TD3 and TD4, subsurface runoff was produced more gradually at a nearly constant rate

Figure 6.9 Available water storage in different TDR profiles in Harp 4-21 during the November 2 and 4, 1992 event.

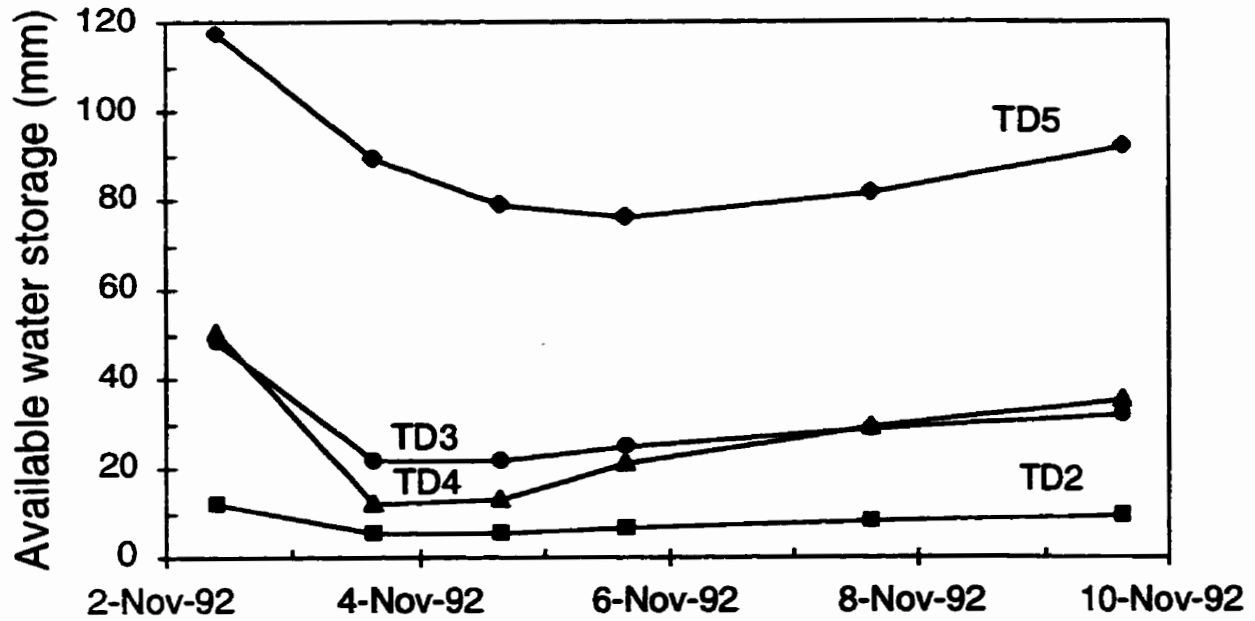
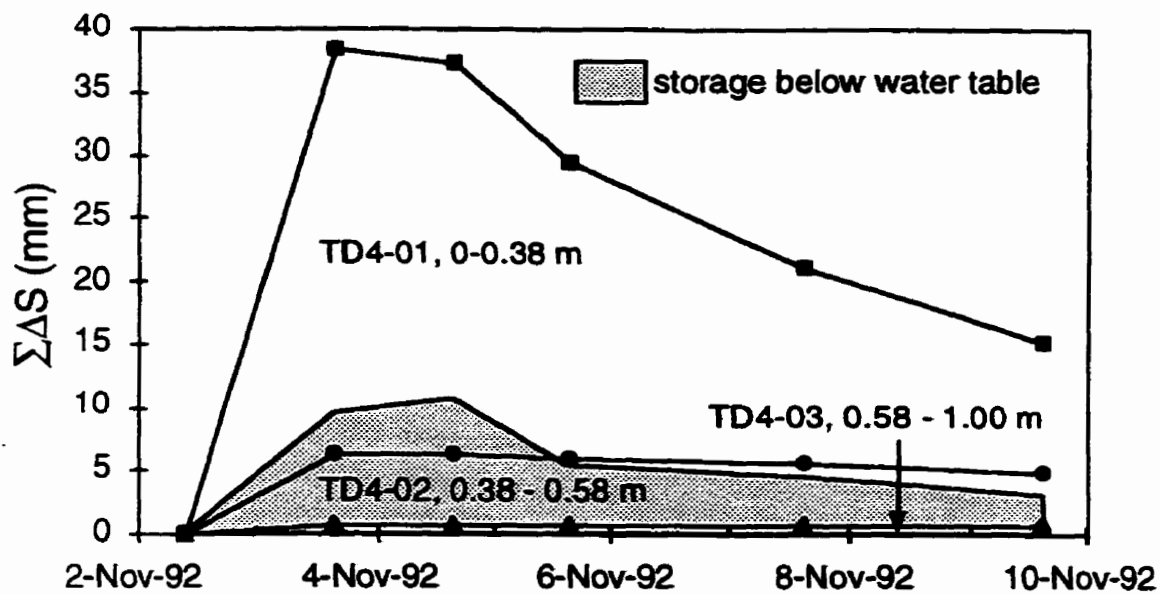


Figure 6.10 Cumulative water storage ($\Sigma\Delta S$) within the TD4 profile during the November 2 and 4, 1992 event. Curves indicate the total $\Sigma\Delta S$ from the lowest horizon (i.e. curve TD4-01 indicates total $\Sigma\Delta S$ from 0 to 1.00 m). Shaded area indicates the $\Sigma\Delta S$ that is stored below the water table.



throughout the event although there was a slight initial delay in the response at TD4. At TD5, subsurface runoff production was delayed several days and occurred predominantly on the falling limb of the second hydrograph.

Cumulative net subsurface runoff ($\Sigma\Delta SSR$) was generally largest where the water table was shallowest and smallest where it was deepest. In Harp 4-21, subsurface runoff ratios (Equation 6.7) were always largest (> 92%) at TD2 where the water table was nearest to the surface. Ratios were smaller (>65%) at TD3 and TD4 where the water table was deeper but remained in the soil horizons. They were smallest (47-56%) at TD5 where the water table was below the soil horizons (Table 6.1). Lower hillslopes and near-stream areas contributed more to subsurface runoff than other portions of the watershed since more runoff was produced from sites TD2, TD3 and TD4 than the observed average stream runoff (Table 6.1, Figure 6.8b).

2) November 2 and 4, 1992 event in Harp 3A

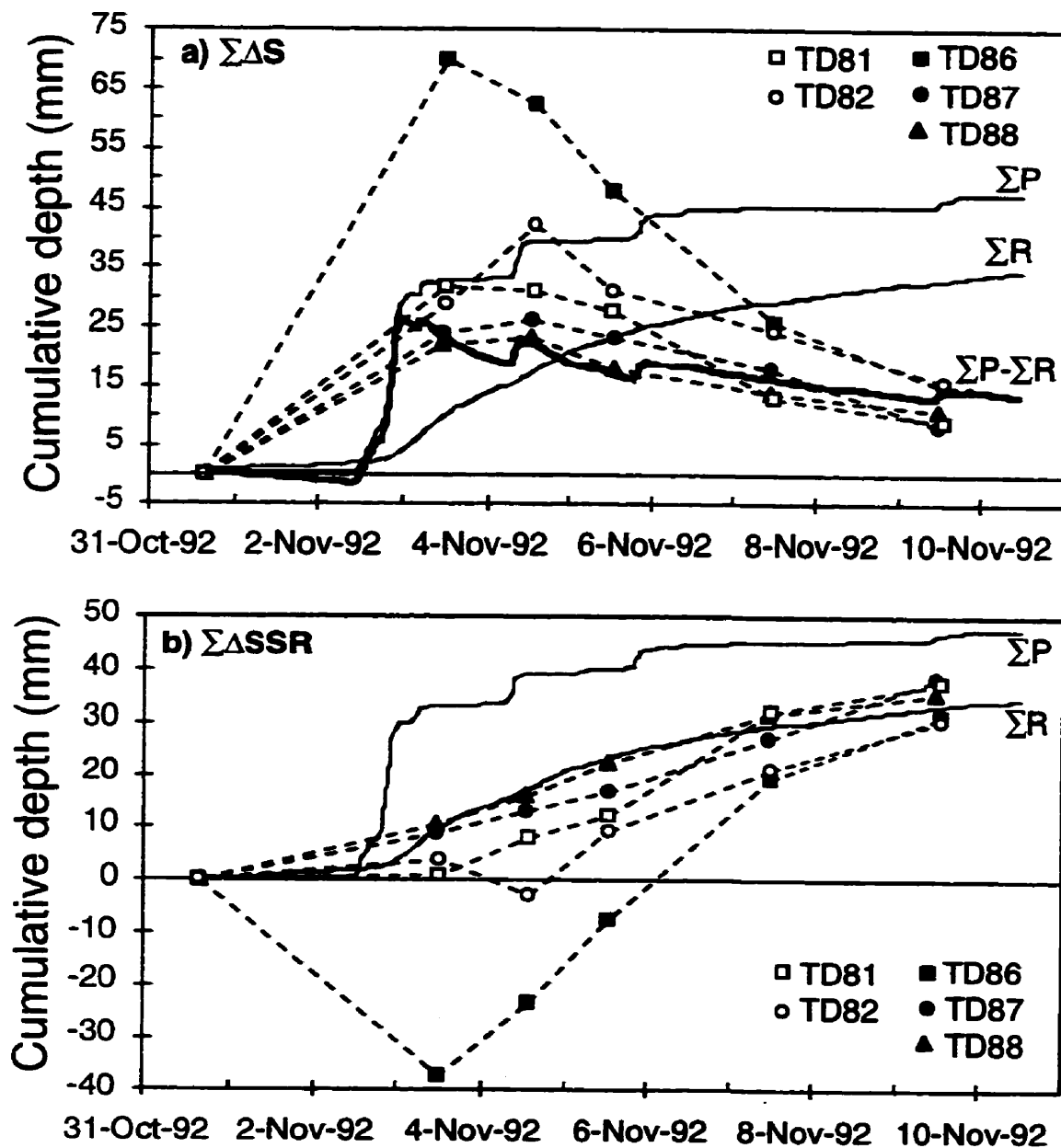
The sites in Harp 3A did not demonstrate distinct spatial and temporal patterns of water storage and subsurface runoff production. At midslope sites TD87 and TD88, the cumulative changes in water storage ($\Sigma\Delta S$) measured by TDR were similar to the average of the watershed as a whole ($\Sigma P - \Sigma R$) (Equation 6.2, Figure 6.11a). At TD81 and TD82, the precipitation from the November 2 storm was entirely stored within the soil. Soils at TD81 began to drain after the storm, but those at TD82 also stored the additional precipitation from the November 4 storm before draining. The initial increase in cumulative storage at TD86 was much greater than the cumulative precipitation for the entire event (Figure 6.11a). This anomalous result could only have occurred if there was a net contribution to water storage by subsurface flow from upslope or if focusing of infiltration occurred above the measurement site. Focusing of infiltration probably did not occur because there was no overland flow at

Table 6.1. Cumulative subsurface runoff ($\Sigma\Delta SSR$) during storms in Harp 4-21.

Storm period		ΣP (mm)	ΣR (mm)	$\Sigma\Delta SSR$ (mm)				
Start	End		S1	TD2	TD3	TD4	TD5	
13-Oct-92 10:45	20-Oct-92 15:48	44.4	17.0	41.0	33.5	28.4	20.9	
2-Nov-92 09:46	9-Nov-92 15:22	47.1	25.7	44.2	30.9	32.0	22.0	
22-May-93 14:52	27-May-93 12:47	36.2	13.8	34.0	30.0	23.4	-	
27-May-93 12:47	30-May-93 16:43	18.0	9.4	17.2	17.2	18.7	10.1	
			$\frac{\Sigma R}{\Sigma P}$	$\frac{\Sigma\Delta SSR}{\Sigma P}$				
13-Oct-92 10:45	20-Oct-92 15:48		0.38	0.92	0.75	0.64	0.47	
2-Nov-92 09:46	9-Nov-92 15:22		0.55	0.94	0.66	0.68	0.47	
22-May-93 14:52	27-May-93 12:47		0.38	0.94	0.83	0.65	-	
27-May-93 12:47	30-May-93 16:43		0.53	0.96	0.96	1.04	0.56	

Spring storms are not corrected for evapotranspiration.

Figure 6.11 Cumulative a) water storage ($\Sigma\Delta S$) and b) cumulative net subsurface runoff ($\Sigma\Delta SSR$) in Harp 3A during the November 2 and 4, 1992 event (dashed lines). Cumulative precipitation (ΣP), depth of stream runoff (ΣR) and change in storage over the entire catchment ($\Sigma P - \Sigma R$) are shown for comparison (solid lines).



TD86 and surface topography was uniform. The absence of nearby trees also precluded the focusing of infiltration by stemflow. Therefore, this site temporarily stored subsurface flow from upslope. After November 3, TD86 drained rapidly and produced a cumulative net change in water storage similar to the catchment average by November 9.

In contrast to Harp 4-21, the increase in storage in Harp 3A occurred mostly in the transiently saturated zone (Figure 6.12) rather than in the unsaturated zone above the rising water table. Infiltrating precipitation rapidly penetrated into the deeper soil horizons and must have flowed through or bypassed available water storage in the upper horizons. The large increase in water storage at TD86 was caused by saturating the lower B horizon (Figure 6.12) which has a steep characteristic curve (approximately 9% decrease in water content between 0 and 0.25 m water table depth, Figure 6.3b).

The different sites in Harp 3A contributed similar depths of subsurface runoff over the duration of the entire event (Table 6.2), but timing of runoff production differed substantially among the sites (Figure 6.11b). TD87 and TD88 produced runoff with similar timing to the catchment average. TD81 was slightly delayed; TD82 was delayed almost until after the November 4 storm. Negative cumulative net subsurface runoff ($\Sigma\Delta SSR$) at TD86 indicates net water storage until November 6.

3) November 10 and 12, 1992 event in Harp 3A

Results for the November 10 and 12 event were similar to those for the November 2 and 4 event in Harp 3A. Cumulative net subsurface runoff ($\Sigma\Delta SSR$) at TD87 and TD88 was similar to cumulative stream runoff (ΣR) at W1; $\Sigma\Delta SSR$ was similar but slightly delayed at TD81, and delayed at TD82 for almost a day after the November 12 storm. Soils at site TD86

Figure 6.12 Cumulative water storage ($\Sigma\Delta S$) within the TD86 profile during the November 2 and 4, 1992 event. Curves indicate the total $\Sigma\Delta S$ from the lowest horizon (i.e. curve TD86-01 indicates total $\Sigma\Delta S$ from 0 to 1.06 m). Shaded area indicates the $\Sigma\Delta S$ that is stored below the water table.

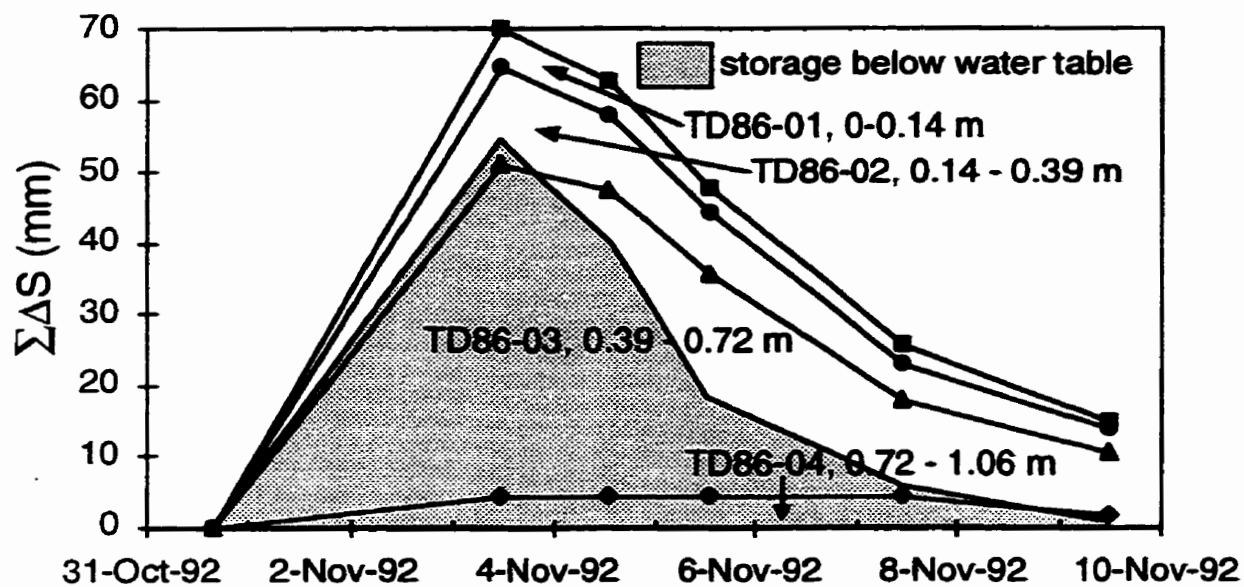


Table 6.2. Cumulative net subsurface runoff ($\Sigma\Delta SSR$) during storms in Harp 3A.

Storm period		ΣP (mm)	ΣR (mm)	$\Sigma\Delta SSR$ (mm)					
Start	End		W1	TD86	TD87	TD88	TD81	TD82	
13-Oct-92 18:24	31-Oct-92 15:54	58.3	33.8	24.3	-	-	-	-	
31-Oct-92 15:54	9-Nov-92 11:54	46.3	33.9	31.4	38.2	35.3	37.5	30.5	
9-Nov-92 11:54	20-Nov-92 10:25	81.9	71.5	70.3	82.0	81.6	78.5	71.8	
22-May-93 11:58	27-May-93 10:39	36.2	6.3	18.4	27.6	16.3	24.2	-	
27-May-93 18:20	30-May-93 15:06	18.0	5.5	14.2	13.5	14.0	16.3	-7.8	
			$\frac{\Sigma R}{\Sigma P}$			$\frac{\Sigma\Delta SSR}{\Sigma P}$			
13-Oct-92 18:24	31-Oct-92 15:54		0.58	0.42	-	-	-	-	
31-Oct-92 15:54	9-Nov-92 11:54		0.73	0.68	0.82	0.76	0.81	0.66	
9-Nov-92 11:54	20-Nov-92 10:25		0.87	0.86	1.00	1.00	0.96	0.88	
22-May-93 11:58	27-May-93 10:39		0.17	0.51	0.76	0.45	0.67	-	
27-May-93 18:20	30-May-93 15:06		0.31	0.79	0.75	0.78	0.91	-0.44	

Spring storms are not corrected for evapotranspiration. Storm periods differ slightly for TD81 and TD82.

again showed net water storage (mostly in the lower B horizon) and delayed subsurface runoff production until after the second rainfall event (Figure 6.13). However, the magnitude of subsurface runoff production was similar at all sites (86 to 100% of precipitation; Table 6.2). Given that stream runoff at W1 was 87% of precipitation, subsurface runoff must have been produced throughout most of the Harp 3A.

4) Water redistribution during dry periods

A period of hot, dry weather during rapid leaf growth (May 2 to 13, 1993) caused water storage to decrease most at sites TD82 and TD88 (> 29 mm) and least at site TD2 (1 mm) (Figure 6.7). Water storage decreased as a result of both subsurface runoff production and evapotranspiration. Very low stream discharge at W5 (see below) indicated that much of the decrease in water storage in Harp 3A was caused by evapotranspiration rather than subsurface runoff. The total amount of $\sum(\Delta\text{SSR} + \text{ET})$ at all sites exceeded the average depth of stream runoff at W5 by 8 to 34 mm. Assuming $\sum\Delta\text{SSR} = \sum\text{R}$ at W5 for this dry weather period, the average evapotranspiration rate for the TDR sites in Harp 3A was 1.9 ± 1.3 mm/day. Energy budget estimates of lake evaporation of up to 2.6 mm/day for Harp Lake over the same time period in previous years demonstrate that this estimate is reasonable (Scheider et al., 1983).

With this estimate of evapotranspiration, it was possible to determine $\sum\Delta\text{SSR}$ at individual sites (Equation 6.4). Although these $\sum\Delta\text{SSR}$ values (corrected for $\sum\text{ET}$) are approximate, upslope sites (TD82 and TD88) indicated net subsurface outflow, ($\sum\Delta\text{SSR} > 0$) whereas downslope sites (TD81, TD86, and TD87) indicated net subsurface inflow ($\sum\Delta\text{SSR} < 0$) (Figure 6.14a). Therefore, drainage of upslope sites displaced water to downslope sites where it was available for evapotranspiration. If the same evapotranspiration rates are assumed for Harp 4-21, $\sum\Delta\text{SSR}$ becomes negative for all sites, and indicates net subsurface inflow

Figure 6.13 a) Cumulative water storage ($\Sigma\Delta S$) and b) cumulative net subsurface runoff ($\Sigma\Delta SSR$) in Harp 3A during the November 10 and 12, 1992 event (dashed lines). Cumulative precipitation (ΣP), depth of stream runoff (ΣR) and change in storage over the entire catchment ($\Sigma P - \Sigma R$) are shown for comparison (solid lines).

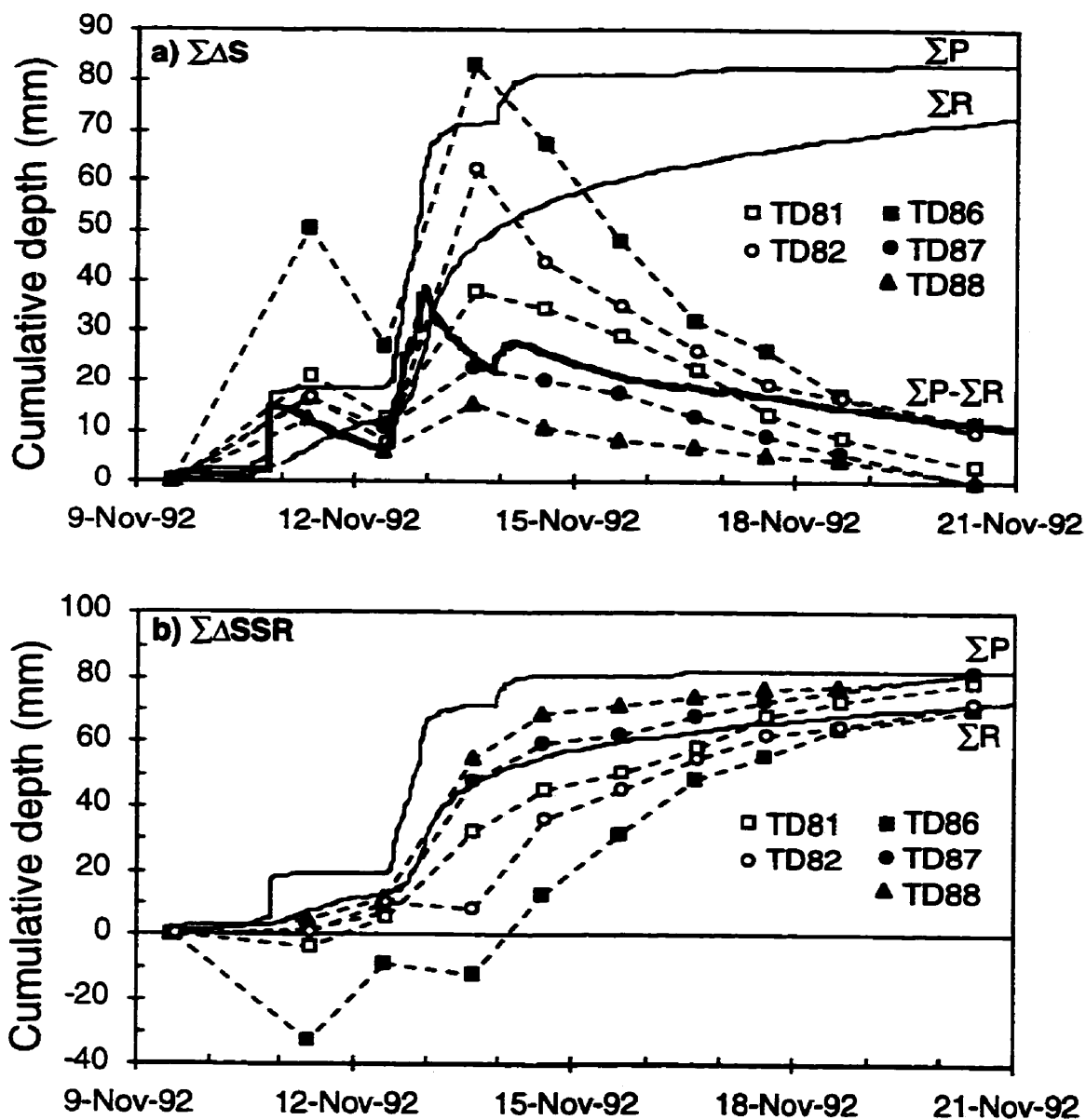
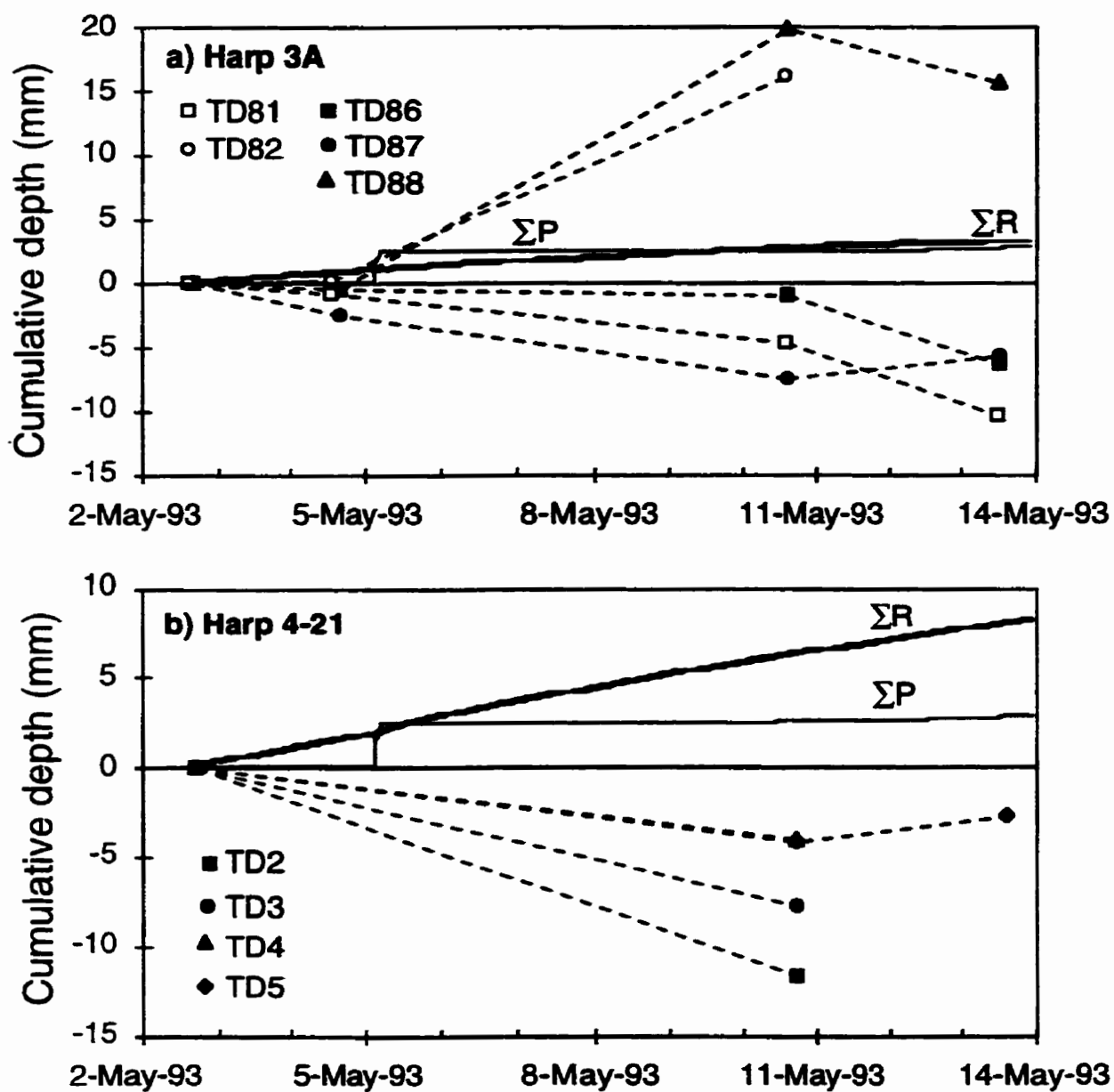


Figure 6.14 Cumulative net subsurface runoff ($\Sigma\Delta SSR$) in a) Harp 3A and b) Harp 4-21 during the dry period in early May, 1993. Net subsurface runoffs have been adjusted for an average evapotranspiration rate of 1.9 mm/d (see text).



(Figure 6.14b). Consequently, stream baseflow during this period was sustained by changes in storage in areas upslope of TD5.

Subsurface flow from upslope influenced groundwater levels and stream baseflow differently in the two catchments. In Harp 3A, the water table declined below the base of the B soil horizon at several sites and disappeared below the piezometer at TD82. During this period, baseflow at W5 decreased fourfold to 0.1 l/s or 0.2 mm/day. In Harp 4-21, stream discharge decreased by only 25% to 0.55 l/s or 1.3 mm/day on May 13. Despite more stream runoff in Harp 4-21, the water table remained within the soil horizon upslope beyond P06 (TD4).

Soil moisture measurements during the summer confirmed that groundwater flow from upslope had a measurable effect on moisture conditions in near-stream areas and lower hillslopes of Harp 4-21. In comparison to the large decreases in soil water storage in Harp 3A (128-173 mm) from late May to late August, water storage in Harp 4-21 decreased by only 23 to 106 mm (from TD2 to TD5, Table 6.3). The smaller decrease in soil water storage at all Harp 4-21 TDR sites demonstrates that subsurface flow from upslope maintained wetter soil conditions throughout the entire lower hillslope and near-stream areas. Although storm water balances were not measured during summer storms, it is evident why no storm runoff was produced in Harp 3A from a storm in late August (Chapter 5). Soil water contents had decreased between 0.10 and 0.21 (m^3/m^3) since the end of May so that there was a large capacity to retain infiltrating precipitation. Since most of the precipitation onto hillslopes in Harp 3A generated subsurface runoff during storms in wet periods (Table 6.2), precipitation from these storms was not stored and could not sustain groundwater levels and baseflow during dry periods.

Table 6.3. Change in soil water storage during the summer.

Harp 3A	Soil water storage (mm)				
	TD86	TD87	TD88	TD81	TD82
30-May-93 15:06	455.0	344.0	484.4	590.8	455.1
26-Aug-93 13:45	294.5	216.2	331.3	417.9	289.3
change	160.4	127.8	153.0	172.9	165.8

Harp 4-21	TD2	TD3	TD4	TD5
	30-May-93 16:43	541.5	421.2	420.2
26-Aug-93 12:13	518.6	369.3	330.6	579.5
change	22.9	51.9	89.6	106.3

5) Spring storm events

Quantitative interpretation of the combined $\Sigma(\Delta\text{SSR} + \text{ET})$ results during the spring storms was complicated by evapotranspiration which was not measured. However, $\Sigma(\Delta\text{SSR} + \text{ET})$ represented the maximum subsurface runoff since $\Sigma\text{ET} > 0$. Some qualitative observations show that the spring storm response was similar to that of autumn storms. Firstly, subsurface runoff production in Harp 4-21 was greatest and most rapid at TD2 and decreased and was more delayed with increasing distance from the stream (Table 6.1). Secondly, the timing of subsurface runoff at TD86 was delayed by temporary storage of runoff from upslope ($\Sigma\Delta\text{S} > \Sigma\text{P}$).

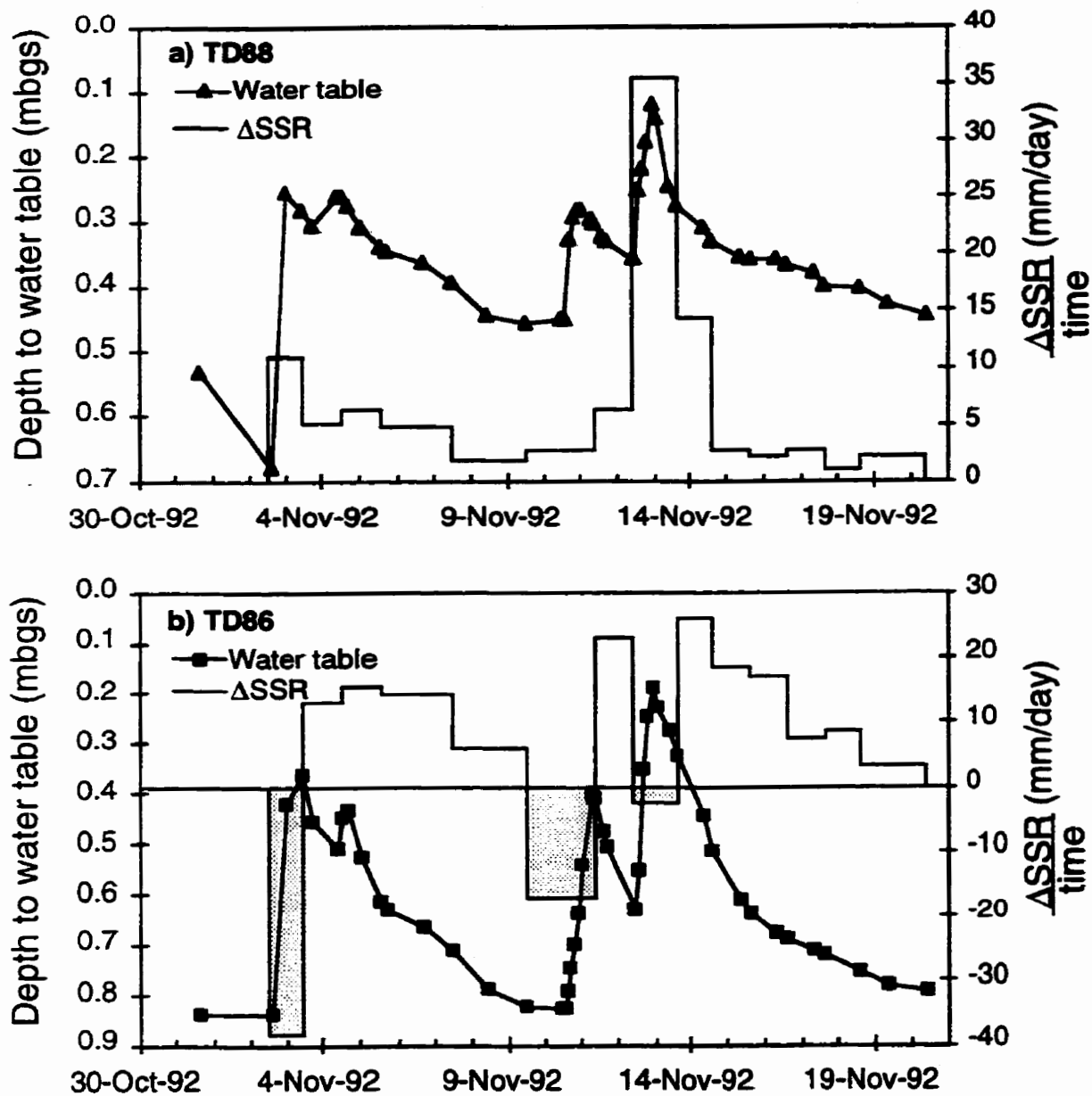
Individual water balances

1) Changes in net subsurface runoff and groundwater levels

Subsurface flow production ($\Delta\text{SSR}/\text{time}$) and water table fluctuations at site TD88 occurred simultaneously for storms in November, 1992 (Figure 6.15a). Since downslope hydraulic gradients were nearly constant (Chapter 5), groundwater levels fluctuated to accommodate subsurface flow from upslope. Therefore, the timing of subsurface flow at TD88 was similar to that generated farther upslope in Harp 3A. Consequently, upslope extrapolation of subsurface runoff production at TD88 is justified. Poor correspondence between groundwater levels and subsurface flow at sites TD82 and TD5 preclude the possibility of extrapolating these results to upslope areas.

Peak subsurface flow from TD86 did not necessarily occur when groundwater levels peaked. In contrast to TD88, most of the subsurface runoff at TD86 was generated when the lower B horizon drained coincidentally with the drop in the water table (Figures 6.15b and 6.12).

Figure 6.15 Net subsurface flow ($\Delta SSR/\text{time}$) and water table fluctuations at a) TD88 and b) TD86 during November, 1992 events. Shaded areas indicate net inflows. mbgs = meters below ground surface.



2) *Total hillslope runoff*

The depth of subsurface runoff produced along the hillslope can be calculated by extrapolating subsurface runoff production at sites TD86, TD87 and TD88 to larger hillslope areas (delimited by the midpoints between successive sites) and summing them (Equation 6.6). The response at TD88 was extrapolated to the top 130 m of the hillslope, at TD87 to 26 m along the midslope region and at TD86 to 14 m along the lower midslope. The bottom 13 m of the hillslope was assumed to produce runoff equivalent to 100% of the precipitation without delay because groundwater levels were close to ground surface. Since the topography of this hillslope transect does not converge or diverge, a unit hillslope width was assumed. The net hydrograph for the hillslope during autumn storms, that was determined from ΔSSR values, correlates to the stream discharge at W1 (calculated for the same time steps) (Figure 6.16) and is further evidence that these soil water balances for individual sites are representative of larger hillslope areas.

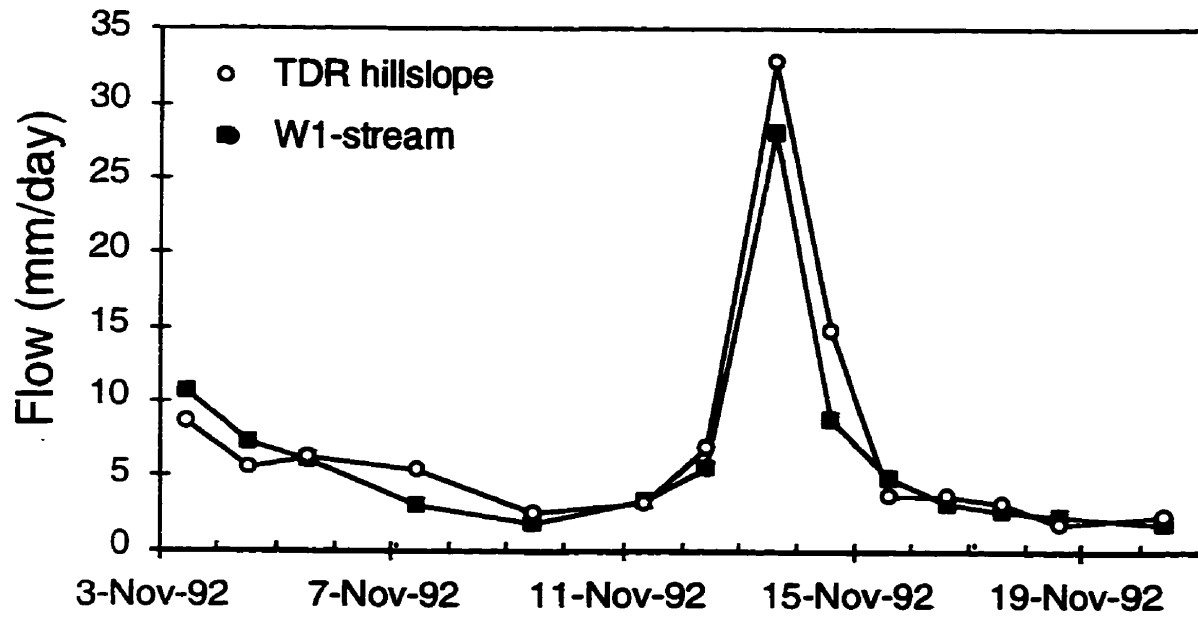
3) *Calculation of hydraulic conductivity*

Subsurface runoff measurements at individual sites can be used to calculate hydraulic conductivities within the soil profiles by Darcy's Law because they are based on water balance data (SSR_n , Equation 6.6) and, therefore, are independent of groundwater level data. Darcy's law can be expressed as:

$$Q = K_s i A_c \quad (6.8)$$

where Q is the volumetric flow rate, K_s is the saturated hydraulic conductivity, i is the hydraulic gradient and A_c is the cross-sectional area. For a 1 m width of hillslope, $A_c = h * 1$

Figure 6.16 Total subsurface flow (SSR/time) from TDR hillslope (TD86-TD87-TD88) and stream discharge for Harp 3A (W1) during November, 1992 events. Total subsurface flow is normalized to hillslope area and stream discharge to catchment area for comparison.



where h is the depth of saturated soil. Equation 6.8 then becomes:

$$K_s = \frac{Q}{h} * \frac{1}{i} \quad (6.9)$$

Since the downslope hydraulic gradients remain nearly constant over time (Chapter 5), K_s will be directly proportional to the slope of a plot between Q (SSR_n/time) and groundwater level. This calculation assumes that all the subsurface flow is produced by saturated flow.

Subsurface flow increased gradually with increasing groundwater levels in the lower portion of the soil profile and rapidly in the upper portion of the profile at sites TD86, TD87 and TD88 (Figure 6.17). The distinctly different slopes within the profile indicate that the hydraulic conductivity of the upper soil horizons were approximately one order of magnitude greater than those in lower horizons (Table 6.4). The large increase in hydraulic conductivity in the upper 0.4 m of the soil profile corresponds approximately to the boundary between the upper and lower B horizons. Higher hydraulic conductivity in the upper B horizon may be related to greater root density, lower bulk density and better soil structure (e.g. aggregation) as a result of greater biological activity (Table 6.5, Lozano et al., 1987).

As groundwater levels rose to saturate upper soil horizons with higher hydraulic conductivities, greater fluxes of subsurface flow were transmitted. Consequently, during the large and intense rainstorm on November 12, 1992 (82 mm), these soils had the capacity to transmit subsurface flow without groundwater levels reaching ground surface.

Discussion

Magnitude and area of subsurface runoff production

The magnitude of cumulative subsurface storm runoff for a given site is determined by the change in soil water storage between the start and the end of a storm (Equation 6.5). The

Figure 6.17 Total subsurface flow (SSR/time) vs. maximum groundwater levels at a) TD88, b) TD87 and c) TD86. Total subsurface flow is expressed per unit width of hillslope. The maximum groundwater level is the highest measured groundwater level in the interval during which SSR is measured. The horizontal scale is selected so that the ground surface plots at the right end of the graph and the bedrock surface on the left.

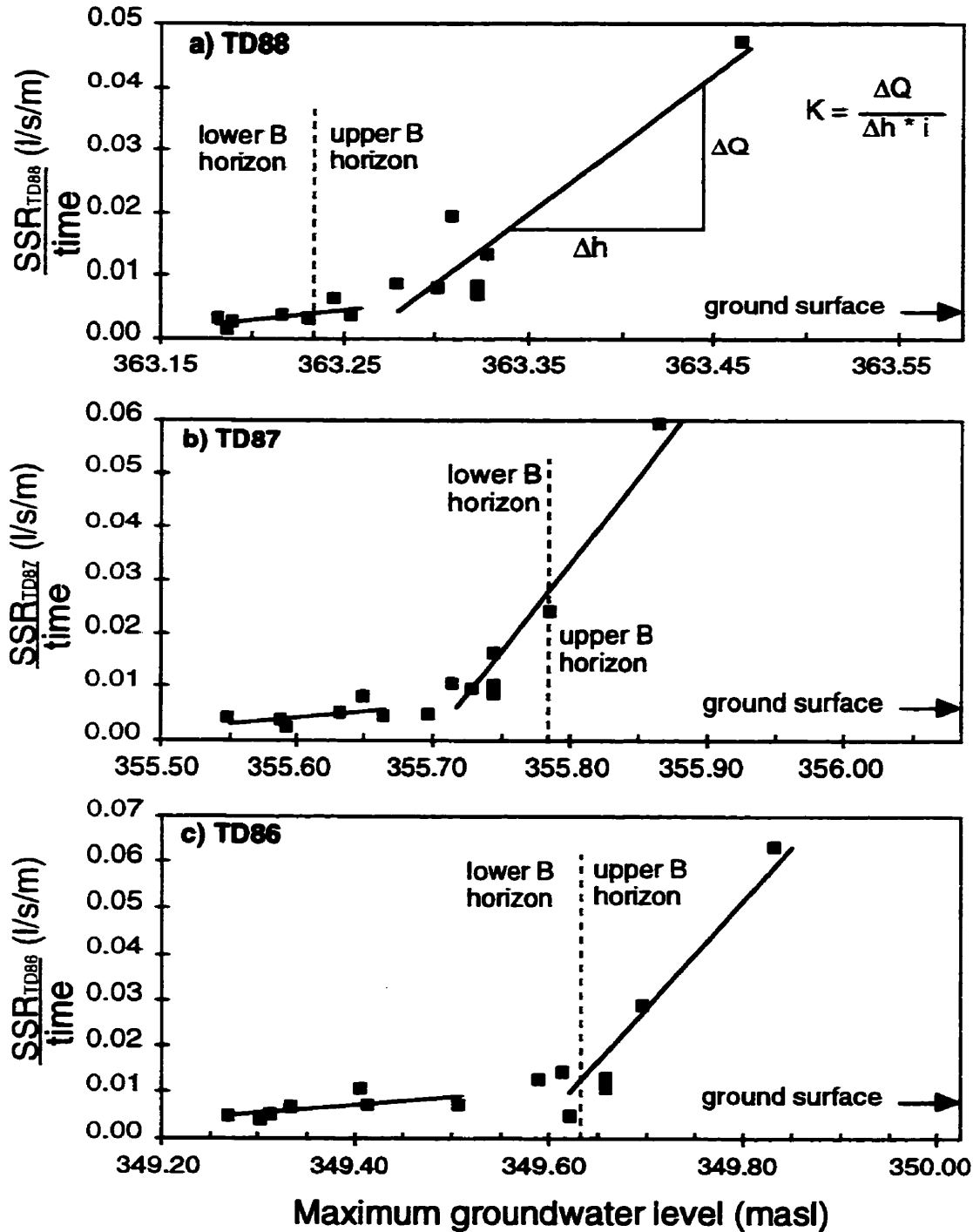


Table 6.4. Hydraulic conductivity profiles calculated from soil water balances (Figure 6.17) and bail tests in piezometers adjacent to TDR sites.

	Hydraulic conductivity (m/s)		
	Soil water balance		Bail test
	Upper B horizon	Lower B horizon	C horizon
TD88	9.4×10^{-4}	1.4×10^{-4}	1.3×10^{-5}
TD87	1.2×10^{-3}	8.6×10^{-5}	5.9×10^{-6}
TD86	1.2×10^{-3}	8.4×10^{-5}	4.8×10^{-6}

Table 6.5. Physical properties of (Orthic Humo-Ferric) Podzolic soils in Harp 4 (Lozano et al., 1987).

Soil horizon	Organic carbon %	Root volume %	Bulk density (g/cm ³)
LFH	40.2 ± 4.2	-	0.01 ± 0.01
Ah	10.2 ± 5.4	1.8 ± 3.5	0.5 ± 0.2
Ahe	5.3	0.8	0.6
Ae	2.3 ± 1.0	0.4 ± 0.6	1.16 ± 0.04
Bf1 (upper B)	3.9 ± 0.8	1.8 ± 0.7	0.8 ± 0.2
Bf2 (lower B)	2.0 ± 0.4	0.4 ± 0.9	1.1 ± 0.2
BC	1.1 ± 0.2	0.5 ± 0.2	1.2 ± 0.3
C	0.6 ± 0.2	0.2 ± 0.05	1.4 ± 0.1

Sample sizes not indicated.

change in soil water storage depends on both hydrological and physical factors. Firstly, subsurface runoff increases with increasing antecedent water storage in soil horizons. Higher initial water contents for a given soil result in higher unsaturated hydraulic conductivities that yield more rapid and effective drainage of infiltrating precipitation. Secondly, soil characteristic curves and unsaturated hydraulic conductivities will affect how rapidly one soil type drains compared to another. Soils with steep characteristic curves (e.g. clean sand) can have large increases in water content during storms, but may drain very rapidly to similar initial water contents; therefore the net change in water storage is small. Conversely, soils with gentle characteristic curves (e.g. silt) may have smaller increases in water content during a storm, but may retain soil moisture more effectively; therefore, the net change in water storage is larger. Thirdly, sites with a deeper water table store more water and, therefore, produce less runoff. With a deep water table, infiltration can produce increases in water content and storage throughout the thick unsaturated zone (Figures 6.5, 6.10 and 6.12). A thicker unsaturated zone (e.g. TD5) results in larger water storage caused by incomplete drainage of soil horizons. Depth to water table was, therefore, a good indicator of the magnitude of subsurface runoff production.

On a catchment scale, the magnitude of stream runoff depends not only on the effectiveness of subsurface runoff production, but also on the proportion of the catchment area that effectively generates runoff. Catchment runoff is the sum of runoff production (surface and subsurface) for the entire catchment area (similar to Equation 6.6). Consequently, determining the magnitude of stream runoff depends greatly on the delineation of areas that do and that do not contribute. Although this chapter has dealt primarily with the efficiency of subsurface runoff production, results from site TD82 in Harp 3A demonstrated that the spatial extent of subsurface runoff production can change. Subsurface runoff at TD82 was generated efficiently during autumn storms when a water table was present in soil horizons but did not

generate any runoff during the May 28, 1993 storm before which the water table was absent from soil horizons (Table 6.2). In Harp 4-21, stream runoff was larger for the November 2 and 4 event than for the October 16, 1992 event despite similar subsurface runoff ratios at TDR sites. This result suggests that the larger runoff may be caused by the expansion of the contributing area rather than by the increased runoff efficiencies from existing contributing areas (Tables 5.3 and 6.1).

Timing of runoff production

The timing of subsurface runoff production at a site can be broadly classified into four groups.

- 1) Precipitation produces runoff with very little or no delay (TD2; Figure 6.8).
- 2) Soils store some precipitation, yet contribute to peak discharge and the falling limb of the storm hydrograph (TD3, TD87, TD88; Figures 6.8, 6.11 and 6.13).
- 3) Soils store most of the infiltrating precipitation and contribute primarily to the falling limb of the storm hydrograph (TD4, TD5, TD81, TD82, TD86; Figures 6.8, 6.11 and 6.13).
- 4) Soils store nearly all of the infiltrating precipitation and contribute primarily to evapotranspiration or to stream baseflow after the storm event (TD82 during the May 28 event; Table 6.2).

Upslope portions of Harp 4-21 and entire hillslopes of Harp 3A during the summer would also likely belong to the fourth group. Although an individual site may be classified differently for different storms, depending on the antecedent moisture or storm size and duration, most sites responded similarly to different storms.

The timing of subsurface runoff production is primarily a function of water storage. Precipitation contributes most rapidly to runoff where it is greater than the available water storage. Some sites have sufficiently high hydraulic conductivities to transmit this excess

precipitation rapidly as subsurface flow such that the water storage never reaches its maximum (TD2); other sites saturate to the surface and produce saturated overland flow (TD1).

Although the flowpaths are different in both cases, the timing and magnitude of runoff production are almost the same. Therefore, the capacity to transmit subsurface flow has little effect on the magnitude and timing of runoff production in these areas but could have an important effect on flowpaths and, hence, water chemistry. For these sites, the timing of the subsurface runoff production was influenced primarily by the timing of precipitation (Figure 6.8b). The onset of subsurface runoff production could be slightly delayed depending on the available water storage, but was more delayed in sites without excess precipitation.

Increases in water storage within the soil profile causes subsurface runoff production to be delayed. Once infiltration or flow from upslope fills unsaturated pore space, subsurface runoff cannot be produced until the pores drain. The factors that control pore drainage also control the timing and magnitude of subsurface runoff. Factors that influence the drainage of pores include the unsaturated hydraulic conductivity (a function of water content), characteristic curves (a function of the pore size distribution) and spatial distribution of these features within a soil profile. Vertical drainage within the unsaturated zone of the soil profile cannot contribute to subsurface runoff because there is no net change in storage.

Consequently, the thickness of the unsaturated zone also controls the timing of subsurface runoff production. For example, at TD3 and TD4, the unsaturated zone was relatively thin, but stored a large proportion of the rainfall temporarily (Figure 6.10). At TD5, the unsaturated zone was much thicker and all the water remained stored within the profile so that subsurface runoff production was delayed for a longer period (Figure 6.8b). Therefore, the delay in runoff production from upslope areas was not directly caused by their distance from the stream, but rather by the increasing depth to the water table with distance from the stream.

Characteristic curves of soil horizons and water table fluctuations controlled the timing of subsurface runoff generation during wet conditions in Harp 3A because the thickness of the unsaturated zone varied little along hillslopes. Since most of the infiltration in Harp 3A was stored below the rising water table (Figure 6.12), sustained subsurface flow from upslope maintained elevated groundwater levels and delayed subsurface runoff production at some sites. For example, the timing of groundwater level fluctuations at TD86 and TD87 was nearly identical (Figure 5.9), yet subsurface flow production was greatly delayed at TD86 (Figures 6.11 and 6.13). The delayed response at TD86 was caused by large water storage in a horizon with a steep characteristic curve immediately above the initial water table. Net subsurface flow was only produced from this horizon when upslope flow decreased and the water table dropped within it (Figures 6.5 and 6.15).

Similar timing of subsurface runoff response does not necessarily imply that similar processes are responsible for the storage and release of infiltrating water. For example, the timing of subsurface runoff generation was similar at sites TD5 and TD82 (Figures 6.8 and 6.11). Although storage in the unsaturated zone at TD5 delayed runoff production, storage in the transiently saturated zone was responsible for delayed runoff production at TD82.

Hydraulic conductivity profile of the soil

The 10-fold increase in hydraulic conductivity from the lower to upper B horizon (Table 6.4) is very important for the production of subsurface flow and is consistent with the transmissivity feedback mechanism of streamflow generation (Chapter 2). It allows for large increases in subsurface flow with relatively small increases in water levels (Figure 6.17) and no change in hydraulic gradients. When water levels rise into the higher conductivity horizon, runoff production becomes very efficient as demonstrated during the November 10 and 12 event, 1992 (Figure 6.13, Table 6.2). Since the hydraulic conductivity of the soil is high, an

increase in infiltration can be easily converted into subsurface runoff with only a small increase in water levels. Without higher hydraulic conductivities in the upper soil profiles, downslope soils could not accommodate the accumulation of subsurface flow from upslope and groundwater would discharge to the ground surface.

The lower permeability of the lower B and C horizons also significantly affects stormflow production by prolonging drainage and saturation within the hillslope. If the high permeability horizon extended to bedrock, hillslopes would drain rapidly, the water table would drop, and both pressure head and water content would decrease. Consequently, more of the infiltrating storm precipitation would be retained by the soil and less storm runoff would occur (e.g. Harp 3A when soils were dry in the summer). In Harp 4-21, the permeability of the tills were sufficiently low to prevent hillslope drainage during the summer and sustain baseflow (Chapter 5).

Conclusions and implications

Differences in the magnitude and timing of streamflow generation between Harp 4-21 and Harp 3A are largely the result of differences in the spatial pattern of water storage and subsurface flow production. In Harp 4-21, runoff production is largest near the stream (92-96%); it decreases and is delayed with increasing distance from the stream. This pattern of runoff production was observed during several storms and is caused by the increasing depth to the water table (and thickness of the unsaturated zone) with distance from the stream. In Harp 3A, a large proportion of precipitation (up to 100%) can produce runoff very rapidly from midslope sites when the water table is within soil horizons. The timing of runoff production in Harp 3A is consistently delayed at one lower hillslope site because water stored in the soil profile cannot drain until subsurface flow from upslope decreases. Soil water balances during

dry weather demonstrate that subsurface flow from upslope has a greater effect on moisture conditions in lower hillslopes of Harp 4-21 than in Harp 3A.

Runoff production calculated from individual soil water balances along a Harp 3A hillslope provided reasonable estimates of stream discharge from the entire watershed during several storms. These results suggest that this approach is useful to quantify not only the magnitude and timing of runoff production at individual sites but also the subsurface fluxes along hillslopes. These fluxes were used to estimate the hydraulic conductivity of soil horizons. The hydraulic conductivities of the upper B horizon (10^{-3} m/s) are one order of magnitude greater than those in the lower B horizon (10^{-4} m/s). Therefore, the permeable upper B horizons can transmit large subsurface fluxes with small fluctuations of the water table.

Streamflow generation was not limited to near-stream areas. This result has several implications for streamflow generation processes and water chemistry. Firstly, conceptual models of streamflow generation must account for the spatial and temporal patterns of subsurface flow production. The groundwater ridging and saturation overland flow models (Chapter 2) cannot explain the subsurface runoff responses observed at TDR sites in this study. Secondly, although it is convenient to state that subsurface runoff from upslope displaces groundwater along the hillslope and into the stream, the controls on these processes have not been fully addressed. For example, downslope displacement of groundwater requires higher groundwater levels and, therefore, also requires consideration of downslope water storage (e.g. at TD86) which can delay this displacement. Thirdly, the implications of this displacement for water flowpaths and residence times within the hillslope, particularly in heterogeneous soils, are also poorly known. Flowpaths and residence times may have important consequences for groundwater and stream chemistry. Lastly, because subsurface flow is generated along the hillslope, fluxes must increase downslope during storms. The

average velocity of subsurface flow through the soils also increases downslope and, therefore, near-stream soils are flushed with more water than are upslope soils. Consequently, increased flushing has implications for the rate of chemical contaminant transport during storms and for soil and water chemistry.

The two most important factors that determine the magnitude of stream runoff are the proportion of the catchment area that produces runoff and the antecedent moisture conditions. The latter factor greatly influenced the proportion of precipitation that produced storm runoff at individual sites. One of the most simple and effective methods to estimate antecedent moisture conditions and to identify areas that produce storm runoff within a catchment is to measure groundwater levels along one or more transects from the stream to the hilltops. Although detailed soil moisture measurements at several locations would be necessary to quantify spatial variations in storm runoff production, water table measurements can effectively delineate catchment areas that respond most significantly to storms by the presence or absence of a water table within soil horizons. Other factors, such as soil characteristic curves, also affect runoff response but to a lesser extent. Till thickness and slope influence storm runoff indirectly through their effects on water table position and antecedent moisture conditions by water redistribution.

This study emphasizes two important aspects of streamflow generation that are usually given little consideration. Firstly, water storage and drainage are critical processes, yet most conceptual models do not explicitly include them (Chapter 2). Soil water retention and unsaturated hydraulic conductivity are commonly studied in soil science, agricultural and hydrogeological research, but are infrequently part of streamflow generation studies. Consideration of such factors would provide greater insight into the magnitude and timing of storm runoff production and baseflow generation. Secondly, spatial differences in the magnitude and timing of subsurface runoff generation can be quantified. Such field data will

become more important in order to develop better spatially-distributed models which are needed to predict stream hydrology and water chemistry with greater accuracy. The method in this study provides the simplest example of an approach in which subsurface runoff is quantified at several locations within a catchment.

There are considerable research opportunities to expand upon this approach. For example, improvements in the automated acquisition of soil moisture measurements by TDR will make more complete data sets available to be analysed (Baker and Allmaras, 1990; Heimovaara and Bouten, 1990). The simultaneous measurement of pressure head and soil water content can be used to obtain characteristic curves that may be more representative of soil water retention in the field (Schaap et al., 1997). Such curves may more clearly demonstrate the influence of soil structure and macropores, as well as the effect of position along drying, wetting and scanning curves, on subsurface flow generation. These data could be used to examine the relative importance of saturated versus unsaturated flow in subsurface runoff generation. Ideally, simultaneous measurement of evapotranspiration would allow complete water balances to be calculated during periods when evapotranspiration is not negligible.

Chapter 7

Streamflow generation in Harp 4-21 and Harp 3A

Introduction

Within the streamflow generation literature, there are five conceptual models of subsurface flow generation: 1) unsaturated flow, 2) groundwater ridging, 3) transmissivity feedback, 4) perched water table, and 5) old water macropore flow. They are described and their implications are discussed in Chapter 2. Several hydrological processes may occur within an individual catchment. Therefore, determining the dominant processes within an individual watershed is necessary to apply conceptual models of streamflow generation.

The main objective of this chapter is to evaluate streamflow generation mechanisms in Harp 4-21 and Harp 3A within the context of existing conceptual models. Since most streamflow in these catchments originates as subsurface flow (unsaturated and groundwater flow), this chapter focuses specifically on subsurface flow processes. The specific goals are: 1) to systematically examine and integrate precipitation, stream discharge, soil moisture, groundwater level, hydraulic conductivity, and isotopic data from storm events in Harp 4-21 and Harp 3A, 2) to determine the dominant mechanism for increased subsurface flow during storms, 3) to identify the most appropriate conceptual model of subsurface flow, and 4) to consider the general implications of the findings for catchments on the Canadian Shield.

Approach: Evaluation of the dominant subsurface flow processes

To determine the dominant processes in Harp 4-21 and Harp 3A, a systematic eight step approach is applied. The approach is based on the classification of conceptual models according to the principal mechanism for the increase in subsurface flow (changes in hydraulic

gradients or water contents), the spatial extent of runoff production, and the physical and hydrological properties of the porous media (Chapter 2).

1. The role of subsurface flow in storm runoff

The relative contributions of surface and subsurface runoff to total storm runoff must first be assessed. This assessment can include qualitative observations of overland flow during storms (particularly when there is little or none, Hewlett and Hibbert, 1967), mapping of saturated areas during storms (Dunne et al., 1975; McDonnell and Taylor, 1987), and quantitative estimates of event and pre-event runoff volumes from isotopic or geochemical hydrograph separations (e.g. Chapter 4). In catchments where surface water storage is minimal (or can be quantified) and Horton (1933) overland flow is not observed, subsurface runoff can be estimated as the total stream runoff minus the volume of precipitation directly onto discharge areas.

The volume of pre-event runoff from isotopic hydrograph separations does not necessarily equal the volume of subsurface flow during the storm. Subsurface storm runoff can exceed pre-event runoff if event water infiltrates the soil and discharges into the stream during the storm. Conversely, pre-event runoff can exceed subsurface storm runoff if ponded pre-event water (i.e. that had discharged to the ground surface prior to the storm) is replaced by precipitation or surface runoff of event water (Buttle and Sami, 1992; Hill and Waddington, 1993; Waddington et al. 1993). Therefore, pre-event runoff can be used as a minimum estimate of subsurface runoff, provided that displacement of ponded pre-event water into the stream by event water during the storm is minimal.

2. Areas that contribute to storm runoff

The minimum contributing area, calculated as the volume of storm runoff divided by the depth of precipitation, provides an estimate of the spatial extent of streamflow generation within a catchment. This calculation assumes that 100% of precipitation onto the minimum contributing area generates runoff. In reality, the contributing area is larger because some precipitation can be stored in the soil, or lost to interception or evapotranspiration within this area. The length of the stream that faces hillslopes (i.e. both sides of the stream) can be used to convert the contributing area into an average length of contributing hillslope. The total volume of storm runoff is typically determined by a graphical hydrograph separation that accounts for the volume of runoff in excess of baseflow. One of the main purposes of calculating contributing areas (or lengths) is to evaluate the relevance of the groundwater ridging model for which the maximum contributing length is limited to approximately 20 m or less (Chapter 2).

3. Spatial extent of water table fluctuations during storm events

Subsurface stormflow generation models can be distinguished, in part, by differences in the spatial extent of water table fluctuations (Chapter 2). Therefore, water table level monitoring during storms provides essential data for interpreting subsurface stormflow generation.

The spatial extent of water table fluctuations can be compared to the contributing area or length (Step 2) to evaluate the suitability of the conceptual models in an individual watershed. For example, if the minimum contributing area is larger than the spatial extent of water table fluctuations during the storm, then unsaturated flow must contribute to storm runoff that reaches the stream (Harr, 1978).

4. Timing of groundwater fluctuations during storms

If groundwater flow is responsible for the increase in stream discharge during storms, then changes in groundwater levels in rapidly contributing portions of the watershed must precede or coincide with changes in stream discharge. The timing of groundwater level fluctuations can also help to distinguish between areas that contribute groundwater rapidly, areas where groundwater contributions are delayed, and areas in which groundwater flow does not contribute to storm runoff.

5. Capillary fringe effect

The capillary fringe effect, can be identified by a water table rise that is not accompanied by a change in water content. Changes in water content can be monitored by repeated non-destructive measurements of soil moisture (e.g. TDR). A rapid water table rise should be comparable to the thickness of the capillary fringe, if present. The air entry pressure from characteristic curves can be used to estimate the expected thickness of the capillary fringe.

As a result of the capillary fringe effect, the water table should rise suddenly, within minutes of the onset of infiltration (Gillham, 1984). After infiltration ceases, the water table should also decline rapidly and re-establish the capillary fringe. Monitoring of groundwater levels in this study could not be used directly to evaluate the capillary fringe effect because it requires nearly continuous monitoring of water levels to detect sudden changes. In addition, water level response in an observation well may be smaller and slightly delayed compared to that measured in tensiometers (Gillham, 1984) because of well (or piezometer) lag time.

6. Changes in hydraulic gradients

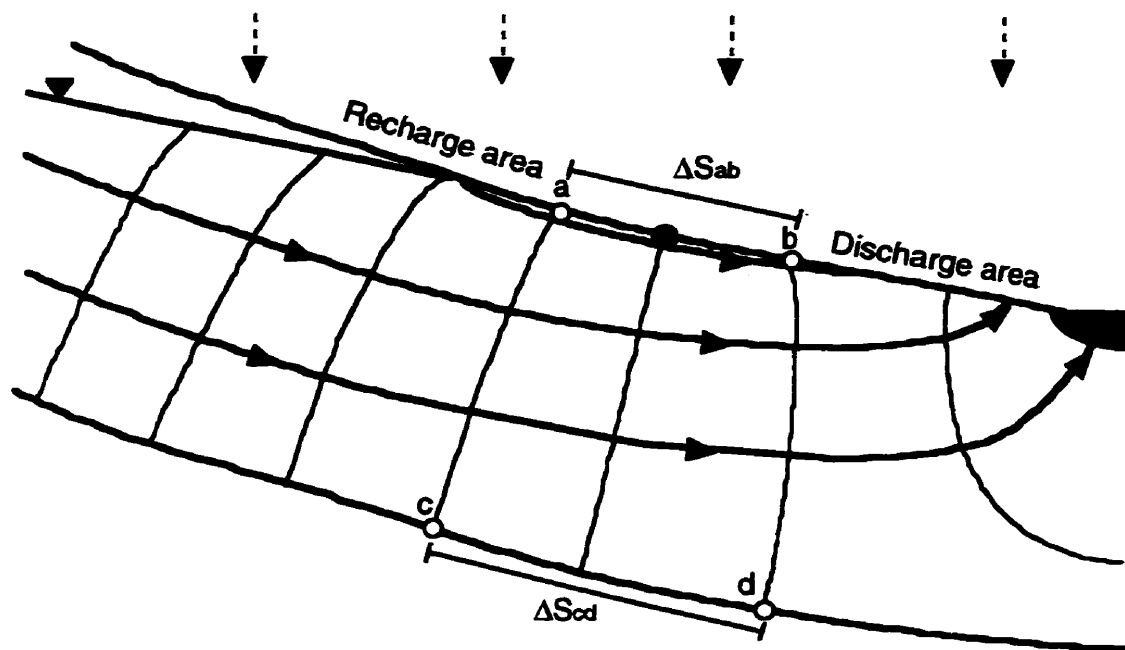
The most definitive test of the groundwater ridging model is to measure the change in hydraulic gradients during storms. In this model, the increase in downslope hydraulic gradients (i.e. change in hydraulic head divided by the distance *along* the slope) from baseflow to stormflow conditions must account for the increase in subsurface flow to the stream. In contrast to Steps 2 and 3, which are based on a comparison of runoff volumes, this step compares subsurface fluxes. Simple water table measurements during the storm event provide the necessary data to calculate changes in hydraulic gradients.

In some catchments, it is possible to estimate the maximum increase in hydraulic gradient at the hinge point by comparing the baseflow hydraulic gradient to the topographic gradient along the ground surface. The hinge point is used for this estimate because it is the location of maximum subsurface flow along the hillslope. Since equipotentials near the hinge point diverge with increasing depth (Figure 7.1), the downslope hydraulic gradient beneath the hinge point (c-d) must be smaller than the topographic gradient along the ground surface at that location (a-b). Therefore, the topographic gradient along the ground surface represents the maximum downslope hydraulic gradient within the profile. Consequently, in some catchments, the comparison of topographic gradients with one measurement of hydraulic gradient at baseflow would be sufficient to demonstrate that the maximum possible increase in hydraulic gradient could only increase subsurface flow marginally.

7. Flow through transiently saturated sediments

If groundwater ridging is not responsible for increased subsurface flow, and the magnitudes of the contributing areas (Step 2) and transiently saturated areas are comparable, then flow through transiently saturated sediments could be the dominant mechanism for

Figure 7.1 Comparison of hydraulic (c-d) and topographic (a-b) gradients at the hinge point.
 Δh = change in hydraulic head, ΔS = distance between equipotentials.



Legend

- Hinge point
- Equipotential
- ➔ Flowline
- ▼ Water table
- ⋮ Precipitation

Hydraulic gradients

$$\Delta h_{ab} = \Delta h_{cd}$$

$$\Delta S_{ab} < \Delta S_{cd}$$

$$\frac{\Delta h_{ab}}{\Delta S_{ab}} > \frac{\Delta h_{cd}}{\Delta S_{cd}}$$

increased subsurface flow. To evaluate the magnitude of flow through transiently saturated sediments requires measurements of their depth, thickness, and saturated and unsaturated hydraulic conductivities. When sufficient hydraulic data from the unsaturated zone are not available, the maximum increase in subsurface flow through transiently saturated sediments can be estimated from measurements of saturated hydraulic conductivity (K_s), assuming negligible unsaturated subsurface flow prior to the storm.

8. Matrix versus dual porosity flow

Subsurface flow can occur within the soil matrix, macropores or both. Subsurface flow that occurs within macropores without interaction with the matrix cannot displace pre-event water to the stream because these pores are mostly air-filled under unsaturated conditions. A qualitative assessment of the relative importance of flow in the matrix and flow in large pores can be obtained from tracers or dyes or by examining secondary porosity in excavations or soil pits (Tsuboyama et al., 1994). However, quantifying the relative flow through the soil matrix and macropores at the hillslope scale would require detailed instrumentation, such as trenches that collect flow from the matrix and macropores separately, and was not included in this study.

The role of matrix and dual porosity saturated flow can be crudely assessed from K_s measurements of both undisturbed sediments and sediments where the secondary porosity (macropores and soil structure) has been destroyed. Although all measurements disturb the soil to some extent, instruments, such as ring infiltrometers, can be used to measure K_s without completely destroying secondary porosity. In contrast, an augered hole will likely destroy secondary porosity adjacent to the piezometer so that piezometers most likely provide K_s values representative of the soil matrix. Therefore, comparison of K_s from ring infiltrometers and piezometers may provide an estimate of the influence of macropores on K_s .

Study site and methods

Instrumentation, methods and monitoring periods for investigations in the Harp 4-21 and Harp 3A catchments (Figure 7.2) were previously described in detail in Chapters 3 and 5. In addition, a series of twelve shallow (0.1 - 0.2 m depth) open holes were used to monitor water levels and the extent of surface saturation in the lower hillslopes of Harp 3A. These holes were located between piezometer nests P80 and P81, the edge of Wetland 3 and P86, and along the southern slope draining into Wetland 3 (Figure 7.2).

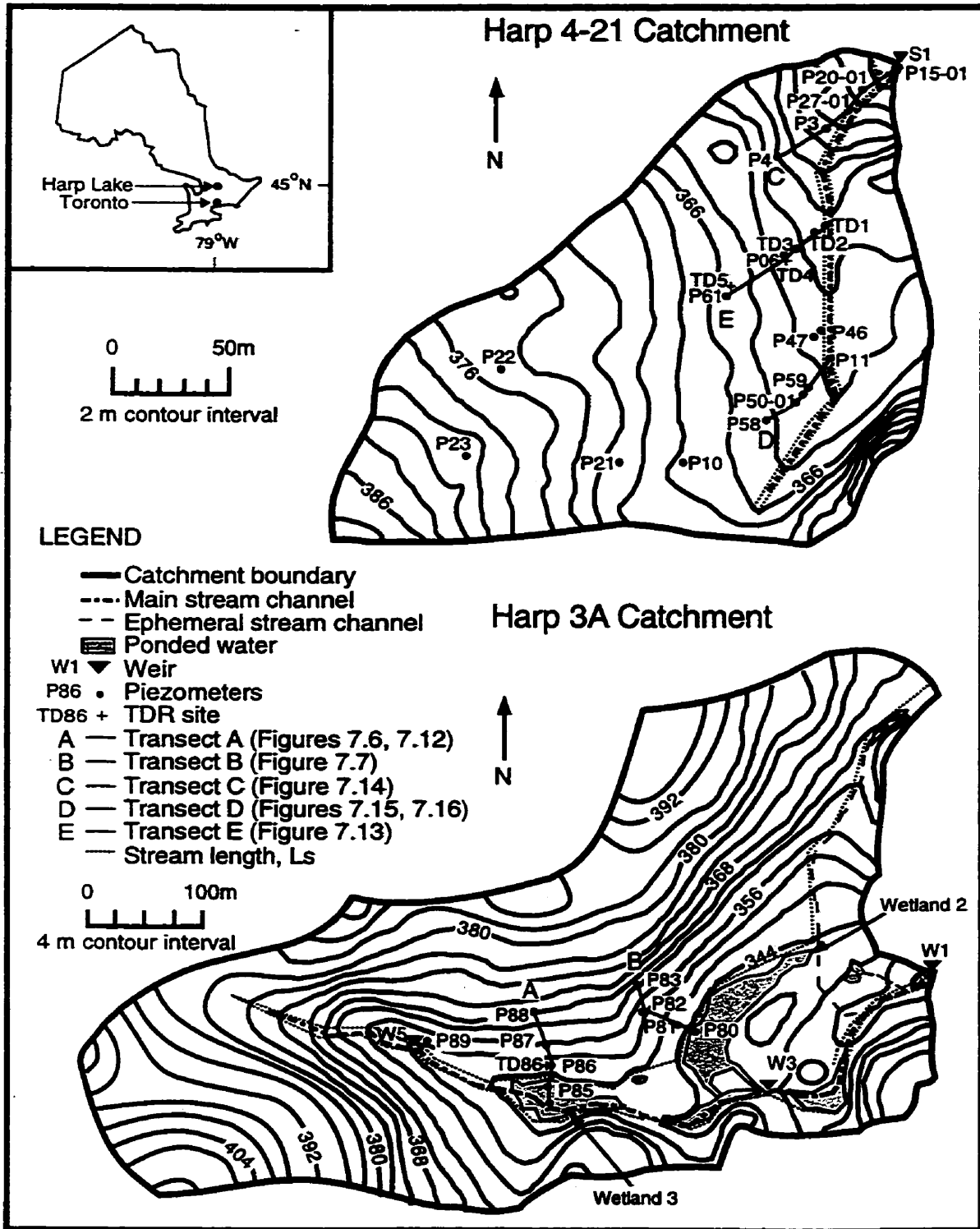
A simple double ring infiltrometer (0.16 and 0.25 m diameter) was used to measure the steady state infiltration into Harp 4-21 soils. Both rings were inserted 1 to 7.5 cm into the A horizon to prevent leakage. Infiltration was initiated in the outer ring to saturate the soil and avoid edge effects. Ponding (<1 cm) was maintained in both rings until the infiltration rate in the inner ring reached steady state.

The minimum contributing area (A_c) was calculated as:

$$A_c = \frac{V_Q}{P} \quad (7.1)$$

where V_Q is the volume of storm runoff and P the depth of precipitation. The volume of runoff was determined by the graphical hydrograph separation method in Chapter 5 except that the duration of the storm was defined by a commonly used, but arbitrary criterion (an increase of $0.05 \text{ ft}^3/\text{s}/\text{mi}^2/\text{hr}$ over pre-storm baseflow discharge; Hewlett and Hibbert, 1967). As demonstrated in the results section, this criterion provides a slightly conservative estimate of storm runoff and, therefore, of A_c in these two catchments. Storm runoff included all the flow in excess of stream baseflow which was estimated during the event with an exponential baseflow recession constant (Bruce and Clark, 1966) that was calculated for a 24 hour period prior to the storm.

Figure 7.2 Instrumentation of the Harp 4-21 and Harp 3A catchments. Figures show piezometer transects A-E and maximum stream lengths, L_s .



The minimum contributing length of hillslope (L_c) can be estimated as:

$$L_c = \frac{(A_c - A_{pw})}{L_s} \quad (7.2)$$

where A_c is the minimum contributing area, A_{pw} is the area of ponded water that includes wetlands and the stream surface, and L_s is the length of the stream (and wetlands) facing hillslopes. A negative (or zero) contributing length ($A_{pw} \geq A_c$) indicates that storm runoff could be produced entirely from precipitation onto areas of ponded water. The contributing length is only intended as an approximation since flowpaths may converge or diverge and flow may not be perpendicular to the stream. Maximum stream lengths for Harp 4-21 and Harp 3A are shown in Figure 7.2. Some portions of the stream and wetlands in Harp 3A were not included in L_s because they have very small contributing areas (into east side of Wetland 2) or because subsurface flow is parallel to the stream (east side of ephemeral channel). A_{pw} was estimated from topographic surveys, measurements of stream width, and water level measurements in Wetland 2.

A more realistic estimate of contributing hillslope area and length can be obtained with soil water balances (Chapter 6) that measure the proportion of precipitation that contributes to runoff. The actual contributing area (A'_c) is calculated as:

$$A'_c = \frac{(A_c - A_{sof})}{\overline{SSRR}} + A_{sof} \quad (7.3)$$

in which A_c is the minimum contributing area, A_{sof} is the area of saturated overland flow where all the precipitation generates runoff (runoff ratio = 1), and \overline{SSRR} is a spatial average of subsurface runoff ratios as defined in Equation 6.7. A_{sof} is estimated as the combined surface area of wetlands, streams, and lower saturated hillslopes. An actual contributing length (L'_c) can be calculated by substituting A'_c for A_c in Equation 7.2.

Actual contributing areas and lengths were calculated (Equations 7.2 and 7.3) at several times during the November 2 and 4, 1992 storm event when subsurface runoff ratios were measured. Since subsurface runoff production was both temporally and spatially variable, average subsurface runoff ratios had considerable uncertainty, particularly early in the storm event when the spatial variability in runoff production was greatest. Average subsurface runoff ratios for Harp 3A hillslopes were calculated as the average of sites TD81, TD87 and TD88. Sites TD82 and TD86 were excluded because they stored subsurface flow from upslope and probably were not representative of large hillslope areas (Chapter 6). Values of A_{sof} were estimated from measurements of A_{pw} and saturation along the piezometer transects. These areas were relatively small (2.2 ha in W1 and 0.26 ha in W5) in comparison to the contributing area for the November 2 and 4 storm event.

Actual contributing areas were difficult to estimate in Harp 4-21 because there was greater spatial variability in subsurface runoff ratios and the proportions of the different corresponding areas were poorly known. The arithmetic average of runoff ratios at TD2 and TD3 overestimated the average subsurface runoff ratios because of their proximity to the stream and, therefore, provided a conservative estimate of actual contributing areas. The value of A_{sof} in Harp 4-21 (0.08 ha) included the perennial discharge area along the lower stream but excluded the areas of saturated overland flow upstream because their high runoff ratios were implicitly considered by including site TD2.

Results

1. The role of subsurface flow in storm runoff

Detailed isotopic hydrograph separations in Harp 4-21 for storms on June 22 and October 31, 1989 (Chapter 4) showed that pre-event water (soil and groundwater) contributed in excess of 75% of the total storm runoff. The volume of subsurface flow must have been

nearly equal to or greater than the volume of pre-event water for two reasons. Firstly, the volume of ponded water prior to the storms was less than 3% of the pre-event storm runoff volume. Secondly, a small proportion of event water undoubtedly reached the stream as subsurface flow because new water continued to contribute several days after the storm. Therefore, subsurface flow was the dominant component of storm runoff.

Subsurface flow in Harp 4-21 did not discharge only into the stream, since groundwater discharge and saturated overland flow were observed within the litter in discharge areas adjacent to the stream. Increased subsurface flow during storms was, therefore, discharged over a wider area than the stream alone.

Most of the storm runoff in Harp 3A was also generated as subsurface flow. Isotopic hydrograph separations (Chapter 5) suggested that pre-event flow was dominant at both W1 and W5. Since there was very little ponded water in W5, subsurface flow must have been equal to or in excess of pre-event runoff. In W1 (Harp 3A), the volume of ponded water prior to storms was significant (370-480 m³) and, therefore, possible displacement of pre-event water from wetlands had to be considered. Expressed as a proportion of the storm runoff at W1, the volume of ponded water was 4%, 43% and 41% of the storm runoff volume for the November 10 and 12, 1992, May 24, 1993 and May 28, 1993 events respectively. However, it is unlikely that pre-event stream discharge during the May storms was simply displaced (or mixed) ponded pre-event water that was replaced by event water. The $\delta^{18}\text{O}$ value of Wetland 2 (which accounted for 60-70% of all ponded water volume) increased from -13.19‰ on May 22 (230 m³) to -12.86‰ on May 30 (300 m³). A theoretical calculation of simple mixing shows that if all the precipitation onto Wetland 2 during the May 24 and May 28 storms (200 m³, -7.18‰ weighted average) had simply displaced ponded pre-event water, the wetland value would have increased to -9.2‰ on May 30. The isotopic water balance for Wetland 2 shows that the maximum volume of precipitation (event water) that could have remained in

the wetland was only 16 m^3 . Since the increase in water storage over the same period was greater (65 m^3), precipitation could not have replaced any of the pre-event water stored in Wetland 2. Therefore, the fluxes of pre-event water at W1 represented minimum subsurface flow in Harp 3A.

Saturation overland flow in Harp 3A was generally limited to the lower few meters of hillslope even during the largest storms. Piezometers and open holes showed that surface saturation only occurred in the lowermost 1-14 m of hillslope in areas downslope of piezometers P81, P86 and P89. During the largest storm (62 mm) on November 12, 1992, the water table did not rise to within 0.1 m of the ground surface at a distance of only 4 m from the edge of Wetland 2. Visual observations in the rest of the catchment confirm that overland flow was restricted to wetlands and the lowermost 15 m of hillslope except immediately south of Wetland 3 where soils are thin ($< 0.2 \text{ m}$ in some areas). Where overland flow was observed on bedrock outcrops, it infiltrated the adjacent soils.

2. Areas that contribute to storm runoff

The minimum contributing area (A_c) varied more among storms in Harp 3A than in Harp 4-21. Storm runoff could be generated from as little as 0.06 ha (600 m^2 , 0.2% of total area) during summer storms to more than 13 ha (60%) of Harp 3A (W1) (Table 7.1). Wide variability was also observed in W5 where A_c ranged from 0.01 ha (0.2%) to 2.6 ha (54%) in the 4.9 ha subcatchment. The range in A_c was much smaller (0.30-1.4 ha, 8-37%) for the same storms in Harp 4-21 (S1).

Runoff production involved much of the Harp 3A hillslopes during wet conditions and almost none during dry conditions. For most conditions in Harp 4-21, runoff was usually generated from lower and middle hillslopes. The flowing length of streams (L_s), 50-300 m in

Table 7.1 Minimum contributing areas and hillslope lengths (Equations 7.1 and 7.2) of storms in catchments W1, W5, and S1.

Date	W1	W1	W5	W5	S1	S1
	Minimum contributing area (ha)	Minimum contributing length (m)	Minimum contributing area (ha)	Minimum contributing length (m)	Minimum contributing area (ha)	Minimum contributing length (m)
22-Jun-89	-	-	-	-	0.81	18
10-Jul-89	-	-	-	-	0.16	3
1-Sep-89	-	-	-	-	0.11	3
10-Oct-89	-	-	-	-	0.16	5
12-Oct-89	-	-	-	-	0.02	0
20-Oct-89	-	-	-	-	0.29	9
31-Oct-89	-	-	-	-	0.31	10
2-Nov-89	-	-	-	-	0.10	3
5-Nov-89	-	-	-	-	0.32	10
12-Jul-92	0.42	<0	-	-	-	-
28-Aug-92	0.06	<0	-	-	0.37	9c
7-Sep-92	0.50	<0	-	-	0.36	9c
10-Sep-92	0.44	<0	-	-	0.30	7c
18-Sep-92	1.6	4	-	-	0.58	13
21-Sep-92	7.3	40	-	-	1.1	24
27-Sep-92	4.5	23	0.74	29	0.97	22
16-Oct-92	4.1	19	0.78	25	0.71	16
23-Oct-92	4.1	19	1.0	33	0.72	16
2-Nov-92 ^a	10.0	55	1.7	57	1.2	27
10-Nov-92 ^b	13.0	73	2.6	86	1.4	31
5-May-93	0.92	0.1	0.01	0.4	0.73	16
14-May-93	1.1	2	0.1	6	0.44	10
24-May-93	2.4	9	0.2	9	0.46	10
28-May-93	4.5	22	0.7	22	0.60	13
30-May-93	4.2	20	0.8	25	0.54	12
Catchment areas (ha)	21.7		4.9		3.7	

^a Includes storm on 4-Nov-92

^b Includes storm on 12-Nov-92

^c Uses an estimated L_s of 400 m

W5, 1000-1700 m in Harp 3A (W1), and 300-440 m in Harp 4-21 (S1), were used to express A_c as minimum contributing lengths, L_c (Table 7.1). Storms in summer 1992 and early May 1993 required little or no runoff response from the hillslopes of Harp 3A to produce the observed stream runoff. In contrast, these hillslopes contributed water from a minimum of 73 to 86 m during the November 10 and 12, 1992 event. In Harp 4-21, L_c never exceeded 31 m and only decreased below 10 m for storms during dry conditions of summer and autumn 1989, and summer 1992.

Stream discharge and precipitation records also demonstrate how rapidly hillslopes can contribute to storm runoff. Figure 7.3 shows the changes in A_c for catchments W1, W5 and S1 during the November 2 and 4, 1992 storm event. Within 24 hours following the start of the first storm, runoff equivalent to precipitation onto 18, 24, and 15 m of hillslopes had already been generated at W1, W5 and S1 respectively.

The graphical hydrograph separation criterion (Hewlett and Hibbert, 1967) used in this analysis provided a reasonable, yet conservative estimate of the minimum contributing area. Although A_c and L_c increased only gradually after the end of the hydrograph separations, by November 9, L_c had increased by an additional 7-15 m (15-27%) over values reported in Table 7.1 (Figure 7.3). Therefore, storm runoff is generated from even greater areas and lengths than shown in Table 7.1.

Although Figure 7.3 appears to indicate that the contributing area expands rapidly during storms, the actual contributing area does not continually expand because the entire area contributes gradually to storm runoff. The actual contributing areas during the November 2 and 4, 1992 storm event ranged from 13 to 20 ha for W1 and from 2.7 to 3.9 ha for W5 (Table 7.2). The corresponding hillslope lengths were similar for W1 and W5 and varied between 73 and 128 m. The increase in average subsurface runoff ratio from 0.21 to 0.80 confirms that

Figure 7.3 Minimum contributing areas (A_C) and hillslope lengths L_C at a) W1, b) W5 and c) S1 during the November 2 and 4 storm events. Arrows indicate the end of storm based on graphical hydrograph separation criterion of Hewlett and Hibbert (1967). A_C values for each time were calculated as the cumulative volume of precipitation to date divided by the cumulative precipitation to date (Equation 7.1). L_C values were calculated from Equation 7.2.

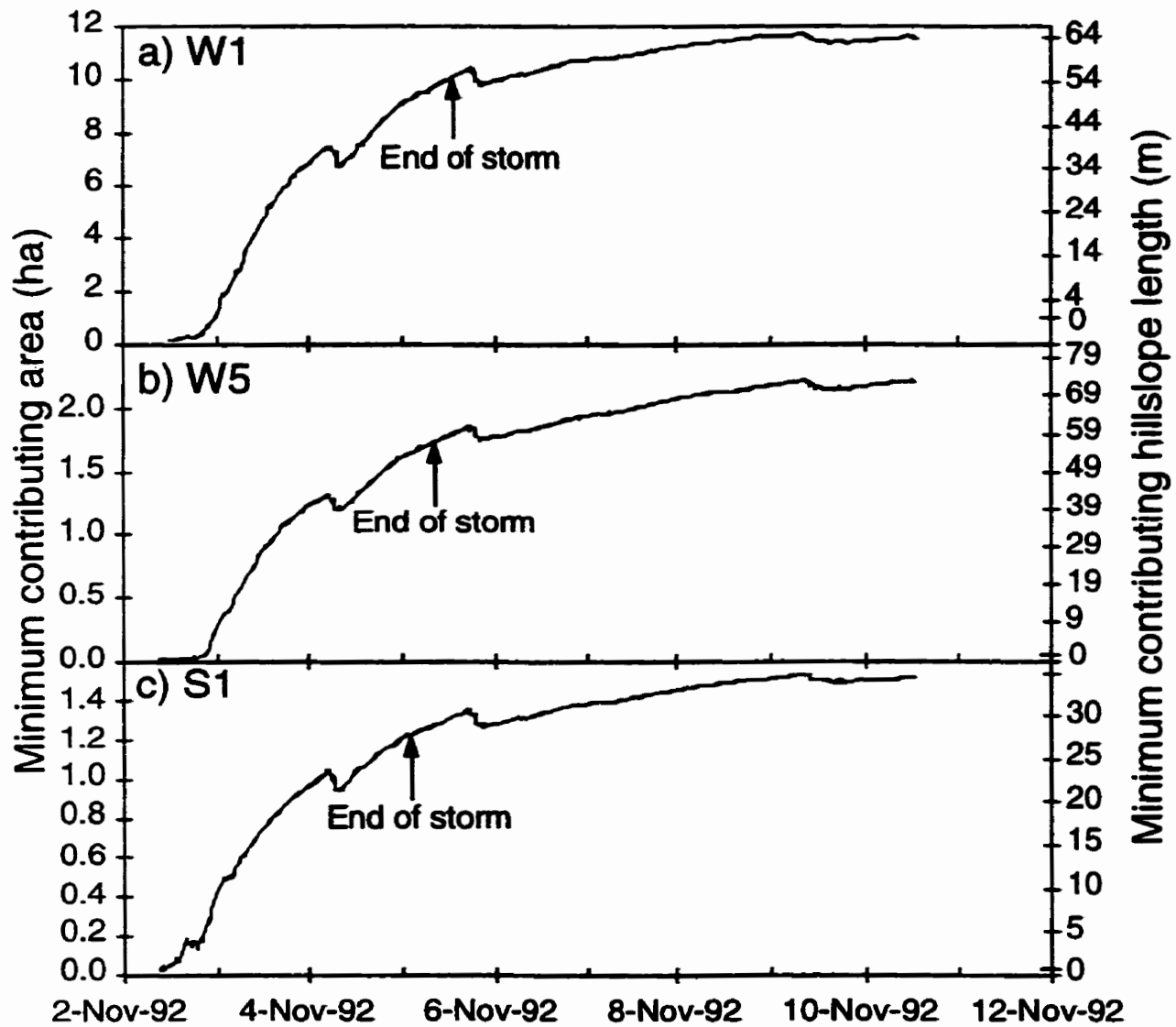


Table 7.2 Actual contributing areas and hillslope lengths during the November 2 and 4, 1992 storm event in catchments W1, W5, and S1.

	SSRR ¹	Minimum contributing area, A _c (ha)	Actual contributing area ² , A' _c (ha)	Actual contributing hillslope length, L' _c (m)
W1				
3-Nov-92 11:21	0.21	4.4	13	73
4-Nov-92 12:55	0.32	7.4	19	107
5-Nov-92 13:15	0.43	10.1	20	119
7-Nov-92 11:03	0.67	10.9	15	87
9-Nov-92 11:54	0.80	11.4	14	78
W5				
3-Nov-92 11:21	0.21	0.8	3.0	101
4-Nov-92 12:55	0.32	1.3	3.6	120
5-Nov-92 13:15	0.43	1.8	3.9	128
7-Nov-92 11:03	0.67	2.0	2.9	95
9-Nov-92 11:54	0.80	2.2	2.7	88
S1				
3-Nov-92 15:15	0.49	0.80	1.5	35
4-Nov-92 15:50	0.58	1.1	1.8	41
5-Nov-92 15:49	0.64	1.3	2.0	46
7-Nov-92 15:02	0.74	1.4	1.9	43
9-Nov-92 15:22	0.80	1.5	1.8	41

$$^1 \overline{\text{SSRR}} = \frac{\sum \Delta \text{SSR}}{\sum P}$$

For W1 and W5, average of sites TD81, TD87, TD88; for S1, average of TD2 and TD3.

$$^2 A'_c = \frac{(A_c - A_{\text{sof}})}{\text{SSRR}} + A_{\text{sof}}$$

A_{sof} = area of saturated overland flow estimated from groundwater levels and visual observations, A_{sof} W1 = 2.23 ha, A_{sof} W5 = 0.26 ha, A_{sof} S1 = 0.08 ha.

this larger area gradually contributed to storm runoff. The slight decrease in actual contributing area during the storm (Table 7.2) was probably not a real decrease, but rather the result of uncertainty in averaging subsurface runoff ratios. The contributing areas near the end of the storm are considered to be most accurate since the runoff ratios were higher and their spatial variability lower (Chapter 6). If sites TD82 and TD86 were included at the end of the storm (November 9), the ratio would be only slightly different (0.75) and would result in similar actual contributing areas for W1 (15 vs. 14 ha) and W5 (2.8 vs. 2.7 ha).

The actual contributing lengths for the November 2 and 4, 1992 storm event in Harp 4-21 are estimated to be approximately 35 to 46 m which are smaller than in Harp 3A (78-128 m; Table 7.2). Since the average distance from the stream to the eastern catchment boundary in Harp 4-21 is 38 m, runoff could have been produced from the entire eastern hillslope and from the lower and midslope areas of the western hillslope.

3. Spatial extent of water table fluctuations during storms

The water table responded to individual storms in over half the catchment area of Harp 4-21. Groundwater levels were measured with sufficient spatial and temporal resolution to produce a map of the maximum change in water level elevations during the June 22, 1989 storm (Figure 7.4). Measured water level fluctuations were less than 0.6 m at all sites. The increase in water levels was generally small near the stream or discharge areas, largest approximately 20 to 40 m upslope, and smaller farther upslope. In upper hillslopes, there was no groundwater response to storms. Figure 7.4 also shows the approximate boundaries of water table fluctuations within the soil or within the till. The upslope extent of the water table fluctuations within the till are poorly defined due to the lack of upslope piezometers. The area where the water table responded to storm runoff was approximately 1.8 ha within the soil and 0.5 ha in the till for a total area of 2.3 ha compared to the total catchment area of 3.7 ha.

The area of water table response in Harp 4-21 was likely smaller for the November 2 and 4, 1992 storm event because initial groundwater levels prior to the event were slightly lower (0.24 m and 0.51 m lower at P06 and P61 respectively) than those prior to the June 22, 1989 storm. Groundwater fluctuations during the November storms were similar (P61) or smaller (P06) than those of the June storm. Since groundwater levels during the November storms were only monitored along the TDR transect, a map similar to Figure 7.4 cannot be prepared.

The spatial extent of water table fluctuations in Harp 4-21 was restricted to lower hillslopes for the storm on October 31, 1989. The area where the water table fluctuated within the soil was approximately 0.6 ha (Figure 7.5). Water table fluctuations within the till could not be delineated spatially because too many piezometers were dry. However, the area of the water table fluctuations within the till was unlikely to extend far beyond that within the soil as demonstrated by piezometer P61 in which the water table response was small (0.03 m), delayed, and would not greatly affect storm runoff production.

In Harp 3A, there were not enough piezometers to define the spatial pattern of water level fluctuations with similar accuracy. However, when conditions were wet in Harp 3A, the timing and magnitude of water level fluctuations were similar between hillslope piezometer transects (Chapter 5).

The water table response at P83 and P88 in autumn (1992) storms indicates that water table fluctuations extended at least 68 m from the base of the hillslope (Figures 7.6a and 7.7a). Although the upslope extent of the water table response beyond these piezometers is not known, observations of surface saturation in depressions along the northern watershed divide suggest that the water table could have responded across the entire watershed during wet periods.

Figure 7.5 Maximum observed increase in groundwater levels in Harp 4-21 during the October 31, 1989 storm event.

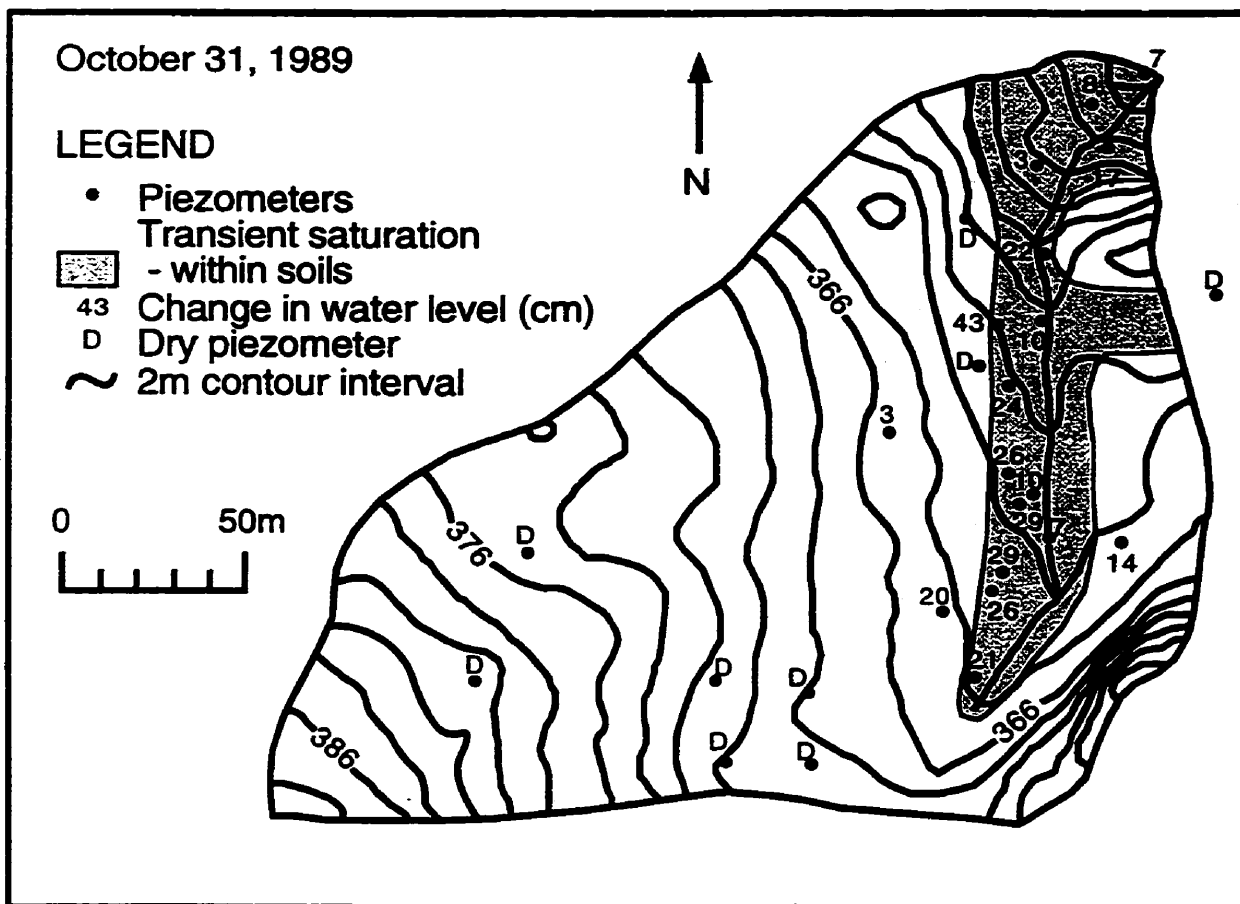


Figure 7.6 Water table profiles along transect A in Harp 3A during the a) November 2, 1992 and b) May 24, 1993 storm events. Transect location is shown in Figure 7.2.

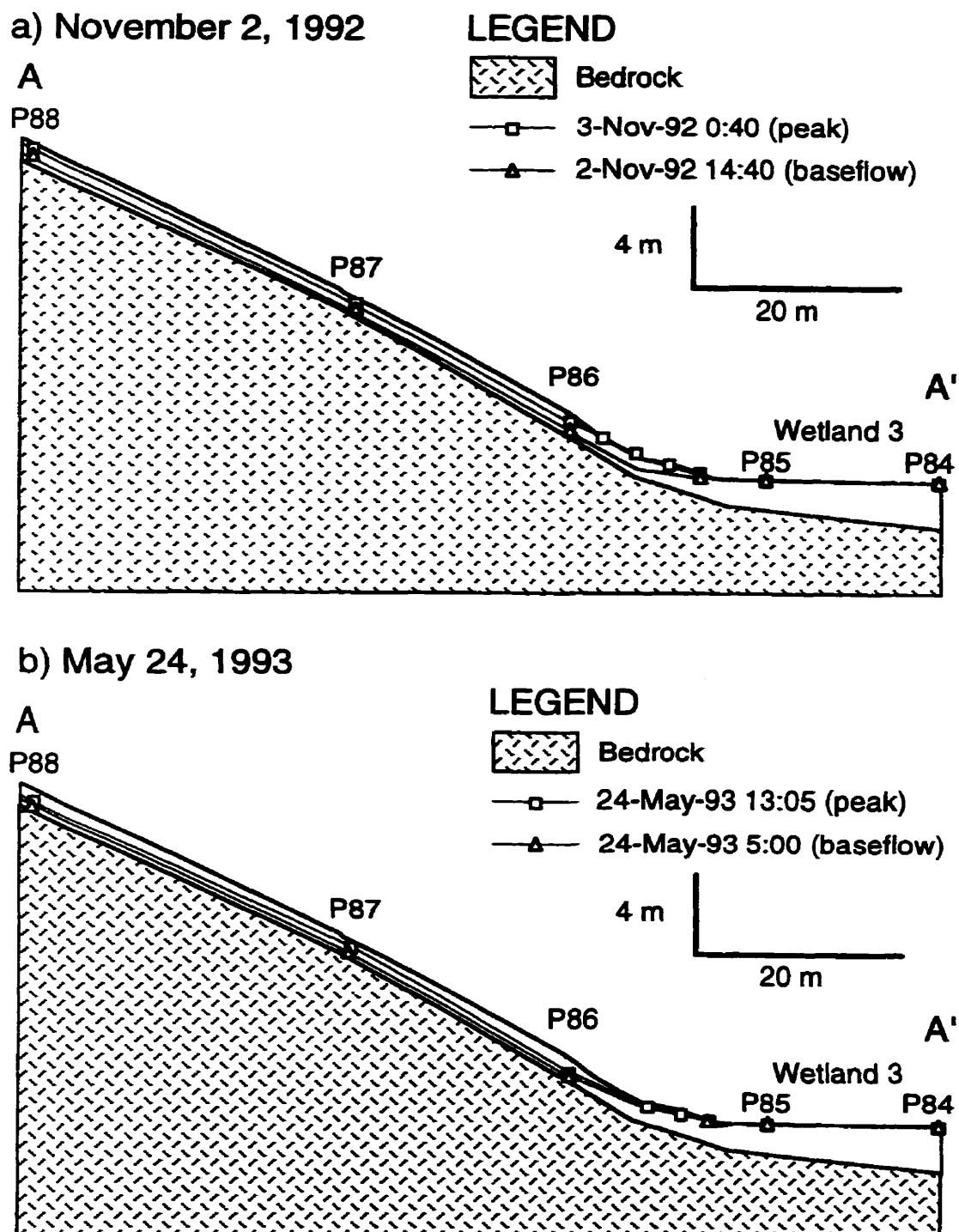
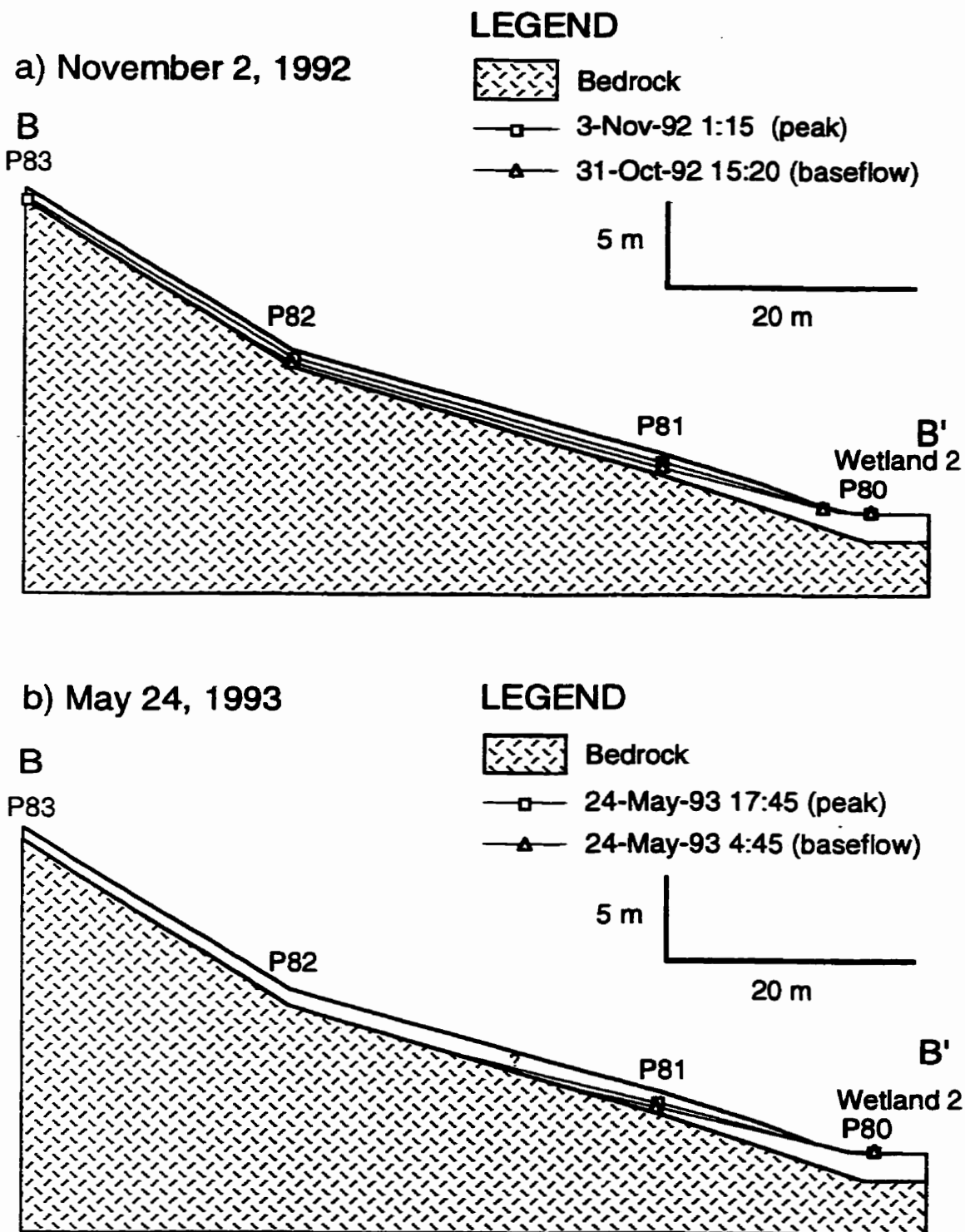


Figure 7.7 Water table profiles along transect B in Harp 3A during the a) November 2, 1992 and b) May 24, 1993 storm events. Transect location is shown in Figure 7.2.



During the May 24, 1993 storm, the water table responded at P88 but not at P82 and P83 (Figures 7.6b and 7.7b). However, during the May 28 storm event, water table responses were observed at P82 and P83 because the preceding storm increased soil water contents. Therefore, the spatial extent of water table fluctuations was smaller during drier conditions.

4. Timing of groundwater fluctuations during storms

Groundwater response to storms throughout the Harp 3A catchment was rapid and coincided with the increase in stream discharge (Figure 7.8). The rapid response of midslope piezometers suggests that even these areas could generate storm runoff in the early portions of a storm event. Rapid runoff generation was also demonstrated in soil water balances at TD88 (Chapter 6). The correlation between groundwater levels at P88 and stream discharge at W5 (Chapter 5) provides further evidence for the simultaneous response over wide areas. Such a good correlation would not exist if groundwater response was delayed compared to stream discharge.

In contrast to Harp 3A, the timing of the groundwater response in Harp 4-21 was not spatially uniform, but there was a progressive delay in water level response with distance upslope (Figure 7.9). During the June 22, 1989 storm, groundwater levels near the stream, such as at P20-01, responded to infiltration simultaneously with the increase in stream discharge. At P50-01, 24 m from the stream, the water levels rose rapidly during the first large peak in streamflow, but reached maximum levels during the second major peak. Maximum groundwater levels were reached approximately one day later at P10 (80 m from the stream), and two days later at P21 (only 21 m farther upslope). Groundwater levels at P22 and P23 declined throughout the entire storm and did not rise again until the following spring. A similar pattern of delayed groundwater response with increasing distance from the stream was

Figure 7.8 Timing of water table fluctuations in Harp 3A during the November 2 and 4, 1992 storm event. Groundwater elevations are plotted at the same scale. Piezometer locations are shown in Figure 7.2.

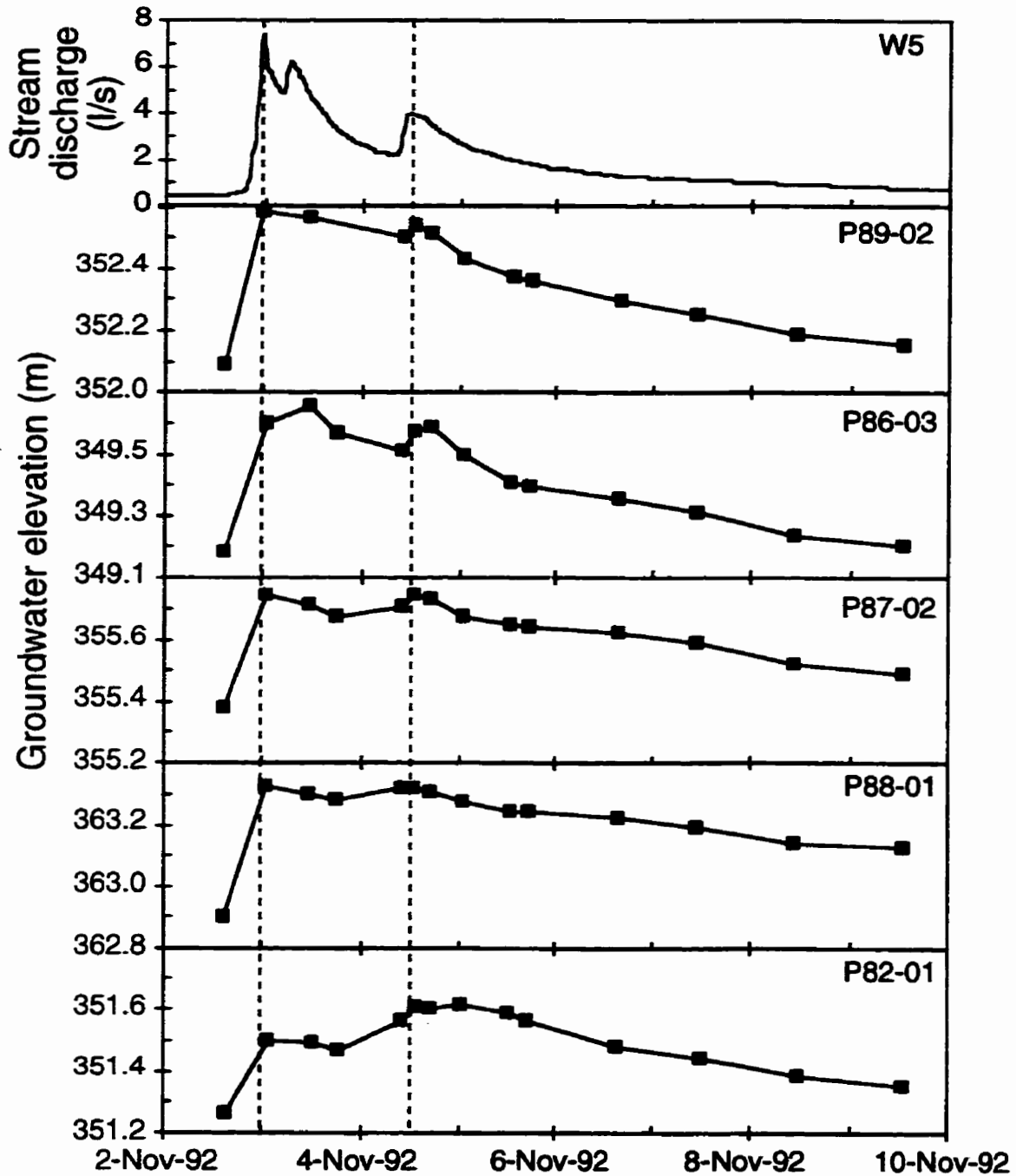
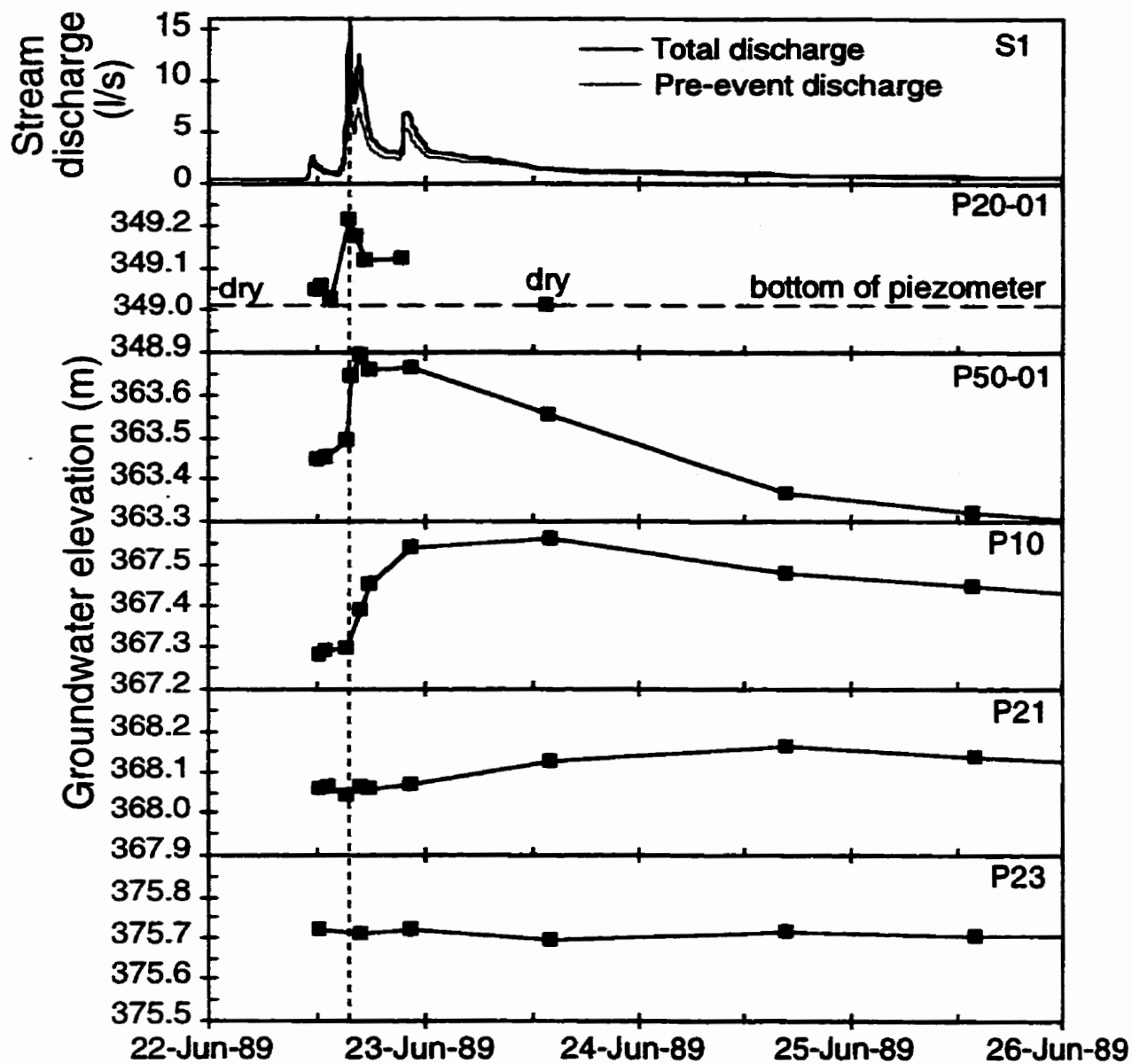


Figure 7.9 Timing of water table fluctuations in Harp 4-21 during the June 22, 1989 storm event. Groundwater elevations are plotted at the same scale. Piezometer locations are shown in Figure 7.2.



also observed during other storm events such as the November 2 and 4, 1992 event (Chapter 5).

5. Capillary fringe effect

The water table response did not result from the capillary fringe effect because water contents changed as groundwater levels rose above TDR waveguides. For example, water contents increased by 13 and 11 percent as the water table rose above the waveguides at TD86 (Harp 3A) during the November 2 and 10, 1992 storms respectively (Figure 7.10). Even when the water table briefly dropped only 0.05 m below the waveguides on November 12, water content decreased by 5.6 percent. At other sites in Harp 3A, increases of 1.2 to 14 percent water content were also observed as the water table rose above waveguides. These results confirm those inferred from the characteristic curves that did not show evidence of a widespread capillary fringe within soils (Chapter 6).

In Harp 4-21, there were also changes in water content as the water table fluctuated above and below the waveguides. Water contents in TD4-02 and TD4-03 changed by more than 1 and 0.6 percent respectively (Figure 7.11). Although these changes are small, they are statistically significant ($p < 0.05$). Even though a capillary fringe did not exist, available water storage was small and resulted in a rapid water table response.

The only characteristic curves that indicated the possible presence of a capillary fringe were P81-04, TD5-02 and TD5-03, but the water table never rose above the waveguides so water contents above and below the water table cannot be compared. At TD5 (P61), the very gradual water table response suggests that there was no capillary fringe immediately above the water table (Chapter 5).

Figure 7.10 Water table levels at P86-03 and water contents at TD86-03 during November 1992 storm events. Periods where the water table position is above the TDR waveguides are indicated by the horizontal lines.

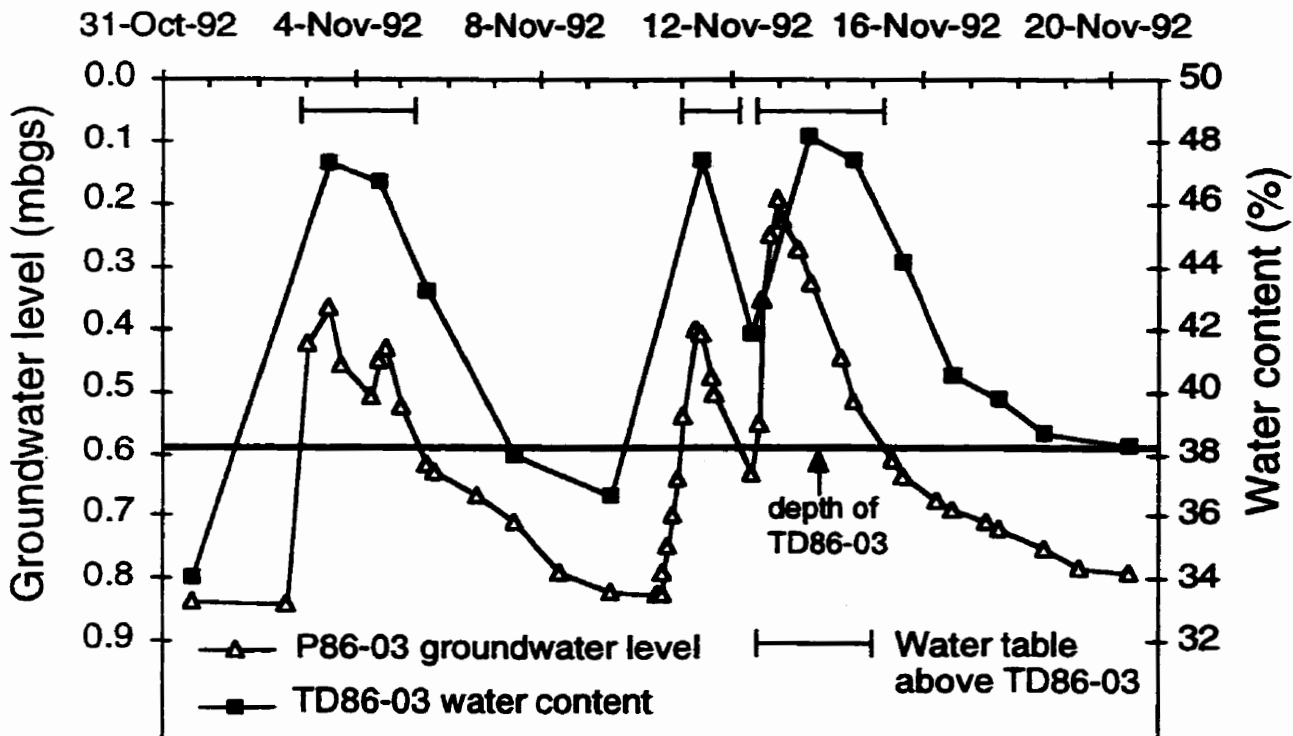
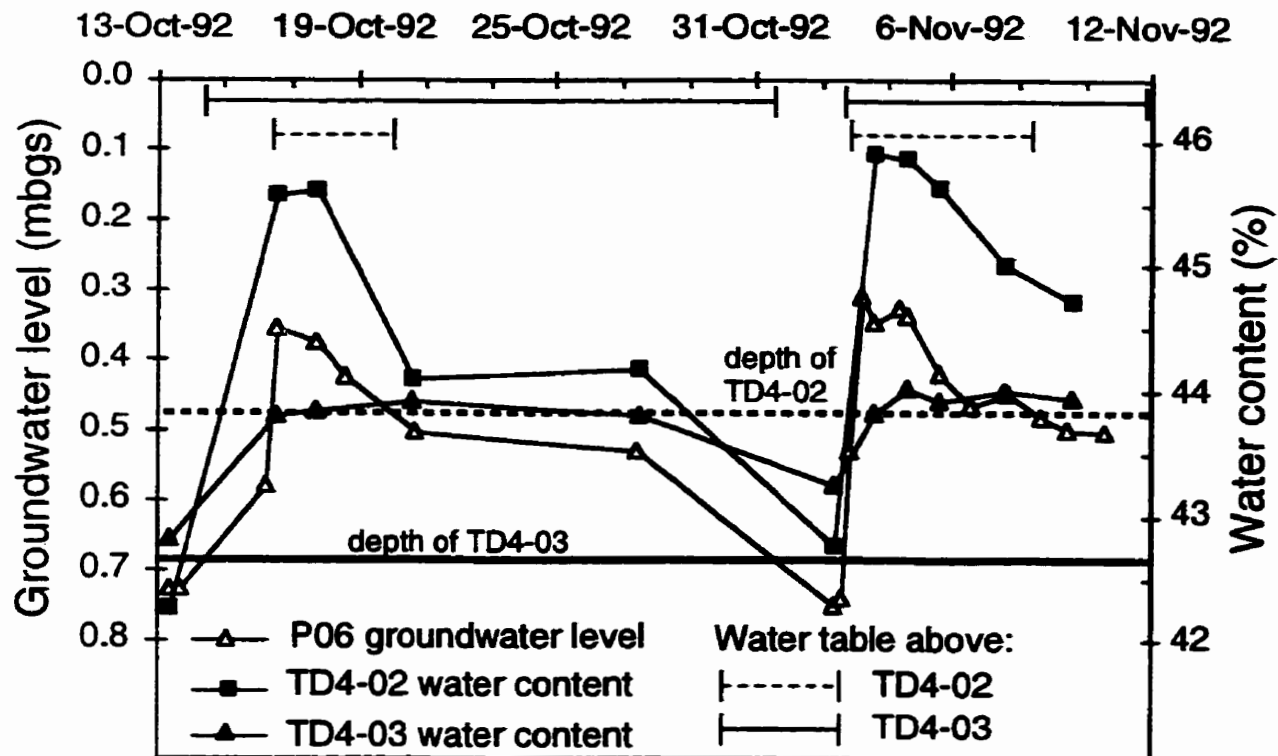


Figure 7.11 Water table levels at P06 and water contents at TD4-02 and TD4-03 during autumn 1992 storm events. Periods where the water table position is above the TDR waveguides are indicated by the horizontal lines.



6. Changes in hydraulic gradients

Downslope hydraulic gradients changed little during storms in both catchments because changes in water table elevation were small in comparison to differences in ground elevations. In Harp 3A, the hydraulic gradients remained nearly constant between P88 and P87 and between P87 and P86 since the water table at these three sites fluctuated simultaneously and by nearly the same amount (Figure 7.12). The hydraulic gradient between P86 and the edge of Wetland 3 increased slightly during storms since the water table rose at P86 but was already at ground surface at the edge of Wetland 3 prior to the storm. However, the maximum increase in hydraulic gradient was only 0.04 m/m. Changes in downslope hydraulic gradients were also small at other sites in Harp 3A and during other storms (Figures 7.6 and 7.7).

In Harp 4-21, changes in downslope hydraulic gradients during storms were also small. The maximum increase in hydraulic gradient near the stream (TD2 to TD1) during the November 2 and 4, 1992 event was 0.02 m/m (Figure 7.13). Changes in hydraulic gradient were also small along the entire hillslope transect (Figure 7.13). Water table profiles adjacent to the Harp 4-21 stream during the June 22, 1989 event are shown in Figures 7.14 and 7.15. The lower portion of Harp 4-21 was a groundwater discharge zone with baseflow groundwater levels in P15-01, P27-01, and P3 very near or above ground surface (Figure 7.14). During the storm, the downslope hydraulic gradient increased from 0.18 to 0.19 m/m between P4 and P3, and from 0.17 to 0.20 m/m between P20-01 and the edge of the hummock. In the upslope portion of Harp 4-21, the change in downslope hydraulic gradient between P59 and P11 increased from 0.08 to 0.09 m/m (Figure 7.15). From Figure 7.15, it is also apparent that there was no increase in hydraulic gradient from P58 to P50-01. Similar results were also observed adjacent to the middle section of the Harp 4-21 stream.

Figure 7.12 Groundwater levels and downslope hydraulic gradients along transect A in Harp 3A, autumn 1992. Transect location is shown in Figure 7.2.

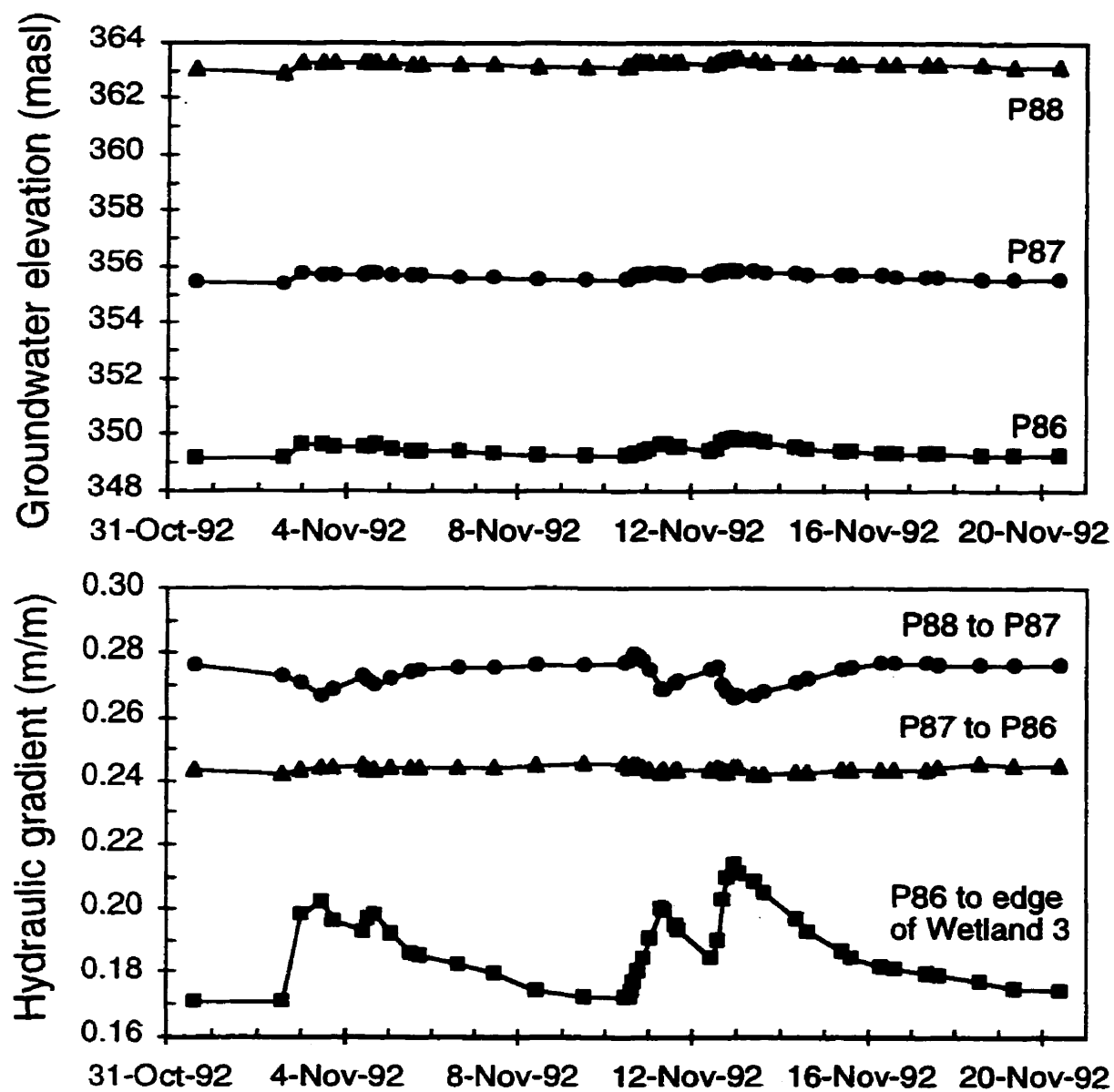


Figure 7.13 Groundwater levels and downslope hydraulic gradients in Harp 4-21, autumn 1992. Transect location is shown in Figure 7.2.

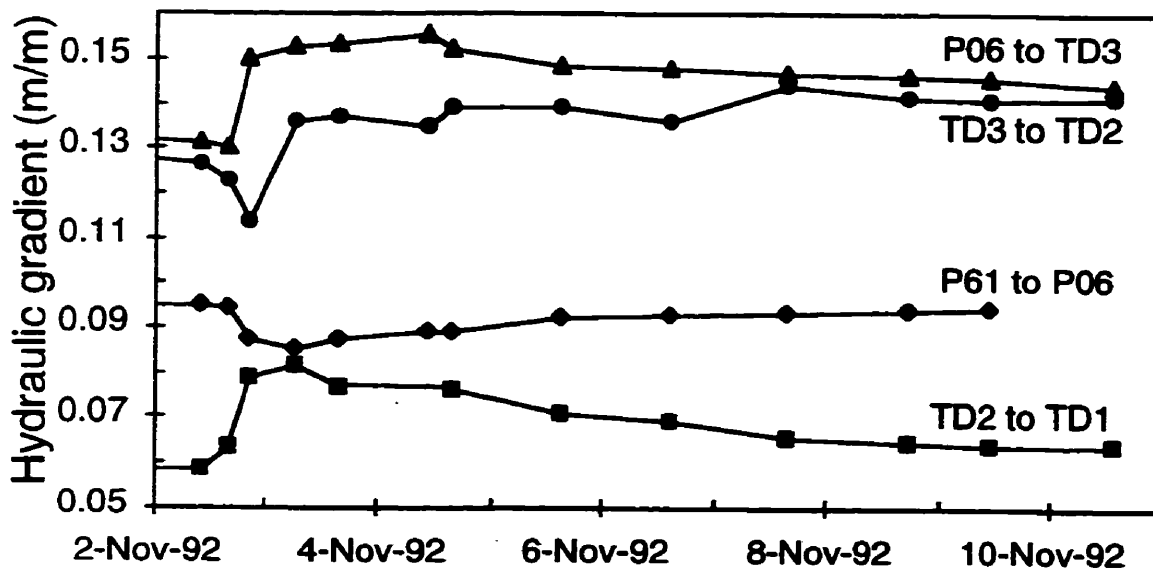
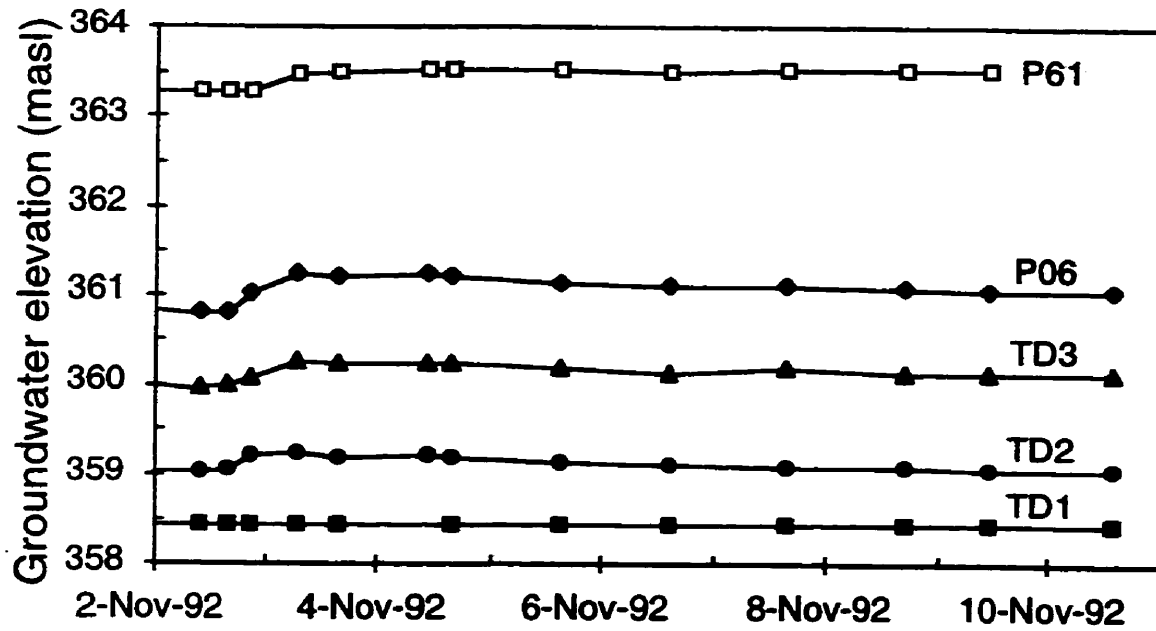


Figure 7.14 Water table profiles along transect C in Harp 4-21 during the June 22, 1989 storm event. Transect location is shown in Figure 7.2.

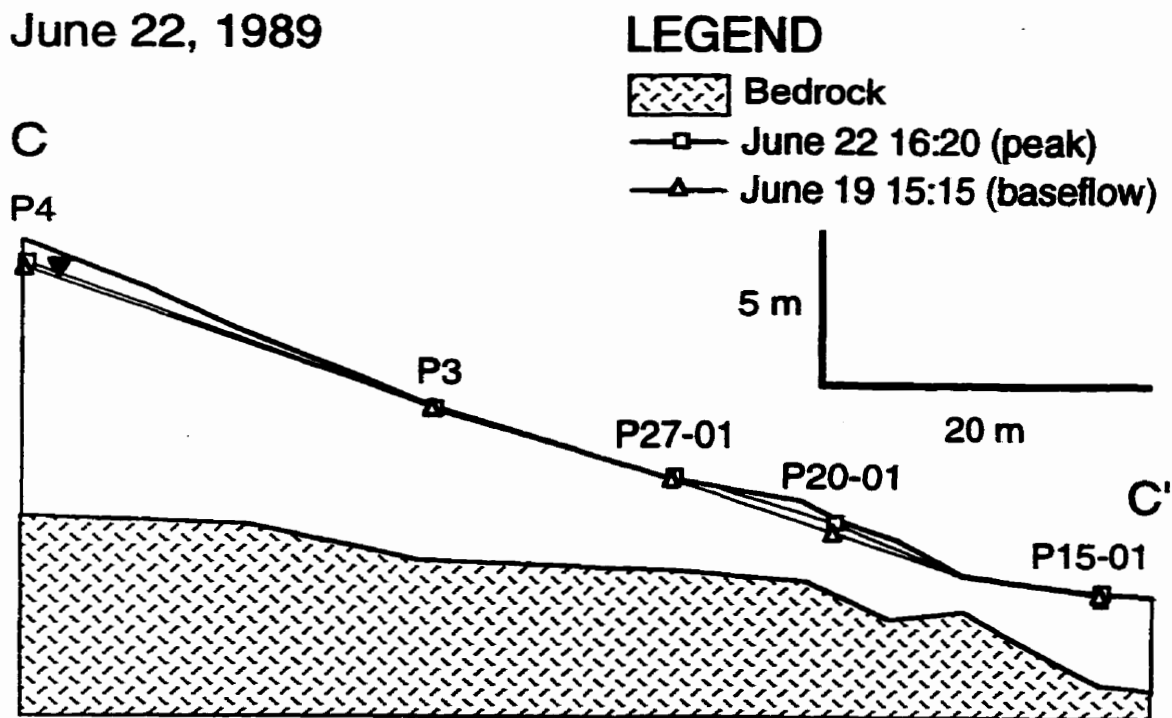
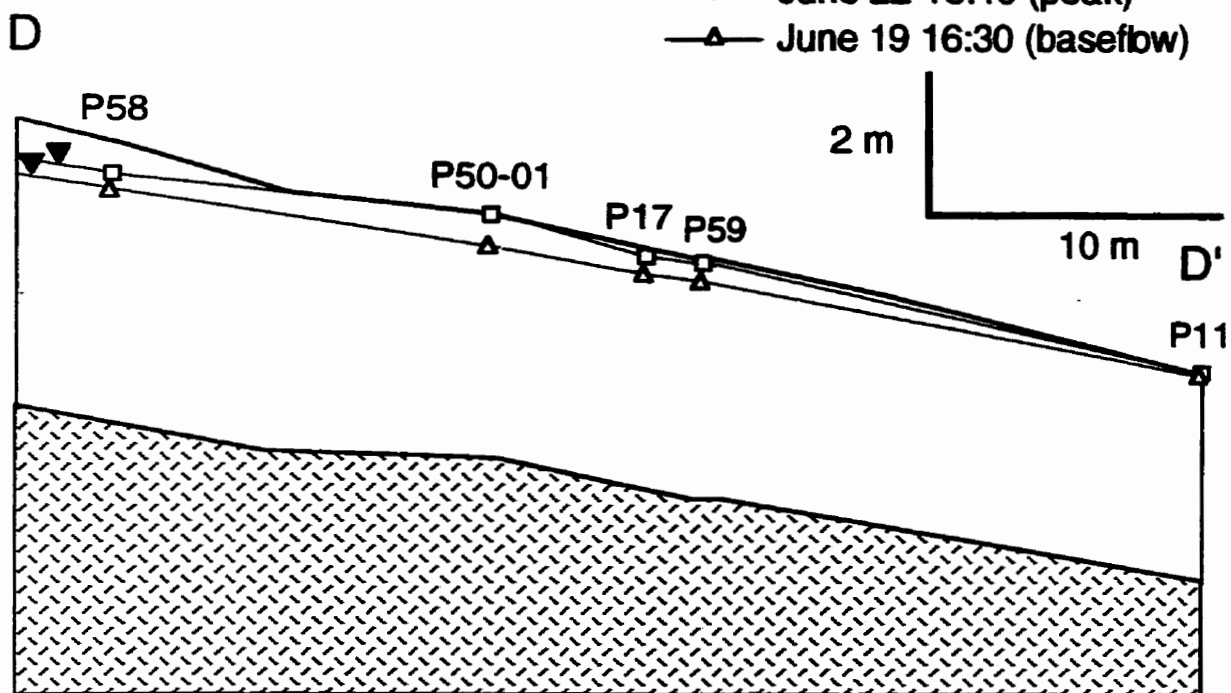


Figure 7.15 Water table profiles along transect D in Harp 4-21 during the June 22, 1989 storm event. Transect location is shown in Figure 7.2.

June 22, 1989

LEGEND

-  Bedrock
-  June 22 16:40 (peak)
-  June 19 16:30 (baseflow)



During drier conditions of autumn 1989, the change in downslope hydraulic gradient during storms was also small (Figure 7.16). The largest increase in gradient (from 0.04 to 0.07 m/m) occurred between P47 and P46. This profile demonstrates that a significant groundwater ridge did not develop during the storm.

If the increase in subsurface flow occurs in the existing saturated zone (ΔQ_A , Chapter 2), the relative changes in hydraulic gradient and groundwater flow should be equal. The maximum relative increase in hydraulic gradient during storms was compared to the relative increase in pre-event discharge (Tables 7.3 and 7.4). The peak pre-event discharge was calculated by multiplying the peak stream discharge with the proportion of pre-event water for the isotopic hydrograph separation closest to the peak discharge (Chapters 4 and 5). These storms represent quite a wide range of antecedent wetness, yet in all cases the relative increase in pre-event discharge (320-2500%) greatly exceeds the relative increase in downslope hydraulic gradients (4-86%).

With a few simple groundwater level measurements during baseflow conditions, it would have been possible to demonstrate that downslope hydraulic gradients could not have increased substantially during storms in both Harp 4-21 and Harp 3A. If the slope of the baseflow water table is compared to the topographic slope, it is apparent that large increases in downslope hydraulic gradients could not have occurred because the increase in hydraulic gradient was limited by the topographic slope (Figures 7.6, 7.7, 7.14, 7.15 and 7.16).

7. Flow through transiently saturated sediments

Since there is little evidence of a capillary fringe, the thickness and the spatial extent of transiently saturated sediments in both Harp 4-21 and Harp 3A are defined by the range of water table fluctuations during storms (Figures 7.4, 7.5, 7.6, 7.7, 7.14, 7.15, 7.16). It is only

Figure 7.16. Water table profiles along transect D in Harp 4-21 during the October 31, 1989 storm event. Transect location is shown in Figure 7.2. Wells P46 and P47 are located 15 m downstream and have been superimposed onto this section while maintaining the distances to the stream and the depths to the water table.

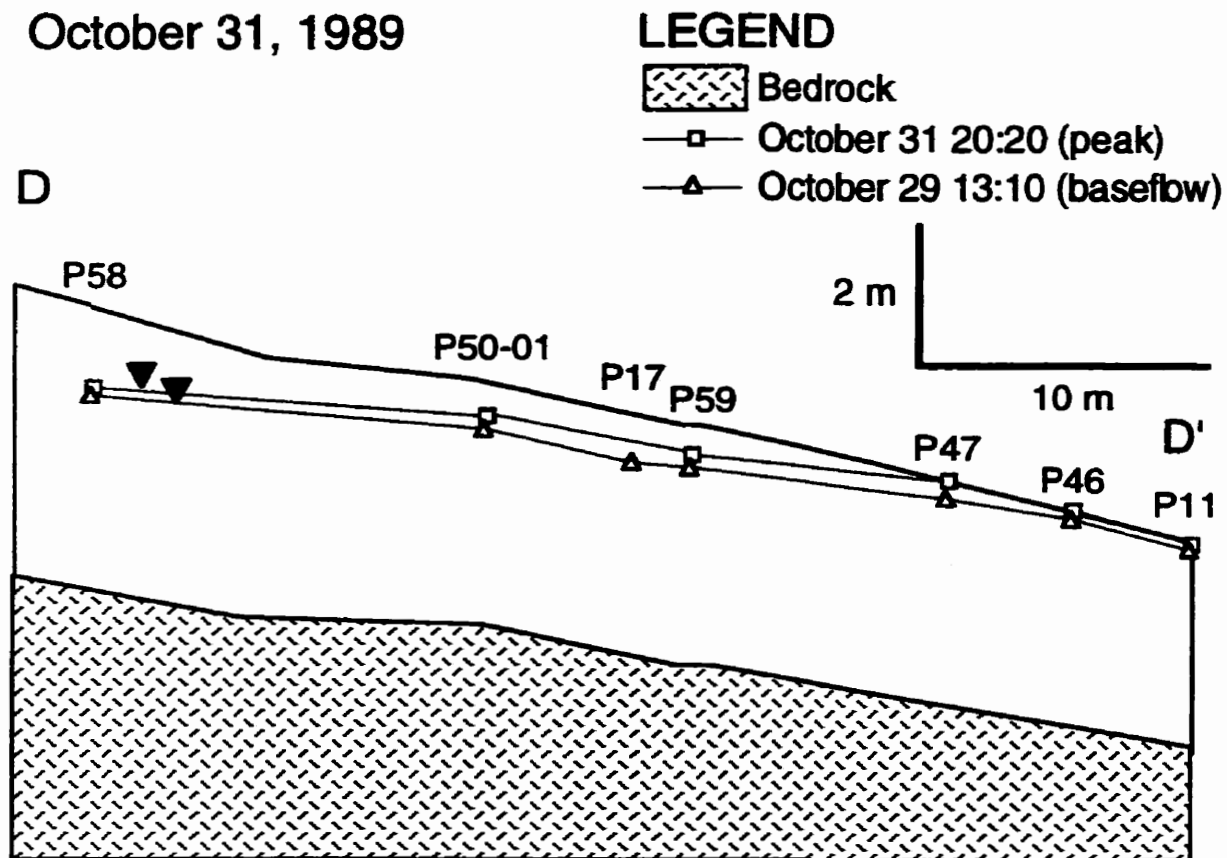


Table 7.3. Change in pre-event discharge and downslope hydraulic gradients in Harp 3A during selected storms.

	Baseflow	Peak	Change (%)
a) November 10, 1992			
Q _p , W1 (l/s)	4.0	22.9	470
gradient P81 to Wetland 2	0.26	0.27	6
gradient P86 to Wetland 3	0.16	0.18	16
b) November 12, 1992			
Q _p , W1 (l/s)	9.4	165	1600
gradient P81 to Wetland 2	0.27	0.30	11
gradient P86 to Wetland 3	0.17	0.20	15
c) May 24, 1993			
Q _p , W1 (l/s)	1.4	13.8	860
Q _p , W5 (l/s)	0.06	1.0	1500
gradient P81 to Wetland 2	0.25	0.27	6
gradient P86 to Wetland 3	0.15	0.17	8
d) May 28, 1993			
Q _p , W1 (l/s)	3.3	13.7	320
Q _p , W5 (l/s)	0.47	2.4	430
gradient P81 to Wetland 2	0.26	0.27	4
gradient P86 to Wetland 3	0.16	0.17	8

Q_p = pre-event discharge

Table 7.4. Change in pre-event discharge and downslope hydraulic gradients in Harp 4-21 during selected storms.

	Baseflow	Peak	Change (%)
a) June 22, 1989			
Q _p , S1 (l/s)	0.40	10.4	2500
gradient P4 to P3	0.18	0.19	6
gradient P6 to P33-01	0.12	0.14	16
gradient P59 to P11	0.08	0.09	14
b) October 31, 1989			
Q _p , S1 (l/s)	0.16	1.76	1000
gradient P59 to P11	0.06	0.08	18
gradient P47 to P46	0.04	0.07	86
c) May 24, 1993			
Q _p , S1 (l/s)	0.53	5.6	960
gradient TD2 to TD1	0.06	0.08	32
d) May 28, 1993			
Q _p , S1 (l/s)	0.72	4.4	510
gradient TD2 to TD1	0.07	0.08	20

Q_p = pre-event discharge

possible to estimate the maximum subsurface flow through transiently saturated horizons in Harp 4-21 and Harp 3A because there are no measurements of unsaturated hydraulic conductivity. In Harp 3A, the maximum subsurface flows have been calculated at P86, P87 and P88 for the same storms considered in Table 7.3 (Table 7.5) with the water table fluctuations shown in Figure 7.17. These calculations used Darcy's law with estimates of K_s from soil water balances in Chapter 6 (upper and lower B horizons) and from bail tests (C horizon).

The maximum increase in subsurface flow through transiently saturated sediments (ΔQ_t) is sufficient to account for most of the increase in pre-event flow to the streams during storms (ΔQ_p). Most ΔQ_t estimates compare, within a factor of 3, to ΔQ_p (Table 7.5). The variability in ΔQ_t estimates between sites likely results from uncertainty in the estimates of K_s . Slightly larger ΔQ_p values are partially attributed to the generation of pre-event flow downslope of piezometer locations. ΔQ_p represents the increase in subsurface flow at the base of the hillslope, whereas ΔQ_t represents the increase in subsurface flow at the piezometer location along the hillslope. Therefore, flow generated downslope of the piezometer would contribute to ΔQ_p but not to ΔQ_t at that piezometer location. The largest relative differences between ΔQ_p and ΔQ_t occurred during the May 24 and 28 storm events. Since the contributing lengths for the May storm events were smaller than the distances from the piezometers to the base of the hillslope, ΔQ_t estimates are expected to be much smaller than ΔQ_p .

Subsurface flow in transiently saturated sediments could also account for much of the increase in pre-event flow in the stream during storms in Harp 4-21. However, calculations of flow through transiently saturated sediments are less meaningful for Harp 4-21 than Harp 3A because more groundwater discharge reaches the stream as saturated overland flow and

Table 7.5 Maximum subsurface flow in transiently saturated horizons in Harp 3A.

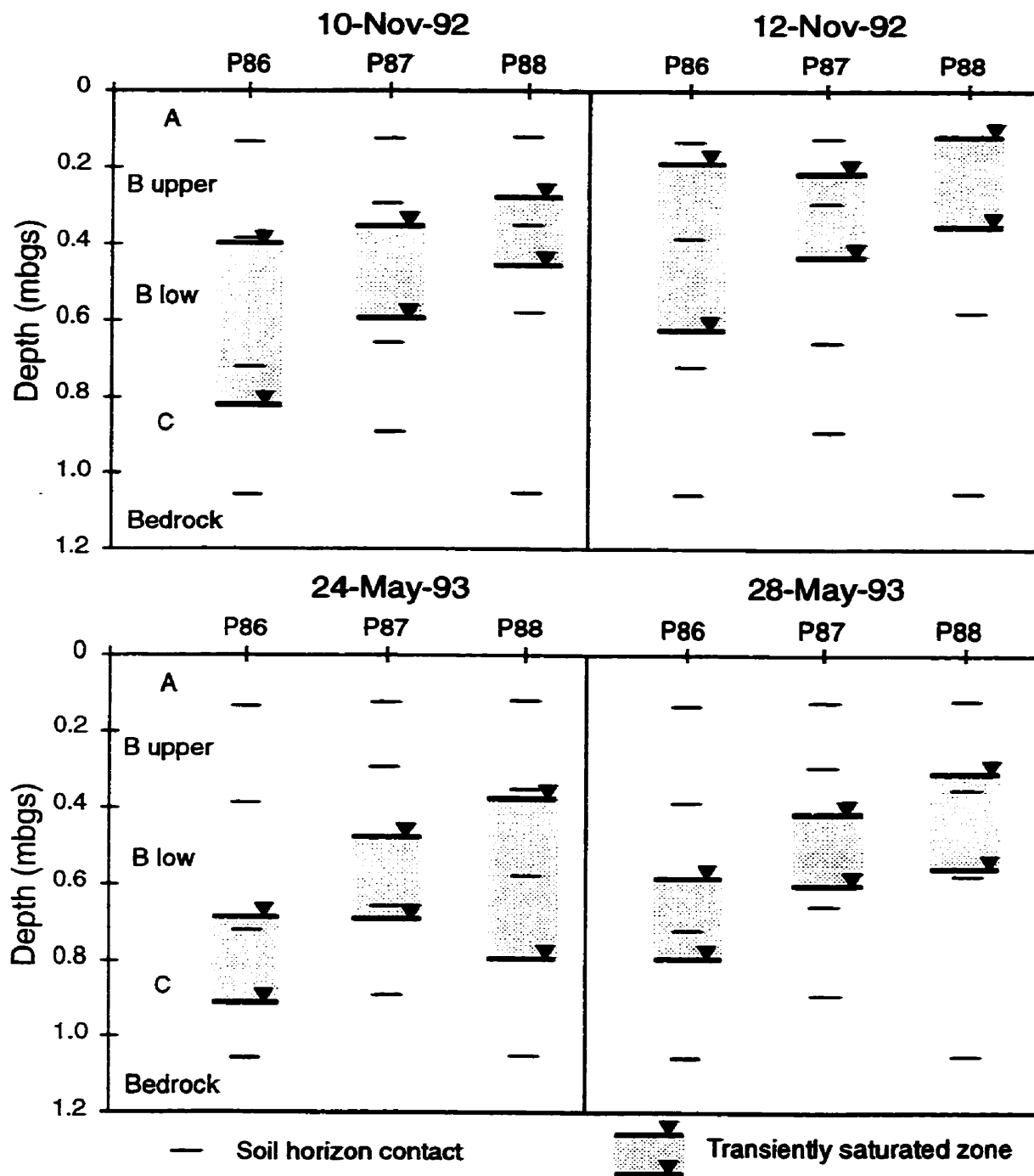
Date	ΔQ_p ¹		ΔQ_t		
	W1	W5	P86	P87	P88
	(L/s per m of stream length)				
10-Nov-92	0.012	-	0.0049	0.0059	0.020
12-Nov-92	0.094	-	0.052	0.030	0.055
24-May-93	0.0075	0.0031	0.0005	0.0044	0.0077
28-May-93	0.0063	0.0064	0.0019	0.0046	0.017

ΔQ_p = increase in pre-event flow to the streams during storms,

ΔQ_t = maximum increase in subsurface flow through transiently saturated sediments.

¹ ΔQ_p from Table 7.3 divided by stream length (L_s).

Figure 7.17 Transiently saturated soil horizons at sites P86, P87 and P88 in Harp 3A. The storms shown are those considered in Tables 7.3 and 7.5.



subsurface flow is more spatially variable. Hydraulic conductivity is the largest possible source of error in these calculations. K_s from bail tests in shallow piezometers near the stream are two to three orders of magnitude smaller than those obtained from surface infiltration experiments (discussed in the following section). Flows that are calculated with piezometer results are much too small to account for the increase in pre-event discharge, whereas flows that are calculated with K_s from infiltration experiments are more consistent with the increase in pre-event discharge (Table 7.6).

8. Matrix versus dual porosity flow

Several observations in Harp 4-21 and Harp 3A suggest that the soils in these catchments behave as a dual porosity medium. However, there is little evidence to suggest that macropores influence flow within the glacial till. Preferential flow through macropores was observed in soil pits and in some discharge zones of Harp 4-21 (MacLean, 1992). These macropores were often associated with root holes and were most common in the A and upper B horizons. The observed change in water contents from small negative to positive pressure heads (as in Figures 7.10 and 7.11) suggest that there were larger pores that became saturated only under positive pressure heads. The K_s values, estimated from soil water balances and infiltration experiments, were high and could not be explained solely by flow through the matrix, given its texture. Soils in Harp 4 are sandy silt, sandy loam and loamy sand with average percentages of silt plus clay that range from $17\pm 3\%$ to $43\pm 10\%$ in different soil horizons (Lozano et al, 1987). Average K_s for soils of similar texture are approximately 5×10^{-6} to 3×10^{-5} m/s (Rawls et al, 1993) and are comparable to those measured in piezometers screened within the upper 0.4 m of Harp 4-21 soils (1×10^{-6} to 7×10^{-6} m/s). Five ring infiltrometers in Harp 4-21 measured steady state infiltration rates that ranged from 2.2×10^{-4} to 4.0×10^{-3} m/s with a geometric mean of 9.8×10^{-4} m/s. In Harp 3A, soil water

Table 7.6 Maximum subsurface flow in transiently saturated horizons in Harp 4-21.

Date	ΔQ_p ¹	ΔQ_t			
		K piezometer		K infiltration	
	S1	P47	TD2	P47	TD2
		(L/s per m of stream length)			
31-Oct-89	0.0036	0.00002	-	0.013	-
24-May-93	0.012	-	0.00005	-	0.0061
28-May-93	0.0084	-	0.00002	-	0.00029

ΔQ_p = increase in pre-event flow to the streams during storms,

ΔQ_t = maximum increase in subsurface flow through transiently saturated sediments.

¹ ΔQ_p pre-event from Table 7.4 divided by stream length (L_s).

balances yielded K_s values from 8.4×10^{-5} to 1.2×10^{-3} m/s in the B horizon. Therefore, it is unlikely that the high K_s is characteristic of matrix flow alone.

Discussion

Conceptual models of subsurface stormflow in Harp 4-21 and Harp 3A

Subsurface flow was the dominant component of runoff during most storms in Harp 4-21 and during storms with wet antecedent conditions in Harp 3A (Chapters 4, 5 and 6). Only after dry antecedent conditions in Harp 3A were contributing areas to storm runoff so small that subsurface flow was minimal; runoff was generated predominantly from direct precipitation onto saturated areas (Table 7.1). The conceptual models of subsurface stormflow generation, summarized in Chapter 2, are considered for Harp 4-21 and Harp 3A.

Groundwater ridging model

The groundwater ridging model is not appropriate for either Harp 4-21 or Harp 3A as demonstrated by several different results. Firstly, groundwater ridges were not observed in groundwater level profiles (Figures 7.6, 7.7, 7.14, 7.15, 7.16). Secondly, evidence for capillary fringes was not observed. Although water table responses were rapid, they were always accompanied by changes in water content (Figures 7.10 and 7.11). Thirdly, the relative changes in downslope hydraulic gradients were small and could not account for the relative increases in pre-event discharge measured in the stream (Tables 7.3 and 7.4). Lastly, the contributing lengths for several storms were much larger than could be explained by groundwater ridging (Tables 7.1 and 7.2). Although storms with drier antecedent conditions had smaller contributing areas, they lacked the water table responses necessary to support the groundwater ridging model.

Transmissivity feedback, perched water table and old water macropore flow models

The increase in water content, in particular the saturation of sediments, was the dominant mechanism responsible for the increase in subsurface flow. Water table responses were rapid enough to produce the observed changes in stream discharge (Figures 7.8 and 7.9). Water table rise and the development of transiently saturated sediments occurred over a sufficiently wide area to account for the volume of storm runoff. For example, in Harp 4-21, the water table responded to the June 22 and October 31, 1989 storms over areas of 2.3 and 0.6 ha respectively, whereas the minimum contributing areas for these storms were 0.8 and 0.3 ha respectively. The actual contributing area for the November 2 and 4, 1992 storm event was estimated to be 1.5 to 2.0 ha (Table 7.2) with a water table response area slightly smaller than that observed on June 22, 1989 (2.3 ha). Similarly, in Harp 3A, minimum contributing hillslope lengths to storm events on November 2 and 4, and November 10 and 12, 1992 were between 55 and 86 m (Table 7.1) and the water table response was shown to extend at least 68 m upslope at two locations (Figures 7.6 and 7.7). Since the extent of groundwater response exceeds the contributing areas and lengths, flow through transiently saturated sediments may explain the observed storm runoff.

Of the different models that propose an increase in saturation as the primary mechanism for increased subsurface stormflow (Chapter 2), the transmissivity feedback model is most consistent with field measurements and observations. Firstly, the maximum subsurface flow through transiently saturated sediments could have caused the increase in pre-event stream discharge (Tables 7.5 and 7.6). Secondly, soil water balances and graphs of stream discharge versus groundwater levels showed that subsurface flow increased with a rising groundwater table, particularly when it rose into shallow soil horizons (Chapters 3, 5 and 6). Soil moisture measurements confirmed that water contents increased with the rising water table (Figures 7.10 and 7.11). Thirdly, perched water tables were not observed in Harp 4-21.

In steep or well drained upslope soils of Harp 3A, a perched water table may have developed and caused the saturation of permeable soil horizons. However, subsurface flow from these areas was probably transmitted downslope in a way similar to the transmissivity feedback model with dual porosity flow. Finally, the old water macropore flow model (McDonnell, 1990) is not applicable in either catchment because precipitation readily infiltrated the soil matrix and Horton overland flow did not occur. However, pre-event water may have been displaced through macropores.

Unsaturated flow model

Although downslope unsaturated flow is not needed to explain subsurface runoff volumes, its importance cannot be assessed because there are few relevant data. The soil water balance approach (Chapter 6) cannot be used to rule out unsaturated flow because saturated flow cannot be distinguished from unsaturated flow. The absence of hillslope runoff from Harp 3A during summer storms (all stream runoff can be accounted for by precipitation onto saturated areas, Table 7.1) suggests that unsaturated flow does not contribute significantly to stream runoff. In contrast, rapid water table responses in most piezometers and large increases in water content in lower soil horizons suggest that vertical unsaturated flow is widespread and rapid.

Role of macropores

Effect of hydraulic conductivity

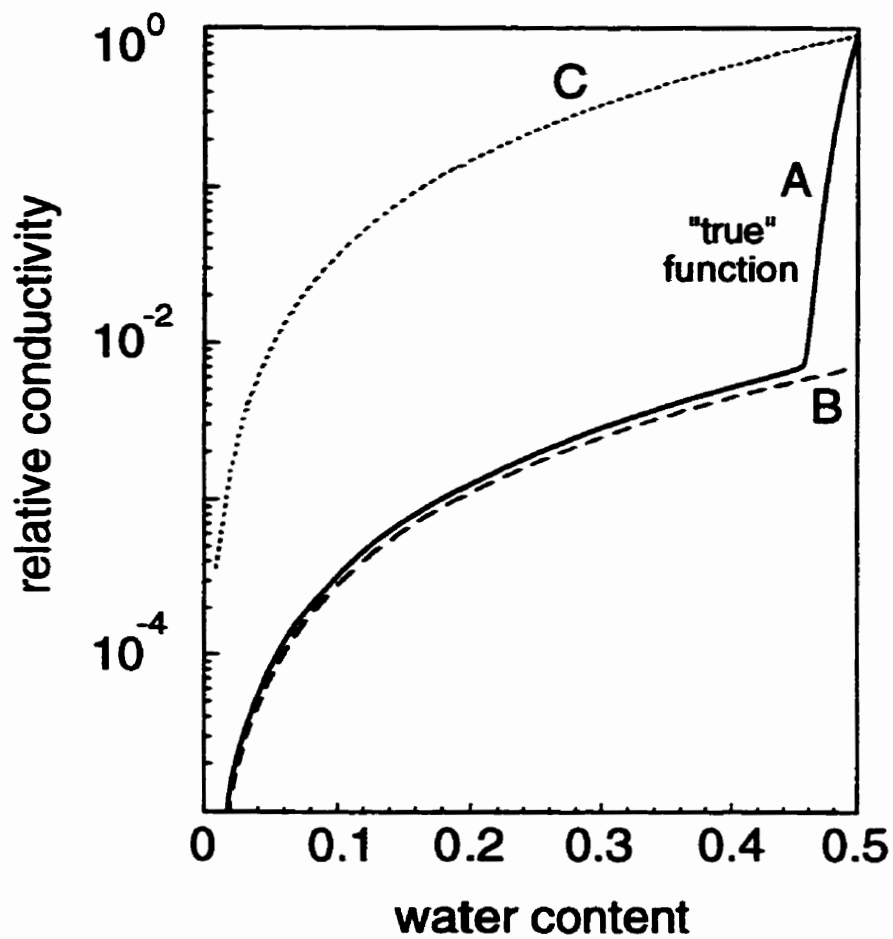
Flow within the transiently saturated zone cannot be strictly matrix flow. The K_s required to produce plausible subsurface flows ($\approx 10^{-3}$ - 10^{-4} m/s, Tables 7.5 and 7.6) are one to three orders of magnitude greater than those measured in piezometers. However, such high estimates of K_s were obtained from soil water balances (Chapter 6) and steady state

infiltration measurements. The discrepancy could be attributed to macropores which have not been disturbed in the measurements used for water balances and infiltration but have been destroyed by augering during piezometer installation. Consequently, the transmissivity feedback model with dual porosity flow appears to be most applicable in the soils. In glacial tills where macropores are less prevalent, the transmissivity feedback model with matrix flow may be most applicable.

Similar discrepancies in K_s were obtained within the Plastic Lake (PC-108) catchment, located about 40 km southeast of Harp Lake (House, 1996). The catchment is similar to Harp 3A but with thinner podzolic soils (average depth 0.3 m) developed on a thin basal till. In contrast to Harp 3A, the dominant vegetation is coniferous. House (1996) compared the K_s of soils at 35 sites within PC-108 using both ring infiltrometers and constant head permeameters on soils cored at several depths. Ring infiltrometer measurements yielded K_s values between 8.2×10^{-5} m/s and 3.9×10^{-3} m/s whereas permeameter measurements yielded K_s values between 6.3×10^{-8} to 7.9×10^{-4} m/s. K_s from ring infiltrometers was consistently one to four orders of magnitude higher than for permeameter tests on cores extracted from the same sites within the valley. Since K_s for cores was representative of the matrix and ring infiltrometers of the bulk forest soils, the discrepancies of K_s were attributed to the presence of macropores by House (1996).

Durner's (1994) model describes the influence of pore size distribution on soil water retention and unsaturated hydraulic conductivity functions. This model considers not only dual porosity media (bimodal pore size) but also soils with heterogeneous pore sizes. Durner (1994) identifies the problems of using unimodal pore size distribution (i.e. matrix flow) models to estimate unsaturated hydraulic conductivity curves of dual porosity sediments (Figure 7.18). Curve A is the "true" relative conductivity function calculated for dual porosity media with Durner's model. The unsaturated hydraulic conductivity function based on the

Figure 7.18 Schematic representation of the conductivity calibration problem for bimodal (dual porosity) pore size distributions. Line A is the conductivity curve for a bimodal pore size distribution. Line B is the conductivity curve for unimodal (matrix) pore size distribution matched to unsaturated conductivity or K_s for the matrix. Line C is the conductivity curve for unimodal (matrix) pore size distribution matched to bulk K_s (adapted from Durner, 1994).



undisturbed bulk K_s (curve C) overestimates unsaturated hydraulic conductivity because large pores drain very rapidly at small negative pressures. The unsaturated hydraulic conductivity function based only on measurements of the saturated and unsaturated hydraulic conductivity of the matrix (curve B) underestimates saturated and nearly saturated hydraulic conductivity because it ignores the influence of large pores on hydraulic conductivity. Incorrect mathematical representation of soil water retention and hydraulic conductivity curves in sediments with bimodal (dual porosity) or heterogeneous pore size distributions can lead to inaccurate results and interpretations in numerical models of subsurface stormflow.

Interaction between the matrix and macropores: pre-event flow in macropores

A more explicit description of hydrological processes in the transmissivity feedback model with dual porosity flow is required to explain the displacement of pre-event water through macropores. In the case of a soil matrix of fine sand, the matrix could have a high water content or could be tension-saturated ≈ 0.5 m above the water table. The macropores above the water table would drain because they are too large to remain saturated for even small tensions. In effect, the matrix could have a capillary fringe whereas the bulk soil would not. Consequently, soil moisture measurements from TDR or neutron probes would indicate a small decrease in water content compared to fully saturated conditions. Macropores that do not extend to the ground surface may saturate with pre-event water rather than event water. Once a small volume of infiltration reaches the top of the tension-saturated (or nearly saturated) zone in the matrix, the water pressure in the pores of the soil matrix becomes positive and water will flow from the soil matrix into the macropores. Therefore, macropores fill with pre-event water from the matrix. Once the macropore is filled, it can greatly increase the K_s of the bulk soil. Since the macropore is the largest pore, it also drains first after infiltration stops, and causes a rapid decrease in K_s . This mechanism is consistent with

observations of rapid water table response and small changes in water content in Harp 4-21 (Figure 7.11).

Another explanation for pre-event water flow through macropores is the maintenance of hydraulic gradients between the matrix and macropores. The transmissivity feedback model with dual porosity flow allows for discontinuous macropores provided that the K_s of the matrix is sufficiently high to sustain flow between them. Since saturated macropores offer less resistance to flow, they may act as localized conduits such that small (centimeter) scale patterns of hydraulic gradients may develop around them. Macropores can have 'recharge' zones where water flows into macropores from the matrix and 'discharge' zones where water flows from the macropores into the matrix or to the ground surface. In effect, flow patterns around individual macropores may be analogous to regional scale groundwater flow in discontinuous high permeability aquifers (Freeze and Witherspoon, 1967). Discontinuous macropores should enhance mixing of event and pre-event water. Given that the volume of event water is small compared to the large volume of pre-event water stored in the soil, such mixing will increase the proportion of pre-event water that reaches the stream.

Spatial extent of runoff production

Variable contributing areas

Although Beven and Kirkby (1979) unfortunately used the term 'variable contributing area' to be synonymous with 'variable source area', these two concepts are distinctly different. Variable source areas are delineated by the expansion and contraction of discharge areas during storm events. The variable source area concept attributes storm runoff to return flow (groundwater discharge that flows overland to the stream) and precipitation directly onto discharge areas (Dunne, 1978). In effect, the variable source area is where water actually becomes storm runoff. The concept is practical because variable source areas are easily

delineated by visual observations (e.g. Dunne et al., 1975). However, the concept does not consider the source area of return flow. Therefore, it does not address the spatial extent of subsurface stormflow production from the hillslopes.

The contributing area is defined here as the area from which precipitation or infiltration actually produces storm runoff. It includes the portions of a catchment that contribute to storm runoff as both surface and subsurface flow. Unlike the variable source area concept, actual contributing areas cannot be identified visually and are more difficult to delineate. In addition, they do not necessarily transform 100 percent of the precipitation into runoff, and therefore, yields must be quantified explicitly. The yield (i.e. subsurface runoff ratio) at a site within a contributing area can be quantified by soil water balances (Chapter 6). Measurements at several sites can be used to delineate the spatial extent and quantity of runoff production. Variable contributing areas are a better representation of the actual source areas of stream discharge. Variable contributing areas are always equal to or larger than variable source areas. They only refer to the same area in the unlikely case that all the storm runoff is generated from precipitation onto saturated areas (i.e. no return flow).

Seasonal variations in contributing areas are related to the spatial extent of the water table within the soil. In Harp 3A, the proportion of hillslope that contributed to storm runoff varied seasonally from zero to as much as 90% of its length. Lengths of contributing hillslopes were zero (or negative) when a water table was not present in the hillslopes, increased when a water table was present in lower hillslopes, and were largest as the water table extended farther upslope (Table 7.1). In Harp 4-21, seasonal variations in contributing area were much smaller as the water table remained within near-stream soils throughout the year. Contributing areas were comparable to the spatial extent of the water table within the soil (Figures 7.4 and 7.5). Therefore, the areal extent of the water table in the soil may be an easily measured proxy

for the contributing areas to storm runoff in studies for which soil water balances are not used to delineate them.

Localized flow systems

In catchments, small isolated flow systems may develop within small topographic ridges in discharge areas. The conceptual models of subsurface flow in Chapter 2 consider flow on a hillslope scale with one recharge area and one discharge area; small topographic features are generally ignored. Within all these models, there is a cumulative increase in subsurface flow along the flowpath with the maximum subsurface flow at the boundary between recharge and discharge areas (hinge line). With only one continuous recharge zone, all the subsurface flow from the hillslope must pass this boundary. An example of a small isolated flow system was observed at piezometer nest P20-01 which is located on a very small ridge approximately 10 m in diameter within the lower portion of Harp 4-21 (Figure 7.14). Groundwater discharged around the edges of the ridge and vertical hydraulic gradients at depth within the nest indicated upward flow. However, the vertical hydraulic gradient at the water table within the ridge indicated downward flow or recharge. Therefore, the ridge is actually a separate flow system with recharge at the surface and discharge downslope. Smaller topographic features, such as hummocks, may also form very small flow systems on the scale of a few meters or less. The area of each hummock does not necessarily have to be large, provided that the vertical flow at the surface is downward. Since these isolated flow systems can occur downslope of the hinge line, estimating subsurface flow across it would underestimate the total subsurface flow.

The subsurface flow models of Chapter 2 also apply within small topographic features. Within the ridge at P20-01, the increase in downslope hydraulic gradient from 0.17 to 0.20 m/m during the June 22, 1989 event was too small to produce a large increase in flow by

groundwater ridging. In general, these small flow systems are probably of minor importance to the total volume of flow generated from the main hillslope. However, since these areas have shallow water tables and are close to the stream, they may generate subsurface runoff more rapidly during early storm periods. Furthermore, the water chemistry of the subsurface discharge from small isolated flow systems could be different from that of the hillslope areas because of the differences in flowpaths and residence times.

Subsurface flow mechanisms in Canadian Shield catchments

Most isotopic and geochemical hydrograph separations in Canadian Shield catchments show the dominance of pre-event water during storms (Fritz et al., 1976; Sklash and Farvolden, 1979; Bottomley et al., 1984, 1986; Sklash, 1986; Moore, 1989; Buttle and Sami, 1992; Renzetti et al., 1992). Event water contributions are usually only important where soils are very thin or absent over much of the catchment (Allan and Roulet, 1994), or are flushed by snowmelt (Wels et al., 1990). The results of Maulé and Stein (1990) during snowmelt in the Lac Laflamme watershed are among the few exceptions. In their study, the large proportion of event water (71%) was generated mostly as saturation overland flow because the water table reached ground surface during a period of very rapid snowmelt. Few of these studies included detailed hydrometric measurements to examine subsurface flow processes directly.

No hydrometric evidence has yet been presented for undisturbed Canadian Shield catchments where the dominant cause for increased subsurface flow to streams during storms is an increase in hydraulic gradient. Based on the results from Harp 4-21 and Harp 3A, increased downslope hydraulic gradients will rarely be sufficient to be the primary cause for increased subsurface flow, and therefore, the groundwater ridging model is not widely applicable within the Canadian Shield. Firstly, large increases in hydraulic gradients are not possible in many catchments. In watersheds with an existing water table in the hillslope, the

water table adjacent to the stream will generally be almost parallel to the ground surface except if the stream is incised (which is uncommon). In watersheds where the water table is absent in hillslopes, most of the increase in subsurface flow will likely be caused by the saturation of sediments as the water table develops rather than by increased hydraulic gradients. Secondly, since much of the southern Canadian Shield is forested, most soils will have macroporosity as a result of root holes and soil structure. As a result, most soils will not develop a capillary fringe and macropores may contribute substantially to the bulk saturated hydraulic conductivity.

The transmissivity feedback model with dual porosity flow may also apply to another watershed, PC-108, on the Canadian Shield. From chemical and isotopic hydrograph separations, Wels et al. (1991b) calculated that 90% of spring runoff (1987) occurred as subsurface flow. From measurements of stream discharge and subsurface flow in hillslope trenches within the same catchment, Renzetti et al. (1992) confirmed that subsurface flow was the dominant source of stream runoff. Subsurface flow occurred predominantly within a perched water table that developed at the soil/bedrock interface. Macropore flow was thought to contribute to subsurface flow because measured subsurface flows exceeded those calculated from measured soil hydraulic conductivity (3.8×10^{-5} m/s). Using their published peak subsurface flow rates (Renzetti et al., 1992), the bulk hydraulic conductivity of the layer above the bedrock surface was calculated to be between 8.2×10^{-5} and 3.4×10^{-4} m/s, which is comparable to K_s measured by House (1996) and in Harp 4-21 and Harp 3A.

Several studies in Canadian Shield catchments suggest that unsaturated flow is a minor component of storm runoff. In PC-108 during a storm on October 10, 1989, the lower slope did not saturate and the trench produced only 0.07% of rainfall (Renzetti et al., 1992). In Harp 4-21 where the water table was present in the soil, the same storm generated 5% of rainfall. Subsequent storms in PC-108 (both larger and smaller) produced between 5 and 14% of

rainfall when a water table was present in the hillslope (Renzetti et al., 1992). In the Lac Laflamme catchment north of Quebec City, Roberge and Plamondon (1987) report that only 0.2 to 6% of the total discharge in the trenches occurred above the water table. At Chalk Lake, Ontario, measurements of unsaturated hydraulic conductivity from deuterium profiles in undisturbed soils yielded values between 6.8×10^{-8} and 1.4×10^{-7} m/s (Sami and Buttle, 1991), which would be too small to produce significant subsurface stormflow as unsaturated flow in most Canadian Shield catchments. These studies suggest that unsaturated flow is a very small component of subsurface stormflow in Canadian Shield catchments.

Conclusions

A systematic assessment of subsurface stormflow processes, such as the one presented in this study, can improve both the planning and interpretation of catchment hydrology research. Prior to installing instrumentation in a watershed, preliminary assessment of the importance of subsurface flow can be made from the observed extent of discharge areas and areas of surface saturation during storms, and from storm hydrograph separations. Similarly, near-stream topography and water levels in a transect of shallow wells, can be used to determine the maximum changes in near-stream hydraulic gradients. Minimum contributing areas can be calculated from rainfall and runoff volumes. These results can indicate whether increased hydraulic gradients are the primary mechanism for increased subsurface stormflow. With this preliminary information, monitoring strategies should be developed according to the expected dominant mechanisms for increased subsurface flow during storms (Chapter 2). In catchments where increases in hydraulic gradients are dominant, investigations should focus on near-stream changes in water table elevations, vertical and horizontal hydraulic gradients, the capillary fringe effect, and the saturated hydraulic conductivity of sediments near the stream. Conversely, in catchments where increases in water content cause increases in subsurface stormflow, investigations should include water table fluctuations, changes in water

content and soil water tension, saturated and unsaturated hydraulic conductivity, water retention curves, and the influence of macropores, for the entire watershed area. Systematic reporting and assessment of data, in particular, contributing areas, changes in hydraulic gradients, water table fluctuations and hydraulic conductivity, would provide a better basis of comparison of results with those from different watersheds.

In this study, subsurface stormflow was the dominant component of storm runoff in Harp 4-21 and Harp 3A and resulted from increased water contents rather than from increased hydraulic gradients. Water table profiles, hydraulic gradients, water contents, and contributing areas clearly demonstrate that the groundwater ridging model is not appropriate in these catchments. Rather, results are most consistent with the transmissivity feedback model with dual porosity flow. Subsurface flow in transiently saturated soil horizons can account for the increase in pre-event stream discharge because soil horizons have very high hydraulic conductivities as estimated from infiltration experiments and soil water balances. These high hydraulic conductivities are only possible if macropores are present; much lower hydraulic conductivities were measured by piezometer bail tests because instrumentation likely compromised the surrounding macropore structures. The perched water table and old water macropore flow models could not fully account for the observed data.

Although subsurface runoff processes may be similar in both Harp 4-21 and Harp 3A, the timing and spatial patterns of subsurface flow generation are different because of differences in depth to the water table. In Harp 3A, subsurface flow is generated from most of the hillslope simultaneously. In Harp 4-21, subsurface runoff is generated progressively from near-stream to midslope areas during the storm because more water is stored for longer periods with increasing depth to the water table. Therefore, streamflow generation studies must identify not only the dominant hydrological processes in watersheds but also the spatial and temporal patterns of runoff production. Few studies, including this one, have adequately

monitored the subsurface response to storms from the edge of the stream to the top of the hillslope. However, such an approach would have been beneficial both for better delineation of the spatial extent of storm runoff production and for testing the significance of unsaturated flow from the upper hillslopes.

The transmissivity feedback model with dual porosity flow has important implications for numerical modelling of subsurface flow during storms because the hydraulic characteristics of single and dual porosity media are different. For example, Freeze's (1972b) unsaturated-saturated models that were coupled with stream discharge suggested that subsurface flow was dominant only when "unrealistic" saturated hydraulic conductivities as high as 4.4×10^{-3} m/s were assumed. However, such values may be reasonable in macroporous forest soils as indicated by results from Harp 4-21, Harp 3A and PC-108. Groundwater modelling that incorporates Durner's (1994) representations of bulk hydraulic properties (unsaturated hydraulic conductivity and characteristic curves) for dual (or multiple) porosity media would likely provide very different results to those for single porosity media (Freeze, 1972a, 1972b). Comparison of these results would make a substantial contribution to the understanding of subsurface flow in streamflow generation. Numerical models that explicitly simulate flow in both the matrix and macropores (or fractures) can also be used to examine the transmissivity feedback model with dual porosity flow (e.g. Beven and Germann, 1981; Gerke and van Genuchten 1993a). This latter approach would be an improvement over the representation of bulk hydraulic properties because water flow and mixing between the matrix and macropores can be explicitly considered and quantified.

Field data from dual porosity media are required to test the transmissivity feedback model with dual porosity flow. Although the data from this study are consistent with this model, they cannot be used to test it explicitly because of the scale of measurement. Field techniques are required to measure bulk hydraulic properties, such as saturated and

unsaturated hydraulic conductivity and characteristic curves, because they ultimately control subsurface flow. Separate sampling and measurements of pressure head and water content from both the macropores and the matrix are necessary to better understand the role of macropores on subsurface stormflow generation. A major challenge in obtaining such measurements is to install instrumentation without disturbing macropore structures.

Results reported for other studies on the Canadian Shield are consistent with those of this study. Saturation of sediments is the primary mechanism for increased subsurface flow during storms. Flow through macropores likely contributes significantly to storm runoff within forested soils. Groundwater ridging is unlikely in most forested catchments on the Canadian Shield. A survey that compares baseflow hydraulic gradients with topographic gradients near the stream (at the hinge point) is needed to establish that increased hydraulic gradients have only a minor role in subsurface storm runoff generation for many catchments on the Canadian Shield. The identification of common elements, such as flow mechanism, among catchments will lead to the development of better and more broadly applicable models.

Chapter 8

The significance of storms for the concentration and export of dissolved organic carbon from Harp 4-21 and Harp 3A

Introduction

The transport of dissolved organic carbon (DOC) through the hydrological cycle affects processes such as carbon cycling (McDowell and Likens, 1988), water acidification (Eshleman and Hemond 1985; Driscoll et al., 1989), soil formation (Dawson et al., 1978), and the sorption, transformation and transport of nutrients, toxic metals and organic compounds (e.g. McDowell, 1985; Jardine et al., 1989). Accurate measurement of the mass of DOC transported in streams is necessary to calculate either the output from a catchment or the input to rivers or lakes. The DOC export in streams varies greatly due to the large spatial and temporal variability in both the availability of DOC within catchments and the water flowpaths that transport much of the DOC to the stream (Cronan, 1990; Easthouse et al., 1992).

Export of DOC is often calculated using regressions of stream discharge and stream DOC concentrations (e.g. Moore, 1989). Stream DOC concentration can be directly (Meyer and Tate, 1983) or inversely related (Hornberger et al., 1995) to stream discharge or even independent of stream discharge depending on the hydrological, biological and geochemical processes operating within catchments. In upland catchments and humid climates, a direct relationship between DOC concentration and stream discharge is frequently observed at scales that vary from small seeps and streams to large continental rivers (Mulholland and Watts, 1982; Thurman, 1985). However, it is also apparent that DOC concentration is influenced by many factors that are poorly related or unrelated to stream discharge such as the availability of leachable organic carbon or adsorption of DOC to soil (e.g. Nelson et al., 1993). Consequently,

stream discharge explains only a portion of the total variability in DOC (generally $0 < r^2 < 0.7$) and may be a poor predictor of DOC concentration. Therefore, it is important to consider the uncertainties resulting from the regression between DOC and stream discharge and the types of catchments in which regressions can be used most successfully.

Many studies examine DOC export over seasonal or annual periods; the significance of individual storms are only briefly, if ever, discussed (e.g. McDowell and Fisher, 1976). However, studies reporting data for individual events frequently demonstrate short term increases in DOC concentrations (McDowell and Likens, 1988). Since DOC increases with discharge in many streams (Meyer and Tate, 1983; Moore, 1989; Eckhardt and Moore, 1990) and stormflow is often a large proportion of the total flow, storm periods may represent a significant proportion of total DOC export budgets. Knowledge of the processes affecting DOC during storms is therefore important for understanding both the short and long term dynamics of DOC cycling in catchments.

Substantial changes in precipitation and evapotranspiration are potential consequences of global warming and climatic change (IPCC, 1990). Any climatic change that significantly influences runoff will also affect DOC export from catchments. Before predicting the effects of climate change on DOC export, it is necessary to consider what types of hydrological changes may lead to altered DOC export and whether it is possible to predict these changes reasonably. For example, the relationship between DOC and stream discharge could be used to predict the possible influences of hydrological changes on DOC export, yet it would be necessary to understand how the relationship between DOC and discharge varies with different hydrological conditions within different catchments.

In this chapter, changes in DOC concentration and DOC export during runoff events in two small catchments are examined. The purposes are: 1) to examine the spatial and temporal

changes in the relationship between DOC concentration and stream discharge and their effect on estimating DOC export; 2) to assess the relative importance of stormflow and baseflow conditions on DOC concentration and DOC export; and 3) to discuss the type of information required to predict the effects of climatic change on DOC export and whether reasonable predictions can be made given the present understanding of DOC dynamics and climate change.

Site description

The two headwater streams under investigation are located in the Harp Lake catchment in central Ontario, Canada. Harp 4-21 is a 3.7 ha catchment covered by a mixed forest of sugar maple (*Acer saccharum*), yellow birch (*Betula alleghaniensis*), poplar (*Populus spp.*), balsam fir (*Abies balsamea*) and hemlock (*Tsuga canadensis*) (Figure 8.1a). Groundwater flow through glacial tills up to 15 m thick maintains perennial stream discharge (Chapter 3). The stream channel is narrow (0.2-1.5 m) with no stagnant water. Soils in Harp 4-21 are Podzolic with poorly developed or absent eluviation in the A horizon. The A horizon is approximately 3-10 cm thick along the hillslopes and becomes approximately 23 cm thick near the stream. The geology, hydrogeochemistry and hydrology of the catchment are described by Jeffries and Snyder (1983), Dankevych (1989), MacLean (1992), and in Chapters 3 and 4.

Harp 3A is a 21.7 ha catchment with two small wetlands (0.4 ha and 0.2 ha) and several other small areas (<0.1 ha) where ponding occurs (Figure 8.1b). The hillslopes are covered predominantly by sugar maple; both cedar (*Thuja occidentalis*) and black spruce (*Picea mariana*) are present in the conifer wetland (Wetland 2). Wetland 3 has a partial canopy of yellow birch and black spruce. Wetland 2 is characterized by hummock-hollow topography with a *Sphagnum* ground layer and by water pools approximately 5 to 25 cm deep. Surface runoff through Wetland 3 occurs both as slow flow across the ponded surface and as poorly channelized flow in the stream. Flow is also channelized through the ponded area downstream of W3. The

Figure 8.1a Location and instrumentation of the a) Harp 4-21 and b) Harp 3A catchments.

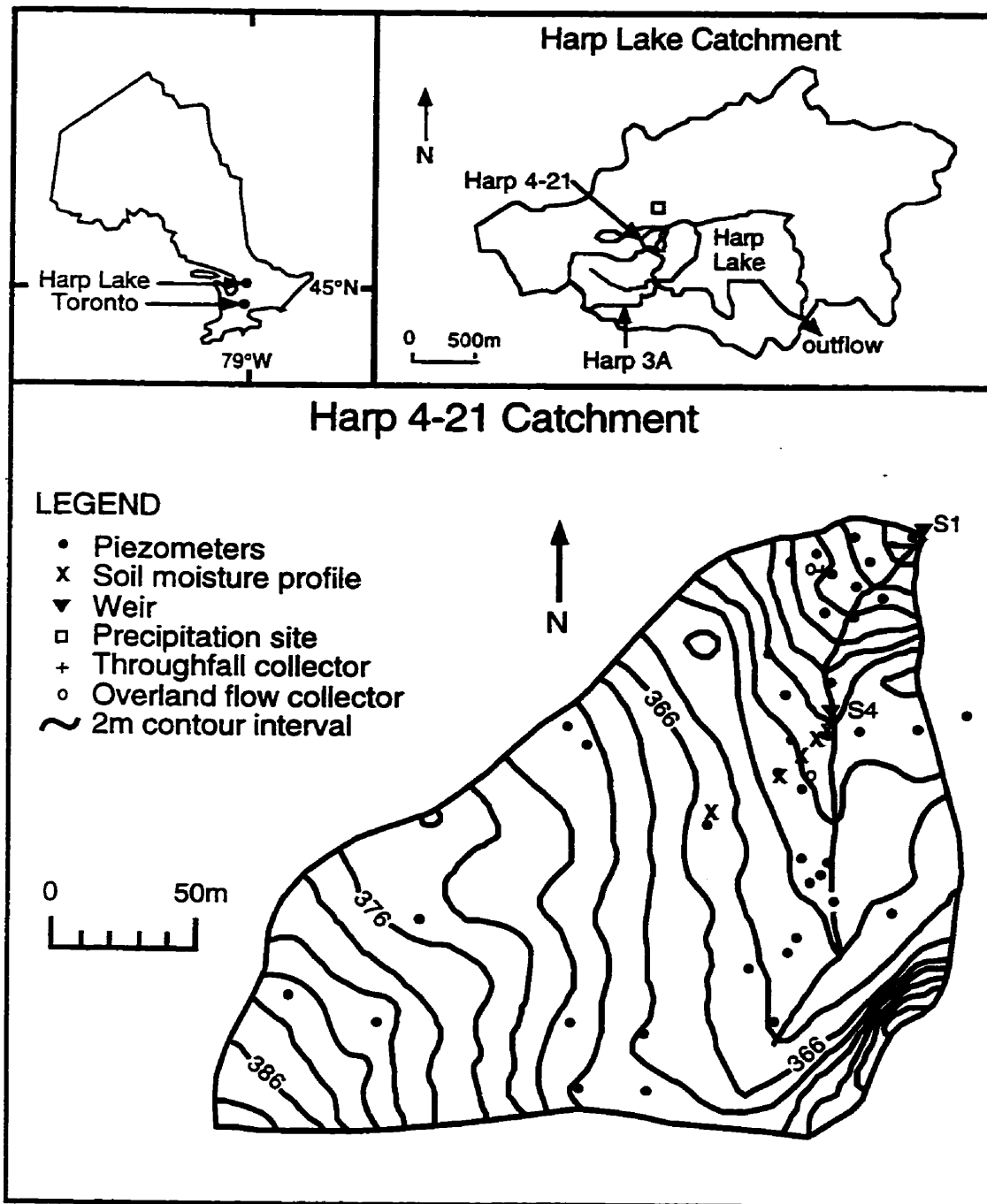
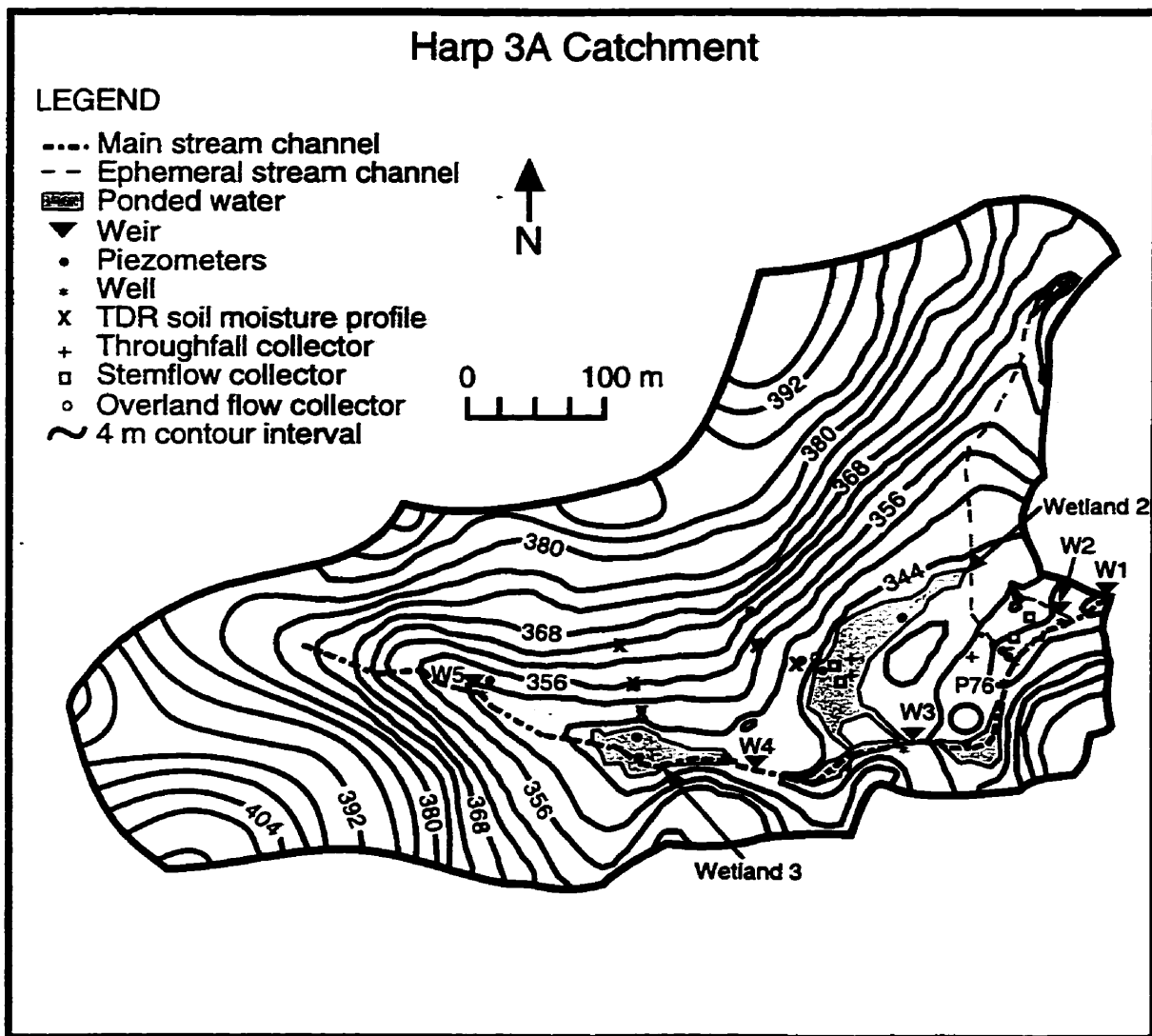


Figure 8.1b Continued.



Podzolic soils in Harp 3A are very similar to those in Harp 4-21 except that the A horizon near the stream is not as thick and does not appear visually to be as humic-rich.

Due to the thinner (<1.5 m) glacial sediments in Harp 3A, there is less water storage in the hillslopes and the water table is absent from most of the hillslopes during the summer. Consequently, all surface ponding disappears and the Harp 3A stream dries out upstream of P76 during the summer. Downstream of P76, groundwater flow through lacustrine silts and clays maintains very low summer baseflow (≈ 0.1 l/s).

Harp 4-21 and Harp 3A are subdivided into two (S1 and S4) and five (W1-W5) subcatchments respectively. Subcatchments S1, S4, W2 and W5 drain hillslopes with little ponded water and small stream surface areas. Hillslopes also comprise most of the area within subcatchments W3 and W4, however, Wetlands 2 and 3 reside in the flat valley bottoms of W3 and W4 (Figure 8.1b). Although subcatchment W1 also drains hillslopes and only has small areas of ponded water, it is influenced by wetland runoff from W3 and W4. Most of catchments in the region are influenced by wetlands.

Methods

Sampling methods

Sampling was conducted from September 27 to November 20, 1992 (autumn season) and from May 2 to June 4, 1993 (spring season) in Harp 3A and from September 27 to November 10, 1992 and from May 2 to May 30, 1993 in Harp 4-21. The autumn season included storms both during and following the leaf fall period (\approx September 27 to October 13). Snowmelt was complete prior to the start of the spring season and spring storms followed leaf-out. The entire length of the Harp 3A stream as well as the secondary channels were flowing during both sampling periods. Each sampling period was further subdivided into stormflow and

baseflow periods. Stream water samples were collected from five weirs in Harp 3A (W1-W5) and two weirs in Harp 4-21 (S1, S4). Previous sampling in Harp 4-21 during spring (May 1 to June 30) and autumn (October 4 to November 11) 1989 storms are used for comparison with the 1992-93 data.

DOC analysis

Stream and groundwater samples were filtered in the field through 80 μm and 44 μm polyester screening into site-designated, opaque polyethylene bottles. All 1992 and 1993 samples were subsequently filtered through 0.45 μm cellulose nitrate filters into glass scintillation vials, acidified with HNO_3 to a pH near 2 to prevent microbial degradation of the DOC and kept refrigerated and in darkness until analysis. DOC concentration was measured using a Dohrmann DC-190 total carbon analyzer at the University of Waterloo (UW). Dissolved inorganic carbon was stripped from the sample, DOC was combusted to CO_2 in a 800°C oven, CO_2 was then dehumidified, passed through a Cu scrubber and measured by an infrared detector. The instrument blank measured 0.1 mg/l.

DOC concentrations reported from 1989 were analyzed by the Ontario Ministry of the Environment (MOE) using the persulfate oxidation method (MOE, 1983). Comparison of 33 split samples analyzed using both methods demonstrated that MOE results were lower by an average of 0.8 ± 0.4 mg/l in the range of 2-12 mg/l. All 1989 MOE results have been adjusted by 0.8 mg/l to correspond to UW values (Appendix 9).

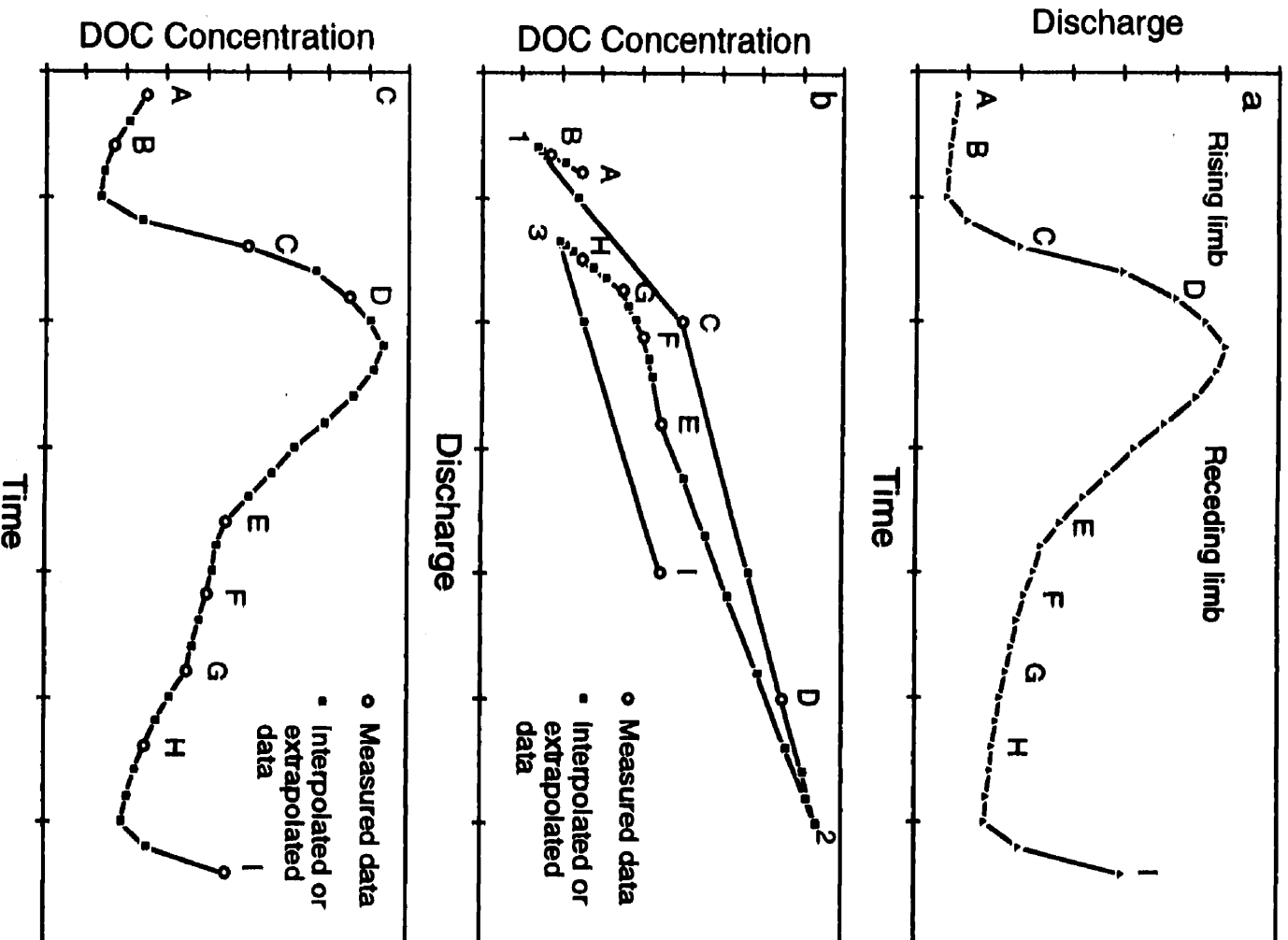
Methods of calculating DOC export

Several methods are available for calculating the nutrient fluxes from catchments based on measurements of stream discharge and stream water chemistry including the period-weighted method and several regression-based procedures (Dann et al., 1986; Johnson, 1979). The method employed becomes important when the concentration is flow dependent. In the period-

weighted method, the average concentration of successive samples is multiplied by the volume of water leaving the catchment during the interval. The total export is obtained by summing the export during individual sampling intervals. In the regression-based methods, a regression between concentration and stream discharge combined with continuous measurements of discharge with time is used to calculate concentration with time. Export can then be calculated easily by multiplying concentration with discharge and summing to obtain the total export. The period-weighted method accounts for changes in flow volume but does not consider changes in concentration with stream discharge. In contrast, the regression-based methods explicitly take into consideration the changes in concentration with discharge. However, since the concentrations are calculated from the regression, this method does not use the measured concentration data to calculate export and errors in the regressions lead to uncertainty in the estimate of DOC export.

This study uses an alternative calculation method that retains the measured concentration data and considers both the changes in concentration with discharge and the volumes of flow associated with successive samples. The method combines both procedures by assuming that DOC concentration varies linearly with discharge between successive samples and will be referred to as the sample-interpolation method. The DOC export is calculated in three steps. Firstly, stream discharge is determined at 20-minute intervals from the continuous measurements of stage as determined from stream charts (Figure 8.2a). Secondly, a linear equation between DOC and stream discharge is calculated for every two successive stream samples (Figure 8.2b). DOC is interpolated at 20-minute intervals to obtain a continuous record of DOC (Figure 8.2c). The interpolated DOC is calculated using the measured stream discharge (from step 1) and the linear equation between DOC and discharge (Figure 8.2b). When a local minimum or maximum in stream discharge exists between two samples (between samples B-C, D-E and H-I), the linear equation between DOC and discharge on the receding limb of the hydrograph is extrapolated to the measured streamflow minimum or maximum (extrapolations 1

Figure 8.2 Schematic example of the sample-interpolation method of calculating DOC concentrations. Panel a shows the continuous measurement of stream discharge divided into discrete time intervals. Panel b shows measured DOC (open circles with letters) plotted against measured stream discharge. DOC is interpolated or extrapolated (squares) between pairs of samples using measured stream discharge. Numbers 1 and 3 indicate data extrapolated from the rising limb and number 2 is extrapolated from the receding limb of the hydrograph. The resulting DOC concentrations are plotted in panel c. The method is discussed further in the text.



and 3). If there are no high-discharge data on the receding limb and better data are available on the rising limb, the equation is extrapolated to the time of peak flow from the rising limb of the hydrograph to avoid large extrapolations (extrapolation 2). Thirdly, DOC exports for each time interval are the products of the calculated DOC and the volumes of discharge that are summed to yield the total export. The average DOC concentration equals the total DOC export divided by the total runoff during the period of interest. This sample-interpolation procedure is only appropriate when many samples have been collected, particularly near each minimum and maximum in stream discharge, to define all the changes in DOC concentration with discharge. This procedure could also be used for the calculation of export of other solutes given sufficient sample collection and a relationship between solute concentration and stream discharge. For the small storm on October 24 during which no samples were collected but discharge was measured, the DOC was calculated using the slope of DOC versus discharge between baseflow and peak discharge from the previous storm on October 16.

Uncertainties in using data collected on a regular sampling interval are quantified for the autumn 1992 data in the Harp 4-21 and Harp 3A catchments at S1 and W1. The interpolated DOC data were subdivided at weekly intervals to simulate weekly sampling. DOC exports were calculated from the weekly data using both the period-weighted and regression methods. The accuracy and precision of the DOC exports were estimated from averages and standard deviations of seven arbitrarily chosen weekly data sets, each offset by an increment of one day. The results are reported as a percentage of the DOC export estimated by the sample-interpolation method used in this study. DOC exports were also calculated using only the measured data to examine the accuracy of the period-weighted and regression methods for intensively sampled storms.

Each sampling season was subdivided into stormflow and baseflow periods. The criterion used to distinguish between these periods is the hydrograph separation method proposed by Hewlett and Hibbert (1967). The start of the stormflow period is defined by an

increase in stream discharge; the end of the period is defined by adding 0.0055 L/s to the stream baseflow for each hectare of catchment area for each hour ($0.05 \text{ ft}^3/\text{s}/\text{mi}^2/\text{hr}$) following the start of stormflow until the receding limb of the hydrograph is intersected (Figure 8.3). Although these criteria are entirely arbitrary, they provide a consistent method to define stormflow periods. Based on these criteria, stormflow generally ends prior to the return to baseflow DOC concentration so that the baseflow period may also include a portion of the receding limb of the storm hydrograph. The term stormflow used in this chapter is distinct from Hewlett and Hibbert's (1967) definition of quickflow in that it includes all runoff during storm periods. Stormflow and baseflow periods were determined at W1 in Harp 3A and applied to the other catchments so that DOC exports from the different catchments can be compared for the same storm duration.

Results and discussion

DOC concentrations as a function of stream discharge

In contrast to stream water concentrations of major ions that are generally diluted during storms (Likens et al., 1977), DOC increases during runoff events at all locations (Figure 8.4). The magnitude of the increase in DOC during individual runoff events ranges from 0.7 to 4.1 mg/l (15% to 100% of baseflow DOC) at W1 and from 3.9 to 11.4 mg/l (123% to 410% of baseflow DOC) at S1.

Regressions between DOC and stream discharge for individual runoff events at W1 and S1 are significant ($p < 0.05$) with r^2 values ranging from 0.56 to 0.98 (except Nov. 10 storm at W1, $r^2 = 0.26$). The positive relationship between DOC and stream discharge during storms suggests the inflow of water with high DOC to the stream and/or increased leaching of organic carbon within the stream. The good correlations also justify the use of the sample-interpolation method for calculating DOC concentration and DOC export. Weaker correlations at wetland sites

Figure 8.3 Criteria for graphical hydrograph separation to define periods of stormflow and baseflow.

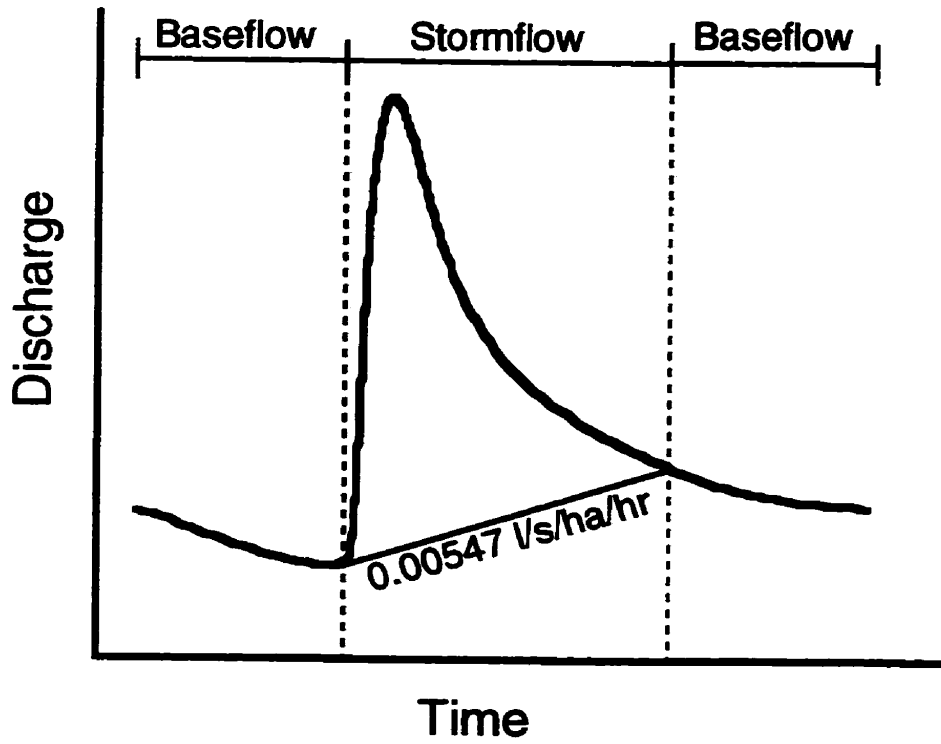
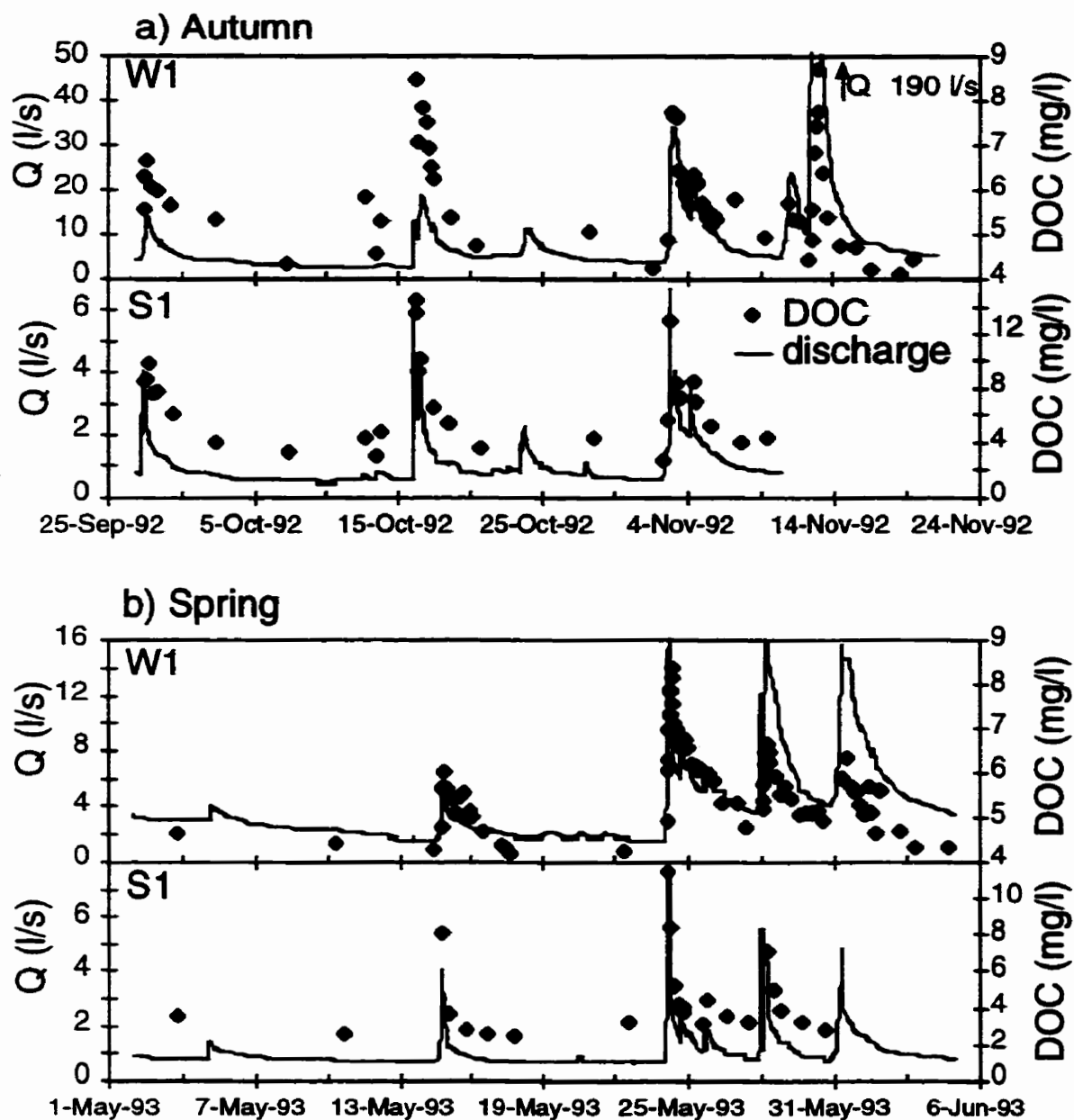


Figure 8.4 Stream discharge (lines) and DOC concentrations (diamonds) during the a) autumn and b) spring sampling seasons at W1 and S1. Note the different vertical scales.



W3 and W4 ($0.12 < r^2 < 0.93$) may result from the influence of flushing DOC from stagnant portions of the wetlands (Chapter 9).

The seasonal regressions between DOC and stream discharge show the highest correlations at S1, S4, W2 and W5 (autumn), lower correlations at W1, and no significant relationship at W3 and W4 (Table 8.1). The lower correlations of the seasonal regressions reflect the variability in the regressions among individual storms (Figure 8.5).

One of the most prominent factors affecting the correlation in the seasonal regressions appears to be the presence or absence of wetlands. Despite increases in DOC during individual storms at W3 and W4, there is no significant correlation when all the data are combined into one seasonal regression. At W3 and W4 the variability in the regressions among storms is large. High DOC is not restricted to periods of high stream discharge. Pondered water with high DOC may be flushed from the wetland at relatively low discharge during smaller storms. Furthermore, other factors such as the input of fresh litter to the wetland surface during the autumn and variable contact time between water and organic matter can lead to additional variability in the seasonal regressions. Similar results are reported in southern Quebec where four catchments containing wetlands show no significant (logarithmic) relationships between DOC and stream discharge and four catchments without wetlands show significant direct correlations (Eckhardt and Moore, 1990).

The variability in the regressions among storms is smallest at S1 and S4, two catchments that lack wetlands. In addition, comparison of soil moisture and groundwater levels in Harp 4-21 and Harp 3A suggest that differences in groundwater flow are a possible explanation for better correlations in Harp 4-21. Groundwater flow through thicker glacial till in the Harp 4-21 catchment (S1 and S4) maintains elevated groundwater levels adjacent to the stream throughout the year and perennial stream baseflow (Chapter 3). Since the soils adjacent to the stream are

Table 8.1 Regressions between DOC concentrations and stream discharge during the autumn and spring sampling seasons.

Site	Autumn 1992 ^a	r ²	Spring 1993 ^b	r ²
W1	[DOC] = 0.021 Q + 5.46	0.32*	[DOC] = 0.145 Q + 4.70	0.43*
W2	[DOC] = 0.403 Q + 3.50	0.83*	-	-
W3	[DOC] = 0.006 Q + 7.33	0.005	[DOC] = 0.137 Q + 7.99	0.06
W4	[DOC] = 0.027 Q + 5.76	0.03	[DOC] = 0.112 Q + 5.56	0.01
W5	[DOC] = 0.102 Q + 3.81	0.71*	[DOC] = -0.076 Q + 3.21	0.01
S1	[DOC] = 1.828 Q + 3.38	0.88*	[DOC] = 1.290 Q + 2.03	0.96*
S4	[DOC] = 3.094 Q + 2.87	0.83*	[DOC] = 1.693 Q + 2.48	0.68*
	Autumn 1989 ^c		Spring 1989 ^d	
S1	[DOC] = 4.540 Q + 2.83	0.83*	[DOC] = 1.048 Q + 4.81	0.81*

DOC concentrations are expressed in mg/l and stream discharges are expressed in l/s.

Sampling seasons:

^a September 27-November 20, 1992 at W1 to W5 and September 27-November 10, 1992 at S1 and S4.

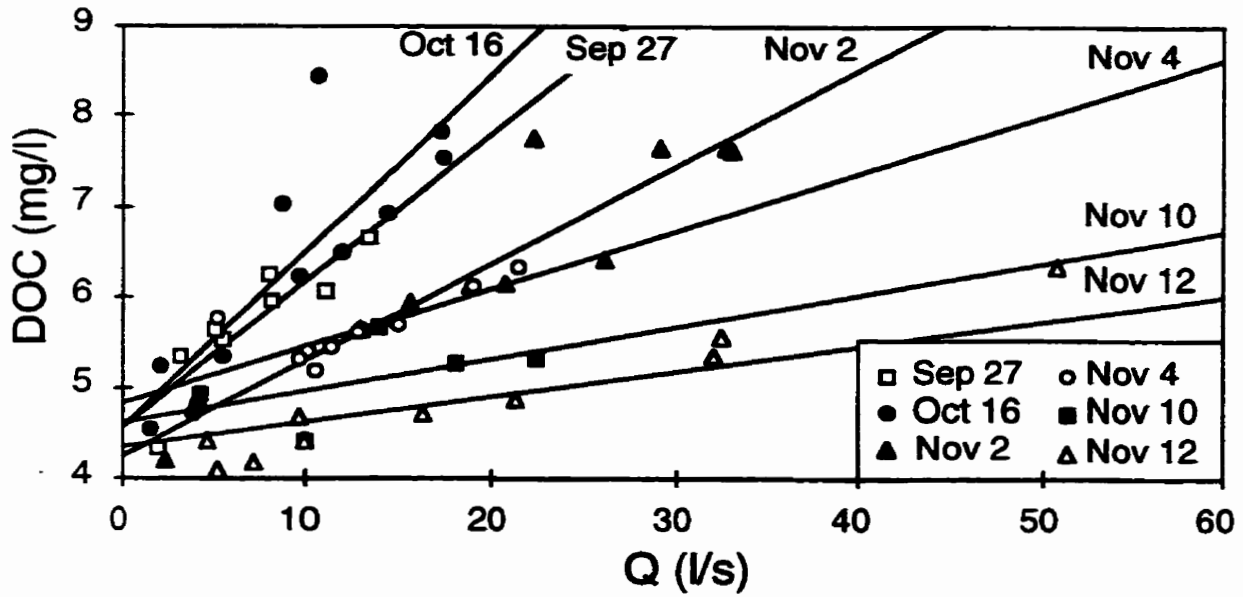
^b May 2-June 4, 1993, at W1; May 2- May 30, 1993, at W3-W5 and S1.

^c October 4-November 11, 1989.

^d May 1-June 30, 1989.

* Significant at p<0.01.

Figure 8.5 Regressions between DOC concentration and stream discharge for individual autumn storm events at W1. r^2 values: Sep. 27 = 0.80, Oct. 16 = 0.70, Nov. 2 = 0.86, Nov. 4 = 0.65, Nov. 10 = 0.26, Nov. 12 = 0.94.



close to saturation prior to each storm (MacLean, 1992), changes in water flowpaths during individual storms are similar and slopes of the regressions for individual storm events show less variation than in Harp 3A. Thin or absent till in the Harp 3A catchment is not able to store sufficient water to sustain groundwater flow within the hillslopes throughout the summer. Consequently, soil moisture and groundwater levels decline and baseflow ceases. During the autumn, soil moisture and groundwater levels vary among storms as infiltration replenishes the depleted soil moisture. Water flowpaths in autumn also change from one storm to the next. The resulting slopes of the regressions between DOC and stream discharge change among storms and the combined seasonal regressions are weaker at W2 and W5 than at S1 and S4. The lack of correlation at W5 in the spring is due, in part, to dry conditions experienced in early May and the small hydrological response to subsequent storms. At W1, the seasonal regressions are significant but weak (Table 8.1), indicating the mixed influence of variable hillslope flowpaths and flow from Wetlands 2 and 3.

The variability in hydrological conditions among years can result in larger errors in calculated DOC than the variability among storms. In Harp 4-21, the seasonal regressions at S1 changed drastically from the dry conditions of autumn 1989 to the wet conditions of autumn 1992 (Table 8.1). The average absolute difference between actual DOC measured at S1 in 1989 and those calculated using the discharges from 1989 with the seasonal regressions from autumn 1992 and spring 1993 are 1.4 mg/l and 2.4 mg/l (22% to 36% of actual DOC respectively) with errors in individual samples of up to 4.9 mg/l (120% of actual DOC). Therefore, data sets spanning several years are not recommended for seasonal regression calculations.

Where individual runoff events have not been sampled intensively, seasonal or annual regressions between DOC and discharge are frequently used to calculate DOC from stream discharge records (Meyer and Tate, 1983; Moore, 1989). Even where seasonal regressions are

relatively good, estimates of individual DOC concentrations using seasonal or annual regressions may have large uncertainties for two important reasons. Firstly, because slopes of the regressions vary among storms at every site, there is a resultant loss of precision in DOC which has been calculated from seasonal regressions that average results from several individual storms. The absolute differences between the actual and calculated DOC averages between 0.3 mg/l and 1.3 mg/l (10% and 22% of actual DOC) for the different subcatchments with errors for individual samples of up to 6.5 mg/l (60% of actual DOC). Because the regressions for individual events diverge with increasing discharge (Figure 8.5), the precision in calculated DOC decreases at high flows when DOC export is greatest.

Secondly, DOC concentrations estimated from seasonal regressions are imprecise because they are often determined from data in which there are few measurements of DOC at high discharges. Samples collected at regular intervals often miss high discharge conditions because of their short duration. Using the interpolated data from the autumn of 1992 as the entire population of samples, the probability of randomly collecting a sample in the upper third of the DOC concentration range was 5% and 0.8% at sites W1 and S1 respectively. Consequently, regressions must either be extrapolated to discharges beyond the sampled range or are biased by the few samples collected at high discharge since the data at high discharge reflect unique conditions of short duration for each storm. High discharge can occur from a variety of weather conditions such as spring snowmelt, rain-on-snow storms, intense thunderstorms or prolonged rainstorms so that different storms are likely to produce different DOC at high discharge.

The problems with annual regressions are demonstrated in Figure 5a in Schiff et al. (1997) which shows all the DOC data collected during two years of routine sampling ($n = 392$) in Harp 4-21 (S1). The regression is poor ($r^2 = 0.17$) because samples were collected over a wide range of hydrological conditions during different storms and seasons. The samples with

the highest DOC (above 6 mg/l) were all collected during the autumn whereas the samples with the highest flows (above 2.5 l/s) were all collected during spring snowmelt. This bias in the regression would tend to overestimate spring DOC export and underestimate autumn DOC export.

Uncertainty in estimating DOC export

Discrete sampling and the method used to calculate DOC export from DOC concentrations and stream discharge generate the largest uncertainties in the estimation of DOC export. Although increased sampling frequency during storms is recommended, the time and expense required for collection and analysis of many samples from individual storms are often prohibitive for long term studies of DOC export. Therefore, it is necessary to consider the uncertainties in DOC exports calculated from less data.

Seasonal regressions based on weekly data yield accurate results (98% and 93% of true export at W1 and S1 respectively) but the uncertainties in any single calculation of the DOC export at the 90% confidence interval are 32% and 33% respectively (Table 8.2). In contrast, the period-weighted results significantly ($p < 0.01$) underestimate DOC export by 14% at W1 and 22% at S1 because high DOC is not adequately represented by weekly sampling. However, when all the measured data were used, the period-weighted method provided accurate estimates of DOC export at both W1 and S1 (100% and 103% respectively). The DOC exports calculated from seasonal regressions using all the measured data underestimate DOC export by 12% but are within the range of uncertainty calculated from weekly data.

Underestimating DOC export in streams could influence DOC budgets for lakes since stream inflows are underestimated whereas the lake outflow is less likely to be underestimated because large and rapid changes in DOC concentrations are not observed. Consequently, the net CO₂ evasion rates calculated from DOC and dissolved inorganic carbon budgets for lakes in this

Table 8.2 Comparison of autumn DOC export at W1 and S1 calculated using period-weighted and seasonal regression methods from all measured data and weekly interval data.

Calculation method	Sampling interval			
	W1		S1	
	All data	Weekly interval	All data	Weekly interval
Period-weighted	100	86±9	103	78±18
Seasonal regression	88	98±32	88	93±33

Results are expressed as a percentage of DOC export obtained using the sample-interpolation method. Uncertainties are expressed as the 90% confidence interval.

area and the magnitude of the in-lake DOC sink may be larger than reported (Dillon and Molot, 1995).

DOC export during runoff events

Contribution of DOC export by stormflow exceeds that by baseflow in autumn. Although stormflow occurs only 21% of the time, storms produced 57% of the flow volume and 64% of the DOC export at W1 during the autumn (Table 8.3). Stormflow DOC export is more important at terrestrial sites W2 and W5 (68% and 65% respectively) than at wetland-influenced sites W3 and W4 (57% and 59% respectively). In the spring, stormflow DOC export was slightly lower at W1 (40%) since the stormflow was a smaller proportion of total runoff (34%) and time (14%) (Table 8.3). Similar results are also observed at S1 (Table 8.3).

Periods of high discharge are responsible for the majority of DOC export (Figure 8.6). For example, autumn stream discharge at W1 exceeds 14.3 l/s only 10% of the time, yet the proportions of flow and DOC export occurring above this discharge are 43% and 50% respectively. Similar results are observed at all the stream sites where between 41% and 57% of the total autumn export of DOC are associated with the upper 10% of discharge values. The November 12 event accounted for 31% of the total autumn DOC export. The export during that single storm (63.4 kg) exceeds the total DOC export during the entire spring sampling period (54.2 kg).

Although much of the DOC export occurs during storms because of high runoff, increased DOC concentration during storms also increases DOC export. Average stormflow DOC is up to 4.2 mg/l greater than average baseflow DOC (Table 8.4). Consequently, the percentage of DOC exported during storms exceeds the percentage of stormflow runoffs by 5%

Table 8.3 Summary of DOC export from W1 and S1 during a) autumn 1992 and b) spring 1993.

	W1			S1		
	Stormflow	Baseflow	Total	Stormflow	Baseflow	Total
a) Autumn 1992						
DOC export (kg)	129 (63.7)	73.3 (36.3)	202	10.6 (56.7)	8.1 (43.3)	18.7
Flow volume (1000 m ³)	19.9 (56.9)	15.1 (43.1)	35.0	1.32 (40.1)	1.97 (59.9)	3.29
Average [DOC] (mg/l)	6.5	4.8	5.8	8.0	4.1	5.7
Duration (days)	11.3 (20.5)	43.7 (79.5)	55.0	7.3 (16.4)	37.2 (83.6)	44.5
b) Spring 1993						
DOC export (kg)	21.5 (39.7)	32.7 (60.3)	54.2	3.3 (39.7)	4.9 (60.3)	8.2
Flow volume (1000 m ³)	3.6 (34.3)	6.9 (65.7)	10.5	0.56 (25.8)	1.61 (74.2)	2.17
Average [DOC] (mg/l)	6.0	4.7	5.2	5.8	3.1	3.8
Duration (days)	4.8 (14.1)	29.2 (85.9)	34.0	3.2 (11.0)	25.8 (89.0)	29.0

Numbers in parentheses are percentages of total values.

Figure 8.6 Cumulative percentage of DOC export as a function of cumulative percentage of flow duration at W1 during the autumn sampling period. 50% of the total DOC export is associated with the highest 10% of discharge values.

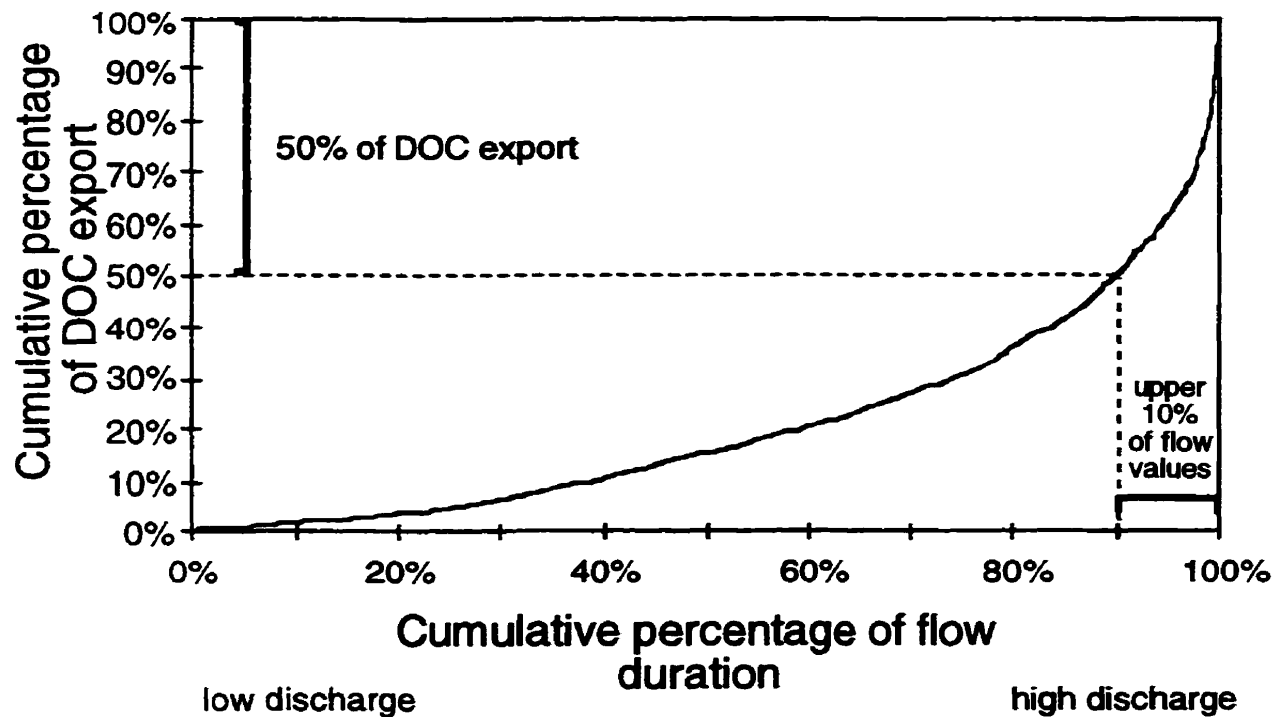


Table 8.4 Average DOC concentrations for periods of stormflow, baseflow and total flow during the autumn and spring sampling periods.

Site	Average DOC concentration (mg/l)					
	Autumn 1992			Spring 1993		
	Stormflow	Baseflow	Total flow	Stormflow	Baseflow	Total flow
W1	6.5	4.8	5.8	6.0	4.7	5.2
W2	5.5	3.4	4.6	-	-	-
W3	7.4	6.4	6.9	8.5	7.6	7.8
W4	6.4	5.0	5.7	5.8	5.1	5.3
W5	5.0	3.6	4.4	3.2	3.2	3.2
S1	8.0	4.1	5.7	5.8	3.1	3.8
S4	7.1	3.9	5.2	-	-	-

to 7% at W1 and 14% to 17% at S1 (Table 8.3). Increased DOC during storms has the largest influence on DOC export at S1 and S4 because baseflow DOC is low and relative increases in DOC from baseflow to stormflow are largest (Table 8.4). In contrast, baseflow DOC is highest at W3 and W4 because wetlands contribute additional DOC to the stream and relative increases in DOC during storms are smaller. Therefore, increased stormflow DOC is less important in catchments with wetlands.

Assessing the potential effects of climate change on DOC concentration and DOC export

Predictions of the hydrological consequences of climate change are necessary to predict changes in DOC export. Such predictions are needed at the catchment scale since changes in runoff resulting from altered precipitation and evapotranspiration will vary among catchments. For example, an increase in summer evapotranspiration would have a small effect on stream runoff and DOC export from Harp 3A (W1) since summer stream runoff is already extremely low (< 2% of summer precipitation). However, increased evapotranspiration could reduce groundwater discharge, stream runoff and DOC export during the summer in Harp 4-21 (S1).

Changes in the seasonal distribution of precipitation will also influence total runoff and DOC export since the runoff response to precipitation, expressed as the effective runoff (the ratio of precipitation to storm runoff), varies seasonally as a function of antecedent soil moisture conditions (MacLean, 1992). Therefore, an increase in precipitation during the wet season would produce a greater increase in runoff and DOC export than a similar increase in precipitation during the dry season. The effect of changes in the seasonal distribution of precipitation would differ among catchments since runoff response to precipitation also varies differently among catchments. Seasonal changes in effective runoffs are larger in Harp 3A than in Harp 4-21; during the November 12, 1992 storm, the effective runoffs were 0.63 at W1 and

0.38 at S1 whereas during the May 24, 1993 storm they were 0.10 and 0.20 at W1 and S1 respectively.

Two potential consequences of climate change are an increase in the size and frequency of extreme events (IPCC, 1990; Gates et al., 1992). Considering the importance of storms and particularly large storms (e.g. November 12, 1992) on DOC export, changes in the frequency and size of large storms could have a large effect on DOC export. Therefore, it is not only important to recognize changes in the averages of climatic variables but also to consider variability in weather patterns leading to large storms.

Even given accurate estimates of the effects of climate change on stream discharge and stream runoff, estimates of the changes in DOC concentration and DOC export would be unreliable because the relationship between DOC and discharge varies substantially among storms (Figure 8.5), seasons and years (Table 8.1). Since the factors influencing these variations are not yet understood, it is not clear how the regression between DOC and discharge may vary under different climatic conditions. Furthermore, other factors such as changes in organic matter production, dissolution, decomposition and biologic activity which alter the availability of soluble organic carbon for leaching will also affect the regression. Therefore, it is difficult to predict the relative importance of changes in stream runoff and changes in regressions on DOC concentration and DOC export. Longer term studies examining DOC concentrations and DOC export during storms over a range of wet and dry seasons should provide additional insight into the important factors affecting stormflow DOC export and the relationship between DOC and discharge.

Conclusions

The relationships between stream DOC and discharge and the comparison of DOC export in the Harp 4-21 and Harp 3A catchments have provided some insight into both the

uncertainties of calculating DOC concentration and DOC export and the role of storms on DOC concentration and DOC export. Unless the stream is sampled intensively enough to define the changes in stream discharge and DOC, the period-weighted method is not recommended for the calculation of DOC export because it does not take into consideration changes in DOC with discharge and DOC export is systematically underestimated. The calculation of DOC export using regressions is preferred, particularly if the storms are shorter than the sampling interval. Uncertainties in the calculation of DOC export using regressions are substantial and arise principally from two sources: variability in the regression between DOC and discharge and lack of samples with high DOC. Provided that sufficient samples have been collected, shorter time periods can be chosen for the regressions to reduce the variability arising from differences among individual storms. High DOC can be sampled by adopting flow-related sampling protocols or by augmenting regular sampling with high discharge samples using automated samplers. Alternatively, proportional samplers have been found to provide representative samples of the volume-weighted average DOC during storms (Meyer and Tate, 1983).

DOC export during storms accounts for a substantial proportion of the total DOC export (Table 8.3), yet few studies specifically examine the processes affecting DOC export during runoff events (Easthouse et al., 1992; Chapter 9). Stream DOC increased during almost every storm at all sites, including wetlands. Consequently, the average stormflow DOC was greater than baseflow DOC (Table 8.4), indicating that the dominant processes controlling DOC concentration and export may differ substantially between baseflow and stormflow periods. Although the consequences of these changes in DOC were not studied, storms may also have substantial effects on the chemical nature of DOC and the abiotic and biotic utilization of DOC in the stream (Kramer et al., 1990; Meyer, 1990). Greater emphasis on understanding DOC dynamics during storms is required.

The significant role of storms on DOC concentration and DOC export makes predictions of the effects of climate change difficult. Predictions would require considerable meteorological and hydrological information such as changes in the frequency and size of storm events and changes in the seasonal distribution of precipitation and runoff. Predictions are further complicated by large variations in regressions between DOC and stream discharge among storms, seasons and years. Until these variations in regressions are related to hydrological, biologic and geochemical characteristics of the catchments, the regressions will not be useful for assessing the possible effects of climate change.

Chapter 9

Sources and flowpaths of dissolved organic carbon during storms in Harp 4-21 and Harp 3A

Introduction

Recent reviews have highlighted the ecological significance of groundwater interactions with streams (Brunke and Gonser, 1997) and the incomplete understanding of the sources, fluxes and pathways of groundwater dissolved organic carbon (DOC) contributions to streams (Kaplan and Newbold, 1993). While several studies have observed groundwater DOC concentrations that exceed stream DOC (Rutherford and Hynes, 1987; Fiebig, 1997) and several authors recognize the significance of subsurface flowpaths (Hemond, 1990; Kaplan and Newbold, 1993), few studies actually relate stream DOC dynamics with groundwater flowpaths (Easthouse et al., 1992).

An issue closely associated with that of groundwater flowpaths is the geographical location of DOC sources within watersheds. Hemond (1990) suggested that in glaciated catchments with shallow soils and bedrock, riparian wetlands and soils are the dominant sources. Using an annual organic carbon budget for a watershed in the Atlantic Coastal Plain, Dosskey and Bertsch (1994) demonstrated that 90% of the DOC originated in riparian wetlands that occupy only 6% of the watershed area. Even though uplands cover a greater area within the watersheds, they are thought to contribute a small proportion of the exported DOC because DOC sorbs to mineral soils prior to reaching the stream.

To examine DOC sources, it is necessary to consider storms since storm runoff exports much of the DOC from small watersheds (Grieve, 1984; Chapter 8). Conceptual hydrological models of stormflow generation emphasize hydrological processes with different water

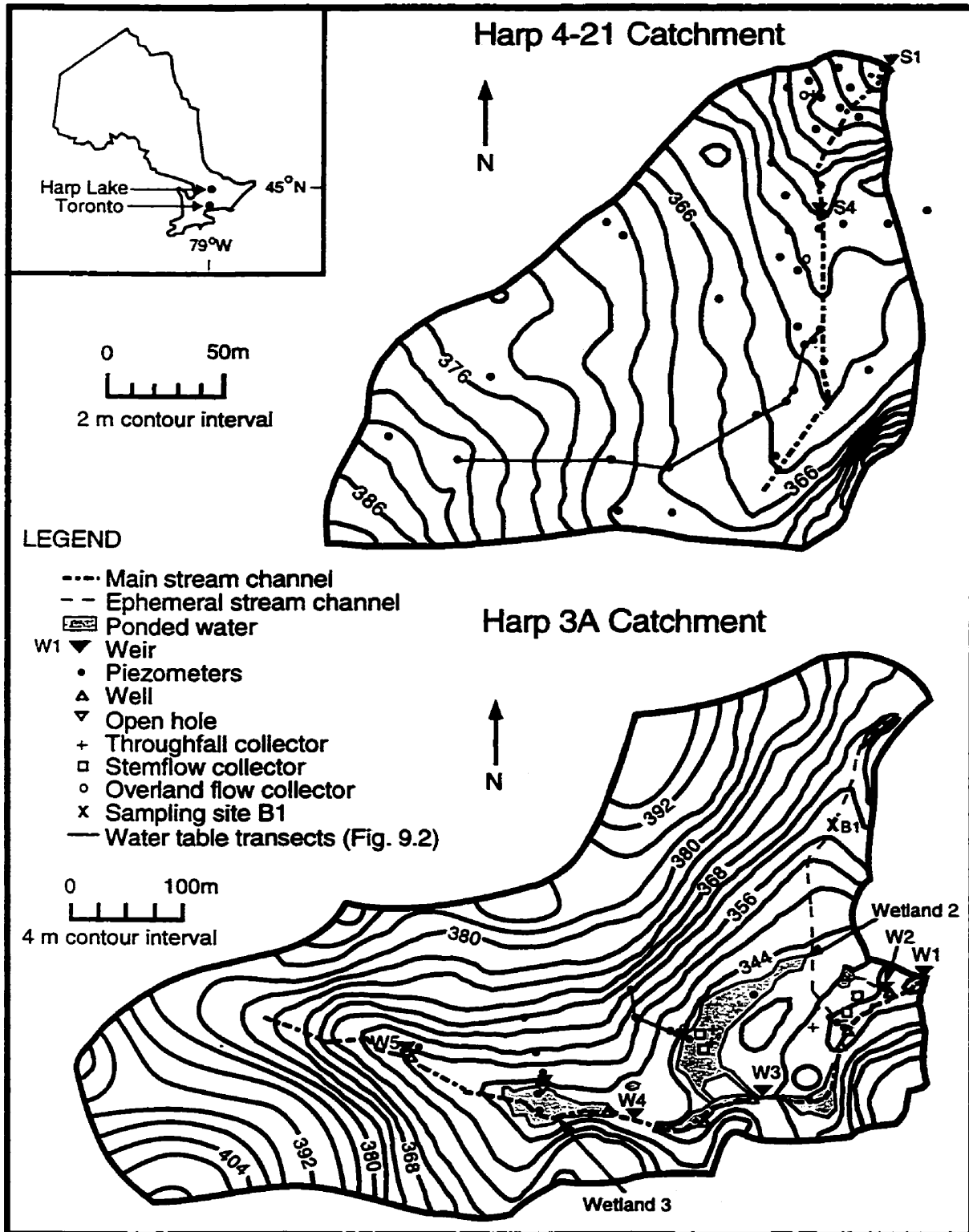
flowpaths in the riparian zone (Freeze, 1974; Ward, 1984; Wood et al., 1990). Hemond (1990) and Kaplan and Newbold (1993) discuss the significance of subsurface flowpaths near the stream on DOC sources and flowpaths. Because the relative importance of water flowpaths through different soil horizons can vary with soil moisture and groundwater levels, DOC pathways and fluxes may differ substantially from baseflow to stormflow conditions and produce changes in both DOC quality and quantity during storms (Jardine et al., 1990; Easthouse et al., 1992). Similarly, the dominant sources and pathways of stream water and DOC may differ among catchments or even within a single catchment during different storms (McDowell and Likens, 1988). Therefore, it is necessary to study DOC dynamics in areas where flowpaths have been delineated.

Harp Lake has been the focus of several investigations examining the hydrological flowpaths (Dankevy, 1989; MacLean, 1993; MacLean et al., 1995; Devito et al., 1996; Chapter 3 and 4) and carbon cycles (Schiff et al., 1990, 1997; Aravena et al., 1992; Trumbore et al., 1992; Molot and Dillon, 1996; Dillon and Molot, 1997; Chapter 8) of watersheds with uplands or wetlands. This chapter examines DOC concentrations and export in relation to water flowpaths during runoff events in two small catchments of Harp Lake. The purposes are 1) to compare the transport of DOC along different hydrological pathways during runoff events; 2) to compare the relative DOC contributions from riparian and upland hillslope areas; and 3) to examine some of the hydrological and physical controls on DOC transport to streams.

Site description

Hydrological response to storms and DOC concentrations were monitored in two small and adjacent catchments in central Ontario, Canada (Figure 9.1). Both catchments, Harp 4-21 with an area of 3.7 ha and Harp 3A with an area of 21.7 ha, have podzolic soils and mixed

Figure 9.1 Location and instrumentation of the Harp 4-21 and Harp 3A catchments.



forests dominated by sugar maple (*Acer saccharum*) (Lozano et al., 1987). Harp 4-21 and the northern half of Harp 3A are underlain by Precambrian Shield amphibolite and schist bedrock, whereas the southern half of Harp 3A is underlain by granitized biotite and hornblende gneiss (Jeffries and Snyder, 1983). The shape and steepness of the hillslopes and the total sediment thickness differs between the catchments. Most hillslopes in Harp 4-21 are gentle to moderately steep (= 8 to 30%) and are slightly concave towards the stream. In Harp 3A, hillslopes are steeper (= 20 to 50%), straighter, and end in nearly flat valley bottoms. Glacial till is up to 15 m thick in Harp 4-21 whereas the soils and till along the hillslopes of Harp 3A rarely exceed 1.5 m. The lower 50 m of the Harp 3A stream is incised in 2 m of sand and is underlain by approximately 2 m of clay.

Harp 4-21 and Harp 3A are subdivided into two (S1 and S4) and five (W1-W5) subcatchments respectively (Figure 9.1). All subcatchments drain predominantly hillslope areas; less than 1% of Harp 4-21 and 4% of Harp 3A are covered by surface water (including streams and wetland ponds). Wetlands 2 and 3 occupy the flat valley bottoms of W3 and W4 respectively. Although subcatchment W1 only has small areas of ponded water, it is influenced by wetland runoff from W3 and W4. An ephemeral stream draining the easternmost hillslopes of Harp 3A flows over a bedrock outcrop at B1.

Methods

Samples of precipitation, throughfall, stemflow, overland flow, groundwater, water ponded in wetlands and stream water were collected in autumn 1992 (September 27 to November 20) and spring 1993 following snowmelt (May 2 to June 4). Throughfall, groundwater and stream samples from Harp 4-21 were also collected during selected storms between March 1989 and April 1990. Precipitation was collected at a meteorological station less than 500 m north of the Harp 4-21 catchment. In 1992 and 1993, throughfall volumes

were measured and samples were collected from four sites: two beneath a deciduous canopy (one in Harp 4-21, one in Harp 3A) representative of hillslopes and two beneath a coniferous canopy of cedars (*Thuja occidentalis*) and black spruce (*Picea mariana*) that predominate in Wetland 2 of Harp 3A. Precipitation and throughfall samples were collected in polyethylene funnels that drained into 20 l glass bottles. Although polyethylene screening (1 mm mesh) was placed at the neck of the funnels to prevent falling leaves from entering the bottles, at least four throughfall samples were likely to have been contaminated by leaves and organic matter that fell into the funnels between or during storms. Stemflow samples were collected from one sugar maple, one white birch (*Betula papyrifera*) and two cedar trees using polyethylene tubing that drained into 1 l polyethylene bottles.

Stemflow from deciduous trees overflowed the 1 l collection bottles except during the smallest storms. For the purpose of calculating DOC fluxes, the depth of stemflow from deciduous trees is estimated from the empirical relationship $SF = 0.062 P - 0.13$ where stemflow (SF) and precipitation (P) are expressed in mm (Helvey and Patric, 1965). Measured water depths of stemflow from the cedars were negligible (<0.2 mm). The empirical relations for throughfall (TF), $TF = 0.92 P - 0.54$ and $TF = 0.88 P - 3.0$ (expressed in mm) for the deciduous and coniferous stands respectively, were calculated on a storm basis and compare well with those of Helvey and Patric (1965).

Overland flow was sampled from two collectors in Harp 4-21 and one collector in Harp 3A. Collectors were made from PVC pipe that was cut in half lengthwise, screened, capped at both ends, inserted at ground surface below the litter, and drained by gravity to 1 l polyethylene bottles.

Groundwater samples were collected from piezometers that were screened at various depths (0.04 to 7.8 m) along the hillslopes, in the streams, in riparian areas and in the

wetlands. Screen lengths varied from 0.08 to 0.5 m and some shallow piezometers were constructed to collect groundwater flowing through the A or upper B soil horizons. Groundwater levels were measured manually in piezometers, wells and shallow (0.15 to 0.2 m) open holes.

Streams were sampled several times during each storm at W1-W5, S1, S4, and B1 during the autumn, and at W1, W3-W5, S1 and S4 during the spring (Figure 9.1). Stream discharge was monitored continuously using V-notch weirs and water level recorders at all sites except B1 where instantaneous measurements of discharge were made. Rating curves were calibrated from numerous instantaneous measurements of discharge and stage during storms. Stream DOC exports were calculated by interpolating DOC concentrations according to stream discharge as described in Chapter 8.

Stream, wetland, stemflow and groundwater samples were prefiltered in the field through 80 μm (44 μm for groundwater) polyester screening into site-designated polyethylene bottles. Precipitation, throughfall and overland flow samples were not prefiltered. All 1992 and 1993 samples were filtered within 24 hours through 0.45 μm Sartorius® cellulose nitrate membranes (25 mm diameter) into glass scintillation vials. Cellulose nitrate membranes were rinsed by passing a minimum of 75 ml of sample through the filter prior to sample collection. Experiments with deionized (Nanopure®) water and with a HCl solution (pH = 4.3) demonstrated that the cellulose nitrate membranes rinsed in this way contributed only 0.04 ± 0.07 mg/l and 0.06 ± 0.03 mg/l respectively to the filtrate (Appendix 9). Samples were acidified with HNO_3 to a pH near 2 and kept refrigerated in darkness until analyzed by high temperature combustion with a Dohrmann DC-190 total carbon analyzer. The instrument blank measured 0.1 mg/l. All results are reported in mg C/l.

DOC concentrations reported from 1989 and 1990 were analyzed by the Ontario Ministry of the Environment (MOE) by the persulfate oxidation method (MOE, 1983). All MOE samples were prefiltered as described above but were not passed through the 0.45 μm membranes. To account for differences in analytical methods, filtering and preservation, 33 pairs of samples were compared. The results demonstrated that MOE samples were lower than the 0.45 μm filtered samples by an average of 0.8 ± 0.4 mg/l in the range of 2-12 mg/l. It is not apparent whether the difference is due to differences in sample treatment or analytical method. All 1989 and 1990 MOE results have been normalized by +0.8 mg/l for comparison with the other analyses (Appendix 9).

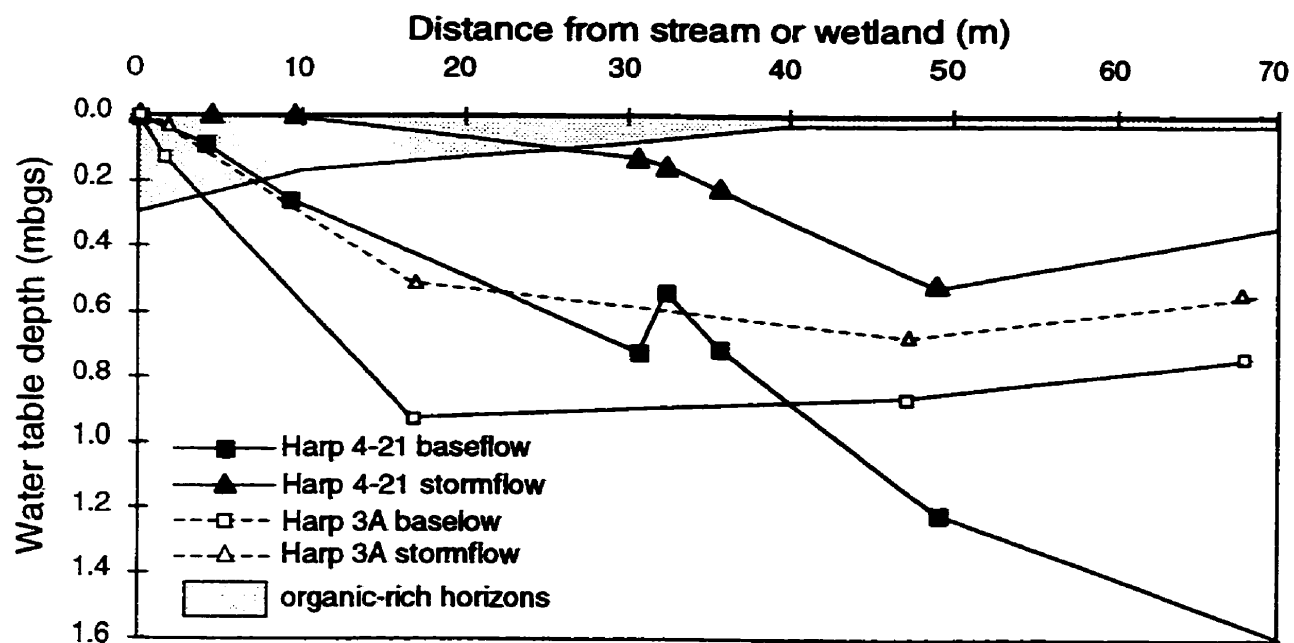
The mass of DOC transported along flowpaths is calculated by multiplying the volume of flow by the average DOC concentration. The volume of water that originated from a particular hillslope between November 2 and 9, 1992 is estimated as the total stream discharge minus the volume of precipitation that fell onto the riparian area. This calculation is justified by time domain reflectometry measurements of soil water in riparian areas which demonstrate that there is almost no net storage of water during storms. The extent of riparian areas was delineated by the occurrence of the water table within the organic-rich soil horizons (A, O and upper B) adjacent to the stream.

Results

Hydrological flowpaths

In Harp 4-21, the depth to the water table increased with increasing distance from the stream. At baseflow, the water table was positioned within the upper B or lower A horizons adjacent to the stream, within the middle to lower B horizon in the lower portion of the hillslopes, and within the till in the upper hillslopes (Figure 9.2) (Chapter 3). Groundwater discharging from the till into the soils near the stream maintained high water table levels,

Figure 9.2 Depth to water table during baseflow and stormflow conditions in Harp 4-21 and Harp 3A. Stippled area shows the approximate depth of organic-rich horizons in Harp 4-21. Locations of transects are shown in Figure 9.1.



creating saturated conditions and maintaining stream baseflow throughout the year along the Harp 4-21 stream. Baseflow was sustained by deep groundwater flowing from the till directly through the stream bed and through the lower B horizons of riparian soils. During storms, groundwater levels near the stream and along the lower hillslope rose into soil horizons so that most of the subsurface flow to the stream passed through shallow soil horizons (A and upper B) (Figure 9.2).

In Harp 3A, the water table remained near the base of the B horizon along the length of the hillslope. The water table generally intersected the A or O horizons for a small distance at the edge of the stream or wetlands (Figure 9.2). During storms, the water table in the hillslope usually remained within the lower B horizon and subsurface flow during storms occurred mostly in the lower B horizon (40-60 cm depth). Riparian water tables and flowpaths varied within Harp 3A and the extent of subsurface flowpaths through shallow soil horizons was limited to the lower 1 to 10 meters of hillslopes in most areas. Only during the very large storms on November 12 (88 mm of precipitation) did hillslope groundwater levels rise into the upper B horizon. During dry summer conditions, the entire hillslopes became unsaturated and most of the Harp 3A stream was dry.

Hydrograph separations using ^{18}O and dissolved Si concentrations demonstrated that more than 75% of the storm runoff in Harp 4-21 consisted of soil water or groundwater (Chapter 4). High Si concentrations in deep groundwaters and stream discharge showed that a significant proportion (up to 70%) of the runoff involved deep groundwater that flowed through the till, discharged into soil horizons near the stream where it mixed with soil water, and flowed to the stream. Hydrograph separations in Harp 3A during the November 2, 1992 storm suggest that groundwater and soil water contributed approximately 85% of peak runoff. Thus, in both Harp 4-21 and 3A, stream stormflow is dominated by subsurface water.

DOC concentrations

The pattern of DOC concentrations through the hydrological cycle (Figure 9.3) are typical of those reported in other catchments (McDowell and Likens, 1988; Moore, 1989). DOC concentrations of precipitation were low; throughfall and stemflow concentrations increased from contact with live vegetation. Overland flow and groundwater in the A horizon typically had similar or higher DOC concentrations than throughfall which indicates production of DOC in litter and high organic matter soil horizons. DOC removal as a result of sorption or decomposition within the soil is suggested by lower DOC concentrations in groundwaters from the B horizon or deeper. In wetlands, groundwater DOC concentrations varied substantially but were generally higher than those in the hillslope. Similarly, higher DOC concentrations in surface water within Wetland 2 may have been caused by production of DOC and/or leaching of litter, organic matter and vegetation within the wetland.

Stream DOC concentrations and concentration changes during storms differed between the subcatchments. Harp 3A subcatchments showed variable increases in DOC concentrations during storms with no response to spring storms at W5 (Figure 9.4, Table 9.1). In Harp 4-21, both S1 and S4 showed larger increases in DOC concentrations during storms (Table 9.1) that were more closely related to discharge. Whereas seasonal regressions between DOC concentration and discharge were significant ($p < 0.01$) at S1 and S4, similar regressions at W3 and W4 (subcatchments with wetlands) were not significant (Chapter 8). In Harp 3A, the wetlands were obvious sources of DOC to the stream as average DOC concentrations increased from W5 to W4 to W3 in both seasons during baseflow and stormflow conditions (Table 9.1).

Groundwater DOC concentrations varied spatially along flowpaths (Table 9.2). In Harp 4-21, the DOC concentrations within the till were low both along the hillslopes (mean =

Figure 9.3 DOC concentrations of waters in Harp 4-21 and Harp 3A (1989-1993) (GW = groundwater, hor. = soil horizon, and n = number of samples).

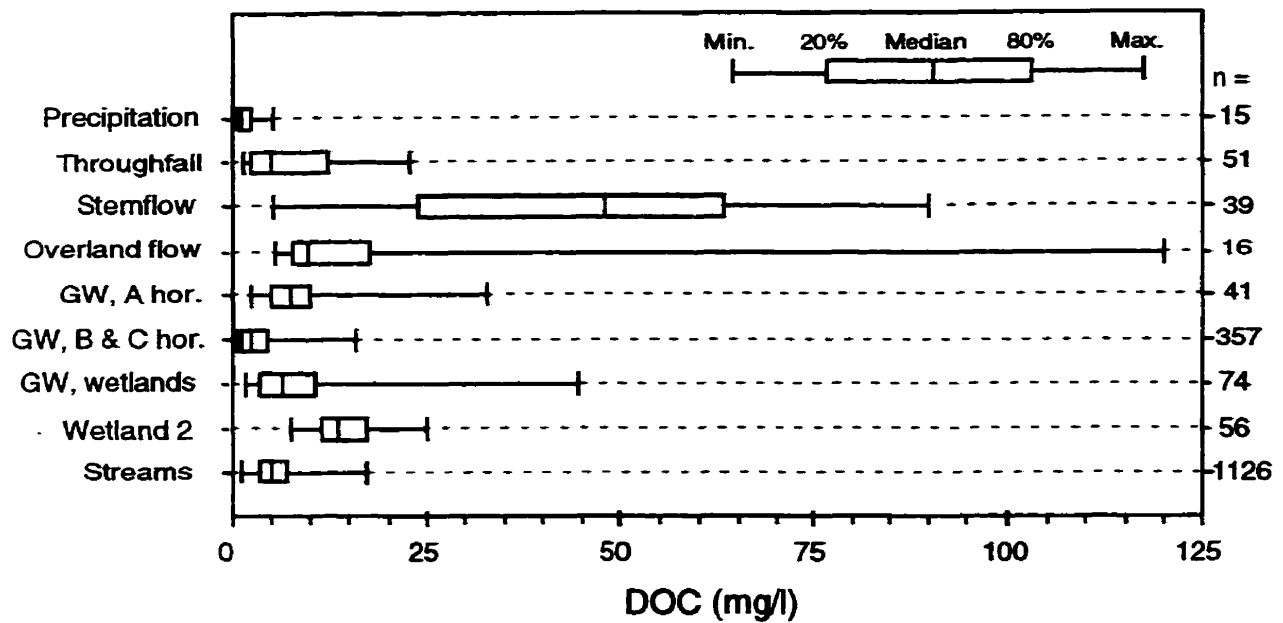


Figure 9.4 Stream DOC concentrations at S1, W5 and W3 during the a) autumn and b) spring sampling periods.

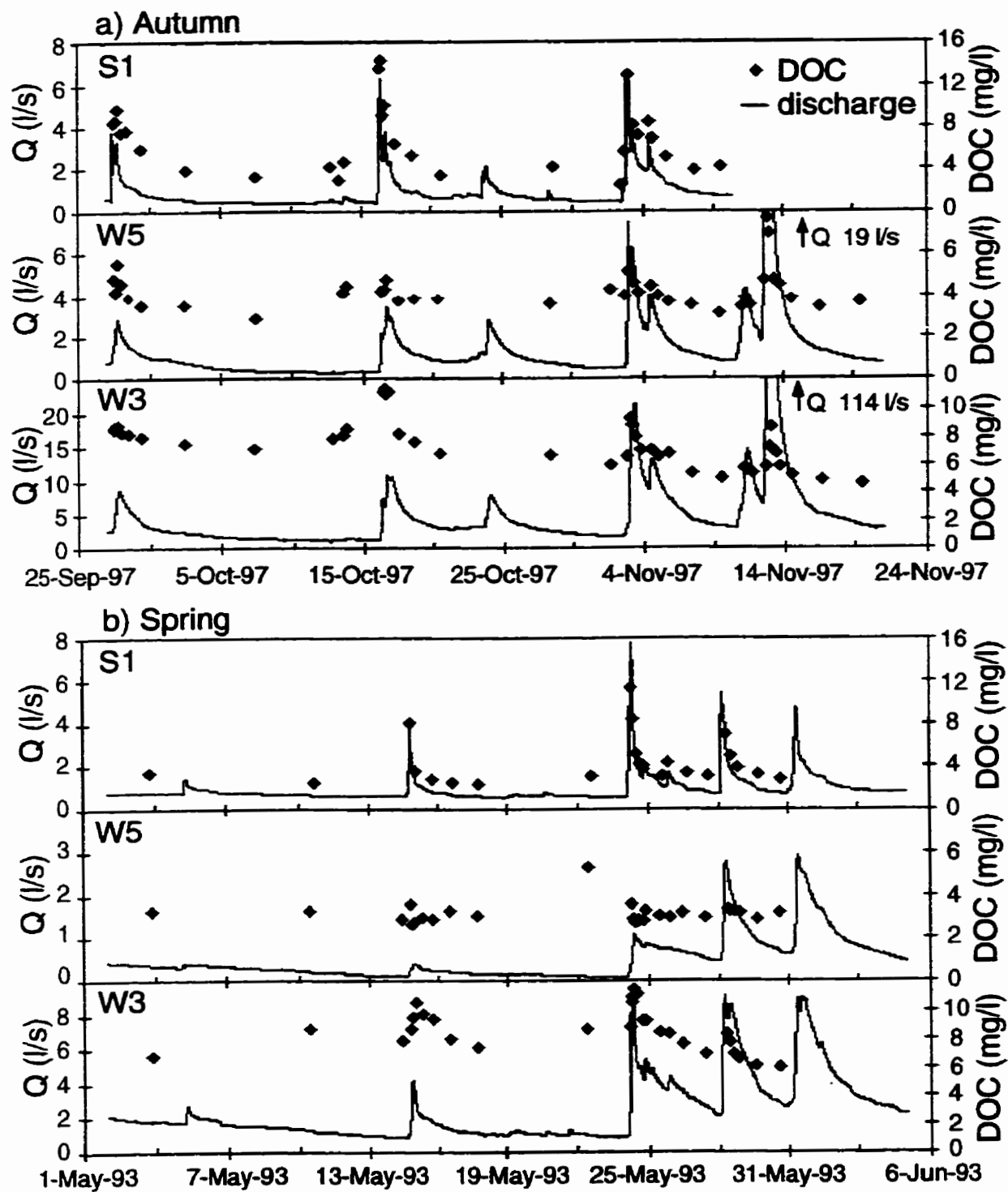


Table 9.1 Flow-averaged DOC concentrations for periods of stormflow, baseflow and total flow during the autumn and spring sampling periods.

Site	Average DOC concentration (mg/l)					
	Autumn 1992			Spring 1993		
	Stormflow	Baseflow	Total flow	Stormflow	Baseflow	Total flow
W1	6.5	4.8	5.8	6.0	4.7	5.2
W2	5.5	3.4	4.6	-	-	-
W3	7.4	6.4	6.9	8.5	7.6	7.8
W4	6.4	5.0	5.7	5.8	5.1	5.3
W5	5.0	3.6	4.4	3.2	3.2	3.2
S1	8.0	4.1	5.7	5.8	3.1	3.8
S4	7.1	3.9	5.2	-	-	-

Table 9.2 Average DOC concentrations of groundwaters and ponded water in Harp 4-21 and Harp 3A.

Harp 4-21	depth range ¹ (m)	Average [DOC] (mg/l)	np	n	Harp 3A	depth range ¹ (m)	Average [DOC] (mg/l)	np	n
Hillslope, till	0.9 - 6.8	2.3 ± 1.3	14	61	Hillslope, B horizon or till	0.27 - 1.6	5.1 ± 2.3	11	56
Riparian, lower B horizon or till	0.69 - 2.9	1.5 ± 0.5	11	100	Riparian and beneath wetlands, C horizon	1.5 - 2.9	2.8 ± 1.3	5	38
Riparian, middle B horizon	0.16 - 0.53	4.7 ± 1.7	7	62	Riparian and lower hillslope, A or upper B horizon	0.04 - 0.08	14.3 ± 13.1	4	11
Riparian, A or upper B horizon	0.12 - 0.13	8.9 ± 3.2	3	27	Wetlands, organic sediments	0.08 - 1.23	7.6 ± 5.7	10	74
					Wetland 2, ponded water	0.00	14.0 ± 3.3	-	56

Mean DOC concentrations of individual piezometers are averaged. Total number of piezometers (np) and samples (n) are indicated.

¹ piezometer mid-screen depths

2.3 mg/l) and in deep piezometers near the stream (mean = 1.5 mg/l) but increased as groundwater flowed through the B (mean = 4.7 mg/l) and A (mean = 8.9 mg/l) soil horizons near the stream. In Harp 3A, there were larger temporal variations in DOC concentrations within individual piezometers and larger spatial variations among piezometers than in Harp 4-21. Piezometers within the lower B horizon and within the till along the hillslopes of Harp 3A had a mean DOC concentration of 5.1 mg/l. Within the sandy horizons beneath the wetlands and the clays in the lower portion of the catchment, the groundwater DOC concentration averaged 2.8 mg/l. However, moderate to low hydraulic conductivities within the wetlands and in the clays suggest that these groundwaters are minor contributors to streamflow. Wetland DOC concentrations were higher with average values of 7.6 mg/l within the organic soils of wetlands, and 14.0 mg/l at the surface of Wetland 2.

DOC contributions along flowpaths

Throughfall and stemflow were minor contributors to stream DOC and discharge. Hydrograph separations using ^{18}O indicate that they contributed 23% of the total runoff during the October 31, 1989 storm onto a leafless canopy in Harp 4-21 (Chapter 4). With a measured throughfall DOC concentration of 4.1 mg/l and an assumed stemflow concentration of 34 mg/l (the volume-weighted mean concentration from autumn 1992 for deciduous trees), the total DOC export that originated from throughfall and stemflow was approximately 18% (12% and 6% respectively). During the dormant season in Harp 3A, the mean throughfall DOC concentrations (2.3-4.0 mg/l) were lower than stream baseflow by 1.0 mg/l to 2.4 mg/l with the exception of one storm (Nov. 4, 1992, 10.4 mg/l) where throughfall samples may have been contaminated by fallen leaves in the collectors. Lower throughfall DOC would contribute to a net dilution of stream DOC yet all these storms exhibited increases in stream DOC concentrations.

Similar calculations for the June 22, 1989 storm indicate that throughfall and stemflow contributions to stream discharge and DOC were also minor in the growing season. Together, they contributed 17% of the total runoff (Chapter 4) and approximately 12% of the total DOC flux in Harp 4-21. The DOC flux was estimated by using the measured throughfall DOC concentration of 2.3 mg/l and the weighted mean stemflow DOC concentration of 55 mg/l from spring 1993. The low throughfall DOC concentration may result from the high rainfall intensity of this storm or spatial variability in throughfall DOC concentrations. In Harp 3A, the small proportion of throughfall and stemflow in stream runoff (<15%) suggests that throughfall and stemflow were also insufficient in volume to contribute much of the total stream DOC export.

Overland flow was observed in both Harp 3A and Harp 4-21 during storm events. Whereas the extent of overland flow varied seasonally in both catchments, the temporal and spatial distribution of overland flow was much more variable in Harp 3A. The overland flow collector in Harp 3A was poorly located and malfunctioned so that only one overland flow sample with a DOC concentration of 90 mg/l was collected from the October 16, 1992 storm. The two overland flow collectors in Harp 4-21 were more successful and collected samples with DOC concentrations that range from 5.5 mg/l to 120 mg/l. Nearly all these results were greater than stream DOC concentrations (Figure 9.3) and suggest that overland flow could have been an important pathway of DOC to streams during storms if the volumes were substantial. The large spatial and temporal variability of overland flow volumes and DOC concentrations make it difficult to estimate reasonably the input of DOC to streams along this flowpath. Because overland flow in these basins includes both groundwater discharge and throughfall, hydrograph separations of the streams cannot be used to distinguish overland flow from soil or groundwater flow.

Groundwater flow through the shallow soil horizons adjacent to the stream represents a major flowpath for DOC in Harp 4-21. If we assume that the entire increase in soil water and groundwater discharge (i.e. above baseflow) during the October 31, 1989 storm flowed through the A and upper B horizons and had the average DOC concentration of 11.0 mg/l (n=6) measured in piezometers P34-01 (0.03-0.19 m depth) and P46-01 (0.06-0.22 m depth) prior to and during that storm, the mass of DOC flowing through the shallow riparian horizons would equal 73% of the total DOC exported by the stream.

Riparian and wetland vs. hillslope sources of DOC

To demonstrate the significance of DOC production in riparian and wetland areas, DOC export from hillslopes and streams are compared for storms between November 2 and 9, 1992 (Table 9.3). The range of hillslope DOC export was calculated by assuming that the average DOC concentration of groundwater in hillslopes ranged between that of stream baseflow (at S1 and W5) and that of hillslope piezometers. In Harp 4-21, the hillslope accounted for between 16 and 27% of the total DOC export from the stream. Therefore, most of the DOC exported during storms must have originated either in riparian areas or within the stream.

Hillslope transport of DOC to the riparian and wetland areas was more important in Harp 3A than in Harp 4-21 and varied between 37 and 68% of the total stream DOC export (Table 9.3). In the subcatchments without wetlands, W1 and W5, between 50-93% and 62-115% respectively of the stream DOC export originated from the hillslope. Even the lower ranges of these estimates in Harp 3A exceeded the upper ranges of estimates from S1 and S4 in Harp 4-21.

The wetlands were a significant source of DOC near the stream in Harp 3A. Whereas riparian areas in W5 contributed less than 38% of DOC export, the riparian areas and wetlands

Table 9.3 Hillslope and stream export of DOC between November 2 and 9, 1992.

	Hillslope			Stream	
	Water volume (m ³)	DOC export ¹ (kg)	% of stream export	Water volume (m ³)	DOC export (kg)
Harp 4-21					
S1	350	0.51 - 0.91	15 - 26	430	3.5
S4	320	0.47 - 0.82	16 - 28	530	3.0
Total	670	0.98 - 1.73	16 - 27	960	6.5
Harp 3A					
W1	1920	5.4 - 9.9	50 - 93	2240	10.7
W3	1260	3.5 - 6.5	22 - 40	1710	16.2
W4	1170	3.2 - 6.0	35 - 64	1570	9.4
W5	1120	3.1 - 5.7	62 - 115	1240	5.0
Total	5470	15.2 - 28.1	37 - 68	6760	41.3

Total precipitation during this period was 46 mm. Results are net values for each subcatchment (e.g. W4 values are calculated from W4 - W5).

¹ Using a range of DOC concentrations based on stream baseflow and groundwater (1.5-2.6 mg/l in Harp 4-21 and 2.8-5.1 mg/l in Harp 3A).

in subcatchments W3 and W4 contributed between 60-78% and 36-65% of the subcatchment stream DOC (Table 9.3). These areas exported 32-46% of the total DOC export from Harp 3A even though they occupy only 8% of the total catchment area. The effect of wetlands and riparian areas on DOC export is also evident when the seasonal DOC yields are compared for the different subcatchments (Table 9.4). The DOC yields from subcatchments with wetlands (W3 and W4) were comparable to those with riparian DOC sources (S1) and were much larger than the yields from subcatchments without wetlands (W1 and W5).

Wetlands and in-stream sources of DOC

The increase in average groundwater DOC concentrations from hillslopes to wetlands to ponded water in Wetland 2 (Table 9.2) suggests that the source of DOC within the wetland originates either from organic matter at the wetland surface or from contact of groundwater with organic matter prior to discharging to the wetland surface. The hydraulic conductivities that were measured within the wetlands decrease rapidly with depth ($\approx 10^{-5}$ m/s near the surface at 0.1 m depth, $\approx 10^{-7}$ to 10^{-6} m/s at depths >0.5 m) and suggest limited groundwater flow through the base of the wetland and greater flow through more permeable shallow organic horizons at the wetland edge.

The response of stream DOC during storms at W3 and W4 suggests DOC production by decomposition and leaching of organic matter by ponded water as a source of DOC and episodic flushing as a transport process of DOC from wetlands to the stream. The clockwise loops in Figure 9.5 show that DOC concentrations were usually higher during the rising limb than on the falling limb of the hydrographs at W3 and W4. Site S1 did not show these loops and site W5 only had small loops during two small autumn storms. Higher DOC concentrations on the rising limbs may have been caused by the flushing of high DOC water from the relatively stagnant portions of the wetland as water levels rose and the pools became

Table 9.4 DOC and water yields within each subcatchment of Harp 3A in the autumn and spring sampling seasons.

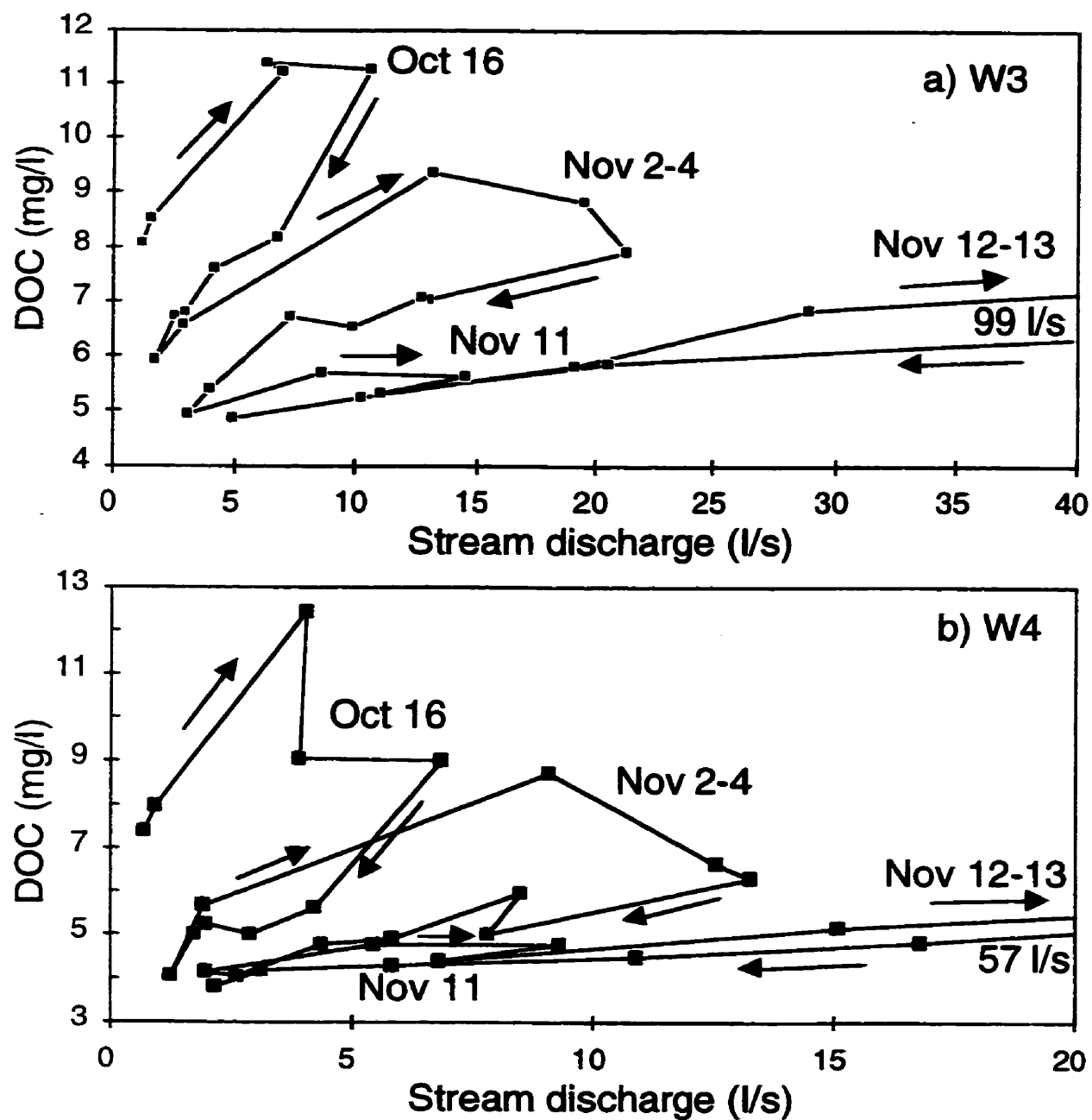
	W1	W3	W4	W5	S1
Autumn ¹ DOC yield (g m ⁻² y ⁻¹)	1.1	8.9	4.8	2.6	4.1
Autumn ¹ water yield (mm)	97	104	82	80	88
Spring ² DOC yield (g m ⁻² y ⁻¹)	-0.1	6.0	2.5	0.8	2.7
Spring ² water yield (mm)	43	42	36	19	58

Results are net values for each subcatchment (e.g. W4 values are calculated from W4- W5).

¹ September 27-November 10, 1992

² May 2-May 31, 1993

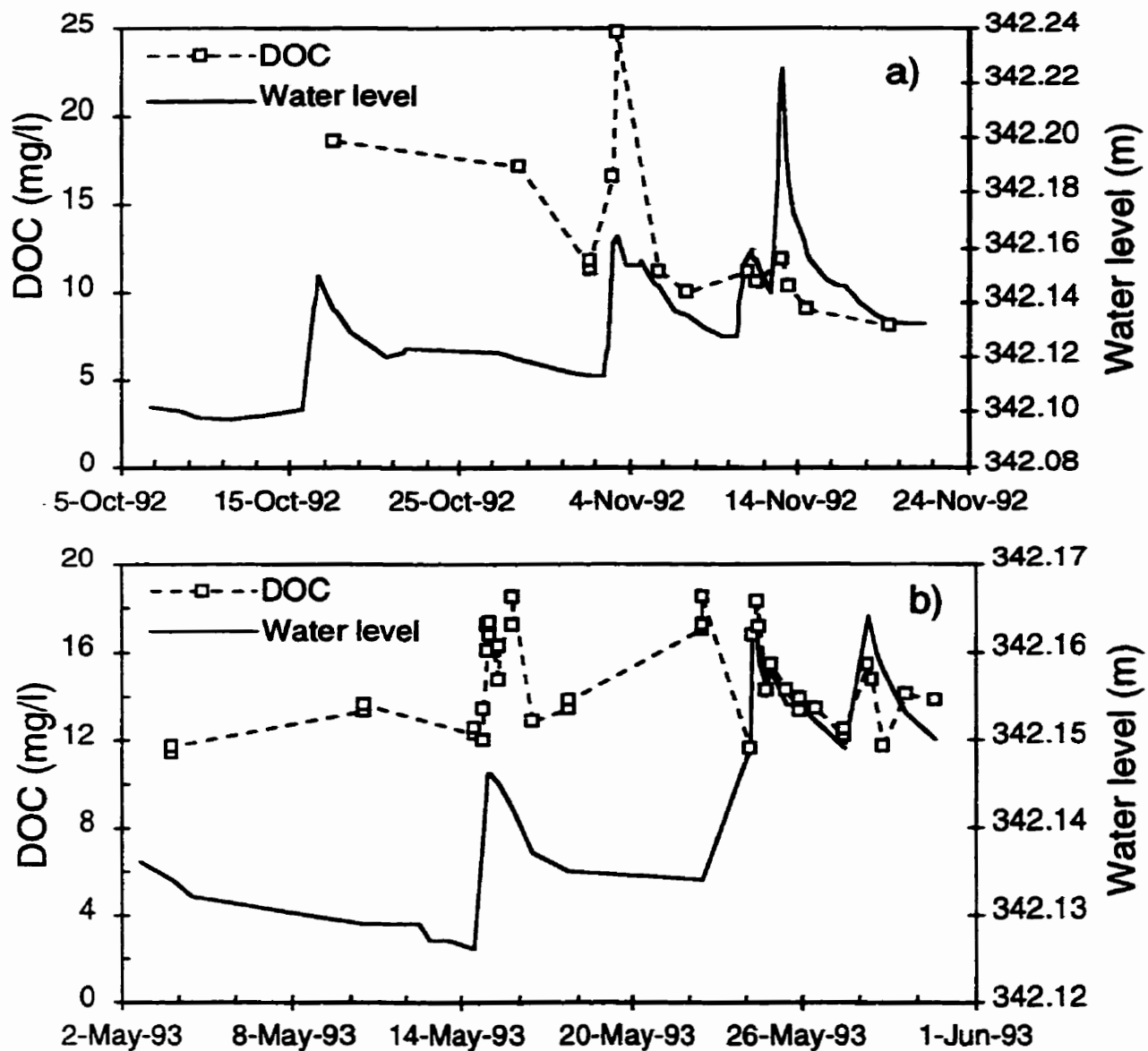
Figure 9.5 DOC concentrations versus stream discharge during autumn 1992 storms at a) W3 and b) W4. Arrows indicate the progression of time.



more interconnected. The DOC concentrations in Wetland 2 during baseflow conditions varied spatially with values that ranged from 5.3 to 17.1 mg/l during one autumn sampling and from 10.3 to 26.5 mg/l during a spring sampling when the pools were poorly interconnected. Samples of water flowing across Wetland 2 collected during storms showed that DOC concentrations initially increased as water levels rose and stagnant pools became connected (Figure 9.6). When water levels were extremely high and all the pools were interconnected during the large storm on November 12, 1992, wetland DOC concentrations remained low as there were no stagnant areas and most pools were continuously flushed. Alternatively, a larger volume of water in the wetland during this storm may simply have diluted the DOC.

With the exception of wetlands, in-stream sources of DOC are unlikely in Harp 3A and Harp 4-21. The stream beds are sandy with little organic matter and no debris dams. In fact, the Harp 3A stream between W3 and W1 was a net sink of DOC. A conservative estimate of the total mass of DOC that entered the stream between W3 and W1 (W3 export + W2 export + B1 stream export + groundwater discharge) exceeded DOC export at W1 by 8 kg in the autumn and 11 kg in the spring or 4% and 27% of total DOC export respectively. In the spring the DOC export at W3 was greater than that measured at W1 so that the loss of DOC between W3 and W1 exceeded the DOC production from the W1 subcatchment to produce a net negative yield (Table 4). Since these estimates only include DOC removal downstream of W3, the total amount of DOC removed along the entire stream length could be larger. Meyer (1990) and Mann and Wetzel (1995) discuss biotic and abiotic utilization of DOC in streams and wetlands. Baseflow sampling along the Harp 4-21 stream did not show downstream increases in DOC concentrations (Hinton, unpublished data).

Figure 9.6 DOC concentrations and water levels in Wetland 2 during a) autumn, and b) spring.



Discussion

DOC concentrations of the different subcatchments clearly demonstrate the effects of different DOC sources and flowpaths in riparian, hillslope and wetland areas (Figure 9.4). DOC mass balances show that riparian and wetland sources contributed most of the stream DOC during storms (Table 9.3), that shallow subsurface flowpaths are capable of contributing most of the stream DOC export, and that in-stream sources of DOC are unlikely. The differences in DOC dynamics among these three areas are examined by comparing results from subcatchments S1 and S4 (riparian), subcatchments W3 and W4 (wetland), and subcatchments W1, W2 and W5 (hillslope). Although wetland areas can be riparian, a distinction between riparian and wetland areas based on the persistence of ponded water in wetland areas is made for the following discussion.

Riparian areas

Riparian areas contributed most of the DOC to the Harp 4-21 stream during storms. Because the DOC originates near the stream, the riparian flowpaths are most important and the hillslope water flowpaths are relatively unimportant. In the riparian areas, the dominant flowpath was lateral saturated flow within the upper soil horizons where hydraulic conductivities are highest. Deeper groundwater from the till is a major contributor to storm runoff. However, discharge of deeper groundwater from the till directly to the stream could not have contributed sufficient discharge during storms to account for streamflow (Chapter 4). Consequently, most of the deeper groundwater flow from the till discharges to riparian soils, mixes with shallower waters and flows rapidly through shallow soil horizons to the stream during storms. Therefore, both shallow flowpaths that originate near riparian areas, and deeper flowpaths that originate in hillslope areas could have similar flowpaths near the stream and reach the stream with similar DOC concentrations.

Despite their similar riparian flowpaths, there is an important difference between these shallow and deeper flowpaths. In riparian areas, water flowing along shallow flowpaths may reach the stream without substantial interaction with lower soil horizons. In hillslope areas, soil water DOC concentrations decreased from approximately 21 mg/l in the litter and A horizons to 2.2 mg/l in the B and C horizons (LaZerte and Scott, 1996). Therefore, waters flowing along deeper flowpaths have been through a cycle of DOC leaching and sorption before they contact riparian soils. This distinction is important for the interpretation of DOC quality. For example, deep groundwater DOC had little modern (bomb) carbon and low ^{14}C activities compared to litter and soil water leachates with higher ^{14}C activities (Trumbore et al., 1992; Schiff et al., 1997). Intermediate stream water ^{14}C activities showed that the stream was composed predominantly of modern, shallow carbon sources but was diluted by old, deeper carbon sources (Schiff et al., 1997). Therefore, quantitative models using chemical fingerprints of DOC (Kaplan and Newbold, 1993) would need to consider such flowpaths where low DOC waters from the hillslopes leach riparian DOC sources. These flowpaths are not represented in schematic diagrams by Kaplan and Newbold (1993) and Boyer et al. (1996) but are possible in the hydrological model for the riparian zone presented by Fiebig et al. (1990).

In the debate of whether groundwater dilutes or contributes to stream DOC and whether groundwater DOC is immobilized in the hyporheic zone (Kaplan and Newbold, 1993), there have been several comparisons of stream and groundwater DOC concentrations (e.g. Rutherford and Hynes, 1987; Ford and Naisman, 1989; Fiebig, 1997). The difficulty with this approach is that groundwater contributes to the stream along different flowpaths with different DOC concentrations. Stream DOC concentrations in Harp 4-21 are largely controlled by the relative contributions of waters from the different horizons in riparian areas. Average baseflow DOC concentrations (Table 9.1) were higher than the deep groundwater (Table 9.2)

which indicates that baseflow is a mixture of flow along deep and shallow groundwater flowpaths. During very dry conditions in late August, mostly deep groundwater contributed to the stream and stream DOC concentration (2.3 mg/l) and ^{14}C activity were similar to deep groundwater DOC (Schiff et al., 1997). Consequently, not only are the positioning of the piezometers and their screen lengths relative to the soil horizons and subsurface flowpaths very important, but the relative flow along different flowpaths will change with fluctuating water levels.

Saturated overland flow could also be a significant flowpath for DOC to the stream, particularly near peak discharges during large storms. As overland flow is a mixture of groundwater discharge, throughfall and stemflow, the contribution of the DOC sources will vary and be difficult to quantify. Higher DOC concentrations in overland flow compared to throughfall and groundwater suggest that the leaching of litter may be the main source of DOC along this flowpath. If this flowpath is significant, most of the DOC would likely originate near the stream or wetlands. Further examination of overland flow DOC is warranted.

Riparian vs. hillslope areas

Riparian areas are far more important to storm DOC export in Harp 4-21 than in subcatchments W1, W2 and W5 of Harp 3A (Table 9.3). The importance of riparian areas depends on the level of the water table relative to the organic-rich soil horizons. During storms there was more flow through high organic matter soil horizons in Harp 4-21 than in Harp 3A. This difference is partly a reflection of the effect of slope angle on the riparian water table. Along the more gentle hillslopes of Harp 4-21, the water table remained closer to ground surface farther from the stream than along the steeper slopes of Harp 3A (Figure 9.2). Therefore, groundwater flowed along shallow flowpaths for a greater distance allowing more contact with organic matter.

Groundwater flow from the hillslopes is also important for its influence on the riparian water table. In Harp 3A, the lack of tills with lower hydraulic conductivities combined with steeper slopes and a rooting zone that extends to bedrock results in faster drainage of the water from the hillslope. Slower groundwater flow through the tills of Harp 4-21 hillslopes maintains high water levels and wetter antecedent conditions near the stream whereas the Harp 3A hillslopes drain more rapidly and dry up in the summer due to lack of flow from hillslope soils and till.

Not all the differences in stream DOC response between Harp 4-21 and Harp 3A can be attributed to differences in riparian flowpaths. There may be differences in soil properties both along the hillslopes and in riparian areas. Groundwater in the lower B horizons of Harp 3A hillslopes had higher DOC concentrations than in Harp 4-21 (Table 9.2). These differences could indicate different DOC sorption capacities along the hillslopes as documented by Nelson et al. (1993) in a paired watershed study. However, there are not any large differences in soil texture or cation exchange capacity that would suggest such differences are due to differences in hillslope soil properties (Lozano et al, 1987). Rather, differences in the thickness and organic content of the riparian soils were observed between Harp 4-21 and Harp 3A, but no thorough investigation of organic matter content or distribution was carried out. Thicker and higher organic matter content in riparian soils of Harp 4-21 probably result from the higher and more persistent saturation. Seasonally dry conditions in Harp 3A allows for more oxidation of organic matter.

Hillslope vs. wetland areas

The subcatchments in Harp 3A have similar topography and vegetation except for the presence of small wetlands in W3 and W4. The DOC concentrations increased from the hillslope to the wetland (Table 9.2), and DOC concentrations at W3 and W4 were consistently

higher than those at W5 during both baseflow and stormflow conditions (Table 9.1). Consequently, the yield of DOC was much greater from subcatchments with wetlands than those without (Table 9.4). The presence of wetlands, even small ones, completely dominated the DOC export during both baseflow and stormflow conditions so that the hillslope areas were relatively unimportant compared to the wetlands (Table 9.3). Therefore, it would be pointless to attempt to relate DOC dynamics in subcatchments W3 and W4 to hillslope flowpaths. This dominance of wetlands over hillslopes as a DOC source is the reason that correlations between wetland area and DOC export are possible (Eckhardt and Moore, 1990; Molot and Dillon, 1996).

Wetland vs. riparian areas

The DOC dynamics of wetland subcatchments (W3 and W4) are different from riparian subcatchments (S1 and S4) in several ways. Baseflow DOC concentrations were lower at S1 and S4 (Table 9.1). During storms, S1 and S4 had larger changes in DOC concentrations that were more closely related to flow (Figures 9.4 and 8.5). Whereas higher groundwater levels during storms generally produced larger peak DOC concentrations for larger discharges at S1 and S4, peak DOC concentrations at W3 and W4 (Figures 9.4 and 9.5) and Wetland 2 (Figure 9.6) were smaller for progressively larger storms. Higher DOC concentrations on the rising limbs of hydrographs (Figure 9.5) suggest that flushing of organic sources at the wetland surface during storms may be important. These results suggest that most of the DOC in W3 and W4 originates at the wetland surface rather than at the wetland edge in a manner similar to riparian areas in S1 and S4. Consequently, the processes and the dynamics of DOC in riparian areas are not the same as those in wetlands, and riparian areas cannot simply be treated as wetland areas.

Conclusions and implications

Riparian and wetland areas were the major sources of stream DOC during storms in two small catchments of glacial sediments. A significant proportion of DOC export originated in these areas (Table 9.3) and DOC yields were highest from these areas (Table 9.4). These results support the hypothesis by Hemond (1990) that 'stream channel wetlands' are the main source of stream DOC. Riparian DOC sources are not restricted to areas of ponded water; most of the DOC export from Harp 4-21 during storms originated in the shallow organic-rich soils adjacent to the stream that do not have ponded water. In this study, the response of stream DOC concentrations during storms were different between riparian and wetland areas because the DOC export in riparian areas is related to flowpaths whereas the DOC export in wetlands is related to DOC production and leaching in ponded water.

The results of this study emphasize the need to focus on the dynamics of DOC in riparian and wetland areas during storms. Some of the important hydrological processes that control DOC dynamics only occur during storms and would not be observed from studies with longer sampling intervals. Because the sources of DOC in watersheds can be localized (within 5-25 meters of the stream channel in Harp 4-21), the geographic locations of instrumentation are very important. Traditionally, most studies have relied on soil lysimeters and piezometers located in midslope positions or have failed to recognize different flowpaths in riparian areas. Recognition of the difference in flowpaths between hillslope and riparian areas needs to be incorporated into project design. Studies are also needed to examine how differences in soil properties in the immediate area near the stream (0-25 m) affect stream DOC dynamics.

DOC sources cannot be equated with water flowpaths. Water flowing along different flowpaths can acquire DOC from similar sources in riparian and wetland areas. The use of multiple organic markers in mixing models as suggested by Kaplan and Newbold (1993) may

be complicated by the discharge of deeper groundwater through shallow riparian flowpaths. First, if groundwater acquires the same concentration as soil water then the marker will not serve to distinguish the two. Second, not all markers will be affected similarly in riparian areas so that the markers may record the degree of interaction with riparian soils rather than the relative fluxes along different flowpaths. Conversely, such markers could help identify interactions in riparian areas.

The importance of riparian soils as a source of DOC ultimately depends on the water flowpaths near the stream. Where flowpaths intersect riparian soils of high organic matter content for a significant distance before discharging to the stream, stream DOC export will be higher. Several hydrological and physical factors affect these flowpaths but the most critical factor is the water table fluctuation near the stream. Where riparian DOC sources are important, DOC dynamics will vary from catchment to catchment and may vary within a catchment during different storms. However, we hypothesize that positive correlations between DOC concentrations and stream discharge will be strongest in watersheds with large riparian DOC sources and without significant wetland areas.

Chapter 10

Conclusions

The role of subsurface flow in streamflow generation was examined in this thesis by field studies of two small catchments on the Canadian Shield, Harp 4-21 and Harp 3A, located in central Ontario. The most significant difference between these catchments is the presence of thicker glacial till in Harp 4-21 (up to 15 m) than in Harp 3A (less than ≈ 0.5 m). Therefore, the hydrological role of glacial till could be evaluated by a paired watershed study. Field studies combined the use of hydrometric measurements, such as stream discharge, groundwater levels and soil water content, with hydrochemical and isotopic data. The purposes of these field measurements were to quantify the temporal and spatial pattern of subsurface contributions to storm runoff and to identify the controlling hydrological processes. Conceptual models of streamflow generation were summarized and refined in the context of subsurface flow. Field data were then used to evaluate the relative importance of these models in Harp 4-21 and Harp 3A. Whenever possible, linkages between hydrological processes and physical and hydrological parameters were identified to allow the extension of results to other catchments on the Canadian Shield. Lastly, the dynamics of dissolved organic carbon (DOC) during storms were studied to assess their importance on export budgets, to identify DOC sources during storms, and to demonstrate how knowledge of the hydrological flowpaths can improve interpretations of hydrochemical variables.

Contributions of this thesis

This thesis has made several contributions to the study of subsurface flow in streamflow generation. These contributions can be classified according to methodology, data collection, data interpretation, and conceptual understanding. Methodological contributions of

this study include: the development of general equations for three-component hydrograph separations (Chapter 4), the use of a water balance approach to quantify the magnitude and timing of runoff from a hillslope (Chapter 6), and the development of a new method to calculate storm export of a hydrochemical variable that is dependent on discharge (Chapter 8). The collection, documentation and interpretation of hydrological and hydrochemical data represents a significant contribution in itself because it provides a database for comparison with other studies and for development of broader generalizations and conceptual models. Although the combined use of hydrological and hydrochemical data from streams and groundwater is not a new development for streamflow generation studies, few studies on the Canadian Shield have reported such combined data (e.g. Buttle and Sami, 1992; Allan and Roulet, 1994; Peters et al., 1995). In this study, a substantial amount of stream, soil moisture, groundwater, and hydrochemical data were collected and reported. Some of the most important results, interpretations, generalizations and conceptual developments of the thesis are summarized in the following sections. Their implications are discussed and suggestions for additional research proposed.

The role of glacial till

Glacial till on the Canadian Shield is coarser grained than till that has incorporated Paleozoic carbonates adjacent to the Shield. Consequently, its hydraulic conductivity is higher (Chapter 3) and flow through it can contribute significantly to stream discharge (Chapter 4). Therefore, the glacial till of Harp 4-21 is considered to be a low yield aquifer rather than an aquitard.

Groundwater flow through glacial till on the Canadian Shield has important hydrological roles both during and between storms. The most important is to provide seasonal water storage and groundwater flow from upslope throughout the year (Chapters 3 and 5).

This flow maintains the groundwater table within soil horizons near the stream, displaces stored water from these soils, and supplies stream baseflow year round. Flow rates from the till during storms do not change greatly and cannot account for the observed increase in stream discharge because the hydraulic conductivity of the till is lower than that of the overlying soils. However, water that flows through the till can still be the dominant component of storm runoff because it is discharged to the soils adjacent to the stream prior to the storm and is rapidly displaced into the stream during the storm (Chapter 4).

The role of soils

Subsurface stormflow generation occurs predominantly within saturated soils because their saturated hydraulic conductivity is much greater than that of the till or the bedrock. This result is probably true for most catchments on the Canadian Shield except where the parent material of the soil is quite permeable ($> \approx 10^{-5}$ to 10^{-6} m/s) as in the case of glaciofluvial or shoreline sediments (e.g. Buttle and Sami, 1992). Macropores that are created by roots and soil structure are likely responsible for the high hydraulic conductivity observed in the study catchments and are important for transmitting subsurface flow through the soils (Chapter 7).

The spatial extent of water table development within the soils is the most important factor that influences the effectiveness of runoff generation. The large temporal variability in the spatial extent of the water table within the Harp 3A soils causes the large variability in runoff response to storms (Chapters 5 and 7). The spatial extent of the water table in soils depends on antecedent soil moisture, slope, hydraulic conductivity of the till, and till thickness.

The water table position with respect to soil horizons is also important because the hydraulic conductivity is higher for shallower horizons as macropores become more prevalent. As water levels rise within the soil, subsurface flow increases greatly as does the relative

importance of flow within soils (Chapter 6). The water table position in soils influences the relative amount of flow through different horizons and, therefore, stream water chemistry (Chapter 9).

Timing and spatial extent of subsurface stormflow generation

As demonstrated by soil water balances in Harp 3A (Chapter 6), subsurface flow can be generated rapidly from middle or upper hillslopes. Infiltrating water ultimately generates subsurface flow and stream runoff by displacing water downslope towards the stream. Consequently, the timing and magnitude of subsurface runoff production at a given slope position depends on storage of infiltrating water, storage of subsurface flow from upslope, and release of stored water. Therefore, the timing of subsurface stormflow generation depends on slope position, not only because of spatial differences in antecedent water storage within the slope, but also because of subsurface flow from upslope. Sites farther upslope can even contribute subsurface runoff more rapidly than downslope sites because water storage within the transiently saturated zone at downslope sites may not decrease until subsurface flow from upslope decreases and the water table drops (Chapter 6).

Role of physical and hydrological conditions on the Canadian Shield

In this thesis, it has been suggested that hydrological responses and processes should be related to the physical and hydrological conditions of individual catchments in order to apply the results more widely to other watersheds. Several relationships between physical and hydrological factors, and hydrological responses and processes have been made in the previous sections and throughout the thesis. However, there are too few studies to formulate broad generalizations of hydrological processes for the different types and thicknesses of overburden on the Canadian Shield without resorting to speculation. This thesis does provide sufficient data to compare differences in hydrological responses for hillslopes with soils and

thick till (Harp 4-21) and hillslopes with soils and thin till (Harp 3A, and PC-108). These results are summarized and compared with those from another Canadian Shield catchment without soils or with thin soils directly on bedrock (Allan and Roulet, 1994) in Table 10.1.

Conceptual models of subsurface stormflow generation

Conceptual models of subsurface stormflow generation were classified according to the mechanism and spatial extent of increased subsurface flow during storms and the zones in which increased flow occurs (unsaturated, transiently-saturated or previously saturated zones, Chapter 2). Increased subsurface flow can result from increased downslope hydraulic gradients and increased water contents. These mechanisms provide a means for distinguishing between different conceptual models and hydrological processes. Consequently, recognition of these different mechanisms are a useful basis for planning streamflow generation studies and for interpreting their results (Chapter 7).

The implications of streamflow generation models on subsurface flow had not previously been adequately considered, particularly with respect to the identification of the physical and hydrological conditions necessary to produce significant subsurface stormflow. A theoretical examination of these physical and hydrological conditions has placed constraints on the type of environments where hydrological processes are likely to dominate. For example, the groundwater ridging model is limited to sediments without macroporosity because of the model's requirement of tension-saturation which cannot occur in soils with macropores (Chapter 2). This limitation invalidates the application of this model to most forested watersheds.

The groundwater ridging model is the only model to emphasize changes in hydraulic gradient and increased flow through previously saturated sediments. Results in the two study catchments demonstrate that changes in downslope hydraulic gradients were small during

Table 10.1 Hydrological response in hillslopes of different sediment thickness on the Canadian Shield. Data for thin or absent soils from Allan and Roulet (1994).

Hydrological variable	Soils thin or absent on bedrock	Soils on thin till or bedrock	Soils on thick tills
Baseflow	none	none or very low when evapotranspiration is high	maintains baseflow throughout year
Runoff ratio	high	high variability, very low in summer, high in wet periods	low variability, lower in summer than wet seasons
Peak discharge	high	high variability	less variability
Groundwater discharge area	small or absent	less evident than for thick tills, may disappear in summer, related to change in topographic slope and convergence	easily observed by summer wetness and vegetation, expand and contract seasonally, related to change in topographic slope, convergence and decrease in sediment thickness
Pre-event water discharge	initially low but increases as pre-event water is displaced from soils	high but can decrease if water storage is replaced by event water	high throughout events
Event water discharge	mostly as Horton overland flow, or as saturated overland flow if soils saturate	mostly as saturated overland flow, or also as subsurface flow if storage is replaced by event water	mostly as saturated overland flow

storms and were insufficient to account for the increase in subsurface flow. Consequently, changes in hydraulic gradient were relatively unimportant for subsurface stormflow generation. These and other results show that the groundwater ridging model is inappropriate for these catchments (Chapter 7).

The increase in subsurface flow in the two catchments results from an increase in water content, specifically, the saturation of the soils (Chapter 7). Unsaturated soils have lower hydraulic conductivity that can increase substantially upon saturation. Consequently, the hydraulic conductivity of sediments that become transiently saturated during storms can transmit much more flow than when unsaturated. This process is the basis of the transmissivity feedback model which is the most appropriate model for both Harp 4-21 and Harp 3A.

Consideration of the hydrological and physical settings conducive to subsurface stormflow generation (Chapter 2) and results of field studies (Chapter 7) have contributed to the improved understanding of hydrological processes within the transmissivity feedback model. Two variations of this model were discussed: matrix flow and dual porosity flow. The dual porosity flow model was proposed as a general explanation that accounts both for the flow of pre-event water through macropores and the role of macropores in the transmissivity feedback model. In dual porosity flow, high saturated hydraulic conductivity is caused by saturation of macropores; in matrix flow, it is caused by saturation of the soil matrix. Since the dual porosity model applies to a wider range of sediment textures, it is more generally applicable provided that macropores are present (Chapter 2). The dual porosity model is most appropriate for forested soils on the Canadian Shield, but may be less appropriate for parent material below the root zone. The high hydraulic conductivity attributed to macropores in

Harp 4-21 and Harp 3A suggests that the transmissivity feedback model with dual porosity is applicable in these catchments (Chapter 7).

The role of storms on DOC

Storms contribute significantly to the total DOC export from the study catchments because storm runoff accounts for a considerable proportion of total runoff and because DOC concentrations increase with stream discharge (Chapter 8). A comparison of different methods to calculate DOC export shows that calculations can introduce errors, particularly when storms have not been sampled at appropriate times. The results emphasize the need for monitoring storms and for understanding the processes that influence DOC export during storms, a research topic that has received relatively little attention given the large amount of published research on DOC.

Study of DOC dynamics during storms in Harp 4-21 and Harp 3A revealed the geographical distribution of DOC sources and demonstrated that water flowpaths can have a large influence on DOC sources to the stream (Chapter 9). In Harp 4-21, most of the DOC originates from riparian areas as groundwater flows through shallow soil horizons before discharging to the stream. In Harp 3A, riparian sources of DOC adjacent to hillslopes are less important because riparian flowpaths do not intersect shallow soil horizons for similar durations and upslope distances as in Harp 4-21. However, DOC from wetlands is important in Harp 3A despite their small areal coverage. Results also show that DOC concentrations and transport during storms are different for wetlands and riparian areas adjacent to hillslopes.

Understanding of flowpaths in Harp 4-21 permitted the interpretation of apparently contradictory results. Isotopic and geochemical hydrograph separations indicated that most of the stream discharge originated as groundwater from the till (Chapter 4), yet DOC concentrations were lowest in the till and increased in the stream during storms (Chapter 9).

The contradiction is resolved by the discharge of till water through shallow riparian soil horizons where it acquires DOC and transports it to the stream. This result is significant because many conceptual models of stream hydrochemistry do not allow for discharge of deep groundwater through shallow soil horizons.

Implications of this study

Hydrological implications

One of the goals of this thesis has been to study streamflow generation with an emphasis on subsurface flow. Streamflow generation has been a research topic for many years within various disciplines such as forest hydrology, geomorphology, ecology and soil science. Although the field work in this study integrated methods from various disciplines, the interpretation of its results has used a predominantly hydrogeological approach where subsurface flow is concerned. This approach is not new (e.g. Sklash and Farvolden, 1979), but it has provided some new insight into and structure to the understanding of subsurface stormflow. For example, conceptual models of subsurface stormflow were summarized according to hydrogeological conditions and were related to physical and hydraulic properties of porous media (Chapter 2). The intent of this thesis has been to guide streamflow generation research towards greater consideration of hydrogeological (and soil physics) principles and processes within the development of conceptual models and the interpretations of subsurface flow.

The soil water balance emphasizes a different approach for considering subsurface stormflow generation (Chapter 6). Whereas most research has focused on water fluxes, this approach also relates runoff generation to changes in water storage. The differences in runoff generation are attributed to different capacities to store water or to the timing of water storage and drainage from the sediments. This approach is very practical because it can be used to

determine the magnitude and timing of runoff contributions at an individual location. It is anticipated that this approach will become more commonly applied with recent technological developments in measurements of soil moisture.

The fact that changes in water content were more important than changes in hydraulic gradients has implications for the methods that are used to study subsurface stormflow. Quantification of the increase in subsurface flow that results from increasing water content requires a greater focus on measurements of the unsaturated properties of sediments. Therefore, subsurface stormflow generation studies not only require the measurement of the groundwater response during storms but also of water content, the soil water retention curve, and unsaturated hydraulic conductivity. Since these properties are greatly affected by macropores, measurements must be made on undisturbed soils.

This study demonstrates that subsurface stormflow generation is not limited to areas near the stream (Chapter 6). Midslope and upslope soils can contribute rapidly to subsurface stormflow by displacing water towards the stream. The implications of this result are both methodological and conceptual. Firstly, catchments should be instrumented to assess runoff contributions from areas distant from the stream. Even in Harp 4-21, where contributions to storm runoff from upper hillslopes are less significant, measurements of soil water balances would have been useful to quantify stormflow contributions by unsaturated flow. Secondly, the concept of a variable source area is useful to consider streamflow contributions by saturated overland flow but does little to advance the understanding of the spatial and temporal contributions of subsurface stormflow. Since runoff contributions at individual sites can be measured, it is possible to define the spatial and temporal variations in the area that contributes to subsurface flow. The concept of a variable contributing area is more inclusive than a variable source area because it also includes subsurface flow.

Hydrochemical implications

Dissolved silica was a very useful tracer on the Canadian Shield because thick till had significantly higher concentrations than soils. These measurements were even more useful when combined with isotopic measurements because soil and till water contributions to stream runoff could be quantified (Chapter 4). However, it is not known whether or not similar differences in dissolved silica concentrations are observed in other catchments and if they are only found within thick till. If so, stream surveys of dissolved silica during baseflow conditions could also be used to identify catchments where till is hydrologically important.

Since silicate weathering is an important source of alkalinity where carbonates are absent (Dankevych, 1989), groundwater flow through the till provides alkalinity to the stream in an environment where alkalinities are low. Consequently, catchments with thick till, such as Harp 4-21, are more capable of buffering acidic deposition than those with thin till, such as Harp 3A and PC-108. Although sediment thickness is only one of many factors that influences alkalinity, the regional distributions of till thickness may help explain some of the wide differences in alkalinity between streams and lakes within the Canadian Shield. The decrease in dissolved silica concentrations in Harp 4-21 during spring snowmelt indicates that the relative contribution of till water to the stream decreases, probably as a result of increased subsurface flow through the soils and flushing of till water from them. Therefore, stream alkalinity (and other hydrochemical fluxes) in Harp 4-21 may not only be dependent on subsurface flowpaths but also on the flushing of till water from soils near the stream.

The value of combining hydrometric, isotopic and geochemical data in streamflow generation studies has been demonstrated in this thesis. High silica concentrations during storms could have been interpreted as large increases in subsurface flow from the till, whereas the hydrometric data showed that such increases were not possible and led to the interpretation

that till water was being rapidly displaced from soils (Chapter 4). The combined data helped define flowpaths in a way that neither tracers nor hydrometric monitoring would have shown individually.

The implications of the transmissivity feedback model on subsurface flowpaths, water mixing and hydrochemistry have not been thoroughly considered. For example, how does water that flows in the transiently saturated zone mix with water in deeper horizons? The answer to this question would be very important for the buffering of acidic precipitation that infiltrates the soil. Alternatively, what does this model imply about the spatial distribution and temporal variations of natural tracers such as ^{18}O within a soil? Many important questions such as these have yet to be addressed fully but have important implications for the interpretations of hydrochemical processes and tracers. One obvious implication of the model is that hydrological flowpaths are very closely related to groundwater levels and hydrological conditions. Therefore, changes in hydrological conditions, such as those related to climate change, could also change water flowpaths and catchment hydrochemistry. The differences between matrix and dual porosity flow in the transmissivity feedback model may also result in different mixing processes and water flowpaths. The implications of this model on hydrological flowpaths, mixing and hydrochemical output of hillslopes require more detailed study.

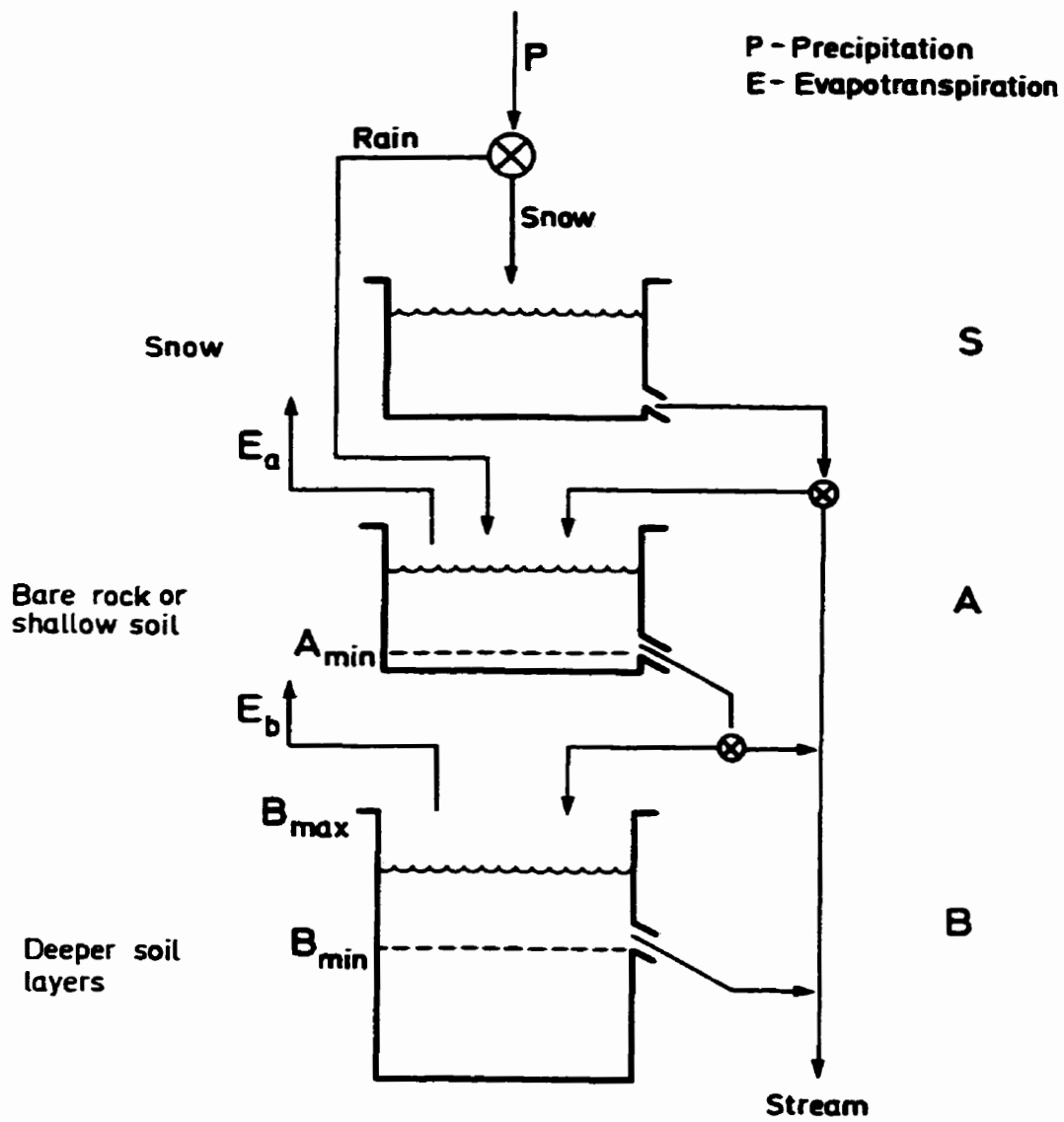
Modelling implications

Mathematical models either implicitly or explicitly incorporate a conceptual model. Mathematical models, like conceptual models, are simplified representations of reality. The value of models depends, in part, on whether or not the simplifications are appropriate. For conceptual models, the simplification often involves the inclusion of only the significant hydrological processes. Much of the study of streamflow generation has been devoted to

determining which processes are most significant for individual catchments. Although studies such as this one can determine which processes and models are most appropriate in a few catchments that have been carefully instrumented and monitored, more widespread application of conceptual or mathematical models requires the identification of possible processes in other catchments. Classification and description of conceptual models according to the hydrological processes and physical environments in Chapter 2 is one step towards making the knowledge that is gained in individual watersheds more widely applicable. One goal of such generalizations is to be able to determine the important hydrological processes in a catchment from the measurement of a minimal amount of physical, hydrological, and hydrochemical data.

Mathematical models of hydrological processes in catchments vary greatly in complexity. Very simple empirical models that treat hydrological flowpaths within a catchment as vertical flow through hydrological reservoirs have been commonly used for modelling the effects of acidic deposition (e.g. Christophersen and Wright, 1981). Such a model was used to predict discharge and sulphate concentrations in the Harp 4 catchment (Figure 10.1, Seip et al., 1985). The results of this thesis can be used to consider some of the simplifications of the hydrological component of this model. The spatial differences in the water table profiles along the stream and the variations in the spatial patterns of runoff production (Chapter 3) suggest that spatially distributed models may be more appropriate than the lumped model shown in Figure 10.1. Even given its simplified nature, this mathematical model is based on a faulty conceptual model. It is apparent that this model cannot represent the observed flowpaths in Harp 4-21 where deep groundwaters (or deep soil layers in this case) discharge through shallow soil horizons before reaching the stream. This hydrological model would not be able to reconcile the isotopic and dissolved silica

Figure 10.1 Hydrological reservoir model (Seip et al., 1985).



concentration data (Chapter 4) with the DOC results (Chapter 9). This example demonstrates the importance of having valid conceptual models in the design of mathematical models.

More recent hydrogeochemical models attempt to incorporate the effects of DOC (Hornberger et al., 1994) and nitrogen flushing (Creed et al., 1996). Although these models incorporate the spatially variable nature of runoff production through the use of TOPMODEL (Beven and Kirkby, 1979), they are also based on a simple conceptual model of hydrological flowpaths. Consequently, interpretations of hydrochemical results could be inappropriate if the hydrological flowpaths of the model are not validated. For example, it may be possible to develop a credible model of DOC in Harp 4-21 based a simple model such as in Figure 10.1. Such a model would emphasize shallow flowpaths that deliver high DOC water to the stream during storms. If other water chemistry data or hydrometric data had not been collected, it would likely not have been possible to recognize the contribution of deeper, high silica and alkalinity groundwater to the stream during storms. Therefore, it is important to collect various types of data that will help constrain and validate hydrological flowpaths.

Slightly more complex mathematical models account for the spatially variable nature of runoff generation (e.g. TOPMODEL, Beven and Kirkby, 1979). However, these models rely on the surface topography as an indicator of subsurface flow. As demonstrated in Chapter 3, this assumption may not be valid in catchments with thick sediments in which groundwater flowpaths are not always perpendicular to topographic contours. In addition, in catchments with thin sediments, bedrock topography may be a more accurate representation of subsurface flow directions (McDonnell et al., 1996).

Even when more complex deterministic mathematical models are used, it is not always possible to incorporate all the hydrological processes of the different conceptual models that are described in Chapter 2. Some of the differences between conceptual models simply

represent different catchment properties and can be incorporated within the input parameters of numerical models. However, some conceptual models, such as those involving macropore flow, may require different numerical models or specific formulations of input parameters. The results of this study suggest that modelling of both the unsaturated and saturated zones in catchments is essential if increased water contents cause the increase in subsurface flow. The results also suggest that dual porosity flow may be an important hydrological process and should also be incorporated into mathematical models of subsurface stormflow as described in Chapter 7.

Ecological implications

Groundwater flow through thick glacial till can have important biological and ecological implications. During extended periods of drought, it provides baseflow to streams which may be refuges for aquatic organisms that require perennial flow. Many streams on the Canadian Shield are intermittent because hillslopes cannot provide baseflow throughout the year. Groundwater discharge not only provides flowing water conditions but may also provide alkalinity, nutrients or proper temperature conditions for some aquatic species (e.g. Curry, 1993; Curry and Noakes, 1995).

The most important ecological role of groundwater discharge may be in the maintenance of water levels in wetlands during the summer. Devito et al. (1996) found higher summer water levels in a wetland where upland catchments supplied perennial baseflow input (Harp 4) than in a wetland within a catchment where upland streams were ephemeral (Plastic Lake, PC1). Water levels in wetlands are very important ecologically and biogeochemically because they largely control the redox conditions that influence the transformation of elements within wetlands and their export (Devito and Dillon, 1993; Devito et al., 1996).

The DOC budgets that were presented in Chapter 8 demonstrate the importance of storms to the DOC export from catchments. The methodological implication of this result is that studies with annual DOC budgets should include careful evaluation both of sampling frequency and timing with respect to changes in stream discharge, and of methods to calculate stream DOC budgets. For some such studies, it may be wise to consider intensive sampling of some storms in different seasons to quantify possible errors in annual DOC budgets.

A potentially more significant implication of large DOC exports during storms is that the sources and processes that influence DOC may not be the same during storms as during baseflow conditions (Chapter 9). Interpretation of data that are collected predominantly during baseflow conditions may preclude the identification of processes that occur only during storms. Furthermore, the recognition of the importance of storm periods may lead to better interpretation of processes or sources that previously may not have been considered fully.

Research opportunities

Several ideas for additional research have emerged from both the interpretation of results from this thesis and the summary of existing research. This section presents these ideas with the intent to stimulate further development and research.

Additional testing of hydrological processes

Although conceptual models of subsurface flow incorporate several hydrological processes (Chapter 2), these processes and some of their hydrochemical implications are not fully understood. These processes should be tested under carefully controlled conditions both in the laboratory and in small field experiments. The experiments of Abdul and Gillham (1984, 1989) and Gillham (1984) are very good examples of this approach to test the groundwater ridging hypothesis and the capillary fringe effect. A similar approach is required

for testing other hydrological processes, particularly those of the transmissivity feedback model, that are associated with increasing subsurface flow in transiently saturated sediments. The interactions between the soil matrix and macropores under both negative and positive pressure heads also require further experimental study. The comparison of flow through sediments without macropores, sediments with a single continuous macropore, and sediments with a single discontinuous macropore in the column experiment of Buttle and Leigh (1997), is another good example of the necessary research to better understand flow processes.

There is also a need to verify the physical and hydrological properties appropriate for various models. The assessment of these properties in Chapter 2 was based predominantly on the theoretical understanding of processes but these properties remain to be verified under controlled field or laboratory conditions.

Field studies

The identification of hydrological processes is not sufficient to explain the hydrological and hydrochemical responses of catchments. It is also necessary to determine how these processes change temporally and spatially during storms. This thesis has placed great emphasis on the examination of spatial differences in hydrological responses. This approach subdivides larger catchments into smaller areas where it is easier to relate hydrological responses to physical properties or hydrological conditions. Furthermore, it is possible to integrate individual responses for smaller areas into a larger catchment response.

The spatial and temporal pattern of subsurface flow generation within a catchment can be measured by the same approach. Soil water balances can be used to determine the timing and magnitude of runoff generation at a given location (Chapter 6). With a sufficient number of sites and frequency of sampling, it would be possible to account for the spatial distribution of stored water within a catchment at several times during a storm. Since the distribution of

water storage would be known, these data implicitly include the net flow rates throughout the catchment. When interpreted in conjunction with other data, such as water table elevations, saturated and unsaturated hydraulic conductivity and hydrochemistry, the hydrological processes can be identified.

Since the fieldwork for this thesis was completed, there have been substantial improvements in the availability and cost of automated soil moisture measurement by TDR. It is possible to measure or estimate automatically all the components of the water balances (including evapotranspiration) in Chapter 6. Although the cost of full automation may still be prohibitive for some studies, automated measurements of water levels, pressure head (tension) and soil moisture at a few sites could provide better temporal resolution and measurements for a greater number of storms over a wide range of hydrological conditions (Baker and Allmaras, 1990; Heimovaara and Bouten, 1990).

Numerical models

One beneficial use of numerical models for streamflow generation research would be to test various conceptual models and determine if they can generate significant fluxes of subsurface water, given realistic estimates of hydraulic parameters. One of the important results of this study is that subsurface flow is attributed to an increase in hydraulic conductivity upon saturation of macroporous soils. Durner's (1994) estimation of the hydraulic conductivity function for soils with heterogeneous pore structure could be used to assess the possible significance of the transmissivity feedback model with dual porosity flow (Chapter 7).

One objective of this thesis was to relate streamflow generation processes to measurable physical or hydrological factors. Although this was done qualitatively with respect to conceptual models of subsurface stormflow generation (Chapter 2), there was no

quantitative attempt to determine the relative importance of different factors, such as soil moisture retention curves. An effective way to consider the quantitative importance of any individual factor is by numerical modelling in which each parameter can be varied independently. Freeze (1972b) used this approach to assess the importance of saturated hydraulic conductivity, soil thickness, topographic slope, slope shape, rainfall intensity and duration. Freeze (1972b, p. 1277) recognized that:

variations in the shape of the characteristic curves for the hillside soils would undoubtedly influence outflow hydrographs, but an analysis of the effect does not seem warranted until more measured curves from near-surface samples are available.

Given that such data are currently available, and mathematical models for the bulk hydraulic properties of soils with heterogeneous pore structures have been developed (Durner, 1994), new simulations are warranted. Their results can be used to assess the potential significance of soil texture and macropores to subsurface stormflow generation.

Processes that affect DOC during storms

This study has shown that, during storms, DOC export is important and DOC sources to stream discharge may vary (Chapters 8 and 9). Given the ecological significance of DOC and the relative lack of studies that focus specifically on DOC during storms, it is clear that additional research is warranted. Since much is already known about the processes that transform organic carbon, a review of the most important processes that may affect DOC during storms is required first. Then, the relative importance of these processes can be evaluated either in simple field experiments or from storm data. Since DOC is very dependent on water flowpaths, such studies should be undertaken in catchments where water flowpaths can be controlled or are well defined.

Summary

This study has investigated and provided insight into the hydrological processes that contribute subsurface flow to storm runoff in two small catchments on the Canadian Shield. These results have several implications for streamflow generation both on the Canadian Shield and in other environments. Although much has been learned about subsurface stormflow, there remain many opportunities for additional research. Both a collaborative approach that integrates several disciplines within and outside hydrology, and an integrated approach that includes modelling, laboratory and field studies will provide the greatest insight into hydrological and hydrochemical processes within watersheds.

References

- Abdul, A. S. and Gillham, R. W., 1984. Laboratory studies of the effects of the capillary fringe on streamflow generation. *Water Resour. Res.*, 20 (6), 691-698.
- Abdul, A. S. and Gillham, R. W., 1989. Field studies of the effects of the capillary fringe on streamflow generation. *J. Hydrol.*, 112, 1-18.
- Agriculture Canada Expert Committee on Soil Survey, 1987. *The Canadian System of Soil Classification*. Agriculture Canada Publication 1646, Supply and Services, Canada, Ottawa, Ont., 2nd Ed.
- Allan, C. J. and Roulet, N. T., 1994. Runoff generation in zero-order Precambrian Shield catchments: the stormflow response of a heterogeneous landscape. *Hydrol. Proces.*, 8, 369-388.
- Amerman, C. R., 1965. The use of unit-source watershed data for runoff prediction. *Water Resour. Res.*, 1, 499-508.
- Anderson, M. G. and Burt, T. P., 1978. Toward more detailed field monitoring of variable source areas. *Water Resour. Res.*, 14 (6), 1123-1131.
- Anderson, M. G. and Burt, T. P., 1978. The role of topography in controlling throughflow generation. *Earth Surf. Proc.*, 3, 331-344.
- Aravena, R., Schiff, S. L., Trumbore, S. E., Dillon, P. J. and Elgood, R., 1992. Evaluating dissolved inorganic carbon cycling in a forested lake watershed using carbon isotopes. *Radiocarbon*, 34 (3), 636-645.
- Baker, J. M. and Allmaras, R. R., 1990. System for automating and multiplexing soil moisture measurement by time domain reflectometry. *Soil Sci. Soc. Am. J.*, 54, 1-6.
- Baker, J. M. and Lascano, R. J., 1989. The spatial sensitivity of time-domain reflectometry. *Soil Sci.*, 147 (5), 378-383.

- Barry, P.J., 1975. *Hydrological studies on a small basin on the Canadian Shield, A final summary of the Perch Lake Evaporation Study 1965-1974*. Atomic Energy of Canada Limited, Chalk River, Ont.
- Bear, J., 1972. *Dynamics of fluids in porous media*. Dover Publications Inc., New York, NY.
- Beven, K. J., 1978. The hydrological response of headwater and sideslope areas. *Hydrol. Sci. Bull.*, 23 (4), 419-437.
- Beven, K. J. and Germann, P., 1981. Water flow in soil macropores II. A combined flow model. *J. Soil Sci.*, 32, 15-29.
- Beven, K. J. and Germann, P., 1982. Macropores and water flow in soils. *Water Resour. Res.*, 18 (5), 1311-1325.
- Beven, K. J. and Kirkby, M. J., 1979. A physically based, variable contributing area model of basin hydrology. *Hydrol. Sci. Bull.*, 24 (1), 42-69.
- Bishop, K.H., 1991. *Episodic increases in stream acidity, catchment flow pathways and hydrograph separation*. Ph.D. thesis, University of Cambridge, Cambridge, England.
- Blowes, D. W. and Gillham, R. W., 1988. The generation and quality of streamflow on inactive uranium tailings near Elliot Lake, Ontario. *J. Hydrol.*, 97, 1-22.
- Bonnell, M., 1993. Progress in the understanding of runoff generation in forests. *J. Hydrol.*, 150, 217-275.
- Bonnell, M., 1998. Selected challenges in runoff generation research in forests from the hillslope to headwater drainage basin scale. *J. Am. Wat. Res. Assoc.*, 34, 765-785.
- Bosch, J. M. and Hewlett, J. D., 1982. A review of catchment experiments to determine the effect of vegetation changes on water yield and evapotranspiration. *J. Hydrol.*, 55, 3-23.
- Bottomley, D. J., Craig, D. and Johnston, L. M., 1984. Neutralization of acid runoff by groundwater discharge to streams in Canadian Precambrian Shield watersheds. *J. Hydrol.*, 75, 1-26.

- Bottomley, D. J., Craig, D. and Johnston, L. M., 1986. Oxygen-18 studies of snowmelt runoff in a small Precambrian shield watershed: implications for streamwater acidification in acid-sensitive terrain. *J. Hydrol.*, 88, 213-234.
- Boyer, E. W., Homberger, G. M., Bencala, K. E. and McKnight, D. M., 1996. Overview of a simple model describing variation of dissolved organic carbon in an upland catchment. *Ecol. Model.*, 86, 183-188.
- Brown, I.C., 1976. Groundwater geology. In: *Geology and economic minerals of Canada*. Douglas, R.J.W. (Ed.), Geological Survey of Canada, Economic geology report No. 1, Ottawa, Ont., p.765-791.
- Bruce, J.P. and Clark, R.H., 1966. *Introduction to hydrometeorology*. Pergammon Press, Toronto, Ont..
- Brunke, M. and Gosner, T., 1997. The ecological significance of exchange processes between rivers and groundwater. *Fresh. Biol.*, 37, 1-33.
- Buttle, J. M., 1994. Isotope hydrograph separations and rapid delivery of pre-event water from drainage basins. *Progress Phys. Geog.*, 18, 16-41.
- Buttle, J. M. and Leigh, D. G., 1997. The influence of artificial macropores on water and solute transport in laboratory soil columns. *J. Hydrol.*, 191, 290-314.
- Buttle, J. M. and Sami, K., 1992. Testing the groundwater ridging hypothesis of streamflow generation during snowmelt in a forested catchment. *J. Hydrol.*, 135, 53-72.
- Carson, R., 1962. *Silent Spring*. Houghton-Mifflin Company, Boston, MA.
- Chapman, L.J., 1975. *The physiography of the Georgian Bay-Ottawa Valley area*. Ontario Division of Mines Geoscience Report 128, Toronto, Ontario.
- Cherry, J.A., Jackson, R.E., McNaughton, D.C., Pikers, J.F. and Woldetensae, H., 1975. Physical hydrogeology of the lower Perch Lake basin. In: *Hydrological studies on a small basin on the Canadian Shield*. Barry, P.J. (Ed.), Atomic Energy of Canada Limited, Chalk River, Ont., p.625-682.

- Chorley, R.J., 1978. The hillslope hydrological cycle. In: *Hillslope hydrology*. Kirkby, M.J. (Ed.), John Wiley & Sons, New York, NY, p.1-42.
- Christophersen, N., Seip, H. M. and Wright, R. F., 1982. A model for streamwater chemistry at Birkenes, Norway. *Water Resour. Res.*, 18 (4), 977-996.
- Christophersen, N. and Wright, R. F., 1981. Sulfate budget and a model for sulfate concentrations in stream water at Birkenes, a small forested catchment in southernmost Norway. *Water Resour. Res.*, 17 (2), 377-389.
- Creed, I. F., Band, L. E., Foster, N. W., Morrison, I. K., Nicolson, J. A., Semkin, R. S. and Jeffries, D. S., 1996. Regulation of nitrate-N from temperate forests: a test of the N flushing hypothesis. *Water Resour. Res.*, 32, 3337-3354.
- Cronan, C.S., 1990. Patterns of organic acid transport from forested watersheds to aquatic ecosystems. In: *Organic acids in aquatic environments*. Perdue, E.M. and Gjessing, E.T. (Eds.), John Wiley & Sons, London, p.245-260.
- Curry, R.A., 1993. *Hydrogeology of brook charr (Salvelinus fontinalis) spawning and incubation habitats: linking aquatic and terrestrial ecosystems*. Ph.D. thesis, University of Guelph, Guelph, Ont..
- Curry, R. A. and Noakes, L. G., 1995. Groundwater and the selection of spawning sites by brook trout (*Salvelinus fontinalis*). *Can. J. Fish. Aqu. Sci.*, 52, 1733-1740.
- Dankevy, S.N., 1989. *Groundwater flow and chemistry in a small acid-stressed sub-catchment of the Canadian Shield*. Master's Project, University of Waterloo, Waterloo, Ont.
- Dann, M. S., Lynch, J. A. and Corbett, E. S., 1986. Comparison of methods for estimating sulfate export from a forested watershed. *J. Environ. Qual.*, 15 (2), 140-145.
- Dawson, H. J., Ugolini, F. C., Hrutfiord, B. F. and Zachara, J., 1978. Role of soluble organics in the soil process of a Podzol, Central Cascades, Washington. *Soil Sci.*, 126, 290-296.

- Devito, K. J. and Dillon, P. J., 1993. The influence of hydrologic conditions and peat oxia on the phosphorous and nitrogen dynamics of a conifer swamp. *Water Resour. Res.*, 29 (8), 2675-2685.
- Devito, K. J., Dillon, P. J. and LaZerte, B. D., 1989. Phosphorous and nitrogen retention in five Precambrian shield wetlands. *Biogeochem.*, 8, 185-204.
- Devito, K. J., Hill, A. R. and Roulet, N., 1996. Groundwater-surface water interactions in headwater forested wetlands of the Canadian Shield. *J. Hydrol.*, 181, 127-147.
- DeWalle, D. R., Swistock, B. R. and Sharpe, W. E., 1988. Three-component tracer model for stormflow on a small Appalachian forested catchment. *J. Hydrol.*, 104, 301-310.
- Dillon, P. J., Jeffries, D. S. and Scheider, W. A., 1982. The use of calibrated lakes and watersheds for estimating atmospheric deposition near a large point source. *Water Air Soil Poll.*, 18, 241-258.
- Dillon, P. J., Lulis, M., Reid, R. A. and Yap, D., 1988. Ten-year trends in sulphate, nitrate and hydrogen deposition in central Ontario. *Atmos. Environ.*, 22 (5), 901-905.
- Dillon, P. J. and Molot, L. A., 1997. Dissolved organic and inorganic carbon mass balances in central Ontario lakes. *Biogeochem.*, 36, 29-42.
- Dillon, P. J., Molot, L. A. and Scheider, W. A., 1991. Phosphorous and nitrogen export from forested stream catchments in Central Ontario. *J. Environ. Qual.*, 20 (4), 857-864.
- Dillon, P. J., Reid, R. A. and deGrosbois, E., 1987. The rate of acidification of aquatic ecosystems in Ontario, Canada. *Nature*, 329, 45-48.
- Dinçer, T., Payne, B. R. and Florkowski, T., 1970. Snowmelt runoff from measurements of tritium and oxygen-18. *Water Resour. Res.*, 6 (1), 110-124.
- Domenico, P.A. and Schwartz, F.W., 1990. *Physical and chemical hydrogeology*. John Wiley & Sons, New York, NY.
- Dosskey, M. G. and Bertsch, P. M., 1994. Forest sources and pathways of organic matter transport to a blackwater stream: a hydrological approach. *Biogeochem.*, 24, 1-19.

- Driscoll, C. T., Fuller, R. D. and Schecher, W. D., 1989. The role of organic acids in the acidification of surface waters in the eastern U.S. *Water Air Soil Poll.*, 43, 21-40.
- Dunne, T., 1978. Field studies of hillslope flow processes. In: *Hillslope hydrology*. Kirkby, M.J. (Ed.), John Wiley & Sons, New York, NY, p.227-293.
- Dunne, T. and Black, R. D., 1970. Partial area contributions to storm runoff in a small New England watershed. *Water Resour. Res.*, 6 (5), 1296-1311.
- Dunne, T. and Black, R. D., 1970. An experimental investigation of runoff production in permeable soils. *Water Resour. Res.*, 6 (2), 478-490.
- Dunne, T., Moore, T. R. and Taylor, C. H., 1975. Recognition and prediction of runoff-producing zones in humid regions. *Hydrol. Sci. Bull.*, 20, 305-327.
- Durner, W., 1994. Hydraulic conductivity estimation for soils with heterogeneous pore structure. *Water Resour. Res.*, 30 (2), 211-223.
- Easthouse, K. B., Mulder, J., Christophersen, N. and Seip, H. M., 1992. Dissolved organic carbon fractions in soil and stream water during variable hydrological conditions at Birkenes, South Norway. *Water Resour. Res.*, 28 (6), 1585-1596.
- Eckhardt, B. W. and Moore, T. R., 1990. Controls on dissolved organic carbon concentrations in stream, southern Quebec. *Can. J. Fish. Aqu. Sci.*, 47, 1537-1544.
- Eshleman, K. N. and Hemond, H. F., 1985. The role of organic acids in the acid-base status of surface waters at Bickford watershed, Massachusetts. *Water Resour. Res.*, 21 (10), 1503-1510.
- Espeby, B., 1989. *Water flow in a forested till slope*. Ph.D. thesis, Dept. of Land and Water Resources, R. Inst. of Technol., Stockholm, Sweden.
- Farvolden, R.N., Pfannkuch, O., Pearson, R. and Fritz, P., 1988. Precambrian Shield. In: *Hydrogeology, The Decada of North American Geology*. Back, W., Rosenshein, J.S. and Seaber, P.R. (Eds.), The Geological Society of North America, Boulder, CO, p.101-114.

- Fiebig, D. M., 1995. Groundwater discharge and its contribution of dissolved organic carbon to an upland stream. *Arch. Hydrobiol.*, 134, 129-155.
- Fiebig, D. M., Lock, M. A. and Neal, C., 1990. Soil water in the riparian zone as a source of carbon for a headwater stream. *J. Hydrol.*, 116, 217-237.
- Ford, T. E. and Naiman, R. J., 1989. Groundwater-surface water relationships in boreal forest watersheds: dissolved organic carbon and inorganic nutrient dynamics. *Can. J. Fish. Aqu. Sci.*, 46, 41-49.
- Freeze, R. A., 1972. Role of subsurface flow in generating surface runoff 1. Base flow contributions to channel flow. *Water Resour. Res.*, 8 (3), 609-623.
- Freeze, R. A., 1972. Role of subsurface flow in generating surface runoff 2. Upstream source areas. *Water Resour. Res.*, 8 (5), 1272-1283.
- Freeze, R. A., 1974. Streamflow generation. *Rev. Geophys.*, 12 (4), 627-647.
- Freeze, R.A. and Cherry, J.A., 1979. *Groundwater*. Prentice Hall, Englewood Cliffs, NJ.
- Freeze, R. A. and Whitherspoon, P. A., 1967. Theoretical analysis of regional groundwater flow: 2. Effect of water-table configuration and subsurface permeability variation. *Water Resour. Res.*, 3, 623-634.
- Fritz, P., Cherry, J.A., Weyer, K.U. and Sklash, M., 1976. Storm runoff analyses using environmental isotopes and major ions. In: *Interpretation of environmental isotopes and hydrochemical data in groundwater hydrology*. IAEA-STI/PUB/429. International Atomic Energy Agency, Vienna, p.111-130.
- Gardner, W. R., Hillel, D. and Benyamini, Y., 1970. Post irrigation movement of soil water: I Redistribution. *Water Resour. Res.*, 6, 851-861.
- Gates, W.L., Mitchell, J.F.B., Boer, G.J., Cubasch, U. and Meleshko, V.P., 1992. Climate modelling, climate prediction and model validation. In: *Climate change 1992. The supplementary report to the IPCC scientific assessment*. Houghton, J.T., Callander, B.A. and Varney, S.K. (Eds.), Cambridge University Press, Cambridge, p.97-134.

- Gerber, R. E. and Howard, K. W. F., 1996. Evidence for recent groundwater flow through late Wisconsinan till near Toronto, Ontario. *Can. Geotech. J.*, 33, 538-555.
- Gerke, H. H. and van Genuchten, M. T., 1993. Evaluation of a first-order water transfer term for variably saturated dual-porosity flow models. *Water Resour. Res.*, 29 (4), 1225-1238.
- Gerke, H. H. and van Genuchten, M. T., 1993. A dual-porosity model for simulating the preferential movement of water and solutes in a structured porous media. *Water Resour. Res.*, 29 (2), 305-319.
- Germann, P. and Beven, K. J., 1981. Water flow in soil macropores I. An experimental approach. *J. Soil Sci.*, 32, 1-13.
- Gherini, S. A., Mok, L., Hudson, R. J. M., Davis, G. F., Chen, C. W. and Goldstein, R. A., 1985. The ILWAS model: formulation and application. *Water Air Soil Poll.*, 26, 425-459.
- Gillham, R. W., 1984. The capillary fringe and its effect on water-table response. *J. Hydrol.*, 67, 307-324.
- Goodrich, D. C. and Woolhiser, D. A., 1991. Catchment hydrology. *Rev. Geophys.*, Supplement, 202-209.
- Grieve, I. C., 1997. Concentrations and annual loading of dissolved organic matter in a small moorland stream. *Fresh. Biol.*, 14, 533-537.
- Harr, R. D., 1978. Water flux in soil and subsoil on a steep forested slope. *J. Hydrol.*, 33, 37-58.
- Heath, R.C, 1988. Hydrogeological setting of regions. In: *Hydrogeology, The Decade of North American Geology*. Back, W., Rosenshein, J.S. and Seaber, P.R. (Eds.), The Geological Society of North America, Boulder, CO, p.15-24.
- Heimovaara, T. J. and Bouten, W., 1990. A computer -controlled 36-channel time domain reflectometry system for monitoring soil water contents . *Water Resour. Res.*, 27, 857-864.
- Helvey, J. D. and Patric, J. H., 1965. Canopy and litter interception of rainfall by hardwoods of eastern United States. *Water Resour. Res.*, 1 (2), 193-206.

- Hemond, H.F., 1990. Wetlands as the source of dissolved organic carbon to surface waters. In: *Organic acids in aquatic ecosystems*. Perdue, E.M. and Gjessing, E.T. (Eds.), John Wiley & Sons, London, p.301-313.
- Hendershot, W. H., Savoie, S. and Courchesne, F., 1992. Simulation of stream-water chemistry with soil solution and groundwater flow contributions. *J. Hydrol.*, 136, 237-252.
- Hewlett, J.D. and Hibbert, A.R., 1967. Factors affecting the response of small watersheds to precipitation in humid areas. In: *Forest hydrology*. Proc. Intern. Symp. on Forest Hydrol., Penn State, August, 1965. Pergammon Press, NY, p.275-290.
- Hill, A. R. and Waddington, J. M., 1993. Analysis of storm run-off sources using oxygen-18 in a headwater swamp. *Hydrol. Proces.*, 7, 305-316.
- Hillel, D., 1971. *Soil and Water: Physical principles and processes*. Academic Press, New York, NY.
- Hinton, M. J., Schiff, S. L. and English, M. C., 1993. Physical properties governing groundwater flow in a glacial till catchment. *J. Hydrol.*, 142, 229-249.
- Hinton, M. J., Schiff, S. L. and English, M. C., 1994. Examining the contributions of glacial till water to storm runoff using two- and three-component hydrograph separations. *Water Resour. Res.*, 30 (4), 983-993.
- Hinton, M. J., Schiff, S. L. and English, M. C., 1997. The significance of storms for the concentration and export of dissolved organic carbon from two Precambrian Shield catchments. *Biogeochem.*, 36, 67-88.
- Hinton, M. J., Schiff, S. L. and English, M. C., 1998. Sources and flowpaths of dissolved organic carbon during storms in two forested watersheds of the Precambrian Shield. *Biogeochem.*, 41, 175-197.
- Hooper, R. P. and Shoemaker, C. A., 1986. A comparison of chemical and isotopic hydrograph separation. *Water Resour. Res.*, 22 (10), 1444-1454.

- Hornberger, G. M., Bencala, K. E. and McKnight, D. M., 1994. Hydrological controls on dissolved organic carbon during snowmelt in the Snake River near Montezuma, Colorado. *Biogeochem.*, 25, 147-165.
- Horton, J.H and Hawkins, R.H., 1964. *The importance of capillary pores in rainwater percolation to the groundwater table*. E.I. du Pont de Nemours and Co., Savannah River Plant, DPSPU 64-30-12.
- Horton, R. E., 1933. The role of infiltration in the hydrological cycle. *Trans. Am. Geophys. Union*, 14, 446-460.
- House, D.A., 1996. *The spatial distribution of infiltration in a forested basin and the role of macropores*. B.Sc. thesis, Trent University, Peterborough, Ontario.
- Hursh, C. R., 1944. Subsurface-flow. *Trans. Am. Geophys. Union*, 743-746.
- Hursh, C. R. and Brater, E. F., 1941. Separating storm-hydrographs from small drainage-areas into surface- and subsurface-flow. *Trans. Am. Geophys. Union*, 863-871.
- Hvorslev, M.J., 1951. *Time lag and soil permeability in groundwater observations*. US Army Corps of Engineers, Waterways Experimental Station, Bull. 36, Vicksburg, MS.
- IPCC, 1990. *Climate change, the IPCC scientific assessment*. Cambridge University Press, UK.
- Jardine, P. M., Weber, N. L. and McCarthy, J. F., 1989. Mechanisms of dissolved organic carbon adsorption on soil. *Soil Sci. Soc. Am. J.*, 53, 1378-1385.
- Jardine, P. M., Wilson, G. V., McCarthy, J. F., Luxmoore, R. J., Taylor, D. L. and Zelazny, L. W., 1990. Hydrogeochemical processes controlling the transport of dissolved organic carbon through a forested catchment. *J. Contam. Hydrol.*, 6, 3-19.
- Jeffries, D.S. and Snyder, W.R., 1983. *Geology and geochemistry of the Muskoka-Haliburton study area. Data Report DR 83/2*. Dorset Research Centre, Dorset, Ont..
- Johnson, A. H., 1979. Estimating solute transport in streams from grab samples. *Water Resour. Res.*, 15 (5), 1224-1228.

- Kaplan, L.A. and Newbold, J.D., 1993. Biogeochemistry of dissolved organic carbon entering streams. In: *Aquatic microbiology: an ecological approach*. Ford, T.E. (Ed.), Blackwell Scientific Publications, Oxford, p.139-165.
- Karrow, P.F., 1979. The texture, mineralogy and petrology of North American tills. In: *Glacial till: an interdisciplinary study*, Legget, R.F. (Ed.), The Royal Society of Canada Spec. Publ. Ser., vol. 12. , Ottawa, Ont.,
- Keller, C. K., van der Kamp, G. and Cherry, J. A., 1988. Hydrogeology of two Saskatchewan tills; I, Fractures, bulk permeability, and spatial variability of downward flow. *J. Hydrol.*, 101, 97-121.
- Kennedy, V. C., 1971. Silica variation in stream water with time and discharge. *Adv. Chem. Ser.*, 106, 94-130.
- Kirkby, M.J., 1978. *Hillslope Hydrology*. John Wiley & Sons, New York, NY.
- Kirkby, M. J. and Chorley, R. J., 1967. Throughflow, overland flow and erosion. *Bull. Int. Assoc. Sci. Hydrol.*, 12, 5-21.
- Kramer, J.R., Brassard, P., Collins, P., Clair, T.A. and Takats, P., 1990. Variability of organic acids in watersheds. In: *Organic acids in aquatic ecosystems*. Perdue, E.M. and Gjessing, E.T. (Eds.), John Wiley & Sons, London, p.127-139.
- Kung, K-J. S., 1990a. Preferential flow in a sandy vadose zone: 1. Field observation. *Geoderma*, 46, 51-58.
- Kung, K-J. S., 1990b. Preferential flow in a sandy vadose zone: 2. Mechanisms and implications. *Geoderma*, 46, 59-71.
- LaZerte, B. D. and Dillon, P. J., 1984. Relative importance of anthropogenic versus natural sources of acidity in lakes and streams of central Ontario. *Can. J. Fish. Aqu. Sci.*, 41 (11), 1664-1677.
- LaZerte, B. D. and Scott, L., 1996. Soil water leachate from two forested catchments on the Precambrian Shield, Ontario. *Can. J. For. Res.*, 26, 1353-1365.

- Likens, G.E., Bormann, H., Pierce, R.S., Eaton, J.S. and Johnson, N.M., 1977. *Biogeochemistry of a forested ecosystem*. Springer, New York, NY.
- Lozano, F.C., Parton, W.J., Lau, J.K.H. and Vanderstar, L., 1987. *Physical and chemical properties of the soils at the southern biogeochemical study site*. . MOE BGC Rep. Ser., BGC-018, Faculty of Forestry, University of Toronto, Ont..
- Lundin, L., 1982. *Soil moisture and ground water in till soil and the significance of soil type for runoff*. Division of Hydrology, Dept. of Physical Geography, Uppsala University, UNGI Report No. 56.
- MacLean, R.A., 1992. *The role of the vadose zone in the generation of runoff from a headwater basin in the Canadian Shield*. M.Sc. Thesis. Wilfrid Laurier University, Waterloo, Ont.
- MacLean, R. A., English, M. C. and Schiff, S. L., 1995. Hydrological and hydrochemical response of a small Canadian Shield catchment to late winter rain-on-snow events. *Hydrol. Proces.*, 9, 845-863.
- Mann, C. J. and Wetzel, R. G., 1995. Dissolved organic carbon and its utilization in a riverine wetland ecosystem. *Biogeochem.*, 31, 99-120.
- Maule, C. P. and Stein, J., 1990. Hydrologic flow path definition and partitioning of spring meltwater. *Water Resour. Res.*, 26 (12), 2959-2970.
- McDonnell, J. J., 1990. A rationale for old water discharge through macropores in a steep, humid catchment. *Water Resour. Res.*, 26 (11), 2821-2832.
- McDonnell, J. J., Bonnell, M., Stewart, M. K. and Pearce, A. J., 1990. Deuterium variations in storm rainfall: implications for stream hydrograph separations. *Water Resour. Res.*, 26 (3), 455-458.
- McDonnell, J. J., Freer, J., Hooper, R., Kendall, C., Burns, D., Beven, K. and Peters, J., 1996. New methods developed for studying hillslopes. *EOS Trans. AGU*, 77, 465-472.
- McDonnell, J. J., Owens, I. F. and Stewart, M. K., 1991. A case study of shallow flow paths in a steep zero-order basin. *Wat. Resour. Bull.*, 27 (4), 679-685.

- McDonnell, J. J., Stewart, M. K. and Owens, I. F., 1991. Effect of catchment-scale subsurface mixing on stream isotopic response. *Water Resour. Res.*, 27 (12), 3065-3073.
- McDonnell, J. J. and Taylor, C. H., 1987. Surface and subsurface water contributions during snowmelt in a small Precambrian Shield watershed, Muskoka, Ontario. *Atm. Ocean*, 25 (3), 251-266.
- McDowell, W. H., 1985. Kinetics and mechanisms of dissolved organic carbon retention in a headwater stream. *Biogeochem.*, 1, 329-352.
- McDowell, W. H. and Fisher, S. G., 1976. Autumnal processing of dissolved organic matter in a small woodland stream ecosystem. *Ecol.*, 57, 561-569.
- McDowell, W. H. and Likens, G. E., 1988. Origin, composition, and flux of dissolved organic carbon in the Hubbard Brook Valley. *Ecol. Mon.*, 58 (3), 177-195.
- McKeague, J. A. and Cline, M. G., 1963. Silica in soil solutions. 1. The form and concentration of dissolved silica in aqueous extracts of some soils. *Can. J. Soil Sci.*, 43, 70-96.
- Meyer, J.L., 1990. Production and utilization of dissolved organic carbon in riverine ecosystems. In: *Organic acids in aquatic ecosystems*. Perdue, E.M. and Gjessing, E.T. (Eds.), John Wiley and Sons, London, p.281-299.
- Meyer, J. L. and Tate, C. M., 1983. The effects of watershed disturbance on dissolved organic carbon dynamics of a stream. *Ecol.*, 64, 33-44.
- Molot, L. A. and Dillon, P. J., 1996. Storage of terrestrial carbon in boreal lake sediments and evasion to the atmosphere. *Global Biogeochem. Cycles*, 10, 483-492.
- Moore, I. D. and Grayson, R. B., 1991. Terrain-based catchment partitioning and runoff prediction using vector elevation data. *Water Resour. Res.*, 27, 1177-1191.
- Moore, R. D., 1989. Tracing runoff sources with deuterium and oxygen-18 during spring melt in a headwater catchment. *J. Hydrol.*, 112, 135-148.
- Moore, T. R., 1989. Dynamics of dissolved organic carbon in forested and disturbed catchments, Westland, New Zealand. 1. Maimai. *Water Resour. Res.*, 25, 1321-1330.

- Mosley, M. P., 1979. Streamflow generation in a forested watershed, New Zealand. *Water Resour. Res.*, 15, 795-806.
- Mosley, M. P., 1982. Subsurface flow velocities through selected forest soils, south island, New Zealand. *J. Hydrol.*, 55, 65-92.
- Mulholland, P. J. and Watts, J. A., 1982. Transport of organic carbon to the oceans by rivers of North America: a synthesis of existing data. *Tellus*, 34, 176-186.
- Nelson, P. N., Baldock, J. A. and Oades, J. M., 1993. Concentrations and composition of dissolved organic carbon in streams in relation to catchment soil properties. *Biogeochem.*, 19, 27-50.
- Novakowski, K. S. and Gillham, R. W., 1988. Field investigations of the nature of water-table response to precipitation in shallow water-table environments. *J. Hydrol.*, 97, 23-32.
- Ontario Ministry of the Environment (MOE), 1983. *Handbook of analytical methods for environmental samples*. Lab. Serv. Branch, Rexdale, Ont.
- Pearce, A. J., Stewart, M. K. and Sklash, M., 1986. Storm runoff generation in humid headwater catchments, 1. Where does the water come from? *Water Resour. Res.*, 22, 1263-1272.
- Peters, D. L., Buttle, J. M., Taylor, C. H. and LaZerte, B. D., 1995. Runoff production in a forested, shallow soil, Canadian Shield basin. *Water Resour. Res.*, 31, 1291-1304.
- Philips, R. E., Quisenberry, V. L., Zeleznik, J. M. and Dunn, G. H., 1989. Mechanism of water entry into simulated macropores. *Soil Sci. Soc. Am. J.*, 53, 1629-1635.
- Pinder, G. F. and Jones, J. F., 1969. Determination of the ground-water component of peak discharge from the chemistry of total runoff. *Water Resour. Res.*, 5, 438-445.
- Rawls, W.J., Ahuja, L.R., Brakensiek, D.L. and Shirmohammadi, A., 1993. Infiltration and soil water movement. In: *Handbook of hydrology*. Maidment, D.R. (Ed.), McGraw-Hill, Inc., New York, p.5.1-5.51.

- Redpath, B., 1973. *Seismic refraction exploration for engineering investigations. Technical Report E-US Army Corps Engineering Waterways Experimental Station. Explosive Research Laboratory, No. E-73-4, Livermore, CA.*
- Renzetti, A. V. E., Taylor, C. H. and Buttle, J. M., 1992. Subsurface flow in a shallow soil Canadian Shield watershed. *Nord. Hydrol.*, 23, 209-226.
- Richards, L. A., 1931. Capillary conduction of liquids through porous mediums. *Physics*, 1, 318-333.
- Richards, L. A., 1950. Laws of soil moisture. *Trans. Am. Geophys. Union*, 31, 750-753.
- Roberge, J. and Plamondon, A. P., 1987. Snowmelt pathways in a boreal forest hillslope, the role of pipe throughflow. *J. Hydrol.*, 95, 39-54.
- Rodhe, A., 1981. Spring flood, meltwater or groundwater? *Nord. Hydrol.*, 12, 21-31.
- Rodhe, A., 1984. Groundwater contribution to stream flow in Swedish forested till soil as estimated by oxygen-18. In: *Isotope Hydrology 1983. IAEA-SM-270/65. International Atomic Energy Agency, Vienna, p.55-66.*
- Rodhe, A., 1987. *The origin of streamwater traced by oxygen-18.* Uppsala University, Department of Physical Geography, Division of Hydrology, Report Series A, No. 41, Uppsala, Sweden.
- Rustad, S., Christophersen, N., Seip, H. M. and Dillon, P. J., 1986. Model for streamwater chemistry of a tributary to Harp lake, Ontario. *Can. J. Fish. Aqu. Sci.*, 43, 625-633.
- Rutherford, J. E. and Hynes, H. B. N., 1987. Dissolved organic carbon in streams and groundwater. *Hydrobiol.*, 154, 33-48.
- Sahin, V. and Hall, M. J., 1996. The effects of afforestation and deforestation on water yields. *J. Hydrol.*, 178, 293-309.
- Sami, K. and Buttle, J. M., 1991. Comparison of measured and estimated unsaturated hydraulic conductivities during snowmelt. *J. Hydrol.*, 123, 243-259.

- Schapp, M. G., Bouten, W. and Verstraten, J. M., 1997. Forest floor water content dynamics in a Douglas fir stand. *J. Hydrol.*, 201, 367-383.
- Scheider, W.A., Cox, C.M. and Scott, L.D., 1983. *Hydrological data for lakes and watersheds in the Muskoka-Haliburton study area (1976-1980)*. Ontario Ministry of the Environment, Dorset, Ontario.
- Schiff, S. L., Aravena, R., Trumbore, S. E. and Dillon, P. J., 1990. Dissolved organic carbon cycling in forested watersheds: a carbon cycle approach. *Water Resour. Res.*, 26, 2949-2957.
- Schiff, S. L., Aravena, R., Trumbore, S. E., Hinton, M. J., Elgood, R. and Dillon, P. J., 1997. Export of DOC from forested catchments on the Precambrian Shield of Central Ontario: Clues from ^{13}C and ^{14}C . *Biogeochem.*, 36, 43-65.
- Schindler, D. W., Bayley, S. E., Curtis, P. J., Parker, B. R., Stainton, M. P. and Kelly, C. A., 1992. Natural and man-caused factors affecting the abundance and cycling of dissolved organic substances in precambrian shield lakes. *Hydrobiol.*, 229, 1-21.
- Scott, J.S., 1979. Geology of Canadian tills. In: *Glacial till: An interdisciplinary study*, Legget, R.F. (Ed.), The Royal Society of Canada Spec. Publ. Ser., vol. 12., Ottawa, Ont.,
- Seip, H. M., Seip, R., Dillon, P. J. and deGrosbois, E., 1985. Model of sulphate concentration in a small stream in the Harp Lake catchment. *Can. J. Fish. Aqu. Sci.*, 42, 927-937.
- Shibatanni, R., 1988. *Meltwater processes and runoff mechanism in a small Precambrian Shield watershed during snowmelt*. Master's thesis, Trent University, Peterborough, Ont.
- Sklash, M., 1986. *Final report on an environmental isotope survey to determine the role of groundwater in snowmelt runoff in the APIOS Harp 5 watershed*. Rep IRI 18-36. Ontario Ministry of the Environment, Toronto, Ont.
- Sklash, M. G. and Farvolden, R. N., 1979. The role of groundwater in storm runoff. *J. Hydrol.*, 43, 45-65.

- Sklash, M. G., Stewart, M. K. and Pearce, A. J., 1986. Storm runoff generation in humid headwater catchments, 2, A case study of hillslope and low-order stream response. *Water Resour. Res.*, 22, 1273-1282.
- Thurman, E.M., 1985. *Organic geochemistry of natural waters*. Martinus Nijhoff/Dr W. Junk Publishers, Dordrecht.
- Topp, G. C., Davis, J. L. and Annan, P., 1980. Electromagnetic determination of soil water content: measurements in coaxial transmission lines. *Water Resour. Res.*, 16, 574-582.
- Topp, G. C. and Davis, J. L., 1985. Measurement of soil water content using Time-domain Reflectometry (TDR): A field evaluation. *Soil Sci. Soc. Am. J.*, 49, 19-24.
- Topp, G. C., Davis, J. L. and Annan, A. P., 1982. Electromagnetic determination of soil water content using TDR: I Applications to wetting fronts and steep gradients. *Soil Sci. Soc. Am. J.*, 46, 672-678.
- Topp, G. C., Davis, J. L. and Annan, A. P., 1982. Electromagnetic determination of soil water content using TDR: II Evaluation of installation and configuration of parallel transmission lines. *Soil Sci. Soc. Am. J.*, 46, 678-684.
- Trumbore, S. E., Schiff, S. L., Aravena, R. and Elgood, R., 1992. Sources and transformation of dissolved organic carbon in the Harp Lake forested catchment: the role of soils. *Radiocarbon*, 34, 626-635.
- Tsuboyama, Y., Sidle, R. C., Noguchi, S. and Hosoda, I., 1994. Flow and solute transport through the soil matrix and macropores of a hillslope segment. *Water Resour. Res.*, 30, 879-890.
- Waddington, J. M., Roulet, N. T. and Hill, A. R., 1993. Runoff mechanisms in a forested groundwater discharge wetland. *J. Hydrol.*, 147, 37-60.
- Ward, R. C., 1984. On the response to precipitation of headwater streams in humid areas. *J. Hydrol.*, 74, 171-189.
- Wels, C., 1989. *Streamflow generation in acidified headwater basins during spring runoff: an isotopic and geochemical approach*. M.Sc. thesis, Trent University, Peterborough, Ont.

- Wels, C., Cornett, J. and LaZerte, B., 1990. Groundwater and wetland contribution to stream acidification: an isotopic analysis. *Water Resour. Res.*, 26, 2993-3003.
- Wels, C., Cornett, J. and LaZerte, B., 1991. Hydrograph separation: a comparison of geochemical and isotopic tracers. *J. Hydrol.*, 122, 253-274.
- Wels, C., Taylor, C. H., Cornett, J. and LaZerte, B., 1991. Streamflow generation in a headwater basin on the Precambrian Shield. *Hydrol. Proces.*, 5, 185-199.
- Wenzel, L.K., 1941. *Tech. Bull. 27*. School Eng. , Pennsylvania State College.
- Weyman, D. R., 1970. Throughflow on hillslopes and its relation to the stream hydrograph. *Bull. Int. Assoc. Sci. Hydrol.*, XV, 25-33.
- Whipkey, R.Z. and Kirkby, M.J., 1978. Flow within the soil. In: *Hillslope hydrology*. Kirkby, M.J. (Ed.), John Wiley & Sons, New York, p.121-144.
- Wills, J., 1992. *Estimating the hydrological and chemical importance of groundwater input into a Precambrian Shield lake, Ontario*. Master's Thesis, University of Waterloo, Waterloo, Ont.
- Wilson, G. V., Jardine, P. M., Luxmoore, R. J. and Jones, J. R., 1990. Hydrology of a forested hillslope during storm events. *Geoderma*, 46, 119-138.
- Wilson, G. V. and Luxmoore, R. J., 1988. Infiltration, macroporosity and mesoporosity distributions on two forested watersheds. *Soil Sci. Soc. Am. J.*, 52, 329-335.
- Wood, E. F., Silvapalan, M., Beven, K. and Band, L., 1988. Effects of spatial variability and scale with implications to hydrologic modelling. *J. Hydrol.*, 102, 29-47.
- Wood, E. F., Silvapalan, M. and Beven, K., 1990. Similarity in scale in catchment storm response. *Rev. Geophys.*, 28, 1-18.
- Wu, L., Vomocil, J. A. and Childs, S. W., 1990. Pore size, particle size, aggregate size and water retention. *Soil Sci. Soc. Am. J.*, 54, 952-956.

Appendix 1

Piezometer data

Table A1.1. Piezometer information for the Harp 4-21 watershed.

Piezometer number	Type ^a	Hydraulic conductivity (cm/s)	Test ^b	Ground elevation (masl)	Stick up above ground (m)	Depth of mid-screen (mbgs)	Screen length (m)
15-01	DP	5.1E-04	B	346.918	1.615	0.275	0.16
15-02	DP	2.4E-05	B	346.925	1.403	1.258	0.16
15-03	DP	2.3E-04	B	346.840	1.328	2.394	0.16
15-04	DP	2.2E-06	B	346.891	0.677	3.078	0.16
16-01	DP	3.9E-06	B	348.067	1.301	0.650	0.16
16-02	DP	5.6E-04	B	348.047	0.783	1.127	0.16
16-03	DP	2.6E-04	B	348.047	1.438	2.287	0.16
17-01	DP	2.1E-04	B	349.938	1.318	0.662	0.16
17-02	DP	2.8E-04	B	350.016	1.603	0.427	0.16
20-01	DP	-	-	349.285	0.999	0.161	0.16
20-02	DP	7.5E-04	B	349.272	1.003	0.687	0.16
20-03	DP	1.5E-03	B	349.219	1.011	1.474	0.16
20-04	DP	8.1E-04	B	349.086	1.129	1.671	0.16
20-05	DP	2.6E-03	B	349.119	1.285	1.945	0.16
20-06	DP	3.1E-04	B	349.186	1.092	2.303	0.16
20-07	DP	8.4E-09	B	348.547	0.513	2.467	0.16
20-08	DP	6.6E-04	B	349.310	1.300	1.189	0.16
25-01	DP	2.4E-06	B	351.127	1.388	0.492	0.16
25-02	DP	2.6E-04	B	351.186	1.153	0.789	0.16
25-03	DP	3.6E-04	B	351.169	1.703	1.980	0.16
26-01	DP	3.1E-05	B	353.041	1.119	0.708	0.16
26-02	DP	-	-	353.082	1.215	1.513	0.16
27-01	DP	5.6E-04	B	350.577	0.673	2.250	0.16
27-02	DP	5.1E-04	B	350.525	0.769	2.871	0.16
28-01	DP	1.0E-04	B	352.063	1.382	0.367	0.16
28-02	DP	1.3E-05	B	352.073	1.454	1.045	0.16
28-03	DP	5.9E-04	S	352.182	1.365	2.180	0.16
30-01	DP	2.1E-05	B	358.390	0.990	0.752	0.16
30-02	DP	8.8E-05	B	358.400	1.362	1.704	0.16
30-03	DP	7.7E-08	B	358.465	0.929	2.570	0.16
30-04	DP	1.3E-04	B	358.367	1.035	2.608	0.16
30-05	DP	1.3E-08	B	358.400	1.025	2.865	0.16
30-06	DP	2.6E-08	B	358.375	1.011	3.609	0.16

Table A1.1 (continued). Piezometer information for the Harp 4-21 watershed.

Piezometer number	Type ^a	Hydraulic conductivity (cm/s)	Test ^b	Ground elevation (masl)	Stick up above ground (m)	Depth of mid-screen (mbgs)	Screen length (m)
31-01	DP	3.6E-06	B	358.606	1.169	0.746	0.16
31-02	DP	9.6E-06	B	358.553	1.149	3.313	0.16
32-00	DP	9.2E-06	S	358.436	1.076	2.706	0.16
32-01	DP	7.0E-07	B	358.246	1.433	0.502	0.16
32-02	DP	7.0E-07	B	358.115	1.469	0.436	0.16
33-01	DP	7.2E-07	B	357.918	1.157	0.633	0.16
33-02	DP	3.6E-06	B	357.933	0.689	1.131	0.16
33-03	DP	8.7E-07	B	357.947	1.531	1.754	0.16
34-01	PVC	-	-	358.602	0.090	0.120	0.16
34-02	PVC	1.9E-04	B	358.607	0.100	0.350	0.16
34-03	PVC	2.4E-04	B	358.647	0.051	0.690	0.16
45-01	DP	3.7E-05	B	360.511	1.361	0.448	0.16
45-02	DP	2.4E-05	B	360.500	0.693	0.997	0.16
45-03	DP	1.4E-04	B	360.520	0.743	2.197	0.16
46-01	PVC	6.8E-04	B	361.081	0.193	0.130	0.16
46-02	PVC	2.3E-04	B	361.093	0.070	0.370	0.16
46-03	PVC	2.3E-04	B	361.194	0.090	0.530	0.16
47-01	PVC	1.2E-04	B	361.594	0.050	0.120	0.16
47-02	PVC	2.5E-04	B	361.687	0.070	0.320	0.16
47-03	PVC	7.6E-04	B	361.720	0.070	0.510	0.16
50-01	DP	2.0E-04	B	363.810	1.173	0.602	0.16
50-02	DP	3.5E-05	B	363.705	1.260	0.710	0.16
50-03	DP	5.8E-06	B	363.741	1.199	1.256	0.16
1	PVC	2.3E-04	S	351.126	1.250	0.720	0.50
2 ^c	PVC	3.3E-05	S	350.909	1.210	0.830	0.50
3	PVC	2.7E-04	S	352.908	1.010	0.750	0.50
4	PVC	3.2E-03	B	359.772	1.030	0.900	0.50
5 ^d	PVC	-	-	359.779	1.200	1.010	0.35
5 ^e	PVC	-	-	359.779	1.205	0.723	1.045
6 ^d	PVC	-	-	361.558	1.255	1.015	0.38
6 ^e	PVC	-	-	361.558	1.315	0.60	1.20

Table A1.1 (continued). Piezometer information for the Harp 4-21 watershed.

Piezometer number	Type ^a	Hydraulic conductivity (cm/s)	Test ^b	Ground elevation (masl)	Stick up above ground (m)	Depth of mid-screen (mbgs)	Screen length (m)
7d	PVC	-	-	360.129	1.175	0.625	0.32
7e	PVC	-	-	361.558	1.065	0.427	0.855
8	PVC	-	-	356.783	0.990	0.590	0.50
9	PVC	dry ^f	-	383.009	1.110	4.370	0.50
10	PVC	7.4E-04	S	367.759	1.040	1.740	0.50
11	PVC	1.7E-04	S	361.430	1.150	0.320	0.50
13	PVC	3.0E-03	S	363.446	1.170	0.730	0.50
14d	PVC	-	-	361.545	1.050	0.570	0.55
14e	PVC	-	-	361.545	0.970	0.422	0.855
15	PVC	dry ^f	-	370.288	1.230	2.680	0.16
16	PVC	dry ^f	-	370.517	1.190	2.870	0.16
17	PVC	3.1E-05	S	363.080	1.300	0.910	0.16
18	PVC	1.8E-07	S	363.003	1.350	0.960	0.16
19	PVC	6.8E-05	S	363.097	1.300	1.770	0.16
20	PVC	9.0E-06	S	369.217	0.550	3.140	0.16
21	PVC	2.5E-06	S	370.452	1.130	4.410	0.16
22	PVC	5.9E-07	S	375.526	0.940	6.760	0.16
23	PVC	-	-	380.556	1.340	4.990	0.16
24	PVC	1.7E-05	S	362.508	1.130	1.410	0.16
29	PVC	9.4E-04	B	353.852	0.900	0.435	0.50
57	ABS	-	-	368.201	0.580	1.140	0.60
58	ABS	3.4E-04	S	364.712	0.440	2.500	0.60
59	ABS	2.4E-04	B	363.048	0.450	2.130	0.60
60	ABS	1.4E-05	B	363.074	0.400	2.920	0.60
61	ABS	9.6E-05	B	365.016	0.450	2.740	0.60
62	ABS	2.9E-05	B	364.933	0.620	4.800	0.60
63	ABS	1.1E-05	B	365.218	0.420	6.690	0.60
TD1 ^g	PVC	-	-	358.457	0.785	0.167	0.335
TD2 ^g	PVC	-	-	359.458	1.057	0.359	0.718
TD3 ^g	PVC	-	-	360.880	1.000	0.535	1.070

Table A1.1 (continued). Piezometer information for the Harp 4-21 watershed.

Notes:

- ^a Type: DP = Drive point piezometer (stainless steel screen diameter = 1.6 cm, riser tube ID = 0.95 cm)
PVC = Polyvinyl chloride piezometer (diameter = 4.0 cm, except for piezometers 2 and 7 with diameters of 5.1 cm)
ABS = Plumbing pipe (diameter = 5.1 cm)
- ^b Test: S = Slug test, B = Bail test
- ^c Piezometer was removed by MacLean (1992) in summer 1990.
- ^d Piezometer was replaced by MacLean (1992) with fully screened well in summer 1990. Measurements prior to replacement.
- ^e Piezometer was replaced by MacLean (1992) with fully screened well in summer 1990. Measurements after replacement.
- ^f Piezometer is dry. A water level was never observed.
- ^g Piezometer installed by MacLean in summer 1990.

masl: meters above sea level

mbgs: meters below ground surface

Table A1.2. Piezometer information for the Harp 3A watershed.

Piezometer number	Type ^a	Hydraulic conductivity (cm/s)	Test ^b	Ground elevation (masl)	Stick up above ground (m)	Depth of mid-screen (mbgs)	Screen length (m)
P65	PVC	1.6E-03	B	334.466	0.925	1.19c	2.38
P70	PVC	7.7E-06	B	334.432	1.295	0.745	0.20
P71-01	plastic	-	-	334.492	0.040	0.135	0.05
P71-02	PVC	5.6E-05	B	334.561	1.261	0.692	0.20
P71-03	PVC	4.5E-07	B	334.561	1.229	1.475	0.20
P71-04	PVC	1.9E-06	B	334.534	1.349	2.901	0.20
P72-01	plastic	-	-	334.917	0.063	0.112	0.05
P72-02	PVC	8.7E-03	B	334.912	1.239	0.511	0.20
P72-03	PVC	3.9E-06	B	334.912	1.090	1.571	0.20
P73-01	plastic	-	-	335.962	0.095	0.080	0.05
P73-02	PVC	-	-	336.010	1.140	0.270	0.20
P73-03	PVC	8.4E-04	B	335.978	1.045	0.759	0.20
P74-01	plastic	-	-	340.003	0.130	0.075	0.05
P74-02	PVC	-	-	340.169	1.105	0.340	0.20
P74-03	PVC	-	-	340.076	0.829	0.506	0.20
P74-04	PVC	5.7E-03	B	340.018	0.971	0.779	0.20
P75-01	plastic	2.4E-03	B	342.166	0.058	0.117	0.05
P75-02	PVC	5.6E-06	B	342.170	0.873	1.227	0.20
P76	PVC	4.9E-03	B	335.841	0.743	0.340c	0.65
P77-01	plastic	7.5E-04	B	338.150	0.084	0.091	0.05
P77-02	PVC	1.0E-02	B	338.143	0.901	0.667	0.20
P78	PVC	7.5E-06	B	340.339	1.120	0.680	0.20
P79	PVC	7.7E-05	B	342.358	1.030	0.560 ³	1.12
P80-01	plastic	4.5E-03	B	342.141	0.069	0.106	0.05
P80-02	PVC	1.4E-05	B	342.141	1.269	0.481	0.20
P80-03	PVC	1.9E-05	B	342.121	0.985	1.570	0.20
P81-01	plastic	-	-	345.744	0.126	0.049	0.05
P81-02	PVC	-	-	345.843	1.325	0.375	0.20
P81-03	PVC	1.8E-03	B	345.823	1.087	1.203	0.20
P82-01	PVC	1.1E-03	B	352.006	0.949	0.771	0.22
P83-01	plastic	-	-	361.835	0.119	0.056	0.05
P83-02	PVC	-	-	361.786	0.825	0.628	0.20
P84-01	PVC	5.9E-05	B	346.494	1.080	0.503	0.20

Table A2.1 (continued). Piezometer information for the Harp 3A watershed.

Piezometer number	Type ^a	Hydraulic conductivity (cm/s)	Test ^b	Ground elevation (masl)	Stick up above ground (m)	Depth of mid-screen (mbgs)	Screen length (m)
P84-02	PVC	5.5E-04	B	346.474	1.323	2.127	0.20
P85-01	plastic	1.1E-04	B	346.638	0.090	0.085	0.05
P85-02	PVC	2.6E-04	B	346.633	0.836	0.574	0.20
P85-03	PVC	7.1E-04	B	346.634	0.799	1.511	0.20
P86-01	plastic	-	-	349.906	0.090	0.085	0.05
P86-02	PVC	-	-	349.880	0.955	0.385	0.20
P86-03	PVC	4.8E-04	B	350.024	1.083	0.797	0.24
P87-01	plastic	-	-	355.283	0.138	0.037	0.05
P87-02	PVC	-	-	355.367	0.942	0.600	0.20
P87-03	PVC	5.9E-04	B	356.086	0.838	0.740	0.20
P88-01	PVC	1.3E-03	B	363.585	1.033	0.697	0.20
P89-01	plastic	-	-	352.669	0.137	0.038	0.05
P89-02	PVC	3.1E-04	B	352.686	0.943	0.829	0.20
P90	PVC	3.2E-05	B	351.551	0.804	0.326	0.20
P91	PVC	1.1E-04	B	346.200	0.520	0.550 ^c	1.00

^a Type: PVC = Polyvinyl chloride piezometer (diameter = 4.0 cm)
plastic = Plastic pipe (diameter = 4.0 cm)

^b Test: B = Bail test

^c Fully screened well

masl: meters above sea level

mbgs: meters below ground surface

Appendix 2

Rating curves

Figure A2.1 Rating curve for weir W1 for stages within the V portion of the weir.

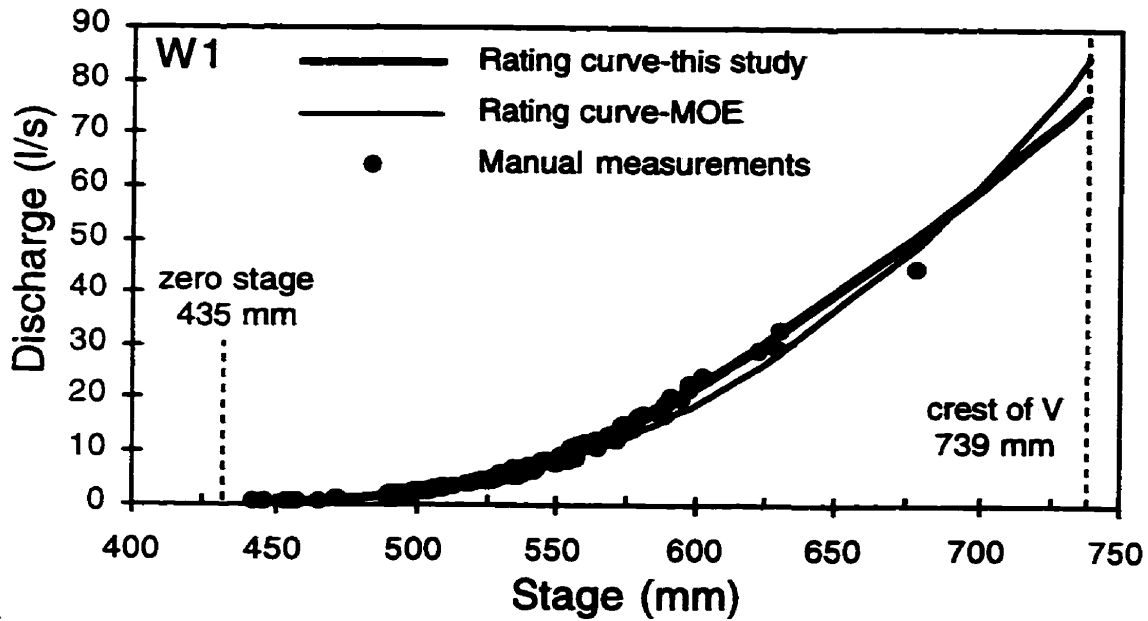


Figure A2.2 Rating curve for weir W1 for stages within the rectangular portion of the weir.

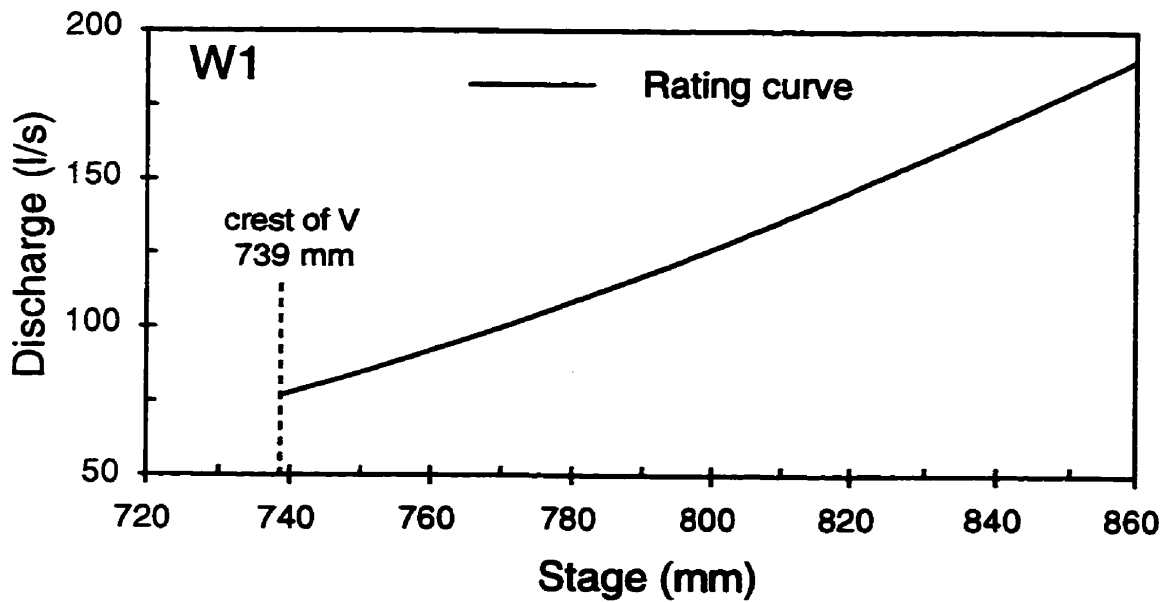


Figure A2.3 Rating curve for weir W2.

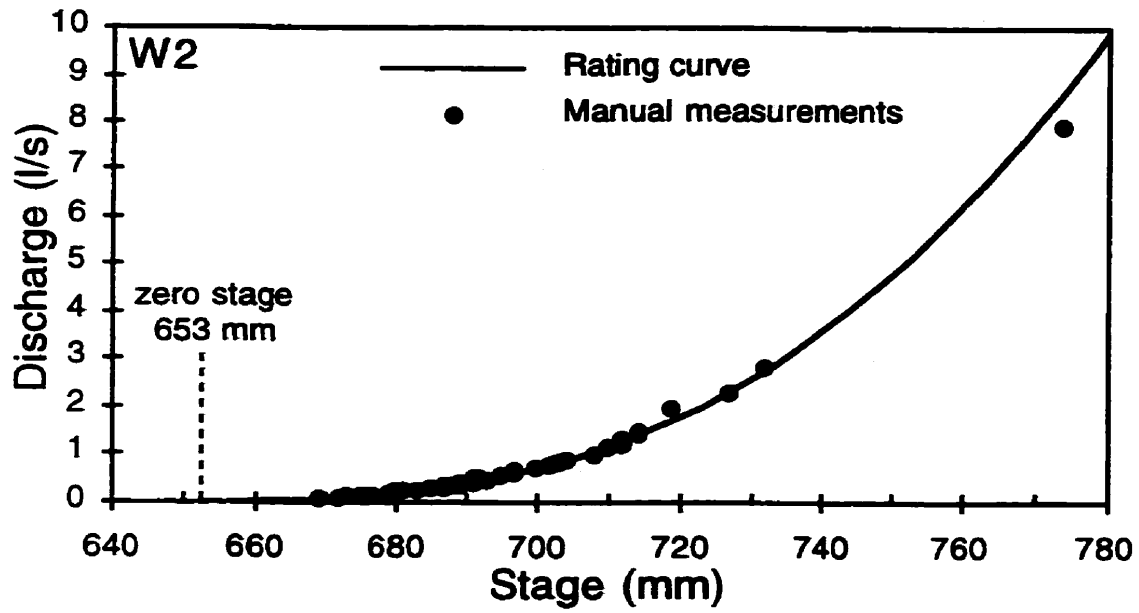


Figure A2.4 Rating curve for weir W3.

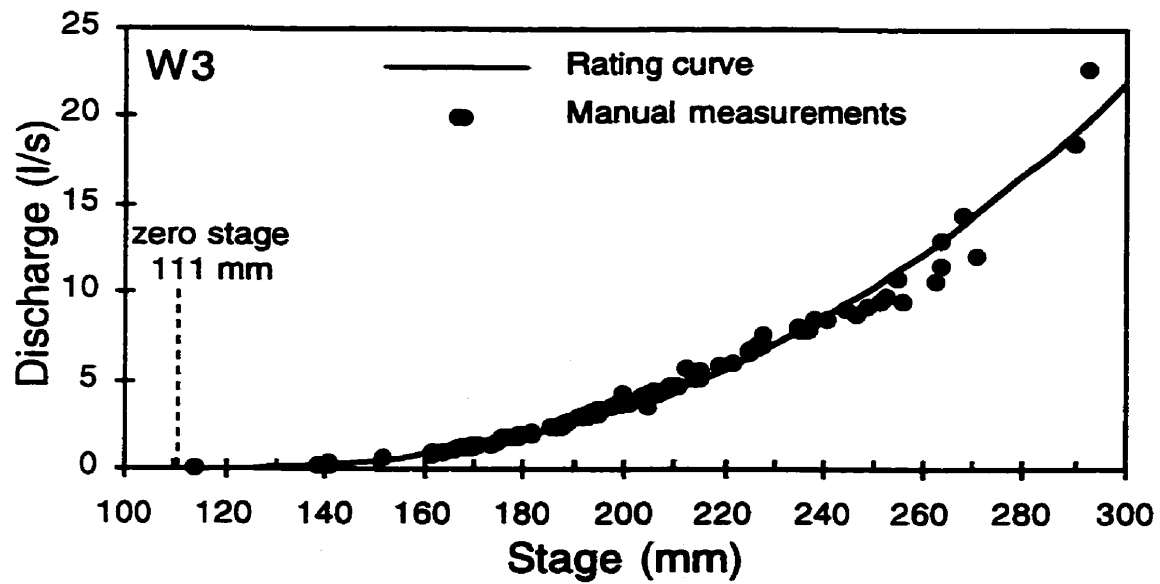


Figure A2.5 Rating curve for weir W4.

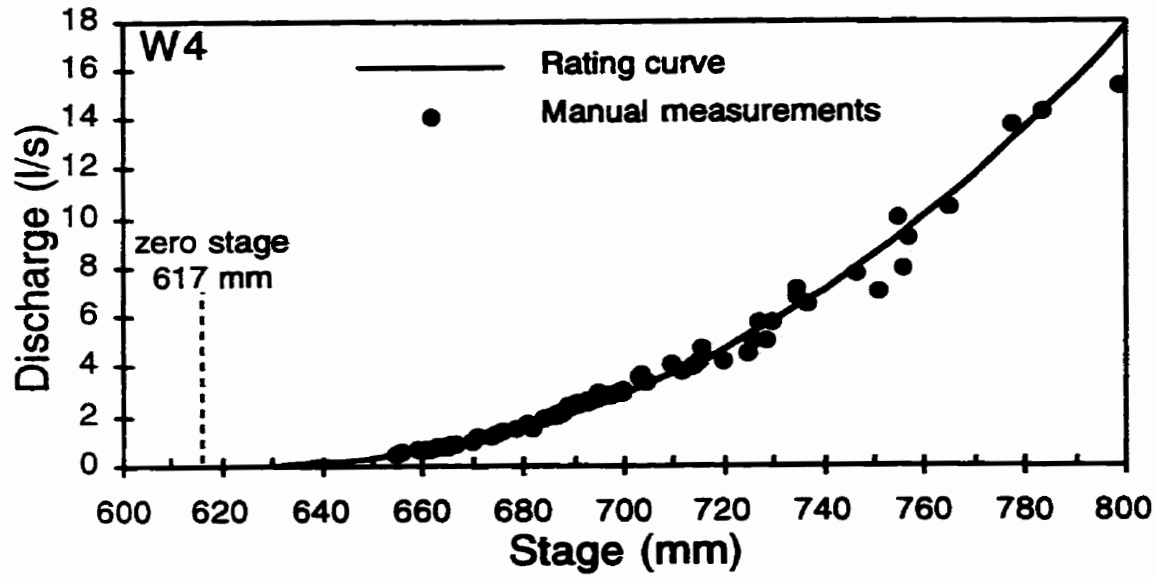


Figure A2.6 Rating curve for weir W5.

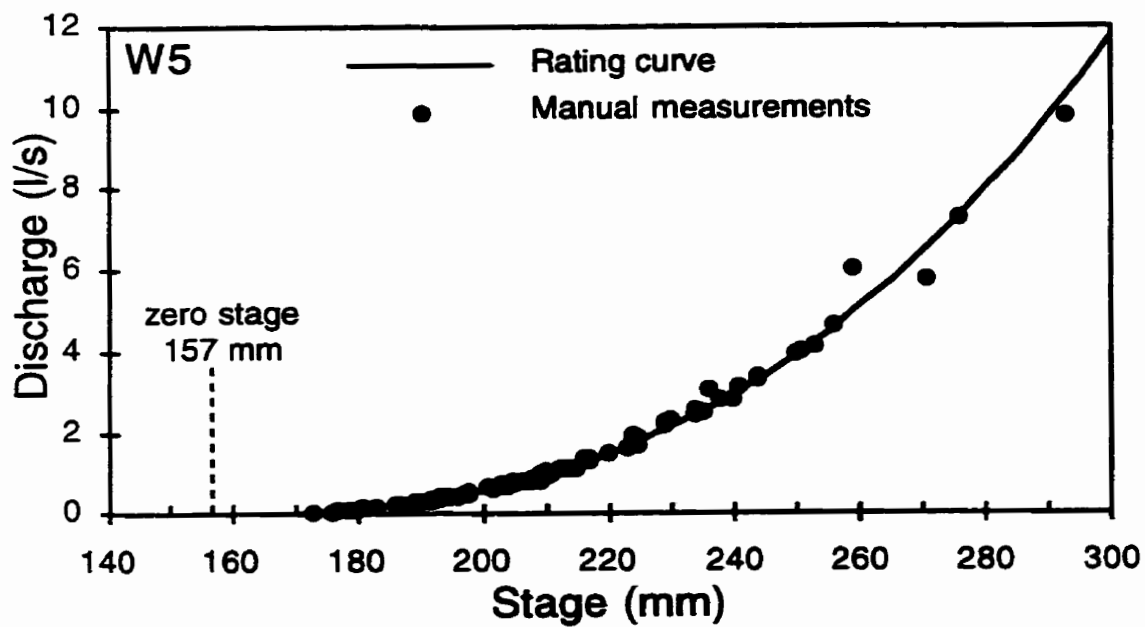


Figure A2.7 Rating curve for weir S1.

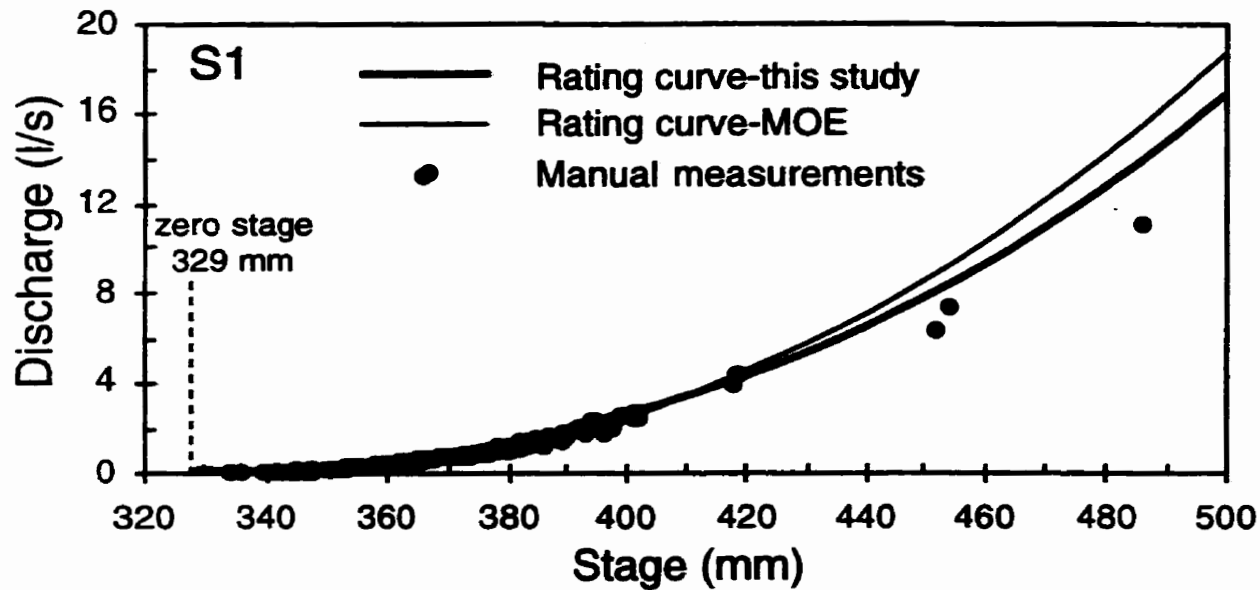


Figure A2.8 Rating curve for weir S3.

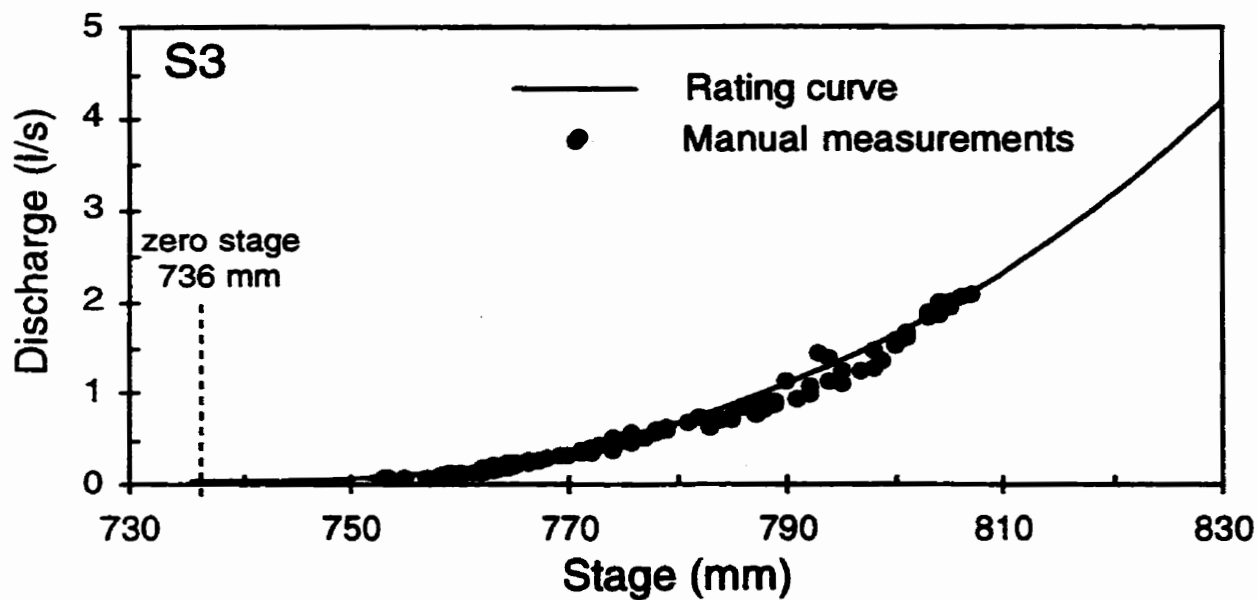


Figure A2.9 Rating curve for weir S4.

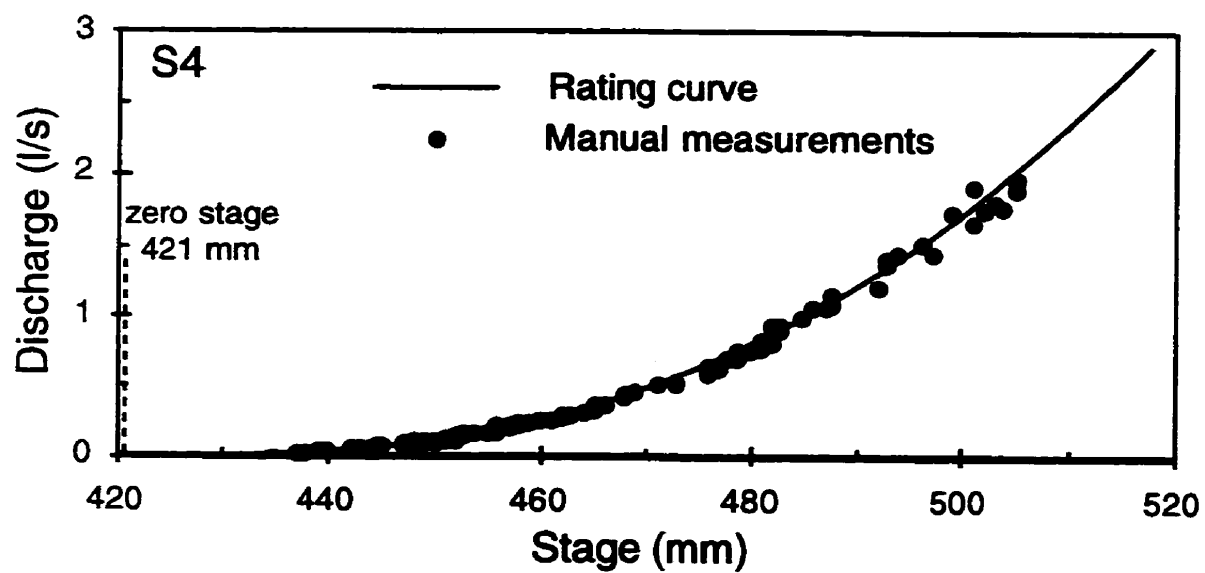
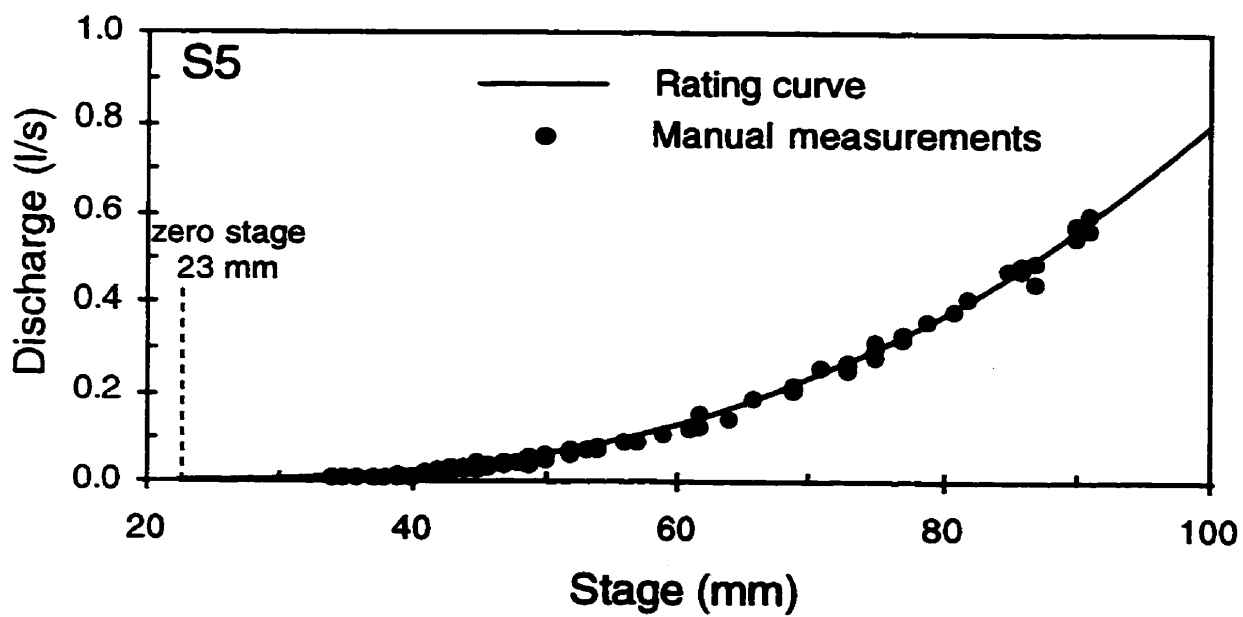


Figure A2.10 Rating curve for weir S5.



Appendix 3

TDR waveguide depths

Table A3.1 TDR waveguide depths and depth intervals for water balance calculations in Harp 3A.

Waveguide number	Depth (m)	Depth interval (m)
TD74-01	0.17	0-0.25
TD74-02	0.33	0.25-0.40
TD74-03	0.46	0.40-0.52
TD74-04	0.73	0.52-1.03
TD81-01	0.08	0-0.15
TD81-02	0.22	0.15-0.22
TD81-03	0.37	0.22-0.37
TD81-04	0.55	0.37-1.35
TD82-01	0.07	0-0.16
TD82-02	0.22	0.16-0.28
TD82-03	0.50	0.28-0.40
TD82-04	0.34	0.40-1.05
TD86-01	0.08	0-0.14
TD86-02	0.23	0.14-0.39
TD86-03	0.58	0.39-0.72
TD86-04	0.74	0.72-1.06
TD87-01	0.08	0-0.21
TD87-02	0.32	0.21-0.38
TD87-03	0.44	0.38-0.66
TD87-04	0.67	0.66-0.89
TD88-01	0.07	0-0.12
TD88-02	0.27	0.12-0.35
TD88-03	0.43	0.35-0.58
TD88-04	0.60	0.58-1.05

Table A3.2 TDR waveguide depths (from MacLean, 1992) and depth intervals for water balance calculations in Harp 4-21.

Waveguide number	Depth (m)	Depth interval (m)
TD1-01	0.08	-
TD1-02	0.16	-
TD1-03	0.28	-
TD2-01	0.08	0-0.13
TD2-02	0.18	0.13-0.24
TD2-03	0.29	0.24-1.00
TD3-01	0.18	0-0.31
TD3-02	0.44	0.31-0.52
TD3-03	0.60	0.52-1.00
TD4-01	0.28	0-0.38
TD4-02	0.48	0.38-0.58
TD4-03	0.68	0.58-1.00
TD5-01	0.27	0-0.42
TD5-02	0.56	0.42-0.69
TD5-03	0.81	0.69-2.00

Appendix 4

Water storage calculations

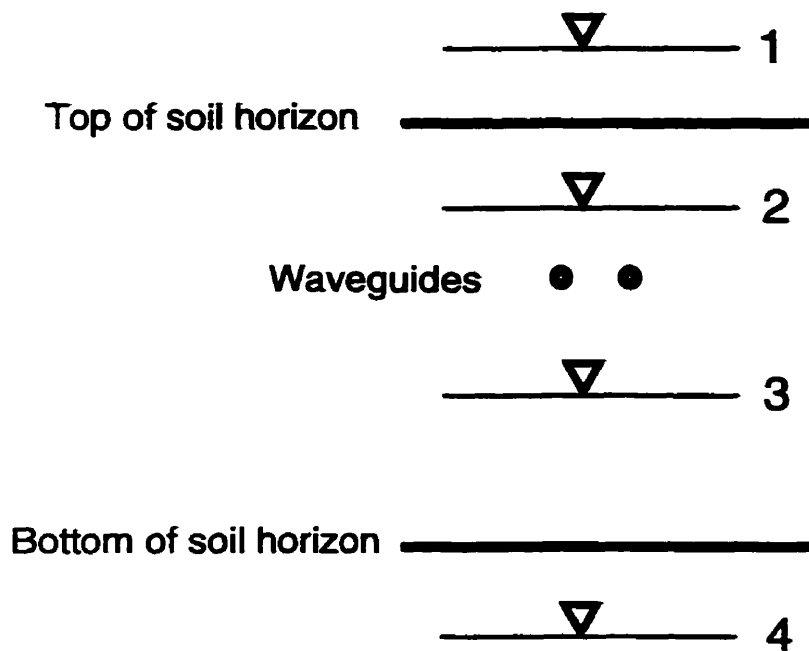
Method

Water contents and groundwater levels were used to calculate the total depth of water stored within individual soil profiles. In Harp 3A, water storage to bedrock was calculated. In Harp 4-21, water storage to an arbitrary depth of 1 m was calculated because the water table never declined below this depth except at TD5 where a total soil depth of 2 m was used. In each soil profile, a range of soil depths that correspond approximately with soil horizons was assigned to each pair of waveguides (Appendix 3). Water storage was calculated for each TDR soil horizon and summed to obtain the total water storage for each soil profile (Appendix 6).

The simplest method to calculate the water storage for each soil horizon would be to multiply the measured water content by the depth of the soil horizon. However, this approach assumes that the water content is either constant with depth or that the measured water content represents an actual depth average. Neither situation is likely to occur particularly when the water table is present within the soil horizon or when the waveguides are located near the top or bottom of the soil horizon. Waveguides could not always be located at the middle of soil horizons because the soil was stony.

The soil moisture profile was estimated according to the position of the water table relative to the soil horizon and the TDR waveguides (Figure A4.1). Four different water table positions are considered: 1) above the top of the soil horizon, 2) above the waveguides but below the top of the soil horizon, 3) within the soil horizon below the waveguides, and 4) below the entire soil horizon.

Figure A4.1 Positions of water table with respect to soil horizon and TDR waveguides for water storage calculations.



The water content profile for each horizon is estimated with one to three curve segments for the different portions of the soil moisture profile relative to the water table and waveguide positions. In position 1, the water content profile was calculated as one segment from the bottom to the top of the soil horizon (Figure A4.2). Two segments were used in position 2: one from the base of the horizon to the water table, the other from the water table to the top of the soil horizon (Figure A4.3). In position 3, the segments extend from the base of the horizon to the water table, from the water table to the waveguides, and from the waveguides to the ground surface (Figure A4.4). Only one segment was needed for position 4 (Figure A4.5).

The water content was approximated with a linear equation for each line segment. Below the water table (positions 1, 2, and 3), the water content was assumed to equal the average saturated water content that was calculated from measurements where the water table was above the waveguides. This value was used instead of the measured water content to reduce changes in soil water storage caused by measurement error. Therefore, the soil water storage for position 1 is constant and equals the maximum soil water storage for the horizon (Figure A4.2).

The matrix-saturated water content was always assumed at the top boundary of the water table. This value was obtained from the intercept of the characteristic curve for the soil horizon with the water content axis. In position 2, the soil water storage in the upper segment was calculated from the characteristic curve between a pressure head of zero (the matrix-saturated value) to a negative pressure head equal to the distance from the water table to the top of the soil horizon (Figure A4.3). Therefore, the soil water storage calculations for positions 1 and 2 do not directly use the measured soil water content except in the calculation of the average saturated water content. Position 2 illustrates the potential error that can result

Figure A4.2 Water storage calculation for water table position 1.

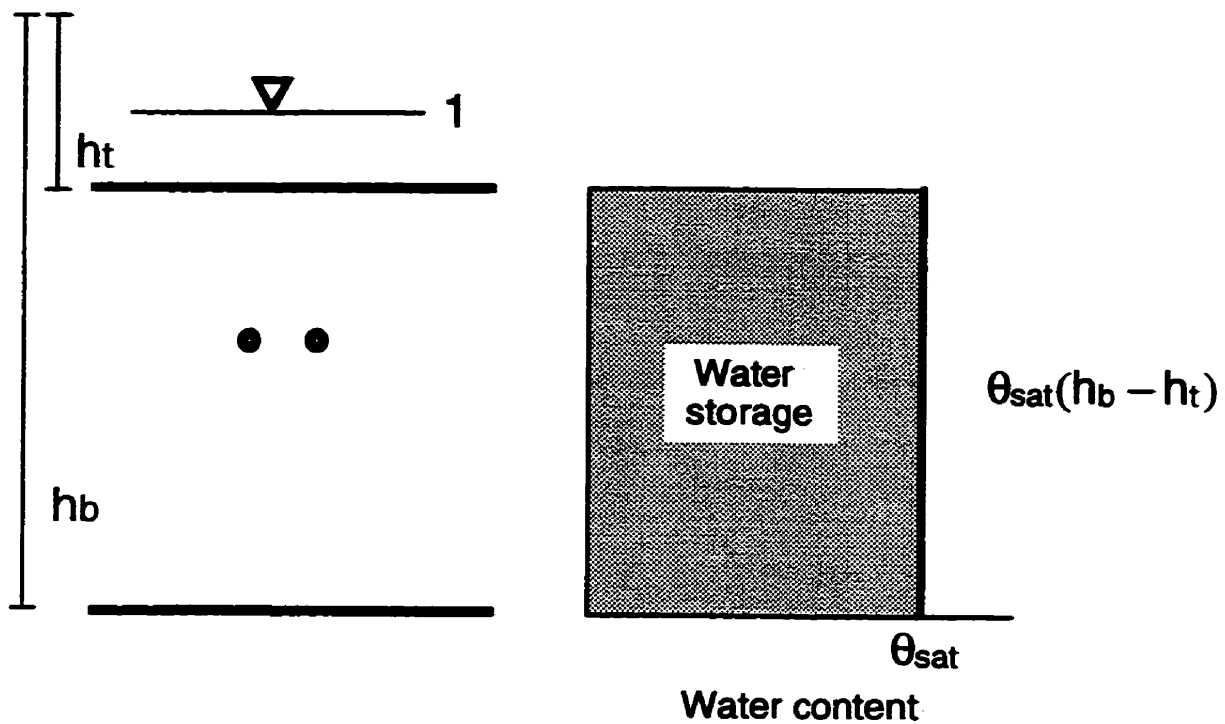


Figure A4.3 Water storage calculation for water table position 2. a) Water table position and soil moisture profile. b) portion of characteristic curve used in calculations.

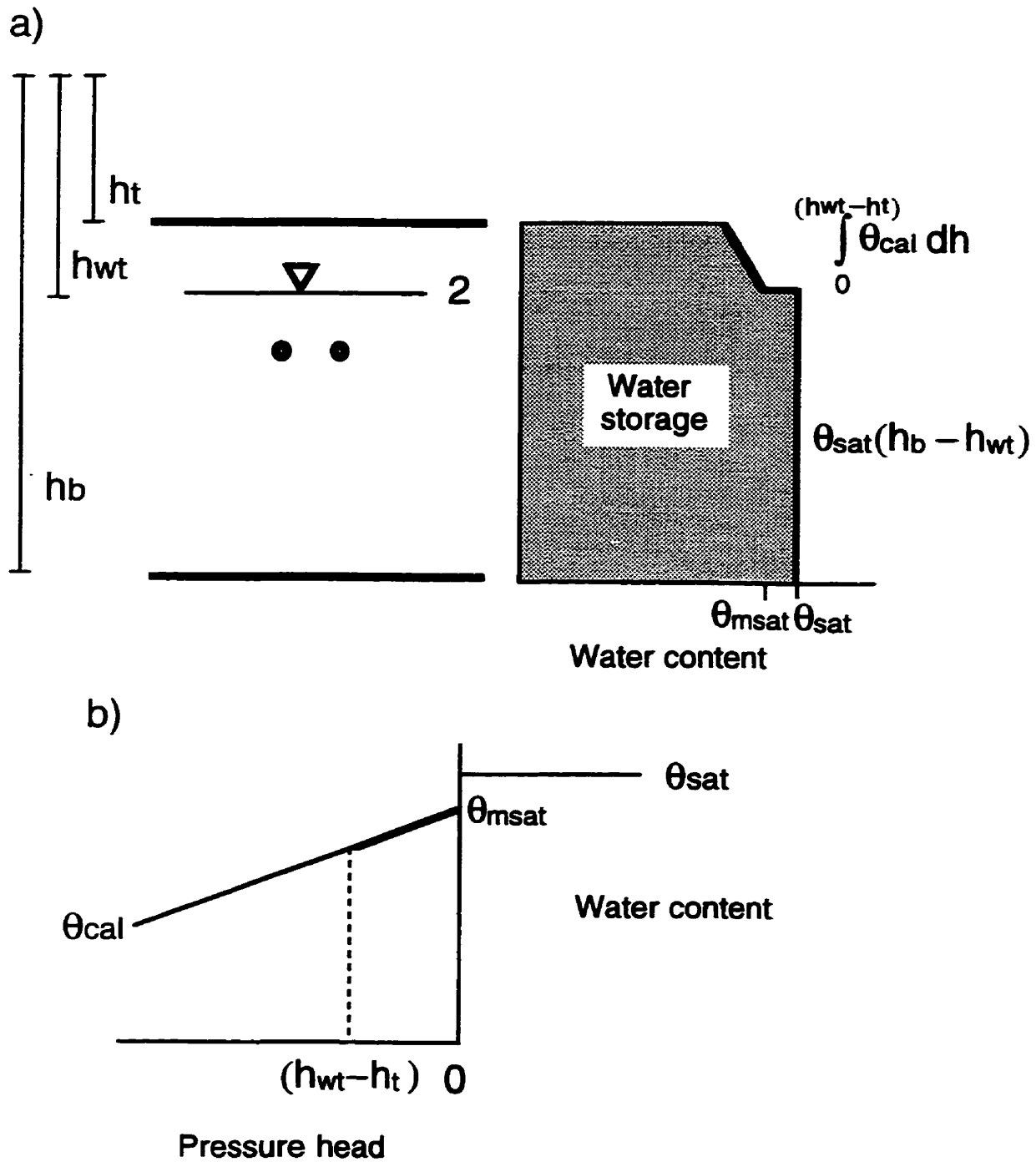


Figure A4.4 Water storage calculation for water table position 3. a) Water table position and soil moisture profile. b) portion of characteristic curve used in calculations.

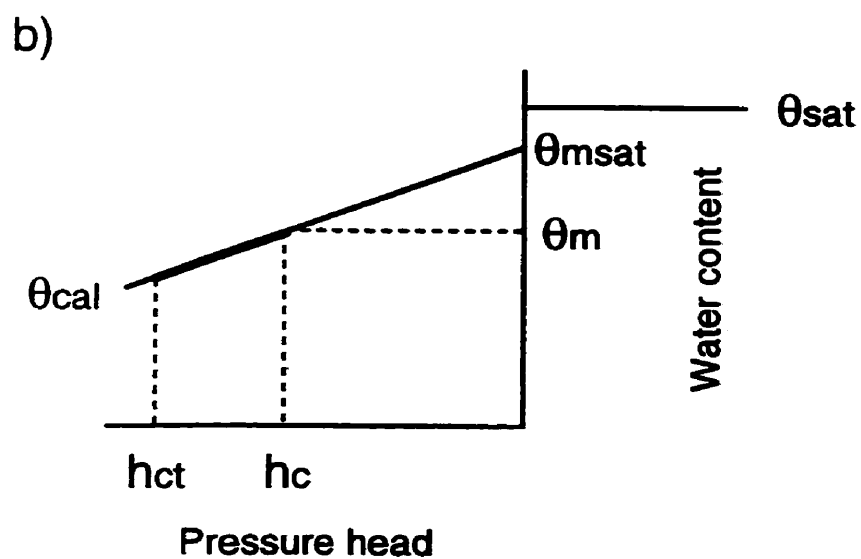
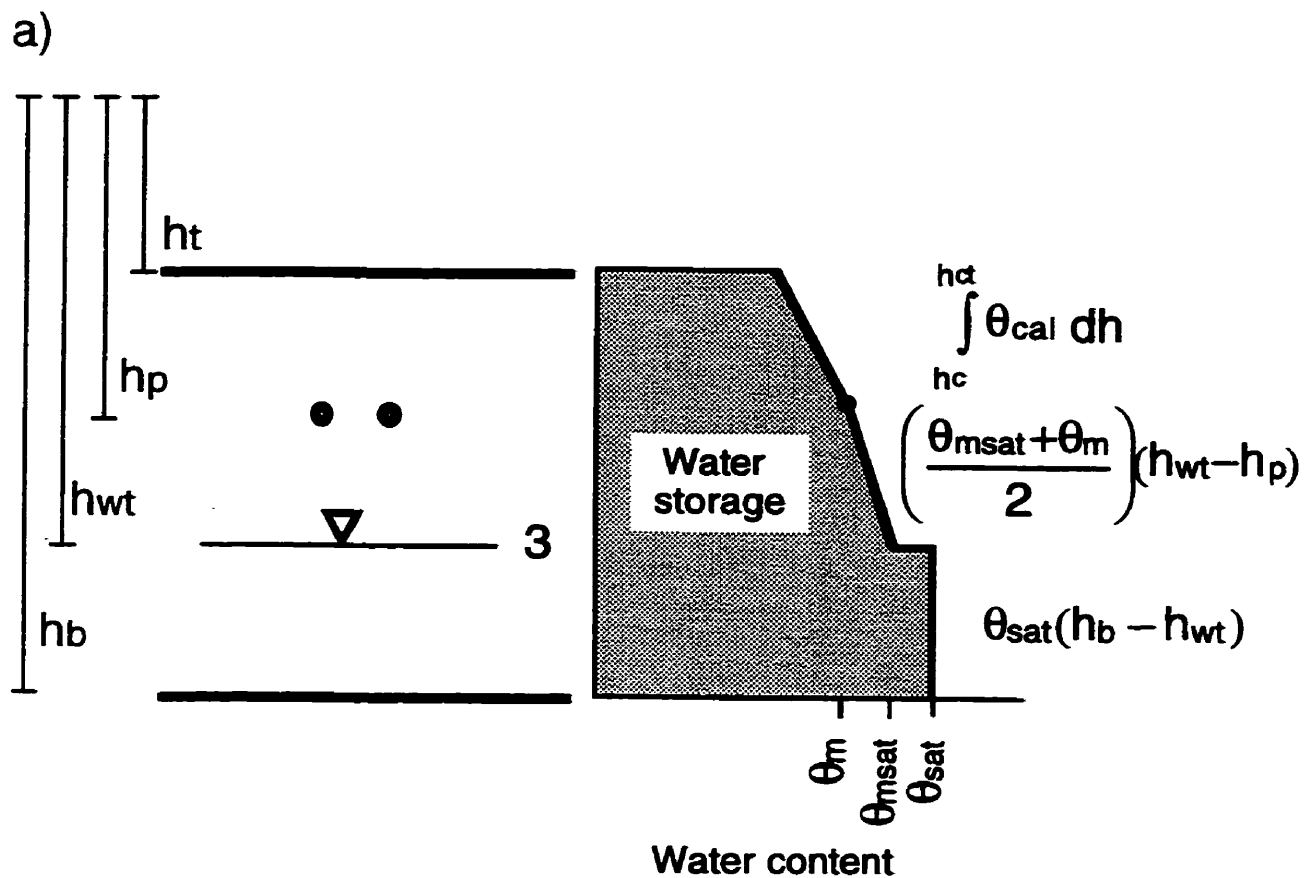
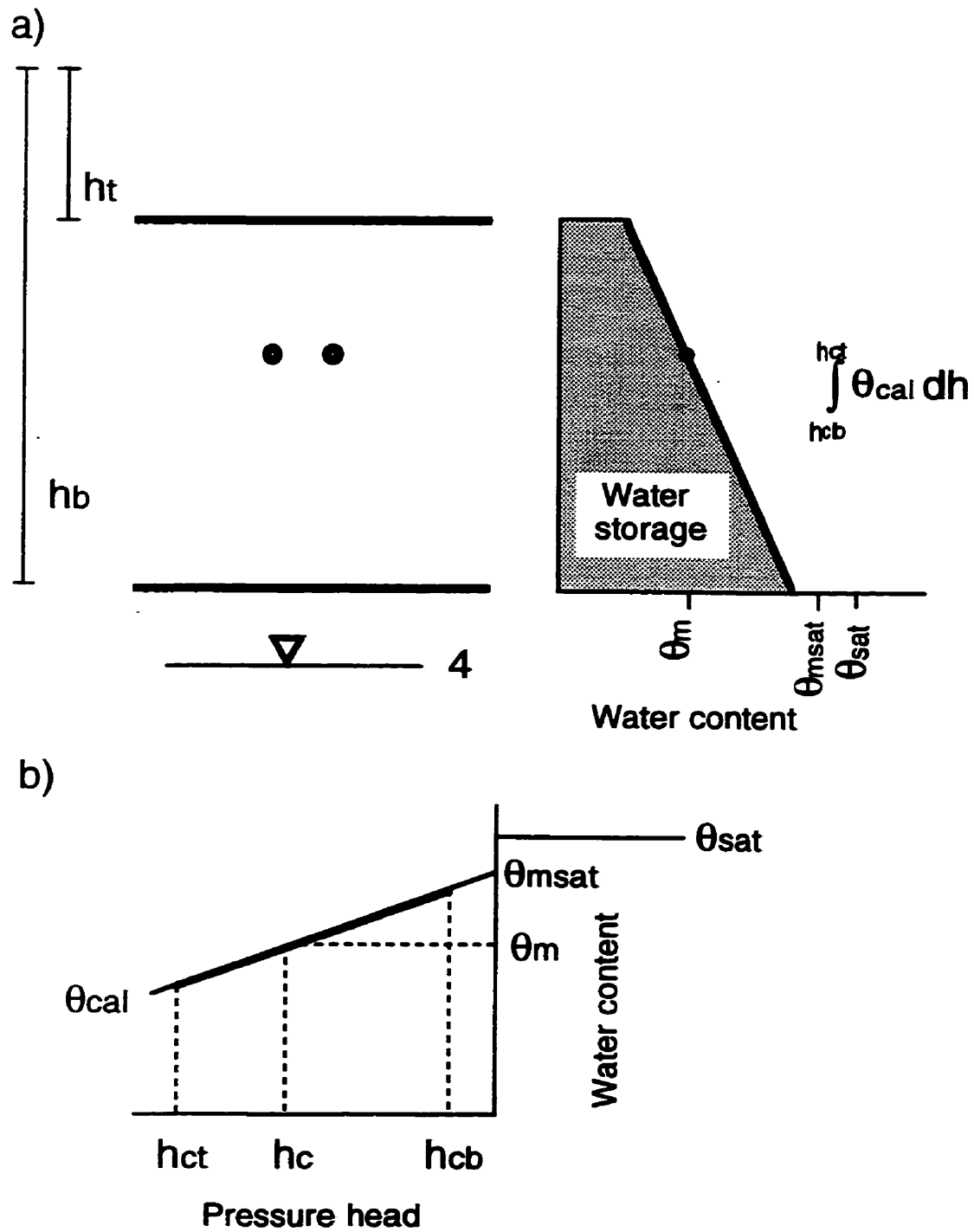


Figure A4.5 Water storage calculation for water table position 4. a) Water table position and soil moisture profile. b) portion of characteristic curve used in calculations.



if water storage was calculated as measured water content multiplied by horizon thickness. Once the water table rises above the waveguides, the entire horizon would be considered saturated (i.e. equivalent to position 1) even though the upper portion of the horizon may remain unsaturated.

Whenever the water table was positioned below the waveguides, the measured water content was used. In position 3, the water content is known at three positions: the measured value at the waveguides (θ_m), the matrix-saturated value at the top of the water table (θ_{msat}) and the fully saturated value below the water table (θ_{sat}). The three segments include these known values (Figure A4.4). The average saturated water content was assumed for the zone below the water table. From the water table to the waveguides, water content is a linear interpolation between the matrix-saturated value and the measured value at the waveguides. If a capillary fringe is observed in the characteristic curve, the linear interpolation joins the top of the capillary fringe to the measured value (adding a fourth line segment that approximates the capillary fringe). The characteristic curve was used to indicate the water content from the waveguides to the top of the soil horizon. To maintain a continuous water content profile across the waveguides, the characteristic curve was calculated from the pressure head that coincides with the measured soil water content. Therefore, the calculated pressure head (h_c) at the waveguides does not necessarily correspond to the distance from the water table to the waveguides.

In position 4, the water content profile is calculated from the characteristic curve with a calculated pressure head (h_c) that corresponds to the measured soil water content at the waveguides (Figure A4.5). The water content at the top of the profile corresponds to the pressure head equal to h_c minus the distance between the waveguides and the top of the horizon ($h_{ct} = h_c - (h_p - h_t)$). Similarly, the water content at the bottom of the profile

corresponds to the pressure head equal to h_c plus the distance between the waveguides and the bottom of the horizon ($h_{cb} = h_c - (h_p - h_t)$). Since the characteristic curve is represented by a linear equation, the soil water storage for position 4 will be the same as the measured water content multiplied by the soil horizon thickness if the waveguides are positioned in the middle of the horizon. Soil water storage would be underestimated if the waveguides were in the upper half of the soil horizon and overestimated if the waveguides were in the lower half of the horizon.

Although these water content profiles are only estimates of the actual water content profiles, they are more appropriate than simply assuming a constant water content for each soil horizon. Most importantly, this method prevents large sudden changes in soil water storage that would occur as the water table rises above or drops below the waveguides. Furthermore, the effects of measurement error are reduced for water storage below the water table. This method makes the best use of the existing data for the calculation of soil water storage.

Errors in water storage calculations

As discussed in Chapter 6, there are several possible sources of error in water storage calculations although the errors of greatest concern are related to incorrect water content profiles. Since water content measurements were not accompanied with measurements of pressure head at the same depth as the TDR waveguides, hydrostatic conditions were assumed to obtain an estimate of the pressure head from the depth of the water table. However, hydrostatic conditions do not apply during storms because vertical flow requires a hydraulic gradient other than zero. This section discusses some of the possible errors that result from the assumption of static hydraulic conditions.

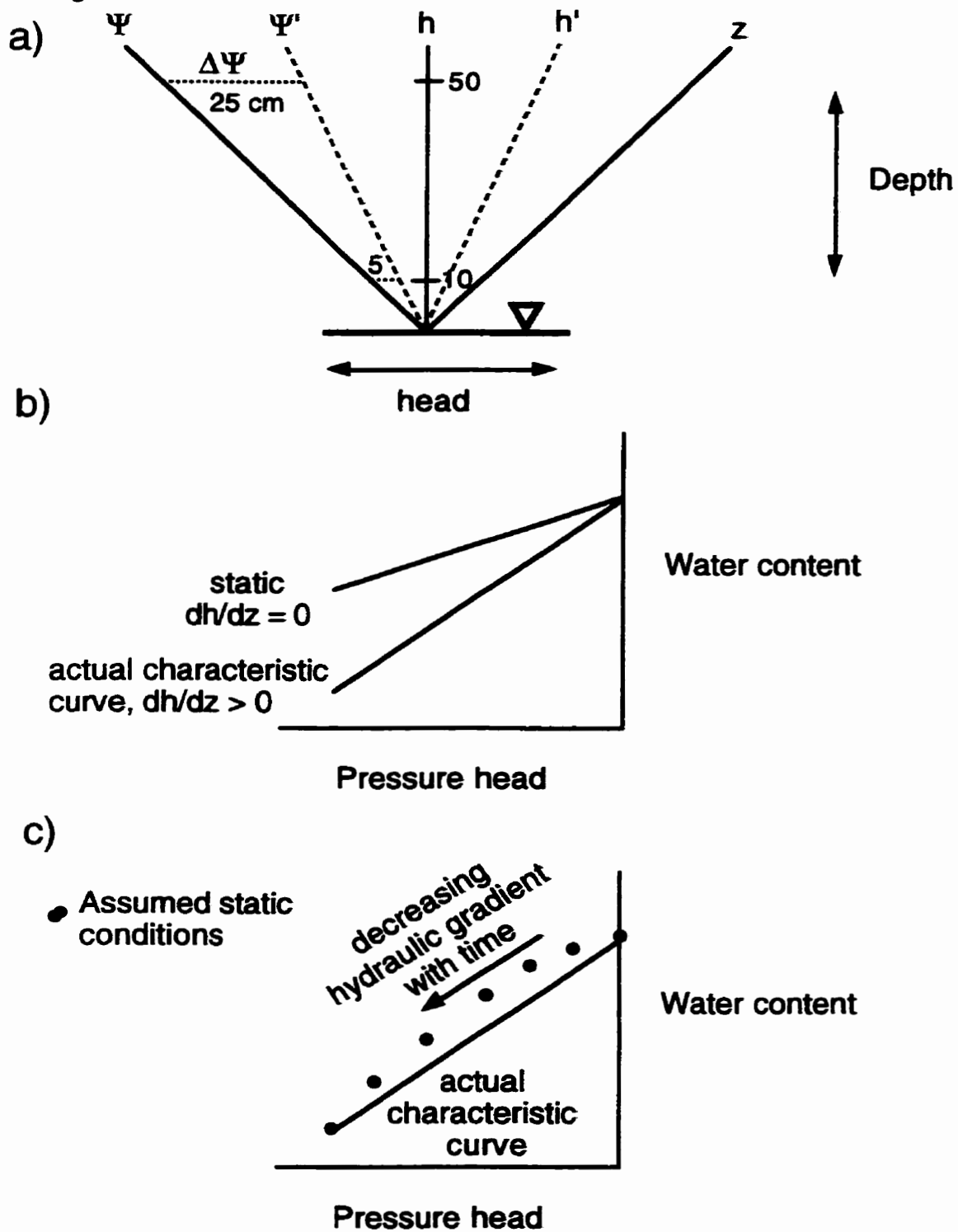
The assumption of static hydraulic conditions will result in errors in the characteristic curves. When there is downward flow, the actual pressure head at any point in the vadose zone

will be larger (a smaller negative value) than the distance to the water table. Therefore, a measured water content would be assigned a pressure head that is too small. The magnitude of this error will increase with both the vertical hydraulic gradient and the distance to the water table. For example, a hydraulic gradient of 0.5 would result in a 5 cm error in pressure head if the water table were 10 cm below the waveguides, but would result in an error of 25 cm if the water table were 50 cm below the waveguides (Figure A4.6a). Therefore, errors in pressure head are likely to be larger in the shallow soil horizons than in the deeper horizons.

If hydraulic gradients were constant, the actual and estimated characteristic curves measured instantaneously (assuming uniform soil water retention within the horizon) would diverge with decreasing pressure head (Figure A4.6b). However, the vertical hydraulic gradients would likely decrease after a storm such that the magnitude of the error in pressure head does not necessarily increase with a deeper water table. In effect, the error will eventually decrease with time and reach zero when hydrostatic conditions re-established. This progression is important since the characteristic curves in this study are calculated for each horizon on the basis of water content measurements at one location over time. Since the characteristic curve is based on several measurements under decreasing vertical hydraulic gradients, the estimated characteristic curve will converge with the actual characteristic curve at smaller pressure heads and the two curves will be approximately parallel (Figure A4.6c). Without knowing the actual pressure heads or vertical hydraulic gradients, it is not possible to quantify the errors in the characteristic curves.

The calculation of soil water storage tends to minimize the effects of errors in the characteristic curves because the soil moisture profile is derived from the measured water content at the waveguides. Although the slope of the characteristic curve (linear in this case) affects the distribution of water content, it usually has a minor influence on water storage. This

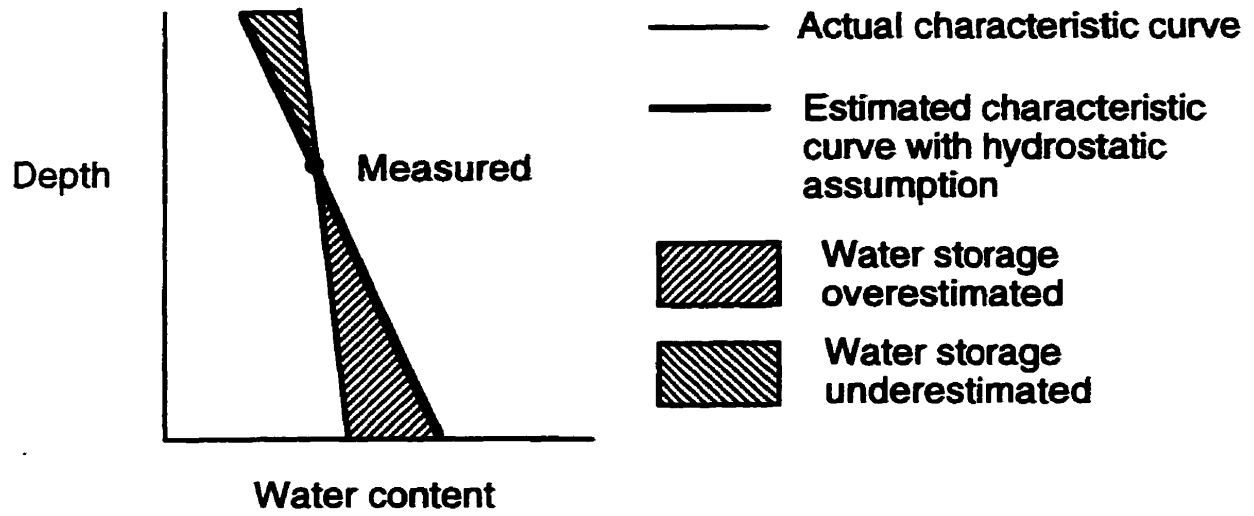
Figure A4.6. Possible errors that result from the assumption of hydrostatic conditions. a) hydraulic head profiles for static and flowing conditions. b) resulting characteristic curves. c) errors caused by monitoring during decreasing hydraulic gradients.



is particularly valid if the waveguides are near the middle of the horizon since the differences in water storage above and below the waveguides cancel each other (Figure A4.7).

Although the errors in the characteristic curves can produce some small errors in the absolute water storage, the effect on the relative changes in water storage may be even smaller. An error in the slope of the characteristic curve will be repeated in every profile and will not produce an error in the change of water storage unless there is a change from unsaturated to saturated conditions within the soil horizon (or vice versa). Although it is not possible to determine the error in water storage caused by vertical flow (i.e. not hydrostatic conditions) since the actual pressure heads are not known, the approximate magnitude of the error can be illustrated by an example. The characteristic curve and soil water storage were recalculated for TD88-02 (where the waveguides were located at the bottom third of the soil horizon) by assuming a vertical hydraulic gradient of 0.75 that gradually decreases to 0.0 at baseflow. The average difference in water storage during the November 1992 storms was 0.1 mm with a maximum difference of 0.5 mm or 0.4% of the total volume of water stored within the horizon. Therefore, the assumption of static conditions did not appear to have a large influence on the water storage, given the procedure used.

Figure A4.7. Errors in water storage caused by errors in the slope of the characteristic curve are partially cancelled.



Appendix 5

Water content data

Table A5.1. Water content and depth to water table data, site TD81.

Date and time	Water content (%) TDR waveguides				Depth to water table (m)
	81-01	81-02	81-03	81-04	
17-Oct-92 16:03	34.6	50.8	49.5	43.8	0.749
20-Oct-92 12:50	34.0	49.5	48.3	43.8	0.877
27-Oct-92 09:38	34.2	50.1	48.6	44.0	0.865
31-Oct-92 15:07	31.8	49.4	47.9	43.2	0.938
3-Nov-92 12:00	35.3	53.9	56.9	43.9	0.630
4-Nov-92 13:35	36.2	53.0	56.1	43.9	0.599
5-Nov-92 12:46	35.1	52.6	55.1	43.9	0.676
7-Nov-92 12:04	34.1	51.5	49.7	43.8	0.768
9-Nov-92 12:51	33.4	50.6	48.8	43.8	0.857
11-Nov-92 10:13	36.2	53.0	55.1	43.7	0.616
12-Nov-92 10:47	35.3	51.7	52.3	43.7	0.696
13-Nov-92 15:57	44.0	55.8	55.8	43.8	0.549
14-Nov-92 15:10	42.9	55.0	55.7	43.6	0.618
15-Nov-92 16:00	41.5a	53.5	55.1	43.4	0.657
16-Nov-92 16:13	40.0	53.0a	53.0	43.3	0.694
17-Nov-92 15:30	38.1	52.4	50.7	43.4	0.728
18-Nov-92 15:14	36.5	51.8	50.1	43.4	0.756
20-Nov-92 11:02	34.4	51.0	49.7	43.4	0.794
3-Mar-93 16:23	26.1	45.4	42.6	37.8	1.338b
14-Apr-93 12:45	36.8	52.8	50.1	44.1	0.740
2-May-93 15:04	33.4	50.0	48.4	43.8	0.883
4-May-93 12:59	32.4	49.7	48.0	43.5	0.912
10-May-93 13:53	32.0	48.7	47.0	42.6	0.965
13-May-93 11:23	32.3	48.4	47.0	42.8	1.015
16-May-93 13:18	32.3	48.7	47.6	42.7	0.961
22-May-93 12:29	29.4	47.3	45.1	41.2	1.078
24-May-93 13:34	33.8	50.0	47.5	43.8	0.807
25-May-93 11:57	32.5	49.6	47.4	44.0	0.791
26-May-93 11:38	32.2	49.5	47.1	43.7	0.822
27-May-93 11:01	31.3	49.2	46.5	43.1	0.894
28-May-93 11:09	34.8	50.8c	49.1	43.9	0.715
29-May-93 15:36	32.6	50.4c	48.7c	43.8	0.822

Table A5.1 (continued). Water content and depth to water table data, site TD81.

Date and time	Water content (%) TDR waveguides				Depth to water table (m)
	81-01	81-02	81-03	81-04	
30-May-93 15:30	31.6	49.0	47.4	42.6	0.894
26-Aug-93 13:25	22.8	36.9	34.1	25.5	1.338 ^b
22-Sep-93 14:00	24.7	41.3	37.5	30.2	1.338 ^b

^a Wave forms were improperly stored. Data are interpolated.

^b Minimum water table depth. Water table is below screen bottom. Depth to screen bottom is reported.

^c Wave forms were improperly stored. Water contents may be overestimated.

Table A5.2. Water content and depth to water table data, site TD82.

Date and time	Water content (%) TDR waveguides				Depth to water table (m)
	82-01	82-02	82-04	82-03	
31-Oct-92 14:57	41.5 ^a	44.9	41.9	36.3 ^b	0.719
3-Nov-92 11:49	43.7	46.0	44.2	39.1 ^b	0.516
4-Nov-92 13:40	44.3	46.5	46.4	45.3	0.402
5-Nov-92 12:50	43.5	46.1	45.8	44.5	0.520
7-Nov-92 12:08	42.8	45.9	45.4	38.6	0.566
9-Nov-92 12:58	42.4	45.5	45.2	38.4	0.652
11-Nov-92 10:17	44.1	46.7	45.7	40.2	0.518
12-Nov-92 10:53	43.3	46.4	45.6	38.3	0.589
13-Nov-92 16:03	52.0	52.7	59.8	47.5	0.207
14-Nov-92 15:14	49.7	50.4	50.1	47.6	0.374
15-Nov-92 16:04	49.0	49.5	47.7	43.5	0.505
16-Nov-92 16:26	47.8	48.7	46.9	41.3	0.572
17-Nov-92 15:41	46.1	48.5	46.3	40.9	0.618
18-Nov-92 15:21	45.9	47.7	46.3	40.6	0.636
20-Nov-92 11:14	44.4	47.6	45.2	39.7	0.659
3-Mar-93 16:34	35.3	40.0	37.2	30.9	0.843 ^c
14-Apr-93 12:57	47.2	49.0	46.7	41.5	0.475
2-May-93 15:25	43.1	47.1	44.7	39.9	0.646
4-May-93 13:13	42.6	46.6	44.6	39.5	0.677
10-May-93 13:59	40.9	45.1	43.2	37.4	0.822
13-May-93 11:32	d	d	43.9	36.8	0.843 ^c
16-May-93 13:24	41.0	44.8	d	36.7	0.843 ^c
17-May-93 18:03	d	d	d	36.3	0.843 ^c
22-May-93 12:35	38.5	42.3	41.0	33.9	0.843 ^c
24-May-93 13:40	42.3	44.6	42.0	37.0	0.843 ^c
25-May-93 12:04	40.7	44.1	41.8	36.5	0.843 ^c
26-May-93 11:46	40.3	44.0	41.9	36.7	0.843 ^c
27-May-93 11:06	39.6	44.0	41.6	36.5	0.843 ^c
28-May-93 11:14	42.3	44.8	42.1	37.6	0.701
29-May-93 15:41	d	d	42.0	38.0	0.662
30-May-93 15:38	41.8	45.2	42.4	38.1	0.652

Table A5.2 (continued). Water content and depth to water table data, site TD82.

Date and time	Water content (%) TDR waveguides				Depth to water table (m)
	82-01	82-02	82-04	82-03	
26-Aug-93 13:25	23.3	23.6	24.7	23.0	0.843 ^c
22-Sep-93 14:00	33.2	36.8	34.7	26.4	0.843 ^c

^a Soil moisture was affected by initial disturbance. Water content was calculated from regression with 82-02.

^b Soil moisture was affected by initial disturbance. Water content was calculated from regression with 82-04.

^c Minimum water table depth. Water table is below screen bottom. Depth to screen bottom is reported.

^d Wave forms were improperly stored. Data are not reported.

Table A5.3. Water content and depth to water table data, site TD86.

Date and time	Water content (%) TDR waveguides				Depth to water table (m)
	86-01	86-02	86-03	86-04	
9-Oct-92 16:15	33.0	42.1	31.8	37.8	0.936a
13-Oct-92 13:28	32.1	41.9	32.2	38.9	0.936a
13-Oct-92 18:24	33.0	41.9	32.0	38.3	0.936a
17-Oct-92 16:40	37.2	44.1	38.2	50.4	0.645
20-Oct-92 12:13	36.0	43.4	36.0	47.8	0.756
27-Oct-92 09:07	36.1	43.7	36.3	47.6	0.755
31-Oct-92 15:54	34.3	42.5	34.0	45.1	0.838
3-Nov-92 11:21	38.2	47.2	47.4	50.3	0.365
4-Nov-92 12:55	37.7	46.7	46.7	50.2	0.451
5-Nov-92 13:15	36.8	46.0	43.3	50.0	0.617
7-Nov-92 11:03	36.1	44.6	38.0	49.5	0.710
9-Nov-92 11:54	35.2	43.9	36.6	47.2	0.822
11-Nov-92 09:24	38.3	46.4	47.4	49.6	0.410
12-Nov-92 10:04	36.4	45.3	41.8	49.2	0.632
13-Nov-92 15:28	45.3	55.9	48.2	50.3	0.327
14-Nov-92 14:27	43.0	51.7	47.4	49.6	0.516
15-Nov-92 15:10	40.9	48.9	44.2	49.6	0.637
16-Nov-92 15:30	39.7	47.2	40.5	48.8	0.689
17-Nov-92 14:45	39.2	46.3	39.8	48.1	0.720
18-Nov-92 14:35	37.8	45.6	38.6	47.3	0.754
20-Nov-92 10:25	37.6	44.5	38.3	46.1	0.791
3-Mar-93 17:07	34.2	40.7	35.1	43.1	0.936a
14-Apr-93 11:41	38.0	46.2	b	49.5c	0.720
2-May-93 15:57	36.8	43.1	38.6	44.8	0.847
4-May-93 15:47	36.6	43.1	38.0	44.4	0.870
10-May-93 14:26	35.9	42.4	37.8	43.9	0.936a
13-May-93 11:57	35.5	42.8	37.6	44.3	0.936a
14-May-93 17:23	35.3	42.6	37.2	43.9	0.936a
14-May-93 22:31	b	b	38.2	44.6	0.936a
16-May-93 12:49	37.1	42.6	38.2	44.6	0.877
17-May-93 17:29	36.1	42.2	38.2	44.5d	0.911
22-May-93 11:58	35.8	41.6	37.1	44.2e	0.936a

Table A5.3 (continued). Water content and depth to water table data, site TD86.

Date and time	Water content (%) TDR waveguides				Depth to water table (m)
	86-01	86-02	86-03	86-04	
24-May-93 13:06	38.7 ^e	44.9 ^e	38.0	49.5 ^c	0.704
25-May-93 11:32	37.6	43.6	38.8	49.5 ^c	0.698
26-May-93 11:08	37.5	43.4	38.8	49.5 ^c	0.716
27-May-93 10:39	37.3	43.0	38.4	45.4	0.773
27-May-93 18:20	37.1	43.2	38.4	44.7	0.801
28-May-93 09:46	38.2	42.9	40.3	47.4	0.641
28-May-93 20:49	38.9	44.3	41.9	48.5	0.604
29-May-93 15:06	38.5	44.0	40.6	48.2	0.682
30-May-93 15:06	37.3	42.9	39.2	45.3	0.759
26-Aug-93 13:45	25.6	29.4	25.4	27.1	0.936 ^a
22-Sep-93 14:00	30.8	36.0	29.9	b	0.936 ^a

^a Minimum water table depth. Water table is below screen bottom. Depth to screen bottom is reported.

^b Wave forms were improperly stored. Data are not reported.

^c Wave forms were improperly stored. Soil horizon was entirely saturated. Average saturated water content reported.

^d Wave form was improperly stored. Datum is interpolated.

^e Wave form was improperly stored. Water content may be overestimated.

Table A5.4. Water content and depth to water table data, site TD87.

Date and time	Water content (%) TDR waveguides				Depth to water table (m)
	87-01	87-02	87-03	87-04	
31-Oct-92 15:44	24.4	40.2 ^a	41.3 ^b	46.6 ^c	0.618
3-Nov-92 11:14	27.6	47.0	45.8	46.2	0.375
4-Nov-92 13:05	28.3	47.5	46.1	46.3	0.342
5-Nov-92 13:26	27.6	46.6	46.0	46.4	0.437
7-Nov-92 11:12	27.3	43.9	45.6	46.6	0.497
9-Nov-92 12:01	26.5	40.8	43.0	46.5	0.599
11-Nov-92 09:31	28.2	46.5	44.9	46.4	0.371
12-Nov-92 10:12	27.0	45.1	44.9	46.8	0.440
13-Nov-92 15:34	29.7	48.3	45.1	46.6	0.300
14-Nov-92 14:35	29.1	47.7	44.5	46.7	0.388
15-Nov-92 15:17	28.8	46.7	44.5	46.6	0.430
16-Nov-92 15:36	27.8	45.4	44.4	46.6	0.453
17-Nov-92 14:55	27.6	43.8	43.9	46.2	0.493
18-Nov-92 14:44	26.9	43.0	43.4	46.5	0.537
20-Nov-92 10:36	26.4	41.2	42.2	46.7	0.563
3-Mar-93 17:13	22.7	35.9	38.1	47.0	0.754 ^d
14-Apr-93 11:52	28.1	43.1	43.9	46.9	0.485
2-May-93 16:05	25.2	39.3	41.1	47.0	0.620
4-May-93 16:08	25.1	39.4	40.5	46.9	0.629
10-May-93 14:39	24.7	38.4	40.1	46.6 ^c	0.655
13-May-93 12:09	21.8	38.3	39.9	46.9	0.689
14-May-93 17:30	24.0	38.0	41.2	47.0	0.695
14-May-93 22:34	25.8	39.3	40.9	47.1	0.604
15-May-93 13:10	24.3	39.3	40.8	46.4	0.620 ^e
16-May-93 12:55	21.9	38.6	40.5	46.6 ^c	0.654
17-May-93 17:34	22.0	f	f	f	0.675
22-May-93 12:05	21.6	38.1	40.0	46.0 ^g	0.705
25-May-93 11:38	23.7	f	f	f	0.552
26-May-93 11:15	23.5	f	f	f	0.546
27-May-93 10:44	22.9	39.9	41.0	46.8	0.593
27-May-93 18:26	22.4	39.9	40.9	46.7	0.607
28-May-93 09:46	23.9	43.8	42.4	46.8	0.422

Table A5.4 (continued). Water content and depth to water table data, site TD87.

Date and time	Water content (%) TDR waveguides				Depth to water table (m)
	87-01	87-02	87-03	87-04	
28-May-93 20:54	24.2	43.6	42.5	47.1	0.441
29-May-93 15:11	23.8	41.3	42.3	46.6 ^c	0.534
30-May-93 15:11	23.8	40.4	41.0	46.7	0.584
26-Aug-93 13:45	17.6	24.4	23.4	28.8	0.754 ^d
22-Sep-93 14:00	19.0	27.5	27.4	34.2	0.754 ^d

^a Soil moisture was affected by initial disturbance. Water content was calculated from regression with 87-01.

^b Soil moisture was affected by initial disturbance. Water content was calculated from regression with water table.

^c Wave form was improperly stored. Soil horizon was entirely saturated. Average saturated water content reported.

^d Minimum water table depth. Water table is below screen bottom. Depth to screen bottom is reported.

^e Interpolated water table.

^f Wave forms were improperly stored. Data are not reported.

^g Wave form was improperly stored. Water content was calculated from regression with water level.

Table A5.5. Water content and depth to water table data, site TD88.

Date and time	Water content (%) TDR waveguides				Depth to water table (m)
	88-01	88-02	88-03	88-04	
31-Oct-92 15:35	31.3a	47.5	46.6a	46.1	0.534
3-Nov-92 11:05	36.1	52.0	49.4	47.9	0.284
4-Nov-92 13:13	36.6	52.7	50.0	47.7	0.262
5-Nov-92 13:33	35.2	50.4	49.1	47.8	0.340
7-Nov-92 11:22	33.7	50.1	48.0	47.8	0.395
9-Nov-92 12:12	33.4	49.7	47.8	48.0	0.458
11-Nov-92 09:38	37.3	52.1	50.4	47.9	0.305
12-Nov-92 10:17	35.1	50.5	50.4	47.6	0.358
13-Nov-92 15:40	39.4	52.3	50.6	48.2	0.276
14-Nov-92 14:41	38.4	50.6	50.6	47.8	0.330
15-Nov-92 15:22	37.3	50.2	50.5	47.8	0.359
16-Nov-92 15:44	36.4	50.2	48.2	47.9	0.368
17-Nov-92 15:02	36.1	50.1	47.9	47.9	0.399
18-Nov-92 14:52	35.9	49.8	47.5	47.9	0.404
20-Nov-92 10:46	35.2	48.9	47.5	47.9	0.444
3-Mar-93 17:23	24.7	42.1	41.9	41.4	0.810b
14-Apr-93 12:02	36.8	49.8	48.2	45.9	0.409
2-May-93 16:16	34.7	48.2	47.6	46.8	0.525
4-May-93 16:18	34.6	47.6	47.3	44.5	0.572
10-May-93 14:52	31.5	45.9	45.6	43.8	0.810b
13-May-93 12:16	31.1	45.2	45.7	44.0	0.810b
14-May-93 17:36	32.7	44.6	45.8	44.1	0.810b
14-May-93 23:46	34.7	45.6	45.7	44.1	0.810b
16-May-93 13:01	33.6	45.6	46.7c	44.2	0.637
17-May-93 17:39	32.7	d	d	d	0.695
22-May-93 12:11	30.4	45.1c	46.0c	44.2c	0.810b
24-May-93 13:17	37.0c	47.6c	47.7c	45.5c	0.632
25-May-93 11:44	36.1	d	d	d	0.385
26-May-93 11:21	35.5	d	d	d	0.431
27-May-93 10:48	34.8	47.5	46.5	45.9	0.537
27-May-93 18:32	34.2	46.9	46.4	44.1	0.565
28-May-93 09:50	38.0	49.7	49.9	48.4	0.312
28-May-93 20:58	36.9	49.0	48.1	48.0	0.359

Table A5.5 (continued). Water content and depth to water table data, site TD88.

Date and time	Water content (%) TDR waveguides				Depth to water table (m)
	88-01	88-02	88-03	88-04	
29-May-93 15:17	34.5	48.8 ^c	47.6 ^e	46.3 ^e	0.438
30-May-93 15:16	34.7	47.7	46.9	45.5	0.530
26-Aug-93 13:45	25.8	34.6 ^c	32.8 ^c	31.0 ^c	0.810 ^b
22-Sep-93 14:00	25.7	38.3	37.9	35.0	0.810 ^b

^a Soil moisture was affected by initial disturbance. Water content was calculated from regression with 88-02.

^b Minimum water table depth. Water table is below screen bottom. Depth to screen bottom is reported.

^c Wave forms were improperly stored. Water contents may be overestimated.

^d Wave forms were improperly stored. Data are not reported.

^e Wave forms were improperly stored. Data are interpolated.

Table A5.6. Water content and depth to water table data, site TD74.

Date and time	Water content (%) TDR waveguides				Depth to water table (m)
	74-01	74-02	74-03	74-04	
11-Oct-92 09:41	34.8	a	a	32.6	0.921 ^b
13-Oct-92 12:06	34.5	45.1	38.4	32.5	0.921 ^b
13-Oct-92 18:39	35.5	45.2	38.4	32.8	0.921 ^b
17-Oct-92 15:28	52.9	56.1	53.5	51.5	0.232
20-Oct-92 13:19	50.9	52.6	53.3	52.0	0.469
27-Oct-92 10:21	50.0	53.0	53.4	53.0	0.512
31-Oct-92 16:45	43.1	50.1	46.7	50.9	0.765
3-Nov-92 12:34	52.3	56.0	53.0	52.2	0.099
7-Nov-92 12:39	51.3	55.4	52.7	52.6	0.306
9-Nov-92 13:34	49.2	52.1	52.2	52.6	0.564
17-Nov-92 16:05	51.7	55.8	51.7	52.9	0.293
14-Apr-93 13:23	51.9	55.1	52.1	53.5	0.303
2-May-93 14:10	44.0	49.9	46.8	51.2	0.740
4-May-93 11:08	41.5	49.2	46.0	46.7	0.779
10-May-93 13:24	39.6	47.9	43.9	41.8	0.921 ^b
13-May-93 11:02	38.8	47.8	43.5	41.0	0.921 ^b
16-May-93 14:05	39.8	48.4	43.9	41.6	0.921 ^b
17-May-93 18:25	39.6	48.3	43.5	41.1	0.921 ^b
22-May-93 13:05	38.6	47.7 ^c	42.7	40.2	0.921 ^b
24-May-93 13:58	51.1	55.0 ^c	52.5	51.9	0.218
25-May-93 12:28	49.8	51.8	52.4	52.0	0.346
26-May-93 12:05	49.2	51.4	51.5	51.9	0.433
27-May-93 11:30	47.6	50.8	50.2	51.7	0.571
28-May-93 11:34	53.7	54.9	51.5	52.3	0.124
29-May-93 16:00	49.5	51.8 ^c	51.5	52.4	0.382
30-May-93 15:55	46.9	50.9	49.6	52.2	0.584
26-Aug-93 13:15	26.8	38.1 ^c	30.4	23.9	0.921 ^b
22-Sep-93 13:00	32.0	42.2	36.3	27.6	0.921 ^b

a Wave forms were improperly stored. Data are not reported.

b Minimum water table depth. Water table is below screen bottom. Depth to screen bottom is reported.

c Wave forms were improperly stored. Water contents may be overestimated.

Table A5.7. Water content and depth to water table data, site TD2.

Date and time	Water content (%) TDR waveguides			Depth to water table (m)
	2-01	2-02	2-03	
10-Oct-92 10:51	47.5	52.7	53.0	0.447
13-Oct-92 10:38	47.6	52.8	52.7	0.445
13-Oct-92 17:26	47.7	52.9	52.9	0.432
16-Oct-92 14:10	48.7	54.3	55.4	0.279
17-Oct-92 17:35	48.6	54.2	54.2	0.323
20-Oct-92 15:51	48.1	53.8	53.4	0.383
27-Oct-92 12:46	47.9	53.5	53.1 ^a	0.408
2-Nov-92 09:49	47.4	53.2	53.0	0.441
3-Nov-92 15:18	48.6	54.6	55.7	0.263
4-Nov-92 15:55	48.8	54.5	55.6	0.265
5-Nov-92 15:53	48.6	54.3	54.8	0.320
7-Nov-92 15:06	48.3	54.1	53.8	0.370
9-Nov-92 15:26	47.9	53.9	53.7	0.393
14-Apr-93 16:42	48.9	55.9	55.7	0.180
2-May-93 16:51	47.8	53.9	54.1	0.433
10-May-93 17:23	47.3	53.4	53.2	0.364
14-May-93 20:16	49.1	54.0	55.3	0.266
16-May-93 17:10	47.9	53.5	53.6	0.374
17-May-93 19:18	47.9	53.5	53.5	0.390
22-May-93 14:46	47.4	53.5	52.8	0.403
24-May-93 11:24	48.4	54.5	55.9	0.280
25-May-93 14:21	48.2	54.5	54.8	0.333
26-May-93 15:10	47.8	54.3 ^a	54.1 ^a	0.355
27-May-93 12:41	47.8	54.1	53.5	0.373
28-May-93 12:43	48.6	54.6	55.8	0.298
30-May-93 16:38	47.9	54.1	54.3	0.380
25-Aug-93 12:07	45.0	50.0	50.0	0.698
21-Sep-93 12:48	45.4	51.6	50.6	0.537

^a Wave forms were improperly stored. Data are interpolated.

Table A5.8. Water content and depth to water table data, site TD3.

Date and time	Water content (%) TDR waveguides			Depth to water table (m)
	3-01	3-02	3-03	
10-Oct-92 10:40	42.7	34.2	42.6	0.828
13-Oct-92 10:43	42.6	33.8	42.2	0.852
13-Oct-92 17:30	41.5a	33.8	42.1	0.844
16-Oct-92 14:06	45.4	36.3	43.5	0.620
17-Oct-92 17:31	44.3	36.6	43.7	0.658
20-Oct-92 15:47	43.8	35.7	43.4	0.744
27-Oct-92 12:40	43.6	35.6	43.5	0.758
2-Nov-92 09:45	41.7	33.5	41.4	0.912
3-Nov-92 15:14	45.3	37.0	45.2	0.653
4-Nov-92 15:49	45.0	37.3	45.2	0.637
5-Nov-92 15:48	44.7	36.6	44.5	0.695
7-Nov-92 15:00	44.2	36.0	44.0	0.707
9-Nov-92 15:21	43.8	35.0	43.9	0.753
14-Apr-93 16:48	45.8	43.1	45.4	0.454
2-May-93 16:43	43.5	37.2	43.8	0.584
10-May-93 17:28	43.0	35.9	43.5	0.644
13-May-93 14:02	42.9	b	b	0.675
14-May-93 20:26	45.0	36.0	43.9	0.623
16-May-93 17:15	43.6	36.7	43.9	0.645
17-May-93 19:23	43.5	36.1	43.8	0.674
22-May-93 14:50	42.7	34.7	43.0	0.702
24-May-93 11:28	45.0	37.4	45.1	0.518
25-May-93 14:25	43.9	36.7	44.2	0.560
26-May-93 15:14	43.7	36.2	44.0	0.618
27-May-93 12:46	43.4	35.9	43.9	0.639
28-May-93 12:47	44.6	37.9	45.4	0.508
30-May-93 16:43	43.4	35.9	43.8	0.647
25-Aug-93 12:12	36.5	28.9	39.3	1.070
21-Sep-93 12:51	39.2	30.9	40.5	0.906

a Wave form was improperly stored. Water content may be overestimated.

b Wave forms were improperly stored. Data are not reported.

Table A5.9. Water content and depth to water table data, site TD4.

Date and time	Water content (%) TDR waveguides			Depth to water table (m)
	4-01	4-02	4-03	
10-Oct-92 10:31	36.5	42.9	43.0	0.688
13-Oct-92 10:48	36.2	42.3	42.8	0.728
13-Oct-92 17:34	35.4	a	a	0.726
16-Oct-92 14:02	40.1	45.6	43.8	0.355
17-Oct-92 17:27	41.9	45.6	43.9	0.375
20-Oct-92 15:43	38.9	44.1	43.9	0.502
27-Oct-92 12:37	38.3	44.2	43.8	0.531
2-Nov-92 09:40	36.3	42.8	43.2	0.750
3-Nov-92 15:10	45.9	45.9	43.8	0.348
4-Nov-92 15:44	45.0	45.9	44.0	0.338
5-Nov-92 15:44	42.6	45.6	43.9	0.421
7-Nov-92 14:55	40.4	45.0	44.0	0.446
9-Nov-92 15:16	39.0	44.7	44.0	0.498
14-Apr-93 16:54	47.2	46.0	43.5	0.221
2-May-93 16:33	42.6	46.0	43.9	0.312
10-May-93 17:39	40.8	45.1	44.1	0.403
14-May-93 20:36	40.5	45.4	44.0	0.322
16-May-93 17:21	40.2	45.1	44.2	0.419
17-May-93 19:26	40.0	44.8	44.2	0.451
22-May-93 14:55	37.3	44.2	43.9	0.522
24-May-93 11:32	43.5	45.9	43.8	0.241
25-May-93 14:30	43.1	45.9	43.9	0.296
26-May-93 15:19	41.5	45.5 ^b	44.1	0.335
27-May-93 12:51	40.2	44.9	44.0	0.394
28-May-93 12:50	46.4	46.2	43.9	0.201
30-May-93 16:43	40.0	a	43.8	0.408
25-Aug-93 12:12	28.8	34.7	36.2	1.175
21-Sep-93 12:51	33.7	40.3	40.2	0.965

^a Wave forms were improperly stored. Data are not reported.

^b Wave form was improperly stored. Soil horizon was entirely saturated. Average saturated water content reported.

Table A5.10. Water content and depth to water table data, site TD5.

Date and time	Water content (%) TDR waveguides			Depth to water table (m)
	5-01	5-02	5-03	
10-Oct-92 10:20	28.2	31.5	28.5	1.656
13-Oct-92 10:52	27.6	31.5	26.3	1.796a
13-Oct-92 17:38	27.3	31.2	26.4	1.809a
16-Oct-92 13:57	32.2	32.9	27.8	1.560
17-Oct-92 17:23	30.8	33.9	29.4	1.595
20-Oct-92 15:37	30.0	33.7	29.7	1.564
27-Oct-92 12:33	30.1	33.8	29.6	1.559
2-Nov-92 09:33	28.1	30.3	27.3	1.700
3-Nov-92 15:04	31.2	33.4	30.2	1.492
4-Nov-92 15:36	31.5	35.7	31.7	1.442
5-Nov-92 15:39	31.3	36.4	32.5	1.446
7-Nov-92 14:50	30.8	35.5	31.9	1.444
9-Nov-92 15:10	30.0	33.7	30.9	1.463
14-Apr-93 17:01	35.1	41.0	35.4	1.092
2-May-93 16:24	32.2	37.6	33.9	1.010
10-May-93 17:45	31.3	35.9	33.6	1.124
13-May-93 14:21	31.2b	34.7	32.6	1.178
14-May-93 20:46	31.1	34.4	32.1	1.142
16-May-93 17:25	30.0	35.0	32.8	1.186
17-May-93 19:30	29.7	34.7	32.1	1.216
24-May-93 11:36	30.6	33.0	29.9	1.125
25-May-93 14:36	29.8	34.5	31.5	1.160
26-May-93 15:24	29.9	35.0	32.1	1.165
27-May-93 12:55	29.4	34.4	31.7	1.208
28-May-93 12:55	30.8	36.1	32.6	1.060
29-May-93 17:09	30.8	36.0	33.0	1.156
30-May-93 16:49	30.3	35.1	32.6	1.175
25-Aug-93 12:22	20.6	23.1c	19.1	1.929
21-Sep-93 12:58	24.0	27.7	25.7	1.877

a Water levels were disturbed by pumping. Water levels are extrapolated from measurements taken on October 10 and 12, 1992.

b Wave form was improperly stored. Datum is interpolated.

c Wave form was improperly stored. Water content may be overestimated.

Appendix 6

Water storage data

Table A6.1. Water storage, site TD81.

Date and time	Water storage (mm)				Total
	81-01	81-02	81-03	81-04	
17-Oct-92 16:03	51.8	76.2	115.0	360.7	603.8
20-Oct-92 12:50	50.9	74.3	112.2	360.7	598.1
27-Oct-92 09:38	51.2	75.2	112.8	360.7	599.9
31-Oct-92 15:07	47.6	74.1	111.2	360.4	593.3
3-Nov-92 12:00	52.9	80.9	130.7	360.7	625.2
4-Nov-92 13:35	54.2	79.6	129.9	360.7	624.5
5-Nov-92 12:46	52.6	79.0	128.7	360.7	621.0
7-Nov-92 12:04	51.0	77.3	117.5	360.7	606.5
9-Nov-92 12:51	49.9	76.0	115.5	360.7	602.1
11-Nov-92 10:13	54.1	79.6	128.7	360.7	623.1
12-Nov-92 10:47	52.8	77.7	123.5	360.7	614.7
13-Nov-92 15:57	65.8	83.8	129.6	360.7	639.9
14-Nov-92 15:10	64.1	82.5	129.5	360.5	636.6
15-Nov-92 16:00	62.0	80.4	128.6	360.2	631.2
16-Nov-92 16:13	59.8	79.6	125.1	359.8	624.3
17-Nov-92 15:30	57.0	78.7	119.9	360.0	615.6
18-Nov-92 15:14	54.5	77.8	118.4	360.1	610.7
20-Nov-92 11:02	51.4	76.6	117.5	360.0	605.5
3-Mar-93 16:23	39.0	68.1	99.1	350.1	556.2
14-Apr-93 12:45	54.9	79.3	116.3	360.7	611.2
2-May-93 15:04	50.0	75.1	112.3	360.7	598.1
4-May-93 12:59	48.6	74.7	111.5	360.6	595.3
10-May-93 13:53	47.8	73.1	109.2	359.9	590.0
13-May-93 11:23	48.3	72.7	109.2	360.1	590.2
16-May-93 13:18	48.4	73.2	110.5	360.0	592.0
22-May-93 12:29	44.1	71.0	104.7	357.3	577.1
24-May-93 13:34	50.6	75.1	110.2	360.7	596.7
25-May-93 11:57	48.6	74.5	110.0	360.7	593.8
26-May-93 11:38	48.2	74.4	109.3	360.7	592.6
27-May-93 11:01	46.9	74.0	108.1	360.3	589.2
28-May-93 11:09	52.1	76.3	114.1	360.7	603.2
29-May-93 15:36	48.8	75.7	113.0	360.7	598.2
30-May-93 15:30	47.3	73.6	110.2	359.8	590.8
26-Aug-93 13:25	34.1	55.4	79.5	248.8	417.9
22-Sep-93 14:00	36.9	62.0	87.4	287.4	473.8

Table A6.2. Water storage, site TD82.

Date and time	Water storage (mm)				Total
	82-01	82-02	82-03	82-04	
31-Oct-92 14:57	66.6	53.8	50.3	273.6	444.4
3-Nov-92 11:49	70.1	55.2	53.0	294.9	473.1
4-Nov-92 13:40	71.1	55.8	55.7	304.1	486.5
5-Nov-92 12:50	69.7	55.3	54.9	295.3	475.3
7-Nov-92 12:08	68.6	55.1	54.5	290.4	468.6
9-Nov-92 12:58	67.9	54.6	54.3	283.4	460.2
11-Nov-92 10:17	70.7	56.1	54.8	295.5	477.0
12-Nov-92 10:53	69.4	55.7	54.8	288.3	468.2
13-Nov-92 16:03	83.5	63.0	71.8	304.2	522.5
14-Nov-92 15:14	79.8	60.5	59.6	304.2	504.1
15-Nov-92 16:04	78.6	59.4	57.2	299.6	494.9
16-Nov-92 16:26	76.8	58.5	56.3	294.4	486.0
17-Nov-92 15:41	74.1	58.2	55.6	291.8	479.6
18-Nov-92 15:21	73.6	57.3	55.5	290.4	476.8
20-Nov-92 11:14	71.2	57.2	54.2	287.7	470.3
3-Mar-93 16:34	56.6	48.0	44.7	247.9	397.2
14-Apr-93 12:57	75.7	58.8	56.1	298.4	489.0
2-May-93 15:25	69.0	56.5	53.6	288.7	467.8
4-May-93 13:13	68.3	55.9	53.6	286.3	464.1
10-May-93 13:59	65.5	54.1	51.9	267.3	438.7
13-May-93 11:32	1	1	52.7	264.1	2
16-May-93 13:24	65.7	53.8	1	263.7	2
17-May-93 18:03	1	1	1	262.7	2
22-May-93 12:35	61.7	50.8	49.2	256.1	417.8
24-May-93 13:40	67.8	53.5	50.4	264.5	436.2
25-May-93 12:04	65.2	53.0	50.2	263.2	431.6
26-May-93 11:46	64.7	52.8	50.3	263.8	431.6
27-May-93 11:06	63.4	52.8	49.9	263.2	429.3
28-May-93 11:14	67.9	53.8	50.5	277.9	450.1
29-May-93 15:41	1	1	50.4	281.8	2
30-May-93 15:38	67.1	54.2	50.9	282.9	455.1
26-Aug-93 13:25	37.3	28.3	29.6	194.1	289.3
22-Sep-93 14:00	53.2	44.2	41.7	206.9	345.9

- ¹ Wave forms improperly stored. Water content data not reported. Water storage not calculated.**
- ² Water storage not reported for one or more horizons. Total water storage not calculated.**

Table A6.3. Water storage, site TD86.

Date and time	Water storage (mm)				
	86-01	86-02	86-03	86-04	Total
9-Oct-92 16:15	46.1	105.9	102.3	137.9	392.2
13-Oct-92 13:28	44.8	105.4	103.7	141.9	395.8
13-Oct-92 18:24	46.0	105.5	103.1	139.8	394.4
17-Oct-92 16:40	52.0	110.9	128.6	168.1	459.6
20-Oct-92 12:13	50.3	109.3	116.0	167.3	442.8
27-Oct-92 09:07	50.4	110.0	117.2	167.3	444.8
31-Oct-92 15:54	48.0	107.0	109.6	163.9	428.5
3-Nov-92 11:21	53.3	120.6	156.4	168.1	498.5
4-Nov-92 12:55	52.6	117.4	152.9	168.1	491.0
5-Nov-92 13:15	51.4	115.8	140.9	168.1	476.2
7-Nov-92 11:03	50.5	112.2	123.4	168.1	454.1
9-Nov-92 11:54	49.1	110.5	118.2	165.6	443.4
11-Nov-92 09:24	53.6	116.6	155.4	168.1	493.7
12-Nov-92 10:04	50.9	114.1	137.3	168.1	470.4
13-Nov-92 15:28	62.9	138.8	156.4	168.1	526.2
14-Nov-92 14:27	60.0	131.5	151.0	168.1	510.6
15-Nov-92 15:10	57.0	124.3	142.0	168.1	491.5
16-Nov-92 15:30	55.3	120.2	131.8	168.1	475.4
17-Nov-92 14:45	54.7	118.0	128.5	168.1	469.2
18-Nov-92 14:35	52.7	116.2	124.4	167.3	460.6
20-Nov-92 10:25	52.4	113.4	123.2	166.0	455.0
3-Mar-93 17:07	47.8	102.5	115.2	155.0	420.4
14-Apr-93 11:41	53.1	117.7	1	1	2
2-May-93 15:57	51.4	108.2	126.5	163.4	449.4
4-May-93 15:47	51.1	108.2	124.7	162.2	446.2
10-May-93 14:26	50.2	106.6	124.2	156.6	437.6
13-May-93 11:57	49.6	107.5	123.2	157.3	437.6
14-May-93 17:23	49.3	107.0	122.1	156.6	435.0
14-May-93 22:31	1	1	125.1	157.8	2
16-May-93 12:49	51.8	107.1	125.2	162.1	446.1
17-May-93 17:29	50.4	106.0	125.1	160.8	442.4
22-May-93 11:58	49.9	104.5	121.7	157.3	433.4
24-May-93 13:06	54.0	112.7	126.9	168.1	461.7
25-May-93 11:32	52.5	109.6	129.4	168.1	459.6
26-May-93 11:08	52.3	109.1	127.9	168.1	457.4

Table A6.3 (continued). Water storage, site TD86.

Date and time	Water storage (mm)				
	86-01	86-02	86-03	86-04	Total
27-May-93 10:39	52.1	108.1	126.1	166.2	452.5
27-May-93 18:20	51.9	108.4	126.0	165.0	451.2
28-May-93 09:46	53.3	107.6	137.1	168.1	466.2
28-May-93 20:49	54.4	111.3	141.9	168.1	475.7
29-May-93 15:06	53.8	110.5	134.8	168.1	467.2
30-May-93 15:06	52.1	107.7	128.6	166.6	455.0
26-Aug-93 13:45	35.7	74.2	83.0	101.6	294.5
22-Sep-93 14:00	43.0	90.8	97.8	1	2

¹ Wave forms improperly stored. Water content data not reported. Water storage not calculated.

² Water storage not reported for one or more horizons. Total water storage not calculated.

Table A6.4. Water storage, site TD87.

Date and time	Water storage (mm)				
	87-01	87-02	87-03	87-04	Total
31-Oct-92 15:44	52.0	67.0	120.1	107.3	346.5
3-Nov-92 11:14	58.7	78.6	125.7	107.3	370.4
4-Nov-92 13:05	60.1	79.3	125.7	107.3	372.5
5-Nov-92 13:26	58.7	78.0	125.7	107.3	369.7
7-Nov-92 11:12	58.1	73.5	125.7	107.3	364.6
9-Nov-92 12:01	56.4	68.2	122.8	107.3	354.6
11-Nov-92 09:31	59.9	77.9	125.7	107.3	370.8
12-Nov-92 10:12	57.5	75.4	125.4	107.3	365.6
13-Nov-92 15:34	63.1	81.0	125.7	107.3	377.1
14-Nov-92 14:35	61.8	79.6	125.7	107.3	374.5
15-Nov-92 15:17	61.1	78.1	125.5	107.3	372.1
16-Nov-92 15:36	59.0	75.9	125.1	107.3	367.4
17-Nov-92 14:55	58.6	73.3	124.6	107.3	363.7
18-Nov-92 14:44	57.1	71.9	123.8	107.3	360.2
20-Nov-92 10:36	56.2	68.8	122.2	107.3	354.5
3-Mar-93 17:13	48.4	59.7	110.0	107.3	325.5
14-Apr-93 11:52	59.7	72.0	124.6	107.3	363.6
2-May-93 16:05	53.6	65.6	117.8	107.3	344.3
4-May-93 16:08	53.4	65.7	116.7	107.3	343.1
10-May-93 14:39	52.7	64.1	115.1	107.3	339.2
13-May-93 12:09	46.4	63.8	114.2	107.3	331.8
14-May-93 17:30	51.0	63.4	117.4	107.3	339.2
14-May-93 22:34	54.9	65.6	118.0	107.3	345.9
15-May-93 13:10	51.7	65.6	117.4	107.3	342.0
16-May-93 12:55	46.5	64.3	115.8	107.3	334.0
17-May-93 17:34	46.8	1	1	1	2
22-May-93 12:05	45.8	63.5	114.4	107.1	330.8
25-May-93 11:38	50.3	1	1	107.3	2
26-May-93 11:15	49.9	1	1	107.3	2
27-May-93 10:44	48.5	66.5	118.5	107.3	340.8
27-May-93 18:26	47.6	66.6	118.0	107.3	339.5
28-May-93 09:46	50.7	73.2	124.7	107.3	355.9
28-May-93 20:54	51.4	72.9	124.0	107.3	355.6
29-May-93 15:11	50.4	68.9	121.7	107.3	348.3
30-May-93 15:11	50.5	67.5	118.7	107.3	344.0

Table A6.4 (continued). Water storage, site TD87.

Date and time	Water storage (mm)				
	87-01	87-02	87-03	87-04	Total
26-Aug-93 13:45	37.4	40.2	67.9	70.7	216.2
22-Sep-93 14:00	40.5	45.6	79.0	83.3	248.4

¹ Wave forms improperly stored. Water content data not reported. Water storage not calculated.

² Water storage not reported for one or more horizons. Total water storage not calculated.

Table A6.5. Water storage, site TD88.

Date and time	Water storage (mm)				Total
	88-01	88-02	88-03	88-04	
31-Oct-92 15:35	37.1	107.8	109.2	225.2	479.2
3-Nov-92 11:05	42.8	118.2	115.2	225.2	501.3
4-Nov-92 13:13	43.5	118.6	115.2	225.2	502.5
5-Nov-92 13:33	41.8	114.9	115.2	225.2	497.0
7-Nov-92 11:22	39.9	113.8	114.1	225.2	493.0
9-Nov-92 12:12	39.6	113.0	112.5	225.2	490.3
11-Nov-92 09:38	44.3	118.1	115.2	225.2	502.8
12-Nov-92 10:17	41.5	114.7	115.0	225.2	496.4
13-Nov-92 15:40	46.6	118.7	115.2	225.2	505.6
14-Nov-92 14:41	45.5	115.4	115.2	225.2	501.2
15-Nov-92 15:22	44.1	114.1	115.0	225.2	498.4
16-Nov-92 15:44	43.0	114.2	114.7	225.2	497.1
17-Nov-92 15:02	42.7	113.8	113.9	225.2	495.5
18-Nov-92 14:52	42.4	113.1	113.8	225.2	494.5
20-Nov-92 10:46	41.6	111.2	112.6	225.2	490.6
3-Mar-93 17:23	29.3	95.6	96.8	195.4	417.1
14-Apr-93 12:02	43.8	113.2	113.7	225.2	495.9
2-May-93 16:16	41.3	109.6	110.7	225.2	486.8
4-May-93 16:18	41.2	108.0	109.2	225.2	483.6
10-May-93 14:52	37.5	104.2	105.4	207.0	454.2
13-May-93 12:16	37.0	102.6	105.5	207.7	452.9
14-May-93 17:36	39.0	101.1	105.7	207.7	453.5
14-May-93 23:46	41.4	103.6	105.5	207.8	458.3
16-May-93 13:01	40.0	103.5	107.9	223.1	474.4
17-May-93 17:39	38.9	1	1	220.9	2
22-May-93 12:11	36.2	102.5	106.2	215.6	460.5
24-May-93 13:17	44.1	108.1	109.5	223.5	485.2
25-May-93 11:44	43.0	1	114.3	225.2	2
26-May-93 11:21	42.3	1	113.1	225.2	2
27-May-93 10:48	41.4	107.8	109.0	225.2	483.4
27-May-93 18:32	40.7	106.5	108.0	225.2	480.4
28-May-93 09:50	45.3	114.6	115.2	225.2	500.2
28-May-93 20:58	44.0	112.0	115.0	225.2	496.1
29-May-93 15:17	41.7	111.5	112.8	225.2	491.1
30-May-93 15:16	40.6	109.0	109.6	225.2	484.4

Table A6.5 (continued). Water storage, site TD88.

Date and time	Water storage (mm)				
	88-01	88-02	88-03	88-04	Total
26-Aug-93 13:45	30.7	78.2	75.9	146.5	331.3
22-Sep-93 14:00	30.5	86.8	87.6	165.4	370.3

¹ Wave forms improperly stored. Water content data not reported. Water storage not calculated.

² Water storage not reported for one or more horizons. Total water storage not calculated.

Table A6.6. Water storage, site TD74.

Date and time	Water storage (mm)				
	74-01	74-02	74-03	74-04	Total
11-Oct-92 09:41	85.3	1	1	177.9	2
13-Oct-92 12:06	84.6	67.6	46.1	177.2	375.4
13-Oct-92 18:39	86.9	67.8	46.1	178.9	379.6
17-Oct-92 15:28	130.3	83.3	62.7	266.7	543.0
20-Oct-92 13:19	125.5	78.8	62.6	266.7	533.6
27-Oct-92 10:21	123.3	79.4	62.7	266.7	532.0
31-Oct-92 16:45	106.0	75.1	56.0	252.3	489.4
3-Nov-92 12:34	131.6	83.3	62.7	266.7	544.3
7-Nov-92 12:39	126.5	82.4	62.7	266.7	538.3
9-Nov-92 13:34	121.2	78.0	62.7	265.8	527.7
17-Nov-92 16:05	127.6	82.7	62.7	266.7	539.6
14-Apr-93 13:23	127.9	82.5	62.7	266.7	539.8
2-May-93 14:10	108.2	74.8	56.2	253.2	492.4
4-May-93 11:08	101.8	73.8	55.2	242.1	472.9
10-May-93 13:24	97.2	71.8	52.6	221.7	443.3
13-May-93 11:02	95.2	71.6	52.2	218.4	437.5
16-May-93 14:05	97.7	72.5	52.7	220.9	443.8
17-May-93 18:25	97.2	72.4	52.2	218.7	440.4
22-May-93 13:05	94.7	71.4	51.2	214.8	432.1
24-May-93 13:58	126.4	83.3	62.7	266.7	539.1
25-May-93 12:28	122.8	79.6	62.7	266.7	531.8
26-May-93 12:05	121.1	77.1	62.7	266.7	527.5
27-May-93 11:30	117.1	76.2	60.2	265.5	519.1
28-May-93 11:34	130.6	83.3	62.7	266.7	543.3
29-May-93 16:00	122.0	78.3	62.7	266.7	529.7
30-May-93 15:55	115.4	76.2	59.5	265.0	516.2
26-Aug-93 13:15	65.1	57.1	36.5	133.7	292.4
22-Sep-93 13:00	78.2	63.3	43.6	152.3	337.3

¹ Wave forms improperly stored. Water content data not reported. Water storage not calculated.

² Water storage not reported for one or more horizons. Total water storage not calculated.

Table A6.7. Water storage, site TD2.

Date and time	Water storage (mm)			
	2-01	2-02	2-03	Total
10-Oct-92 10:51	61.6	58.0	417.6	537.2
13-Oct-92 10:38	61.7	58.1	417.3	537.2
13-Oct-92 17:26	61.9	58.3	417.7	537.9
16-Oct-92 14:10	63.2	59.8	421.2	544.1
17-Oct-92 17:35	63.1	59.6	420.4	543.1
20-Oct-92 15:51	62.4	59.2	419.0	540.6
27-Oct-92 12:46	62.2	58.9	418.4	539.5
2-Nov-92 09:49	61.5	58.6	417.7	537.8
3-Nov-92 15:18	63.0	60.1	421.3	544.4
4-Nov-92 15:55	63.3	60.0	421.3	544.5
5-Nov-92 15:53	63.1	59.7	420.8	543.6
7-Nov-92 15:06	62.6	59.6	419.6	541.8
9-Nov-92 15:26	62.2	59.3	419.2	540.7
14-Apr-93 16:42	63.5	61.3	421.5	546.2
2-May-93 16:51	62.0	59.3	419.3	540.5
10-May-93 17:23	61.3	58.7	419.2	539.2
14-May-93 20:16	63.7	59.5	421.3	544.4
16-May-93 17:10	62.1	58.9	419.4	540.3
17-May-93 19:18	62.1	58.9	419.0	540.0
22-May-93 14:46	61.5	58.9	418.2	538.5
24-May-93 11:24	62.8	60.0	421.1	544.0
25-May-93 14:21	62.5	60.0	420.7	543.2
26-May-93 15:10	62.0	1	1	2
27-May-93 12:41	61.9	59.5	419.3	540.8
28-May-93 12:43	63.0	60.1	420.9	544.0
30-May-93 16:38	62.0	59.6	419.9	541.5
25-Aug-93 12:07	58.3	55.0	405.2	518.6
21-Sep-93 12:48	58.9	56.9	412.0	527.7

¹ Wave forms improperly stored. Water content data not reported. Water storage not calculated.

² Water storage not reported for one or more horizons. Total water storage not calculated.

Table A6.8. Water storage, site TD3.

Date and time	Water storage (mm)			
	3-01	3-02	3-03	Total
10-Oct-92 10:40	131.5	71.0	210.1	412.6
13-Oct-92 10:43	131.1	70.3	209.0	410.5
13-Oct-92 17:30	127.8	70.2	208.9	406.9
16-Oct-92 14:06	139.7	75.8	213.1	428.7
17-Oct-92 17:31	136.5	76.1	213.0	425.6
20-Oct-92 15:47	134.9	74.3	212.2	421.4
27-Oct-92 12:40	134.7	74.0	212.2	420.9
2-Nov-92 09:45	128.3	69.6	206.4	404.3
3-Nov-92 15:14	139.4	77.1	214.5	431.0
4-Nov-92 15:49	138.6	77.5	214.5	430.6
5-Nov-92 15:48	137.7	76.1	213.8	427.7
7-Nov-92 15:00	136.0	74.8	213.2	424.0
9-Nov-92 15:21	134.9	72.8	212.9	420.5
14-Apr-93 16:48	140.9	86.3	214.6	441.8
2-May-93 16:43	133.7	77.3	214.1	425.0
10-May-93 17:28	132.2	74.6	213.0	419.8
13-May-93 14:02	131.9	1	1	2
14-May-93 20:26	137.1	75.0	213.5	425.5
16-May-93 17:15	133.0	76.4	213.4	422.7
17-May-93 19:23	132.8	75.1	213.0	420.9
22-May-93 14:50	130.3	72.1	211.8	414.2
24-May-93 11:28	138.3	78.3	214.6	431.2
25-May-93 14:25	134.9	76.2	214.4	425.5
26-May-93 15:14	134.4	75.2	213.6	423.2
27-May-93 12:46	133.5	73.6	213.4	420.4
28-May-93 12:47	137.0	79.8	214.6	431.5
30-May-93 16:43	133.4	74.7	213.2	421.2
25-Aug-93 12:12	112.2	59.9	197.3	369.3
21-Sep-93 12:51	120.5	64.3	203.6	388.3

¹ Wave forms improperly stored. Water content data not reported. Water storage not calculated.

² Water storage not reported for one or more horizons. Total water storage not calculated.

Table A6.9. Water storage, site TD4.

Date and time	Water storage (mm)			Total
	4-01	4-02	4-03	
10-Oct-92 10:31	133.4	85.8	181.6	400.8
13-Oct-92 10:48	132.3	84.5	181.4	398.3
13-Oct-92 17:34	129.1	1	1	2
16-Oct-92 14:02	148.8	91.0	182.7	422.5
17-Oct-92 17:27	153.8	91.0	182.7	427.5
20-Oct-92 15:43	142.7	89.0	182.7	414.3
27-Oct-92 12:37	140.2	88.7	182.7	411.6
2-Nov-92 09:40	132.8	85.5	181.8	400.1
3-Nov-92 15:10	164.8	91.0	182.7	438.5
4-Nov-92 15:44	163.7	91.0	182.7	437.4
5-Nov-92 15:44	156.3	90.6	182.7	429.5
7-Nov-92 14:55	148.3	90.3	182.7	421.3
9-Nov-92 15:16	142.9	89.7	182.7	415.2
14-Apr-93 16:54	165.2	91.0	182.7	438.9
2-May-93 16:33	158.6	91.0	182.7	432.3
10-May-93 17:39	149.8	90.8	182.7	423.3
14-May-93 20:36	151.8	91.0	182.7	425.5
16-May-93 17:21	147.5	90.6	182.7	420.8
17-May-93 19:26	146.7	90.2	182.7	419.5
22-May-93 14:55	136.6	88.8	182.7	408.1
24-May-93 11:32	163.8	91.0	182.7	437.5
25-May-93 14:30	160.5	91.0	182.7	434.2
26-May-93 15:19	154.3	91.0	182.7	428.0
27-May-93 12:51	147.3	90.9	182.7	420.9
28-May-93 12:50	166.6	91.0	182.7	440.3
30-May-93 16:43	146.7	90.8	182.7	420.2
25-Aug-93 12:12	104.3	69.4	156.9	330.6
21-Sep-93 12:51	122.7	80.6	174.1	377.4

¹ Wave forms improperly stored. Water content data not reported. Water storage not calculated.

² Water storage not reported for one or more horizons. Total water storage not calculated.

Table A6.10. Water storage, site TD5.

Date and time	Water storage (mm)			Total
	5-01	5-02	5-03	
10-Oct-92 10:20	115.8	84.8	454.5	655.1
13-Oct-92 10:52	113.1	84.8	449.7	647.6
13-Oct-92 17:38	111.9	84.0	450.0	645.9
16-Oct-92 13:57	132.3	88.7	453.0	674.0
17-Oct-92 17:23	126.6	91.4	456.5	674.5
20-Oct-92 15:37	123.2	90.7	457.1	671.0
27-Oct-92 12:33	123.8	91.2	456.8	671.8
2-Nov-92 09:33	115.2	81.5	451.9	648.6
3-Nov-92 15:04	128.4	90.0	458.2	676.6
4-Nov-92 15:36	129.5	96.1	461.3	686.9
5-Nov-92 15:39	128.6	98.2	463.1	689.8
7-Nov-92 14:50	126.6	95.7	461.8	684.2
9-Nov-92 15:10	123.2	90.8	459.7	673.7
14-Apr-93 17:01	144.8	110.5	469.3	724.6
2-May-93 16:24	132.8	101.4	470.0	704.1
10-May-93 17:45	129.0	96.8	469.3	695.1
13-May-93 14:21	128.2	93.5	466.7	688.4
14-May-93 20:46	127.9	92.5	465.6	686.0
16-May-93 17:25	123.4	94.3	467.2	684.8
17-May-93 19:30	122.2	93.4	465.4	681.0
24-May-93 11:36	126.0	88.9	460.2	675.0
25-May-93 14:36	122.4	92.9	464.0	679.3
26-May-93 15:24	123.0	94.2	465.5	682.7
27-May-93 12:55	120.7	92.7	464.6	678.0
28-May-93 12:55	126.6	97.3	466.9	690.8
29-May-93 17:09	126.7	97.0	467.7	691.4
30-May-93 16:49	124.5	94.5	466.8	685.8
25-Aug-93 12:22	83.8	62.2	433.5	579.5
21-Sep-93 12:58	98.2	74.6	449.8	622.6

Appendix 7

Isotope data

Table A7.1 Isotope data.

Date and time	Site	$\delta^{18}\text{O}$ (‰ SMOW)	$\delta^{18}\text{O}$ repeat (‰ SMOW)
28-Mar-89	HPZT6 Bhf	-11.90	
30-Mar-89	HPZT6 Bhf	-12.44	-12.27
14-Mar-89	P20-03	-12.18	
29-Mar-89 12:40	P20-03	-12.30	
29-Mar-89 13:40	P59	-11.65	
28-Mar-89 18:30	Precipitation	-7.10	
20-Mar-89	S1	-11.12	
28-Mar-89 13:15	S1	-14.11	
28-Mar-89 21:10	S1	-12.91	-12.85
29-Mar-89 12:00	S1	-12.34	-12.37
3-Apr-89 12:30	S1	-12.11	-12.17
28-Mar-89 21:58	S3	-13.43	
29-Mar-89 12:10	S3	-12.76	
28-Mar-89 13:35	S5	-14.12	
28-Mar-89 22:30	S5	-12.86	-12.66
29-Mar-89 12:20	S5	-11.85	
28-Mar-89 17:00	Snow lysimeter 1	-16.81	
28-Mar-89 17:07	Snow lysimeter 2	-15.80	
10-Jun-89 01:30	Precipitation	-10.69	
10-Jun-89 11:30	Precipitation	-13.20	
12-Jun-89 17:15	P11	-12.51	
23-Jun-89 16:00	P11	-12.31	
23-Jun-89 15:45	P20-03	-12.26	
23-Jun-89 15:20	P20-05	-12.34	-12.54
12-Jul-89 14:28	P59	-12.18	
22-Jun-89 13:20	Precipitation	-5.75	
22-Jun-89 23:15	Precipitation	-5.76	-5.84
22-Jun-89 11:32	S1	-11.20	
22-Jun-89 13:13	S1	-11.85	
22-Jun-89 15:08	S1	-10.75	
22-Jun-89 16:27	S1	-9.42	-9.35
22-Jun-89 17:07	S1	-9.93	-10.03
22-Jun-89 18:09	S1	-10.37	-10.51
22-Jun-89 20:25	S1	-10.92	
22-Jun-89 22:50	S1	-10.52	

Table A7.1 Isotope data (continued).

Date and time	Site	$\delta^{18}\text{O}$ (‰ SMOW)	$\delta^{18}\text{O}$ repeat (‰ SMOW)
23-Jun-89 02:46	S1	-11.11	
23-Jun-89 17:15	S1	-11.32	
25-Jun-89 13:00	S1	-11.56	
30-Jun-89 13:30	S1	-12.27	
23-Jun-89 14:50	Seep near S2	-10.22	-10.28
31-Oct-89 17:15	P20-01	-11.34	
31-Oct-89 17:45	P20-02	-12.37	
23-Oct-89 18:15	P20-05	-12.39	
2-Nov-89 11:50	P20-05	-12.45	
29-Oct-89 11:55	P46-01	-11.44	
31-Oct-89 21:40	P46-01	-11.39	
29-Oct-89 11:40	P46-03	-11.40	
2-Nov-89 16:10	P59	-11.34	
31-Oct-89 14:50	Precipitation	-5.66	
31-Oct-89 16:35	Precipitation	-6.18	
31-Oct-89 22:40	Precipitation	-6.43	
29-Oct-89 09:30	S1	-11.83	
31-Oct-89 15:15	S1	-10.62	
31-Oct-89 15:55	S1	-9.93	
31-Oct-89 20:50	S1	-10.27	
2-Nov-89 10:00	S1	-11.66	-11.70
29-Oct-89 09:45	S2	-12.02	-12.13
31-Oct-89 15:17	S2	-10.66	
31-Oct-89 16:00	S2	-10.31	
31-Oct-89 21:00	S2	-10.69	
2-Nov-89 10:10	S2	-11.84	
29-Oct-89 10:15	S3	-11.77	-11.69
31-Oct-89 15:22	S3	-10.29	
31-Oct-89 16:02	S3	-9.82	
31-Oct-89 21:15	S3	-10.4	
2-Nov-89 10:15	S3	-10.91	
2-Nov-89 10:15	S3 (different submission)	-10.83	
29-Oct-89 10:30	S4	-11.62	
31-Oct-89 15:28	S4	-9.58	
31-Oct-89 16:10	S4	-9.94	

Table A7.1 Isotope data (continued).

Date and time	Site	$\delta^{18}\text{O}$ (‰ SMOW)	$\delta^{18}\text{O}$ repeat (‰ SMOW)
31-Oct-89 21:25	S4	-10.24	
2-Nov-89 10:25	S4	-11.47	
29-Oct-89 10:45	S5	-11.71	-11.64
31-Oct-89 15:35	S5	-9.13	
31-Oct-89 16:20	S5	-9.16	
31-Oct-89 21:30	S5	-10.08	
2-Nov-89 10:35	S5	-11.33	
1-Apr-90 14:50	P59	-12.62	
14-Apr-90 16:35	P20-05	-12.13	
16-Apr-90 10:05	S1	-13.26	
16-Apr-90 18:02	S1	-13.65	-13.37
16-Apr-90 16:45	Snow lysimeter 3	-15.35	
2-Nov-92 09:05	S1	-11.29	
2-Nov-92 20:10	S1	-11.11	
4-Nov-92 10:50	S1	-10.44	
22-May-93 14:15	S1	-12.47	
24-May-93 05:45	S1	-10.89	
28-May-93 06:45	S1	-11.75	
3-Nov-92 14:50	TF1	-12.72	-12.73
4-Nov-92 15:35	TF1	-9.06	
11-Nov-92 12:15	TF1	-14.00	
13-Nov-92 06:30	TF1	-13.15	
24-May-93 15:45	TF1	-6.18	
28-May-93 13:15	TF1	-8.82	
1-Nov-92 14:35	W1	-10.03	
3-Nov-92 07:10	W1	-10.23	
4-Nov-92 11:50	W1	-10.02	-10.00
9-Nov-92 09:15	W1	-10.11	
11-Nov-92 06:15	W1	-10.07	
12-Nov-92 23:40	W1	-10.43	-10.57
19-Nov-92 10:30	W1	-10.33	
22-May-93 10:20	W1	-13.06	
24-May-93 07:40	W1	-12.15	-12.22
28-May-93 06:30	W1	-12.49	
1-Nov-92 15:55	W5	-9.89	

Table A7.1 Isotope data (continued).

Date and time	Site	$\delta^{18}\text{O}$ (‰ SMOW)	$\delta^{18}\text{O}$ repeat (‰ SMOW)
2-Nov-92 23:45	W5	-10.05	
4-Nov-92 12:50	W5	-9.74	
22-May-93 11:30	W5	-14.19	
24-May-93 09:55	W5	-14.08	-14.06
28-May-93 08:15	W5	-13.58	
1-Nov-92 16:25	Wetland 2	-9.72	
19-Nov-92 11:30	Wetland 2	-10.22	-10.27
22-May-93 11:00	Wetland 2	-13.19	
30-May-93 14:30	Wetland 2	-12.86	

Appendix 8

Dissolved silica data, 1989-90

Table A8.1 Dissolved silica data, 1989-90.

Date and Time	Site	Si (mg/l)	Date and Time	Site	Si (mg/l)
3-Aug-89 00:00	P01	10.9	5-Oct-89 17:50	P20-02	10.9
11-Aug-89 12:00	P01	10.9	10-Oct-89 11:00	P20-02	9.90
16-Aug-89 11:20	P01	12.1	10-Oct-89 21:00	P20-02	9.60
24-Aug-89 12:00	P01	10.6	12-Oct-89 11:30	P20-02	10.7
30-Aug-89 09:50	P01	12.4	15-Oct-89 21:45	P20-02	10.5
2-Nov-89 16:30	P01	9.08	17-Oct-89 15:45	P20-02	11.0
10-Nov-89 16:30	P01	8.96	20-Oct-89 17:00	P20-02	10.6
14-Apr-90 11:15	P01	8.28	23-Oct-89 12:40	P20-02	10.5
19-Apr-90 18:10	P01	8.14	29-Oct-89 15:00	P20-02	10.5
6-Jun-89 12:40	P03	10.6	31-Oct-89 17:45	P20-02	10.6
14-Jul-89 15:00	P03	11.2	2-Nov-89 11:30	P20-02	10.4
24-Aug-89 14:10	P03	10.9	7-Nov-89 10:15	P20-02	10.4
6-Jun-89 13:00	P04	4.34	8-Nov-89 16:15	P20-02	10.2
2-Jun-89 10:15	P05	3.34	16-Apr-90 22:30	P20-02	8.88
13-Jul-89 18:00	P05	3.88	29-Mar-89 12:45	P20-03	9.30
2-Jun-89 10:00	P06	3.74	3-Apr-89 16:30	P20-03	10.0
19-Apr-90 16:50	P07	3.16	17-Apr-89 10:55	P20-03	10.9
5-Jun-89 16:20	P10	3.00	6-Jun-89 15:00	P20-03	10.7
12-Jul-89 15:00	P10	3.26	14-Jul-89 14:50	P20-03	11.6
5-Jun-89 17:30	P11	5.98	5-Oct-89 17:00	P20-03	10.7
10-Jun-89 10:50	P11	5.32	10-Oct-89 11:45	P20-03	10.5
12-Jun-89 17:15	P11	6.20	10-Oct-89 21:05	P20-03	10.7
20-Jun-89 15:25	P11	6.16	12-Oct-89 11:25	P20-03	11.5
23-Jun-89 16:00	P11	6.56	15-Oct-89 21:35	P20-03	11.3
12-Jul-89 14:00	P11	7.32	17-Oct-89 16:30	P20-03	11.5
12-Jul-89 14:00	P11	7.42	20-Oct-89 17:10	P20-03	11.4
5-Oct-89 17:20	P11	8.44	23-Oct-89 16:00	P20-03	11.2
12-Oct-89 17:30	P11	5.78	29-Oct-89 15:00	P20-03	11.3
17-Oct-89 14:10	P11	5.98	31-Oct-89 19:05	P20-03	11.2
23-Oct-89 16:00	P11	6.06	2-Nov-89 11:40	P20-03	11.1
2-Nov-89 16:00	P11	6.10	7-Nov-89 11:10	P20-03	11.0
10-Nov-89 14:00	P11	6.60	8-Nov-89 16:30	P20-03	10.9
14-Apr-90 14:05	P11	5.20	10-Nov-89 16:00	P20-03	11.1
19-Apr-90 16:40	P11	5.48	14-Apr-90 10:30	P20-03	9.40
6-Jun-89 12:30	P15-01	5.74	16-Apr-90 22:41	P20-03	9.58
14-Jul-89 15:20	P15-03	10.7	5-Oct-89 17:05	P20-04	10.8
20-Oct-89 16:45	P20-01	10.1	29-Mar-89 12:15	P20-05	9.70
31-Oct-89 17:15	P20-01	12.5	3-Apr-89 16:30	P20-05	10.4
7-Nov-89 09:00	P20-01	11.2	17-Apr-89 10:50	P20-05	11.2
16-Apr-90 22:20	P20-01	4.90	17-May-89 13:00	P20-05	10.0

Table A8.1 Dissolved silica data, 1989-90 (continued).

Date and Time	Site	Si (mg/l)	Date and Time	Site	Si (mg/l)
21-May-89 13:30	P20-05	10.1	4-Nov-89 15:40	P34-02	7.16
6-Jun-89 14:25	P20-05	10.3	7-Nov-89 11:30	P34-02	6.98
10-Jun-89 11:30	P20-05	10.3	8-Nov-89 15:55	P34-02	6.96
12-Jun-89 17:45	P20-05	10.4	16-Apr-90 21:48	P34-02	5.88
20-Jun-89 15:15	P20-05	10.5	20-Oct-89 16:10	P34-03	7.98
23-Jun-89 15:20	P20-05	10.5	23-Oct-89 16:30	P34-03	7.86
14-Jul-89 15:05	P20-05	10.8	29-Oct-89 15:00	P34-03	7.82
3-Aug-89 00:00	P20-05	10.9	31-Oct-89 19:35	P34-03	7.82
11-Aug-89 09:55	P20-05	11.0	4-Nov-89 15:50	P34-03	7.52
16-Aug-89 09:00	P20-05	10.9	7-Nov-89 11:35	P34-03	7.36
24-Aug-89 10:30	P20-05	10.9	8-Nov-89 16:05	P34-03	7.32
30-Aug-89 09:45	P20-05	11.1	16-Apr-90 21:58	P34-03	6.80
5-Oct-89 17:50	P20-05	11.1	31-Oct-89 21:40	P45-01	5.78
12-Oct-89 18:10	P20-05	11.0	29-Oct-89 11:30	P45-02	5.36
17-Oct-89 16:45	P20-05	10.9	5-Oct-89 18:10	P46-01	7.30
23-Oct-89 16:00	P20-05	11.0	5-Oct-89 23:00	P46-01	6.08
2-Nov-89 11:50	P20-05	10.7	10-Oct-89 16:15	P46-01	6.20
10-Nov-89 16:15	P20-05	11.0	10-Oct-89 21:15	P46-01	5.76
14-Apr-90 10:00	P20-05	9.92	11-Oct-89 12:30	P46-01	5.96
19-Apr-90 18:30	P20-05	10.1	12-Oct-89 11:45	P46-01	5.86
29-Mar-89 12:25	P20-06	11.5	12-Oct-89 17:55	P46-01	5.56
5-Oct-89 17:10	P20-06	11.1	15-Oct-89 20:50	P46-01	5.90
13-Jul-89 10:36	P21	6.50	17-Oct-89 13:55	P46-01	5.84
14-Jul-89 15:25	P27-01	11.5	20-Oct-89 12:40	P46-01	5.62
6-Jun-89 15:20	P27-02	10.0	23-Oct-89 15:10	P46-01	5.54
14-Jul-89 15:20	P27-02	10.6	29-Oct-89 11:30	P46-01	5.98
14-Jul-89 15:40	P27-02	11.4	4-Nov-89 14:05	P46-01	5.10
6-Jun-89 15:25	P27-03	10.0	7-Nov-89 09:20	P46-01	5.06
20-Oct-89 15:50	P34-01	7.18	8-Nov-89 13:30	P46-01	5.22
23-Oct-89 16:30	P34-01	7.24	16-Apr-90 21:45	P46-01	5.00
29-Oct-89 15:00	P34-01	7.70	5-Oct-89 18:15	P46-02	6.28
31-Oct-89 19:15	P34-01	5.64	5-Oct-89 23:05	P46-02	5.94
4-Nov-89 15:30	P34-01	7.14	10-Oct-89 16:20	P46-02	5.48
7-Nov-89 11:25	P34-01	5.54	10-Oct-89 21:25	P46-02	5.48
8-Nov-89 15:45	P34-01	6.72	11-Oct-89 12:40	P46-02	5.48
16-Apr-90 22:05	P34-01	5.06	12-Oct-89 11:50	P46-02	5.46
20-Oct-89 16:00	P34-02	7.40	15-Oct-89 21:00	P46-02	5.36
23-Oct-89 16:30	P34-02	7.38	17-Oct-89 13:45	P46-02	5.44
29-Oct-89 15:00	P34-02	7.46	20-Oct-89 12:50	P46-02	5.26
31-Oct-89 19:25	P34-02	7.38	23-Oct-89 15:10	P46-02	5.26

Table A8.1 Dissolved silica data, 1989-90 (continued).

Date and Time	Site	Si (mg/l)	Date and Time	Site	Si (mg/l)
31-Oct-89 21:50	P46-02	5.50	31-Oct-89 22:10	P47-03	4.68
4-Nov-89 13:55	P46-02	5.24	4-Nov-89 14:10	P47-03	4.64
7-Nov-89 09:30	P46-02	5.14	7-Nov-89 10:50	P47-03	4.48
8-Nov-89 13:35	P46-02	5.14	8-Nov-89 13:45	P47-03	4.60
16-Apr-90 21:35	P46-02	4.76	16-Apr-90 21:08	P47-03	4.16
5-Oct-89 18:20	P46-03	6.66	5-Jun-89 17:00	P58	7.18
5-Oct-89 23:15	P46-03	6.62	12-Jul-89 14:50	P58	8.08
10-Oct-89 16:30	P46-03	6.40	23-Aug-89 11:45	P58	8.34
10-Oct-89 21:35	P46-03	6.24	29-Mar-89 13:40	P59	5.40
12-Oct-89 11:55	P46-03	6.16	3-Apr-89 18:00	P59	5.70
15-Oct-89 21:10	P46-03	6.06	17-Apr-89 13:00	P59	5.90
17-Oct-89 13:40	P46-03	6.12	25-Apr-89 00:00	P59	5.84
20-Oct-89 13:00	P46-03	5.98	17-May-89 14:10	P59	4.94
23-Oct-89 15:10	P46-03	5.86	5-Jun-89 16:50	P59	5.46
29-Oct-89 11:30	P46-03	5.60	12-Jul-89 14:28	P59	6.72
31-Oct-89 22:00	P46-03	6.04	23-Aug-89 10:10	P59	7.88
4-Nov-89 13:45	P46-03	5.78	5-Oct-89 17:35	P59	7.24
7-Nov-89 09:35	P46-03	5.66	12-Oct-89 17:50	P59	6.86
8-Nov-89 13:40	P46-03	5.62	17-Oct-89 14:20	P59	6.64
16-Apr-90 21:30	P46-03	5.08	23-Oct-89 16:00	P59	6.32
20-Oct-89 08:35	P47-01	5.44	2-Nov-89 16:10	P59	6.14
31-Oct-89 22:30	P47-01	6.10	10-Nov-89 14:15	P59	5.84
7-Nov-89 10:30	P47-01	6.02	14-Apr-90 14:50	P59	4.10
16-Apr-90 21:25	P47-01	3.46	3-Apr-89 18:00	P60	11.0
11-Oct-89 14:20	P47-02	5.26	25-Apr-89 00:00	P60	11.3
20-Oct-89 13:20	P47-02	5.02	5-Jun-89 16:40	P60	10.9
23-Oct-89 15:10	P47-02	5.10	12-Jun-89 17:30	P60	10.8
31-Oct-89 22:20	P47-02	5.34	12-Jul-89 14:28	P60	11.6
4-Nov-89 14:20	P47-02	5.16	3-Aug-89 00:00	P60	12.0
7-Nov-89 10:40	P47-02	5.14	11-Aug-89 12:20	P60	12.1
8-Nov-89 13:55	P47-02	5.12	16-Aug-89 10:05	P60	12.2
16-Apr-90 21:15	P47-02	4.08	23-Aug-89 10:25	P60	12.1
10-Oct-89 21:45	P47-03	5.04	30-Aug-89 10:15	P60	10.5
11-Oct-89 13:00	P47-03	4.38	17-Oct-89 15:20	P60	12.6
12-Oct-89 12:50	P47-03	4.30	23-Oct-89 16:00	P60	12.4
15-Oct-89 20:40	P47-03	4.52	2-Nov-89 16:20	P60	12.4
17-Oct-89 13:30	P47-03	4.46	10-Nov-89 14:30	P60	11.9
20-Oct-89 13:10	P47-03	4.36	14-Apr-90 15:10	P60	10.3
23-Oct-89 15:10	P47-03	4.28	29-Mar-89 13:20	P61	9.60
29-Oct-89 11:30	P47-03	4.88	2-Jun-89 10:40	P61	4.32

Table A8.1 Dissolved silica data, 1989-90 (continued).

Date and Time	Site	Si (mg/l)	Date and Time	Site	Si (mg/l)
13-Jul-89 15:06	P61	5.16	29-Mar-89 14:30	S1	4.80
23-Aug-89 11:00	P61	5.70	29-Mar-89 17:50	S1	3.96
3-Apr-89 17:10	P62	10.1	29-Mar-89 18:30	S1	5.00
17-Apr-89 11:40	P62	10.9	29-Mar-89 20:25	S1	4.00
17-May-89 14:20	P62	9.64	29-Mar-89 23:50	S1	3.52
2-Jun-89 11:05	P62	9.58	3-Apr-89 12:30	S1	6.22
13-Jul-89 15:20	P62	9.92	4-Apr-89 08:10	S1	5.42
2-Jun-89 11:15	P63	11.4	4-Apr-89 10:20	S1	4.78
13-Jul-89 14:00	P63	11.6	4-Apr-89 12:00	S1	4.56
23-Aug-89 11:20	P63	11.3	4-Apr-89 14:00	S1	4.54
21-May-89 15:15	Precipitation	0.08	16-Apr-89 12:45	S1	5.86
22-Jun-89 15:35	Precipitation	0.00	16-Apr-89 16:15	S1	4.48
22-Jun-89 17:00	Precipitation	0.00	17-Apr-89 00:22	S1	4.32
2-Aug-89 10:40	Precipitation	0.10	17-Apr-89 03:22	S1	4.40
30-Aug-89 11:30	Precipitation	0.10	17-Apr-89 06:22	S1	4.52
11-Oct-89 11:00	Precipitation	0.12	17-Apr-89 09:40	S1	4.82
12-Oct-89 17:10	Precipitation	0.10	24-Apr-89 14:30	S1	3.62
17-Oct-89 17:00	Precipitation	0.08	24-Apr-89 23:59	S1	3.52
21-Oct-89 09:30	Precipitation	0.00	25-Apr-89 06:00	S1	3.80
1-Nov-89 09:50	Precipitation	0.12	25-Apr-89 10:45	S1	3.98
2-Nov-89 16:30	Precipitation	0.00	25-Apr-89 12:00	S1	3.34
6-Nov-89 13:45	Precipitation	0.00	25-Apr-89 17:00	S1	2.96
9-Nov-89 10:30	Precipitation	0.00	1-May-89 13:00	S1	4.86
11-Nov-89 17:00	Precipitation	0.00	17-May-89 13:10	S1	5.26
5-Nov-88 01:00	S1	7.24	21-May-89 13:10	S1	4.98
5-Nov-88 02:00	S1	7.34	30-May-89 10:10	S1	6.62
5-Nov-88 03:00	S1	7.44	8-Jun-89 13:00	S1	6.46
5-Nov-88 04:00	S1	7.54	9-Jun-89 23:50	S1	6.34
5-Nov-88 05:00	S1	7.50	10-Jun-89 01:47	S1	6.44
5-Nov-88 06:00	S1	7.56	10-Jun-89 09:10	S1	4.74
5-Nov-88 07:00	S1	7.68	10-Jun-89 11:50	S1	5.22
5-Nov-88 08:00	S1	7.72	10-Jun-89 13:35	S1	5.38
5-Nov-88 08:00	S1	7.80	10-Jun-89 15:35	S1	5.58
5-Nov-88 09:30	S1	7.14	10-Jun-89 17:20	S1	6.68
5-Nov-88 11:00	S1	7.14	10-Jun-89 17:30	S1	5.74
28-Mar-89 15:15	S1	3.60	12-Jun-89 16:10	S1	7.06
28-Mar-89 22:00	S1	2.80	19-Jun-89 14:05	S1	7.54
29-Mar-89 11:00	S1	4.50	20-Jun-89 08:45	S1	6.14
29-Mar-89 12:00	S1	3.50	20-Jun-89 10:25	S1	6.26
29-Mar-89 13:50	S1	3.40	20-Jun-89 11:40	S1	6.34

Table A8.1 Dissolved silica data, 1989-90 (continued).

Date and Time	Site	Si (mg/l)	Date and Time	Site	Si (mg/l)
20-Jun-89 13:50	S1	6.50	23-Aug-89 15:50	S1	10.6
22-Jun-89 11:32	S1	5.74	28-Aug-89 09:50	S1	10.9
22-Jun-89 11:40	S1	5.62	29-Aug-89 09:40	S1	9.78
22-Jun-89 12:36	S1	5.82	4-Oct-89 09:40	S1	9.70
22-Jun-89 13:13	S1	5.98	5-Oct-89 22:20	S1	9.72
22-Jun-89 14:34	S1	6.00	10-Oct-89 14:50	S1	9.60
22-Jun-89 15:08	S1	5.26	10-Oct-89 18:00	S1	8.62
22-Jun-89 15:44	S1	3.64	10-Oct-89 19:05	S1	8.04
22-Jun-89 16:27	S1	3.62	10-Oct-89 20:00	S1	8.00
22-Jun-89 17:07	S1	3.60	11-Oct-89 00:35	S1	8.38
22-Jun-89 18:09	S1	3.94	11-Oct-89 05:02	S1	8.54
22-Jun-89 19:25	S1	4.12	11-Oct-89 08:02	S1	8.30
22-Jun-89 20:25	S1	4.18	11-Oct-89 09:30	S1	8.80
22-Jun-89 21:25	S1	4.10	11-Oct-89 12:50	S1	6.14
22-Jun-89 22:50	S1	3.78	11-Oct-89 17:50	S1	8.98
22-Jun-89 23:46	S1	3.86	12-Oct-89 09:50	S1	8.34
23-Jun-89 00:46	S1	3.84	12-Oct-89 10:45	S1	8.10
23-Jun-89 02:46	S1	3.86	12-Oct-89 12:10	S1	8.36
23-Jun-89 04:46	S1	3.92	12-Oct-89 15:25	S1	8.68
23-Jun-89 10:16	S1	3.90	12-Oct-89 18:20	S1	8.90
23-Jun-89 12:45	S1	4.02	13-Oct-89 10:30	S1	9.34
23-Jun-89 12:45	S1	4.04	15-Oct-89 13:25	S1	9.12
23-Jun-89 17:15	S1	3.92	16-Oct-89 14:20	S1	8.60
24-Jun-89 01:02	S1	4.02	16-Oct-89 15:40	S1	8.52
24-Jun-89 11:40	S1	3.96	18-Oct-89 08:50	S1	9.04
24-Jun-89 17:10	S1	3.64	20-Oct-89 09:40	S1	7.50
25-Jun-89 03:00	S1	3.96	20-Oct-89 10:25	S1	7.34
25-Jun-89 13:00	S1	4.76	20-Oct-89 11:45	S1	7.58
26-Jun-89 15:00	S1	4.94	20-Oct-89 15:00	S1	7.74
30-Jun-89 13:30	S1	7.86	20-Oct-89 18:30	S1	7.52
11-Jul-89 15:15	S1	8.78	21-Oct-89 00:08	S1	7.94
17-Jul-89 14:05	S1	10.1	21-Oct-89 05:08	S1	8.02
24-Jul-89 09:30	S1	10.2	21-Oct-89 08:40	S1	8.08
31-Jul-89 09:25	S1	10.6	22-Oct-89 11:15	S1	8.52
2-Aug-89 09:30	S1	8.96	23-Oct-89 11:45	S1	8.76
3-Aug-89 14:00	S1	10.4	29-Oct-89 09:30	S1	9.08
8-Aug-89 09:10	S1	10.3	31-Oct-89 15:15	S1	6.08
14-Aug-89 11:05	S1	10.7	31-Oct-89 15:55	S1	5.68
15-Aug-89 11:10	S1	10.1	31-Oct-89 17:50	S1	6.92
21-Aug-89 11:05	S1	10.6	31-Oct-89 20:50	S1	6.80

Table A8.1 Dissolved silica data, 1989-90 (continued).

Date and Time	Site	Si (mg/l)	Date and Time	Site	Si (mg/l)
1-Nov-89 03:00	S1	7.66	29-Mar-89 11:10	S2	5.50
1-Nov-89 06:00	S1	7.78	29-Mar-89 12:05	S2	3.50
1-Nov-89 08:45	S1	8.04	3-Apr-89 12:40	S2	6.96
1-Nov-89 16:30	S1	8.22	4-Apr-89 10:30	S2	4.54
2-Nov-89 10:00	S1	8.42	4-Apr-89 14:10	S2	4.86
2-Nov-89 14:25	S1	7.80	16-Apr-89 12:55	S2	5.34
2-Nov-89 20:10	S1	7.88	16-Apr-89 16:25	S2	4.10
3-Nov-89 00:17	S1	7.86	17-Apr-89 09:50	S2	5.80
3-Nov-89 03:17	S1	7.90	24-Apr-89 14:30	S2	3.60
3-Nov-89 09:17	S1	8.02	25-Apr-89 10:45	S2	4.56
3-Nov-89 14:20	S1	8.40	25-Apr-89 17:00	S2	3.60
4-Nov-89 14:15	S1	8.46	1-May-89 00:00	S2	6.02
5-Nov-89 16:15	S1	8.06	17-May-89 14:50	S2	7.02
6-Nov-89 06:30	S1	6.46	21-May-89 13:20	S2	5.90
6-Nov-89 08:15	S1	6.66	30-May-89 10:20	S2	8.12
6-Nov-89 11:45	S1	7.06	30-May-89 10:30	S2	8.02
6-Nov-89 16:30	S1	7.36	8-Jun-89 13:10	S2	8.86
7-Nov-89 11:30	S1	7.94	9-Jun-89 00:00	S2	7.86
8-Nov-89 11:05	S1	8.12	10-Jun-89 09:15	S2	5.98
9-Nov-89 08:30	S1	7.72	10-Jun-89 17:35	S2	7.70
11-Nov-89 08:10	S1	7.40	12-Jun-89 16:15	S2	8.76
11-Nov-89 14:40	S1	7.26	19-Jun-89 14:15	S2	9.04
23-Nov-89 00:00	S1	7.50	20-Jun-89 08:50	S2	7.74
16-Apr-90 10:05	S1	4.70	20-Jun-89 14:00	S2	8.26
16-Apr-90 13:03	S1	4.62	30-Jun-89 13:45	S2	9.62
16-Apr-90 14:53	S1	4.18	11-Jul-89 15:20	S2	10.3
16-Apr-90 18:02	S1	3.98	17-Jul-89 14:20	S2	8.54
16-Apr-90 22:32	S1	4.12	24-Jul-89 10:15	S2	8.92
16-Apr-90 23:05	S1	4.08	31-Jul-89 09:45	S2	9.20
17-Apr-90 00:05	S1	3.74	2-Aug-89 09:50	S2	9.48
17-Apr-90 00:58	S1	3.62	3-Aug-89 14:15	S2	10.9
17-Apr-90 02:58	S1	3.32	8-Aug-89 09:35	S2	10.7
17-Apr-90 04:58	S1	3.34	14-Aug-89 11:20	S2	11.0
17-Apr-90 06:58	S1	3.50	15-Aug-89 11:25	S2	10.8
17-Apr-90 08:30	S1	3.68	21-Aug-89 11:25	S2	11.1
17-Apr-90 19:20	S1	4.32	28-Aug-89 11:30	S2	11.1
18-Apr-90 09:10	S1	4.84	29-Aug-89 10:10	S2	10.4
19-Apr-90 17:05	S1	3.40	4-Oct-89 10:00	S2	10.4
28-Mar-89 15:20	S2	2.70	5-Oct-89 22:25	S2	10.0
28-Mar-89 22:05	S2	3.10	10-Oct-89 14:55	S2	9.80

Table A8.1 Dissolved silica data, 1989-90 (continued).

Date and Time	Site	Si (mg/l)	Date and Time	Site	Si (mg/l)
10-Oct-89 18:05	S2	9.04	9-Nov-89 08:35	S2	8.66
10-Oct-89 19:10	S2	8.56	11-Nov-89 08:15	S2	8.42
10-Oct-89 20:10	S2	8.70	11-Nov-89 14:45	S2	8.18
11-Oct-89 00:40	S2	9.24	16-Apr-90 13:07	S2	6.20
11-Oct-89 09:35	S2	9.48	16-Apr-90 14:56	S2	5.34
11-Oct-89 17:55	S2	9.62	16-Apr-90 18:11	S2	5.58
12-Oct-89 09:55	S2	8.68	16-Apr-90 23:10	S2	5.66
12-Oct-89 10:48	S2	8.62	17-Apr-90 08:35	S2	5.16
12-Oct-89 12:15	S2	9.06	17-Apr-90 19:24	S2	5.88
12-Oct-89 15:30	S2	9.32	19-Apr-90 17:10	S2	4.44
12-Oct-89 18:25	S2	9.44	28-Mar-89 15:25	S3	3.00
13-Oct-89 10:40	S2	9.60	28-Mar-89 22:10	S3	2.60
15-Oct-89 13:35	S2	9.84	29-Mar-89 11:20	S3	4.00
16-Oct-89 15:45	S2	9.12	29-Mar-89 12:10	S3	3.50
18-Oct-89 08:55	S2	9.80	3-Apr-89 12:50	S3	5.50
20-Oct-89 09:45	S2	7.92	4-Apr-89 10:35	S3	4.34
20-Oct-89 10:30	S2	7.82	4-Apr-89 14:20	S3	4.12
20-Oct-89 11:47	S2	8.36	16-Apr-89 13:05	S3	5.04
20-Oct-89 15:05	S2	8.48	16-Apr-89 16:35	S3	4.04
21-Oct-89 08:45	S2	9.10	17-Apr-89 10:00	S3	4.34
22-Oct-89 11:20	S2	9.40	24-Apr-89 14:30	S3	3.08
23-Oct-89 11:45	S2	9.54	25-Apr-89 10:45	S3	3.62
29-Oct-89 09:30	S2	9.76	25-Apr-89 17:00	S3	2.66
31-Oct-89 15:17	S2	6.54	1-May-89 13:10	S3	4.18
31-Oct-89 16:00	S2	6.44	17-May-89 13:35	S3	4.42
31-Oct-89 17:55	S2	7.66	21-May-89 13:30	S3	4.36
31-Oct-89 21:00	S2	7.78	30-May-89 10:40	S3	5.50
1-Nov-89 08:55	S2	9.06	8-Jun-89 13:20	S3	6.34
1-Nov-89 16:35	S2	9.22	10-Jun-89 00:10	S3	5.40
2-Nov-89 10:10	S2	9.58	10-Jun-89 09:20	S3	4.28
2-Nov-89 14:42	S2	8.50	10-Jun-89 17:40	S3	5.12
2-Nov-89 20:20	S2	8.90	12-Jun-89 16:20	S3	6.14
3-Nov-89 14:25	S2	9.42	19-Jun-89 14:30	S3	6.48
4-Nov-89 14:25	S2	9.34	20-Jun-89 08:55	S3	5.40
6-Nov-89 06:35	S2	7.30	20-Jun-89 14:20	S3	5.70
6-Nov-89 08:18	S2	7.66	30-Jun-89 13:40	S3	6.96
6-Nov-89 11:50	S2	8.16	11-Jul-89 15:30	S3	8.02
6-Nov-89 16:35	S2	8.44	17-Jul-89 14:30	S3	8.54
7-Nov-89 11:35	S2	8.86	24-Jul-89 10:35	S3	8.90
8-Nov-89 11:10	S2	9.10	31-Jul-89 10:00	S3	9.26

Table A8.1 Dissolved silica data, 1989-90 (continued).

Date and Time	Site	Si (mg/l)	Date and Time	Site	Si (mg/l)
2-Aug-89 09:45	S3	8.34	2-Nov-89 10:15	S3	7.82
3-Aug-89 14:25	S3	9.16	2-Nov-89 14:50	S3	7.12
8-Aug-89 09:15	S3	9.08	2-Nov-89 20:35	S3	7.36
14-Aug-89 11:30	S3	9.38	3-Nov-89 14:40	S3	7.64
15-Aug-89 12:20	S3	9.18	4-Nov-89 14:45	S3	7.76
21-Aug-89 11:55	S3	9.30	6-Nov-89 06:45	S3	6.06
28-Aug-89 11:50	S3	9.22	6-Nov-89 08:27	S3	6.22
29-Aug-89 10:45	S3	8.76	6-Nov-89 12:00	S3	6.60
4-Oct-89 10:20	S3	8.72	6-Nov-89 16:40	S3	6.86
5-Oct-89 22:30	S3	8.56	7-Nov-89 11:50	S3	7.34
10-Oct-89 15:00	S3	8.38	8-Nov-89 11:20	S3	7.52
10-Oct-89 18:10	S3	7.82	9-Nov-89 08:40	S3	7.24
10-Oct-89 19:20	S3	7.42	11-Nov-89 08:30	S3	6.90
10-Oct-89 20:11	S3	7.40	11-Nov-89 14:52	S3	6.82
11-Oct-89 00:50	S3	7.78	16-Apr-90 13:13	S3	4.20
11-Oct-89 09:50	S3	8.06	16-Apr-90 15:06	S3	3.80
11-Oct-89 18:00	S3	8.24	16-Apr-90 18:16	S3	3.70
12-Oct-89 10:00	S3	7.56	16-Apr-90 23:15	S3	3.66
12-Oct-89 10:50	S3	7.58	17-Apr-90 08:40	S3	3.72
12-Oct-89 12:20	S3	7.76	17-Apr-90 19:28	S3	4.00
12-Oct-89 15:35	S3	7.94	19-Apr-90 17:20	S3	3.16
12-Oct-89 18:30	S3	8.02	28-Mar-89 15:30	S4	2.90
13-Oct-89 10:50	S3	8.18	28-Mar-89 22:15	S4	2.60
15-Oct-89 13:40	S3	8.40	29-Mar-89 11:30	S4	3.80
16-Oct-89 15:50	S3	8.00	29-Mar-89 12:15	S4	3.40
18-Oct-89 09:05	S3	8.36	3-Apr-89 13:00	S4	5.14
20-Oct-89 09:50	S3	7.08	4-Apr-89 10:40	S4	4.10
20-Oct-89 10:35	S3	6.96	4-Apr-89 14:30	S4	3.94
20-Oct-89 11:55	S3	7.12	16-Apr-89 13:20	S4	4.60
20-Oct-89 15:15	S3	7.28	16-Apr-89 16:45	S4	3.82
21-Oct-89 08:55	S3	7.52	17-Apr-89 10:10	S4	4.12
22-Oct-89 11:30	S3	7.90	24-Apr-89 14:30	S4	2.90
23-Oct-89 11:45	S3	8.08	25-Apr-89 10:45	S4	3.40
29-Oct-89 09:30	S3	8.40	25-Apr-89 17:00	S4	2.74
31-Oct-89 15:22	S3	5.62	1-May-89 13:20	S4	3.96
31-Oct-89 16:02	S3	5.70	17-May-89 13:25	S4	4.00
31-Oct-89 18:10	S3	6.40	21-May-89 13:40	S4	4.12
31-Oct-89 21:15	S3	6.50	30-May-89 10:50	S4	5.10
1-Nov-89 09:10	S3	7.52	8-Jun-89 13:30	S4	6.08
1-Nov-89 16:40	S3	7.64	10-Jun-89 00:20	S4	5.02

Table A8.1 Dissolved silica data, 1989-90 (continued).

Date and Time	Site	Si (mg/l)	Date and Time	Site	Si (mg/l)
10-Jun-89 09:25	S4	4.14	20-Oct-89 15:20	S4	6.98
10-Jun-89 17:45	S4	4.88	21-Oct-89 09:00	S4	7.30
12-Jun-89 16:30	S4	5.84	22-Oct-89 11:35	S4	7.70
19-Jun-89 14:45	S4	6.22	23-Oct-89 11:45	S4	7.90
20-Jun-89 09:00	S4	5.10	29-Oct-89 09:30	S4	8.20
20-Jun-89 14:40	S4	5.42	31-Oct-89 15:28	S4	4.76
30-Jun-89 13:45	S4	6.68	31-Oct-89 16:10	S4	5.44
11-Jul-89 15:40	S4	7.94	31-Oct-89 18:20	S4	6.24
17-Jul-89 14:40	S4	8.52	31-Oct-89 21:25	S4	6.60
24-Jul-89 10:55	S4	8.84	1-Nov-89 09:20	S4	7.28
31-Jul-89 10:30	S4	9.04	1-Nov-89 16:50	S4	7.44
2-Aug-89 09:50	S4	7.86	2-Nov-89 10:25	S4	7.48
3-Aug-89 14:50	S4	9.12	2-Nov-89 14:57	S4	6.92
8-Aug-89 09:45	S4	8.94	2-Nov-89 20:40	S4	7.16
14-Aug-89 11:15	S4	9.00	3-Nov-89 14:50	S4	7.50
15-Aug-89 12:00	S4	8.84	4-Nov-89 14:55	S4	7.66
21-Aug-89 12:05	S4	9.06	6-Nov-89 06:52	S4	5.88
28-Aug-89 11:40	S4	8.74	6-Nov-89 08:32	S4	6.02
29-Aug-89 10:25	S4	8.32	6-Nov-89 12:05	S4	6.42
4-Oct-89 10:30	S4	8.56	6-Nov-89 16:45	S4	6.64
5-Oct-89 22:40	S4	8.16	7-Nov-89 12:00	S4	7.10
10-Oct-89 15:10	S4	8.02	8-Nov-89 11:30	S4	7.34
10-Oct-89 18:15	S4	7.10	9-Nov-89 08:50	S4	6.96
10-Oct-89 19:25	S4	6.70	11-Nov-89 08:40	S4	6.64
10-Oct-89 20:20	S4	7.00	11-Nov-89 15:00	S4	6.54
11-Oct-89 01:05	S4	7.62	16-Apr-90 13:18	S4	3.84
11-Oct-89 10:05	S4	7.94	16-Apr-90 15:11	S4	3.48
11-Oct-89 18:10	S4	8.12	16-Apr-90 18:23	S4	3.46
12-Oct-89 10:05	S4	6.98	16-Apr-90 23:23	S4	3.36
12-Oct-89 11:00	S4	7.22	17-Apr-90 08:46	S4	3.32
12-Oct-89 12:30	S4	7.52	17-Apr-90 19:34	S4	3.68
12-Oct-89 15:45	S4	7.76	19-Apr-90 17:30	S4	2.98
12-Oct-89 18:35	S4	7.86	28-Mar-89 15:35	S5	2.90
13-Oct-89 11:00	S4	8.04	28-Mar-89 22:20	S5	2.70
15-Oct-89 14:00	S4	8.30	29-Mar-89 11:40	S5	3.70
16-Oct-89 15:55	S4	7.66	29-Mar-89 12:20	S5	3.40
18-Oct-89 09:15	S4	8.18	3-Apr-89 13:10	S5	4.64
20-Oct-89 09:55	S4	6.52	4-Apr-89 10:50	S5	3.90
20-Oct-89 10:40	S4	6.58	4-Apr-89 14:40	S5	3.84
20-Oct-89 12:00	S4	7.00	16-Apr-89 13:30	S5	4.60

Table A8.1 Dissolved silica data, 1989-90 (continued).

Date and Time	Site	Si (mg/l)	Date and Time	Site	Si (mg/l)
16-Apr-89 16:55	S5	3.76	20-Oct-89 10:00	S5	4.70
17-Apr-89 10:20	S5	3.96	20-Oct-89 10:45	S5	5.26
24-Apr-89 14:30	S5	2.86	20-Oct-89 12:05	S5	5.58
25-Apr-89 10:45	S5	3.22	20-Oct-89 15:21	S5	5.40
25-Apr-89 17:00	S5	2.70	21-Oct-89 09:15	S5	6.00
1-May-89 13:30	S5	3.68	22-Oct-89 11:45	S5	6.56
17-May-89 13:50	S5	4.10	23-Oct-89 11:45	S5	6.88
21-May-89 13:50	S5	3.96	29-Oct-89 09:30	S5	7.38
30-May-89 11:00	S5	4.94	31-Oct-89 15:35	S5	3.80
8-Jun-89 13:40	S5	4.78	31-Oct-89 16:20	S5	3.86
10-Jun-89 00:30	S5	4.74	31-Oct-89 18:25	S5	4.44
10-Jun-89 09:30	S5	4.18	31-Oct-89 21:30	S5	5.32
10-Jun-89 17:50	S5	4.72	1-Nov-89 09:30	S5	6.04
12-Jun-89 16:40	S5	4.76	1-Nov-89 17:00	S5	6.24
19-Jun-89 15:00	S5	4.98	2-Nov-89 10:35	S5	6.44
20-Jun-89 09:05	S5	4.78	2-Nov-89 15:05	S5	5.56
20-Jun-89 14:50	S5	4.86	2-Nov-89 20:50	S5	5.92
30-Jun-89 13:50	S5	5.30	3-Nov-89 15:00	S5	6.42
11-Jul-89 16:00	S5	5.96	4-Nov-89 15:05	S5	6.56
17-Jul-89 14:45	S5	6.68	6-Nov-89 06:58	S5	4.96
24-Jul-89 11:20	S5	7.18	6-Nov-89 08:39	S5	5.20
31-Jul-89 11:00	S5	9.04	6-Nov-89 12:10	S5	5.50
2-Aug-89 10:00	S5	5.72	6-Nov-89 16:50	S5	5.66
5-Oct-89 22:45	S5	7.02	7-Nov-89 12:10	S5	6.16
10-Oct-89 15:20	S5	6.76	8-Nov-89 11:40	S5	6.42
10-Oct-89 18:25	S5	5.10	9-Nov-89 09:00	S5	6.10
10-Oct-89 19:45	S5	4.94	11-Nov-89 08:50	S5	5.78
10-Oct-89 20:30	S5	5.40	11-Nov-89 15:10	S5	5.60
11-Oct-89 01:20	S5	6.06	16-Apr-90 13:28	S5	3.40
11-Oct-89 10:20	S5	6.50	16-Apr-90 15:18	S5	3.16
11-Oct-89 18:20	S5	6.84	16-Apr-90 18:30	S5	3.20
12-Oct-89 10:10	S5	5.06	16-Apr-90 23:30	S5	3.08
12-Oct-89 11:05	S5	5.82	17-Apr-90 08:53	S5	3.18
12-Oct-89 12:40	S5	6.20	17-Apr-90 19:38	S5	3.30
12-Oct-89 15:55	S5	6.48	19-Apr-90 17:40	S5	2.82
12-Oct-89 18:45	S5	6.62	12-Jun-89 16:00	S6	7.06
13-Oct-89 11:10	S5	6.90	19-Jun-89 15:10	S6	6.46
15-Oct-89 14:10	S5	7.36	30-Jun-89 13:55	S6	6.70
16-Oct-89 16:05	S5	6.22	17-Jul-89 14:55	S6	8.50
18-Oct-89 09:30	S5	7.26	24-Jul-89 09:40	S6	10.1

Table A8.1 Dissolved silica data, 1989-90 (continued).

Date and Time	Site	Si (mg/l)	Date and Time	Site	Si (mg/l)
3-Aug-89 15:00	S6	10.4	17-May-89 14:40	Seep above P03	6.58
8-Aug-89 09:20	S6	10.4	12-Oct-89 13:30	Seep near P27	9.02
14-Aug-89 11:10	S6	10.7	23-Jun-89 14:50	Seep near S2	0.66
15-Aug-89 11:10	S6	10.2	21-May-89 13:50	Seep above P03	6.18
21-Aug-89 11:05	S6	10.6	1-May-89 15:20	Seep above P03	6.60
28-Aug-89 09:50	S6	10.8	17-Apr-90 16:45	Snow lysimeter 3	0.00
29-Aug-89 09:50	S6	9.90			
4-Oct-89 09:50	S6	9.74			
15-Oct-89 14:40	S6	8.50			
16-Oct-89 01:25	S6	8.58			
16-Oct-89 16:15	S6	8.10			
18-Oct-89 09:45	S6	8.66			
20-Oct-89 09:50	S6	7.16			
20-Oct-89 10:32	S6	7.04			
20-Oct-89 11:50	S6	7.20			
20-Oct-89 15:08	S6	7.36			
21-Oct-89 08:50	S6	7.84			
22-Oct-89 11:23	S6	8.16			
23-Oct-89 11:45	S6	8.32			
29-Oct-89 09:30	S6	8.92			
31-Oct-89 15:18	S6	5.98			
31-Oct-89 16:05	S6	6.36			
31-Oct-89 18:00	S6	6.26			
31-Oct-89 21:10	S6	6.86			
1-Nov-89 09:00	S6	7.72			
1-Nov-89 16:38	S6	7.78			
2-Nov-89 10:05	S6	8.00			
2-Nov-89 14:47	S6	7.36			
2-Nov-89 20:30	S6	7.56			
3-Nov-89 14:30	S6	7.98			
4-Nov-89 14:35	S6	8.06			
6-Nov-89 06:38	S6	6.14			
6-Nov-89 08:21	S6	6.36			
6-Nov-89 11:55	S6	6.68			
6-Nov-89 16:38	S6	7.02			
7-Nov-89 11:43	S6	7.54			
8-Nov-89 11:13	S6	7.68			
9-Nov-89 08:35	S6	7.34			
11-Nov-89 08:20	S6	7.08			
11-Nov-89 14:50	S6	7.00			

Appendix 9

DOC analyses

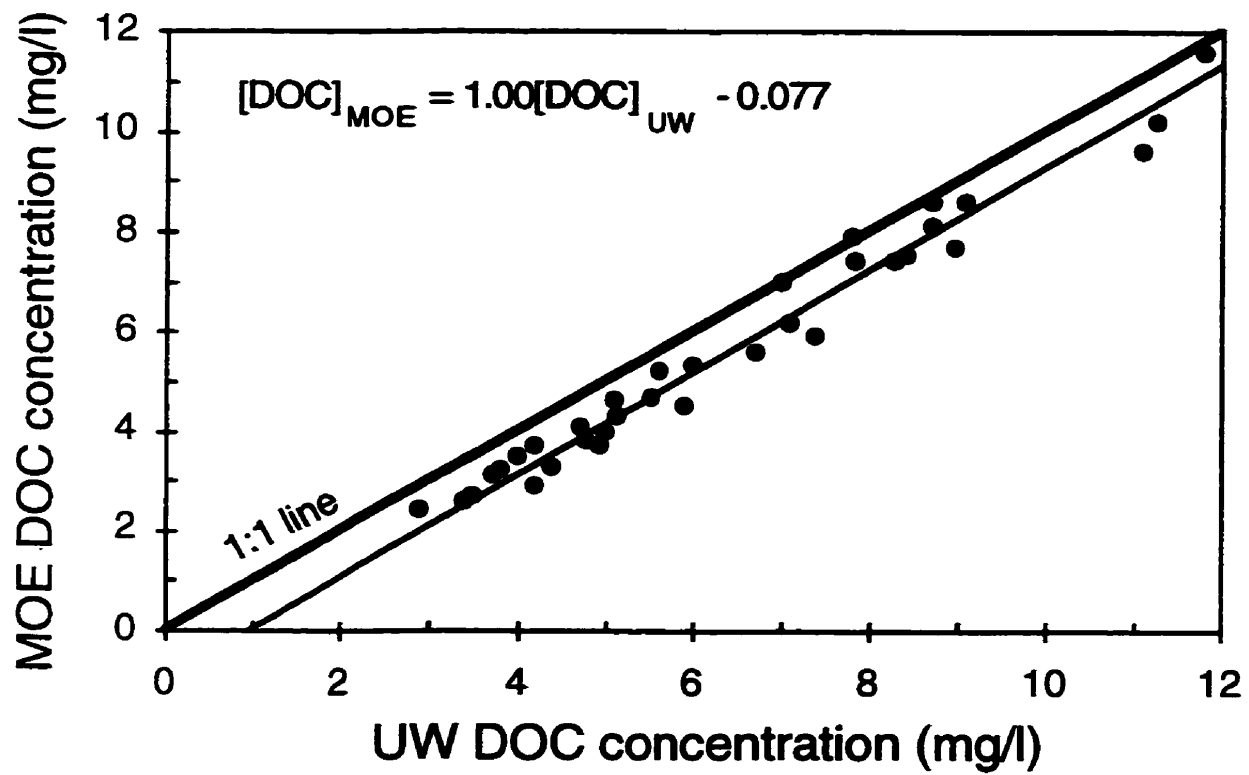
Comparison of dissolved organic carbon analyses

Dissolved organic carbon (DOC) samples collected in 1989 and 1990 were sampled and analysed differently than those collected in 1992 and 1993. This section compares 34 pairs of samples that were collected and analysed with both methods.

The methodology for sample collection and analysis is described in Chapter 9. Samples collected in 1989 and 1990 were pre-filtered with 80 µm (44 µm for groundwater) polyester screens but were not filtered further with 0.45 µm filters according to the most common definition of DOC (Thurman, 1982). These samples were analysed by the persulfate oxidation method at the Dorset Laboratory of the Ontario Ministry of the Environment (MOE). Samples collected in 1992 and 1993 were pre-filtered by the same method as the previous samples but were also filtered using 0.45 µm membranes. These samples were analysed at the University of Waterloo (UW) with a Dohrmann DC-190 total carbon analyser.

The DOC concentrations that were obtained from both procedures are presented in Figure A9.1. On average, the DOC concentrations of the MOE samples were 0.8 ± 0.4 mg/l lower than the UW samples. As the linear regression demonstrates, the difference in concentration is independent of DOC concentration in the range from 2-12 mg/l. It is not apparent whether the difference is caused by differences in sample treatment or analytical method. All 1989 and 1990 data have been adjusted by +0.8 mg/l to be consistent with the 1992 and 1993 data.

Figure A9.1. Comparison of MOE and UW DOC concentrations.



Cellulose nitrate filters

DOC samples that were collected in 1992 and 1993 were filtered with Sartorius® 0.45 µm cellulose nitrate membranes. Although DOC samples are commonly filtered with glass fibre filters (Kaplan, 1994), these filters were too expensive given the large number of samples to be collected and the small budget of the project. Two simple experiments were conducted to test whether the cellulose nitrate filters would contribute DOC to the sample.

In the first experiment, deionized (Nanopure®) water was filtered through new cellulose nitrate filters. The filtrate was collected in 10 ml aliquots from 0-70 ml with another aliquot from 70-75 ml. Then a 25 ml aliquot (75-100 ml) was collected and analysed. This last aliquot was intended to represent the field sample since a minimum of 75 ml of sample was passed through the filter before field samples were collected. The DOC concentration of unfiltered deionized water (blank) was measured and subtracted from the filtrate DOC concentration to obtain the DOC contributed by the cellulose nitrate filter membrane. This experiment was repeated four times although for the fourth filter (Filter 4) only the final 75-100 ml aliquot was analysed (Table A9.1).

The results of this experiment demonstrate that the first 10 ml of filtrate is enriched by approximately 0.5 mg/l DOC and that the subsequent filtrates are enriched by 0.2 mg/l or less (Table A9.1). The sample aliquot of 75-100 ml had an average DOC concentration of 0.04 ± 0.07 mg/l greater than the blank.

The second experiment was similar to the first except that a dilute solution of HCl (pH = 4.3) was used to verify if an acid solution would leach more DOC from the filter. This pH is lower than the pH of all DOC samples in Harp 3A and Harp 4-21 during the 1992 and 1993 sampling periods. This experiment was repeated three times, although only the first and last

Table A9.1 Experiment 1: DOC contributed to deionized water by 0.45 μm cellulose nitrate filter membrane.

Aliquot (ml)	DOC contributed by filter (mg/l)				Average
	Filter 1	Filter 2	Filter 3	Filter 4	
0-10	0.48	0.49	0.59	-	0.52
10-20	0.18	0.23	0.08	-	0.17
20-30	0.26	0.14	0.14	-	0.18
30-40	0.20	0.17	0.08	-	0.15
40-50	0.13	0.00	0.05	-	0.06
50-60	0.18	0.07	0.17	-	0.14
60-70	0.31	0.10	0.23	-	0.21
70-75	0.03	0.12	0.04	-	0.06
75-100	-0.01	0.15	0.01	0.02	0.04 \pm 0.07

Contributed [DOC] = [DOC] of aliquot - [DOC] of blank

aliquots were collected for the third filter (Filter 7, Table A9.2). The results of this experiment were similar to the first. The first aliquot was enriched by 0.5 mg/l, subsequent aliquots were enriched by 0.1 mg/l or less, and the last sample aliquot (75-100 ml) was enriched by 0.06 ± 0.03 mg/l. These two simple experiments suggest that the cellulose nitrate membranes did not contribute appreciable amounts of DOC to the samples in this study.

Table A9.2 Experiment 2: DOC contributed to dilute HCl solution by 0.45 μm cellulose nitrate filter membrane.

Aliquot (ml)	DOC contributed by filter (mg/l)			Average
	Filter 5	Filter 6	Filter 7	
0-10	0.50	0.45	0.54	0.50
10-20	0.11	0.09	-	0.10
20-30	-0.02	0.03	-	0.00
30-40	-0.09	0.11	-	0.01
40-50	-0.11	0.07	-	-0.02
50-60	0.00	-0.05	-	-0.02
60-70	-0.09	-0.05	-	-0.07
70-75	-0.07	-0.16	-	-0.11
75-100	0.08	0.05	0.02	0.06 \pm 0.03

Contributed [DOC] = [DOC] of aliquot - [DOC] of blank

Appendix 10

DOC data, 1992-93

Table A10.1 DOC data, 1992-93.

Sample date	Location	DOC (mg/l)	Sample date	Location	DOC (mg/l)
27-Sep-92 12:30	B1	5.3	14-Nov-92 13:00	B1	3.3
27-Sep-92 12:30	B1	5.4	16-Nov-92 14:15	B1	3.3
27-Sep-92 14:33	B1	5.1	19-Nov-92 10:50	B1	2.9
27-Sep-92 18:31	B1	6.7	14-Apr-93 00:00	B1	3.9
28-Sep-92 01:28	B1	5.6	04-May-93 11:35	B1	4.7
28-Sep-92 10:50	B1	7.2	10-May-93 10:10	B1	3.3
29-Sep-92 09:47	B1	4.3	28-Sep-92 11:02	OF 1	8.3
29-Sep-92 09:47	B1	4.2	10-Oct-92 13:00	OF 1	5.5
02-Oct-92 10:55	B1	4.4	13-Oct-92 10:25	OF 1	7.7
07-Oct-92 10:25	B1	4.2	17-Oct-92 10:10	OF 1	10.3
13-Oct-92 19:07	B1	5.8	22-Oct-92 16:15	OF 1	8.2
16-Oct-92 08:10	B1	8.3	27-Oct-92 15:00	OF 1	12.5
16-Oct-92 11:30	B1	6.5	02-Nov-92 21:00	OF 1	12.7
16-Oct-92 16:30	B1	6.9	24-May-93 08:35	OF 1	7.0
17-Oct-92 13:10	B1	4.6	25-May-93 16:55	OF 1	6.9
18-Oct-92 14:51	B1	6.0	28-May-93 13:20	OF 1	9.6
20-Oct-92 09:55	B1	4.0	02-Jun-93 09:00	OF 1	8.9
28-Oct-92 09:30	B1	4.2	17-Oct-92 10:00	OF 2	9.8
01-Nov-92 15:05	B1	3.8	27-Oct-92 16:45	OF 2	119.5
01-Nov-92 15:05	B1	4.0	02-Nov-92 20:45	OF 2	23.4
02-Nov-92 16:55	B1	5.4	09-Nov-92 14:30	OF 2	17.4
02-Nov-92 22:50	B1	9.6	17-Oct-92 16:00	OF 3	90.1
03-Nov-92 07:17	B1	6.1	28-May-93 10:15	OF near P72	5.6
03-Nov-92 07:17	B1	6.0	09-Nov-92 16:40	P07-01	3.6
03-Nov-92 07:17	B1	5.9	25-May-93 16:15	P07-01	2.3
03-Nov-92 17:20	B1	4.9	09-Nov-92 16:30	P07-02	2.8
04-Nov-92 12:17	B1	5.1	25-May-93 16:30	P07-02	2.7
05-Nov-92 00:05	B1	4.1	09-Nov-92 16:20	P07-03	1.9
05-Nov-92 16:50	B1	4.0	25-May-93 16:20	P07-03	1.8
07-Nov-92 09:00	B1	3.6	09-Nov-92 16:10	P07-04	2.4
09-Nov-92 09:30	B1	3.2	25-May-93 16:35	P07-04	3.0
09-Nov-92 09:30	B1	3.2	17-Sep-92 19:00	P20-02	1.7
11-Nov-92 00:05	B1	4.5	17-Sep-92 18:55	P20-05	1.2
11-Nov-92 06:45	B1	4.8	09-Nov-92 16:50	P20-05	0.9
11-Nov-92 15:55	B1	4.0	05-Jun-93 19:00	P20-05	0.6
12-Nov-92 15:05	B1	6.8	17-Aug-93 17:00	P20-05	1.3
12-Nov-92 21:00	B1	8.3	25-May-93 16:45	P45-01	4.8
13-Nov-92 00:25	B1	7.8	17-Sep-92 19:25	P45-03	1.3
13-Nov-92 09:00	B1	4.7	07-Oct-92 16:55	P45-03	1.4
13-Nov-92 17:00	B1	4.2	17-Aug-93 17:25	P45-03	1.0

Table A10.1 DOC data, 1992-93 (cont.).

Sample date	Location	DOC (mg/l)	Sample date	Location	DOC (mg/l)
07-Oct-92 17:05	P46-01	5.1	17-Sep-92 11:50	P76	4.5
07-Oct-92 17:10	P46-02	3.7	17-Sep-92 12:00	P77-01	5.3
07-Oct-92 17:15	P46-03	5.6	18-Oct-92 09:30	P77-01	4.5
17-Aug-93 11:35	P65	3.4	01-Nov-92 10:30	P77-01	3.9
17-Sep-92 18:55	P70	6.1	04-May-93 12:10	P77-01	3.8
17-Sep-92 18:55	P70	6.3	04-Jun-93 14:35	P77-01	3.8
04-May-93 19:10	P70	4.3	17-Sep-92 12:05	P77-02	4.7
04-May-93 19:10	P70	4.4	18-Oct-92 09:55	P77-02	4.9
17-Sep-92 18:20	P71-02	3.3	01-Nov-92 10:15	P77-02	4.4
04-Jun-93 13:30	P71-02	1.8	04-May-93 12:05	P77-02	4.5
04-Jun-93 13:30	P71-02	2.1	04-Jun-93 14:50	P77-02	4.3
04-Jun-93 13:25	P71-03	3.6	04-Jun-93 14:50	P77-02	4.4
17-Sep-92 18:30	P71-04	1.1	17-Sep-92 17:30	P78	3.0
04-Jun-93 13:10	P71-04	1.6	17-Sep-92 16:55	P80-01	44.5
17-Sep-92 18:15	P72-02	3.4	28-Sep-92 15:01	P80-01	28.6
04-Jun-93 14:10	P72-02	3.2	08-Oct-92 11:50	P80-01	23.5
17-Sep-92 18:10	P72-03	3.2	08-Oct-92 11:50	P80-01	26.5
04-Jun-93 13:50	P72-03	14.9	18-Oct-92 10:20	P80-01	18.7
04-Jun-93 13:50	P72-03	14.6	01-Nov-92 10:50	P80-01	16.4
18-Oct-92 08:55	P73-01	4.4	08-Nov-92 15:55	P80-01	13.7
04-May-93 19:05	P73-01	4.1	21-Nov-92 09:45	P80-01	11.3
18-Oct-92 08:50	P73-02	5.0	04-May-93 12:50	P80-01	14.5
04-May-93 19:00	P73-02	4.4	04-May-93 12:50	P80-01	13.9
18-Oct-92 08:45	P73-03	5.2	25-May-93 15:20	P80-01	14.9
01-Nov-92 09:30	P73-03	3.2	17-Sep-92 17:00	P80-02	36.7
01-Nov-92 09:30	P73-03	3.4	28-Sep-92 15:15	P80-02	22.0
04-May-93 11:20	P73-03	4.9	08-Oct-92 12:00	P80-02	19.2
04-Jun-93 16:10	P73-03	3.1	18-Oct-92 16:25	P80-02	10.6
17-Sep-92 17:55	P75-01	9.5	01-Nov-92 18:00	P80-02	8.4
18-Oct-92 09:05	P75-01	9.6	08-Nov-92 16:00	P80-02	10.6
01-Nov-92 10:00	P75-01	5.6	21-Nov-92 15:10	P80-02	9.9
04-May-93 11:40	P75-01	6.7	04-May-93 18:30	P80-02	9.3
04-May-93 11:40	P75-01	6.9	25-May-93 18:10	P80-02	7.2
04-Jun-93 15:30	P75-01	8.9	17-Aug-93 13:55	P80-02	11.0
17-Sep-92 17:50	P75-02	6.0	17-Sep-92 17:10	P80-03	8.6
18-Oct-92 16:55	P75-02	2.1	28-Sep-92 15:25	P80-03	8.3
01-Nov-92 18:30	P75-02	2.2	08-Oct-92 12:15	P80-03	5.6
04-May-93 18:50	P75-02	2.8	18-Oct-92 16:20	P80-03	4.1
04-Jun-93 17:55	P75-02	9.0	18-Oct-92 16:20	P80-03	4.2
17-Sep-92 11:50	P76	4.5	01-Nov-92 17:55	P80-03	3.5

Table A10.1 DOC data, 1992-93 (cont.).

Sample date	Location	DOC (mg/l)	Sample date	Location	DOC (mg/l)
08-Nov-92 16:10	P80-03	3.3	18-Oct-92 15:50	P85-01	7.1
21-Nov-92 10:15	P80-03	4.8	01-Nov-92 17:00	P85-01	6.7
04-May-93 18:40	P80-03	2.9	08-Nov-92 15:00	P85-01	6.5
04-May-93 18:40	P80-03	5.7	08-Nov-92 15:00	P85-01	7.2
25-May-93 18:00	P80-03	2.8	20-Nov-92 15:25	P85-01	10.5
17-Aug-93 14:00	P80-03	4.8	04-May-93 17:55	P85-01	6.3
21-Nov-92 09:30	P81-01	33.0	02-Jun-93 16:15	P85-01	5.1
28-Sep-92 15:30	P81-02	4.1	02-Jun-93 16:15	P85-01	5.3
21-Nov-92 09:15	P81-02	13.4	17-Sep-92 14:25	P85-02	3.5
08-Oct-92 12:30	P81-03	3.2	28-Sep-92 14:55	P85-02	3.7
18-Oct-92 10:50	P81-03	3.8	08-Oct-92 10:45	P85-02	3.5
01-Nov-92 11:05	P81-03	3.4	18-Oct-92 15:45	P85-02	3.1
08-Nov-92 12:30	P81-03	4.0	01-Nov-92 17:05	P85-02	3.0
21-Nov-92 09:00	P81-03	5.2	08-Nov-92 15:05	P85-02	3.0
04-May-93 13:15	P81-03	3.1	21-Nov-92 14:45	P85-02	6.0
25-May-93 15:00	P81-03	2.7	14-Apr-93 15:50	P85-02	3.1
01-Nov-92 17:45	P82-03	15.6	04-May-93 17:50	P85-02	7.5
08-Nov-92 15:45	P82-03	7.2	02-Jun-93 16:50	P85-02	2.9
08-Nov-92 15:45	P82-03	7.8	17-Aug-93 16:00	P85-02	3.6
21-Nov-92 11:10	P82-03	7.9	17-Sep-92 14:30	P85-03	2.0
04-May-93 18:15	P82-03	4.0	17-Sep-92 14:30	P85-03	2.0
17-Sep-92 16:40	P83	7.2	28-Sep-92 15:00	P85-03	2.0
18-Oct-92 16:00	P84-01	2.8	08-Oct-92 10:55	P85-03	2.0
01-Nov-92 16:45	P84-01	2.2	08-Oct-92 10:55	P85-03	2.0
08-Nov-92 15:30	P84-01	2.2	18-Oct-92 15:35	P85-03	1.5
21-Nov-92 14:30	P84-01	2.7	01-Nov-92 17:10	P85-03	1.6
04-May-93 17:40	P84-01	1.7	08-Nov-92 15:10	P85-03	1.6
02-Jun-93 18:00	P84-01	1.7	08-Nov-92 15:10	P85-03	1.6
17-Aug-93 15:30	P84-01	2.1	20-Nov-92 15:35	P85-03	3.5
17-Sep-92 13:50	P84-02	3.1	14-Apr-93 15:35	P85-03	4.8
18-Oct-92 11:35	P84-02	1.8	04-May-93 16:00	P85-03	1.8
01-Nov-92 12:45	P84-02	2.1	02-Jun-93 16:40	P85-03	1.2
08-Nov-92 15:20	P84-02	1.8	02-Jun-93 16:40	P85-03	1.6
21-Nov-92 14:25	P84-02	3.5	17-Aug-93 16:15	P85-03	1.6
04-May-93 15:50	P84-02	1.6	18-Oct-92 11:50	P86-03	3.7
02-Jun-93 15:50	P84-02	1.2	01-Nov-92 17:20	P86-03	3.1
17-Aug-93 15:30	P84-02	1.3	08-Nov-92 13:45	P86-03	3.4
17-Sep-92 16:20	P85-01	7.9	20-Nov-92 14:40	P86-03	4.5
28-Sep-92 14:50	P85-01	7.5	14-Apr-93 16:10	P86-03	3.3
08-Oct-92 10:30	P85-01	7.1	05-May-93 12:00	P86-03	3.2

Table A10.1 DOC data, 1992-93 (cont.).

Sample date	Location	DOC (mg/l)	Sample date	Location	DOC (mg/l)
02-Jun-93 14:20	P86-03	2.7	03-Nov-92 14:20	Precipitation	0.9
02-Jun-93 14:20	P86-03	3.1	04-Nov-92 15:15	Precipitation	5.3
20-Nov-92 13:50	P87-01	13.6	09-Nov-92 07:00	Precipitation	1.8
01-Nov-92 17:25	P87-03	5.2	11-Nov-92 12:00	Precipitation	2.1
08-Nov-92 13:05	P87-03	3.5	11-Nov-92 12:00	Precipitation	2.3
20-Nov-92 13:40	P87-03	4.0	13-Nov-92 06:06	Precipitation	1.2
14-Apr-93 14:50	P87-03	4.1	15-May-93 09:25	Precipitation	1.6
05-May-93 12:10	P87-03	3.9	24-May-93 15:00	Precipitation	1.7
02-Jun-93 14:40	P87-03	3.1	25-May-93 17:10	Precipitation	3.4
02-Jun-93 14:40	P87-03	3.0	26-May-93 14:40	Precipitation	1.6
02-Jun-93 14:40	P87-03	3.3	28-May-93 12:15	Precipitation	0.9
17-Sep-92 15:50	P88	5.8	02-Jun-93 08:30	Precipitation	2.3
04-May-93 17:25	P88-01	5.6	15-Sep-92 10:55	S1	4.6
01-Nov-92 11:45	P88-02	3.7	27-Sep-92 12:40	S1	8.4
08-Nov-92 12:50	P88-02	3.9	27-Sep-92 14:48	S1	8.6
20-Nov-92 13:25	P88-02	4.9	27-Sep-92 18:40	S1	9.8
14-Apr-93 14:30	P88-02	3.3	28-Sep-92 01:40	S1	7.5
04-May-93 18:10	P88-02	3.5	28-Sep-92 10:00	S1	7.8
02-Jun-93 15:30	P88-02	3.1	29-Sep-92 10:03	S1	6.0
02-Jun-93 15:30	P88-02	3.2	02-Oct-92 11:07	S1	4.0
07-Oct-92 11:30	P89-01	13.1	07-Oct-92 10:45	S1	3.3
18-Oct-92 12:20	P89-01	4.8	12-Oct-92 17:50	S1	4.3
08-Nov-92 11:15	P89-01	5.8	13-Oct-92 09:45	S1	2.9
20-Nov-92 16:00	P89-01	6.2	13-Oct-92 17:05	S1	4.8
04-May-93 17:10	P89-01	5.3	16-Oct-92 06:40	S1	13.5
02-Jun-93 17:25	P89-01	5.0	16-Oct-92 07:30	S1	14.3
02-Jun-93 17:25	P89-01	4.8	16-Oct-92 10:30	S1	9.1
17-Sep-92 16:05	P89-02	4.0	16-Oct-92 15:10	S1	10.0
18-Oct-92 12:30	P89-02	4.1	17-Oct-92 09:30	S1	6.5
01-Nov-92 13:15	P89-02	3.3	17-Oct-92 18:15	S1	12.5
08-Nov-92 11:30	P89-02	3.5	18-Oct-92 13:30	S1	5.4
20-Nov-92 16:15	P89-02	5.0	20-Oct-92 16:25	S1	3.5
04-May-93 17:00	P89-02	4.8	28-Oct-92 14:50	S1	4.2
02-Jun-93 17:40	P89-02	3.6	02-Nov-92 09:05	S1	2.6
02-Jun-93 17:40	P89-02	3.8	02-Nov-92 15:45	S1	5.6
17-Sep-92 12:15	P90	3.1	02-Nov-92 20:10	S1	12.9
28-Oct-92 11:50	Pond nr W4	18.0	03-Nov-92 06:10	S1	8.2
17-Oct-92 18:40	Precipitation	2.2	03-Nov-92 15:36	S1	7.2
22-Oct-92 16:00	Precipitation	1.9	04-Nov-92 10:50	S1	8.4
27-Oct-92 14:30	Precipitation	4.5	04-Nov-92 15:45	S1	6.9

Table A10.1 DOC data, 1992-93 (cont.).

Sample date	Location	DOC (mg/l)	Sample date	Location	DOC (mg/l)
05-Nov-92 15:00	S1	5.2	27-Sep-92 14:33	S4	7.8
07-Nov-92 15:30	S1	3.9	27-Sep-92 18:57	S4	8.0
09-Nov-92 10:50	S1	4.3	28-Sep-92 01:40	S4	6.3
14-Apr-93 00:00	S1	3.7	28-Sep-92 10:25	S4	5.5
03-May-93 18:35	S1	3.5	29-Sep-92 10:15	S4	6.0
10-May-93 17:00	S1	2.7	02-Oct-92 11:21	S4	5.2
10-May-93 17:00	S1	2.6	07-Oct-92 11:15	S4	5.4
10-May-93 17:00	S1	2.5	12-Oct-92 17:36	S4	5.1
14-May-93 20:00	S1	7.7	13-Oct-92 09:55	S4	3.7
14-May-93 20:00	S1	8.3	13-Oct-92 17:12	S4	5.7
15-May-93 01:35	S1	3.4	16-Oct-92 06:45	S4	14.7
15-May-93 01:35	S1	3.7	16-Oct-92 07:34	S4	15.0
15-May-93 19:40	S1	2.6	16-Oct-92 10:45	S4	8.2
15-May-93 19:40	S1	2.9	16-Oct-92 15:20	S4	10.0
16-May-93 16:50	S1	2.5	17-Oct-92 09:40	S4	4.5
16-May-93 16:50	S1	2.5	17-Oct-92 18:20	S4	7.7
17-May-93 19:00	S1	2.2	18-Oct-92 13:35	S4	3.4
17-May-93 19:00	S1	2.6	20-Oct-92 16:55	S4	3.4
22-May-93 14:15	S1	3.1	28-Oct-92 15:10	S4	2.9
24-May-93 05:45	S1	11.4	02-Nov-92 09:20	S4	2.4
24-May-93 08:05	S1	8.4	02-Nov-92 15:55	S4	5.3
24-May-93 11:10	S1	5.2	02-Nov-92 20:20	S4	12.7
24-May-93 15:15	S1	4.1	03-Nov-92 06:20	S4	7.0
24-May-93 19:00	S1	3.8	03-Nov-92 15:42	S4	4.7
24-May-93 19:30	S1	4.0	04-Nov-92 11:00	S4	7.4
25-May-93 14:00	S1	3.1	04-Nov-92 15:50	S4	5.0
25-May-93 20:10	S1	4.3	05-Nov-92 15:10	S4	4.4
25-May-93 20:10	S1	4.4	07-Nov-92 15:45	S4	3.1
26-May-93 14:50	S1	3.5	09-Nov-92 20:00	S4	2.8
27-May-93 12:20	S1	3.1	14-Apr-93 00:00	S4	4.0
28-May-93 06:45	S1	7.0	14-Apr-93 00:00	S4	4.0
28-May-93 12:25	S1	7.2	10-May-93 17:10	S4	3.1
28-May-93 19:15	S1	3.9	10-May-93 17:10	S4	3.2
29-May-93 16:40	S1	3.2	14-May-93 20:05	S4	7.6
30-May-93 16:20	S1	2.7	14-May-93 20:05	S4	8.6
16-Aug-93 14:25	S1	2.9	14-May-93 20:55	S4	6.5
15-Sep-92 11:40	S2	3.3	14-May-93 20:55	S4	6.5
15-Sep-92 11:50	S3	3.0	15-May-93 01:45	S4	3.8
15-Sep-92 11:50	S4	3.8	15-May-93 01:45	S4	4.2
27-Sep-92 12:50	S4	8.0	15-May-93 19:50	S4	2.8

Table A10.1 DOC data, 1992-93 (cont.).

Sample date	Location	DOC (mg/l)	Sample date	Location	DOC (mg/l)
15-May-93 19:50	S4	3.1	25-May-93 12:45	SF 1	48.2
16-May-93 17:00	S4	2.2	28-May-93 16:10	SF 1	54.4
16-May-93 17:00	S4	2.6	02-Jun-93 09:30	SF 1	28.8
16-May-93 17:00	S4	2.8	13-Oct-92 15:05	SF 2	60.9
16-May-93 17:00	S4	2.9	16-Oct-92 10:00	SF 2	18.0
17-May-93 19:05	S4	2.3	16-Oct-92 10:00	SF 2	18.7
17-May-93 19:05	S4	2.3	17-Oct-92 18:44	SF 2	32.6
22-May-93 14:30	S4	4.2	27-Oct-92 16:00	SF 2	64.5
24-May-93 05:50	S4	10.5	03-Nov-92 03:00	SF 2	11.6
24-May-93 08:15	S4	7.8	03-Nov-92 03:00	SF 2	12.5
24-May-93 11:15	S4	4.8	11-Nov-92 14:45	SF 2	13.6
24-May-93 15:20	S4	3.8	11-Nov-92 14:45	SF 2	13.4
24-May-93 19:05	S4	4.1	13-Nov-92 07:35	SF 2	5.2
24-May-93 19:05	S4	4.6	15-May-93 00:00	SF 2	88.7
24-May-93 19:05	S4	4.6	24-May-93 16:10	SF 2	80.1
24-May-93 19:38	S4	4.5	24-May-93 16:25	SF 2	62.3
25-May-93 14:05	S4	3.5	25-May-93 12:50	SF 2	72.5
25-May-93 20:15	S4	3.7	28-May-93 16:05	SF 2	27.9
26-May-93 15:00	S4	2.7	02-Jun-93 09:41	SF 2	27.4
27-May-93 12:30	S4	2.6	03-Nov-92 17:15	SF 3	30.1
28-May-93 06:50	S4	5.9	09-Nov-92 14:25	SF 3	30.8
28-May-93 12:35	S4	3.6	13-Nov-92 08:05	SF 3	11.3
28-May-93 12:35	S4	3.5	24-May-93 16:35	SF 3	154.2
28-May-93 19:20	S4	3.8	28-May-93 15:00	SF 3	50.0
28-May-93 19:20	S4	3.8	02-Jun-93 12:30	SF 3	41.6
29-May-93 16:45	S4	2.8	15-May-93 13:30	SF 4	67.2
30-May-93 16:30	S4	2.8	24-May-93 16:30	SF 4	56.0
16-Aug-93 14:25	S4	4.0	28-May-93 15:01	SF 4	51.2
15-Sep-92 12:00	S5	3.6	02-Jun-93 12:35	SF 4	67.3
13-Oct-92 15:00	SF 1	35.4	17-Oct-92 13:01	Stream near MP66	6.7
17-Oct-92 00:20	SF 1	57.0	17-Oct-92 13:02	Stream near P70	6.7
17-Oct-92 00:20	SF 1	55.6	17-Oct-92 13:04	Stream near P76	7.0
22-Oct-92 17:00	SF 1	31.8	28-Oct-92 09:20	Stream near P76	5.3
27-Oct-92 15:50	SF 1	57.7	17-Oct-92 13:30	Stream near P77	8.7
03-Nov-92 03:10	SF 1	52.4	28-Oct-92 11:40	Stream near P83	4.9
11-Nov-92 13:35	SF 1	48.1			
11-Nov-92 13:35	SF 1	47.6			
13-Nov-92 07:30	SF 1	67.0			
15-May-93 18:30	SF 1	30.4			
24-May-93 10:10	SF 1	90.0			

Table A10.1 DOC data, 1992-93 (cont.).

Sample date	Location	DOC (mg/l)	Sample date	Location	DOC (mg/l)
17-Oct-92 13:00	Stream near W2	6.5	02-Jun-93 02:40	TF 4	6.1
28-Sep-92 10:20	TF 1	8.1	16-Sep-92 09:40	W1	4.2
13-Oct-92 10:00	TF 1	48.2	27-Sep-92 11:30	W1	5.5
15-Oct-92 19:40	TF 1	10.2	27-Sep-92 13:45	W1	6.2
17-Oct-92 10:25	TF 1	2.7	27-Sep-92 17:37	W1	6.6
27-Oct-92 14:50	TF 1	2.3	28-Sep-92 00:26	W1	6.1
03-Nov-92 14:50	TF 1	1.9	28-Sep-92 11:15	W1	6.0
04-Nov-92 15:35	TF 1	12.6	29-Sep-92 08:40	W1	5.6
11-Nov-92 12:15	TF 1	1.6	02-Oct-92 08:35	W1	5.3
13-Nov-92 06:30	TF 1	1.5	07-Oct-92 08:15	W1	4.3
15-May-93 10:50	TF 1	4.8	12-Oct-92 18:45	W1	5.7
24-May-93 15:45	TF 1	2.0	12-Oct-92 18:45	W1	6.2
25-May-93 16:50	TF 1	4.1	12-Oct-92 18:45	W1	5.6
26-May-93 15:35	TF 1	2.0	13-Oct-92 11:40	W1	4.6
28-May-93 13:15	TF 1	2.5	13-Oct-92 11:40	W1	4.5
02-Jun-93 08:50	TF 1	3.5	13-Oct-92 20:14	W1	5.3
02-Jun-93 08:50	TF 1	3.3	13-Oct-92 20:14	W1	5.2
03-Nov-92 16:25	TF 2	3.4	16-Oct-92 07:55	W1	8.5
04-Nov-92 16:35	TF 2	8.2	16-Oct-92 11:15	W1	7.0
11-Nov-92 13:50	TF 2	6.3	16-Oct-92 16:10	W1	7.8
13-Nov-92 07:40	TF 2	3.4	17-Oct-92 00:00	W1	7.5
15-May-93 12:15	TF 2	20.1	17-Oct-92 00:00	W1	7.6
24-May-93 16:15	TF 2	19.9	17-Oct-92 04:00	W1	6.7
25-May-93 12:40	TF 2	20.1	17-Oct-92 04:00	W1	7.1
27-May-93 11:40	TF 2	16.4	17-Oct-92 08:00	W1	6.3
28-May-93 16:00	TF 2	8.0	17-Oct-92 08:00	W1	6.7
02-Jun-93 09:45	TF 2	8.2	17-Oct-92 12:45	W1	6.1
03-Nov-92 17:05	TF 3	2.8	17-Oct-92 12:45	W1	6.4
04-Nov-92 16:45	TF 3	9.1	18-Oct-92 14:25	W1	5.2
11-Nov-92 14:20	TF 3	3.8	18-Oct-92 14:25	W1	5.5
13-Nov-92 08:00	TF 3	2.4	20-Oct-92 09:20	W1	4.9
15-May-93 13:25	TF 3	16.5	20-Oct-92 09:20	W1	4.8
24-May-93 16:25	TF 3	20.1	20-Oct-92 09:20	W1	4.4
25-May-93 12:15	TF 3	15.0	28-Oct-92 08:55	W1	5.0
24-May-93 16:30	TF 4	8.8	28-Oct-92 08:55	W1	5.1
25-May-93 12:10	TF 4	13.9	01-Nov-92 14:35	W1	4.2
27-May-93 11:15	TF 4	11.4	02-Nov-92 16:35	W1	4.9
28-May-93 16:05	TF 4	5.6	02-Nov-92 22:25	W1	7.7
28-May-93 16:05	TF 4	5.8	03-Nov-92 02:15	W1	7.7
			03-Nov-92 06:00	W1 ISCO	7.2

Table A10.1 DOC data, 1992-93 (cont.).

Sample date	Location	DOC (mg/l)	Sample date	Location	DOC (mg/l)
03-Nov-92 06:00	W1 ISCO	7.4	13-Nov-92 16:40	W1	5.4
03-Nov-92 06:00	W1 ISCO	7.9	14-Nov-92 12:40	W1	4.7
03-Nov-92 07:10	W1	7.6	15-Nov-92 14:45	W1	4.7
03-Nov-92 12:00	W1 ISCO	6.4	16-Nov-92 14:00	W1	4.2
03-Nov-92 16:10	W1	5.9	18-Nov-92 13:35	W1	4.1
03-Nov-92 16:10	W1	6.4	19-Nov-92 10:30	W1	4.5
03-Nov-92 18:00	W1 ISCO	5.9	19-Nov-92 10:30	W1	4.4
03-Nov-92 18:00	W1 ISCO	6.3	04-Jan-93 00:00	W1	3.9
04-Nov-92 00:00	W1 ISCO	5.9	04-Jan-93 00:00	W1	4.2
04-Nov-92 06:00	W1 ISCO	5.6	14-Apr-93 00:00	W1	4.7
04-Nov-92 11:50	W1	6.0	03-May-93 18:50	W1	4.6
04-Nov-92 11:50	W1	6.4	10-May-93 09:45	W1	4.4
04-Nov-92 12:00	W1 ISCO	6.5	14-May-93 10:00	W1	3.9
04-Nov-92 18:00	W1 ISCO	6.1	14-May-93 10:00	W1	4.3
04-Nov-92 23:47	W1	5.4	14-May-93 10:00	W1	4.5
04-Nov-92 23:47	W1	5.3	14-May-93 18:30	W1	4.7
05-Nov-92 00:00	W1 ISCO	5.9	14-May-93 18:30	W1	4.8
05-Nov-92 00:00	W1 ISCO	6.2	14-May-93 19:45	W1	5.7
05-Nov-92 06:00	W1 ISCO	5.6	14-May-93 19:45	W1	5.6
05-Nov-92 12:00	W1 ISCO	5.5	14-May-93 21:35	W1	5.7
05-Nov-92 16:30	W1	5.0	14-May-93 21:35	W1	5.9
05-Nov-92 16:30	W1	5.4	14-May-93 21:35	W1	6.4
05-Nov-92 18:00	W1 ISCO	5.4	14-May-93 23:15	W1	5.4
06-Nov-92 00:00	W1 ISCO	5.3	14-May-93 23:15	W1	5.8
07-Nov-92 08:25	W1	6.0	15-May-93 01:00	W1	5.5
07-Nov-92 08:25	W1	5.6	15-May-93 01:00	W1	5.6
09-Nov-92 09:15	W1	5.0	15-May-93 01:00	W1	5.4
09-Nov-92 09:15	W1	4.8	15-May-93 02:30	W1 ISCO	10.4
10-Nov-92 23:30	W1	5.7	15-May-93 02:30	W1 ISCO	10.8
11-Nov-92 06:15	W1	5.5	15-May-93 02:30	W1 ISCO	10.9
11-Nov-92 06:15	W1	5.1	15-May-93 04:00	W1 ISCO	5.4
11-Nov-92 15:30	W1	5.3	15-May-93 04:00	W1 ISCO	5.4
12-Nov-92 07:10	W1	4.4	15-May-93 05:30	W1 ISCO	5.3
12-Nov-92 13:15	W1	4.8	15-May-93 05:30	W1 ISCO	5.6
12-Nov-92 14:45	W1	5.6	15-May-93 07:15	W1	5.0
12-Nov-92 18:30	W1	6.8	15-May-93 07:15	W1	5.1
12-Nov-92 20:40	W1	7.4	15-May-93 07:15	W1	5.1
12-Nov-92 23:40	W1	8.7	15-May-93 12:05	W1	5.4
13-Nov-92 02:30	W1	7.7	15-May-93 14:00	W1 ISCO	5.6
13-Nov-92 08:30	W1	6.3	15-May-93 14:00	W1 ISCO	5.7

Table A10.1 DOC data, 1992-93 (cont.).

Sample date	Location	DOC (mg/l)	Sample date	Location	DOC (mg/l)
15-May-93 14:00	W1 ISCO	5.2	24-May-93 15:00	W1 ISCO	6.8
15-May-93 16:00	W1 ISCO	5.5	24-May-93 16:00	W1 ISCO	6.7
15-May-93 16:00	W1 ISCO	5.6	24-May-93 17:20	W1	6.6
15-May-93 18:00	W1 ISCO	5.2	24-May-93 19:00	W1 ISCO	8.2
15-May-93 18:10	W1	4.7	24-May-93 19:00	W1 ISCO	8.3
15-May-93 18:10	W1	4.8	24-May-93 19:00	W1 ISCO	8.1
15-May-93 18:10	W1	4.9	24-May-93 20:10	W1	6.6
15-May-93 22:00	W1 ISCO	5.1	24-May-93 20:10	W1	6.5
16-May-93 02:00	W1 ISCO	5.0	24-May-93 21:00	W1 ISCO	6.7
16-May-93 11:45	W1	4.7	25-May-93 01:00	W1 ISCO	6.8
17-May-93 06:00	W1 ISCO	4.3	25-May-93 01:00	W1 ISCO	6.2
17-May-93 12:00	W1 ISCO	4.3	25-May-93 05:00	W1 ISCO	6.2
17-May-93 16:25	W1	4.1	25-May-93 09:00	W1 ISCO	6.0
17-May-93 16:25	W1	4.2	25-May-93 09:00	W1 ISCO	6.2
22-May-93 10:20	W1	4.2	25-May-93 10:30	W1	6.2
24-May-93 04:20	W1	4.9	25-May-93 10:30	W1	5.9
24-May-93 05:00	W1 ISCO	6.2	25-May-93 13:00	W1 ISCO	6.1
24-May-93 05:00	W1 ISCO	5.9	25-May-93 20:40	W1	5.9
24-May-93 05:30	W1 ISCO	6.3	26-May-93 02:00	W1 ISCO	5.8
24-May-93 06:00	W1 ISCO	7.2	26-May-93 10:10	W1	5.3
24-May-93 06:00	W1 ISCO	6.7	27-May-93 02:00	W1 ISCO	5.5
24-May-93 06:20	W1	7.3	27-May-93 02:00	W1 ISCO	5.1
24-May-93 06:20	W1	7.2	27-May-93 09:35	W1	4.8
24-May-93 06:30	W1 ISCO	7.3	28-May-93 02:00	W1 ISCO	5.2
24-May-93 07:00	W1 ISCO	7.3	28-May-93 02:30	W1 ISCO	5.3
24-May-93 07:30	W1 ISCO	7.7	28-May-93 03:30	W1 ISCO	5.7
24-May-93 07:40	W1	8.0	28-May-93 04:30	W1 ISCO	6.2
24-May-93 07:40	W1	8.1	28-May-93 05:30	W1 ISCO	6.5
24-May-93 08:00	W1 ISCO	7.7	28-May-93 06:30	W1 ISCO	6.9
24-May-93 08:00	W1 ISCO	7.8	28-May-93 06:30	W1 ISCO	6.3
24-May-93 08:00	W1 ISCO	8.0	28-May-93 07:15	W1	5.9
24-May-93 08:30	W1 ISCO	8.1	28-May-93 07:15	W1	6.0
24-May-93 08:30	W1 ISCO	8.7	28-May-93 09:00	W1 ISCO	6.3
24-May-93 09:00	W1	8.1	28-May-93 09:00	W1 ISCO	6.6
24-May-93 10:00	W1 ISCO	7.5	28-May-93 10:05	W1	6.2
24-May-93 11:00	W1 ISCO	7.1	28-May-93 14:30	W1	5.9
24-May-93 12:00	W1 ISCO	6.9	28-May-93 19:55	W1	5.4
24-May-93 12:10	W1	7.0	28-May-93 19:55	W1	5.5
24-May-93 13:00	W1 ISCO	7.0	29-May-93 01:00	W1 ISCO	5.7
24-May-93 14:00	W1 ISCO	6.9	29-May-93 06:00	W1 ISCO	5.4

Table A10.1 DOC data, 1992-93 (cont.).

Sample date	Location	DOC (mg/l)	Sample date	Location	DOC (mg/l)
29-May-93 13:50	W1	5.0	13-Oct-92 20:05	W2	4.9
29-May-93 22:00	W1 ISCO	5.4	16-Oct-92 08:00	W2	4.2
29-May-93 22:00	W1 ISCO	4.8	16-Oct-92 11:20	W2	4.0
30-May-93 04:00	W1 ISCO	4.9	16-Oct-92 11:20	W2	4.0
30-May-93 04:00	W1 ISCO	5.2	16-Oct-92 16:20	W2	5.0
30-May-93 10:00	W1 ISCO	5.1	16-Oct-92 16:20	W2	5.2
30-May-93 14:10	W1	5.0	17-Oct-92 12:55	W2	3.6
30-May-93 14:10	W1	4.8	17-Oct-92 12:55	W2	3.8
31-May-93 08:40	W1 ISCO	5.9	18-Oct-92 14:35	W2	3.6
31-May-93 10:00	W1 ISCO	5.9	18-Oct-92 14:35	W2	3.7
31-May-93 14:00	W1 ISCO	6.3	20-Oct-92 09:30	W2	3.2
31-May-93 18:00	W1 ISCO	5.7	20-Oct-92 09:30	W2	3.4
31-May-93 22:00	W1 ISCO	5.4	28-Oct-92 09:10	W2	3.5
31-May-93 22:00	W1 ISCO	5.8	28-Oct-92 09:10	W2	3.5
01-Jun-93 02:00	W1 ISCO	5.3	01-Nov-92 14:45	W2	3.0
01-Jun-93 06:00	W1 ISCO	5.0	02-Nov-92 16:45	W2	3.5
01-Jun-93 10:00	W1 ISCO	5.9	02-Nov-92 22:35	W2	5.1
01-Jun-93 10:00	W1 ISCO	5.4	03-Nov-92 08:03	W2	4.8
01-Jun-93 14:00	W1 ISCO	5.1	03-Nov-92 16:20	W2	3.8
01-Jun-93 18:00	W1 ISCO	4.6	04-Nov-92 12:00	W2	4.0
01-Jun-93 22:00	W1 ISCO	5.5	04-Nov-92 23:55	W2	3.9
01-Jun-93 22:00	W1 ISCO	5.7	05-Nov-92 16:40	W2	3.4
02-Jun-93 16:35	W1	4.6	07-Nov-92 08:40	W2	3.1
03-Jun-93 08:45	W1	4.3	09-Nov-92 09:20	W2	3.1
04-Jun-93 16:15	W1	4.0	09-Nov-92 09:20	W2	3.1
04-Jun-93 16:15	W1	4.6	11-Nov-92 00:10	W2	3.4
16-Aug-93 14:25	W1	4.2	11-Nov-92 06:30	W2	3.7
27-Sep-92 11:40	W2	4.1	11-Nov-92 15:45	W2	3.5
27-Sep-92 11:40	W2	4.2	12-Nov-92 14:55	W2	4.9
27-Sep-92 13:55	W2	4.5	12-Nov-92 20:50	W2	7.7
27-Sep-92 17:45	W2	4.4	13-Nov-92 00:15	W2	9.1
28-Sep-92 00:34	W2	4.4	13-Nov-92 08:40	W2	4.2
28-Sep-92 11:20	W2	3.8	13-Nov-92 16:50	W2	4.0
29-Sep-92 08:45	W2	3.4	14-Nov-92 12:50	W2	3.6
02-Oct-92 08:45	W2	4.0	16-Nov-92 14:05	W2	3.2
07-Oct-92 08:50	W2	2.8	19-Nov-92 10:40	W2	3.5
07-Oct-92 08:50	W2	2.7	14-Apr-93 00:00	W2	3.9
13-Oct-92 11:45	W2	3.5	04-May-93 12:00	W2	2.9
13-Oct-92 11:45	W2	3.5	04-May-93 12:00	W2	3.8
13-Oct-92 20:05	W2	4.4	10-May-93 09:55	W2	2.6

Table A10.1 DOC data, 1992-93 (cont.).

Sample date	Location	DOC (mg/l)	Sample date	Location	DOC (mg/l)
28-May-93 10:10	W2	2.9	05-Nov-92 17:05	W3	6.7
16-Sep-92 10:15	W3	8.4	07-Nov-92 09:15	W3	5.4
16-Sep-92 10:15	W3	8.7	09-Nov-92 09:45	W3	4.9
27-Sep-92 11:45	W3	8.5	09-Nov-92 09:45	W3	5.0
27-Sep-92 11:45	W3	8.7	11-Nov-92 00:20	W3	5.7
27-Sep-92 14:00	W3	8.7	11-Nov-92 07:00	W3	5.6
27-Sep-92 17:55	W3	8.7	11-Nov-92 16:10	W3	5.3
28-Sep-92 00:45	W3	8.3	12-Nov-92 15:20	W3	5.8
28-Sep-92 11:30	W3	8.3	12-Nov-92 21:10	W3	7.3
29-Sep-92 09:00	W3	7.9	13-Nov-92 00:35	W3	8.7
02-Oct-92 09:00	W3	7.5	13-Nov-92 09:20	W3	6.8
07-Oct-92 09:15	W3	7.1	13-Nov-92 17:10	W3	5.8
12-Oct-92 19:05	W3	7.8	14-Nov-92 13:10	W3	5.2
12-Oct-92 19:05	W3	7.9	16-Nov-92 14:30	W3	4.9
13-Oct-92 12:30	W3	8.0	19-Nov-92 11:00	W3	4.7
13-Oct-92 12:30	W3	8.1	14-Apr-93 00:00	W3	6.0
13-Oct-92 19:40	W3	8.6	14-Apr-93 00:00	W3	6.3
13-Oct-92 19:40	W3	8.5	03-May-93 19:05	W3	6.8
16-Oct-92 08:15	W3	11.2	10-May-93 10:30	W3	9.0
16-Oct-92 11:50	W3	11.4	10-May-93 10:30	W3	8.3
16-Oct-92 16:40	W3	11.2	14-May-93 10:10	W3	7.8
16-Oct-92 16:40	W3	11.3	14-May-93 10:10	W3	8.0
17-Oct-92 13:20	W3	8.0	14-May-93 18:40	W3	8.7
17-Oct-92 13:20	W3	8.3	14-May-93 21:45	W3	9.3
18-Oct-92 15:00	W3	7.6	14-May-93 21:45	W3	9.7
18-Oct-92 15:00	W3	7.7	15-May-93 00:50	W3	9.9
20-Oct-92 10:10	W3	6.7	15-May-93 00:50	W3	10.8
20-Oct-92 10:10	W3	6.8	15-May-93 07:25	W3	9.6
28-Oct-92 09:55	W3	6.5	15-May-93 07:25	W3	9.8
28-Oct-92 09:55	W3	6.9	15-May-93 18:20	W3	8.9
01-Nov-92 15:20	W3	5.9	15-May-93 18:20	W3	9.7
02-Nov-92 17:05	W3	6.6	16-May-93 12:00	W3	8.0
02-Nov-92 23:10	W3	9.3	17-May-93 16:35	W3	7.2
03-Nov-92 02:30	W3	8.8	17-May-93 16:35	W3	7.6
03-Nov-92 07:25	W3	7.8	22-May-93 10:30	W3	9.2
03-Nov-92 07:25	W3	8.1	22-May-93 10:30	W3	8.6
03-Nov-92 16:25	W3	7.0	22-May-93 10:30	W3	8.4
04-Nov-92 12:22	W3	7.1	22-May-93 10:30	W3	8.3
05-Nov-92 00:20	W3	6.5	24-May-93 04:30	W3	9.1
05-Nov-92 00:20	W3	6.6	24-May-93 04:30	W3	8.6

Table A10.1 DOC data, 1992-93 (cont.).

Sample date	Location	DOC (mg/l)	Sample date	Location	DOC (mg/l)
24-May-93 04:30	W3	8.7	28-Sep-92 11:35	W4	5.5
24-May-93 06:30	W3	10.7	29-Sep-92 09:12	W4	5.4
24-May-93 06:30	W3	10.5	02-Oct-92 09:30	W4	4.7
24-May-93 07:30	W3	10.8	07-Oct-92 09:35	W4	7.6
24-May-93 07:30	W3	10.9	13-Oct-92 13:00	W4	7.4
24-May-93 09:10	W3	11.4	13-Oct-92 19:24	W4	7.9
24-May-93 09:10	W3	11.5	16-Oct-92 08:25	W4	12.4
24-May-93 12:20	W3	10.9	16-Oct-92 12:05	W4	9.0
24-May-93 12:20	W3	11.3	16-Oct-92 16:50	W4	9.0
24-May-93 17:30	W3	9.4	17-Oct-92 13:50	W4	5.6
24-May-93 17:30	W3	9.2	18-Oct-92 15:25	W4	5.0
24-May-93 20:20	W3	9.3	20-Oct-92 10:30	W4	5.2
24-May-93 20:20	W3	9.3	28-Oct-92 10:15	W4	4.7
25-May-93 10:40	W3	8.5	28-Oct-92 10:15	W4	5.2
25-May-93 10:40	W3	8.4	01-Nov-92 15:35	W4	4.0
25-May-93 20:45	W3	8.2	02-Nov-92 17:20	W4	5.6
25-May-93 20:45	W3	8.3	02-Nov-92 23:30	W4	8.7
26-May-93 10:20	W3	7.6	02-Nov-92 23:30	W4	8.7
26-May-93 10:20	W3	7.7	03-Nov-92 02:45	W4	6.6
27-May-93 09:45	W3	7.0	03-Nov-92 07:39	W4	6.3
27-May-93 09:45	W3	6.9	03-Nov-92 16:45	W4	5.0
28-May-93 07:30	W3	8.4	04-Nov-92 12:35	W4	5.9
28-May-93 07:30	W3	8.1	05-Nov-92 00:55	W4	4.6
28-May-93 10:20	W3	7.6	05-Nov-92 00:55	W4	5.1
28-May-93 10:20	W3	7.8	05-Nov-92 17:40	W4	4.8
28-May-93 14:40	W3	7.0	07-Nov-92 09:50	W4	4.0
28-May-93 14:40	W3	6.6	09-Nov-92 10:00	W4	4.1
28-May-93 14:40	W3	7.2	11-Nov-92 00:35	W4	4.7
28-May-93 20:05	W3	6.6	11-Nov-92 07:10	W4	4.7
28-May-93 20:05	W3	6.6	11-Nov-92 16:20	W4	4.3
28-May-93 20:05	W3	6.5	12-Nov-92 15:30	W4	5.1
29-May-93 14:05	W3	6.1	12-Nov-92 21:25	W4	6.8
29-May-93 14:05	W3	6.0	13-Nov-92 00:45	W4	7.7
30-May-93 14:20	W3	6.0	13-Nov-92 00:45	W4	8.8
16-Sep-92 10:35	W4	7.3	13-Nov-92 09:35	W4	4.8
27-Sep-92 12:00	W4	6.0	13-Nov-92 17:50	W4	4.5
27-Sep-92 14:05	W4	7.8	14-Nov-92 13:35	W4	4.3
27-Sep-92 14:05	W4	6.8	16-Nov-92 14:45	W4	4.2
27-Sep-92 18:01	W4	6.8	19-Nov-92 11:40	W4	3.8
28-Sep-92 01:00	W4	5.9	14-Apr-93 00:00	W4	4.8

Table A10.1 DOC data, 1992-93 (cont.).

Sample date	Location	DOC (mg/l)	Sample date	Location	DOC (mg/l)
14-Apr-93 00:00	W4	5.0	16-Oct-92 08:35	W5	4.2
03-May-93 19:30	W4	5.3	16-Oct-92 12:20	W5	4.3
10-May-93 11:25	W4	5.1	16-Oct-92 17:00	W5	4.8
14-May-93 10:45	W4	4.9	17-Oct-92 14:05	W5	3.7
14-May-93 18:55	W4	6.7	18-Oct-92 14:25	W5	3.8
14-May-93 22:05	W4	7.6	20-Oct-92 10:55	W5	3.8
15-May-93 00:25	W4	6.5	28-Oct-92 10:30	W5	3.4
15-May-93 07:40	W4	5.7	28-Oct-92 10:30	W5	3.7
15-May-93 18:40	W4	5.0	01-Nov-92 15:55	W5	4.3
16-May-93 12:20	W4	5.1	01-Nov-92 15:55	W5	4.9
17-May-93 17:00	W4	4.7	02-Nov-92 17:30	W5	3.9
22-May-93 11:15	W4	6.7	02-Nov-92 23:45	W5	5.1
24-May-93 04:50	W4	8.1	03-Nov-92 07:53	W5	4.6
24-May-93 06:55	W4	10.3	03-Nov-92 16:52	W5	4.1
24-May-93 09:30	W4	8.6	04-Nov-92 12:50	W5	4.4
24-May-93 12:40	W4	6.9	05-Nov-92 01:20	W5	3.9
24-May-93 17:50	W4	6.4	05-Nov-92 18:10	W5	3.6
24-May-93 20:40	W4	6.1	07-Nov-92 10:15	W5	3.5
25-May-93 11:05	W4	5.1	09-Nov-92 10:10	W5	3.0
25-May-93 21:00	W4	5.2	09-Nov-92 10:10	W5	3.1
26-May-93 10:40	W4	4.4	11-Nov-92 00:45	W5	3.4
27-May-93 10:10	W4	4.2	11-Nov-92 07:20	W5	3.8
28-May-93 07:55	W4	6.0	11-Nov-92 16:30	W5	3.5
28-May-93 10:40	W4	5.1	12-Nov-92 15:45	W5	4.8
28-May-93 15:20	W4	4.8	12-Nov-92 21:40	W5	7.7
28-May-93 20:30	W4	4.5	13-Nov-92 00:55	W5	7.0
29-May-93 14:30	W4	4.2	13-Nov-92 09:55	W5	4.8
30-May-93 14:40	W4	4.2	13-Nov-92 17:30	W5	4.5
16-Sep-92 10:55	W5	4.5	14-Nov-92 13:50	W5	3.8
27-Sep-92 12:10	W5	4.8	16-Nov-92 14:55	W5	3.4
27-Sep-92 14:20	W5	4.2	19-Nov-92 11:50	W5	3.6
27-Sep-92 18:16	W5	5.6	14-Apr-93 00:00	W5	3.9
28-Sep-92 01:10	W5	4.6	14-Apr-93 00:00	W5	3.8
28-Sep-92 11:50	W5	3.9	03-May-93 19:45	W5	3.2
29-Sep-92 09:25	W5	3.5	10-May-93 11:50	W5	3.3
02-Oct-92 10:00	W5	3.5	14-May-93 11:10	W5	2.9
07-Oct-92 09:55	W5	2.9	14-May-93 19:10	W5	3.6
13-Oct-92 14:15	W5	4.0	14-May-93 22:15	W5	2.7
13-Oct-92 14:15	W5	4.3	15-May-93 00:05	W5	2.7
13-Oct-92 19:52	W5	4.4	15-May-93 08:00	W5	3.0

Table A10.1 DOC data, 1992-93 (cont.).

Sample date	Location	DOC (mg/l)	Sample date	Location	DOC (mg/l)
15-May-93 19:00	W5	2.8	14-Apr-93 00:00	Wetland 2	7.4
15-May-93 19:00	W5	3.0	14-Apr-93 00:00	Wetland 2	7.5
16-May-93 12:30	W5	3.2	03-May-93 19:20	Wetland 2	11.4
16-May-93 12:30	W5	3.4	03-May-93 19:20	Wetland 2	11.7
17-May-93 17:10	W5	3.0	10-May-93 11:15	Wetland 2	13.6
22-May-93 11:30	W5	5.5	10-May-93 11:15	Wetland 2	13.3
22-May-93 11:30	W5	5.2	14-May-93 10:30	Wetland 2	12.3
22-May-93 11:30	W5	5.2	14-May-93 10:30	Wetland 2	12.5
24-May-93 05:10	W5	3.6	14-May-93 18:45	Wetland 2	12.0
24-May-93 07:15	W5	2.7	14-May-93 18:45	Wetland 2	13.4
24-May-93 07:15	W5	3.0	14-May-93 22:00	Wetland 2	16.1
24-May-93 09:55	W5	2.7	14-May-93 22:00	Wetland 2	17.2
24-May-93 12:50	W5	2.8	15-May-93 00:35	Wetland 2	16.7
24-May-93 18:05	W5	2.8	15-May-93 00:35	Wetland 2	17.3
24-May-93 20:50	W5	3.2	15-May-93 07:30	Wetland 2	14.8
25-May-93 11:15	W5	3.1	15-May-93 07:30	Wetland 2	16.3
25-May-93 21:10	W5	2.9	15-May-93 18:30	Wetland 2	17.2
26-May-93 10:55	W5	3.2	15-May-93 18:30	Wetland 2	18.5
27-May-93 10:20	W5	3.0	16-May-93 12:10	Wetland 2	12.8
28-May-93 08:15	W5	3.4	17-May-93 16:45	Wetland 2	13.8
28-May-93 08:15	W5	3.3	17-May-93 16:45	Wetland 2	13.4
28-May-93 10:50	W5	3.2	22-May-93 11:00	Wetland 2	17.2
28-May-93 15:40	W5	3.2	22-May-93 11:00	Wetland 2	17.0
28-May-93 20:40	W5	3.2	22-May-93 11:00	Wetland 2	18.5
29-May-93 14:45	W5	2.9	22-May-93 11:00	Wetland 2	18.5
30-May-93 14:50	W5	3.2	24-May-93 04:40	Wetland 2	11.6
17-Oct-92 13:32	Wetland 2	18.6	24-May-93 06:40	Wetland 2	16.8
28-Oct-92 12:30	Wetland 2	17.1	24-May-93 09:20	Wetland 2	18.3
01-Nov-92 16:25	Wetland 2	11.8	24-May-93 12:30	Wetland 2	17.2
01-Nov-92 16:25	Wetland 2	11.3	24-May-93 17:40	Wetland 2	14.3
03-Nov-92 01:00	Wetland 2	16.5	24-May-93 20:30	Wetland 2	15.4
03-Nov-92 07:35	Wetland 2	24.7	25-May-93 10:55	Wetland 2	14.3
05-Nov-92 17:20	Wetland 2	11.1	25-May-93 20:55	Wetland 2	13.9
07-Nov-92 09:35	Wetland 2	10.0	25-May-93 20:55	Wetland 2	13.3
11-Nov-92 01:25	Wetland 2	11.1	26-May-93 10:30	Wetland 2	13.4
11-Nov-92 16:50	Wetland 2	10.6	27-May-93 10:00	Wetland 2	12.2
13-Nov-92 01:16	Wetland 2	11.8	27-May-93 10:00	Wetland 2	12.4
13-Nov-92 10:15	Wetland 2	10.3	28-May-93 07:45	Wetland 2	15.4
14-Nov-92 13:25	Wetland 2	9.0	28-May-93 10:30	Wetland 2	14.8
19-Nov-92 11:30	Wetland 2	8.1	28-May-93 20:15	Wetland 2	11.7

Table A10.1 DOC data, 1992-93 (cont.).

Sample date	Location	DOC (mg/l)
29-May-93 14:20	Wetland 2	14.1
30-May-93 14:30	Wetland 2	13.8
28-Oct-92 13:10	Wetland 2, inflow	5.0
10-May-93 11:00	Wetland 2, low confl	26.5
28-May-93 10:25	Wetland 2, low confl	16.9
28-Oct-92 12:50	Wetland 2, lower confluence	14.2
28-Oct-92 12:55	Wetland 2, middle	10.8
10-May-93 11:05	Wetland 2, middle	14.1
28-Oct-92 13:30	Wetland 2, near P75	10.2
10-May-93 10:25	Wetland 2, near P75	10.3
28-Oct-92 12:40	Wetland 2, upper confluence	16.9
10-May-93 10:50	Wetland 2, upper confluence	23.8
17-Oct-92 16:49	Wetland 3	3.7
28-Oct-92 11:35	Wetland 3	4.2
01-Nov-92 16:10	Wetland 3	3.7
01-Nov-92 16:10	Wetland 3	3.8
03-Nov-92 00:15	Wetland 3	5.7
03-Nov-92 07:46	Wetland 3	4.4
03-Nov-92 07:46	Wetland 3	4.5
05-Nov-92 17:50	Wetland 3	3.7
07-Nov-92 10:00	Wetland 3	4.1
28-Oct-92 11:30	Wetland 3, near P85	4.5
10-May-93 11:40	Wetland 3, near P85	5.2

Note: Samples listed more than once
represent repeat analyses.